METAGENOMICS TO EXPLORE THE BIOTECHNOLOGICAL POTENTIAL OF CRYOSPHERIC BACTERIA

by
Melanie Claire Hay

Department of Geography and Earth Sciences
and
Institute of Biological, Environmental and Rural Sciences
Aberystwyth University

This dissertation is submitted for the degree of Doctor of Philosophy

September 2020

To my parents, siblings, and niece

DECLARATION

Word Count of thesis: 84 690

DECLARATION

This work has not previously been accepted in substance for any degree and is not being concurrently submitted in candidature for any degree.

Candidate name Melanie Claire Hay

Signature:

Date 14 September 2020

STATEMENT 1

This thesis is the result of my own investigations, except where otherwise stated. Where *correction services have been used, the extent and nature of the correction is clearly marked in a footnote(s).

Other sources are acknowledged by footnotes giving explicit references. A bibliography is appended.

Signature:

Date 14 September 2020

STATEMENT 2

I hereby give consent for my thesis, if accepted, to be available for photocopying and for inter-library loan, and for the title and summary to be made available to outside organisations.

Signature:

Date 14 September 2020

SUMMARY

Bioprospecting is the process by which organisms are investigated for natural products (NPs) that can be of societal benefit. The cryosphere is a prime region for bioprospecting because it has extreme environmental conditions that increase the probability of NP novelty, it is underexplored, and it is threatened by global climate change. Initially, 16S rRNA gene amplicon analysis was used to identify environments with high bioprospecting potential in a Svalbard glacier system (**Chapter 3**). Bacteria showed strong habitat preference, suggesting niche specialisation and subsequent vulnerability to climate change. Phylotypes do not provide functional information about microbes, therefore, shotgun metagenomics was used to understand the high potential environments better. Following the construction and testing of a bioinformatics workflow (**Chapter 8**), a collection of 74 metagenome assembled genomes (MAGs) from Svalbard cryoconite, soil and seawater (**Chapter 4)** and 121 MAGs from the Scărișoara Ice Cave (**Chapter 7**) were constructed. These MAGs were taxonomically classified, revealing several novel species. The spatial distribution of MAGs across several sites, together with identification of genes in major biogeochemical pathways was explored to understand microbe nutrient needs and look for signs of cooperation between co-occurring MAGs. Genome-mining was used to screen the MAGs for potentially useful secondary metabolites (**Chapter 5**). The MAGs were rich in biosynthetic gene clusters (BGCs) for exopolysaccharides (EPS), carotenoids, and non-ribosomal peptide synthases (NRPS), all of which find utility in the food, cosmetic and pharmaceutical industries. Bioinformatics predictions are limited by information in databases, and functional studies are needed to describe novel functions. Therefore, a functional metagenomic screen was conducted to search for novel cold-active polymerases by cloning soil and cryoconite environmental DNA into cold-sensitive *E. coli* mutants (**Chapter 6**). This thesis confirmed enormous diversity and novelty in cryospheric bacteria. Furthermore, adaptations that enable survival in the extreme conditions lend themselves to biotechnological applications.

ACKNOWLEDGEMENTS

This research was funded by a Marie Curie MicroArctic ITN grant. I am eternally grateful for the generous financial support as well as the many incredible opportunities that being part of this network has afforded me. I treasure the memories created at training events and meetings, and hope to stay connected to the wonderful group of ESRs and PIs.

I am incredibly grateful to my supervisors, Dr Arwyn Edwards and Dr Andy Mitchell for their mentorship. This was a wonderful adventure. Thank you for indulging my ideas, giving me so much independence, and providing advice, calm, reason, motivation, and support over all the years, as well as some genuinely fun fieldwork trips and discussions.

I am thankful to several people who were generous with their time, expertise, and equipment. Thank you to Dr Matt Hegarty for assisting with shotgun and 16S rRNA amplicon sequencing, Prof Luis Muir, Dr Manfred Beckmann, Dr Sumana Bhowmick, and Dr Jason Finch for all the help with metabolomics, Pauline Rees Stevens for letting me use equipment for DNA extraction and Dr Karen Reed and Shelley Rundle at Wales Gene Park for answering questions and assisting with shotgun metagenome sequencing. I would like to acknowledge those who assisted with sample collection or provided me with samples and data. Thanks to Diana Carolina Mogrovejo, Nora Els, Andy Mitchell, and Arwyn Edwards for your assistance with sample collection in Ny Ålesund, Svalbard in June/ July 2017 and Aliyah Debbonaire and Arwyn Edwards for sample collection in June / July 2018. Special thank you to Nick Cox and the NERC Arctic Research station for hosting me in the summers of 2017 and 2018. I would also like to thank Dr Cristina Purcarea for providing the Scărișoara Ice Cave metagenome sequences. I would like to acknowledge the help I received from Andre Soares conducting bioinformatics analyses, and Pallavee Srivastava, who taught this non-microbiologist how to culture bacteria. I would also like to acknowledge Meren, (of anvi'o) and Kai Blin (of MIBiG) who responded to GitHub issues and tweets, but more than that, created incredible tools, and created excellent resources on how to use their tools.

I had two secondments during my PhD that were both wonderful experiences. Thank you to Prof Tim Vogel, Dr Catherine Larose, Dr Laure Franqueville and Benoit Bergk Pinto at the Environmental Microbial Genomics Group at École Centrale de Lyon, who hosted me in their lab, trained me in new techniques and made me feel absolutely welcome and at home. I would also like to sincerely thank Dr David Rooke, Colin Bright, Sandeep, and Karl for making my visit to Dynamic Extractions in Tredegar such a warm, informative, and friendly experience.

The daily reality of the PhD, with all is highs and lows, has been navigated with the best lab mates, and dear friends that a person could hope to find. My eternal gratitude, love, and loyalty to the 'Four Musketeers', which includes André Soares, Aliyah Debbonaire and Pallavee Srivastava. Thanks for the coffees, beers, wines (and whines), work talk, life talk, silly talk, and serious advice. I learned and gained and grew so much from knowing you. I would also like to thank the other members of F36 who provided friendship, a few good nights out and serious laughs, Karen Cameron, Alvaro Garcia, Eleanor Furness, and Joe Dean.

To Morgan Commins, my wonderful friend- it is impossible not to acknowledge your role in my life and academic journey over the 14 years since we met. Thank you for believing in me, encouraging me, regularly feeding me great food, and all the adventures.

Finally, I would like to thank my family. My father, Malcolm Hay, encouraged my love of science from a young age, and financially supported much of my studies. You believed in me and instilled in me the belief that I can do anything. I also want to thank my mother, Wendy Hay, who is kindness, gentleness, and acceptance personified. I would not have completed this PhD without my twin sister, Michelle Hay (Shelly). You have been there through literally everything. Your support, in academics and life is constant and absolute. Thank you to Michelle and my brother-in-law, Andrew Bowman for the cosiest, happiest, most encouraging space a person could hope for during a combined pandemic/ PhD write-up. Likewise, I had shelter from my youngest sister, Kirsten Hay and my brother-in-law, Timothy Fischer, during December and January 2019. Kirst, it has been a long time since you sent me handwritten and decorated letters at Rhodes, but your support, thoughtfulness and generosity over the years has not wavered. Finally, my brother Alastair Hay, and my sister-in-law Mai, your messages never fail to make me smile, especially since Alexandra Ida Hay joined the world last year.

TABLE OF CONTENTS

LIST OF TABLES

LIST OF FIGURES

List of Abbreviations and Acronyms

Measurements and units

°	degrees
µL	microlitre
µm	micrometer
µM	micromolar
Da	dalton
g	Relative Centrifugal Force
km²	Square kilometers
C	Celsius
L	Litres
M	Molar (Mole per Litre)
m	metres
m/z	mass to charge ratio
mg	milligrams
min	minutes
mL	millilitres
mM	milliMolar
mm	millimetres
ng	nanograms
nm	nanometers
nM	nanoMolar
pM	picoMolar
s	second
E	East/Eastings
N	North/Northings

Acronyms

AA	Amino acid
AB	Austre Brøggerbreen
AFP	Anti-Freeze Protein
Amp	Ampicillin
ANI	Average Nucleotide Identity
ANOVA	Analysis of Variance
antiSMASH	Antimicrobial Secondary Metabolite Analysis Shell
AP	Anabaenopeptin
ASV	Amplicon Sequence Variant
BSC	Biological Soil Crust
BGC	Biosynthetic Gene Cluster
BLAST	Basic Local Alignment Search Tool
BP	Bioplastics
bp	base pairs
Ca2+	Calcium ion

$CaCl_2$	Calcium chloride
CAP	Canonical Analysis of Principal co-ordinates
cDNA	complimentary Deoxyribonucleic Acid
CER	Closest Environmental Relative
Chl a	Chlorophyll a
Cl-	Chloride ion
CLIMB	Cloud Infrastructure for Microbial Bioinformatics
CNR	Closest Named Relative
CO	Carbon monoxide
CO_2	Carbon dioxide
COG	Cluster of Orthologous Groups
coxLMS	Carbon monoxide dehydrogenase (L, M and S subunits)
CP	Cyanopeptolin
CPR	Candidate Phyla Radiation
DEM	Digital Elevation Model
DHA	Docosahexaenoic acid
DNA	Deoxyribonucleic Acid
dNTP	deoxynucleotide triphosphate
EB	Elution Buffer
eDNA	Environmental (metagenomic) DNA
eggNOG	Evolutionary genealogy of genes: Non-supervised Orthologous Groups
EPA	Eicosapentaenoic acid
EPS	Extracellular Polymeric Substances
FA	Fatty acid
FDR	False Discovery Rate
Fe^{2+}	Ferrous ion (Iron)
FI-ESI-MS	Flow Infusion Electrospray Ionisation Mass Spectrometry
GNPS	Global Natural Products Social Molecular Networking
GPS	Global Positioning System
GTDB	Genome Taxonomy Database
GTDB-tk	Genome Taxonomy Database toolkit
H_2O	Water
HCl	Hydrochloric acid
HMM	Hidden Markov Model
HPLC	High Performance Liquid Chromatography
IBP	Ice-Binding Protein
KEGG	Kyoto Encyclopaedia of Genes and Genomes
LB	Luria-Bertani broth
LAP	Linear azol(in)e-containing peptides
LC-MS	Liquid chromatography–mass spectrometry
MAG	Metagenome assembled genome
MAA	Mycosporine-like amino acids
MC	Microcystin
MDS	Multidimensional scaling

MG	Microginin
Mg^{2+}	Magnesium ion
MIBiG	Minimum Information about a Biosynthetic Gene Cluster database
ML	Midtre Lovénbreen
N	Nitrogen
NCBI	National Centre for Biotechnology Information
NGS	Next Generation Sequencing
NH_3	Ammonia
nifDHK	Nitrogenase genes
nmda	NDMA-dependent methanol dehydrogenase
NO_2-	Nitrite ion
NO_{3-}	Nitrate ion
NP	Natural Product
NRPS	Non-ribosomal peptide synthetase cluster
O_2	Oxygen
OD	Optical density
O/N	Overnight
ORF	Open Reading Frame
OTU	Operational Taxonomic Unit
PBS	Phosphate Buffered Saline
PCA	Principal Components Analysis
PCB	Polychlorinated biphenyls
PCO	Principal Co-Ordinates Analysis
PCR	Polymerase Chain Reaction
PERMANOVA	Permutational Analysis of Variance
PKS	Polyketide Synthase
PolA	DNA Polymerase A
POP	Persistent organic pollutant
PpyS-KS	PPY-like pyrone cluster
PUFA	Polyunsaturated fatty acid
QIIME	Quantitative Insights into Microbial Ecology
RA	Relative Abundance
Rbs	ribosome binding site
RED	Relative evolutionary divergence
rRNA	Ribosomal Ribonucleic Acid
RiPP	Ribosomally synthesised and post-translationally modified peptide product
Rpf	Resuscitation promotion factor
Rpm	Revolutions per minute
S_2	Disulphide
SCG	Single-copy Core Gene
SD	Standard Deviation
smdh	S-(hydroxymethyl)mycothiol dehydrogenase
SO_4^{2-}	Sulphate ion
T1PKS	Type I Polyketide synthase

T2PKS	Type II Polyketide synthase
T3PKS	Type III Polyketide synthase
TBE	Tris-borate-EDTA
TBP	Toxic Bioactive Peptides
TCA	Tricarboxylic Acid
TE	Tris-EDTA
Thy	Thymine
TNF	Tetranucleotide frequencies
UV	Ultraviolet
VB	Vestre Brøggerbreen
VL	Vestre Lovénbreen

1 LITERATURE REVIEW

"It was for the best, so Nature had no choice but to do it." -Marcus Aurelius

1.1 Bioprospecting

Bioprospecting is the process by which organisms are investigated for natural products (NPs) that can be of societal benefit. These benefits range from bioactive compounds that can act as life-saving drugs in the pharmaceutical industry (Lo Giudice and Fani, 2016; Lyutskanova et al., 2009) to freeze-resistant genes in genetically modified crops (Muñoz et al., 2017), to cold-active enzymes in large-scale industrial processes (Ferrer et al., 2016; Santiago et al., 2016). NPs are especially attractive to the pharmaceutical industry because they have evolved over millions of years to fulfil a variety of roles in diverse organisms, and therefore offer unrivalled chemical diversity, structural complexity and proven biological potency (Knight et al., 2003).

1.1.1 Bioprospecting encourages biodiversity conservation

While bioprospecting is usually done for commercial profit, recent agreements such as the Nagoya Protocol (https://www.cbd.int/abs/), have done much to ensure that this is not synonymous with exploitation or biopiracy (Buck and Hamilton, 2011). Instead, bioprospecting is frequently cited as a possible solution to natural resource degradation and biodiversity loss because it promotes investment in biodiversity conservation (Ding et al., 2006).

1.1.2 Bioprospecting provides solutions to emerging global challenges

There has been an increase in bioprospecting worldwide as scientists turn to microorganisms to try solve many of the worlds emerging challenges, such as the rise of anti-microbial resistance (Ventola, 2015), global climate change and the need for green energy (Cavicchioli et al., 2019), the accumulation of plastic waste (Wei and Zimmermann, 2017), and environmental contamination (Grannas et al., 2013) to name but a few. The utility of microorganisms as solutions to these problems may lie in their use as communities as a whole (Bell et al., 2013; Yergeau et al., 2009) in pure culture as cell factories (Hauksson et al., 2000; Muñoz et al., 2017), or by the heterologous expression of the products of single genes (like enzymes) (De Santi et al., 2014; Jeon et al., 2009; Vester et al., 2014) or gene clusters (secondary metabolites) (Feng et al., 2012; Komatsu et al., 2013; Owen et al., 2015; Zhang et al., 2010).

1.1.3 Bioprospecting in the cryosphere

While all environments are explored, from deep sea hydrothermal vents (Stokke et al., 2020), to the Amazon rainforest (Pereira et al., 2017) to the stomachs of various ruminants (Hess et al., 2011; Singh et al., 2019), several factors are contributing to increased bioprospecting interest in the Arctic cryosphere (Figure 1-1). Firstly, the Arctic is an extremely harsh environment with several unique environmental stressors that prove challenging to life, such as low temperatures, high summer UV radiation, low winter light and low liquid water availability (Maccario et al., 2015) (Section 1.4). The organisms that inhabit this icy environment therefore warrant our attention because their metabolic, physiological and structural adaptations to these inhospitable conditions may offer unique solutions (Section 1.5). Secondly, the Arctic is a relatively unexplored environment due to logistical difficulty and expense in accessing this region (Edwards et al., 2016; Gowers et al., 2019). One of the great balancing acts in bioprospecting is to maximise novelty, while minimising redundancy and the rediscovery of strains and NPs (Demain and Sanchez, 2009). Therefore, the relative lack of research in this region bodes well for novel discoveries. Thirdly, global climate change is rapidly altering this environment (Barry, 2017; Fountain, 2012), at a rate that twice the global average (Graversen et al., 2008). There is therefore a sense of urgency to explore the environment before it is irrevocably altered.

1.2 The habitats of the global cryosphere

The cryosphere is defined as regions of the Earth where water is in its solid form and includes glaciers, icecaps and ice-sheets, as well as sea ice, frozen inland water bodies, snow and permafrost (Margesin and Collins, 2019). The cryosphere is one of the Earth's largest biomes, covering approximately 10% of the Earth's surface, and is home to an enormous variety of microorganisms from all domains of life (Anesio et al., 2017; Anesio and Laybourn-Parry, 2012; Boetius et al., 2015; Hodson et al., 2008). In the following section the characteristics of some of the major cryospheric environment types and the microorganisms that inhabit them are reviewed.

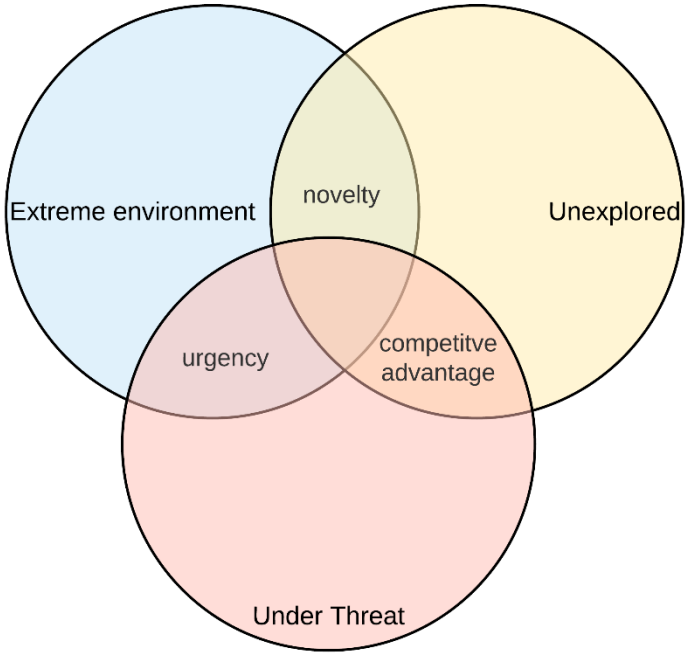

Figure 1-1: Factors that make the cryosphere attractive for bioprospecting. The cryosphere is an extreme environment and relatively unexplored, which increases the chances of novel NPs. The cryosphere is seriously threatened because of global climate change, and there is therefore an urgent need to explore these environments soon.

1.2.1 Glacial ecosystems

Ice sheets, ice caps and glaciers are large bodies of frozen freshwater. Glaciers are defined by their underlying topography while ice caps and sheets override their underlying topography, with a 50,000 km^2 cut-off between cap and sheet. The types and densities of microbial life supported by different glaciers will be shaped by environmental and physical attributes, such as water content, nutrient abundance, ionic strength, solar radiation and pH conditions, which can differ regionally, such as between different glacier sites or within different glacial zones (Hodson et al., 2008).

Glaciers themselves can be divided into three main glacial ecosystems: the supraglacial, englacial and subglacial systems (Figure 1-2) (Hodson et al., 2008). The supraglacial system consists of the surface habitats of the glacier, such as snow, meltwater streams and cryoconite holes (Anesio and Laybourn-Parry, 2012; Hodson et al., 2008). The englacial system consists of deep ice and the moulins and crevasses that bring meltwater from the glacier surface to the subglacial system and is unlikely to support the diversity and abundance of life of the other glacial zones (Hodson et al., 2008). The subglacial system occurs at the interface of the ice-bed with the underlying geology and may consist of basal ice, till mixtures and subglacial lakes.

It is estimated that $10^{25} – 10^{29}$ microbial cells are trapped in glacial ice world-wide (Irvine-Fynn and Edwards, 2014), and it has been suggested that $10^{17} – 10^{21}$ viable microorganisms are liberated annually by global glacier melt (Hodson et al., 2008). All three domains of life are represented; bacteria, archaea and eukarya; with bacteria and eukarya making up the vast majority, and archaea detected less frequently in surface habitats (Cook et al., 2016b; Hodson et al., 2008; Zarsky et al., 2013), but more commonly in subglacial habitats (Hamilton et al., 2013; Stibal et al., 2012). The supraglacial zone itself contains a series of distinct surface habitats such as clean snow, green snow, red snow, biofilms, clean ice, dirty ice and cryoconite holes (Lutz et al., 2016). In a summary of cell density in several different cryosphere habitats, supraglacial and permafrost habitats had the highest cell density, at 10^4 - 10^8 per ml and 10^5 - 10^8 per ml respectively (Boetius et al., 2015). Of these supraglacial habitats, cryoconite holes are the most biodiverse and active (Hodson et al., 2008).

1.2.2 Cryoconite

Cryoconite is a dark, granular sediment comprising biotic (organic) and abiotic (inorganic) material that commonly discolours the surface of glacial ice (Cook et al., 2016b; Hodson et al., 2008). The dark colour of cryoconite granules lowers the albedo of the ice, resulting in localised warming and melting (Box et al., 2012). This melting causes the formation of cylindrical holes, filled with meltwater, which can be tens of centimetres deep (Cook et al., 2016b; Hodson et al., 2008). The most common location of these cryoconite holes is in the ablation zone of glaciers (Cook et al., 2016b; Hodson et al., 2008), however they can also be found in glacial streams (hydroconite) and in a thickened, anoxic form, termed a cryoconite ‘mantle’, which differs substantially from open cryoconite holes (Hodson et al., 2008).

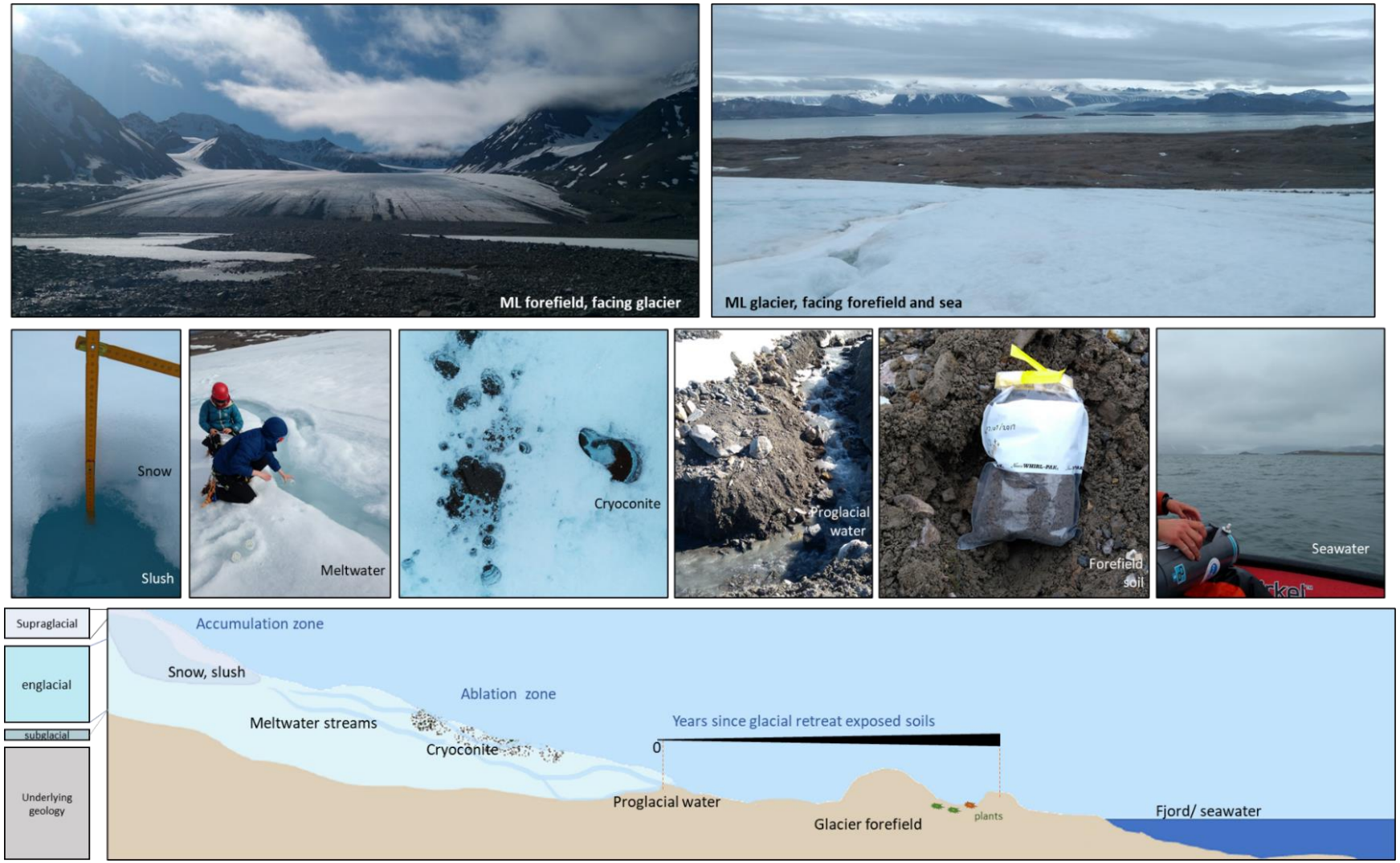

Figure 1-2: Diagram showing some of the habitats of a glacier ecosystem.

Cryoconite granules can be of varying size and comprise a variety of different minerals and organisms in various proportions, depending on local factors (Cook et al., 2016a). In addition to living cyanobacteria and heterotrophic bacteria, granules contain organic matter from decomposition of dead bacteria and biogenic material from local and distant sources (Cook et al., 2016a, 2016b). The amount of organic matter in cryoconite is likely a combination of primary production via photosynthesis, supplemented by windblown allochthonous organic material from surrounding environments, autochthonous material washed-in from the glacier surface or remnants of organic matter from the past, when primary production was much higher, are all possible sources (Telling et al., 2012). The source of living organisms is unclear, but there is strong evidence for the deposition of organisms from an Aeolian biome (Cameron et al., 2020a; Cook et al., 2016b; Cuthbertson et al., 2017).

The microstructure of cryoconite consists of many internal layers, surrounded by filamentous cyanobacteria (Hodson et al., 2010a). The filamentous cyanobacteria are important organisms in establishing cryoconite granules because they weave around smaller particles and bind them together physically, as well as secrete extra cellular polymeric substances (EPS) that act as a glue between particles (Chrismas et al., 2016a; Hodson et al., 2010a). Inorganic mineral fragments are usually present and often consist of phyllosilicate, tectosilicate and quartz, with some variations due to local geology (Cook et al., 2016b). The source of inorganic solutes is likely to be from marine aerosol, which supplies Na^+, Cl^-, K^+ and NO_3^- and carbonate weathering of debris, which provides minerals such as Ca^{2+} and Mg^{2+}(Hodson et al., 2010a). Other sources of inorganic minerals, pollutants and black carbon is via the deposition of wind-blown fine dusts.

1.2.2.1 Spatial and temporal variation

Both spatial and temporal (seasonal) differences in environmental factors affect the activity and structure of microbial communities (Cameron et al., 2012a; Hell et al., 2013). Cameron et al showed that the microbial community structure at various glaciers in the Arctic (Svalbard and Greenland) and the Antarctic were significantly different, suggesting local environmental differences shape community structure (Cameron et al., 2012a); while Edwards et al. showed that the bacterial communities of cryoconite are distinct and differ compared to nearby ice-marginal habitats (Edwards et al., 2013b). This suggests that site-specific environmental variables selects for the types of microbial communities that flourish (Cameron et al., 2012a). However, there is additional complexity because the microbial community can also change the local environment. For example, cryoconite hole morphology responds to environmental

changes such as changes in light intensity and sediment deposition (Cook et al., 2016a, 2010). Specifically, cryoconite holes deepen in response to increased sunlight and broaden in response to additional sediment deposit (Cook et al., 2016a).

There is also evidence of succession of microbial communities over time. Edwards et al demonstrated a reciprocal relationship between Alphaproteobacteria and Betaproteobacteria classes and hypothesises that early-colonizing opportunistic Betaproteobacteria that reproduce quickly and prolifically, are replaced by the Alphaproteobacteria, which establish equilibrium (Edwards et al., 2014). The bacterial communities that initially establish themselves may alter the local environment via their metabolic activities; resulting in an increase or decrease in certain nutrients, or a change in pH, that makes it more suitable for other organisms. For example, numerous studies have shown that the pH of water inside cryoconite holes is increased when there is net autotrophy (Stibal et al., 2008; Stibal and Tranter, 2007).

1.2.2.2 Cryoconite-associated bacteria

Previous studies have shown that there are both inter-regional (Cameron et al., 2012a) and interglacial (Edwards et al., 2011) differences in cryoconite bacterial communities. Early studies on microbial biodiversity on Svalbard relied on techniques such as microscopy and spectroscopy to identify organisms (Hodson et al., 2010a; Kaštovská et al., 2007, 2005; Langford et al., 2010; Säwström et al., 2002, 2002; Stibal et al., 2008, 2006; Stibal and Tranter, 2007; Takeuchi, 2002). As such, all early studies tended to characterise the cyanobacteria as the most abundant species. With the single exception of Kaštovská, 2007, who used fatty acid analysis to identify Actinobacteria (Kaštovská et al., 2007), there were no other phyla of bacteria recognised until after 2010 (Table 1-1). Edwards et al were the first to use 16S rRNA terminal restriction fragment length polymorphisms (tRFLP) to classify bacterial species (Edwards et al., 2011). Studies of cryoconite consistently report Cyanobacteria and Proteobacteria as the most abundant phyla (Cameron et al., 2012a; Edwards et al., 2011, 2014; Gokul et al., 2016). Recently, Gokul et al sampled 37 sites on the Foxfonna ice-cap in central Svalbard and demonstrated that cryoconite bacterial communities are strongly dominated by a small number of core taxa which are both ubiquitous and abundant (Gokul et al., 2016). The core taxa include representatives of Actinobacteria, Cyanobacteria, Proteobacteria, Bacteroidetes, Chloroflexi and Gemmatimonadetes (Gokul et al., 2016). Notably, an OTU belonging to the filamentous cyanobacterial genus *Leptolyngbya* was present at all of the sites at a mean relative abundance four times greater than the next most dominant OTUs, which corroborates the hypothesis that filamentous bacteria are important ecosystem engineers, and play a vital role in the formation of granules. Archaea are very rarely detected in Svalbard,

however, Nitrososphaera from the ammonia-oxidising archaeal phylum Thaumarchaeota (Zarsky et al., 2013), as well as Nitrosophaerales and Methanobacteriales have been detected in Svalbard cryoconite (Lutz et al., 2016). Table 1-1 shows common bacterial phyla in Svalbard cryoconite. There have been a few reviews that have tried to summarise the biodiversity of cryoconite across all geographic locations (Kaczmarek et al., 2016).

Table 1-1 Table of common Bacterial phyla in Svalbard cryoconite

Study	Method	Acidobacteria	Actinobacteria	Bacteroidetes	Chloroflexi	Cyanobacteria	Firmicutes	Gemmatimonadetes	Plantomycetes	Proteobacteria						Verrucomicrobia
										α	β	γ	δ	ε	ζ,	
(Säwström et al., 2002)	M					■										
(Takeuchi, 2002)	M					■										
(Kaštovská et al., 2005)	M					■										
(Stibal et al., 2006)	M					■										
(Kaštovská et al., 2007)	M, FA		■			■										
(Stibal and Tranter, 2007)	M					■										
(Stibal et al., 2008)	M					■										
(Hodson et al., 2010a)	M					■										
(Langford et al., 2010)	M					■										
(Edwards et al., 2011)	TRFLP, C	■	■	■	■	■			■	■	■	■	■	■	■	
(Cameron et al., 2012b)	PCR, N+C					■				■	■	■	■			
(Cameron et al., 2012a)	TRFLP, C	■	■	■		■	■			■	■	■	■	■	■	■
(Edwards et al., 2013c)	TRFLP	■	■			■			■	■	■	■	■	■	■	
(Zarsky et al., 2013)	qPCR 16S	■	■	■		■	■			■	■	■	■	■	■	■
(Edwards et al., 2014)	TRFLP, 454 16S	■	■	■		■	■			■	■	■	■	■	■	
(Singh et al., 2014a)	I, 16S		■	■							■	■				
(Singh et al., 2014b)	I, 16S		■	■							■	■				
(Gokul et al., 2016)	TRFLP, 16S PCR	■	■	■	■	■		■		■	■	■	■	■	■	
(Lutz et al., 2016)		■	■	■		■				■	■	■	■	■	■	

Methods of classification is denoted as follows: M, microscopy, R, 16S rRNA RFLP, C, clone library, I- isolates from clones. The phyla with > 1% abundance are indicated in each study.
cL-cbbL, aA- amoA, nG narG/ napA, NS- NirS

1.2.3 Soil

Soil is considered to harbour the most diverse communities of bacteria of any environment on Earth (Roesch et al., 2007), and this diversity can vary dramatically across micro-, meso- and macro scales (Bach et al., 2018). A review of the biogeography of Arctic soils showed large scale differences in community structure across Alaska, Canada, Greenland, Svalbard, Finland and Siberia (Malard and Pearce, 2018). In a study of 200 independent Arctic soil samples from 43 sites, including Svalbard, the most abundant phyla were the Proteobacteria (20%), Planctomycetes (15%) and Acidobacteria (13%) while Actinobacteria, Bacteroidetes,

Chloroflexi and Verrucomicrobia each accounted for 4–6% of the community (Malard et al., 2019). However, the specific species within these phyla differed between samples and sites, suggesting significant heterogeneity and endemism in Arctic soils. The major factors driving soil biogeography are pH and vegetation cover (Malard et al., 2019; Malard and Pearce, 2018). Vegetation in turn can be established only when nutrients are available to support plant growth.

One of the major processes in the Arctic is the exposure of new soils as glaciers lose volume and retreat (Bradley et al., 2014; Yoshitake et al., 2018). These recently exposed soils are generally extremely oligotrophic and contain few bacteria. It takes years to decades for communities to take hold and flourish and there is a development of the community over time as well as succession of the bacterial taxa that make up that community (Schulz et al., 2013). The initial source of nutrients in recently exposed glacier forefields is established by allochthonous inputs from the supraglacial and subglacial environments, precipitation and aerial deposition (Hodson et al., 2010b), mammal and bird droppings and adjacent ecosystems such as marine systems and vegetated soils (Bradley et al., 2014).

In a study of the Austre Brøggerbreen (AB) glacier forefield, changes in microbial community were found to be rapid in the first few years after deglaciation, and then stabilise and change much more slowly (Yoshitake et al., 2018). The first colonizers in newly exposed soils tend to be Cyanobacteria, green algae, lichens, mosses and fungi, which often conglomerate and form biological soil crusts (BSCs) (Schulz et al., 2013). These early colonisers change the soil nutrient content and increase the availability of biologically available carbon and nitrogen. A study of four sites in Svalbard found that filamentous cyanobacteria belonging to the Leptolyngbyaceae family were the most abundant cyanobacteria in BSCs (Pushkareva et al., 2015). When two sites from the forefield of Midtre Lovénbreen (ML) glacier, Svalbard were investigated using shotgun metagenomics, they were found to contain 28 different phyla, the most dominant phyla of which were the Proteobacteria and Actinobacteria with Planctomycetes, Firmicutes, Verrucomicrobia, Acidobacteria, Cyanobacteria, Bacteroidetes, Chloroflexi making up less abundant community members (Seok et al., 2016). Studies of microbial communities of Svalbard soil is shown in Table 1-2.

Table 1-2 Table of common Bacterial phyla in Svalbard soil

Study	Method	Other	Acidobacteria	Actinobacteria	Bacteroidetes	Chloroflexi	Cyanobacteria	Firmicutes	Gemmatimonadetes	Plantomycetes	Proteobacteria						Verrucomicrobia
											α	β	γ	δ	ε	ζ	
(Lee et al., 2013)	TRFLP	N,T,A															
(Tveit et al., 2013)	rRNA, mRNA																
(Schostag et al., 2015)	16S RNA	A3															
(Seok et al., 2016)	Shotgun																
(Malard et al., 2019)	16S RNA																

Other phyla: N; Nitrospira, T: Thermobaculum, A: Armatimonadetes, A3: AD3,

1.2.4 Seawater

The open fjords of Svalbard's jagged coastline are subject to contrasting environmental conditions due to freshwater inputs from glacial meltwater, terrestrial runoff and marine water mass exchanges (Conte et al., 2018). In addition, there is vast variability in water physical-chemical properties, such as temperature, nutrient content, oxygen saturation, hydrodynamism and light penetration (Conte et al., 2018). The bacterial communities of Fjord water and subtidal fjord sediments in Svalbard have previously been investigated (Conte et al., 2018; Thomas et al., 2020). Fjord water near Ny Ålesund was found to contain predominantly Alphaproteobacteria, Gammaproteobacteria, Bacteroidetes, Firmicutes and Parcubacteria, as well as Gemmatimonadetes, Nitrospirae, Acidobacteria and Chloroflexi (Conte et al., 2018). The fjord water near the Vestre Brøggerbreen (VB) glacier outlet was found to predominantly contain Alphaproteobacteria, Flavobacteriia (Bacteroidetes), Verrucomicrobia, Gammaproteobacteria and Acidimicrobiia (Thomas et al., 2020).

Table 1-3 Table of common Bacterial phyla in Svalbard seawater

Study	Method	Acidobacteria	Actinobacteria	Bacteroidetes	Chloroflexi	Cyanobacteria	Firmicutes	Gemmatimonadetes	Plantomycetes	Proteobacteria						Verrucomicrobia
										α	β	γ	δ	ε	ζ	
(Thomas et al., 2020)	16S rRNA															
(Conte et al., 2018)	16S rRNA															
(Zeng et al., 2017)	16S 454															
(Jain and Krishnan, 2017)	16S rRNA															

1.3 Investigated Regions

The geographic regions of investigation in this thesis was limited to the region surrounding Ny-Ålesund, on Spitsbergen, Svalbard, and the Scărișoara Ice Cave, Romania.

1.3.1 Svalbard

Svalbard is a Norwegian archipelago, situated between 74° - 81° N and 10° - 35° E, about midway between continental Norway and the North Pole. Spitsbergen is the largest island of the Svalbard archipelago, and comprises an area of 39 044 km^2. Svalbard has an Arctic climate, but it is heavily moderated by the warm North Atlantic Current, which means that is has a summer temperature of 4° to 6°C and winter average temperature of -12°C to -16°C.

Figure 1-3 Map of Svalbard. Svalbard is a Norwegian archipelago, situated between 74° - 81° N and 10° - 35° E. The largest island of the Svalbard archipelago is Spitsbergen. Figure by **(Räisänen, 2008)**

1.3.2 Scărișoara Ice Cave

The Scărișoara ice cave in Romania is an example of a non-Arctic cryospheric environment and is included in this thesis because it embodies an example of a habitat that is extremely unique, isolated form other cryospheric habitats and severely threatened by both climate change and anthropogenic activity (tourism). The Scărișoara Ice Cave is one of the oldest and largest perennial underground ice-blocks in the world, being older than 3500 years and greater than 100 000 m^3 in volume. The cave is located in the Bihor Mountains of North West Romania (46°29’23”N, 22°48’35”E) at an altitude of 1165m (Iţcuş et al., 2016). The Scărișoara ice block differs from surface glaciers and glacier caves because it is not formed by snow accumulation (Holmlund et al., 2005). Rather it grows via the annual freezing of a layer of water that trickles into the cave during summer months, forming a shallow lake on top of the existing ice block. This layer, which can be up to 20 cm deep, freezes every winter, trapping at its bottom a layer of sediment deposited during the summer. The ice block therefore consists of sequential layers of ice of variable thickness, separated by organic- and organic-rich sediment layers.

Figure 1-4 Map of the Scărișoara Ice Cave location in Romania. The cave is located in the Bihor Mountains of North West Romania (46°29’23”N, 22°48’35”E) at an altitude of 1165m.

1.4 Extreme environmental parameters

The cryosphere is considered an 'extreme environment' because it has several environmental parameters considered limiting for the development of life (Maccario et al., 2015). These life-limiting parameters include low temperatures, high UV radiation and low liquid water availability (Maccario et al., 2015). However, microorganisms have displayed significant resilience in adapting to these environments.

1.4.1 Low temperatures

The cryosphere, from the Greek work *cryos* meaning "cold" or "ice" consists of regions where temperatures are sufficiently low that water is in a frozen state. Although air temperatures can rise above 0°C, temperatures in the ice tend to range from 0°C as a maximum in the summertime during melting, to - 50°C in the Arctic winter (Maccario et al., 2015). The temperature range is therefore extremely variable, and can differ significantly depending on other conditions, such as wind, which tends to lower the surface temperature, or snow cover, which tends to increase the temperature by insulating the ice (Maccario et al., 2015). Generally, organisms are classified into two groups according to the cardinal (minimum, optimal and maximum growth) temperatures of the organism (Casanueva et al., 2010). Some organisms, called psychrophiles, clearly prefer or require cold environments; and have cardinal temperatures in the range <0°C, 15°C and 20°C (Casanueva et al., 2010). While other organisms, called psychrotrophs, could more accurately be described as "cold-adapted mesophiles" and have cardinal temperature ranges of >0°C, >20°C and >30°C (Casanueva et al., 2010). Some psychrophiles may need to adapt to enormous temperature fluctuations, and will require mechanisms to do so, while others will be exposed to constant low temperature (Casanueva et al., 2010). Among the adaptations to low temperatures, are: cold active enzymes that are active at low temperature (Section 1.5.1), an increase in unsaturated fatty acids, (including polyunsaturated fatty acids), which help maintain membrane fluidity in the cold (Section 1.5.3), and anti-freeze proteins and ice-nucleation proteins that help protect organisms from ice-injury (Section 1.5.2).

1.4.2 High UV radiation

The polar regions are subjected to continuous light in the summer, and continuous dark in the winter. During summer, the polar regions experience continuous daylight and receive increased ultraviolet (UV) exposure due to ozone depletion (Maccario et al., 2015). UV radiation is generally known to be damaging to cells. The type of damage that is caused is

wavelength dependent. UV-B (290-320 nm) results in direct damage to DNA, where it causes the formation of thymine dimers (Setlow et al., 1963). In addition, there is a scattering effect in the ice and snow, which results in photolysis of compounds in the snow, and the release of reactive gases in the snow-boundary layer (Maccario et al., 2015). These highly reactive gases tend to raise the levels of reactive oxygen species (ROS), making this a highly reactive environment (Maccario et al., 2015). Among the adaptations to the high UV radiation are UV screens, pigments, and antioxidants (Section 1.5.4).

1.4.3 Low liquid water availability

Liquid water is vital for all living organisms, as it the medium in which the metabolic reactions of the cell take place. Due to the low temperature of glacial environments, water is mainly found in solid form (ice), with the exception of meltwater streams, water films, or veins and pockets (Hodson et al., 2008). These veins and pockets tend to be hypersaline or hyper-acidic, because they contain all the elements that are excluded from the ice-crystals as freezing takes place (Barletta et al., 2012; Dani et al., 2012; Maccario et al., 2015). Microorganisms in ice may, therefore, undergo desiccation as a consequence of low liquid water availability and high osmotic pressure (Maccario et al., 2015). Adaptations to this environmental stress includes the formation of EPS (Section 1.5.5) and compatible solutes.

1.5 Biotechnology

The focus of Section 1.5 will be how innovative physiological and metabolic adaptations to the environmental stressors highlighted in (Section 1.4) may be harnessed in biotechnology to create products and solutions that are useful to industry (Casanueva et al., 2010; D'Amico et al., 2006; Santiago et al., 2016, Maccario et al., 2015). According to a report by the United Nations University of Advanced Studies (UNU-IAS), in 2008, there were already 43 companies involved in the development of biotechnology products based on Arctic genetic resources (Leary, 2008). In addition, there were 31 patents or pending patents based on these Arctic microbial resources in 2008 (Leary, 2008); this number is undoubtedly much higher in 2020. The potential use of psychrophilic organisms in biotechnology has been reviewed previously (see (Arrigo, 2014; Casanueva et al., 2010; Larose et al., 2013a; Maccario et al., 2015; Margesin and Miteva, 2011; Miteva, 2008)).

Table 1-4. The potential uses of psychrophilic microorganisms in biotechnology

Product	Microorganism source	Application	Section
Cold-active enzymes	Psychrophilic bacteria and fungi	Food industry, detergents	1.5.1 Cold-active enzymes
Polyunsaturated fatty acids	Cold-adapted bacteria	Dietary supplements for humans, livestock, and fish	1.5.3 Polyunsaturated Fatty acids
Ice nucleation proteins	Psychrophilic bacteria and fungi	Food industry, synthetic snow	1.5.2 Anti-freeze proteins (AFPs) and ice-binding proteins (IBPs)
Antifreeze proteins and solutes	Psychrophilic bacteria and fungi	Cryoprotectants, food industry	
UV screens, pigments, and antioxidants	Psychrophilic bacteria and fungi	Biomedical, pharmaceutical, food technology and cosmetics	1.5.4 UV screens, pigments and UV screens, pigments, and antioxidants
Exopolysaccharide	Psychrophilic bacteria (cyanobacteria)	Biomedical, pharmaceutical, food technology and cosmetics	1.5.5 Exopolysaccharides/ extra cellular polymeric substances

The following subsections discuss (i) the various challenges posed by the environment, (ii) the biological adaptations to these challenges that make life possible, and (iii) the potential applications of these adaptive strategies in biotechnology.

1.5.1 Cold-active enzymes

Recently, the World Enzymes to 2017 Report forecast that enzyme demand would rise by 6.4 % to 6.9 billion p.a. in 2017 (http://www.rnrmarketresearch.com/world-enzymes-to-2017-market-report.html). There are several advantages to the use of enzymes to catalyse chemical reactions as opposed to purely chemical and physical methods. Cold-active enzymes have utility in many industries, and help to reduce carbon emmisions in large-scale industrial processes (Casanueva et al., 2010; Cavicchioli et al., 2002; D'Amico et al., 2006; Maccario et al., 2015; Santiago et al., 2016). Biological enzymes are efficient and highly selective catalysts, and they are generally more energy efficient, safer, and better for the environment (Santiago et al., 2016). The heating of reactants, which is a requirement of many chemical reactions, is an energy-intensive process that is both financially undesirable to businesses and environmentally unsustainable (Santiago et al., 2016). The enzymes of psychrophiles allow reactions to take place at lower temperatures, reducing the need for heating. In a time of growing concern over environmental sustainability, this makes low-temperature enzymes an attractive solution for industry. In fact, it has been estimated that by 2030, up to 40% of the bulk chemical synthesis processes requiring environmentally damaging substances, and high energy inputs could be replaced by enzymatic catalysts (Ferrer et al., 2016).

Low-temperature enzymes have several additional advantages in industry. The low temperature of the reaction may reduce or prevent many undesirable chemical reactions that occur spontaneously at higher temperatures. This allows a greater specificity of reaction and potentially a higher yield. Finally, low-temperature enzymes are unstable or denatured at higher temperatures. This enables reactions to be terminated by heat-inactivation, allowing for the sequencing of reactions through multi-stage chemical transformations without the need for purification steps, and removing the need for chemical inactivation methods (Santiago et al., 2016).

The Arrhenius law suggests that reaction rates should decrease with temperature, due to the decreased kinetic energy of the reacting molecules, which results in fewer interactions of the substrate with the active site (Casanueva et al., 2010; Santiago et al., 2016). Therefore, to maintain high activity, psychrophilic organisms must compensate for the reduced number of active site-substrate collisions, by increasing the likelihood of successful collisions. The structural and functional differences between thermophilic, mesophilic, and psychrophilic enzymes are due to changes in the amino acids that make up the enzyme. These changes can be in the form of amino acid substitutions, insertions and deletions (Santiago et al., 2016). The type of change, as well as the location of the change, have different consequences for the thermal stability of the molecule. As a general rule, it appears that there is a trade-off between protein thermostability and conformational flexibility, with high conformational rigidity resulting in the high thermostability seen in thermophiles, and the high conformational flexibility in psychrophiles leading to decreased thermostability (Casanueva et al., 2010; Santiago et al., 2016; Siddiqui and Cavicchioli, 2006). There is evidence that the increased flexibility occurs mainly at the active site, and is not necessarily present throughout the whole protein (Casanueva et al., 2010). Some structural features of cold-adapted proteins include fewer ion pairs resulting in fewer salt bridges, fewer polar, H-bond-forming residues, fewer arginine residues, fewer proline residues in protein loops, and fewer aromatic interactions than those in mesophilic proteins (Grzymski et al., 2006).

Several cold-active enzymes isolated from Arctic bacteria are described in Table 1-5 and cold-active enzymes from Antarctic bacteria are listed in Appendix Table A-1. These include several lipases, esterases and β-galactosidases which lend themselves to applications from laundry and detergent industry, to bioremediation, to biofuel production to the food and pharmaceutical industries (Table 1-5, and references therein).

Table 1-5: Sources of cold-active enzymes from Arctic microorganisms

Target Product	Location	Environment source	Phylum	Source Organism	Discovery approach	Application	Reference
Esterase	Spitsbergen island, Svalbard	Soil	Gammaproteo bacteria	*Pseudomonas* sp. S9	Genomic DNA library, phenotype screening, specific primers, followed by heterologous expression	Additives in food processes, laundry detergents, and bioremediation.	(Wicka et al., 2016)
Protease	Spitsbergen, Svalbard	Seawater	Gammaproteo bacteria	*Shewanella arctica*	Genomic DNA library, phenotype screening, specific primers, followed by heterologous expression	Chemical, cosmetics, and pharmaceutical industries.	(Qoura et al., 2015)
Pullunase	Spitsbergen, Svalbard	Seawater	Gammaproteo bacteria	*Shewanella arctica*	Genomic DNA library, phenotype screening, specific primers, followed by heterologous expression	Starch degradation for ethanol-based biofuel production.	(Elleuche et al., 2015)
β-galacto-sidase	South-West Greenland	Ikka columns	Firmicutes	*Alkalilactibacillus ikkense*	Genomic DNA library, phenotype screening, specific primers, followed by heterologous expression	Production of lactose-free dairy products as yogurt, sour cream, and some cheeses.	(Schmidt and Stougaard, 2010)
Esterase	Kolyma lowland region, Siberia	Cryopeg within Permafrost	Gammaproteo bacteria	**Psychrobacter cryohalolentis* K5(T)	Genome mining and specific primers followed by heterologous expression	Detergent preparations and bioremediation of polluted soils and waters in cold regions.	(Novototskaya-Vlasova et al., 2012)
Esterase	Kolyma lowland region, Siberia	Permafrost	Gammaproteo bacteria	**Psychrobacter cryohalolentis* K5(T).	Genome mining and specific primers followed by heterologous expression	Whole cell biocatalysts in organic synthesis and bioremediation at low temperatures, cell surface display platform.	(Petrovskaya et al., 2015)
Lipase	Kolyma lowland region, Siberia	Cryopeg within Permafrost	Gammaproteo bacteria	**Psychrobacter cryohalolentis* K5(T)	Genome mining and specific primers followed by heterologous expression	Production of pharmaceuticals, food, detergents, and fine organic synthesis.	(Novototskaya-Vlasova et al., 2013)

Target Product	Location	Environment source	Phylum	Source Organism	Discovery approach	Application	Reference
Esterase	Hadsel Fjord, North Norway	Atlantic hagfish stomach, seafloor	Actinobacteria	*Rhodococcus sp*. AW25M09	Genome mining and specific primers followed by heterologous expression	Additive for detergent production and biocatalyst for regio- and stereoselective reactions in chemical synthesis.	(De Santi et al., 2014)
Esterase	Vestfjorden area, Northern Norway	Sea fan (*Paramuricea placomus*) collected sea floor	Alphaproteo-bacteria	*Thalassospira* sp. GB04J01	Genome mining and specific primers followed by heterologous expression	Novel synthetic applications, including enzymes operating in low water activity and organic solvents for applications in bioenergy and biotechnology.	(De Santi et al., 2016)
β-Galactosi-dase	Kongsfjorden at Ny Ålesund, Svalbard	Fjord sediment	Gammaproteo bacteria	*Enterobacter ludwigii MCC 3423*	Phenotypic screen of isolate, followed by genome mining, specific primers	Dairy product manufacture, efficient hydrolysis of lactose in milk; reduce the risk of contamination, save energy during the industrial process.	(Alikkunju et al., 2016; Alikunju et al., 2018)
type II α-glucosidase	Kongsfjorden, Arctic Ocean	Deep-sea sediment	Gammaproteo bacteria	*Pseudoalteromo nas* sp. K8	Genome mining and degenerated primers followed by heterologous expression.	Industrial production of glucose, and other sugar compounds.	(Li et al., 2016)
β-galactos-idases, α-amylases, phosphatase	Greenland	Ikaite columns	Gammaproteo bacteria, Actinobacteria	*Unkown; Pseudoalteromo nas haloplanctis, Brachybacteriu m faecium*	Phenotypic screen of isolate library and functional screen of a metagenomic library	Food and feed, textile, waste management, medical and detergent industries.	(Vester et al., 2014)
Esterases	Kongsfjorden, Ny-Ålesund	Sediment sample from seashore	Bacteria	Metagenomic origin: unknown	Functional metagenomic screen of fosmid library	Organic chemicals, detergents, biosurfactants, oleochemical, dairy, agrochemical, paper manufacture, nutrition, cosmetics, and pharmaceutical processing industries.	(Jeon et al., 2009)

Target Product	Location	Environment source	Phylum	Source Organism	Discovery approach	Application	Reference
Esterase	Kapp Wijk, Svalbard	Intertidal zone sediment	Bacteria	Unknown (similarity to *Vibrio caribbenthicus*)	Functional metagenomic screen of fosmid library	Detergent, food, pharmaceutical, paper, textile, leather, and fine chemicals industries	(Fu et al., 2013)
Serine hydroxymethyl transferase	Arctic Ocean	Sea ice	Gammaproteobacteria	*Psychromonas ingrahamii*	Genome mining of isolate, synthesis of gene and heterologous expression.	Catalyse reactions in the synthesis of pharmaceuticals, agrochemicals, and food additives.	(Angelaccio et al., 2012)
Alkaline phosphatase	Reykjavik, Iceland	Seawater	Gammaproteobacteria	*Vibrio sp. G15-21*	Isolate screen, followed by enzyme purification by affinity-resin column.	Molecular biology tool.	(Hauksson et al., 2000)
DNA Polymerases	Northern Schneeferner, Germany	Glacial ice	Bacteroidetes, Gammaproteobacteria, Actinobacteria	*Algoriphagus, Pedobacter, Microscilla, Thermus, Acinetobacter, Rhodococcus*	Functional metagenomic screen of fosmid library on cold-sensitive *E. coli* mutant.	Molecular biology tool	(Simon et al., 2009a)

* Example of a single genome being mined for multiple enzymes

Abbreviations: Thin Layer Chromatography (TLC), Eicosapentaenoic Acid (EPA), Liquid Chromatography-Mass Spectrometry (LC-MS), Minimum Inhibitory Concentration (MIC)

1.5.2 Anti-freeze proteins (AFPs) and ice-binding proteins (IBPs)

The formation of ice crystals in cells can cause rupture of cell membranes and the death of the organism (Lorv et al., 2014). Psychrophiles have had to establish ways to lower the freezing point of the cytoplasm and prevent the formation of ice-crystals at temperatures at which water is usually frozen. Adaptations that prevent ice crystal formation include the accumulation of antifreeze proteins (AFPs) and ice-binding proteins (IBPs) and the synthesis of highly soluble poly-hydroxyl solutes, such as glycine, betaine, glycerol, trehalose, mannitol and sorbitol, which reduce the freezing point of the cytoplasm and act as cryoprotectant (Casanueva et al., 2010).

AFPs and IBPs find many uses in industry. For example, they are used in the cryopreservation of biological tissues (Bar Dolev et al., 2016), a common process in fertility treatment, where sperm, oocytes and embryos may be frozen for storage, and thawed at the appropriate time. They also have the potential for use in cryosurgery, where ice-nucleation proteins may be used to ablate cancer cells, by forming the characteristic ice spicules that puncture and shear cells during freezing (Bar Dolev et al., 2016). The food industry also has a multitude of uses for AFPs and IBPs, where they are used to prevent the unfavourable changes and loss of quality in food when it is frozen and thawed.

AFPs and IBPs both play a role in ice-crystal development; however, each protein class is involved in a different stage of the freezing process (Lorv et al., 2014). IBPs trigger ice-nucleation events, while AFPs inhibit growth of ice-crystals by binding to the ice-crystal nucleation centres and preventing the further accretion of ice (Bar Dolev et al., 2016; Lorv et al., 2014). AFPs have already been used with some success by Unilver to keep ice-cream from losing its creamy texture (Bar Dolev et al., 2016; Muñoz et al., 2017). AFPs may also be used in agriculture to improve crops resilience to frost and prevent the accumulation of ice on surfaces, such as roads, aircraft, air turbine blades, air-conditioners and freezers (Bar Dolev et al., 2016). Genes from Arctic bacteria that have potential biotechnological applications are listed in Table 1.6.

Table 1-6 Table of ice-nucleation-active bacteria

Antifreeze proteins						
Product	**Location**	**Environment type**	**Domain**	***Microorganism***	**Approach**	**Reference**
Antifreeze protein	Antarctica	Sediment and ice samples	Bacteria	*Sphingomonas, Plantibacter* and *Pseudomonas*	Phenotypic screening of isolates for freeze-thaw tolerance, TH measurement, protein purification, WGS and annotation, food preservation tests.	(Muñoz et al., 2017)
Antifreeze protein	Midre Lovénbreen glacier, Ny-Ålesund, Svalbard	Cryoconite holes	Bacteria	*Cryobacterium. psychrotolerans, Cryobacterium. psychrophilum, Pseudomonas ficuserectae, Subtercola frigoramans)*	Phenotypic screening of isolates for anti-freeze activity, protein purification and activity assays	(Singh et al., 2014a)
Antifreeze protein (extracellular ice-binding glycoprotein)	Tvillingvatnet Pond, Ny-Ålesund, Svalbard	Ice core from frozen freshwater pond	Yeast	*Leucosporidium sp*	Phenotypic screen, followed by genome sequencing, specific primers, cloning and sequence confirmation	(Lee et al., 2010)
Antifreeze protein with ice-nucleation activity	Canadian High Arctic	Plant roots in soil	Bacteria	*Pseudomonas putida GR12-2*	Amino acid sequencing, followed by PCR and expression in a heterologous host	(Muryoi et al., 2004)
Antifreeze protein	Ace Lake, Pendant Lake, Triple Lake, Deep Lake and Club Lake, Vestfold Hills and Larsemann Hills, Antarctica	Water from lakes with range of salinity and nutrients	Bacteria	*Mar. protea, Pseudoalteromonas, Pseudomonas fluorescens, Stenotrophomonas maltophilia, Sphingomonas*	Phenotypic screen of isolates, Splat assay, sequencing of 16S rRNA gene.	(Gilbert et al., 2004)

TH: thermal hysteresis, Splat assay ((Knight et al., 1988)), WGS: whole genome sequencing

1.5.3 Polyunsaturated fatty acids

Cellular membranes are vital components of all cells, as they control the internal composition of the cytoplasm by selectively allowing the transport of molecules into and out of the cell via passive, facilitated and active transport. Membrane-fluidity generally decreases with temperature, which decreases membrane permeability (D'Amico et al., 2006). The lower the density of fatty acid (FA) chains in the membrane, the lower the temperature at which the membrane transitions from the liquid crystalline, to the gel phase (Casanueva et al., 2010). Generally, microorganisms have adapted membranes that reduce the packing efficiency of FA chains by means of an increased proportion of unsaturated FAs, decreased average FA chain length, increased methyl branching and an increased antesio: iso branching ratio (Casanueva et al., 2010; Chattopadhyay, 2006). For example, an analysis of the FA profiles of *Cryobacterium* and *Micrococcus* isolates from cryoconite holes in Svalbard showed a higher concentration of branched fatty acids than saturated or unsaturated fatty acids (Singh et al., 2014b).

Genes involved in increasing the fluidity of cell membranes; that may have biotechnological potential include: polyunsaturated fatty acid (PUFA) synthesis genes, desaturases and dioxygen lipid desaturases (Casanueva et al., 2010). PUFA can be divided into ω6 and ω3 FAs, depending on whether the first double bond is at the 3rd or 6th carbon position, from the methyl end group of the FA chain. Mammals, including humans, are unable to synthesize the ω6 FA, linoleic acid (LA), and the ω3 FA, α-linoleic acid (ALA), and so they rely on dietary sources of the essential fatty acids. Furthermore, several of the other biologically important PUFA such as eicosapentaenoic acid (EPA) and docosahexaenoic acid (DHA) can be synthesised from ALA; however, the conversion from ALA to EPA and DHA Is low, and it is still preferable to obtain EPA and DHA from dietary sources. ALA is used in the biosynthesis of arachidonic acid (AA), which is in turn used in the biosynthesis of some prostaglandins, prostacyclin, leukotrienes, and thromboxane (Abedi and Sahari, 2014).

PUFA are essential to optimal human health and play a role in maintaining several important body functions. For example, long-chain PUFA help to regulate the immune system, and may help prevent autoimmune diseases such as rheumatoid arthritis, ulcerative colitis, and Crohn's disease, while ω3 fatty acids are beneficial in the management of skin disease, asthma, arthritis, lupus erythematosus and multiple sclerosis (Abedi and Sahari, 2014). DHA is essential for proper brain function, and directly influences the activity of serotonergic and cholinergic neurotransmitters (Abedi and Sahari, 2014; Bazinet and Layé, 2014). PUFA

have traditionally been sourced from fish oils; however, as fish stocks plummet worldwide, other alternative and more sustainable sources of PUFAs are required (Abedi and Sahari, 2014). PUFA form aquatic species also carry other risks, such as contamination with teratogenic, carcinogenic, and mutagenic chemicals such as DDT and dioxin-like polychlorinated biphenyls (Abedi and Sahari, 2014). Aquatic species also tend to accumulate methyl mercury and heavy metals such as Pb, Cr, Hg, Cd, and As, and antibiotics (Abedi and Sahari, 2014).

The production of PUFA from bacteria is therefore a promising avenue for investigation (Ochsenreither et al., 2016; Ratledge, 2004). There are two main lineages of marine bacteria appear to produce PUFA, the Gammaproteobacteria genera (*Shewanella* (EPA), *Colwellia* (DHA), *Moritella* (DHA), *Psychromonas* and *Photobacterium* (EPA)) and several species within two genera of the Cytophaga-Flavobacterium-Bacteroides (CFB) grouping (*Flexibacter* (EPA) and *Psychroserpens*) (Allen and Bartlett, 2002; Nichols, 2003; Nichols and McMeekin, 2002). EPA might be a vital component of the cell membrane in selected cold-adapted bacteria, as disruption of the EPA synthesis genes in the halophilic, psychrophilic strain *Shewanella livingstonensis* Ac10 resulted in a cold-sensitive mutant with decreased growth rate and filamentous cells (Dai et al., 2012; Sato et al., 2008).

A survey of metabolites produced by the microorganisms of several surface glacial habitats revealed that several algal species were positively correlated with the presence of PUFAs, and PUFAs were especially high in red snow (Lutz et al., 2016).

Table 1-7 Potential sources of PUFA from Cryospheric microorganisms

Product	Location	Environment	Phylum	Organism	Method	References
EPA, DHA	Svalbard	Amphipods, fish, bivalves, and shrimp in seawaters	Gammaproteobacteria	*Pseudomonads, Vibrio*	Cultured isolates, fatty acid analysis.	(Jøstensen and Landfald, 1997)
EPA, DHA, AA	Antarctica	Sea ice	Gammaproteobacteria	*Shewanella (6 species)*	Cultured isolates, fatty acid analysis.	(Nichols and McMeekin, 2002)
EPA	Antarctica	Sea ice	Proteobacteria	*Shewanella (4 species)*	Cultured isolates, fatty acid analysis	(Bowman et al., 1997)
DHA	Antarctica	Sea-ice diatom assemblages	Proteobacteria	*Colwellia (5 species)*	Cultured isolates, whole fatty acid analysis	(Bowman et al., 1998)
DHA	Japan Trench	Seawater sediments, 6,356m depth	Proteobacteria	*Moritella japonica*	Cultured isolates, fatty acid analysis.	Nogi et al, 1998
High amounts of EPA	Arctic Ocean, Spitsbergen, Svalbard; South-West Norway	Seawater	Protista (Diatoms)	*Phaeodactylum tricornutum*, and *Attheya septentrionalis*	Single cell isolation for clonal isolate, upscaling and culturing of proliferating strains, batch growth experiments	(Steinrücken et al., 2017)
PUFA	Svalbard, Sweden	Glacier surface habitata	Algae (metagenoimica)	*Chlamydomonadaceae, Raphidonema sempervirens*	Total DNA extraction from glacial habitats, Fatty acid analysis and statistical correlations between metabolites and species.	(Lutz et al., 2016)

1.5.4 UV screens, pigments, and antioxidants

At low temperatures, oxygen is more soluble in water, which means that there is a greater threat from reactive oxygen species (ROS). In addition, Arctic environments experience high UV radiation, which can be directly damaging to DNA, as well as causing increased ROS via photolysis (Casanueva et al., 2010). To prevent potentially lethal DNA damage from UV radiation and ROS, microorganisms have adapted a range of DNA repair mechanisms, UV screens and antioxidants (enzymes and metabolites) (Maccario et al., 2015; Mandelli et al., 2012; Sajjad et al., 2020). These antioxidant enzymes and metabolites may be useful in the cosmetic pharmaceutical and biomedical fields (Mandelli et al., 2012; Sajjad et al., 2020; Yabuzaki, 2017).

For example, psychrophilic bacteria have an increase in the number of catalases, superoxide dismutases (SODs) as well as other antioxidants such as rubreyrythrin, and rubredoxin oxidoreductase and dioxygen-consuming lipid desaturases (Casanueva et al., 2010). Microbial mats, dominated by Cyanobacteria, in the Canadian High Arctic, produce several natural UV-absorbing/screening compounds like carotenoids, mycosporine-like amino acids (MAAs) and phycobiliproteins (PBPs)(Mueller et al., 2005). Scytonemin is a Cyanobacterial indole alkaloid compound that has UV protectant, anti-inflammatory, anti-proliferative, and antioxidant activity. MAAs act as sunscreens, and antioxidants and can be used as UV protectors in skin-care products, or as photo-stabilizing additives in paints, plastics, and varnishes (Fuentes-Tristan et al., 2019; Pathak et al., 2020).

A survey of supraglacial habitats revealed that carotenoids were abundant (Lutz et al., 2016), and are a probably responsible for the darkening of snow and ice that causes melting. Cyanobacterial mats in the Canadian High Arctic were also a source of abundant chlorophylls, carotenoids, scytonemins, MAAs and phycobiliproteins and MAA metabolites (Mueller et al., 2005; Quesada et al., 1999).

Table 1-8 Microbial sources of antioxidants, pigments and UV screens

Product	Location	Habitat	Phylum *	Species	Activity/ Application	Reference
Antioxidant (unknown metabolites)						
Strong antioxidant (unknown)	Ny-Ålesund, Svalbard	*Symbionts of Lichen Ochrolechia sp.*	*A*lphaproteo bacteria	*PAMC26625, Sphingomonas sp*.	Free radical scavenging activity.	(Kim et al., 2014)
Antioxidant Enzymes						
Glutathione synthetase	Antarctic	Seawater	*Gammaproteo bacteria*	*Pseudoalteromonas haloplanktis*	Antioxidant, clinical applications; used as a pharmaceutical compound and can be used in food additives and the cosmetic industries.	(Albino et al., 2012)
Glutaredoxin	Antarctic	Sea ice	*Gammaproteo bacteria*	*Pseudoalteromonas* sp. *AN178*	New and potential sources of oxidative stress-inducible enzymes.	(Wang et al., 2014)
Glutathione S-transferase	Antarctic	Sea ice	*Gammaproteo bacteria*	*Pseudoalteromonas* sp. ANT506	Gene engineering strategies involving GSTs could improve plant's salt tolerance.	(Shi et al., 2014)
Carotenoids, Mycosporine-like amino acids (MAAs) and phycobiliproteins (PBPs						
Chlorophylls, carotenoids, scytonemins and (MAAs)	Ward Hunt Ice Shelf, High Arctic Canada	Microbial mat	Cyanobacteria	Whole microbial mat community, comprising Cyanobacteria and heterotrophic bacteria.	UV screening in a variety of organisms, use in cosmetic, pharmaceutical, and biomedical fields.	(Mueller et al., 2005)
Lipophilic pigments, phycobiliproteins and MAA	Canadian Arctic: (Ellesmere Island; Cornwallis Island	Semi-aquatic environments	Cyanobacteria	*Nostoc* spp., *Oscillatoria* spp *Scytonema* spp, *Phormidium* spp, *Anabaena*, *Nodularia*, *Calothrix*, *Schizothrix* and *Synechococcus*	Sunscreens, and antioxidants, UV protectors in skin-care products, or as photo-stabilizing additives in paints, plastics, and varnishes.	(Quesada et al., 1999)

1.5.5 Exopolysaccharides/ extra cellular polymeric substances (EPS)

As mentioned in Section 1.4.3, microorganisms in ice environments are subject to desiccation stress due to low water availability and high osmotic pressure. Adaptation to these stressors include the use of osmoprotectants and exopolysaccharides (EPS). EPS are high molecular weight carbohydrate polymers that constitute a significant component of the extracellular polymers surrounding most microbial cells, where they are usually found as capsular polysaccharides (covalently bound to the cell surface), and or as slime polysaccharides (loosely attached to the cell surface or in the extracellular medium) (Poli et al., 2010). Most EPS are heteropolysaccharides, consisting of three or four different monosaccharides arranged in groups of 10 or less to form repeating units (Poli et al., 2010).

The material properties of these EPSs make them useful in the food industry as a thickening agent, in the pharmaceutical industry, and in the cosmetic industry (Poli et al., 2010). In addition to their ability to produce slime and biofilms, exopolysaccharides also have potential applications as anticoagulant, antithrombotic, immunomodulation, anticancer and as bioflocculants due to their interactions with the immune system (Nwodo et al., 2012). In cold environments EPSs may have a role in freeze-thaw tolerance (Kim and Yim, 2007), and also provide a site for the localisation of UV protective compounds such as scytonemin and MAAs and allow for the scavenging of metal cations in oligotrophic conditions (Chrismas et al., 2016a; Pereira et al., 2009).

EPS is likely to play an important role in the formation of cryoconite granules (Chrismas et al., 2016a; Hodson et al., 2010a; Langford et al., 2010), therefore, the cyanobacteria of cryoconite is particularly interesting as a source of novel EPS.

Table 1-9 The use of EPSs in biotechnology

Product	Location	Habitat	Phylum	Species	Properties	Industrial use	References
EPS: N-acetyl glucosamine, mannose and glucuronic acid residues bound by heterogeneous linkages.	Arctic	Brown alga *Laminaria*	*Bacteriodetes*	P*olaribacter* sp. SM1127	Antioxidant, UV protection and extreme moisture-retaining properties.	Food, cosmetic, pharmaceutical, and biomedical fields.	(Sun et al., 2015, 2020)
EPS: galactose and glucose, at a ratio of 1:1.5.	King George Island, Antarctica	Sediment	*Gammaproteo bacteria*	*Pseudoalteromonas arctica*	Confers protection against free-thaw cycles.	Cryoprotectant in medical applications and food industries.	(Kim and Yim, 2007)
EPS: highly complex α-mannan polysaccharide.	Arctic	Sea ice	*Gammaproteo bacteria*	*Pseudoalteromonas* sp. SM20310	Protection against high salinity and freeze-thaw injury.	Use as cryoprotectant.	(Liu et al., 2013)
Structure not described.	Greenland Ice Sheet.	Cryoconite	*Cyanobacteria*	*Phormidesmis priestleyi BC1401*			(Chrismas et al., 2016a)

1.6 Novel antimicrobial compounds

Since the discovery of penicillin by Alexander Fleming in 1928, more than 23 000 NPs have been characterised (Katz and Baltz, 2016). NPs have also been developed into a great number of drugs, able to treat infection and disease in plants, animals and humans (Katz and Baltz, 2016; Knight et al., 2003). The majority of drugs are bioactive secondary metabolites, which have obscure functions in the organisms which produce them, but which have may have evolved in response to competition between microbes (Bérdy, 2005; van Bergeijk et al., 2020).

1.6.1 Advantages and challenges

NP-based drug-discovery has several advantages over its synthetic chemistry counterpart. NP resources remain largely unexplored and as new discovery strategies are developed, and new environments are sampled, many novel bioactive compounds may emerge (Knight et al., 2003; Zhang and Demain, 2005). NPs have been selected by nature for specific biological interactions; therefore, they have evolved to bind to proteins and have drug-like properties. Because NPs have evolved over billions of years to fulfil a variety of roles in diverse organisms, natural products offer unrivalled chemical diversity, structural complexity, and proven biological potency. However, there are several challenges that have hindered the true potential of discovery antimicrobial compounds from environments from being realised (Knight et al., 2003). Firstly, much of the environmental sampling has consisted of random sampling and has missed the true potential of many regions. Secondly, the major barriers to a truly systematic evaluation of environmental microbes is the difficulty in isolating and cultivation of up to 99% of the microbes present in any sample (Head et al., 1998; Pham and Kim, 2012; Stewart, 2012). Despite the massive number of uncultivated microbes, the easily cultured microbes have been characterised a number of times, resulting in a redundancy of strains and compounds within many NP extract libraries (Demain and Sanchez, 2009). In addition, the entire process from characterization and isolation of the active compounds from NP extracts are extremely labour intensive and time-consuming; and once a compound has been discovered; the production of adequate amounts of the compound generally requires massive scale-up.

The drug discovery process has always been limited by the technological and biological knowledge of the time. From the late 1930s to the 1970’s, drug discovery was mainly conducted via phenotypic screening (Katz and Baltz, 2016). In this technique, fermentation

broths and purified products were deposited on filter paper discs and placed on agar plates seeded with a test organism (Katz and Baltz, 2016). Areas that showed growth inhibition (bacteriostatic) and cell death (bactericidal) activity indicates the presence of a potential antimicrobial (Katz and Baltz, 2016). In this way, more than 20 novel classes of antibiotics were discovered between 1930 and 1962 (Coates et al., 2011). From the 1970's onwards, the approach shifted to "knowledge-based approaches", as knowledge of molecular biology grew, and specific targets for drugs were identified (Katz and Baltz, 2016). Despite the many advances in the field, only two new classes of antimicrobials have made it to market since 1962, a startlingly low figure (Coates et al., 2011). Recently, genome- and metagenome-mining techniques have heralded another paradigm shift in drug discovery, and been used to discover several new antibiotics, such as haloduracin (McClerren et al., 2006), lactocillin (Donia et al., 2014) and taromycin A (Yamanaka et al., 2014). Halduracin, a complex comprising two separate ribosomally encoded and post-translationally modified peptides (RiPPs), prevents transglycosylation and inhibits cell wall biosynthesis in Gram-positive bacteria by binding to lipid II4 (Oman et al., 2011). Lactocillin is also a RiPP that targets Gram-positive organisms. Taromycin A is a nonribosomal peptide derived from a marine actinomycete *Saccharomonospora* sp. CNQ-490(Yamanaka et al., 2014). The screening of soil environmental DNA in heterologous hosts has also resulted in the discovery of the antibiotics Fasamycin A and B (Feng et al., 2012), Tetarimycin A (Kallifidas et al., 2012) and Utahmycins A and B (Bauer et al., 2010).

1.6.2 Drugs from polar organisms

The cryosphere is an excellent environment to search for antimicrobials because there is a high amount of competition in nutrient-poor environments and they have not been fully explored. Furthermore, bioprospecting using metagenomics approaches is ideal because the cultivation of polar organisms is especially time-consuming and difficult. Table 1.10 details some of the potential antimicrobials isolated from polar organisms. To date, antimicrobial compounds have been identified from Arctic (Al-Zereini et al., 2007; Kim et al., 2014; Lyutskanova et al., 2009; Macherla et al., 2005; Wietz et al., 2012; Yuan et al., 2014; Zhang et al., 2004) and Antarctic (Asthana et al., 2009; Bruntner et al., 2005; Learn-Han Lee et al., 2012; L.-H. Lee et al., 2012; Mojib et al., 2010; O'Brien et al., 2004; Tedesco et al., 2016; Wong et al., 2011) environments (Table 10). These antimicrobial producing bacteria were isolated from soil (Lyutskanova et al., 2009; O'Brien et al., 2004), seawater (Tedesco et al., 2016; Wietz et al., 2012), and freshwater (Mojib et al., 2010).

Table 1-10 Antimicrobial products from cryospheric microorganisms

Product	Location	Environment	Organisms	Approach	Reference
Three main antimicrobial compounds with activity against Gram-positive and Gram-negative bacteria, yeasts, and fungi	Spitsbergen, Svalbard	Permafrost soils	*Streptomyces* spp. SB9, SB72 and SB81, Streptomyces spp. SB33 andSB47	Screening of isolates for antimicrobial activity, followed by TLC of extracts.	(Lyutskanova et al., 2009)
Arthrobacilins A, B and C. Antibacterial activity against *Vibrio anguillarum* and *S. aureus*	Arctic Ocean (Above 80°N)	Sea ice surface and deep water	*Pseudoalteromonas sp.* (4), *Arthrobacter* (7), P*sychrobacter* sp. (2), *Vibrio sp.* (3)	Ethanol and ethyl acetate extracts, antibacterial screening, and LC-MS total ion chromatogram.	(Wietz et al., 2012)
Antibacterial and/or antifungal activity (11 strains), activity against *Bacillus subtilis and C. albicans* (7 strains)	Chukchi Shelf, Arctic Ocean	deep-sea sediments	*Streptomyces, Nocardiopsis and Microlunatus.strains*	PCR-based screening biosynthetic pathway genes, Antimicrobial Activity Testing by Agar Diffusion (Inhibition Zones).	(Yuan et al., 2014)
2-Nitro-4-(2'-nitroethenyl)-phenol with antimicrobial and cytotoxic activity	Arctic Ocean	Arctic sea-ice floe	*Salegentibacter sp*. T436	Isolation and purification of the Compounds from fermentation of isolates, Antimicrobial activities, determined in the serial dilution assay, and inhibition of germination and growth.	(Al-Zereini et al., 2007)
Antibacterial activities against Gram positive (*S. aureus, B. subtilis, and M. luteus*) and Gram negative (*E. cloacae, P. aeruginosa, and E. coli*)	Ny-Ålesund, Svalbard, Dasan Korean Arctic Station	*Bacterial symbionts of Lichen Ochrolechia sp.*	*26605 Sphingomonas sp., 26606 Burkholderia sp., 26607 Burkholderia sp., 26608 Burkholderia sp. 26625 Sphingomonas sp.*	Metabolite extraction from isolates, antimicrobial screens against test organisms, paper disk diffusion test, MIC.	(Kim et al., 2014)
Three new pyrrolosesquiterpenes Moderately cytotoxic glyciapyrroles A, B, and C;	Alaska	Marine sediments	*Streptomyces sp. (NPS008187)*	Analytical HPLC with photodiode array (PDA) detection.	(Macherla et al., 2005)
Cyclic acylpeptides Mixirin A, Mixirin B, Mixirin C Cytotoxic against human colon tumour cells (HCT-116)	Arctic ocean	Sea mud	*Bacillus sp*	Silica gel, Sephadex LH-20 column chromatography and reversed-phase HPLC.	(Zhang et al., 2004)

Product	Location	Environment	Organisms	Approach	Reference
Violacein and flexirubin, with antimycobacterial against *M. tuberculosis*	Schirmacher Oasis, East Antarctica	Freshwater lakes	*Janthinobacterium sp. Ant5-2 (J-PVP), Flavobacterium sp. Ant342 (F-YOP)*	Pigments were extracted from isolates, purified by liquid chromatograph, concentrated then purified using reverse phase flash column reverse phase HPLC column	(Mojib et al., 2010)
Three rhamnolipids with antimicrobial activity against Bcc (*Burkholderia cepacia* complex) strains	Ross Sea, Antarctica	Sub-sea sediments	*Pseudomonas BNT1*	Bioassay-guided purification employing SPE and HPLC. Finally, LC-MS and NMR	(Tedesco et al., 2016)
4-[(5-carboxy-2-hydroxy)-benzyl]-1,10-dihydroxy-3,4,7,11,11-pentamethyl-octahydro cyclopenta <a> naphthalene antibacterial against *M. tuberculosis*, *S.aureus*, *S. typhi*, *P. aeruginosa*, *E. coli*, *E. aerogenes*	Antarctica	unknown	*Nostoc CCC 537*	HPLC, UV, IR, 1H NMR, EIMS, and ESIMS	(Asthana et al., 2009)
Metabolites active against *C. albicans* and *S. aureus and P. aeruginosa*.	Barrientos Island, Antarctica	Soil	*Brevibacterium casei (2), Brevibacterium sanguinis (2), Demetria terragena (2), Gordonia sputi (2), Janibacter melonis, Kocuria palustris, Lapillicoccus jejuensis, Micromonospora marina, Micromonospora tulbaghiae, Nocardioides ganghwensis, Rhodococcus yunnanensis*	Isolates were grown in fermentation broth, and aliquots of the of the fermentation supernatant were tested against *C. albicans*; *S. aureus* and *P. aeruginosa*.	(Learn-Han Lee et al., 2012)
Metabolites active against *C. albicans* and *S. aureus*	Barrientos Island, Antarctica	Soil	*Bradyrhizobium (9), Paracoccus (1), Sphingomonas (1), Methylobacterium (2)*	Isolates were grown in fermentation broth, and aliquots of the of the fermentation supernatant were tested against C. albicans; S. aureus and P. aeruginosa.	(L.-H. Lee et al., 2012)
Angucyclinone, Frigocyclinone, antibacterial against Gram-positive bacteria	Antarctica (Terra Nova Bay at Edmundson Point	Soil	*Streptomyces griseus strain NTK 97*	Amberlite XAD-16 column, adsorption chromatography using a column of silica gel 60, purification on a Sephadex LH-20 column, ESI-TOF MS spectrum, NMR data including DEPT-135, 1D and 2D NMR data	(Bruntner et al., 2005)

Product	Location	Environment	Organisms	Approach	Reference
Proteinaceous compounds active against *Listeria innocua, Pseudomonas fragi and Brochothrix thermosphacta*	East Antarctica	Soil	*Arthrobacter sp. HPH17, Planococcus sp. CHF8 and Pseudomonas sp. CrCD21*	Replica plates were overlaid with soft TSA containing indicator organisms. Zones of clearance surrounding the producer colony following incubation indicated the presence of an antagonistic agent.	(O'Brien et al., 2004)
Metabolites that inhibit the growth of pathogens from Escherichia, Salmonella, Klebsiella and Enterobacter and Bacillus, and Vibrio genera	King George Island, Antarctica	Soil	*Pseudomonas sp. MTC3, WEK1, WEA1, MA2 and CG21, and Pedobacter sp. BG5*	Bacteria colonies on the agar plate were overlaid with molten nutrient agar containing indicator bacteria. Zones of clearing around the bacteria after 2 days of incubation indicated the presence of inhibitors. I	(Wong et al., 2011)

Escherichia coli, Staphylococcus aureus, Mycobacterium tuberculosis, Pseudomonas aeruginosa, Enterobacter aerogenes, Salmonella typhi.
Number of isolates is indicated in brackets (n)
MDR, multi-drug resistant

1.7 Biomining, bioremediation and plastic degradation

In low nutrient glacial environments, microorganisms play a vital role in recycling nutrients to ensure the sustained availability of a variety of nutrients (Bradley et al., 2014; Cameron et al., 2012b). Adaptation to extreme, nutrient-poor conditions, may have selected for innovative metabolic processes for metabolising non-conventional compounds in efficient ways. These unique metabolic pathways may lead to novel means of storage, transformation or export of minerals and nutrients (Cook et al., 2016b).

1.7.1 Bioremediation: degradation of contaminants

The successful bioremediation of contaminated soils requires that there are microorganisms that can degrade the offending pollutants, and that the environmental conditions at the site of contamination are conducive to the growth of those bacteria (Aislabie et al., 2006). The isolated polar regions have experienced pollution at or near scientific and military bases, due to the reliance of these human settlements on petroleum for power and heat generation and the operation of transport vehicles (Aislabie et al., 2006). A second cause of pollution in polar regions is the result of industrial activity and the emission of pollutants which can travel vast distances in the atmosphere and be deposited with snow into Arctic environments (Papale et al., 2017). In addition, persistent organic pollutants (POPs) with mutagenic and carcinogenic potential can be incorporated into cryoconite (Cook et al., 2016b).

It was recently shown that microbial communities in Greenland cryoconite have resistance to, and the potential to degrade several anthropogenic pollutants, such as the heavy metals mercury and lead, persistent toxic compounds such as polychlorinated biphenyls (PCB) and dichloro-diphenyl-trichloroethane as well as polyaromatic hydrocarbons (PAH) (Hauptmann et al., 2017). Isolates from seawater and sediment from the Kongsfjorden fjord, Svalbard belonging to the genera *Algoriphagus, Devosia, Salinibacterium* and *Gelidibacter* were also efficient at degrading PCBs (Papale et al., 2017). Bacteria able to degrade alkanes are typically from *Rhodococcus* or *Pseudomonas* genera, while *Sphingomonas* and *Pseudomonas* tend to degrade aromatic compounds (Baraniecki et al., 2002) (Table 1.11).

Table 1-11 Bacteria with ability to grow on hydrocarbon sources, with potential application for bioremediation

Origin/ Source	Phylum/ Class	Organism	Hydrocarbon growth substrates	Reference
Antarctic soil, Jubany Station (King George Island, South Shetland Islands)	*Gammaproteobacteria*	*Acinetobacter* ADH-1	Crude oil, aromatic gas oil, hydrogenated gas oil, kerosene, dodecane, hexadecane, cyclohexane	(Cormack and Fraile, 1997)
Antarctic soil	Actinobacteria	*Arthrobacter protophormiae* MTCC 688	Hexadecane	(Pruthi and Cameotra, 1997)
Arctic tundra, northern coast of Ellesmere Island	*Alphaproteobacteria*	*Sphingomonas* DhA-95	Jet A-1 jet fuel, dodecane, pristane	(Yu et al., 2000)
	Gammaproteobacteria	*Pseudomonas* DhA-91	Jet A-1 jet fuel, octane, dodecane	
		Pseudomonas IpA-92	Toluene	
		Pseudomonas IpA-93	Toluene, benzene	
Scott Base, Antarctica	Actinobacteria	*Rhodococcus* 5/1, 5/14, 7/1	JP8 jet fuel, C_6–C_{20}*n*-alkanes, pristane	(Bej et al., 2000)
Northeastern tip of Ellesmere Island	*Gammaproteobacteria*	*Pseudomonas* Ps 8	Jet A-1 fuel, hexadecane, pristane	(Thomassin-Lacroix et al., 2001)
	Actinobacteria	*Rhodococcus* Rho10	Jet A-1 jet fuel, dodecane	
Marble Point, Antarctica	*Gammaproteobacteria*	*Pseudomonas* sp.5B	JP-8 jet fuel[1], hexane	(Eckford et al., 2002)
		Pseudomonas stutzeri 5A	JP-8 jet fuel[1], benzene, toluene, *m*-xylene	
Scott Base, Ross Island, Antarctica	Actinobacteria	*Rhodococcus* 43/02	JP5 jet fuel, dodecane, hexadecane, pristane	(Saul et al., 2005)
	Alphaproteobacteria	*Sphingomonas* 43/03, 44/02	Phenanthrene	
Saglek, Labrador, Canada	*Gammaproteobacteria*	*Pseudomonas* PK4	Pyrene, dodecane, hexadecane	(Eriksson et al., 2002)
		Pseudomonas K319	Pyrene	
Wright Valley, Antarctica	*Gammaproteobacteria*	*Pseudomonas* 30-3	JP8 jet fuel, C_8–C_{13}*n*-alkanes, toluene, *m*- and *p*-xylene, 1,2,4-trimethyl benzene	(Panicker et al., 2002)
Coastal soils of the Ross Sea region of Antarctica	*Gammaproteobacteria*	*Pseudomonas* Ant 5	JP8 jet fuel, NAH, 2MNAH	(Aislabie et al., 2000)
		Pseudomonas Ant 7	JP8 jet fuel, *p*-xylene, 1,2,4-trimethyl benzene naphthalene, 1-methyl naphthalene and 2-methyl naphthalene	
		Pseudomonas 7/22	JP8 jet fuel, toluene, *m*- and *p*-xylene, 1,2,4-trimethyl benzene	
	Alphaproteobacteria	*Sphingomonas* Ant 20	JP8 jet fuel, 1-methyl naphthalene, phenanthrene	
	Alphaproteobacteria	*Sphingomonas* Ant 17	JP8 jet fuel, *m*-xylene, 1-methyl naphthalene and 2-methyl naphthalene, dimethylnaphthalene, 2-ethylnaphthalene, fluorene, phenanthrene	(Baraniecki et al., 2002)

[1] Pseudomonas 5A and 5B could only metabolise JP-8 jet fuel in the presence of NH_4Cl (Eckford et al., 2002)

1.7.2 Plastic Degradation

Petroleum-based plastics are ubiquitous and are used in virtually all areas of human life (Wei and Zimmermann, 2017). Unfortunately, many of these plastics are recalcitrant to degradation and persist in the environment for many years, leading to the massive accumulation of plastic in landfills and oceans (Danso et al., 2019). It was estimated that 192 coastal countries generated 275 million metric tons (MT) of plastic waste in 2010, which resulted in 4.8 to 12.7 million MT entering the ocean (Jambeck et al., 2015). That number is only expected to have grown. Unfortunately, nearly 60% of the plastic waste generated in Europe is from packaging materials, single-use disposable plastic and other short-lived items that are discarded within a year (Wei and Zimmermann, 2017). Together, Polyethylene (PE), polypropylene (PP), polystyrene (PS), polyvinyl chloride (PVC), polyethylene terephthalate (PET) and polyurethane (PUR) account for over 80% of the Europe's plastic demand (Wei and Zimmermann, 2017). Plastics also use 8% of the total global fossil fuel production to provide the raw materials or energy for their manufacture (Wei and Zimmermann, 2017). There is virtually no location on the planet untouched by the problem of plastic waste. Even as far north as Spitsbergen, Svalbard, there is human debris in the form of wood, glass, plastic bottles, tins, bulbs, clothing, bags, plastic tape fishing nets and rope (Bergmann et al., 2019; Urbanek et al., 2017).

Conventional plastics are extremely resistant to biodegradation. What biodegradation does take place is incredibly slow and relies on the presence of various abiotic factors such as UV irradiation, the presence/ absence of oxygen, temperature and the presence of chemical oxidants (Wei and Zimmermann, 2017). Chemical and structural factors affecting the biodegradability of plastics include their hydrophobicity, degree of crystallinity, surface topography and the molecular size of the synthetic polymers (Wei and Zimmermann, 2017).

A study of the microbiomes associated with different sized plastic debris types and sizes used a network building approach to define the core taxa associated with the plastic surface of each debris category (Debroas et al., 2017). Interestingly, although samples were collected from the North Atlantic Ocean (subtropical gyre), most of the species present were associated with non-marine ecosystems, suggesting that they are hitchhikers. Keystone species came from the Rhodobacterales, Rhizobiales, Streptomycetales and Cyanobacteria. The colonization also appeared to be polymer specific, with poly(ethylene terephthalate) (PET) and polystyrene (PS) mesoplastics being significantly dominated by

Alphaproteobacterial and Gammaproteobacteria. Polyethylene (PE) mesoplastics were dominated by Alphaproteobacteria, Gammaproteobacteria and Actinobacteria, and the majority of polyethylene microplastics were dominated by Betaproteobacteria (Debroas et al., 2017).

Enzymes capable of degrading PE include certain laccases, manganese peroxidase and lignin peroxidase. A thermostable laccase from the actinomycete, *Rhodococcus ruber* C208 was able to degrade PE films in culture supernatants and cell-free extracts in the presence of copper and when UV-irradiated (Santo et al., 2013). Polyurethane (PUR) can be enzymatically depolymerised by microbial ureases, esterases and proteases (Wei and Zimmermann, 2017).

Bioplastics (BP) are an alternative to the non-degradable conventional plastics. BPs contributed roughly 2 million tons or approximately 1% of the world's annual plastic production in 2014 (Urbanek et al., 2017). However, this is expected to increase four-fold to approximately 8 million tons by 2019 (Urbanek et al., 2017). BPs can be divided into two types: renewable resource-based BPs and petroleum-based BPs. Renewable resource-based BPs can be obtained from organic waste material, crops, microorganisms, or genetically modified plants. Examples include polyhydroxyalkanoates (PHAs) and poly(lactic acid) (PLA). Alternatively, three examples of petroleum-based BPs are poly(butylene succinate-co-adipate) (PBSA), poly(butylene succinate) (PBS) and poly(ε-caprolactone) (PCL). Recently, 121/313 isolates from 52 soil samples from Spitsbergen were shown to degrade BPs (Urbanek et al., 2017). The number of isolates that could clear PBSA, PBS and PCL were 116, 73 and 102, respectively. Moreover, 56 of the isolates were able to grow on PLA agar plates. The bacterial strains with the highest ability for biodegradation were *Pseudomonas* and *Rhodococcus* species (Urbanek et al., 2017).

There is some thought that the use of living microorganisms rather than isolated enzymes may be better for plastic degradation. Even more promising is the use of bacterial communities, made up of defined microbial strains, which have shown better performance than single organisms (Wei and Zimmermann, 2017).

Table 1-12 Bacteria capable of plastic degradation

Type of plastic	Environment	Enzyme	Phylum	Organism	Study Type	Reference
PE	Soil	Laccase	Actinobacteria	*Rhodococcus ruber*	Isolate.	(Santo et al., 2013)
	Crude-oil contaminated beach soil	Alkane Hydroxylase (AH)	Proteobacteria (Gammaproteobacteria)	*Pseudomonas sp. E4, Pseudomonas aeruginosa E7*	Alkane hydroxylase gene (*alkB*) expressed in Escherichia coli BL21	(Jeon and Kim, 2015; Yoon et al., 2012)
PS		Hydroquinone peroxidase	Proteobacteria (Gammaproteobacteria)	*Azotobacter beijerinckii*	Two-phase system- dichloromethane and water. Rapid conversion to soluble products in 5 minutes at 30°C organic phase containing hydrogen peroxide and tetramethylhydroquinone	Nakamiya et al, 1997
PBs (PBSA, PBS and PCL)	Soil samples	Unknown	Gammaproteobacteria, Actinobacteria	*Pseudomonas and Rhodococcus species*	Isolates capable of clear zone formation on emulsified PBSA, PBS and PCL and PLA agar plates.	(Urbanek et al., 2017)

PE: Polyethylene: Made up of monomers of ethylene with the formula (C2H4) n and is the most common plastic containing a C-C backbone.
PS: polystyrene: An aromatic polymer made up of monomers of styrene.
PBSA: poly(butylene succinate-co-adipate), PBS: poly(butylene succinate), PCL: poly(ε-caprolactone),PLA: poly(lactic acid)

1.8 Metagenomics

It is well established that only a small fraction of the species in environmental microbial communities can be cultivated in the laboratory using traditional cultivation techniques (Culligan et al., 2014; Head et al., 1998; Yarza et al., 2014; Yu et al., 2000). This discrepancy has previously been termed "The Great Plate Count Anomaly" (Staley and Konopka, 1985) and the uncultivatable organisms have earned the monicker "microbial dark matter". The field of metagenomics is a field of study and a set of techniques (Culligan et al., 2014) that were developed to address this problem of "microbial dark matter". Currently, there are several different methods and techniques that can be used to identify genes, enzymes, and bioactive molecules. Metagenomics typically consist of the following steps: DNA extraction from an environmental sample, sequencing of the metagenome, bioinformatics analyses and annotate of genes and/or the expression of selected genes in a heterologous host to confirm function (Thomas et al., 2012; Vester et al., 2015) (Figure 1-5). Each strategy has advantages and disadvantages, and the approach depends on the type of sample, the resources available and the question that is being asked. This thesis will use a mix of bioinformatics and functional screening approaches.

1.8.1 Challenges

The following section will highlight several major challenges in microbiology research that metagenomics helps to address.

1.8.1.1 Organisms not yet cultivated

Since the arrival of next-generation sequencing (NGS), and now third-generation sequencing, 16S rRNA sequences representing several hundred thousand new species have been deposited annually into databases (Yarza et al., 2014). An analysis, based on thresholds for 16S rRNA sequence similarity, suggest that there as many as ~ 1350 phyla, ~2200 classes, ~4200 orders, ~9600 families and ~61 000 genera (Yarza et al., 2014). This is vastly more than the number of taxa that have currently been described. For example, approximately 2000 genera have currently been described, of the more than 60 000 genera that are suspected to exist (Yarza et al., 2014). Additionally, although there are more than 1000 estimated phyla, the bacteria cultivated to date are almost completely dominated by just four phyla, the Actinobcteria, Bacteriodetes, Firmicutes and Proteobacteria (Culligan et al., 2014), although debate still exists over whether the Proteobacteria are just one phyla, or several (Yarza et al., 2014).

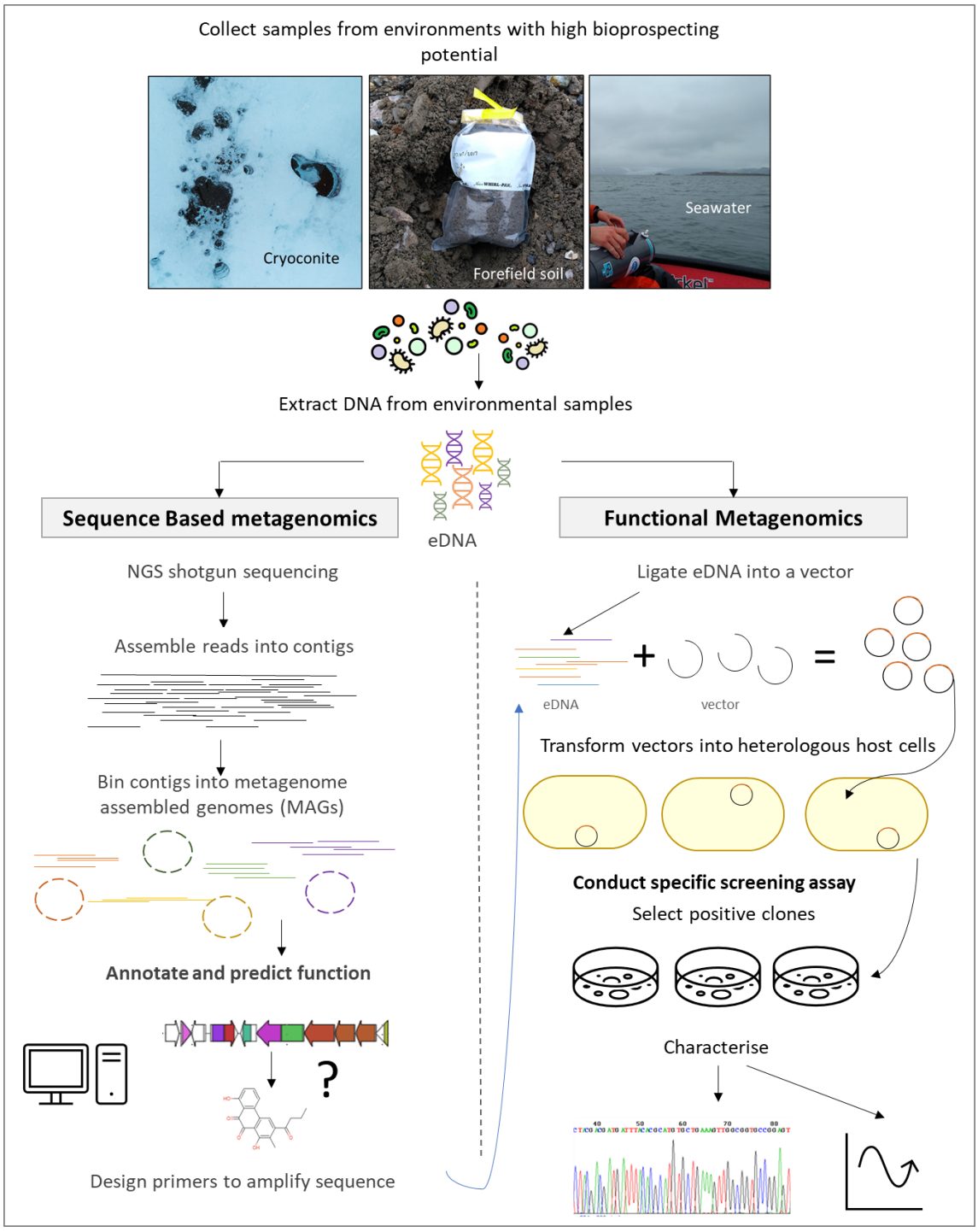

Figure 1-5 Simplified and general overview of culture-dependent and metagenomic methods for bioprospecting. Bioprospecting is an innovative field, beset by many challenges that are being imaginatively overcome by technological advances.

Even prior to the revelation provided by the dawn of metagenomics, a clear mismatch existed between what has been observed under the microscope, and what grows in culture. A study of cryoconite on Svalbard glaciers experienced difficulty isolating cyanobacterial and algal species observed under the microscope, yet managed to culture species that had

not been directly observed (Stibal et al., 2006). This highlights the problem that what is cultured in the lab is very seldom the most abundant or ecologically important species, and the cultivation of strains from an environmental sample is therefore a poor representation of community structure (Vester et al., 2015).

Although many organisms have not yet been cultivated, this doesn't mean that it won't one day be possible. Organisms may be uncultivatable due to a difference between the original environment and the laboratory conditions (Mu et al., 2020). For example, temperature, pH, nutrients, salinity or any number of other factors may inhibit growth. Additionally, many microorganisms are in symbiotic relationships with each other, and are dependent on the presence of other microbes, (and the secondary metabolites they secrete/produce)(Brown et al., 2015).

1.8.1.2 Unexpressed or undetectable proteins

In 2017, the (2017_01) UniProt database contains more than 73 million sequence entries, of which only 0.17 % have evidence at the protein level, and only 1.44% have evidence at the trancript level (http://www.ebi.ac.uk/uniprot/TrEMBLstats) (accessed 24/01/2017). This suggests that a significant number of proteins may not be expressed, or are present at levels below detection (Vester et al., 2015). In addition, the number of hypothetical proteins and proteins of unknown function form the majority of many organisms' genomes (Vanni et al., 2020). Where functions have been ascribed, these are themselves based on predictions using homology to known genes (El-Gebali et al., 2019; Galperin et al., 2015; Huerta-Cepas et al., 2017; Mistry et al., 2013).

1.8.1.3 Undetectable secondary metabolites

As mentioned in Section 1.6, bioactive secondary metabolites are an excellent source of novel drugs to treat a myriad of human, animal, and crop diseases. Recent advances have enabled the complex chemical structure of a secondary metabolite to be discerned from the enzymes encoded by a particular set of genomic sequences (McAlpine et al., 2005). A cryptic biosynthetic gene cluster (BGC) is a cluster of genes that synthesise an unknown compound (Butler et al., 2016). An analysis of the genomes of 1154 archaeal and bacterial organisms predicted 33 351 putative BGCs, many of which encode secondary metabolites that have never been detected (Cimermancic et al., 2014). In addition, it is suspected that the current list of BGCs currently vastly underestimates the true number present. Not only are there many non-detectable BGCs, but those that are detected using bioinformatics may not be expressed in culture. Systematic surveys of

thousands of sequenced microbial genomes showed that silent clusters outnumber expressed clusters in laboratory cultures suggesting enormous untapped potential in the genomes of cultured microbes (Butler, 2004). Metagenome mining studies have revealed that BGCs encoding compound classes that are commonly found in the genomes of uncultivated bacteria are rarely found in the genomes of cultivatable bacteria (Butler et al., 2016). Therefore, there has been a rise in genome mining and metagenome mining as strategies for drug discovery, as the discovery paradigm has shifted from "microbial metabolites" discovered via metabolite detection to "biosynthetic gene cluster" detection together with predictions of their potential products (Butler, 2004).

1.8.2 Sequence-based methods

1.8.2.1 Comparative genomics

When dealing with small datasets it is difficult to interpret whether changes in amino acids in proteins have occurred as an adaptive response to the cold, or whether the changes are purely the result of evolution and genetic drift. However, the use of large metagenomic datasets to compare psychrophilic, mesophilic and thermophilic organisms from cold, moderate and hot environments respectively, can highlight common trends in cold-adapted organisms that are more likely to be due to adaptations to the extreme environment, as opposed to the random background noise of evolution (Casanueva et al., 2010; Siddiqui and Cavicchioli, 2006). For this reason, metagenomic sequence datasets derived from snow and ice habitats have provided a wealth of information about adaptations to the cryospheric conditions (Edwards et al., 2013a; Simon et al., 2009b).

1.8.2.2 Metagenome-assembled genomes (MAGs)

Metagenome-assembled genomes (MAGs) are reconstructed genomes from metagenomic DNA and represent a major advancement in the understanding of uncultivated bacteria because MAGs can be annotated and mined using the same tools as those previously restricted to cultivated organisms. Thanks to a rise in third generation sequencers, such as the MinION™ Nanopore, reads are longer than ever (B. L. Brown et al., 2017). Longer reads not only mean that assembly is less time consuming, as some contigs can span entire genome lengths; but hybrid assembly of long reads from Nanopore and short-reads from Illumina data are enabling the construction of closed, complete genomes from metagenomic data (Moss et al., 2020; Overholt et al., 2019; Singleton et al., 2020).

1.8.3 Functional screening methods

Functional metagenomics refers to the study of a metagenome via the construction of a clone library and the expression of individual genes (or clusters of genes) in a foreign host to asses activity (Vester et al., 2015). However, genes from a library will not automatically be expressed, and the low hit rate achieved to date may be less to do with the low prevalence of these enzymes and products in the environment, and more to do with inappropriate lysis methods, choices of vectors and choice of expression host. There are minimum requirements for gene transcription to occur, including the presence of a promoter, and the appropriate transcription factors to recognise the promoter (Gabor et al., 2004). In addition, successful transcription, does not guarantee translation. The minimum requirements for translation include a ribosome binding site (rbs) in the -20 to -1 region upstream of the start codon for initiation of translation, as well as an initiation codon that is recognisable in the host. Assuming translation at the ribosome, the peptide may require chaperones, cofactors, and various modifications to ensure proper folding, and then an appropriate secretion machinery in order to express the enzyme and prevent the formation of inclusion bodies (Ferrer et al., 2016).

1.8.3.1 Vectors

There are several types of cloning vectors, such as plasmids, fosmids, cosmids and bacterial artificial chromosomes (BACs). The choice of vector depends on the length of the genomic fragments that are obtained from the environmental sample, which in turn depends largely on the extraction method. Plasmids can accept inserts of up to 15kb, fosmids can accept 25-35 kb, cosmids can accept 25 – 40kb fragments and BACs can accept fragments from 100-200kb in size (Rashid and Stingl, 2015; Vester et al., 2015). The advantage of using plasmids to construct small-insert libraries, is that the plasmids can have a high copy number, containing many copies of the insert per cell. In addition, the plasmids typically contain strong promoters, which result in good transcription (Rashid and Stingl, 2015). Together, this makes the detection of even weakly expressed proteins and enzymes possible. In addition, because the insert sizes are smaller, fewer genes will be expressed in each clone (Rashid and Stingl, 2015), which is useful when wanting to screen single enzymes or proteins. An advantage of using BACS, is that large inserts can contain multiple genes or entire operons (Rashid and Stingl, 2015), which is useful when looking for biosynthetic gene clusters that produce novel secondary metabolites (Gabor et al., 2004). However, successful screening of these libraries may be more difficult because they single-copy, and therefore may express products in extremely

low, or undetectable amounts. In addition, unlike the promoters in plasmids, the genes in a BAC insert are usually still under the control of their native promoters. This means that these inserts rely on the transcription factors, cofactors and signalling pathways of the host, which may result in many genes remaining unexpressed.

1.8.3.2 Expression-hosts

To amplify, synthesise, purify, and characterise enzymes, a host is transformed with the vectors containing genomic fragments, and then expressed. The selection of both vector and host are non-trivial matters, as successful expression relies on the transcriptional regulators encoded in the metagenome fragment being recognised by and compatible with the RNA polymerases in the host. In recognition of the need to consider host compatibility and silenced gene clusters, a number of heterologous hosts have been engineered, with the specific intention of maximising secondary metabolite production (Zhang et al., 2010). These include strains of *Streptomyces coelicolor* (Gomez-Escribano and Bibb, 2014), *S. albus* (Seipke, 2015), *S. lividans*, *S avermitillis* (Komatsu et al., 2013), *S. antibioticus*, and *S. parvalus*, from the Actinobacteria, as well as engineered organisms from other phyla, such as *Escherichia coli*, *Bacillus subtilis*, *Pseudomonas putida*, *Saccharomyces cerevisiae* and *Apergillus nidulans* (Gomez-Escribano and Bibb, 2014; Park et al., 2020; Zhang et al., 2010).

One of the most common hosts is *Escherichia coli (E. coli)*. The optimum growth temperature of *E. coli* is 37°C, which is significantly higher than the optimum temperature of psychrophiles, and thus also significantly warmer than the ideal temperature for cold-active enzymes, which presents a number of problems for heterologous expression. If the optimum temperature of the *E. coli* host is used, there may be misfolding or denaturation and a loss of functional ability of the enzymes. However, if the optimum temperature of the enzyme is used, the metabolic reactions of *E.coli* may be 16–80 times lower (Vester et al., 2015). Agilent Technologies have attempted to address this problem, by engineering a strain of *E.coli* (Arctic Express) to include chaperones from a psychrophilic bacterial strain, *Oleispira antarctica* (Vester et al., 2015). An alternative to genetically engineering *E. coli*, is to simply use a psychrophiles as an expression host. *Pseudoalteromonas haloplanktis* TAC125 is an Antarctic bacterium that is used as a system for expression and secretion of proteins (Cusano et al., 2006; Parrilli et al., 2008). *P. haloplanktis* TAC125 has increased solubility and secretion of protein products due to disruption of its *gspE* gene (Parrilli et al., 2008).

1.8.3.2.1 Multiple hosts

The use of a few alternative screening hosts from a variety of taxa may also increase the number of positive clones that can be detected. In a study to try quantify the accessibility of the metagenome by random expression cloning techniques, statistical models were used to assess the percentage of genes from a variety of bacterial taxa that would be detectable in *E.coli* (Gabor et al., 2004). Three scenarios for successful gene expression were defined, (i) independent gene expression where both promoter and ribosome binding site (rbs) are provided by the insert (IND), expression where only the rbs, but not the promoter, is located on the insert (TRANSC) and (iii) expression dependent on both a promoter and rbs provided by the vector (DEP). They found that about 40% of the genes from 32 analysed genomes would be recoverable via the IND method if expressed in *E.coli* (Gabor et al., 2004). However, this varied widely by phyla, with only 7% recoverable from *Actinobacteria*, and up to 73% recoverable from *Firmicutes*. The TRANSC fraction of genes required an optimum insert size of only 15 kb, and this was the largest fraction in Actinobacteria (~58%), and *Proteobacteria* (~38%). The DEP fraction represents DNA that is virtually inaccessible and represents approximately 48% of *Actinobacterial* genes are dependent on this expression type.

This theoretical prediction has been verified experimentally by testing the expression of the same metagenomic library in different hosts. In a screen for secondary metabolites, a library was expressed in both *E. coli* and *Streptomyces lividans* via the creation of a cosmid vector that could be conjugated between *E. coli* and *S. lividans*. They found that the library hosted in *S. lividans* contained 12 functionally active clones, none of which had been detected when using *E.coli* as the host (McMahon et al., 2012). Even more illuminating, Craig et al., screened a metagenomic library in six proteobacterial hosts, *E. coli* and five others; *Agrobacterium tumefaciens, Burkholderia graminis, Caulobacter vibrioides, Pseudomonas putida,* and *Ralstonia metallidurans* and found that there was only one case where the same small-molecule-producing clone (containing a six-gene operon for the production of the carotenoid β-carotene) was identified using two different host species (*R. metallidurans* and *A. tumefaciens*) (Craig et al., 2010). Interestingly, *R. metallidurans* belongs to the *Betaproteobacteria* class and *A. tumefaciens* belongs to the *Betaproteobacteria* class, yet other *Alpha-* and *Betaproteobacteria* hosts in this experiment did not express this operon (Craig et al., 2010).

1.8.3.3 Screening methods

Once a clone library has been constructed, the clones need to be screened for the activity of interest. The hit rate of these screens is notoriously low (Culligan et al., 2014). The following methods have been developed to attempt to either improve expression of psychrophilic NPs or increase the number of positive hits and screen for a larger variety of functions and activities than previously possible.

One possibility is to use traditional chromogenic and substrate-based assays, but simply but incubate the plates at a low temperature (Vester et al., 2015). A second approach is heterologous complementation screening, which involves the use of an expression host that has a mutation such that only clones containing genes that complement or restore that function will be able to grow (Rashid and Stingl, 2015; Vester et al., 2015). This approach was used to identify several cold-active polymerases from glacial ice in Germany (Simon et al., 2009b).

Substrate-induced expression screening (SIGEX) is a means to screen libraries for clones that are able to catabolise a substrate (compound) of interest (Uchiyama and Watanabe, 2008). In this method, a cloning vector is used that contains a fluorescence gene such as green fluorescing protein (GFP), located immediately downstream of the cloning site. Upon the induction of gene(s) in the insert by the substrate of interest, the GPF is co-expressed, signifying the presence of an induced gene (Uchiyama and Watanabe, 2008). Positive clones can then be selected by fluorescence-activated cell sorting (FACS)(Uchiyama and Watanabe, 2008).

Product-induced gene expression (PIGEX) extends the work of SIGEX. Rather than relying on the presence of a substrate to induce GFP expression, PIGEX relies on the presence of the product to induce expression (Uchiyama and Miyazaki, 2010). This is achieved by pairing a product-responsive transcriptional regulator, with a reporter gene like GFP (Uchiyama and Miyazaki, 2010). A huge advantage of this method is that it identifies clones that have the enzyme activity of interest. However, the selection of a sensor gene that is sensitive to the product, and not the substrate or precursor is challenging. Likewise, this assay will only work on those products that are not produced as part of the normal metabolism of the host cell.

1.8.4 Strategic cultivation and expression

Challenges in the field of metagenomics-based bioprospecting from natural environments are therefore (i) trying to get an accurate representation of the species that exist, in their correct proportions, (ii) characterising the enzymes and proteins these organisms are capable of synthesising, and (iii) designing an expression system that can successfully express the NP of interest. The use of bioinformatics to reconstruct uncultivated bacteria from diverse environments, will open new avenues to address each of these challenges, and will pave the way for strategic cultivation and heterologous expression.

1.9 Aims and objectives

The aims of this thesis are:

1. Conduct a taxonomic survey of a range of cryospheric environments to prioritise environments for further research (**Chapter 3**).
2. Construct high quality metagenome-assembled genomes (MAGs) from Svalbard soil, cryoconite and soil metagenomes (**Chapter 4**) and the Scărișoara Ice cave (**Chapter 7**) which will form the basis for:
    2.1.1. Identifying novel species from these environments,
    2.1.2. Describing the distribution of these MAGs across different sites,
    2.1.3. Identifying nutrient sources of the MAGs by looking for key genes in major biogeochemical cycles
    2.1.4. Exploring the MAGs for BGCs capable of synthesising novel secondary metabolites
3. Explore the secondary metabolites of the Svalbard metagenomes by linking the metabolome (detected using LC-MS) in soil and cryoconite to the predicted metabolic profiles of the MAGs (**Chapter 6**).
4. Use functional metagenomics to look for cold-active enzymes by cloning soil and cryoconite DNA into cold-sensitive *E.coli* mutants (**Chapter 7**).
5. Develop and optimise a Bioinformatics workflow for bioprospecting from shotgun metagenomic data (**Chapter 8**).

In addition, there are three outputs of this thesis, in the form of data and a clone library, that form the basis of further research in this area.

1) A collection of MAGs from Svalbard.
2) A collection of MAGs from the Scărișoara Ice Cave.
3) Clone libraries of soil and cryoconite DNA, in DH10B and HCS1 and cs2-29 that can be screened for Natural Products.

2 MATERIALS AND METHODS

2.1 Sampling sites, sample collection, transportation, and storage

The samples included in this thesis were collected from locations in Ny-Ålesund, Svalbard in late June and early July 2017 and 2018 (See Appendix B-1 for sample name, type, collection date, GPS coordinates and chapter inclusion). The environments sampled included cryoconite, snow, slush and meltwater from glacial surfaces, proglacial water from the glacier snout, soil from a glacial forefield, and seawater from the fjord in front of Midtre Lovénbreen (ML). Most samples were collected from the ML glacier and its surrounds. However, cryoconite was also collected from Vestre Brøggerbreen (VB), Austre Brøggerbreen (AB) and Vestre Lovénbreen (VL). The locations of sample sites are shown in Figure 2-1.

2.1.1 Soil sample collection

Soil from the forefield of the ML glacier was collected over three days. Sample sites were arranged in three transects of five time points for a total of 15 unique samples. Samples were collected into sterile Whirl-Pak® bags (Nasco) using a shovel or scoop that was pre-contaminated by soil immediately adjacent to the sample site by scooping and discarding the adjacent soil multiple times before sample collection.

2.1.2 Cryoconite sample collection

Cryoconite was collected from ML and VB in 2017 and ML, VB, AB and VL in 2018. Cryoconite was aspirated into sterile 15 mL or 50 mL Falcon Tubes or Whirl-Pak® bags (Nasco) using a turkey baster pre-contaminated with nearby cryoconite. The granules were allowed to settle, and the excess water poured off until the tube was full. For cryoconite collected in 2018, GPS co-ordinates, photos and hole and water depth measurements were taken on site.

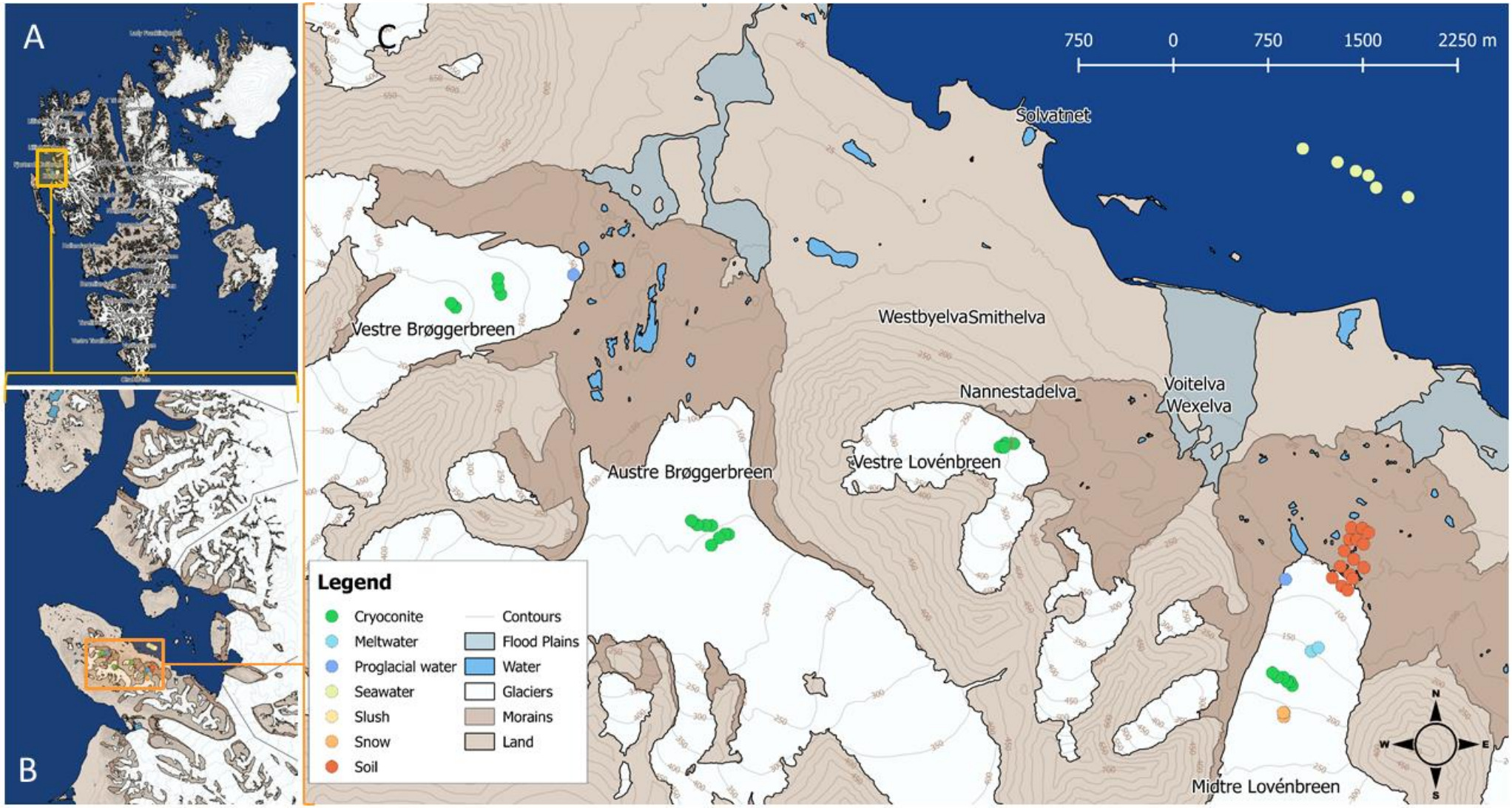

Figure 2-1 Map of sampling sites included in this thesis. Samples of cryoconite were collected from four glaciers (ML, VB, VL and AB). Soil was collected from the ML glacier forefield in three transects of five time points. Snow, slush, and meltwater was collected from ML, and seawater was collected from Kongsfjorden ford.

2.1.3 Glacial water and seawater sample collection

Snow and slush samples from the ML glacier surface were aseptically collected into 2 L sterile Whirl-Pak® bags (Nasco) using a scoop pre-contaminated with snow or slush. Water from glacial meltwater streams on ML and proglacial water from ML and VB was collected in 2L Nalgene bottles that had been bleached, rinsed in HCl, and autoclaved in the lab. Each Nalgene was also pre-contaminated by filling and completely emptying the Nalgene in the stream water five times before taking the sample. Seawater was collected from open water in front of the ML forefield at two depths using a Niskin bottle. The Niskin bottle was cast three times at 1 m and 15 m depth at each sampling location, and 2 L of water was collected in two sterile 1 L Nalgenes after each sampling event.

2.1.3.1 Filtering of liquid samples

Snow and slush samples were left in the sealed bags to melt in the dark in the NERC Arctic Station lab before filtering. All liquid samples were filtered into Sterivex GP 0.22 µm polyethersulfone filters (Millipore, MA, USA) using a peristatic pump. The Sterivex filters were filled with RNAlater ™ Stabilization Solution (Invitrogen, Catalog AM7020), the ports sealed and placed at -20°C at the NERC Arctic Station.

2.1.4 Storage and transport

Cryoconite and soil samples were returned to the NERC Arctic station and stored at -20°C together with Sterivex filters from the filtered liquid samples. Samples were transported to the UK in insulated chilled containers. All samples were then placed at -20°C for long-term storage.

2.2 DNA Extraction

Extraction from complex environments such as soil only recovers a fraction of the cells present (Busi et al., 2020; Trevors and van Elsas, 1995). For example, certain groups of organisms resist separation from soil, such as methanotrophic bacteria from peat, and ammonium-oxidising bacteria in clay loam soils (Bakken and Lindahl, 1995). In addition, DNA purified from soil microorganisms often contains humic and fulvic acids which can inhibit enzymes, such as Taq DNA polymerase, used in downstream assays. Numerous DNA extraction kits and methods were therefore tested to optimise yield and minimise PCR inhibitors. The Extraction methods used for different samples types, and different analyses are listed in Table 2-1.

Table 2-1 Table of DNA Extraction Kits used in different chapters

Kit	Section	Chapter	Application	Samples
Qiagen DNEasy PowerWater	2.2.2	3	16S rRNA gene amplicon Analysis	Snow, slush, meltwater, proglacial water, seawater
		4	Metagenomes	Seawater
Qiagen DNeasy PowerSoil	2.2.3	4	Metagenomes	Cryoconite
MP Biomedicals FastDNA Spin Kit for Soil	2.2.4	3	16 Amplicon analysis	Soil, Cryoconite
		4	Metagenomes	Soil (F3T3_FD)
MO BIO PowerMax Soil DNA Isolation Kit	2.2.7	4	Metagenomes	Soil (F3T3_PM)
		6	Cloning	Soil
MasterPure Complete DNA & RNA Purification Kit	2.2.5	6	Cloning optimisation	Soil
Ludox Density Gradient centrifugation	2.2.6	4	Metagenomes	Soil (F3T3_Lud)
		6	Cloning optimisation	Soil
ZymoBIOMICS DNA Minikit	2.2.8	6	Strain confirmation	*E.coli* isolates

Table listing different DNA Extraction kits, the chapters, and samples for which each kit was used and the purpose for which the DNA was extracted.

2.2.1 DNA Extraction for 16S rRNA gene amplicon analysis

A survey of the taxonomic diversity of a range of cryospheric environment types was conducted using16S rRNA gene amplicon-based analysis (Chapter 3). This study included liquid and solid environment samples; therefore, more than one DNA extraction kit was required due to the differing quantities and properties of the samples collected. DNA from all liquid samples, such as snow, slush, meltwater, proglacial water and seawater were extracted using the DNEasy PowerWater Kit (Section 2.2.2) in a clean room, while wearing a Tyvek suit to minimise contamination of low biomass samples. Some experimentation was required to select the DNA extraction kit for the solid samples because some of the soil sites, particularly those with high clay content, yielded extremely low DNA concentrations. Various kits and modified buffers were tested to optimise DNA yield from these sites. The FastDNA Spin Kit for Soil (MP Biomedicals) resulted in the highest yield from clay soils, which is in agreement with previous published studies (Dineen et al., 2010). Therefore, to reduce bias from using

different kits, all solid samples, including cryoconite, were extracted using the FastDNA Spin Kit for Soil (Section 2.2.4). Extractions from each sample site were performed in triplicate in randomised batches so that DNA from no sample site was extracted twice in a single batch and a control extraction was included in each extraction batch.

2.2.2 Qiagen DNEasy PowerWater

The Qiagen DNeasy® PowerWater® Sterivex™ Kit was used to extract DNA from snow, slush, glacial meltwater, proglacial water, and seawater samples that had been filtered through Sterivex filters (Millipore cat. no. SVGPL10RC).

Prior to use, Solution ST1A was added to Solution ST1B, and mixed well. Inlet and outlet caps were removed to extract the RNA*later*™ Stabilization Solution (ThermoFischer Scientific) which had been added to the Sterivex filters for storage. Liquid was removed using a syringe with a tubing connector that had been washed in bleach, HCl and ddH_2O. The outlet cap was replaced and 0.9 mL of Solution ST1B was added using a pipette tip. Thereafter, the inlet was recapped and the Sterivex filter were secured horizontally to a vortex adapter, with the inlet facing outwards. The filters were vortexed at minimum speed for 5 min, after which they were rotated 180 degrees from the original position, while maintaining their orientation with inlet facing outwards, and vortexed for an additional 5 minutes. The Sterivex filter units were positioned with the inlet facing up, the inlet caps were removed, and 0.9 mL of Solution MBL (prewarmed to 65℃) was added to each unit using a pipette tip. The inlets were recapped, and the Sterivex filter units were incubated at 90ºC for 5 minutes. The filters were cooled for 2 minutes and then secured horizontally, with the inlet facing outwards to a vortex adapter and vortexed at maximum speed for 5 minutes. The lysate was removed from the Sterivex filters by pulling back the plunger of a 3 mL syringe to fill the barrel with 1 mL of air, and then attaching it to the inlet of Sterivex filter unit. The air was pushed into the unit until there was resistance, and then the plunger was released and slowly pulled back to remove as much of the lysate as possible. The syringe was detached from the Sterivex filter unit and the lysate added to 5 mL glass PowerBead Tubes. The PowerBead Tubes were secured horizontally to a vortex adapter and vortexed at maximum speed for 5 minutes. The tubes were centrifuged at 4000 x g for 1 minute and the supernatants transferred to clean 2.2 mL collection tubes. Thereafter, 300 µL of Solution IRS was added to the tubes, which were vortexed briefly to mix, and then incubated in an ice-bucket (approximately 4 °C) for 5 minutes. The tubes were

centrifuged at 13,000 x g for 1 minute and the supernatants were transferred to clean 5 mL collection tubes.

For each sample, a tube extender was placed firmly into an MB Spin Column and the tube extender/MB Spin Column unit was attached to a VacConnector and VacValve (VV) on the QIAvac 24 Plus Manifold. Solution MR, which had been prewarmed to 65 °C, was retrieved and 3 mL was immediately added to the Collection Tubes containing supernatant and vortexed to mix. The entire 4.5 mL of supernatant was then loaded into the tube extender/MB Spin Column. The vacuum source was turned on and the VV of the port opened, allowing the lysate to pass through. Once the lysate had passed through completely, the VV was closed. While keeping the MB Spin Column attached to the VV the tube extenders were removed and discarded. Following this, 0.8 mL of ethanol was added to the MB Spin Column, the VV was opened and the ethanol allowed to pass through the column completely. The VV was closed and then 0.8 mL of Solution PW (mixed thoroughly by shaking) was added to the MB Spin Column. The VV was opened and Solution PW allowed to pass through the column completely. The vacuum was maintained for another minute to dry the membrane. The VV was closed and 0.8 mL of ethanol was added to the MB Spin Column. The VV was opened and a vacuum was applied until the ethanol had passed through the MB Spin Column completely. The vacuum was maintained for another minute to dry the membrane, then closed. The vacuum source was turned off and an unused port as opened to vent the manifold. The MB Spin Column was removed and placed in a 2.2 mL collection tube. The tube was centrifuged at 13,000 x g for 2 min to completely dry the membrane. The MB Spin Column was transferred to a new 2.2 mL collection tube and 100 µL of Solution EB was added to the centre of the white filter membrane. Finally, the tubes were centrifuged at 13,000 x g for 1 minute at room temperature to elute the DNA and the MB Spin Columns were discarded. DNA concentration and quality were tested using Qubit and agarose gel electrophoresis before long-term storage at -20 °C.

2.2.3 Qiagen DNeasy PowerSoil

The Qiagen DNeasy® PowerSoil® Kit was used to extract DNA from soil and cryoconite. Cryoconite DNA from these extractions were used for the shotgun metagenomes (Chapter 4) and clone libraries (Chapter 6).

Briefly, approximately 0.25 g of soil or cryoconite was added to PowerBead tubes and vortexed briefly to mix. Solution C1 was pre-warmed to 60 °C and 60 µL was added to

each tube. The tubes were then secured horizontally to a Vortex Adapter and vortexed at maximum speed for 15 minutes. The samples were centrifuged at 10 000 x g for 30 seconds and the supernatant transferred to 2 mL collection tubes to which 250 µL of Solution C2 had been pre-aliquoted. The samples were vortexed for 5 seconds and then incubated in an ice-bucket (4 °C) for 5 minutes. The samples were centrifuged at 10 000 x g for 1 minute and 600 µL of the supernatants were added to a 2 mL collection tube to which 200 µL of Solution C3 had been pre-aliquoted. The tubes were vortexed to mix, incubated in an ice-bucket (4 °C) for 5 minutes and then centrifuged at 10 000 x g for 1 minute. Carefully avoiding the pellet, 750 µL of supernatant was transferred to 2 mL collection tubes to which 1200 µL of vigorously mixed Solution C4 had been pre-aliquoted. The samples were vortexed briefly to mix and then 675 µL was added onto an MB Spin Column and centrifuged at 10 000 x g for 1 minute. The throughflow was discarded and the same step repeated twice more until all the sample had been processed. Thereafter, 500 µL of Solution C5 was added to the Spin Column and the samples were centrifuged for 30 seconds at 10 000 x g. The flow through was discarded and the Spin Column was centrifuged for a further minute at 10 000 x g. Following this, the Spin Column was carefully transferred to a clean 2 mL collection tube and 100 µL of Solution C6 (10 mM Tris-HCl, pH 8.5) was added to the centre of the filter membrane and left for 5 minutes at room temperature. The DNA was eluted by centrifugation for 30 seconds at 10 000 x g. The Spin columns were discarded, and the DNA concentration and quality were tested using Qubit and agarose gel electrophoresis before long-term storage at -20 °C.

2.2.4 FastDNA™ Spin Kit for Soil

The FastDNA™ Spin Kit for Soil (MP Biomedicals) was used to extract DNA from glacier forefield soils and cryoconite collected in July 2017. The DNA extracted using this kit was used to create the 16S rRNA gene amplicon Libraries in Chapter 3 (Appendix Figure C-1). The Kit was selected because it yielded higher concentrations of DNA than the Qiagen DNEasy PowerSoil, particularly for the high clay-content soils close to the glacier snout.

Extractions from forefield soil were performed following the manufacturer's instructions with small modifications. Approximately 500 mg of soil was weighed and added to Lysing Matrix E tubes, to which 978 µL of Sodium Phosphate Buffer and 122 µL of MT Buffer was added. The samples were then put on ice and homogenized in the

FastPrep24 Instrument for three cycles of 30 seconds at a speed setting of 6.0, with 30 seconds of cooling on ice between cycles. The tubes were centrifuged for 15 minutes at 14 000 x g to pellet debris. Following this, the supernatant was transferred to a clean 2mL microcentrifuge tube, to which 250 µL PPS (Protein Precipitation Solution) was added. The tubes were inverted 10 times to mix, followed by 5 minutes centrifugation at 14 000 x g to pellet the precipitate. The supernatant was then carefully transferred to 15ml flacon tubes. The Binding Matrix suspension was mixed thoroughly using a vortex, and 1 mL was added to the supernatant in each 15 mL tube. Tubes were inverted by hand for 2 minutes, and then placed in a rack for 3 minutes for the silica matrix to settle. Thereafter, 500 µL of supernatant was removed and discarded, avoiding the silica pellet. The Binding Matrix was gently resuspended in the remaining supernatant and approximately 600 µL was added to Spin™ Filter. The Spin™ Filter was centrifuged at 14 000 x g for 1 minute, and the catchment tube was emptied. The remaining supernatant was added to the Spin™ Filter, and the centrifugation and emptying step was repeated. The pellet on the filter was gently resuspended using 500 µL SEWS-M (to which ethanol had been added at first use). The Spin™ Filter tube was then centrifuged at 14 000 x g for 1 minute, the catchment tube was emptied and replaced, followed by a second centrifugation of 2 minutes at 14 000 x g to dry the matrix. The catch tube was discarded and replaced with a new catch tube. The Spin™ Filter was then allowed to air dry at room temperature for 5 minutes. Finally, the Binding Matrix was gently resuspended in 100 µL DES (DNase/ Pyrogen-Free Water) and the tubes were centrifuged for 1 minute at 14 000 x g to elute the DNA, after which the Spin™ Filters were discarded. The DNA concentration and quality were tested using Qubit and agarose gel electrophoresis before long-term storage at -20 ℃.

2.2.5 MasterPure Complete DNA & RNA Purification Kit

The MasterPure™ Complete DNA & RNA Purification Kit was selected to try to extract high molecular weight DNA for cloning because this extraction method does not rely on bead beating, which shears genomic DNA.

2.2.5.1 Extraction

Each extraction used 50 mL of PBS with 0.1% Tween 20 per sample. After sifting soil to remove large stones, 1 g of wet soil was placed in a 50 mL screw-cap conical tube to which 10 mL of PBS with 0.1% Tween 20 was added. The tubes were mixed by vortexing at maximum speed for 1 minute to disperse and dissociate the soil particles. The soil

suspension was centrifuged at 1,600 x g for 4 minutes and the supernatant was poured into a new 50-mL tube. An additional 20 mL of PBS with 0.1% Tween 20 was added to the original soil pellet and mixed by vortexing at maximum speed for 1 minute. The soil suspension was centrifuged at exactly 900 x g for 3 minutes in a tabletop centrifuge and the supernatant was combined with the previously collected supernatant. The soil pellet was extracted again with an additional 20 mL of PBS + 0.1% Tween and centrifugation. The pooled supernatant was centrifuged at 900 x g for 2 minutes in a tabletop centrifuge and the supernatant was transferred to a fresh 50-mL tube.

2.2.5.2 Filtration

The entire collected supernatant (50 mL) was poured through four layers of bleached and autoclaved Miracloth filtration material (Calbiochem). The sample was then prefiltered through a 1.2-µm filter membrane using a Nalgene® 300-4000 250mL Vacuum Filter Holder with Funnel and Receiver (Thermo Scientific™) with a handheld vacuum pump. The filtrate was collected then passed through a 0.22-µm filter membrane to trap the microbial mass on the filter. Using forceps and scissors pre-soaked in 70% ethanol, the membrane was removed from the filter apparatus, cut in half, and each half placed rounded side down along the side near the bottom of a 50-mL sterile conical tube. The upper surface of the filter faced the centre of the tube and was not allowed to dry out. Filter Wash Buffer was prepared immediately before use (by adding 1.5 µL of Tween20 to 1.5 mL of PBS), and 1.5 mL was added to the filter pieces in the tube. The tube was vortexed at the low speed setting to rewet the filter pieces, then the setting was increased to the highest speed. The 1.5 mL cell suspension was transferred to a clean microcentrifuge tube, then centrifuged at 14,000 x g for 2 minutes to pellet the cells.

2.2.5.3 Lysis, and Protein Precipitation

The supernatant was discarded, and the cell pellet resuspended in 300 µL of TE Buffer, to which 2 µL of Ready-Lyse Lysozyme Solution and 1 µL of RNase A was added. The suspension was mixed, centrifuge briefly then incubated at 37°C for 30 minutes. After incubation, 300 µL of 2x Tissue and Cell Lysis Solution and 1 µL of Proteinase K was added to the tube and mixed by vortexing. After a brief pulse-centrifuge to ensure that all the solution is in the bottom of the tube, the suspension was incubated at 65°C for 15 minutes. The tubes were cooled on ice for 3-5 minutes, then 350 µL of MPC Protein Precipitation Reagent was added to the tube and mixed by vortexing vigorously for 10

seconds. The cell debris was pelleted by centrifugation for 10 minutes at 20,000 x in a microcentrifuge at 4°C. The supernatant was transferred to a clean 1.7-mL microcentrifuge tube and 570 µL of isopropanol was added. The contents of the tube were mixed by inverting the tube several times. Thereafter the DNA was pelleted by centrifugation for 10 minutes at 20,000 x g at 4°C. The isopropanol was removed with a pipette tip, being careful not to dislodge the DNA pellet. Once dry, 500 µL of 70% ethanol was added to the pellet, followed by centrifugation for 5 minutes at 20,000 x g at 4°C.21. A pipet tip was used to remove the ethanol without dislodging the DNA pellet. The DNA pellet was then air-dried for 8 minutes at room temperature. Finally, the DNA pellet was resuspended in 40 µL of TE Buffer. The quality (size) and concentration of the isolated DNA was checked by gel electrophoresis on a 1% agarose gel and Qubit, respectively.

2.2.6 Ludox Density Gradient centrifugation

To scale up the number of cells that could be separated for lysis, density gradient centrifugation was tried instead of filtering. The method was based on the protocol described by Bakken who separated cells using a colloidal silica gradient (Percoll) (Bakken and Lindahl, 1995). The size of Percoll particles is approximately 35 nm, whilst the size of Ludox HS 40 particles is approximately 12 nm. Although high losses of cells from clay loam cells due to sedimentation through the gradient were reported (Bakken and Lindahl, 1995), the large amount of soil that could be processed might compensate for a relative increase in cell loss. Moreover, although Bakken reported that the direct loading of cell homogenate on top of a Percoll density gradient was not promising, as the cell yield was low, and the gradient contained many contaminating substances; it was speculated that the greater size difference between Ludox HS particles and bacterial cells would allow for easier removal of the silica particles from the bacterial cell pellet.

According to procedures recommended by Bakken & Lindahl, 1995, 60 – 72 g of soil was added to PBS with 0.1% Tween20 or distilled water and homogenized in a waring-type blender for 3 x 1 minute at maximum speed. The slurry was then poured into two sterile 50 mL Falcon Tubes. Thereafter, 100 mL was added, and the process repeated two more times for a total of 6 x 50 mL Falcon Tubes containing 300 mL of slurry. The Tubes were centrifuged at 900 x g for 2 minutes to pellet large soil particles and transferred to a

new tube. The Falcon tubes were then centrifuged at 3857 x g for 30 minutes and the supernatant was discarded. The pellet was resuspended in 3.5 mL PBS.

The microbial cell fraction was separated from soil particles using density gradient centrifugation with LUDOX HS 40. Exactly 30 mL of Ludox HS 40 was added to sterile 50 mL Falcon Tubes. The supernatant from three Tubes was loaded onto a single column and the Falcon Tube was centrifuged for 30 minutes at 3857 x g. At this point, the cell fraction formed a visible layer on within the Ludox column, which was collected by pipetting and transferred into a new 50 mL Falcon Tube.

Up to 40 mL of PBS was added to the Tubes, which were then centrifuged for 15 minutes at maximum speed (3857 x g). The supernatant was poured off and the step repeated five times to try and dilute and remove the LUDOX silica particles. After the fifth centrifugation, the supernatant was poured off and the pellet was resuspended in 2 mL PBS and added to a 2 mL microcentrifuge tube. The tube was centrifuged at 10 000 x g for 2 minutes and the supernatant poured off. The pellet was finally resuspended in 300 µL TE. The DNA was then extracted followed the method described in Section 2.2.5.3. This method was successful at extracting high molecular weight DNA of the right size for fosmid packaging but did not yield the concentration of DNA expected from the mass of starting material.

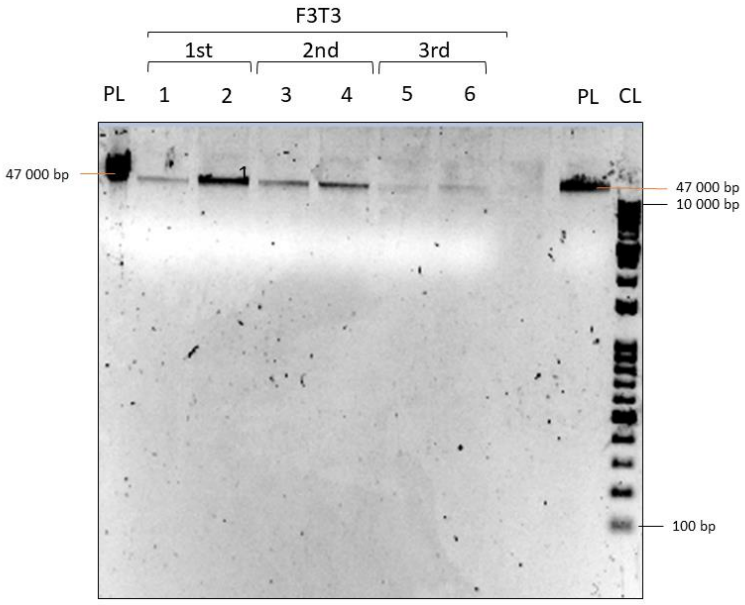

Figure 2-2 Gel of High Molecular Weight DNA extracted using Ludox HS-40. PL is Phage DNA (47 kb). CL is Cleaver Scientific Broad Range Ladder. The numbered lanes 1-20 refer to 1st, 2nd and 3rd 100 mL aliquots of soil slurry). Gel is 0.8% agarose in 0.5 X TBE.

2.2.7 MO BIO PowerMax Soil DNA Isolation Kit

The DNA extracted using the MO BIO PowerMax Soil Kit was used in the Soil Shotgun metagenome library in Chapter 4 and was also used to construct the soil clone library in Chapter 6.

Solution C1 was warmed to 60 °C before starting. Fifteen mL of PowerBead Solution was added to a PowerBead Tube followed by10 g of soil sample (from which large stones had been removed). After vortexing for 1 minute, 1.2 mL of Solution C1 was added to the PowerMax® Bead Solution Tube and vortexed vigorously for 30 seconds. The PowerMax® Bead Solution Tubes were then secured horizontally to a vortex and vortexed for 10 minutes at the highest speed, then centrifuged at 2500 x g for 3 minutes at room temperature. The supernatants were transferred to a clean Collection Tube, to which 5 mL of Solution C2 was added, inverted twice to mix, and incubated at 4°C for 10 minutes. The tubes were centrifuged at 2500 x g for 4 minutes at room temperature, then the supernatant was transferred to a clean Collection Tube, avoiding the pellet. Four mL of Solution C3 was added and the mixture was inverted twice to mix, followed by incubation at 4°C for 10 minutes. The tubes were centrifuged at 2500 x g for 4 minutes at room temperature and the supernatant was transferred to a clean Collection Tube. Solution C4 was mixed by shaking and 30 mL was added to the supernatant and inverted twice. The Spin Filter was filled with the Solution C4/ supernatant mix and centrifuged at 2500 x g for 2 minutes at room temperature. The flow through was discarded and the previous step was repeated twice more with the remaining supernatant. Once the final through-flow has been discarded, 10 mL of Solution C5 was added to Spin Filter and centrifuged at 2500 x g for 3 minutes at room temperature and the flow through discarded. The Spin Filter was centrifuged at 2500 x g for 5 minutes at room temperature, then carefully placed in a new Collection Tube. To elute, 5 mL of sterile Solution C6 was added to the centre of Spin Filter membrane and centrifuged at 2500 x g for 3 minutes at room temperature. The Spin Filter was discarded, and the DNA was further concentrated. To concentrate the DNA, 0.2 mL of 5M NaCl was added and the tube was inverted 3-5 times to mix. Next, 10.4 mL of 100% cold ethanol was added and inverted 3-5 times to mix. The solution was centrifuged at 2500 x g for 30 minutes at room temperature. All liquid was decanted. The DNA pellet was then washed with 70% cold ethanol, the liquid decanted, and the residual ethanol allowed to evaporate in ambient air. Finally, the precipitated DNA was resuspended in sterile 10 mM Tris.

2.2.8 ZymoBIOMICS DNA Minikit

The ZymoBIOMICS DNA Minikit (ZymoResearch, Catalog No. D4300) was used to extract DNA from *E. coli* HCS1 and cs2-29 colonies prior to PCR to confirm the *fcsA29* mutation in the *polA* gene.

DNA was extracted from *E.coli* colonies by scraping single colonies into ZR BashingBead™ Lysis Tubes (0.1 & 0.5 mm) to which 750 µL ZymoBIOMICS™ Lysis Solution was added. The tubes were secured to a vortex adapter with a 2 mL tube holder and vortexed at maximum speed for 5 minutes. The ZR BashingBead™ Lysis Tubes were then centrifuged at ≥ 10,000 x g for 1 minute. Up to 400 µL of the supernatant was transferred to a Zymo-Spin™ IV Spin Filter (Orange Top) in a clean Collection Tube and centrifuged at 7,000 x g for 1 minute. Thereafter, 1,200 µL of ZymoBIOMICS™ DNA Binding Buffer was added to the filtrate. Up to 800 µL at a time of the mixture was added to a Zymo-Spin™ IIIC-Z Column in a Collection Tube, centrifuged at 10,000 x g for 1 minute, and the through-flow discarded, until all the filtrate had been processed. The Zymo-Spin™ IIIC-Z Column was placed in a new Collection Tube to which 400 µL ZymoBIOMICS™ DNA Wash Buffer 1 was added. The Tube was centrifuge at 10,000 x g for 1 minute, the flow-through was discarded and 700 µL ZymoBIOMICS™ DNA Wash Buffer 2 was added to the Zymo-Spin™ IIIC-Z Column in the same Collection Tube. The tube was centrifuged at 10,000 x g for 1 minute, the flow-through discarded and 200 µL ZymoBIOMICS™ DNA Wash Buffer 2 was added to the Zymo-Spin™ IIIC-Z Column and centrifuged at 10,000 x g for 1 minute. The Zymo-Spin™ IIIC-Z Column was transferred to a clean 1.5 mL microcentrifuge tube and 100 µL ZymoBIOMICS™ DNase/RNase Free Water was added directly to the column matrix and incubated for 1 minute. The Tube was centrifuged at 10,000 x g for 1 minute to elute the DNA. In a final step to remove PCR inhibitors, a Zymo-Spin™ IV-HRC Spin Filter (Green Top) was prepared by snapping off the base of the Zymo-Spin™ IV-HRC Spin Filter (Green Top) and placing it into a clean Collection Tube. The tube was centrifuged at 8,000 x g for 3 mins and the flow-through discarded. The cap was removed and 400 µL DNase/RNase Free Water was added to the Zymo-Spin™ IV-HRC Spin Filter and centrifuged at 8,000 x g for 2 minutes. Finally, the eluted DNA was transferred to a prepared Zymo-Spin™ IV-HRC Spin Filter in a clean 1.5 mL microcentrifuge tube. The Zymo-Spin™ IV-HRC Spin Filter was loosely capped and centrifuged at exactly 8,000 x g for 1 minute.

2.3 DNA Quality and concentration

2.3.1 Agarose gel electrophoresis for DNA visualisation

Agarose gel electrophoresis was used for the visualisation of DNA from genomic and metagenomic DNA extraction, PCR amplifications, plasmid minipreps and restriction digestions. Briefly, agarose gels were made using agarose and 0.5X TBE (Tris Borate-EDTA) Buffer. Agarose concentrations ranged from 0.8% (for very large DNA fragments) to 1.5 % for small amplicons. Gels were run in a gel tank for variable lengths of time, depending on fragment size, gel concentration and required band resolution for visualisation. The most used stain was SybrSafe, in a concentration between 2 and 8 μL per 100 mL gel. Appropriate ladders were used, depending on the DNA fragment sizes and resolution required.

2.3.2 Qubit to assess DNA concentration

DNA concentration of samples was measured using the Qubit® dsDNA HS (High Sensitivity) Assay (Invitrogen™, Catalog no. Q32854) and the Qubit® 2.0 Fluorometer (Invitrogen™, Catalog no. Q32866). Samples were prepared in Qubit® assay tubes (Invitrogen™, Catalog. no. Q32856). The working solution was prepared by diluting the Qubit® dsDNA HS Reagent 1:200 in Qubit® dsDNA HS Buffer. Standards were prepared and calibration done for each batch of samples. Working solution (190 – 199 μL) and sample DNA (10 – 1 μL) was mixed to a final volume of 200 μL and briefly vortexed to mix. Calibration was performed with the standards and samples were measured following the Qubit® 2.0 instructions.

2.4 Polymerase Chain Reaction (PCR)

2.4.1 Optimisation of 16S rRNA gene PCR

In the extraction and amplification of DNA from Svalbard, habitats there were several obstacles to overcome. In a comparative study, it is best to minimise the number of potential confounding factors introduced by methodological differences that may introduce bias. However, in a survey of these many diverse habitat types, there is no method that is optimal for all sample types. The samples from different environment types had different starting concentrations of DNA, different inhibitors, and different taxonomic profiles.

However, a common processing method, except where impossible, was used. Therefore, many polymerases, and many iterations of cycling conditions were tried to amplify the greatest number of samples. A high-fidelity polymerase is preferable in 16S rRNA gene amplicon sequencing studies, however, after several attempts, the HiFi polymerases seemed to be sensitive to inhibitors in many of the samples.

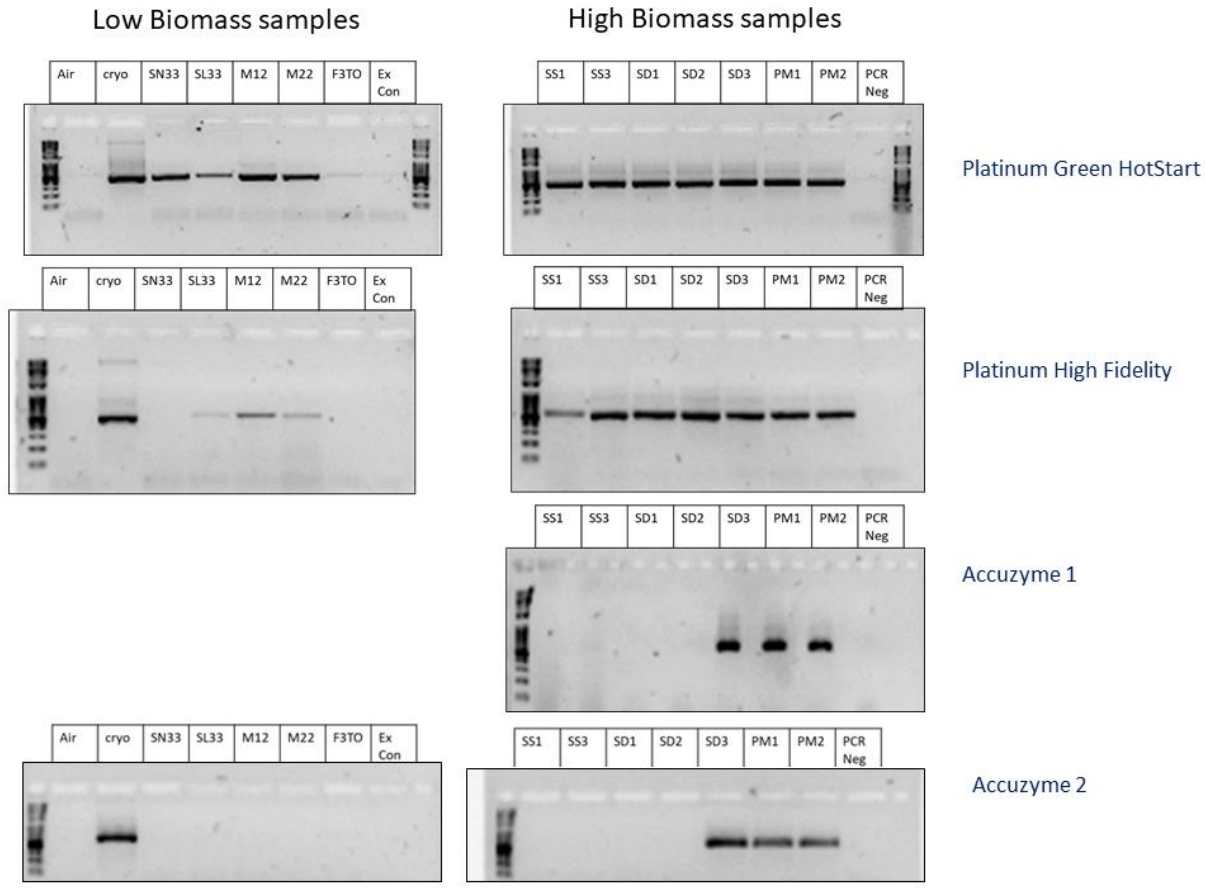

Figure 2-3 Comparison of different polymerases on amplification of a range of environment types. The High-Fidelity polymerases (Accuzyme and Platinum High Fidelity) were completely inhibited by samples that amplified robustly using Platinum Green Hot Start.

2.5 DNA Clean-up and Purification

2.5.1 Ampure bead clean-up

Agencourt AMPure XP beads were used to remove primers and PCR reagents from PCR products during the preparation of 16S rRNA amplicon libraries (Section 2.6.1), shotgun metagenome libraries (Section 2.6.2) and ahead of Sanger sequencing (Section 2.6.3). It was also occasionally used to try remove suspected PCR inhibitors from samples that would not amplify, and to concentrate very low concentration DNA.

Briefly, the AMPure XP solution was vortexed to mix and left for 30 minutes at room temperature. AMPure XP solution was added in a ratio of 1.8 μL AMPure XP: 1 μL of sample. The sample and beads were pipetted to mix and incubated for a few minutes to allow the DNA fragments to bind to the paramagnetic beads. The 96 well plate was then placed on a magnetic plate holder to allow the separation of beads and DNA fragments from contaminants. While the beads + DNA were attached to the tube wall by the magnet, the liquid was removed from the wells, and then the washed twice with 200 μL freshly-made 70 - 80% ethanol to remove contaminants All of the ethanol was removed and the beads allowed to air-dry for a few minutes. The 96 well plate was removed from the magnetic rack and 10mM Tris was added and the beads gently washed into solution and allowed to incubate at room temperature for 5 minutes. The plate was then placed back on the rack and the purified DNA fragments could be removed from the wells and transferred to a new plate.

2.6 DNA Sequencing

2.6.1 Illumina MiSeq of 16S rRNA gene Amplicons

The v3-v4 region of the 16S rRNA gene was amplified because it has been evaluated as the most promising bacterial primer pair for bacterial diversity studies (Klindworth et al., 2013). PCR amplification was performed using the recommended Illumina 16S rRNA PCR Forward 5' [TCGTCGGCAGCGTCAGATGTGTATAAGAGACAGCCT ACGGGNGGCWGCAG] 3’ and Reverse Primers 5' [GTCTCGTGGGCTCGGAGATG TGTATAAGAGACAGGACTACHVGGGTATCTAATCC] 3’. The PCR reaction was performed in two 96 well plates. Samples were split between high and low concentration plates based on the starting concentration of the samples (Appendix Figure C-5 and Figure C-6). This was done to lower the risk of cross contamination of extremely low biomass samples by highly concentrated samples. The PCR reactions were set up in a volume of 50 μL as follows: 25μL Invitrogen Platinum HotStart Green PCR Mix (2x), 10 μL PCR FWD primer (1 μM), 10 μL PCR REV primer (1 μM), 1-5 μL environmental DNA and 0-4 μL PCR water to volume. The amount of DNA added depended on the starting concentration of the extracted DNA and the suspected presence of inhibitors.

Samples were then amplified on a thermal cycler using the following program: 95ºC for 3min, 34 cycles of: 95ºC for 30s, 55ºC for 30s and 72ºC for 30s, followed by a final

72ºC step for 5min. In addition, eight PCR controls were run, in which ultra-pure Milli-Q water was added instead of sample. Amplification success was confirmed by running 5µL of product on a 1% agarose gel (Appendix Figure C-2). Amplification products were then cleaned-up with Ampure® beads (Section 2.5.1) followed by agarose gel electrophoresis to confirm successful clean-up (Appendix Figure C-3).

Using a multichannel pipette, 5 µL from each well was transferred to a new 96-well plate. The Index 1 and 2 primers were arranged in a rack (TruSeq Index Plate Fixture) using the arrangements described in Appendix Table C-1. The second stage PCR reaction to add indexes was set up in a total volume of 25 µL with 2.5 µL DNA, 2.5 µL Nextera XT Index Primer 1 (N7xx), 2.5 µL Nextera XT Index Primer 2 (S5xx), 12.5 µL Accuzyme Mix (2x) and 5 µL PCR-grade water. The PCR was run on a thermal cycler using the following program: 95°C for 3 minutes, followed by 8 cycles of: 95°C for 30 seconds, 55°C for 30 seconds, 72°C for 30 seconds and final elongation step at 72°C for 5 minutes, followed by hold at 4°C. The second stage PCR products were run on a gel and compared to first stage PCR products to confirm the size shift from approximately 550 bp to 630 bp (Appendix Figure C-4). The second stage PCR products were once again cleaned up using AmpureBeads (Section 2.5.1) and 3 µL was run on an agarose gel to check for PCR product with no remaining primers. The samples were then measured using an EPOCH (BioTek Instruments, Inc) or Qubit to determine exact concentrations for pooling.

2.6.2 Illumina Nextera shotgun sequencing

The environmental DNA was tagmented by adding 10 µL Tagment DNA buffer (TD) to the 5ul of normalised DNA and then adding 5µl of Amplicon Tagment Mix (ATM) to the wells and mixing well. The PCR plate was then centrifuged at 280 x g at room temperature for 1 minute to make sure all sample was in the bottom of the well. The mix was then rapidly transferred to a pre-programmed and pre-warmed thermocycler set at 55° C and incubated for 5 minutes exactly, followed by rapid cooling to 10 °C. As soon as the thermocycler reached 10 °C the plate was removed and 5 µL of Neutralize Tagment (NT) Buffer was added to stop the tagmentation reaction. The plate was then centrifuged at 280 x g at room temperature for 1 minute, then incubated for an additional 5 minutes at room temperature.

The libraries were amplified and indexed using a limited-cycle PCR. The indexes for each library (Appendix Table D-1) were arranged in a 96-well PCR plate; 5 µL of Index 1 (i7) was added down each column using a multichannel pipette, followed by the addition of 5

µL of Index2 (i5) across each row. Thereafter, 15 µL of Nextera PCR Master Mix (NPM) was added to each well and mixed by pipetting, followed by a brief centrifugation at 280 x g for 1 minute at room temperature. The libraries were then amplified in a thermocycler set to the following cycle conditions: 72 °C for 3 minutes, 95 °C for 30 seconds, followed by 15 cycles of 95 °C for 10 seconds, 55°C for 30 seconds and 72 °C for 30 seconds, followed by a final elongation step of 5 minutes at 72 °C. A 1.5% agarose gel was run to confirm successful amplification of metagenomic libraries (Appendix Figure D-1). The resulting indexed libraries were cleaned up using Ampure beads (Section 2.5.1) and resuspended in 37.5µL of Resuspension Buffer. Cleaned, indexed metagenomic libraries were equimolarly pooled to 40 nM in a final volume of 50µL. To provide a final library concentration of 4nM, 5µL of the previous solution were diluted in 10mM Tris 0.05% TWEEN. The pooled libraries were sequenced at Wales Gene Park (Cardiff University) in an Illumina NextSeq® in High Output mode, generating 2 x 150bp paired end reads.

2.6.3 Sanger sequencing

The PCR products from amplification of pJET2.1/blunt vector inserts, the 16S rRNA gene and polA gene sequences were sent for Sanger Sequencing. Briefly, the PCR products were cleaned up using Ampure beads. Thereafter, 5- 25 ng DNA in 6 µL was added to 4 µL BigDye™ Terminator Ready Reaction Mix (Applied Biosystems™) and 1.6 pmol of FWD primer and sent for sequencing on an ABI 3730 DNA analyser (Applied Biosystems™).

3 HABITAT PREFERENCE OF BACTERIA FROM A HIGH ARCTIC GLACIAL ECOSYSTEM INDICATES CLIMATE VULNERABILITY

3.1 Introduction

The cryosphere is one of the Earth's largest biomes, covering approximately 10% of the Earth's surface, and includes glaciers, icecaps and ice-sheets, as well as sea ice, frozen inland water bodies, snow and permafrost (Margesin and Collins, 2019). This biome has been identified an attractive region for bioprospecting (Cavicchioli et al., 2002; Leary, 2008) because it is an extreme environment (Maccario et al., 2015), difficult to access and therefore relatively unexplored (Edwards et al., 2016; Gowers et al., 2019) and under threat from global warming (Stibal et al., 2020). The potential loss of biodiversity due to climate change represents a tragic squandering of undiscovered biological novelty and identifying the most vulnerable environments is therefore an urgent priority.

Within the cryosphere, glaciers and glacial systems are attractive ecosystems for bioprospecting because they contain within them different habitat types (snow, slush, cryoconite, meltwater, proglacial water) and are adjacent to influencing environments such as moraines, marine systems and freshwater lakes (Cameron et al., 2020b; Lutz et al., 2016; Thomas et al., 2020). Each habitat contains distinct microbial communities (bacterial, fungal, and algal) adapted to specific local conditions (Anesio and Laybourn-Parry, 2012; Boetius et al., 2015; Hodson et al., 2008). These microbial communities vary in complexity and heterogeneity, and this heterogeneity can be present at the micro, meso and macroscales (Bay et al., 2020; Edwards et al., 2020; Malard et al., 2019). This system is therefore subject to strong gradients in local selection pressures and has high heterogeneity, which makes it a likely biodiversity hotspot.

The microbial communities of glacial systems are also responsive and dynamic, with spatial and temporal variation demonstrated in forefield soil (Bradley et al., 2014; Rime et al., 2016, 2015), snow (Hell et al., 2013; Larose et al., 2013a; Lutz et al., 2014, 2016), slush (Lutz et al., 2014), meltwater (Cameron et al., 2020b; Kohler et al., 2020) and cryoconite (Cook et al., 2016a; Edwards et al., 2013c; Gokul et al., 2016) communities.

The high sensitivity and adaptability of some microorganisms to changing environmental conditions suggest that communities contain specialists that thrive or dominate only under specific conditions (Allison and Martiny, 2008). Alternatively, some taxa are relatively stable both spatially and temporally due to an ability to adapt to a wide range of conditions. These highly prevalent and stable taxa can be considered the core 'keystone' taxa because they persist either in a wide range of spatially separate environments of the same type, or over seasonal changes. Keystone taxa have been identified in cryoconite (Gokul et al., 2016) and soil (Malard et al., 2019) and likely represent highly adaptable generalists. However, in addition to the highly abundant and prevalent keystone taxa, there is a long tail of low abundance taxa. This long tail of low abundance species may represent a reservoir of biodiversity, with specialist taxa that may either thrive and become the new keystone species under different conditions, or go extinct should conditions change beyond the habitable range for that species. Alas, due to practices in dataset processing, the rare tail is often removed during a decontamination step, when rarefying libraries to equal library sizes (McMurdie and Holmes, 2014), or is obscured by OTU clustering (Bay et al., 2020).

With the threat of climate change, understanding the biogeography of the region, as well as the factors that influence it, is a race against time. Specialists, with narrow environmental windows are the most threatened , as perturbations caused by climate change could lead to local extinctions (Stibal et al., 2020). One of the easiest ways to identify specialist species is to determine their prevalence across different sites and environmental gradients. In glacial ecosystems, there is a constant spread or inoculation of taxa from one environment to downstream environments. The seeding and succession of microbial community members into new environments can occur over long time scales, such as the development of a glacier forefield soils (Bradley et al., 2014; Rime et al., 2016), or over shorter time period, such as the flow of microbial assemblages from supraglacial habitats to subglacial, proglacial (Kohler et al., 2020), forefield and marine (Thomas et al., 2020) environments via meltwater (Cameron et al., 2020b; Kohler et al., 2020) or aeolian transfer. In light of the vast amount of meltwater being lost annually due

to climate change, several studies on the consequences of the release of glacial microbial assemblages on downstream environments have been conducted in Arctic environments, from Disco Island, Greenland (Cameron et al., 2020) to Ny Ålesund Svalbard (Thomas et al., 2020). In particular, there has been a focus on the seeding of downstream ecosystems and determining the 'directionality' of the flow of microbial species from glacial surface snow and bare ice to meltwater, to downstream soil, freshwater and marine ecosystems (Cameron et al., 2020b). Environment-agnostic species that can survive in physically linked environments despite harsh 'environmental' boundaries, such as sharp changes in pH, salinity, or light exposure tend to be generalists, and will likely dominate more and more as global climate change continues to alter environments. The habitat or site-specific species represent a vulnerable group that may soon be lost due to climate change.

One of the requirements for this study is a high level of resolution of individual community members within and across sites. As technology has improved, the resolution to which we can resolve community structure has improved from microscopy (Stibal et al., 2006; Takeuchi, 2002), to RFLP analysis (Cameron et al., 2012a; Edwards et al., 2011, 2013c), to cloning amplicons (Cameron et al., 2012a), and finally to the arrival of NGS sequencing (Cameron et al., 2020b; Gokul et al., 2016; Thomas et al., 2020) and soon 3rd Generation sequencing (Edwards et al., 2016; Gowers et al., 2019). However, it has been shown that not just sequencing technology, but also bioinformatics methodologies can weaken the ability to detect biogeographical patterns (Bay et al., 2020). In particular, the clustering of sequences at 97% identity threshold (OTUs) and/or filtering the rare biosphere (sequences lower than 0.05% relative abundance) were both found to obscure biogeographic patterns (Bay et al., 2020). In this study, we describe the biogeography of an Arctic glacier system at a fine resolution, by using amplicon sequence variants (ASVs) rather than OTUs and by retaining the rare microbiome.

In this chapter, samples from a range of cryospheric environments surrounding Ny-Ålesund, Spitsbergen, Svalbard were collected over two weeks. The environment types included snow, slush, glacial meltwater, proglacial water, forefield soil, seawater and cryoconite.

3.1.1 Aims and objectives

The aims of this study were as follows:

1. Increase the resolution for investigating biogeographic trends by using ASVs rather than OTUs and using statistical methods to remove contaminants.
2. Determine the phylogenetic diversity and species-richness of each sampled environment.
3. Identify whether here are ‘keystone’ taxa which are highly abundant and prevalent members of an environment type.
4. Identify community members that are unique to, or shared between, different environments.
5. Create a co-occurrence network to determine the extent to which ASVs co-occur and visualise how these occur within or across environment types.

3.2 Methods

3.2.1 Sample collection

Sampling was conducted on, and in the vicinity of, the Midtre Lovénbreen (ML) and Vestre Brøggerbreen (VB) glaciers in the Kongsfjorden area of Spitzbergen, Svalbard in late June to early July 2017 (Figure 1). Many cryospheric environment types were sampled including air, snow, slush, meltwater, cryoconite, proglacial water, soil, and seawater. GPS co-ordinates are available in Appendix Table B-1.

3.2.1.1 Snow and slush

The snow and slush were collected on 29 June, 3 July, and 7 July, from mid-way between stake 4 and stake 5 on ML. Two litres of snow and two litres of slush were collected from three pits, located approximately three meters apart on each of the three days. The snow and slush from each pit were melted overnight in the dark and filtered through a Millipore Sterivex filter within 36 hours.

3.2.1.2 Meltwater

Six litres of water were collected in sterile 1 litre Nalgene's from a flowing meltwater stream in line with stake 3 on ML on the 29 June, 3 July, and 7 July. Two Nalgene's (2 litres) were filtered through a Millipore Sterivex using a peristaltic pump within 24 hours of collection. The Sterivex filter was filled with DNA Later, sealed, and stored at -20 °C until DNA extraction. A 50 mL falcon tube of filtered meltwater was collected, without any air bubbles, and stored at 4°C until chemical analysis could be done.

3.2.1.3 Proglacial water

Proglacial water was collected in six sterile 1 L Nalgene's from flowing streams at the snout of each of ML and VB glaciers. Two litres of water were filtered through a single Sterivex to get 3 replicates for each proglacial stream.

3.2.1.4 Seawater

Seawater was collected from open water in front of the ML glacier forefield at two depths using a Niskin bottle. The Niskin bottle was dropped three times at 1m and 15 meters each, and 2 litres of water was collected in sterile 1L Nalgenes after each sampling event.

3.2.1.5 Soil

Soil from the forefield of the ML glacier was collected in three transects perpendicular to the snout of the glacier. Samples were collected into Whirl Pak bags at five time points for a total of 15 unique samples, which were extracted in triplicate.

3.2.1.6 Cryoconite

Cryoconite was collected from ML by Nora Els and from VB by Dr Arwyn Edwards and Nora Els. GPS coordinates for cryoconite on the map are approximate, based on descriptions of the collection points relative to landmarks.

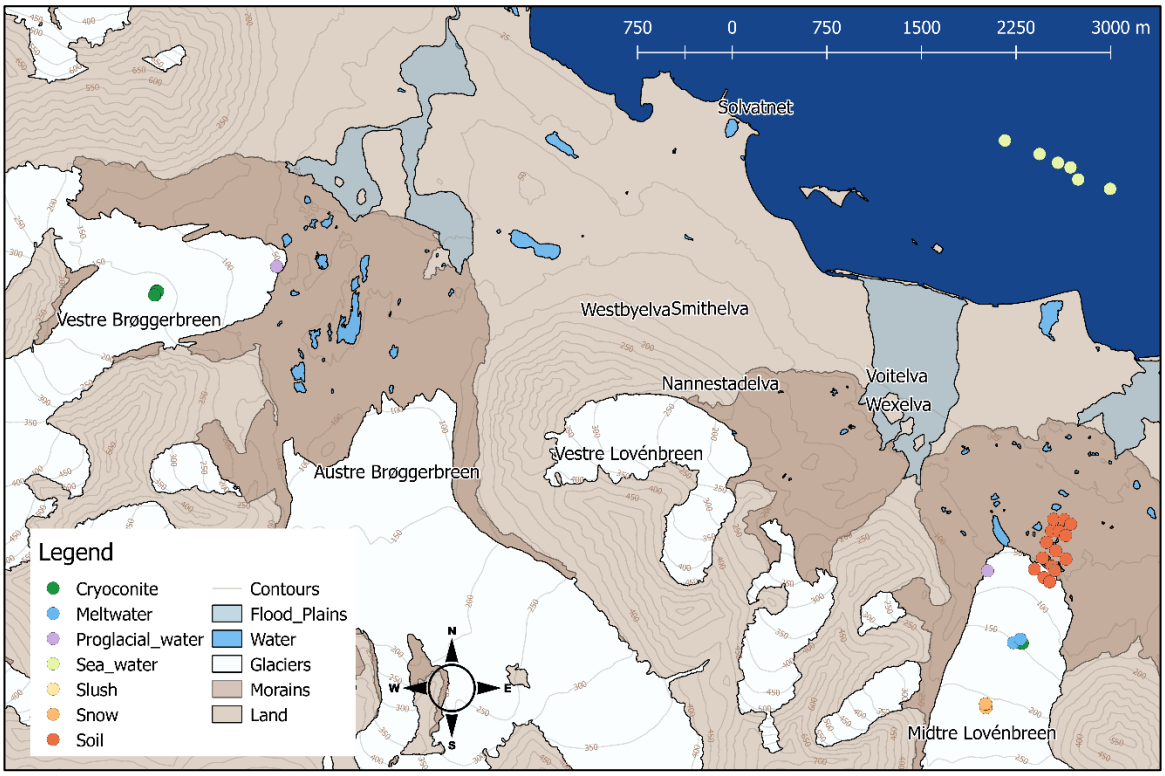

Figure 3-1 Map showing sampling sites in Ny-Ålesund, Spitsbergen, Svalbard.

3.2.2 DNA extraction

The high clay content of soils from the ML Glacier forefield proved challenging for DNA extraction. Several kits and protocols with various modifications were attempted to optimise yield (Section 2.2.1). Based on yield comparisons, the DNA from soil and cryoconite samples were extracted using the MP Biomedicals FastDNA kit for soil according to manufacturer's instructions, with a few modifications (Section 2.2.4). The air, snow, slush, meltwater, proglacial water and sea water was filtered through Sterivex filters, topped with RNA Later and stored at -20 °C. DNA extractions were done using the Qiagen PowerWater Kit according to manufacturer's instructions (Section 2.2.2). Because the samples were low biomass, extractions were performed in a clean room,

while wearing sterile Tyvek suits and masks. All samples from the FastDNA and PowerWater extractions were eluted in 100 µL. DNA quality and quantity were checked by running 4µL- 8µL of genomic DNA on a 1.5% agarose gel and using Qubit (Section 2.3.2) to determine concentration. DNA was aliquoted and stored at -20°C.

3.2.3 Library preparation and sequencing

Samples were prepared for 16S rRNA amplicon sequencing using the Illumina 16S rRNA metagenomic sequencing library preparation protocol (Section 2.6.1). The 16S rRNA PCR was performed using Invitrogen's Platinum Green Mastermix because it succeeded at amplifying more samples in the dataset than the High Fidelity Polymerases we tested (Section 2.4.1). Briefly, a first-stage PCR was performed using the Illumina recommended FWD (5' TCGTCGGCAGCGTCAGATGTGTATAAGAGACAGCC TACGGGNGGCWGCAG 3') and REV (5' GTCTCGTGGGCTCGGAGATGTGTATA AGAGACAGGACTAC HVGGGTATCTAATCC 3') primers for the V3-V4 region of the 16S rRNA gene. Samples were then amplified on a thermal cycler using the following program: 95ºC for 3 min, 34 cycles of: 95ºC for 30s, 55ºC for 30s and 72ºC for 30s, followed by a final 72ºC step for 5 min. Amplicons were cleaned-up with Ampure® beads at a 1.8x ratio (Section 2.5.1) before a second PCR to add indexes (Appendix Table C-1). The conditions for the second stage PCR were: 95ºC for 3 min, 8 cycles of: 95ºC for 30s, 55ºC for 30s and 72ºC for 30s, followed by a final 72ºC step for 5 min. The second stage PCR products were cleaned up using a 1.8x Ampure® beads ratio, and the sample concentrations were quantified on an EPOCH machine. Finally, cleaned-up indexed amplicons pooled in equimolar concentrations in a solution of 10mM Tris-HCl (pH 8) and 0.1% TWEEN® and sequenced using an Illumina MiSeq® at Aberystwyth University. The sequencing run was done using 2 x 300 bp paired-end sequencing, to sequence the entire ~460bp V3-V4 region with enough overlap to merge samples.

3.2.4 Bioinformatics analysis

3.2.4.1 Removing adapters and quality trimming

Raw reads were demultiplexed on Illumina BaseSpace. Various parameters were tested during quality control to optimise read quality and number. Adapters and primer sequences were removed from raw reads using Cutadapt (version 2.4: https://cutadapt.readthedocs.io/en/v2.4/) (Martin, 2011) using pair-ended trimming to remove linked adapters. The 5' adapter + 16S FWD primer and the reverse complement

of the 16S REV primer + adapter were used to trim forward reads and the 5' adapter + 16S REV primer and reverse complement of the 16S FWD primer and adapter were used to trim the reverse reads. The 3' ends were trimmed using a Phred score of 10 (-q 10) and paired reads in which at least one of the paired reads was shorter than 150bp were removed (-m 150).

3.2.4.2 Taxonomic assignment using DADA2

Reads were assigned to amplicon sequence variants (ASVs) using DADA2 (v. 1.14.0) (Callahan et al., 2016). After checking the QualityProfile plots (Appendix Section C-1), FilterAndTrim() was used to truncate the R1 reads to 270 bp and the R2 reads to 220 bp. Reads that had been trimmed shorter than these lengths by Cutadapt were lost at this stage. The learnErrors() function was run with randomize=TRUE, as samples were ordered by environment type and the error model needed to be based on a range of samples types. The Error Plots can be viewed in Appendix Section C-2. The sample inference was run using pool="pseudo". Pooling allows information to be shared across samples, which makes it easier to resolve rare variants that were seen just once or twice in one sample but many times across samples (https://benjjneb.github.io/dada2/pseudo.html#Pseudo-pooling). Pooling is computationally expensive, therefore "pseudo-pooling" was used. Pseudo-pooling is a two-step process in which independent processing is performed first on the raw data alone, and then on the raw data a second time, informed by priors generated from the first round of processing. The R1 and R2 reads were merged using mergePairs() with the default overlap settings. Chimeras were removed using removeBimeraDenovo(). Thereafter, taxonomic assignment was performed to genus level using training fasta files derived from the Silva Project's version 132 release (Quast et al., 2013).

3.2.4.3 Decontamination

Previous studies have shown that contamination can be a major factor in low biomass samples (de Goffau et al., 2018; Salter et al., 2014). Sources of contamination range from DNA extraction kit reagents, to PCR water, PCR reagents (Iulia et al., 2013) or contaminants introduced by human error. To check for contamination, DNA extraction controls and PCR negative controls were sequenced together with samples and used to infer contamination. Contaminants were identified and removed from the samples using the Decontam (v.1.6.0) package in R (Davis et al., 2018) which takes into account the DNA concentrations of samples because contamination is more likely in low

concentration samples (Details in Appendix Table C-2, Section C-5 and Section C-6). Prior to decontam, the dataset was split into subsets containing all samples of a specific environment type, relevant extraction controls and all the PCR negative controls used in each plate. Data was split because the Decontam package recognises outliers, and sequences in low biomass samples as contaminants. Due to the vast differences in DNA concentration, and community diversity in different environment types, the samples were split to compare like with like. The samples were processed using a prevalence of 0.5 (except for the glacial waters, which also made use of frequency). The frequency parameter was omitted because the dataset contained samples of different environment types, some of which were low biomass. The frequency parameter therefore mistakenly excludes real taxa.

3.2.5 Statistical analysis and plotting of 16S rRNA abundance data

The 16S rRNA abundance data was filtered and analysed and using Phyloseq (V. 1.30.0) (McMurdie and Holmes, 2013) in R (R-3.6.1), available at (https://github.com/joey711/phyloseq). Rarefaction was avoided as far as possible to avoid the loss of information or the loss of samples (McMurdie and Holmes, 2014). To account for library size differences, the abundance values were converted to relative abundance (RA) wherever doing so was justified. Occasionally filtering steps were required to see trends in abundant taxa. Wherever filtering steps were applied, the relative effect of the filtering step on library size is recorded. For measures of alpha diversity, the unrarefied and rarefied data is compared. Common taxa shared between environment types were plotted using UpSetR (Conway et al., 2017; Lex et al., 2014) available at (https://github.com/hms-dbmi/UpSetR). Taxa belonging to each environment were considered sets, and intersections between sets reflect shared taxa between groups.

3.2.6 Co-occurrence network analysis

Co-occurrence network analysis was performed using modified R and Python scripts as described in (Hu et al., 2017; Ju et al., 2014; Ju and Zhang, 2015) and available at https://github.com/RichieJu520/Co-occurrence_Network_Analysis. Networks were visualised in Gephi 0.9.2 (https://gephi.org/) (Bastian et al., 2009; Jacomy et al., 2014) using Java V8 (build 1.8.0_241-b07).

3.3 Results

3.3.1 Sequencing results

There were 12,957,386 paired reads sequenced by the MiSeq run. However, 1 629 793 paired reads from the Illumina MiSeq run could not be demultiplexed and assigned to a sample. This represents a significant fraction of the dataset (12.6%) and analysis of the undetermined reads shows these reads either contained unexpected index combinations (evidence of index-switching) or belonged to the PhiX Control. There was a large variation in the library size of different samples (Appendix Section C-3), and potential explanatory factors such as extraction method (Appendix Section C 4-1), environment (Appendix Section C 4-2), extraction batch (Appendix Section C 4-3) and PCR plate, column and row (Appendix Section C 4-4) were explored.

3.3.2 Taxonomic assignment

Prior to decontamination there were 59 135 unique sequence variants detected by DADA2 in 138 samples made up of 116 environmental samples and 22 controls.

3.3.1 Decontamination

One of the main aims of this study was to investigate the extremely rare specialist community. We therefore wanted to retain low abundance ASVs, while removing true contaminants. Simply removing ASVs that occur in negative controls from the dataset risks removing true ASVs because high abundance members of adjacent samples are the most likely source of contamination, and some of the species likely to contaminate laboratory reagents (kitome) are similar to those found in the highly oligotrophic snow, slush and meltwater environments (oligotrophic, stored in the fridge or freezer) (Edwards et al., 2020; Salter et al., 2014). Decontam identifies contaminants based on their prevalence in samples vs negative controls, and/or by their higher frequency in samples with low starting concentrations, such as low biomass samples, which are more likely to be contaminated (Davis et al., 2018).

The snow, slush and meltwater samples were especially tricky to decontaminate because they were both low biomass and most likely to be contaminated by kitome contaminants, but also the environment most likely to legitimately contain common kitome species. To address this concern, the snow, slush, and meltwater samples were combined into a subset (glacial waters) and decontaminated using the combined method, (threshold = 0,5) which

considers both prevalence and frequency. This means that ASVs were considered contaminants if they occurred in the lower concentration samples and were more prevalent in controls. The remaining environmental samples were higher biomass and far less likely to contain kitome contaminants and were therefore decontaminated using the prevalence method, with a threshold of 0.5, which identifies ASVs present in a higher proportion of negative controls than samples. The two air samples were removed due to high contamination levels, and one snow sample (SN31) was removed because it has 0 reads. After decontamination, there were 58 880 true ASVs remaining in 113 samples.

3.3.1.1 Snow, slush, and meltwater decontamination

Of 1511 ASVs in the snow (n=8), slush (n=9) and meltwater (n=9) samples, 78 were identified as contaminants using the combined method (threshold = 0.5) of the Decontam tool. The mean proportion of reads kept after the removal of the identified contaminant ASVs was close to 88% (n =26, mean = 0.8784, SD = 0.2245, median= 0.9797) in the samples, and close to 21% (n =15, mean =0.2130, SD = 0.3339, median = 0.0574) in the negative controls. There was a greater reduction of reads in the snow samples (mean = 0.6476), which had lower starting DNA concentrations and smaller library sizes than the slush (0.9807) and meltwater (0.9813) libraries.

3.3.1.2 Cryoconite decontamination

Of 12 697 ASVs in the combined cryoconite samples, 57 were identified as contaminants using the prevalence method (threshold = 0.5) of the decontam tool. The mean proportion of reads kept after the removal of the indentified contaminant ASVs was close to 100% (n =30, mean = 1.0000, SD = 0.0001, median= 1.0000) in the cryoconite samples, and close to 27% (n =15, mean = 0.2723, SD = 0.3289, median = 0.1225) in the negative controls.

Table 3-1 Table of contaminants and true ASVs in environmental subsets

Subsets		Samples and controls			Number of ASVs				Decontam				Final Dataset	
Environment type	**Controls**	**No of samples**	**No. of controls**	**Combined**	**Sample ASVs**	**Control ASVs**	**Combined ASVs**	**Shared ASVs**	**Method**	**Threshold**	**Contaminant ASVs**	**True ASVs**	**True ASVs in samples**	**Difference**
Glacial waters (snow, slush, and meltwater)	[1] [3]	26	15	41	1323	272	1511	84	Comb	0.5	78	1433	**1245**	78
Proglacial - ML	[1] [3]	3	15	18	2593	272	2846	19	Prev	0.5	64	2782	**2587**	6
Proglacial - VB	[1] [3]	3	15	18	3163	272	3395	40	Prev	0.5	57	3338	**3150**	13
Seawater	[1] [3]	6	15	21	1658	272	1920	10	Prev	0.5	67	1853	**1657**	1
Soil	[1] [2]	45	15	60	40122	226	40257	91	Prev	0.5	88	40169	**40045**	77
Cryoconite	[1] [2]	30	15	45	12483	226	12697	12	Prev	0.5	57	12622	**12478**	5

Subset: the dataset was divided into subsets for decontamination. Several combinations were tested.
Controls: [1] PCR negative controls (n=8), [2] Fast DNA extraction controls (n=7), [3] Sterivex DNA extraction controls (n=7).
Combined ASVs: ASVs in the combined subset. Combined ASVs is less than the sum of the ASVs in samples and controls because several ASVs occur in both the samples and controls.
Shared ASVs: The number of ASVs that are present in both samples and controls.
Method: The method used in the Decontam tool. Prev: uses ASV prevalence in samples and controls to distinguish contaminants. Comb: combined method uses prevalence and frequency. Frequency takes account of the starting concentration of samples in which ASVs are detected because low concentration samples are more likely to contain contaminants.
True ASVs in samples: The number of ASVs in the decontaminated dataset (minus the controls).
Difference: The number of ASVs that have been removed from the subset [Sample ASVs -True ASVs in samples].

3.3.1.3 Proglacial water decontamination

The proglacial water samples from VB and ML were decontaminated together and separately to test the effect of combined and separate decontamination. When combining samples, 21 ASVs were removed, whereas separate decontamination resulted in the removal of 6 and 13 ASVs from ML and VB, respectively. Samples from each glacier were therefore decontaminated separately. Of 2864 ASVs in the ML proglacial water samples (n=3), 64 were identified as contaminants using the prevalence method (threshold = 0.5) of the Decontam tool. Of 3395 ASVs in the VB proglacial water samples (n=3), 57 were identified as contaminants using the prevalence method (threshold = 0.5) of the Decontam tool. The mean proportion of reads kept after the removal of the identified contaminant ASVs was close to 100% (n =6, mean = 0.9983, SD = 0.0016, median = 0.9983) in the proglacial water samples, and approximately 20% (n =15, mean = 0.2036, SD = 0.3384, median = 0.0513) in the negative controls.

3.3.1.4 Soil decontamination

Of 40257 ASVs in the combined forefield soil samples, 88 were identified as contaminants using the prevalence method (threshold = 0.5) of the Decontam tool. The mean proportion of reads kept after the removal of the identified contaminant ASVs was close to 91% (n =45, mean = 0.9096, SD = 0.2410, median = 0.9989) in the soil samples, and approximately 12% (n =15, mean = 0.1247, SD = 0.1873, median = 0.0292) in the negative controls. Notably, the largest proportional drop in reads occurred in the Soil-0 samples (n=9), collected closest to the glacier snout, which had the lowest starting DNA concentrations and were most likely to suffer contamination.

3.3.1.5 Seawater decontamination

Of 1920 ASVs in the seawater samples, 67 were identified as contaminants using the prevalence method (threshold = 0.5) of the decontam tool. The mean proportion of reads kept after the removal of the identified contaminant ASVs was 100% (n =6, mean = 1.00, SD = 0.00, median = 1.00) in the seawater samples, and approximately 16.25% (n =15, mean = 0.1625, SD =0.2606, median =0.0513) in the negative controls. Interestingly, only one of the identified contaminants was present in any seawater samples.

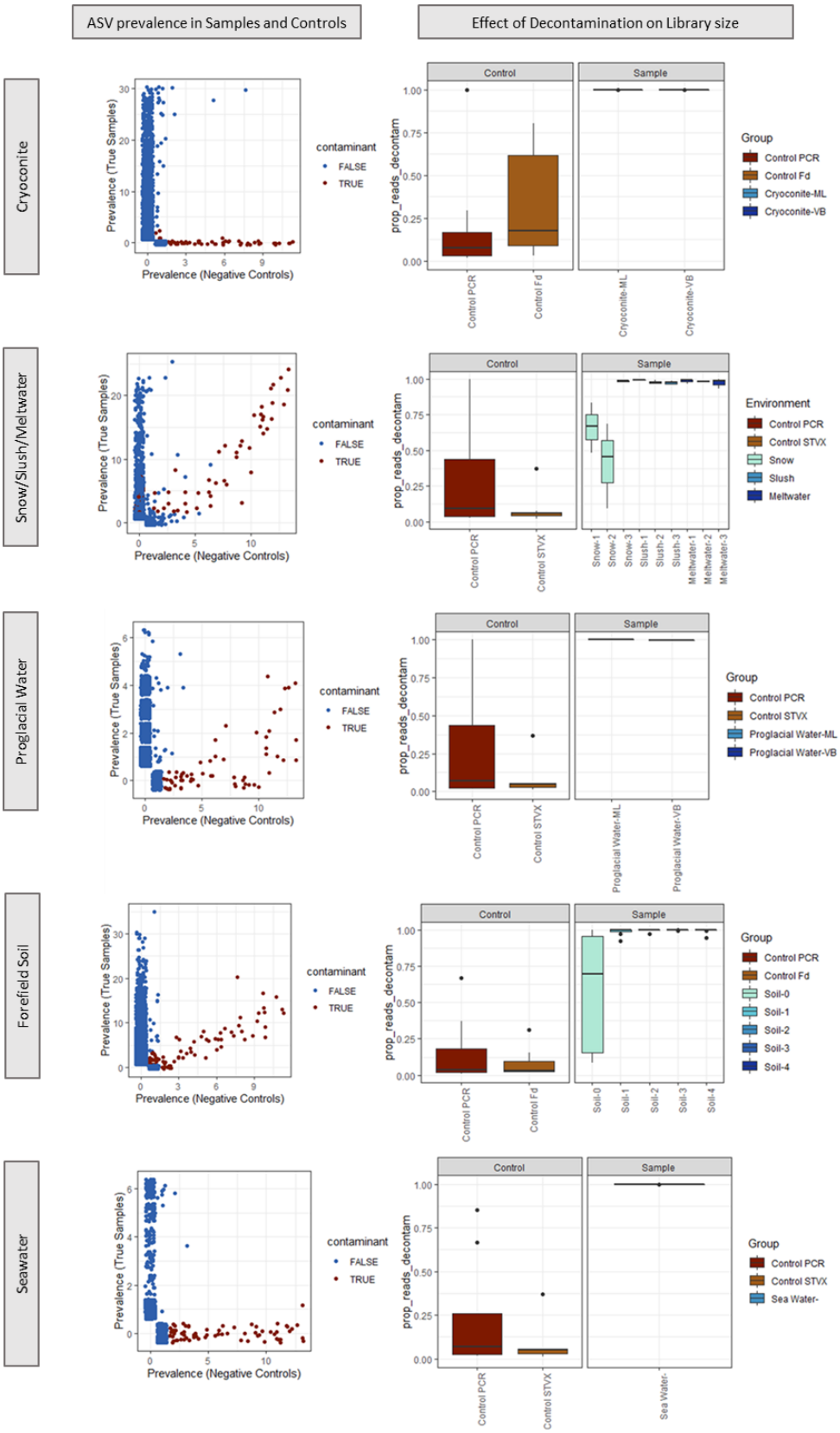

Figure 3-2 Decontamination of the Svalbard dataset. ASVs coloured red are contaminants due to their high prevalence in negative controls, and low prevalence in environmental samples. Blue points are true ASVs, detected in a high proportion of samples, and in a low proportion of the negative controls. Boxplots showing the proportion of reads remaining in samples vs controls after decontamination.

3.3.1 Phylogenetic diversity of different environments

Diversity was investigated in terms of both species richness, and in terms of the phylogenetic distance of the species in the communities. Across all cryospheric habitats, there were ASVs from 37 phyla, 137 classes, 315 orders, 549 families and 1221 genera (Figure 3-3). Phyla describe the most phylogenetically distant groups, therefore the greater the number of phyla the more diverse the community in an environment. Proglacial water contained the most phyla (combined=37, ML=33, VB=32), which is possible because it represents a 'meeting point' of supraglacial, subglacial and soil communities. The soil community was also extremely diverse, with an increase in diversity from recently deglaciated soil (Soil-0) to more developed soils (Soil 1-4). Soil also contained the most diversity at the genus level. The cryoconite from VB and ML are similar in composition, although VB did contain ASVs belonging to a greater number of groups across all taxonomic ranks. Cryoconite was dominated by Cyanobacteria, with Actinobacteria, Chloroflexi, Proteobacteria and WPS-2 making up less abundant members of the community. The supraglacial snow, slush and meltwater communities had the fewest phyla (combined = 21, snow=19, slush = 17, meltwater = 19). The Proteobacteria were the most abundant phylum in snow, slush, and meltwater, with Cyanobacteria, Bacteroidetes, Actinobacteria and Acidobacteria making up less abundant community members. The seawater bacterial community was the least diverse, containing mainly Proteobacteria, Bacteroidetes and Cyanobacteria, with a total of 11 phyla and 15 classes represented.

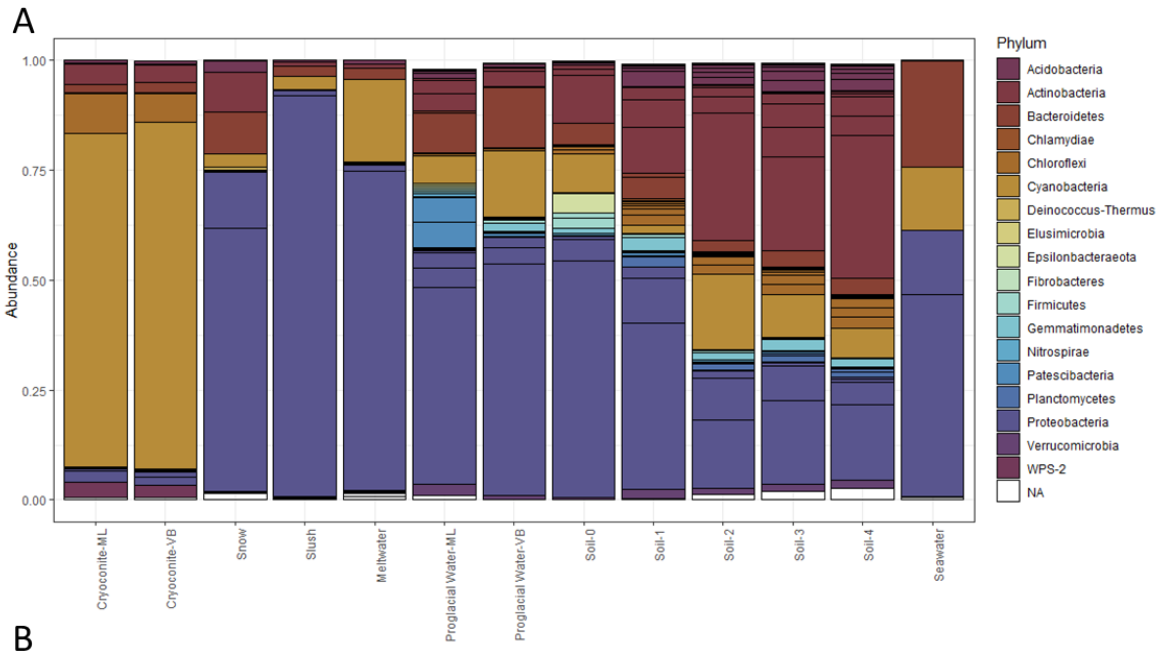

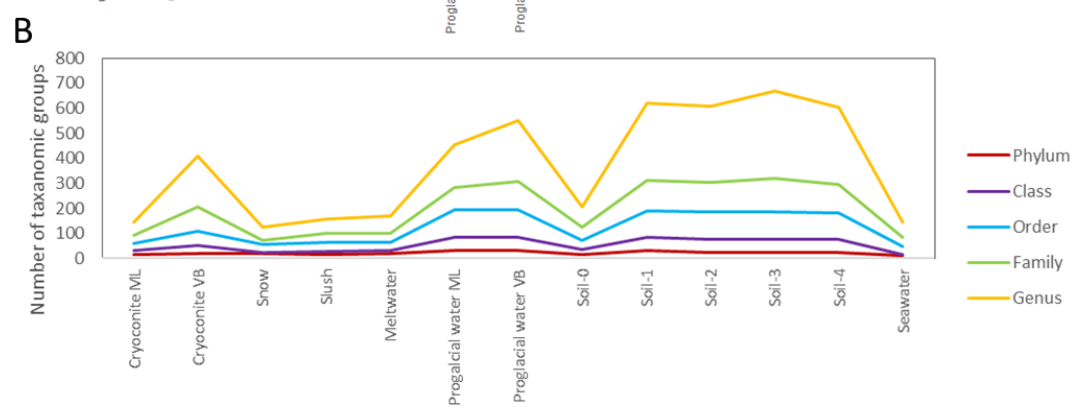

C

	Cryoconite ML	Cryoconite VB	Snow	Slush	Meltwater	Progalcial water ML	Proglacial water VB	Soil-0	Soil-1	Soil-2	Soil-3	Soil-4	Seawater
Phylum	16	21	19	17	19	33	32	17	31	25	24	25	11
Class	32	50	25	29	31	83	84	37	86	77	77	75	15
Order	62	108	54	65	65	192	196	71	191	184	186	180	49
Family	91	205	72	101	99	285	308	124	312	303	318	297	85
Genus	144	409	126	159	169	455	552	207	619	609	668	602	147

	Cryoconite-ALL	Glacial water	Proglacial -ALL	Soil-ALL	sea-ALL	Combined
Phylum	21	21	37	32	11	37
Class	50	39	103	100	15	117
Order	110	91	239	256	49	315
Family	207	149	369	433	85	549
Genus	414	254	658	934	147	1221

Figure 3-3 The phylogenetic diversity of different environment types in Svalbard. A) Bar plot showing the RA of phyla in the different environments. Samples were merged by environment, and ASVs were agglomerated to Class level and only the top 50 classes are shown. Colours represent the different phyla. The thin horizontal lines represent different classes within each phylum. RA does not equal 1, because only the top 50 of 117 classes are plotted. **B)** Line graph showing the number of phyla, classes, orders, families, and genera in each environment type. **C)** Table of phyla, classes, order, families, and genera across different environments, and also showing the totals for the combined soil (soil-0, soil-1, soil-2, soil3 and soil4), glacial waters (snow, slush and meltwater), and the merged proglacial and cryoconite samples from ML and VB.

3.3.1.1 Alpha Diversity

Alpha diversity (species richness) was determined by counts of the number of observed species, Shannon Index (H) and Simpson's Diversity index (D). These measures were applied to decontaminated, but unfiltered data (ASVs = 58880) (Figure 3-4 **A**), to data that had been filtered to remove ASVs not present in at least three samples (ASVs = 3647) (Figure 3-4 **B**) and to rarefied data (reads=3483, ASVs=27643, samples = 95) (Figure 3-4 **C**).

The use of rarefaction in microbiome analysis is growing increasingly controversial (McMurdie and Holmes, 2014), and since the focus of this study is on the rare microbiome, a rarefaction step would almost certainly obscure the very patterns we are trying to identify (Bay et al., 2020). However, the effect of library size/sampling depth is a serious confounding factor because large libraries are likely to have more ASVs than small libraries. In this study, we chose to use the unfiltered dataset because we had already observed that libraries of the lowest number of reads (Soil) had the highest diversity of ASVs (Appendix Section C-7). Therefore, skipping the rarefying skip was unlikely to introduce a confounding factor for species richness, except maybe to underestimate diversity in soil. The significant drop in number of observed species in the filtered data reflects the heterogeneity of the environment, particularly evident in soil. Rarefying to 3483 reads resulted in the loss of 18 samples, and 53% of the ASVs.

Diversity indexes were used to understand species richness in these samples, but also to understand whether sampling depth adequately captured representative diversity. Simpson's Diversity Index (D) was selected as a diversity measure because it considers species richness, as well as the RA of each species. As species richness and evenness increase, so diversity increases. The value of D is close to 1 (representing infinite diversity) for almost all environment types, except for cryoconite (Cryoconite-ML, $D=0.663 \pm 0.043$, Cryoconite-VB, $D=0.663 \pm 0.145$) and Meltwater ($D=0.881 \pm 0.030$). The high D values suggest that sampling depth failed to capture true diversity. The cryoconite samples on the other hand (except for cryoconite from a specific site on VB) had D values close to 0.6, due to the dominance of this environment type by a single species (low evenness).

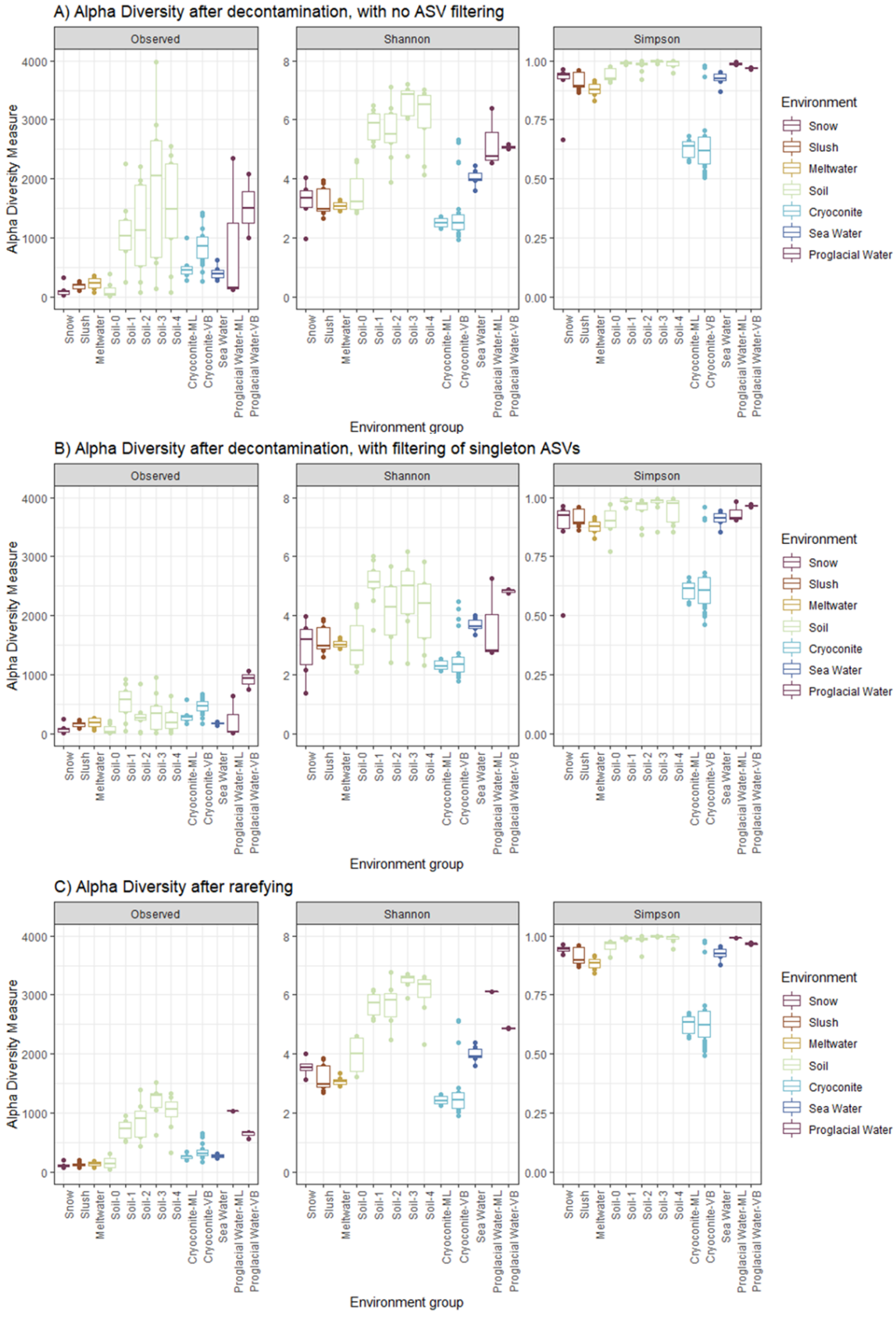

Figure 3-4 Alpha Diversity of environment groups from Svalbard cryospheric environments. See details in Table 3-2.

Table 3-2 Table of alpha diversity measure for different environment groups

	Observed		Shannon		Simpson (D)		
X12_group	Mean	Sd	Mean	Sd	Mean	Sd	n
Cryoconite-ML	270.33	50.55	2.483	0.153	0.633	0.043	6
Cryoconite-VB	360.58	118.99	2.765	0.960	0.663	0.145	24
Meltwater	142.50	44.85	3.075	0.128	0.881	0.030	8
Proglacial Water-ML	1009.00	NA	6.036	NA	0.992	NA	1
Proglacial Water-VB	651.67	68.09	4.932	0.045	0.969	0.003	3
Sea Water	277.50	34.52	3.990	0.280	0.922	0.029	6
Slush	129.44	35.11	3.181	0.476	0.909	0.037	9
Snow	125.75	59.82	3.580	0.386	0.943	0.020	4
Soil-0	162.00	112.98	3.952	0.712	0.954	0.031	4
Soil-1	720.88	175.00	5.659	0.426	0.990	0.006	8
Soil-2	877.57	346.07	5.725	0.717	0.980	0.025	7
Soil-3	1181.00	272.54	6.481	0.244	0.996	0.001	7
Soil-4	1001.38	328.09	6.037	0.754	0.987	0.016	8

NA: There were only 3 Proglacial Water-ML samples to start with. After rarefying, there were not enough samples to calculate mean and sd.

3.3.1.2 Beta Diversity

Beta diversity refers to the ratio between local or alpha diversity and regional diversity. This is the diversity of species between two habitats or regions. Similar patterns of beta diversity were observed using a range of distance measures (Appendix Figure C-23). Beta diversity is shown using MDS ordination of Bray Curtis distance (Figure 3-5). The seawater samples cluster closely together in the centre of the plot, having no overlap with any other environment types and being equally different to all other environment types. There are three main branches on the plot: cryoconite, soil and a cluster of snow, slush, and meltwater. Cryoconite almost always forms a tight cluster, whereas soil forms a long gradient. Most of the snow, slush and meltwater samples cannot be distinguished from each other and form a cluster together. Habitat type is more important, than glacial origin for explaining distance, which can be seen in the clustering of proglacial water from VB and ML clustering together, and cryoconite from VB and VL clustering together.

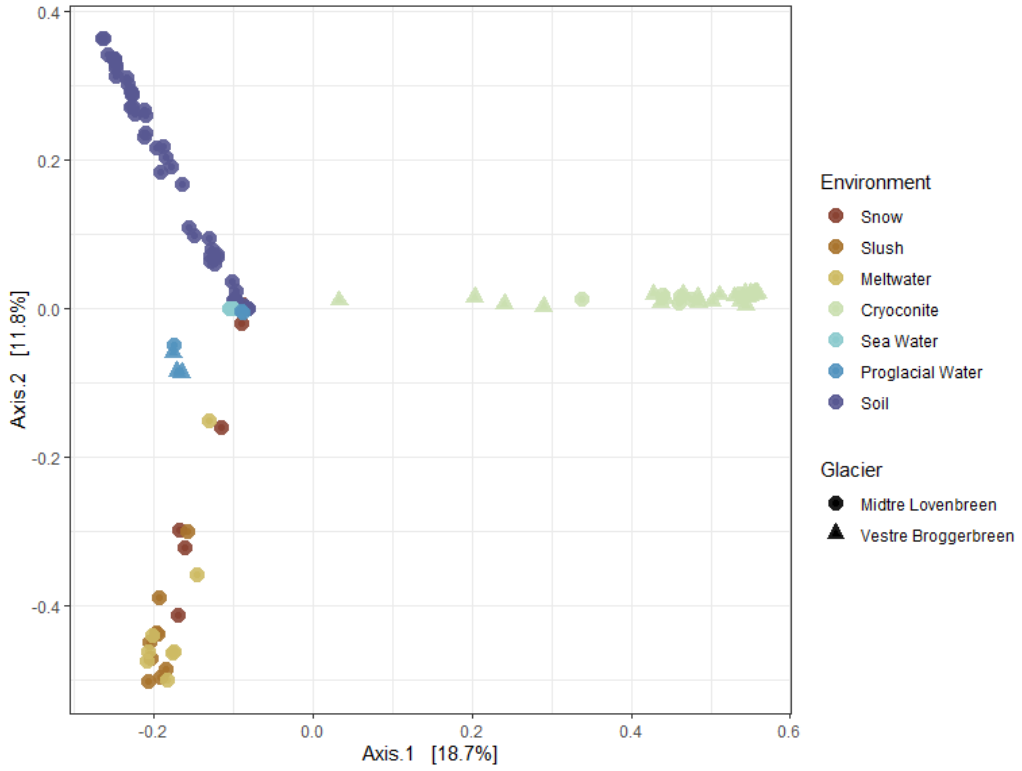

Figure 3-5 MDS Ordination showing Beta Diversity using Bray Curtis distance.

3.3.2 Community composition by environment

3.3.2.1 Cryoconite

Cryoconite was collected from VB (n=24) and ML (n=6) glaciers. In addition, the samples from VB were collected from both open (n=6) and closed (n=6) cryoconite holes. After decontamination, there were 12 478 unique ASVs in cryoconite samples. Technical replicates (ACVBO3-1 and ACVB03-2) from one of the VB open cryoconite holes (ACVB03) was particularly abundant in rare taxa. This species richness is not a consequence of differences in library size (Appendix Figure C-22**).** To detect large scale trends in community structure, and identify keystone taxa, the cryoconite samples were filtered to include on those ASV with more than 20 reads in at least 6 (>20%) or more of the samples. After filtering, 350 ASVs were retained in the dataset. Filtering out rare taxa reduced the dataset to just 2.8% of the original ASV diversity, and reduced the mean library size to 0.949 ± 0.006 for ML and 0.8819004 ± 0.157291348 for VB (Figure 3-6 **A)**. This suggest that about 10% of the cryoconite community consist of rare taxa.

The ASVs in the filtered dataset was agglomerated at the genus level to identify the most abundant genera (Figure 3-6). The most common genera by far was *Phormidesmis_ANT.L52.6* which had a mean RA of 79.89% across the cryoconite samples.

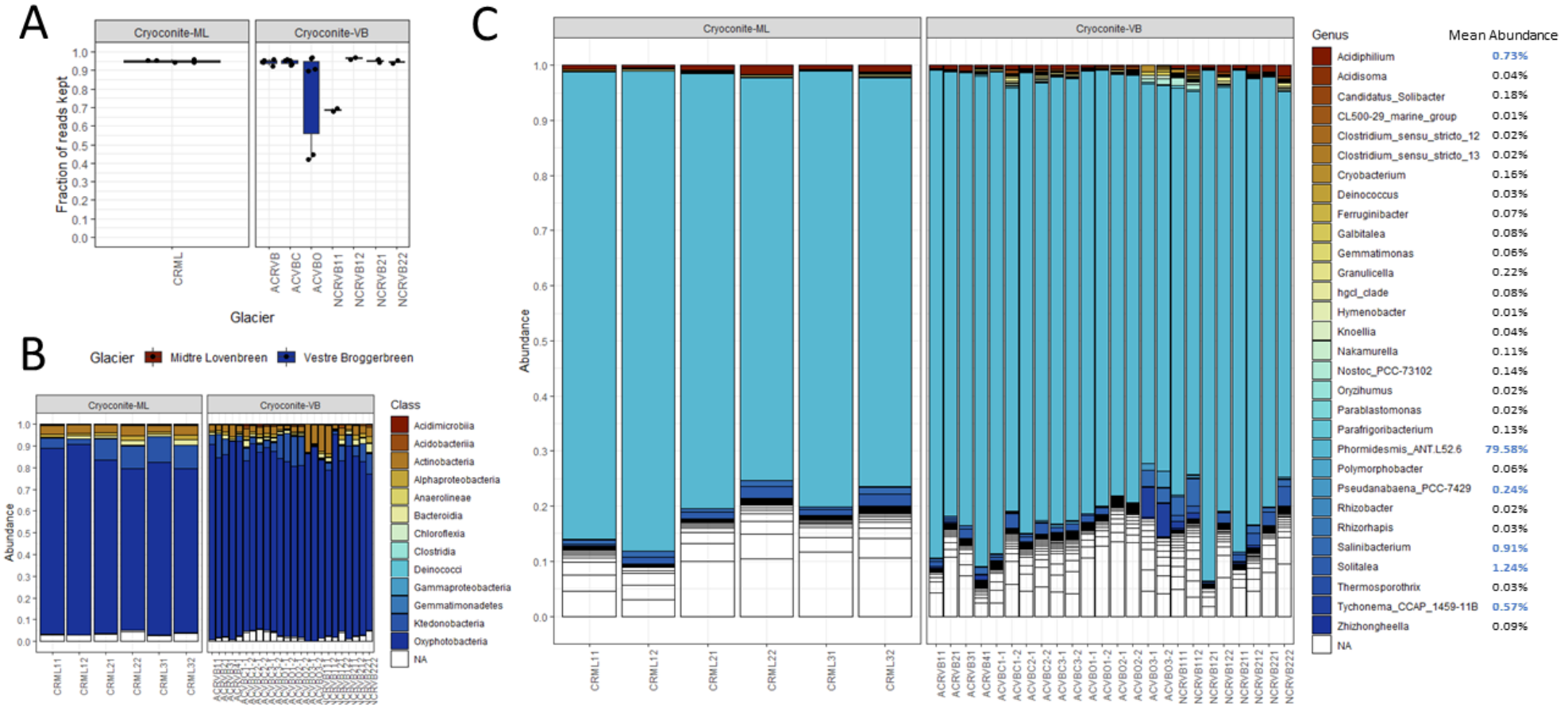

Figure 3-6 Relative abundance of the most abundant taxa in cryoconite samples from Midtre Lovénbreen and Vestre Brøggerbreen. (A) Proportion of reads remaining after filtering out ASVs with less than (x > 20) in at least 6 samples. **(B)** Relative abundance of filtered samples by class. **(C)** Relative abundance of filtered samples by Genus.

Other abundant genera were *Solitalea* (1.21%), *Salinibacterium* (0.93%), *Acidiphilium* (0.72%) *Tychonema*_CCAP_1459-11B (0.59%), *Pseudanabaena*_PCC-7429 (0.25%) and *Granulicella* (0.22%). However, 15.04% of the ASVs were unassigned at the genus level. At the class level, Ktednobacteria, Actinobacteria, Alphaproteobacteria and Bacteroidia were common. Finally, the cryoconite keystone taxa was analysed at the highest resolution by looking at the abundance and prevalence of particular ASVs across all cryoconite samples (Figure 3-7). There were 64 ASVs in the filtered cryoconite dataset of 350 ASVs that were present in 90% of samples. (Appendix Table C-12).

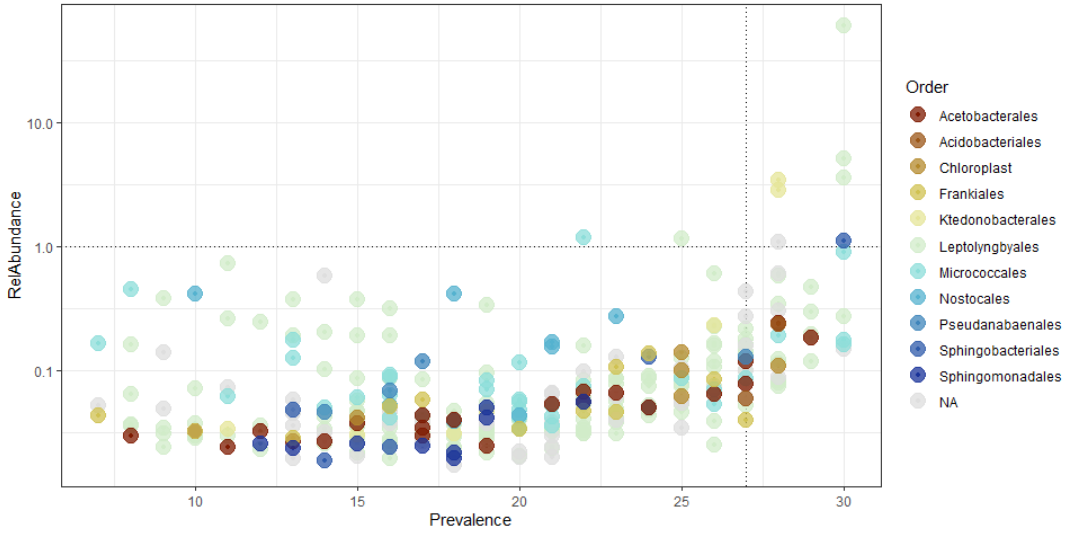

Figure 3-7 Scatter plot of the most prevalent and abundant ASVs in cryoconite, by Order. X-axis is the prevalence of each ASV (number of samples in which each ASV occurs). Y-axis is $\log_{10}$ of the mean RA of the ASVs across all samples in the cryoconite dataset. Points are coloured by Order.

A single ASV, (ASV1) was present across all 30 of the samples belonged to the genus *Phormidesmis_ANT.L52.6* at a mean RA of 59.98%. There were two additional *Phormidesmis_ANT.L52.6* ASVs that were present in all samples at a mean RA of more than 3% (ASV9 (5.142%) and ASV 13 (3.584%)). Other highly prevalent and abundant ASVs include ASV27 (1.094%), genus *Solitalea* and ASV40 (0.900) belonging to the family Microbacteriaceae. We also identified several ASVs that highly abundant members of the community at a specific site (Appendix Table C-13). Examples include ASVs from the order Nostocales (ASV319 and ASV539) were detected only in VB cryoconite, and were not found in ML cryoconite.

3.3.2.2 Glacial waters

Three biological replicates of snow, slush, and meltwater were collected from ML on three separate days during the summer melt season. After decontamination, there were

1245 unique ASVs in supraglacial (snow, slush, and meltwater) samples. To detect large-scale trends in community structure, the samples were filtered to include ASVs with more than 10 copies in 5 or more (>19%) of the samples. After filtering, 231 ASVs were retained in the dataset. The effect of filtering on library size is shown in Figure 3-8 A.

After initial data analysis, snow, slush and meltwater collected on the same day resembled each other more closely than samples of the same environment collected over the three days, suggesting that temporal changes had a greater influence than environment type (Figure 3.8). A high abundance of *Pseudomonas* in slush and meltwater on day one, decreases dramatically on day two and three, concomitant with an increase in *Polaromonas*. *Glaciimonas* is present in low abundance on day one but increases in abundance on day two and three in snow, slush, and meltwater samples. The most common genus was *Actimicrobium* which had a mean RA of 34.51% across the snow, slush and meltwater samples and is present in all environments across all three sampling days. Other abundant genera were *Massilia* (19.73%), *Polaromonas* (13.19%), *Pseudomonas* (5.43%) *Glaciimonas* (2.37%), *Acidiphilium* (1.87%) and *Acinetobacter* (1.63%). However, 9.87% of the ASVs were unassigned at the genus level.

The most prevalent ASVs in snow, slush and meltwater were tabulated and their presence and absence patters were examined taking into account the type of environment (snow, slush and meltwater) and the day of collection during melt (day 1, 2, 3) (Appendix Table C-14). There was a single highly abundant ASV belonging to the genus *Actimicrobium* (ASV2) that was present in 25 of the 27 samples at a mean RA of 26.01%. Several other *Actimicrobium* ASVs (ASV137, ASV25, ASV133, ASV49, ASV28 and ASV73) were present in more than 20 of the samples at mean abundances that ranged from 0.32% to 2.31%. The second most abundant ASV (ASV3) belongs to *Polaromonas* and was present in 23 of the samples at a mean RA of 8.94%. Other *Polaromonas* ASVs present in more than 20 samples include ASV11 and ASV31, present at 3.52% and 1.24% respectively. There were five highly abundant and prevalent *Massilia* ASVs (ASV4, ASV6, ASV24, ASV29, ASV34) present in more than 21 samples with mean RAs ranging from 1.64% - 8.58%. Other notably prevalent and abundant ASVs belong to *Glaciimonas* (ASV16), *Rhodoferax* (ASV37), *Rhodanbacter* (ASV64) and several ASVs from the family

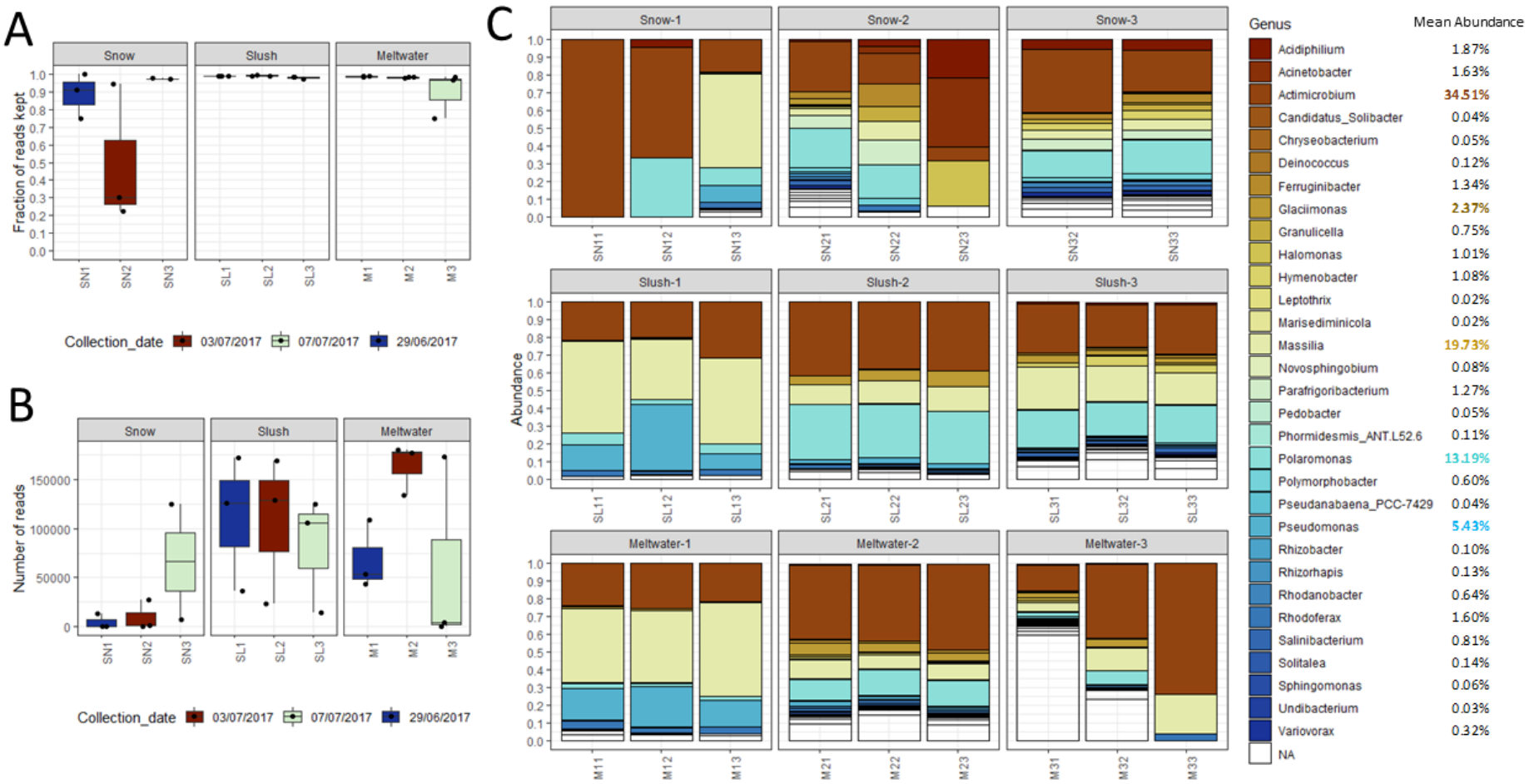

Figure 3-8 Relative abundance of the most abundant taxa in snow, slush and meltwater samples from Midtre Lovénbreen (A) Proportion of reads remaining after filtering out ASVs without at least 10 reads in 5 or more samples. **(B)** Boxplot of number of reads in included libraries. **(C)** Relative abundance of filtered samples by Genus.

Burkholderiaceae (ASV21, ASV41). ASV7, belonging to the order Chloroplast was present at 3.65% in 20 of the samples, and is likely an algae species. Of note, there is a Burkholderiaceae ASV (ASV159) that is present in just 1/9 of the snow samples, but in 9/9 and 6/9 of the slush and meltwater samples, respectively.

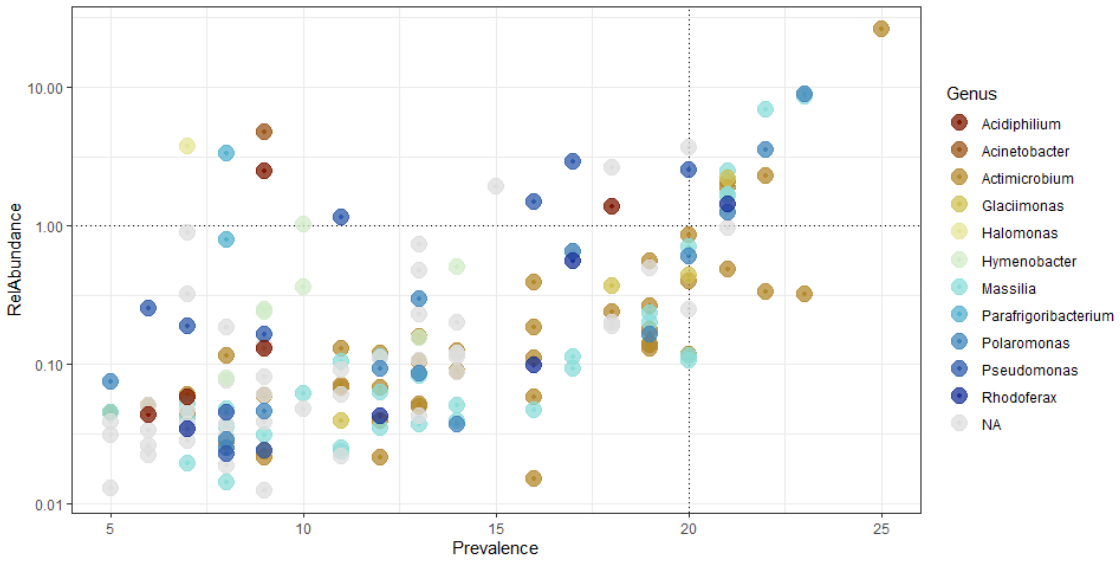

Figure 3-9 Scatter plot of the most prevalent and abundant ASVs in supraglacial habitats) snow, slush and meltwater, by Genus. X-axis is the prevalence of each ASV (number of samples in which each ASV occurs). Y-axis is $\log_{10}$ of the mean relative abundance of the ASVs across all samples in the glacial water (snow, slush, meltwater) dataset. Points are coloured by Genus.

3.3.2.3 Proglacial water

Proglacial water was collected from both ML on day two of the snow, slush, meltwater collection (n=3) and from VB (n=3). After decontamination, there were 5224 ASVs remaining in the proglacial samples. The libraries from samples collected from VB were significantly larger than those collected from ML. Both PM2 and PM3 were less than 1000 sequences before filtering. Therefore the number of reads required in each library was reduced to a minumum of 4 reads in two or more libraries. After filtering the dataset to include only ASVs with four or more copies in two or more samples, there were 945 ASVs remaing in the dataset. The effect of filtering on library size was much more significant in the ML samples than in the VB samples.

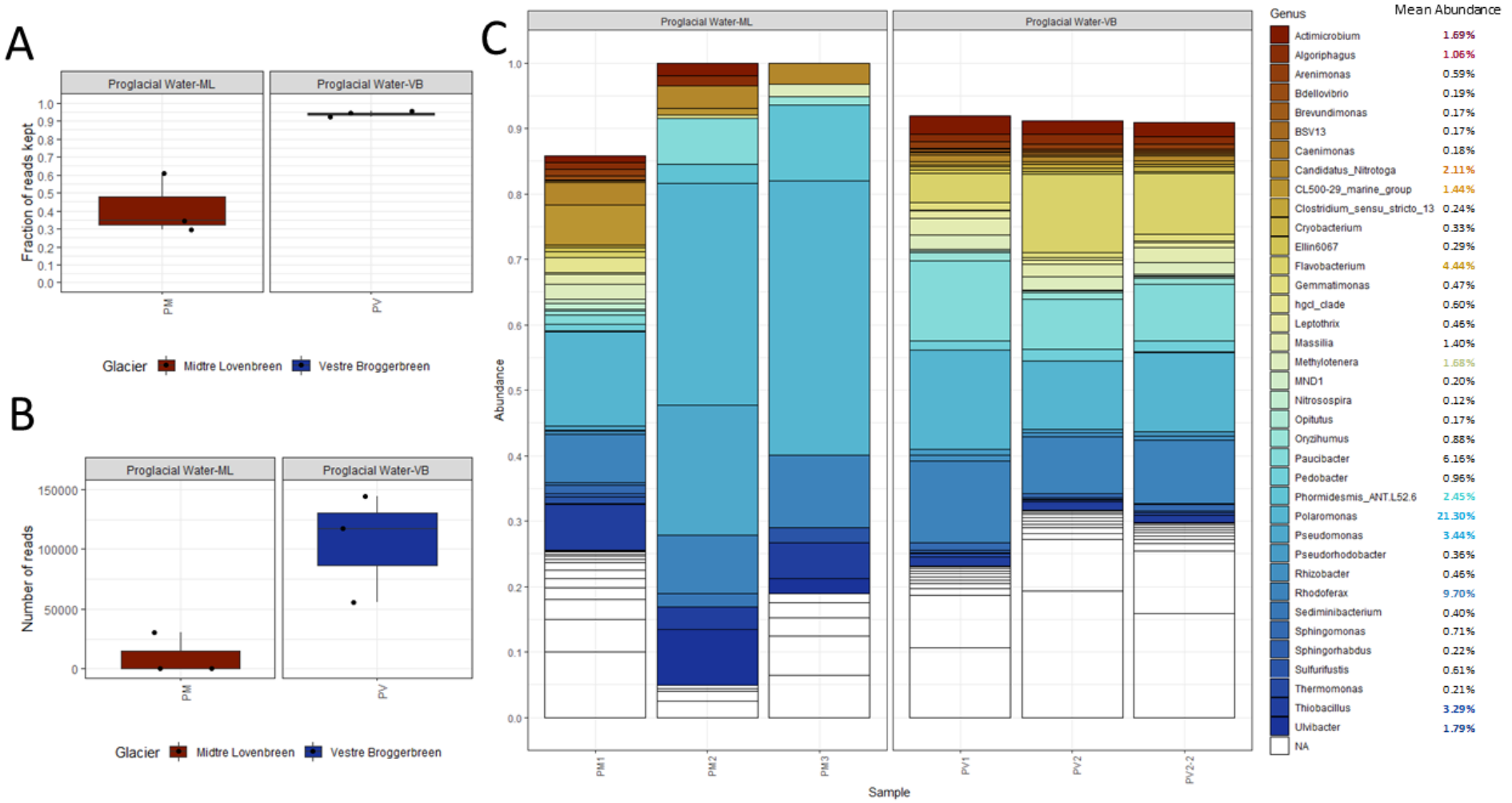

Figure 3-10 Relative abundance of bacterial genera in proglacial water from Midtre Lovénbreen and Vestre Brøggerbreen. (A) Proportion of reads remaining after filtering out ASVs without at least 4 reads in 2 or more samples. **(B)** Boxplot of number of reads in included libraries. **(C)** Relative abundance of filtered samples by Genus.

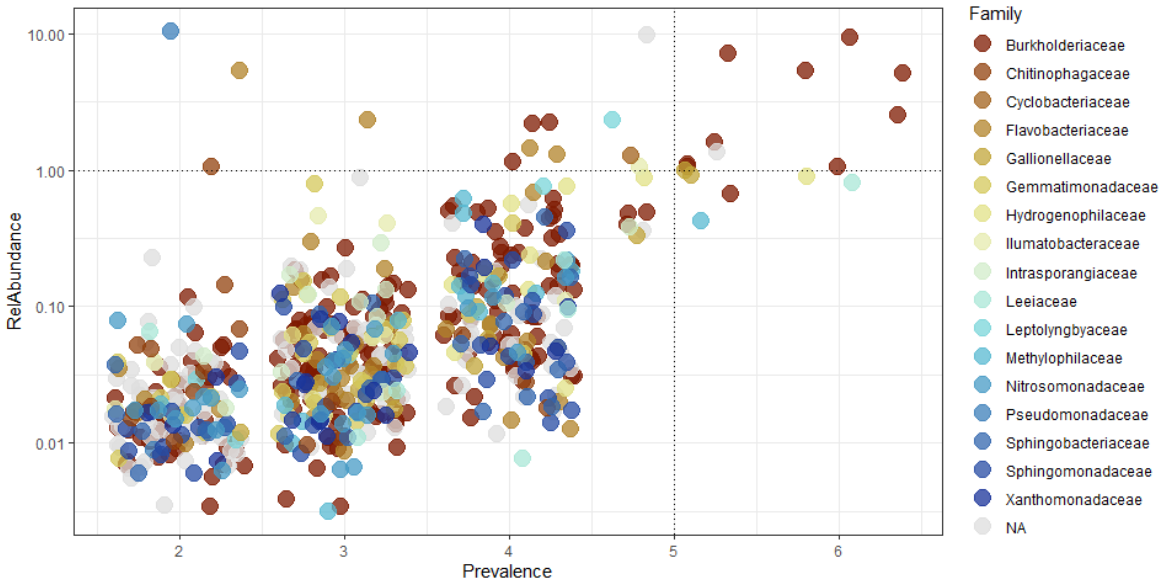

Figure 3-11 Scatter plot of the most prevalent and abundant ASVs in proglacial water by Family. X-axis is the prevalence of each ASV (number of samples in which each ASV occurs). Y-axis is log10 of the mean relative abundance of the ASVs across all samples in proglacial water. Points are coloured by Family.

In the proglacial samples, there is evidence of ASV sharing between environments. The highly abundant *Polaromonas* ASV (ASV11) from snow, slush and meltwater is the most abundant ASV in proglacial water, occurring in all six samples at a mean RA of 9.29% (Appendix Table C-15). Five of the proglacial water samples also contained the *Phormidesmis_ANT.L52.6 ASV* (ASV1) at a mean RA of 2.33%. In addition, there were several highly prevalent ASVs belonging to the genus *Candidatus_Nitrotoga* (ASV219, ASV395, ASV1026) and *Thiobacillus* (ASV26, ASV2425) that hint at a subglacial community input. There were also some site-specific ASVs that occurred in high abundance at a specific site. Although ML had smaller library sizes than VB, there we several ASVs at relatively high abundance in ML samples only, such as *Pseudomonas* (ASV17, 10.31%), *Ulvibacter* (ASV86, 5.38%) and *Sediminibacterium* (ASV5130, 1.05%) (Appendix Table C-16).

3.3.2.4 Soil

After decontamination, there were 40045 ASVs remaining in the forefield soil samples. This enormous species richness is despite relatively small library sizes compared to other environment types (Appendix Figure C-22 and Figure 3-4). To detect large-scale trends in community structure, the samples were filtered to include ASVs with more than 10 reads in three or more of the samples. After filtering, only 1281 ASVs were retained in the dataset.

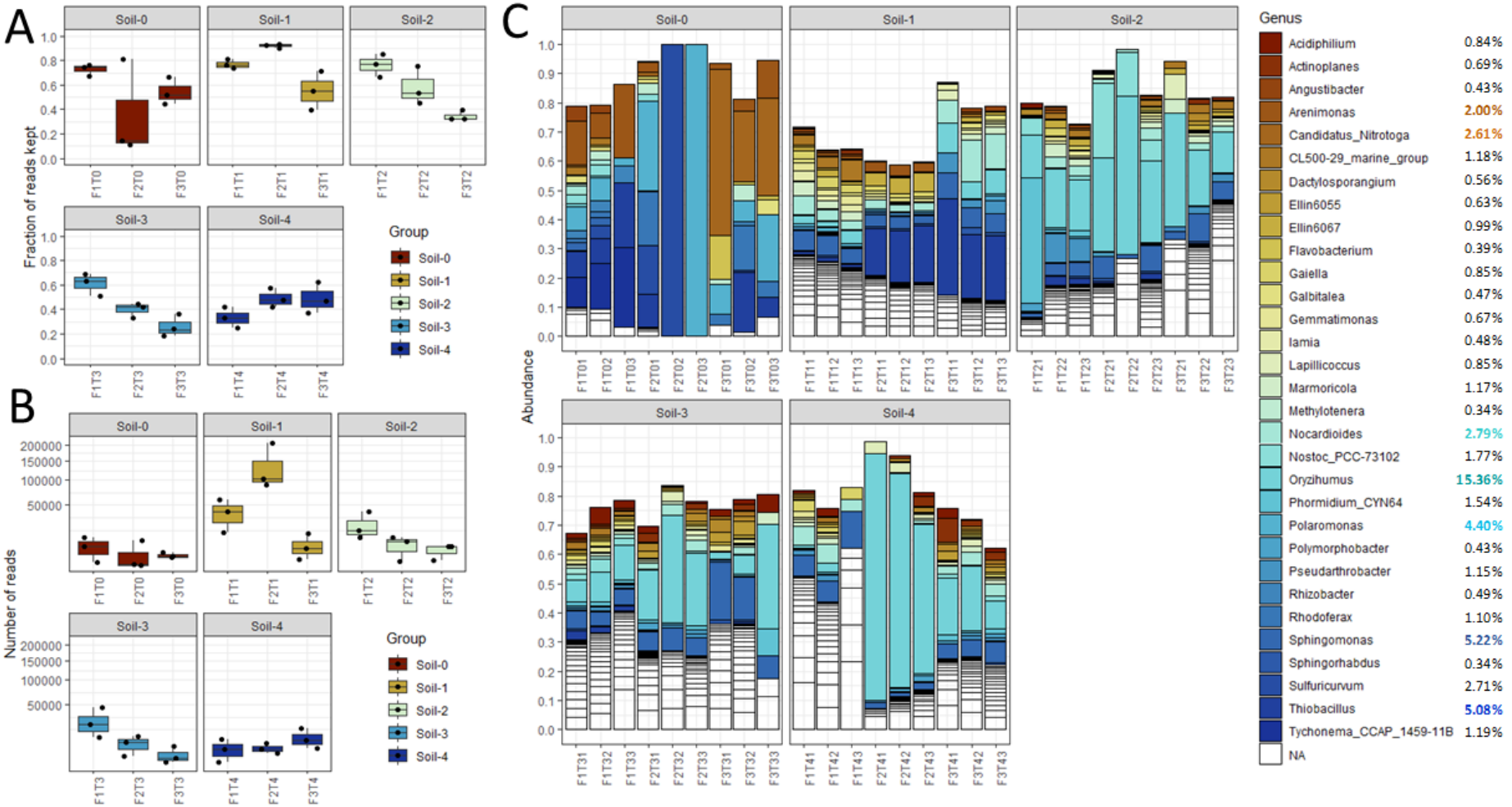

Figure 3-12 Relative abundance of genera in glacier forefield soil samples. (A) Proportion of reads remaining after filtering out ASVs without at least 10 reads in 3 or more samples. **(B)** Boxplot of number of reads in included libraries. **(C)** Relative Abundance of filtered samples by Genus.

The dramatic effect of filtering on library size is shown in Figure 3-8 A. With three replicates from each site, the loss of such a large proportion of ASVs and reads from each library suggest enormous heterogeneity, not only between glacial forefield sites, but even replicates from the same site). The heterogeneity of soil samples in the glacial forefield is further illustrated by plotting the prevalence and abundance of ASVs in the dataset (Figure 3-13).

The most abundant genus was the *Oryzihumus* from the Actinobacteria, with a mean RA of 15.36%, which was more abundant in developed soils (Soil -2, -3, -4). The second most abundant genus was the *Sphingomonas* (5.22 %), present to some degree across all time points. The four genera *Thiobacillus* (5.08%), *Arenimonas* (2.00%), *Candidatus_Nitrotoga* (2.61%) and *Sulfuricurvum* (2.71%) were present mainly in the recently deglaciated Soil-0. There was a large proportion of ASVs that could not be resolved to genus level.

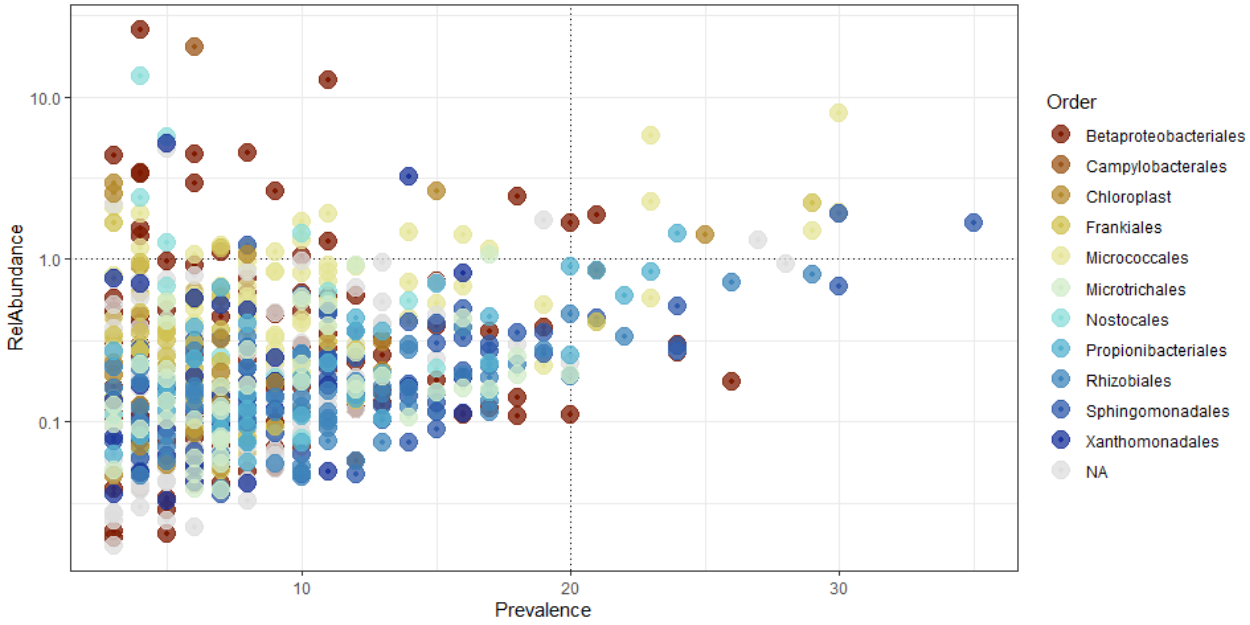

Figure 3-13 Scatter plot of the most prevalent and abundant ASVs in glacial forefield soil (n=45), by order. X-axis is the prevalence of each ASV (number of samples in which each ASV occurs) The axis is shortened from 45 to 35, and there were 0 ASVs present in all 45 samples. Y-axis is log10 of the mean relative abundance of the ASVs across all samples**.** Points are coloured by Order.

The most prevalent ASVs in the soil samples, by time point and by transect, are tabulated in Appendix Table C-17 and the most abundant ASVs in Appendix Table C-18. From a total of 45 samples and 40 045 ASVs, there were only five ASVs present in 30 or more of the samples. A *Sphingomonas* ASV (ASV69) was present in 35 of the samples at a mean RA of 1.58%, and two more *Sphingomonas* ASVs (ASV76 and ASV152) were present in 30 of the samples at a mean RA of 1.92% and 0.68% respectively. The other ASVs in more than 30 of the samples were

Oryzihumus ASVs (ASV48 and ASV114) from the family *Micrococcales*, which were present at a mean RA of 7.99% and 1.94%, respectively. Of the remaining 26 ASVs present in more than 20 of the samples, there were an additional three *Oryzihumus* ASVs (ASV150, ASV83 and ASV334), three *Sphingomonas* ASVs (ASV340, ASV301, ASV460). The remainder were from family Rhizobiales (ASV135, ASV154, ASV45), Frankiales (ASV157, ASV257), Propionibacteriales (ASV101, ASV129, ASV411, ASV363), Betaproteobacteriales (ASV1359, ASV229, ASV403, ASV65, ASV45).

To further investigate soil heterogeneity across the forefield, the ASVs that were prevalent at a single site were examined (Appendix Table C-19). This was done by looking for ASVs that occurred in all three replicates of a single site, and not in any other samples. Site specific ASVs were identified at 6 of 15 sample sites: F1T1 (5), F2T1 (13), F1T2 (1), F1T3 (3), F2T3 (1), and F3T4 (2). Many of the taxa that appeared 'unique to one site' came from the site F2T1. The libraries from this site were much larger in size than the libraries from different sites. This suggests that perhaps the presence of these ASVs in all three replicates are a result of greater sampling depth at this site. Site-specific ASVs were occasionally abundant community members at those sites. For example, ASV39, belonging to genus *Ellin6067*, which was present at a mean RA of 4.371% at F2T2, an *Oryzihumus* ASV (ASV393) was present at a mean RA of 2.11% at site F1T2, and two ASVs from the order Chloroplast (ASV797, ASV976), which may be algal species, were present at 2.96% and 2.53% ate sites F2T3 and F3T4 respectively.

It is unclear whether the clay samples collected from the glacier snout are low in diversity or whether the low diversity reflects the difficulty inherent in extracting DNA from clay soils, which adsorb DNA. Interestingly the library sizes, made from extraction replicates from each site are similar in size, despite each replicate being extracted in different batches on different days.

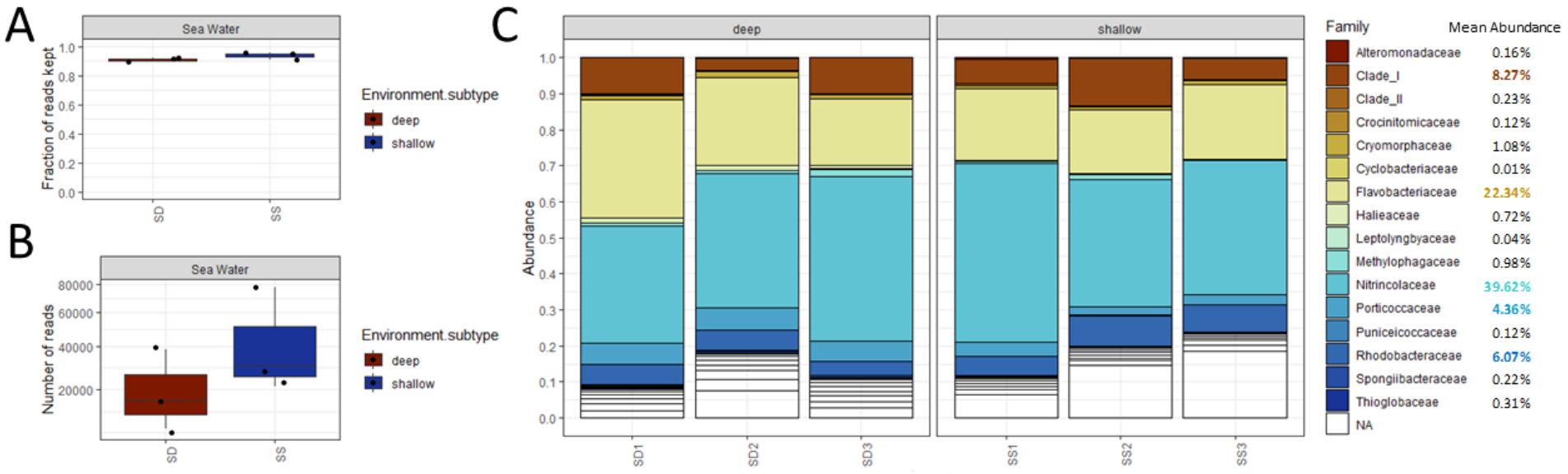

Figure 3-14 Relative abundance of bacterial families in sea water samples collected from 1m and 15m depth from the Kongsfjorden, in front of ML. (A) Proportion of reads remaining after filtering out ASVs without at least 10 reads in 2 or more samples. **(B)** Boxplot of number of reads in included libraries. **(C)** Relative Abundance of filtered samples by Genus.

3.3.2.5 Seawater

Seawater was collected from both 1m depth (n=3) and from 15m depth (n=3) from the fjord in front of ML and there is no clear visible difference between the shallow and deep samples. After decontamination, there were 1657 ASVs remaining in the seawater samples. Following filtering of the dataset to include only ASVs with more than 10 copies in two or more samples, there were 204 ASVs remaing in the dataset. The effect of the filtering step on library size is shown in Figure 3-15 A. The seawater samples were the most unique samples, with very little overlap with any of the other environment types. The most abundant Family were the Nitrincolaceae (39.62%) (from Gammaproteobacteria), followed by the Flavobacteriaceae (22.34%) (from Bacteroidetes), members of Clade I (8.27%) (from the SAR11_clade within Alphaproteobacteria), Rhodobacteraceae (6.07%) (from Alphaproteobacteria) and Porticoccaceae (4.36%) (from Gammaproteobacteria).

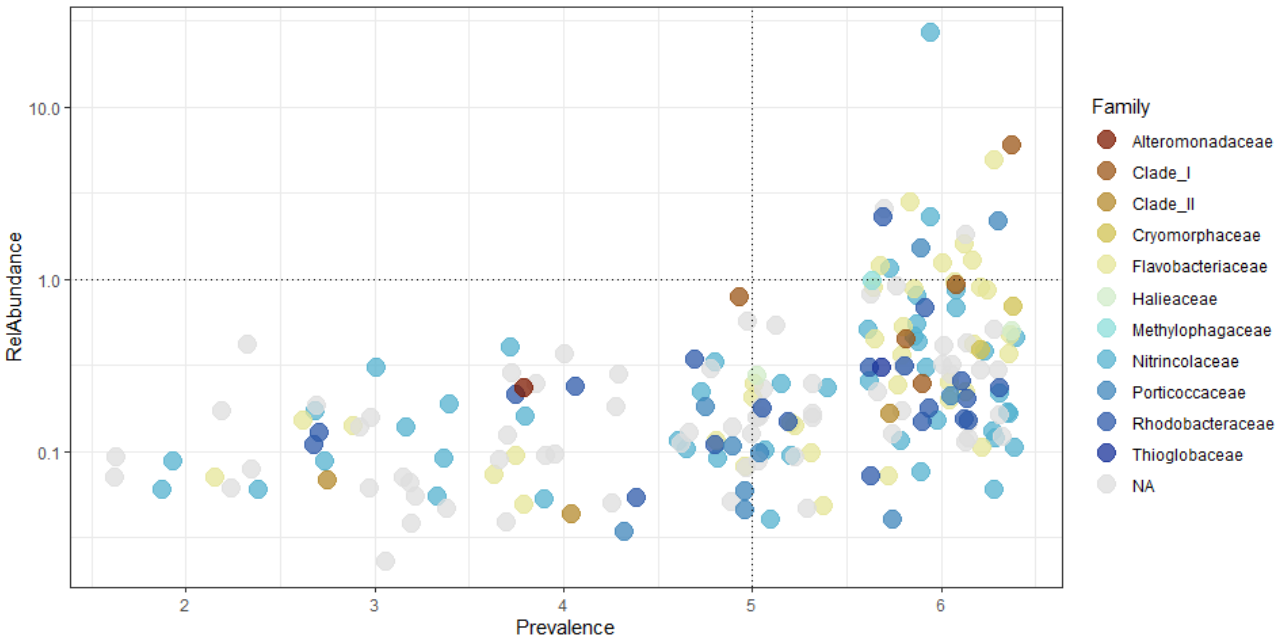

Figure 3-15 Scatter plot of the most prevalent and abundant ASVs in seawater (n=6), by order. X-axis is the prevalence of each ASV (number of samples in which each ASV occurs). Y-axis is log10 of the mean relative abundance of the ASVs across all samples**.** Points are coloured by Order.

The seawater samples were very similar to each other, with 96 of the 204 ASVs present in all six of the samples. In addition, 59.81% of the RA was made up of just 15 highly abundant ASVs, each of which individually had a mean RA > 1% (Appendix Table C-20). A single ASV (ASV18) from the family Nitrincolaceae was present at a mean RA of 26.85%. Other highly abundant ASVs belonged to *Clade_Ia* (ASV61, 5.99%), *Polaribacter_1* (ASV81, 4.88%), *Ulvibacter* (ASV86, 2.79%), *Sulfitobacter* (ASV111, 2.28%) and *SAR92_clade* (ASV179, 2.17%).

There was an apparent trend with ASV88 and ASV126, both of which were of the order Chloroplast, were present at a higher RA in shallow samples than in deep samples, likely due to the greater penetration of sunlight at 1m vs 15m depth. The opposite was true of ASV81 and ASV287 belonging to the genus *Polaribacter_1*, which were present at a higher RA in deep samples vs shallow samples. There were eight ASVs present in of the shallow samples and none of the deep samples, and one ASV present only in the deep samples (Appendix Table C-21). Considering the smaller library sizes of deep-sea samples, the presence of ASV 5401 (f_ Nitrincolaceae) in deep sea libraries only suggests that this may be a specialist species with a narrow tolerance for depth/pressure or sunlight or a correlated environmental pressure.

3.3.3 Comparison/ Relationship between environments

3.3.3.1 Unique taxa and shared taxa between environments

UpsetR was used to show the number of ASVs that are unique to each environment or shared between environment types (Figure 3-17). The plot is based on a filtered dataset (ASVs = 3958) in which ASVs with ≧ 5 copies in at least two samples are included. The requirement for ASVs to occur in at least two samples will result in an underestimation of unique ASVs in heterogenous and complex environments but gives better resolution for understanding shared ASVs. This filtering step results in a proportionally larger decrease in soil library size compared to cryoconite for example (Figure 3-16).

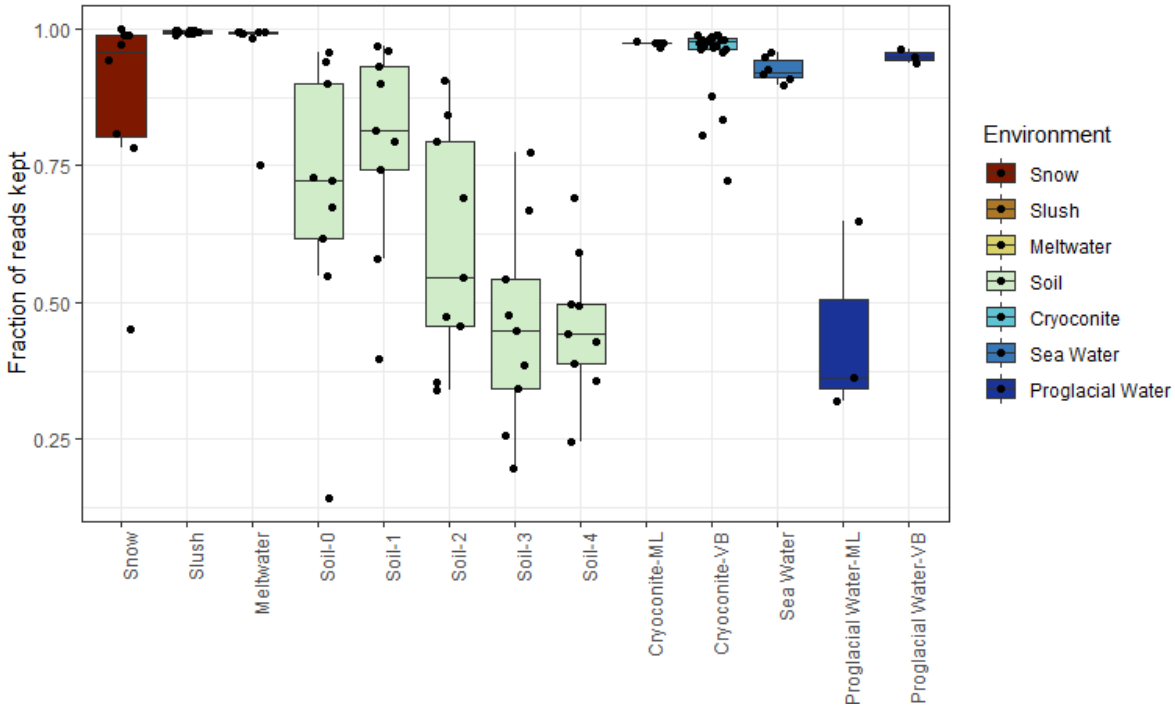

Figure 3-16 Bar plot showing effect of filtering on library size. The removal of ASVs without ≧ 5 copies in at least two samples resulted in a reduction in library size across the different samples. Environments with high heterogeneity and greater diversity (like soil) suffered the greatest reduction in size.

The UpsetR plot shows how several ASVs are shared between environments that are adjacent and/or similar (Figure 3-17). Even though they are physically distant, the largest set is intersection of the cryoconite from VB and ML (n=539). Several sets describe direct flow from one habitat to another, such as the 52 ASVs shared only between VB cryoconite and VB proglacial water, and 23 shared ASVs between proglacial water from ML and Soil-0 from the ML forefield (near the glacier snout). From this plot, large intersections occur between adjacent environments such as the supraglacial habitats of snow, slush and meltwater (65 ASVs), some of which also flow into ML proglacial water (23), or chronological soil sites (soil 1,2,3,4 (169), Soil 2,3,4 (151), Soil-3,4 (148) or soil-1,2 (111)), or from snow, slush, meltwater and cryoconite (14 ASVs). Of note is also a number of sets of ASVs that occur in a single site. They are important because they represent ASVs that are prevalent within a single site (and therefore part of this dataset), but not between sites. Therefore, although they are not rare taxa, they likely represent specialists. Examples include the 248 ASVs unique to Soil-0 and 127 ASVs unique to VB proglacial water and 319 ASVs present only in cryoconite from VB. Seawater is the only environment type that shares 0 ASVs with any other environment.

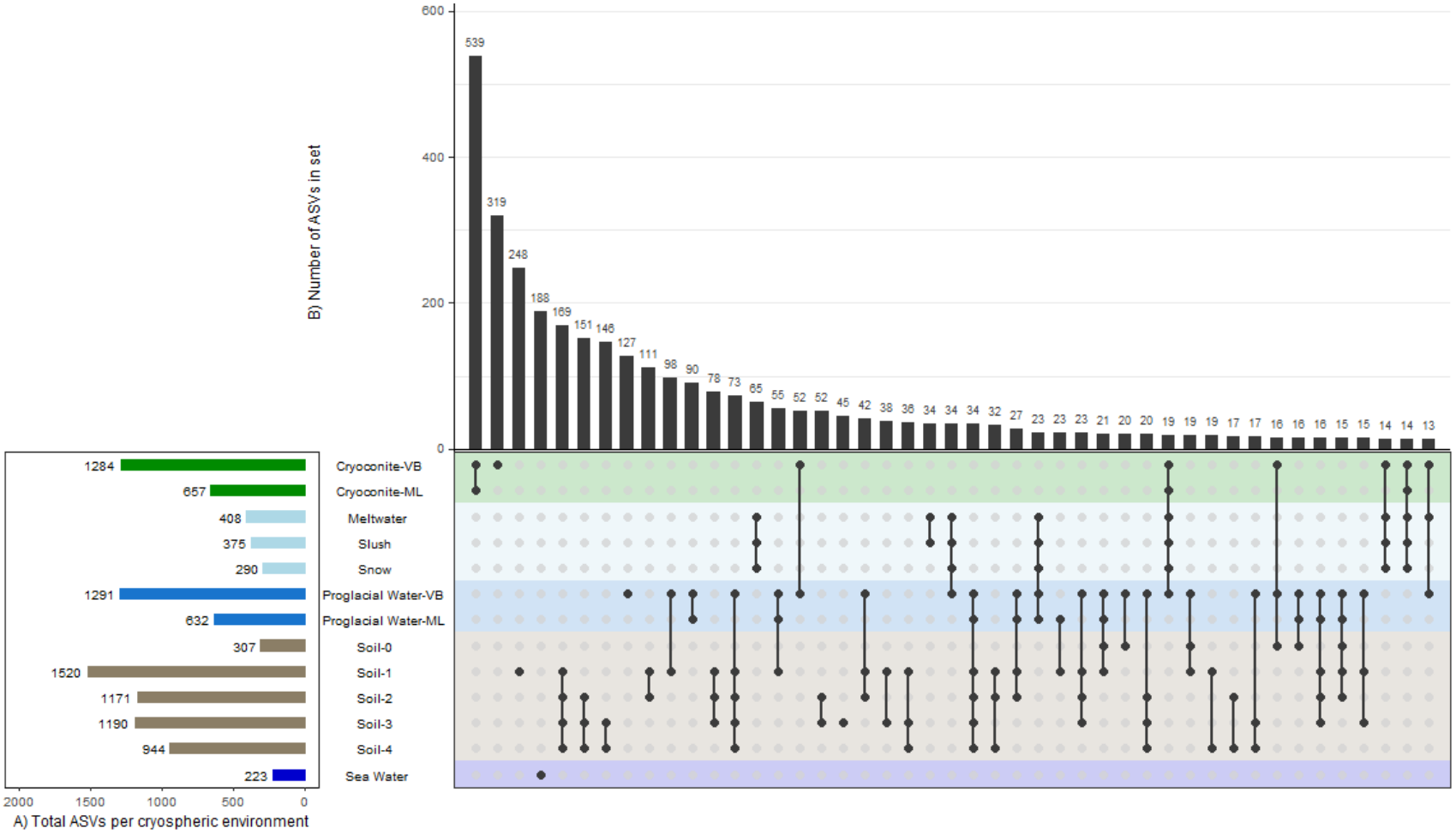

Figure 3-17 UpSetR Diagram showing number of unique and shared ASVs between different environments. Each environment group is a set (**Barplot A**). The number of ASVs in each set and intersection of sets are shown in **Barplot B** above the matrix. The black circles indicate the environments sharing ASVs. Sets are arranged in an environmental gradient and reflect proximity between environments. Only intersections involving 13 or more ASVs are shown.

3.3.3.2 Network analysis between samples

For network analysis, samples with n < 100 reads after decontamination were removed, leaving a dataset of 108 samples containing 58870 ASVs. The data was then filtered to contain only taxa that had >15 reads in three or more samples (ASVs = 2431).

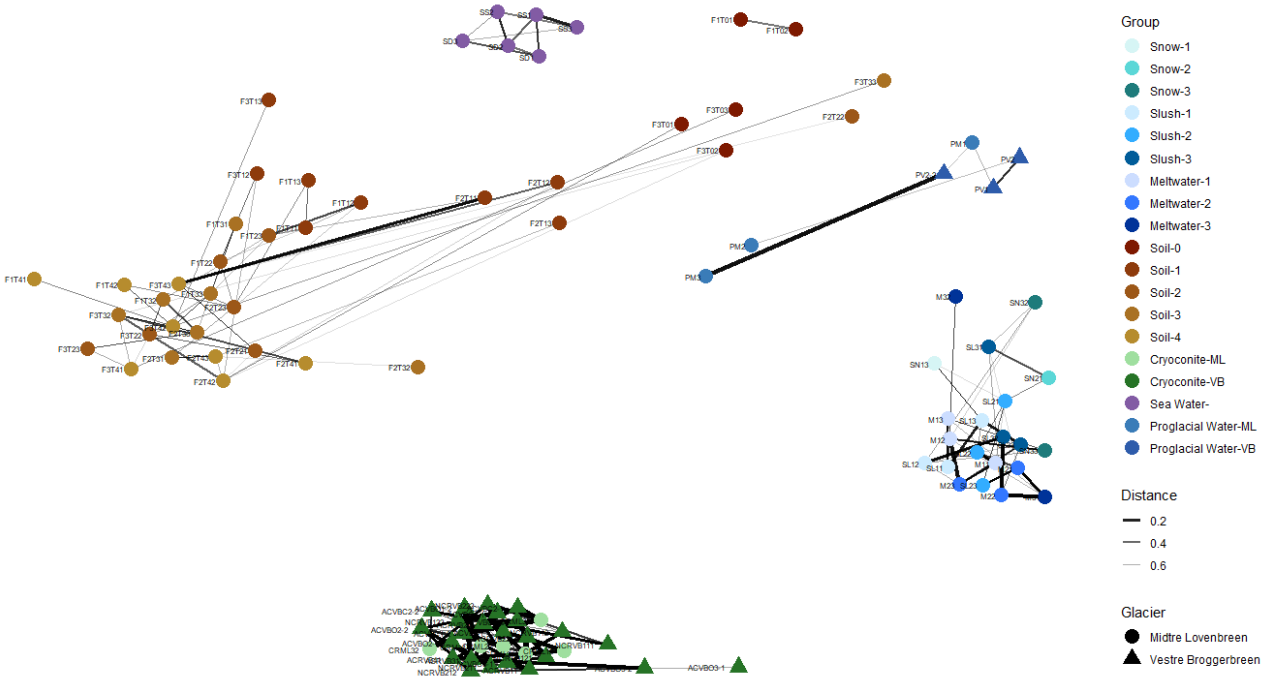

Figure 3-18 Network analysis of samples based on Bray-Curtis distances. Network created using a maximum distance threshold of 0.7 for connecting vertices with an edge. The network layout method is Fruchterman Reingold. The colour of groups is based on environment subgroup, shape is based on glacier of origin and points are labelled.

Samples clearly cluster based on environment type, with environment type playing a more prominent role than proximity. The proglacial water samples from VB are more like proglacial water from ML than they are to cryoconite collected from VB. The snow, slush and meltwater samples form a cluster, with a potential gradient (light-coloured samples from day 1 tend to cluster closely regardless of environment type). The cryoconite samples are similar and tightly clustered, whereas the soil samples are more distributed.

3.3.3.3 Network analysis between taxa

The decontaminated dataset (ASVs = 58 880) was filtered to include only ASVs with more than 40 reads in six or more samples (ASVs = 526). A co-occurrence network described the probability of taxa being found together. There are four main clusters detected, (modularity = 0.592), which correspond roughly to sea, cryoconite, soil, and glacial surface communities.

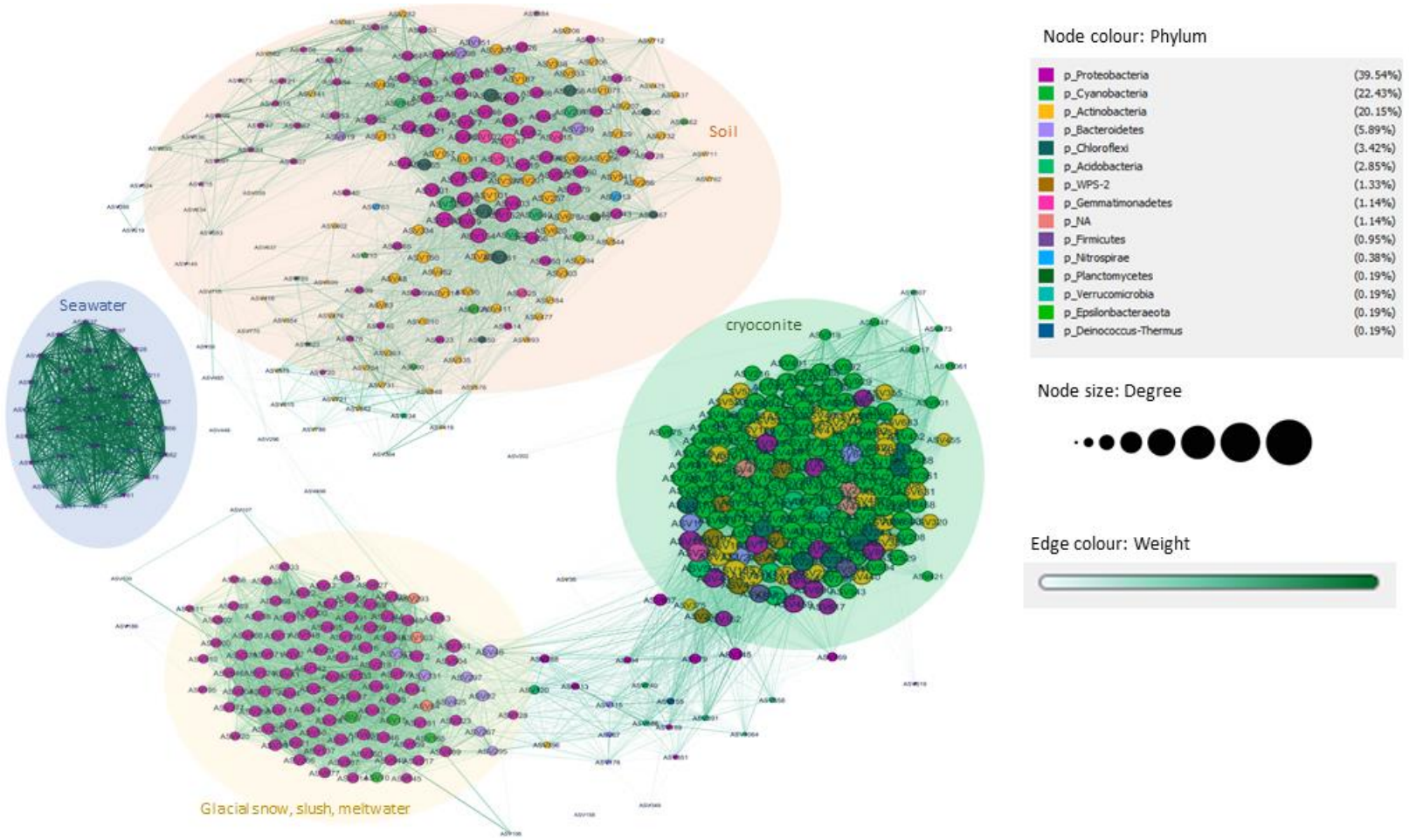

Figure 3-19 Co-occurrence network of ASVs in Svalbard. The decontaminated dataset (ASVs = 58 880) was filtered to include only ASVs with more than 40 reads in six or more samples (ASVs = 526). A correlation analysis was run based on Spearman's co-efficient, with a correlation coefficient cut-off of 0.5 and P-value cut-off of 0.05. Network visualisation performed in Gephi, layout is Fruchterman Reingold. Node colour refers to Phylum membership, Size of node reflects Degree, and edge colour shows weight. There are four clusters main clusters detected, (modularity = 0.592), which correspond roughly to sea, cryoconite, soil, and glacial surface communities.

3.4 Discussion

In this study, the taxonomic profiles of several environment habitats of a glacial system in Ny Ålesund, Svalbard were investigated, with a focus on identifying specialist members of Arctic microbial communities. Specialists are adapted to an extremely narrow environmental niche and are therefore spatially constrained and most threatened by the consequences of global climate change. The use of ASVs was preferred over the use of OTUs (Callahan et al., 2017), as this precise level of resolution improves the ability to detect community members unique to specific environmental niches, regardless of close relatedness to species in nearby environments.

3.4.1 The Decontam tool was able to successfully remove contaminants

Two common methods used to remove contaminants from 16S rRNA amplicon datasets are i) the removal of all sequences present in control samples and ii) the removal of very rare taxa that fall below a certain threshold. Both methods have their drawbacks; in the first case, removal of all ASVs that occur in negative controls can inadvertently remove legitimate environmental ASVs that are also present in the kitome due to similar conditions. In addition, one of the most likely sources of contaminants in negative controls is cross-contamination from environmental samples: the ASVs most likely to contaminate negative controls are the most abundant ASVs in the high biomass environmental samples. The second strategy of removing rare taxa is also flawed as it skews downstream analyses of species richness, particularly in microbially diverse and heterogenous samples. Since specialist species are likely to be rare and low-abundance members of a community, some effort was spent on decontaminating the dataset to preserve the rare microbiome. In this study, the Decontam tool was able to remove most sequences from control samples, whilst having minimal effect on environmental samples (Appendix Figure C-21). As expected, the low abundance samples (snow and clay soil from the glacier snout) were most effected by decontamination, likely due to legitimately high levels of contamination in samples with low starting concentrations.

3.4.2 There is a continuum between the snowpack, slush, meltwater, and proglacial water.

Using a variety of methods, the supraglacial environments of snow, slush and meltwater were similar in community structure (Figure 3-17, Figure 3-18, Figure 3-19). An UpsetR plot (Figure 3-17) showed that there are more shared ASVs between snow, slush and meltwater (n=65) than there are sets of ASVs unique to any of those environment types. However, multivariate analysis

of variance revealed that differences in community structure between environments was still significant, and explained up to 16.5% of the variation (Adonis, F.model = 1.9819, R2= 0.16541, Pr(>F) 0.0161). There was no significant difference between the bacterial diversity of snow, slush and meltwater samples collected on the same day. However, there was a small change in community composition due to time. Using Adonis to perform multivariate analysis of variance, there were significant differences in environmental communities due to sampling date (Date of collection, F.model= 2.6792, R2 = 0.21131, Pr(>F) =0.0014). In fact, time explained more of the variance than environment type, which is similar to previous studies of supraglacial habitat communities (Hell et al., 2013).

A microbial community associated with snow environments is increasingly recognized (Carpenter et al., 2000; Amato et al., 2007; Xiang et al., 2009a; Larose et al., 2010; Chuvochina et al., 2011; Harding et al., 2011). Snow bacterial abundance in Svalbard ranges between 2 x 10^4 cells·ml^{-1} in the accummulation snow layer of glaciers, 6 x 10^4 cells mL^{-1} in seasonal snow bordering the sea, and 2 x 10^5 cells mL^{-1} in the summer layer, where higher temperatures enables rapid mutiplication (Amato et al., 2007). Previous studies of snow show the presence of *Alphaproteobacteria*, *Betaproteobacteria* and *Gammaproteobacteria*, *Firmicutes* and *Actinobacteria* (Amato et al., 2007), with one genus, *Polaromonas*, showing a particularly high abundance (Hell et al., 2013). Although the bacterial communities of surface snow, snow, slush and near-surface ice are distinct, they have a significant capacity for rapid change in response to changing environmental conditions (Hell et al., 2013). This study corroborates these findings, with members of *Actimicrobium, Polaromonas, Glaciimonas and Massilia* making up a core community of abundant and prevalent ASVs in snow, slush, and meltwater (Appendix Table C-14, Figure 3-8). *Massilia* was previously found to be specific to glacial snow, and is thus highlighted as a vulnerable species due to glacier and snowpack loss induced by climate change (Zhang et al., 2015). The most abundant genus and ASV was *Actimicrobium* (ASV1), which has previously been found in a glacial snowpack (Terashima et al., 2017). Interestingly, there is only one characterised species of *Actimocrobium, Actimicrobium antarcticum,* discovered in Antarctic sea water in 2011 (Kim et al., 2011). The presence of this genus in such high abundance, and the number of ASVs related to this genus suggest an opportunity to investigate the possibility of new species of this genus. The high abundance of chloroplast sequences is potentially derived from green algae in the snow.

3.4.3 Proglacial water is an intersection of multiple environment inputs

Proglacial water is expected to be an amalgam of subsurface, surface and forefield communities, and was the most biodiverse habitat type in the dataset, with the greatest number of phyla (Figure 3-3). In the UpSetR plot, the proglacial water from ML was more like forefield samples (65 ASVs), and the proglacial water from VB was more like the glacial surface communities. Strikingly, the proglacial water from ML most resembled the proglacial water from VB, which is agreement with several other sources that identify a similar microbial communities in subglacial environments globally (Dubnick et al., 2017). Phylotypes unique to the subglacial outflow samples were dominated by bacteria in the phyla *Bacteroidetes*, *Actinobacteria*, *Firmicutes, Acidobacteria* and *Proteobacteria* (Dubnick et al., 2017).

3.4.4 Soil is extremely heterogenous

The glacial forefield soil was extremely heterogenous, but there is evidence of gradients affecting species composition. The number of singleton ASVs in soil shows that it is potentially both a heterogeneous and under-sampled environment (Figure 3-4, Figure 3-12, Appendix Figure C-22). In addition, ASVs present at high abundance, but only in specific sites (Appendix Table C-19), suggest that sampling deeply (i.e. large library sizes at a single site) and widely (lots of different sites across the forefield) would be necessary to accurately describe microbial communities. Early-stage glacial soil sampled from the ML glacier snout was extremely different to soil at all other time points (Figure 3-12 and Appendix Table C-17). The forefields of glaciers often show signs of succession, with soils closer to the glacier snout having lower biodiversity and little plant life, and later successional stage soils have significantly more biodiversity and plant life. The co-occurrence network Figure 3-19 shows that the soil co-occurrence network has two ‘arms’, possibly related to soil development and the presence of plants. Although the microbial communities that dominate in Arctic soils can be influenced by a variety of factors, including the local geology, the presence or absence of seasonal or permanent permafrost and their location in relation to glaciers; pH and vegetation of soils has been shown to have the greatest influence on biodiversity (Malard and Pearce, 2018). A recent study of the biogeography of Arctic sites which took into account 200 independent Arctic soil samples from 43 sites, found that of the 48 147 bacterial taxa, a core microbiome composed of only 13 taxa that were ubiquitously distributed and present within 95% of samples was identified (Malard et al., 2019). Together, the high heterogeneity across the ML forefield in this study, and the vast heterogeneity across multiple Arctic sites suggests high levels of endemism in Arctic soils. A review of Arctic soils found that Proteobacteria and, specifically, Nitrogen-fixing Rhizobiales (Alphaproteobacteria), Burkholderiales (Betaproteobacteria),

Xanthomonadales (Gamma-proteobacteria) and Myxococcales (Deltaproteobacteria) dominated Arctic soil bacterial communities. The dominant phyla in the ML forefield belonged to the Proteobacteria, Cyanobacteria, Actinobacteria, Acidobacteria, Bacteroidetes and Gemmatimonadetes. Specific genera included *Oryzihumus*, *Sphingomonas*, *Thiobacillus*, *Arenimonas*, *Candidatus_Nitrotoga* and *Sulfuricurvum*.

3.4.5 Seawater does not share ASVs with other environments

Seawater has various gradients, such as temperature, pressure, oxygen saturation and light penetration which can all affect bacterial community structure. A study of free-living and particle-associated bacterial communities and their spatial variation in Kongsfjorden, found that all samples were dominated by Proteobacteria, followed by Bacteroidetes, Firmicutes and Actinobacteria (Jain and Krishnan, 2017) and Fjord water near Ny Ålesund as found to contain predominantly Alphaproteobacteria, Gammaproteobacteria, Bacteroidetes, Firmicutes and Parcubacteria, as well as Gemmatimonadetes, Nitrospirae, Acidobacteria and Chloroflexi (Conte et al., 2018). The high prevalence of Nitrincolaceae (39.62%) (from Gammaproteobacteria), followed by the Flavobacteriaceae (22.34%) (from Bacteroidetes), members of Clade I (8.27%) (from the SAR11_clade within Alphaproteobacteria), Rhodobacteraceae (6.07%) (from Alphaproteobacteria) and Porticoccaceae (4.36%) (from Gammaproteobacteria) is similar to the community structure described in the fjord waters near the VB glacier snout (Thomas et al., 2020). There was absolutely no evidence that ASVs from the glacier or forefield were present in seawater (Figure 3-17, Figure 3-19). However, this may differ in glacial ecosystems that end in marine outlets.

3.4.6 Cryoconite communities on VB and ML are similar

Cryoconite is a dark, granular sediment comprising biotic (organic) and abiotic (inorganic) material that commonly discolours the surface of glacial ice (J. Cook et al., 2016; Hodson et al., 2008). Previous studies have shown that there are both inter-regional (Cameron et al., 2012a) and interglacial (Edwards et al., 2011) differences in cryoconite bacterial communities. Proteobacteria and Cyanobacteria are consistently the most abundant phyla detected in cryoconite (Edwards et al., 2011) (Cameron et al., 2012a; Edwards et al., 2014; Gokul et al., 2016). Cryoconite bacterial communities from the nearby Foxfanna glacier are strongly dominated by a small number of core taxa, include representatives of Actinobacteria, Cyanobacteria, Proteobacteria, Bacteroidetes, Chloroflexi and Gemmatimonadetes which are both ubiquitous and abundant (Gokul et al., 2016). Notably, an OTU belonging to the filamentous cyanobacterial genus *Leptolyngbya* was present at

all of the sites at a mean RA four times greater than the next most dominant OTUs, which corroborates the hypothesis that filamentous bacteria are important ecosystem engineers, and play a vital role in the formation of granules. In this study, we found the same, a single ASV (ASV1) was found in all the cryoconite samples at mean RA of 59.98%, and a core microbiome of bacteria common to all cryoconite sites included in the study could be identified (Appendix Table C-12). The dominance of the habitat type by a single ASV resulted in a lower Simpson index compared to the other environments (Table 3-2). The cryoconite communities of ML and VB were more similar to each other (UpsetR, 539 ASVs) than supraglacial, meltwater and glacial forefield samples upstream and downstream respectively (Figure 3-17). This suggests that the cryoconite community is a unique supraglacial habitat type, and corroborates previous studies showing that the bacterial communities of cryoconite are distinct and differ compared to nearby ice-marginal habitats (Edwards et al., 2013b). Although robust and diverse, it does not spread easily beyond the supraglacial environment.

3.4.7 High bioprospecting potential due to rare and specialist taxa

It has been suggested that the cryospheric biome is attractive for bioprospecting because it is extreme, difficult to access and therefore relatively unexplored and under threat from global warming. In this chapter, the enormous breadth of diversity in this glacial environment has been highlighted (Figure 3-3). The rare microbiome is enormous, with a significant proportion of communities being composed of rare taxa endemic to specific environments or even specific sites. As a result, sampling depth was inadequate to describe the community completely (Figure 3-4, Figure 3-16, Appendix Figure C-22). This biodiversity is hypothesized to translate to novelty because even in communities that are functionally similar, a greater number of species represents more biological variations in the enzymes and pathways that undertake those functions. Therefore, the more species, the more potential for biological novelty and unique biotechnological tools. In addition, analysis revealed that many of these environments are unique, where ‘uniqueness’ in this case is determined by how many bacterial species occur exclusively in that environment and not in any others. By filtering out ASVs that occur at only a single site, it was shown that soil is extremely heterogenous, with many ASVs that are not shared even between samples extracted from the same site (Figure 3-16). Cryoconite was remarkable for how many ASVs were shared between different sites on the same and different glaciers; nonetheless it did not share ASVs with adjacent environments (Figure 3-6, Figure 3-17, Figure 3-19, Appendix Table C-12). In terms of bioprospecting, environments that share many species represent redundancy and duplication of sampling effort. There are several environments in this study that are especially attractive because

they occur only in and around glaciers. Examples include cryoconite and recently exposed deglaciated soils (Soil-0). Bacterial adaptation to new environmental conditions is also much slower in the cryosphere, because of longer generation times at lower temperatures.

3.4.8 Recommendations

This study attempted to increase the resolution at which the biogeography of glacial environmental habitats in Svalbard was analysed, but using ASVs rather than OTUs, and preserving the rare taxa in the analysis. However, there are several ways in which the data could be improved in future investigations. Firstly, the library size distribution in this study was quite varied (Appendix Figure C-10). There are two ways to decrease variance in library size- the first is using Illumina indexed adapters attached to PCR primers, which removes the need for a second-stage PCR entirely, and ensures that DNA concentration calculations are only measuring indexed reads. It also has the added benefit of decreasing opportunities for contamination because if the index is added in the first PCR, the cross-contamination of wells during further steps and processing has no bearing on the library membership of the amplicon. A second approach is a qPCR of the indexes to determine index concentrations prior to pooling. A qPCR of indexes, rather than amplicons, will prevent the overestimation of library size based on a high DNA concentration library that contains unindexed amplicons. Secondly, the calculation of absolute abundance measures, can help in data preparation, sequencing, and results interpretation. Finally, the sequencing technology can be improved- the use of Nanopore to sequence the entire 16S rRNA operon will allow even better identification of unique ASVs and will also allow a more rapid sampling.

3.5 Conclusions

The extent to which glacial habitat types, and the communities therein, may change because of global climate change is currently a matter of intense research and great concern (Cauvy-Fraunié and Dangles, 2019; Stibal et al., 2020). This study reveals an extensive rare microbiome consisting of highly specialist bacterial communities that have a narrow ecological niche. In addition, some dominant and abundant community members, such as the communities that colonise cryoconite, are widespread across different glaciers, but do not spread easily to adjacent habitats. The implication of this is that glacial communities do not survive outside of glacial conditions, and that glacier loss means the irrevocable loss of these community members. This is additional evidence that changes wrought by climate change may have enormous, unknowable, and potentially irreversible changes on community structure. There may well be a bacterial extinction event decimating rare species of bacteria that are delimited to extremely narrow environmental windows.

4 METAGENOME ASSEMBLED GENOMES FROM SVALBARD CRYOCONITE, SOIL, AND SEAWATER ARE PHYLOGENETICALLY AND FUNCTIONALLY DIVERSE

4.1 Introduction

The cryosphere has been identified as a region with exceptional bioprospecting potential because it is considered an extreme environment (Cavicchioli et al., 2002; Santiago et al., 2016; Vester et al., 2015), it is relatively unexplored, and it is under threat from global climate change (Graham et al., 2017; Graversen et al., 2008). Svalbard is located 74° - 81° N and 10° - 35° E and experiences extreme cold, as well as continuous summer light and winter dark due to its far North latitude. These unique environmental stressors increase the likelihood of novel species and natural products.

Numerous studies have attempted to describe the community profiles of various cryospheric habitats using amplicon sequencing of the 16S rRNA gene (Chapter 3) (Anesio et al., 2017). However, amplicon-based studies have numerous pitfalls, including amplification bias, the fact that bacterial, fungal, archaeal, and algal communities need to be sequenced separately, and the failure of primers to amplify divergent 16S rRNA sequences, such as those present in much of the candidate phyla radiation (CPR) (Brown et al., 2015). Perhaps most importantly, phylotypes are unable to provide reliable functional predictions that would help tell us the putative metabolic potential of the microbial community (Edwards et al., 2020). MAGs are reconstructed genomes that inevitably represent the most abundant members of a community, because they are constructed from the longest contigs with the deepest coverage, proportional to their abundance in the original sample. The MAGs allow the identification of novel species that are unique to the environment,

can then be mined in same was as traditional genomes for genes and genomes clusters that synthesise useful and novel secondary metabolite clusters.

This thesis suggests that resolving metagenomes from these environments in a vital step that provides insight into the ecology of the region and establishes a foundation on which strategic bioprospecting can be based. There are several advantages of genome-centric metagenomics. Firstly, genome-level resolution and classification provides information about novel species and their phylogenetic relationships to known species (Parks et al., 2018). Secondly, mapping reads back to contigs (and MAGs) can be used to estimate the abundance of the species of interest across several sites. This is useful in its own right for providing ecological insights but is also a useful tool as to prioritise locations when a specific target is identified. Finally, functional information, provided by the annotation of metabolic functions and biogeochemical pathways, and co-occurrence at various sites, allows inferences to be made about symbiotic relationships which in turn can inform decision making about co-culturing.

To date, there have been numerous attempts to reconstruct genomes from rare environments in order to gain insights into phylogenetic diversity (Vavourakis et al., 2016), biogeochemical cycling potential (Anantharaman et al., 2016; Linz et al., 2018; Yaxin Xue et al., 2020), contaminant degradation potential (Hauptmann et al., 2017) and even secondary metabolites with antimicrobial potential (Cuadrat et al., 2018). The Arctic is still underexplored, but it has not been neglected. MAGs have been reconstructed from Greenland cryoconite (Hauptmann et al., 2017), Svalbard permafrost (Yaxin Xue et al., 2020) and Canadian glacier metagenomes (Trivedi et al., 2020). For example, 29 MAGS were identified from 34 cryoconite samples collected from five different locations around Greenland (Hauptmann et al., 2017). These genomes showed potential resistance to and degradation of contaminants such as polychlorinated biphenyls (PCB), polycyclic aromatic hydrocarbons (PAHs), and the heavy metals mercury and lead. In addition, the presence of the resistance and degradation genes was spatially variable, which the authors hypothesized may indicate local contamination at specific sites.

Cyanobacteria are important ecosystem engineers in cryoconite on the glacial surface (Gokul et al., 2016; Hodson et al., 2010a) and in the development of soils in glacial forefield (Pushkareva et al., 2015). Indeed, *Phormidesmis Priestleyi* is the major species present in cryoconite from Midtre Lovénbreen and Austre Brøggerbreen (Takeuchi et al., 2019), Foxfanna in Svalbard (Gokul et al., 2016), and is also found in cryoconite in Greenland (Chrismas et al., 2016b) and elsewhere (Segawa et al., 2017). Although the single cultured isolate resembling the *Phormidesmis Priestleyi* in Svalbard was isolated in Greenland (Chrismas et al., 2016a), this specific Cyanobacterial MAG

was notably missing from the Greenland cryoconite metagenome, which had *Nostoc* as its only cyanobacterial bin (Hauptmann et al., 2017). Several closely related bacteria has been sequenced from non-axenic cultures from several sub-polar habitats (Cornet et al., 2018), but abundance and highly prevalent species *Phormidesmis Priestleyi* has not yet been sequenced from metagenomic samples.

4.1.1 Aims and Objectives

The aims of this chapter are as follows:

1. Construct high quality metagenome-assembled genomes (MAGs) from soil, cryoconite and soil metagenomes.
2. Classify the MAGs using phylogenomic methods and identify novel species from these environments.
3. Use read mapping and coverage information to visualise the distribution of these species across different sample sites and identify species that co-occur at specific locations.
4. Use HMMER to detect the presence of genes involved in biogeochemical recycling of major nutrients at specific sites.
5. Create a pangenome of related Cyanobacterial MAGs to evaluate their relatedness to reference sequences, and to each other, and determine whether their accessory genome has genes involved in habitat adaptation.

4.2 Materials and methods

4.2.1 Sample collection

Samples were collected as previously described: seawater from Kongsfjorden Fjord (Section 3.2.1.4), cryoconite from Austre Brøggerbreen (AB), Midtre Lovénbreen (MB), Vestre Brøggerbreen (VB) and Vestre Lovénbreen (VL) (Section 3.2.1.6) and soil from the moraines in front of ML (Section 3.2.1.5). The location and types of samples included in this study are shown in Figure 4-1 and Table 4-1.

Table 4-1 Table of sample type, collection date and GPS coordinates

Sample name	Environment	Year	Date	Glacier	NORTH Y	EAST X
AB1804	Cryoconite	2018	06/07/2018	Austre Brøggerbreen	78d 53' 44"	11d 49' 54"
VL1801	Cryoconite	2018	07/07/2018	Vestre Lovénbreen	78d 54' 14	11d 56' 27
VB1802	Cryoconite	2018	09/07/2018	Vestre Brøggerbreen	78d 54' 40	11d 43' 60
ML1802	Cryoconite	2018	11/07/2018	Midtre Lovénbreen	78d 53' 17	12d 02' 49
CRML21	Cryoconite	2017	12/07/2017	Midtre Lovénbreen	78d 53' 32	12d 03' 18
NCRVB211	Cryoconite	2017	10/07/2017	Vestre Brøggerbreen	78d 54' 41	11d 43' 58
F1T3	Soil	2017	07/07/2017	ML Forefield	78d 53' 54	12d 03' 58
F1T41	Soil	2017	07/07/2017	ML Forefield	78d 53' 57	12d 04' 0
F2T21	Soil	2017	03/07/2017	ML Forefield	78d 53' 49	12d 04' 05
F2T41	Soil	2017	07/07/2017	ML Forefield	78d 53' 57	12d 04' 14
F3T11	Soil	2017	01/07/2017	ML Forefield	78d 53' 44	12d 04' 05
F3T31	Soil	2017	07/07/2017	ML Forefield	78d 53' 53	12d 04' 17
SS1	Seawater	2017	05/07/2017	Fjord	78d 55' 27	12d 03' 59
SS2	Seawater	2017	05/07/2017	Fjord	78d 55' 24	12d 04' 10
SS3	Seawater	2017	05/07/2017	Fjord	78d 55' 22	12d 04' 53

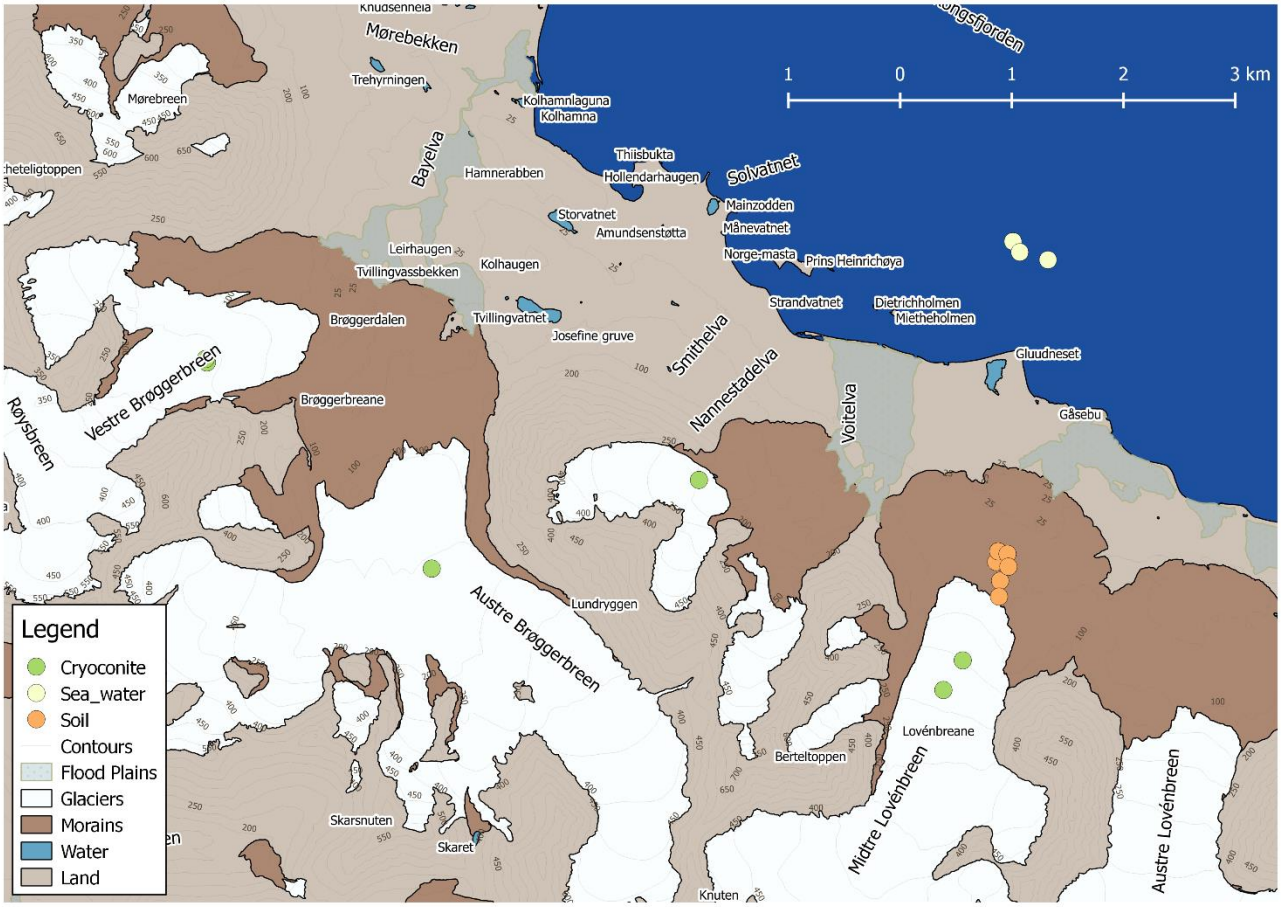

Figure 4-1 Map of sampling sites for shotgun libraries included in this study. Orange points are the soil sites, yellow points are the sea samples and green points are cryoconite samples.

4.2.2 DNA extraction

DNA from seawater was extracted using the Qiagen DNEasy Sterivex PowerWater kit (Section 2.2.2). DNA from soil samples was extracted using a variety of methods: the FastDNA Kit for soil (Section 2.2.4), the Qiagen DNEasy PowerSoil kit (Section 2.2.7), and a Ludox density gradient centrifugation (Section 2.2.6) to separate cells followed by lysis using the Epicentre MasterPure Complete DNA and RNA extraction kit (Section 2.2.5). Cryoconite DNA was extracted using the Qiagen DNEasy PowerSoil kit (Section 2.2.3). DNA from the same location (Soil: Transect 3, Time 3) was extracted using the three different methods and sequenced to evaluate kit bias.

4.2.3 Library preparation and sequencing

Sequencing was performed using the Illumina Nextera Kit according to manufacturer's instructions. Briefly, environmental DNA from cryoconite, soil and seawater was quantified using Qubit (Section 2.3.2), then diluted with DNAse-free water to a concentration of 0.2 ng/µL in a final volume of 5µl in a 96 well plate. The environmental DNA was tagmented by adding 10 µL Tagment

DNA buffer (TD) to the 5uL of normalised DNA and then adding 5µL of Amplicon Tagment Mix (ATM) to the wells and mixing well. The PCR plate was then centrifuged at 280 x g at room temperature for 1 minute to make sure all sample was in the bottom of the well. The mix was then rapidly transferred to a pre-programmed and pre-warmed thermocycler set at 55° C and incubated for 5 minutes exactly, followed by rapid cooling to 10 °C. As soon as the thermocycler reached 10 °C the plate was removed and 5 µL of Neutralize Tagment (NT) Buffer was added to stop the tagmentation reaction. The plate was then centrifuged at 280 x g at room temperature for 1 minute, then incubated for an additional 5 minutes at room temperature.

The libraries were amplified and indexed using a limited-cycle PCR. The indexes for each library (Appendix Table D-1) were arranged in a 96-well PCR plate; 5 µL of Index 1 (i7) was added to each column using a multichannel pipette, followed by the addition of 5 µL of Index2 (i5) across each row. Thereafter, 15 µL of Nextera PCR Master Mix (NPM) was added to each well and mixed by pipetting, followed by a brief centrifugation at 280 x g for 1 minute at room temperature. The libraries were then amplified in a thermocycler set to the following cycle conditions: 72 °C for 3 minutes, 95 °C for 30 seconds, followed by 15 cycles of 95 °C for 10 seconds, 55°C for 30 seconds and 72 °C for 30 seconds, followed by a final elongation step of 5 minutes at 72 °C.

A 1.5% agarose gel was run to confirm successful amplification of metagenomic libraries (Appendix Figure D-1). The resulting indexed libraries were cleaned up using Ampure beads (Section 2.5.1) and resuspended in 37.5µL of Resuspension Buffer. Cleaned, indexed metagenomic libraries were equimolarly pooled to 40 nM in a final volume of 50µL. To provide a final library concentration of 4nM, 5µL of the previous solution were diluted in 10mM Tris 0.05% TWEEN. The pooled libraries were sequenced at Wales Gene Park (Cardiff University) in an Illumina NextSeq® in High Output mode, generating 2 x 150bp paired end reads.

4.2.4 Reads processing and quality control

Paired end libraries were uploaded to KBase (https://www.kbase.us/) (Arkin et al., 2018), assessed using FastQC (J. Brown et al., 2017), trimmed using Trimmomatic (Bolger et al., 2014) to remove adapters and low-quality reads and the checked using FastQC a second time. The quality-controlled libraries for each environment type were combined and co-assembled on KBase using MEGAHIT (D. Li et al., 2015). MEGAHIT was selected as the assembly tool because it was computationally efficient and performed on par with other assemblers, as determined by optimisation, described in Chapter 8 Section 8.3.3.1. The assembly and the trimmed libraries for individual samples were then downloaded for further analysis.

4.2.5 Taxonomic assignment

Reads-based taxonomic assignment was performed on KBase on individual libraries and on pooled environmental libraries using Kaiju (v.15.0) in Greedy mode, against the NCBI BLAST nr + EUK database (Menzel et al., 2016).

4.2.6 Metagenome-assembled genomes (MAGs)

Most analysis was conducted on instances hosted on servers at CLIMB (https://www.climb.ac.uk/) (Connor et al., 2016). Metagenome assembled genomes were constructed using anvi'o (v 6.1 – Esther) (Eren et al., 2015). A contigs database was created from the assembly fasta file by running anvi-gen-contigs-database which and identifies open reading frames (ORFs) using Prodigal (Hyatt et al., 2010). To estimate the number of bacterial genomes in the metagenome, anvi'o runs HMMER against a series of single-copy gene databases. In anvi'o-6.1, these include HMM profiles for Archaea (76 genes), Protista (83 genes), Bacteria (71 genes). The scripts to detect candidate phyla radiation (CPR) rely on the single copy gene HMM dataset from Campbell et al, therefore, we included this dataset, together with the three profiles with anvio-6.1 in the HMMer scan (Campbell et al., 2013). The contigs were also functionally annotated with ncbi COG functions (Section 8.2.4.1.2), KEGG pathway information (Section 8.2.4.1.3) and eggNOG information (Section8.2.4.1.4). Taxonomy information for each gene call and contig was also classified using Kaiju (Section 8.2.4.2.1).

4.2.7 Binning and refinement of MAGs

The contigs database of 162,105 contigs (divided into 163,249 splits) was too large to run anvi-interactive with hierarchical clustering and run manual binning. Therefore, the contigs were binned using anvi-cluster-contigs as part of the anvi'o workflow using CONCOCT, MaxBin2 and MetaBAT2 (Section 8.2.5.1). The DAS Tool was then run on all three collections, using DIAMOND as a search engine. The taxonomic classification of the bins from each binning method (collection) were checked using anvi-estimate-scg-taxonomy, using the contigs database, merged profile, and each of the collections. The SCG taxonomy is a courtesy of The Genome Taxonomy Database (GTDB), which is the new gold standard taxonomy for bacterial classification (Parks et al., 2018).The bins from the DAS Tool collection were then refined using anvi-refine. The resulting bins from each tool were exported as collections, merged to create a data-frame of bin-association per contig and exported as a data layer into anvi'o. Anvi-interactive was run with the collection DAS Tool, ordered by mean-coverage, and viewed using 'detection' which shows proportion of the contig (or bin) which has at least 1 X coverage.

4.2.7.1 Screen for Candidate Phyla Radiation genomes

To screen for candidate phyla radiation (CPR), which often contain reduced genomes (Brown et al., 2015), anvi-script-gen-CPR-classifier was run on the Campbell taxonomy (Campbell et al., 2013).

4.2.7.2 Criteria for inclusion as a MAG

The dataset was trimmed to contain high quality MAGs. The genomes had to be larger than 1.8 MB, have greater 80% completion and less than 10% redundancy (Bowers et al., 2017).

4.2.7.3 Check genome quality with CheckM and GTDB-Tk

The refined MAGs were exported and the contigs were uploaded as assemblies to KBase for quality checking using CheckM (https://github.com/Ecogenomics/CheckM) (Parks et al., 2015). The MAGs were also submitted to GTDB-Tk on KBase for taxonomic assignment. The Genome Taxonomy Database Toolkit (GTDB-Tk) (https://ecogenomics.github.io/GTDBTk/), provides taxonomic classification of bacterial and archaeal genomes by placing them into domain-specific, concatenated protein reference trees (Chaumeil et al., 2020). GTDB-Tk uses the same criteria of relative evolutionary divergence (RED) and average nucleotide identity (ANI) for establishing taxonomic ranks as the recently proposed rank-normalized taxonomy in GTDB (Parks et al., 2018).

4.2.8 Phylogenomic Tree

The phylogenomic relationship of the MAGs was compared by following the tutorial: http://merenlab.org/tutorials/infant-gut/#chapter-iii-phylogenomics. Briefly, using the HMM hits from a curated collection of single copy core genes (Bacteria_71, Appendix Table D-10) for the GToTree workflow (Lee, 2019) were compared in a phylogenomic analysis. To do this, the selected genes from each MAG in the collection were concatenated, translated and aligned by running anvi-get-sequences-for-hmm-hits with default settings plus the additional parameters: (--concatenate-genes --return-best-hit --get-aa-sequences). The anvi-get-sequences command uses MUSCLE to align the genes (Edgar, 2004). The phylogenomic tree was calculated using anvi-gen-phylogenomic-tree, which infers approximately-maximum-likelihood phylogenetic trees from FASTA files using FastTree (Price et al., 2010).

4.2.9 Spatial distribution of the MAGs across sample sites

The spatial distribution of MAGs was visualised using heatmaps of max-normalised ratio (number of reads recruited to a contig divided by the maximum number of reads recruited to that contig in any sample) and abundance (mean coverage of each MAG divided by that sample's overall mean coverage across all the MAGs). The heatmaps were created using the R package ComplexHeatmap (http://www.bioconductor.org/packages/devel/bioc/html/ComplexHeatmap.html) (Gu et al., 2016). Max-normalised ratio considers one contig across all samples, where the value is normalized to the single maximum value for that contig. The sample containing the contig that contributed the max value will always equal 1, and the value for that contig in the other samples will be the fraction of that max.

4.2.10 Biogeochemical cycles

The fasta files from the MAGs were analysed for major metabolic pathways using MetabolisHMM (https://github.com/elizabethmcd/metabolisHMM) (McDaniel et al., 2019). In this analysis, the fasta files of the genomes are formatted, annotated using prodigal and then a HMMER search is run against a curated list of genes involved in important biogeochemical pathways. The list of genes, their HMM profiles and their accessions are available in Appendix Table D-15.

4.2.11 Phormidesmis pangenome

A pangenome of *Phormidesmis* genomes was constructed using nine genomes downloaded from NCBI genbank and refseq by searching for complete *Phormidesmis* genomes on the GTDB database (https://gtdb.ecogenomic.org/). These were compared to the MAGs resolved in this dataset using a workflow described (http://merenlab.org/2016/11/08/pangenomics-v2/) and (http://merenlab.org/tutorials/infant-gut/#chapter-iv-pangenomics). The phylogenetic relationships of genera and families are constantly being shuffled with new information (See Appendix Table D-13 comparing ncbi and GTDB-Tk phylogeny). Therefore, all six cyanobacterial genomes and their closest hits (Appendix Table D-12) were compared in a pangenome analysis (Appendix Figure D-3). Based on this initial analysis, three cyanobacterial bins: CC_mag_060_Nodoslinea. MB_mag_047 and CC_mag_055, were investigated further.

The external genomes (Table 4.9) were downloaded from ncbi, and the fasta files were converted to contigs.db in the anvi'o workflow using anvi-script-FASTA-to-contigs-db. The scripts anvi-run-hmms and anvi-run-ncbi-cogs was then run to make the external genomes comparable to the MAGS. The internal MAGs and external genomes downloaded from GTDB were made into a

genomes storage database that stores information about genomes using anvi-gen-genomes-storage. The pangenome was generated by running anvi-pan-genome, which makes used of DIAMOND (Buchfink et al., 2015) and MCL (Enright et al., 2002). The pangenome was also generated using blastp (--use-ncbi-blast), which is slower than DIAMOND, but which gives better annotation. The average nucleotide identity (ANI) of the MAGs and external genomes was calculated within anvi'o using PyANI (Pritchard et al., 2015). Inkscape (available from https://inkscape.org/) was used to finalize figures.

4.3 Results

4.3.1 Library Statistics

Table 4-2 Characteristics of the Svalbard Soil, Seawater and Cryoconite datasets after trimming

				Read Length		Duplicate reads		Quality		
Environment	**Sample**	**Reads**	**No Bases**	**mean**	**std dev**	**Number**	**%**	**mean**	**std dev**	**GC%**
Soil	F3T3_Lud	40,079,596	5,866,959,800	146.38	17.23	595,443	1.49	34.05	4.75	57.43
Soil	F3T3_PM	44,915,524	6,576,965,385	146.43	17.22	43,387	0.10	34.05	4.76	62.47
Soil	F3T3_FD	113,754,008	16,645,206,349	146.33	17.43	594,826	0.52	34.04	4.77	61.04
Soil	F1T3-3	37,684,166	5,477,450,552	145.35	18.97	121,309	0.32	33.89	5.01	61.17
Soil	F1T4-2	38,762,496	5,660,342,037	146.03	17.92	881,337	2.27	34.00	4.85	57.65
Soil	F2T2-1	29,116,044	4,232,776,792	145.38	19.00	310,829	1.07	33.88	5.02	56.75
Soil	F3T1-3	35,482,472	5,166,716,509	145.61	18.70	336,628	0.95	33.92	4.97	58.63
Soil	F2T4-2	35,085,040	5,124,389,299	146.06	17.92	74,333	0.21	34.00	4.83	58.69
Sea	SS1	51,330,724	7,191,372,496	140.10	25.89	1,100,183	2.14	34.20	4.54	50.69
Sea	SS2	55,019,496	7,445,759,578	135.33	32.31	1,412,286	2.57	33.89	5.02	49.25
Sea	SS3	35,985,822	4,971,626,677	138.16	29.48	775,768	2.16	33.96	4.92	49.01
Cryoconite	ML-17	28,795,356	4,194,553,943	145.67	18.57	441,991	1.53	33.89	5.02	55.16
Cryoconite	VB-17	34,504,862	5,049,762,759	146.35	17.40	601,414	1.74	34.05	4.77	54.68
Cryoconite	ML-18	28,471,672	4,149,307,242	145.73	18.46	471,631	1.66	33.94	4.93	54.46
Cryoconite	VB-18	29,787,650	4,347,438,702	145.95	18.08	384,887	1.29	33.94	4.93	55.41
Cryoconite	AB-18	64,909,032	9,494,783,816	146.28	17.54	131,932	0.20	34.02	4.81	56.75
Cryoconite	VL-18	14,939,536	2,184,519,311	146.22	17.69	78,246	0.52	34.04	4.78	54.47

Library statistics are reported after quality trimming using Trimmomatic. The untrimmed library information can be viewed in Appendix Table D-2.

4.3.2 Reads-based taxonomy

The taxonomy of reads from each library was determined using Kaiju.

4.3.2.1 Cryoconite

Approximately 60% of the reads in the cryoconite libraries could be classified. A small minority of these reads could not be assigned at the phylum level. The majority of reads belonged to bacterial phyla. The Cyanobacteria were the most abundant, followed by Proteobacteria, Actinobacteria and Bacteroidetes. Other phyla present across all the samples include the Acidobacteria, Chloroflexi, Firmicutes, Plantomycetes and Gemmatimonadetes. The Ascomycota were the most abundant phylum from the Fungal kingdom and Chlorophyta were the most abundant phylum from the Viridiplantae (Green Algae). There were also viruses detected in all samples.

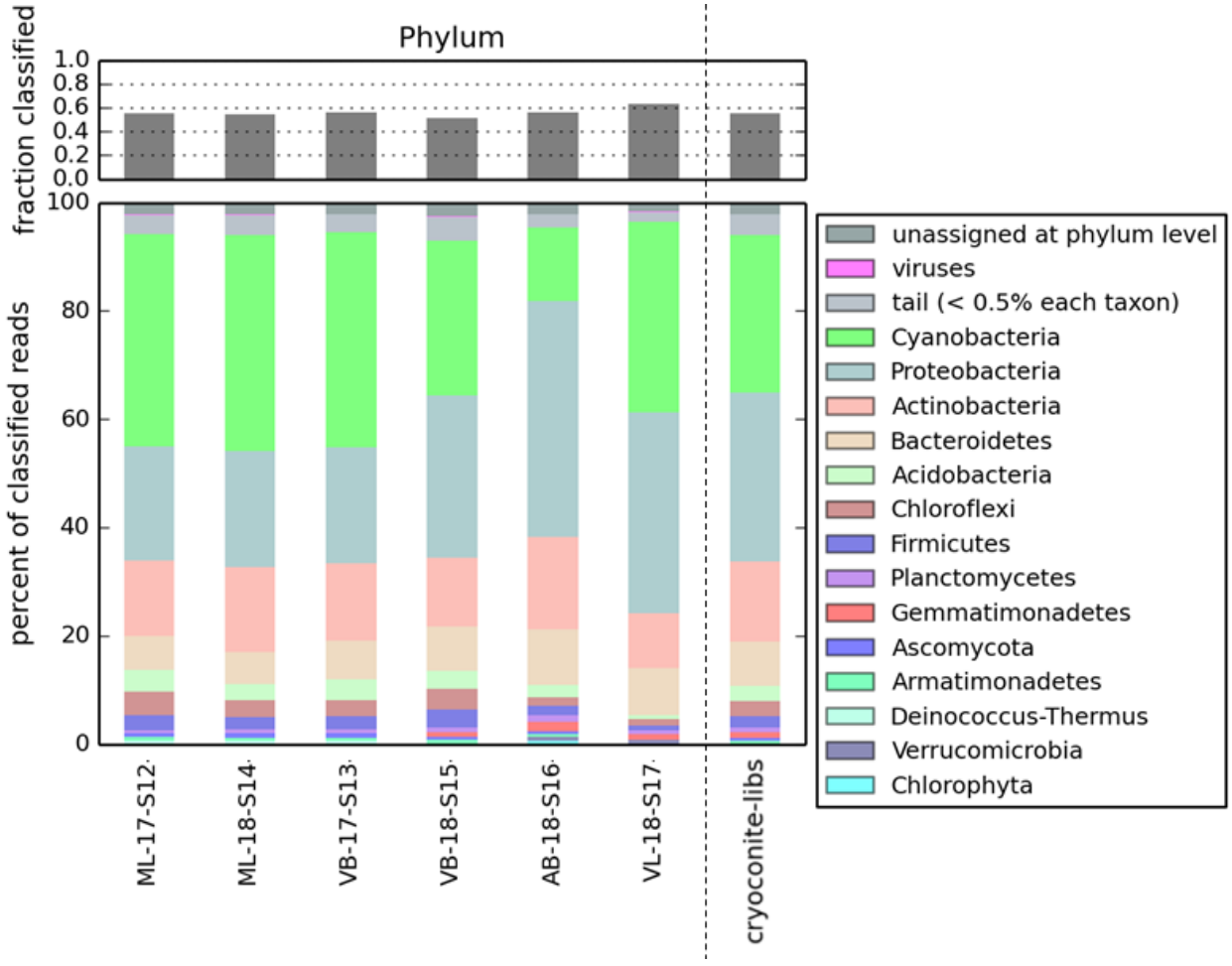

Figure 4-2 Reads-based taxonomic assignment of cryoconite libraries at the Phylum level using Kaiju. Cryoconite libraries are listed on the x-axis. A dashed lined separates the combined cryoconite library from the individual libraries.

At the genus level, the VB library and ML library from 2017 and 2018 resemble each other closely. *Phormidesmis* is the most abundant genus in the ML-17 (33.92%), ML-18 (33.81%), VB-17 (33.69%) and VB-18 (24.12%) samples. Although members of *Phormidesmis* are present in AB (6.23%) and VL (6.00%), they represent a smaller fraction of the community. Other genera present in significant numbers include *Ktedonobacter* which were found in ML-17, ML-18, VB-17, and VB-18. VL is notable for its high proportion of *Nostoc* (7.28%) which was present at higher abundance than *Phormidesmis* (6.00%).

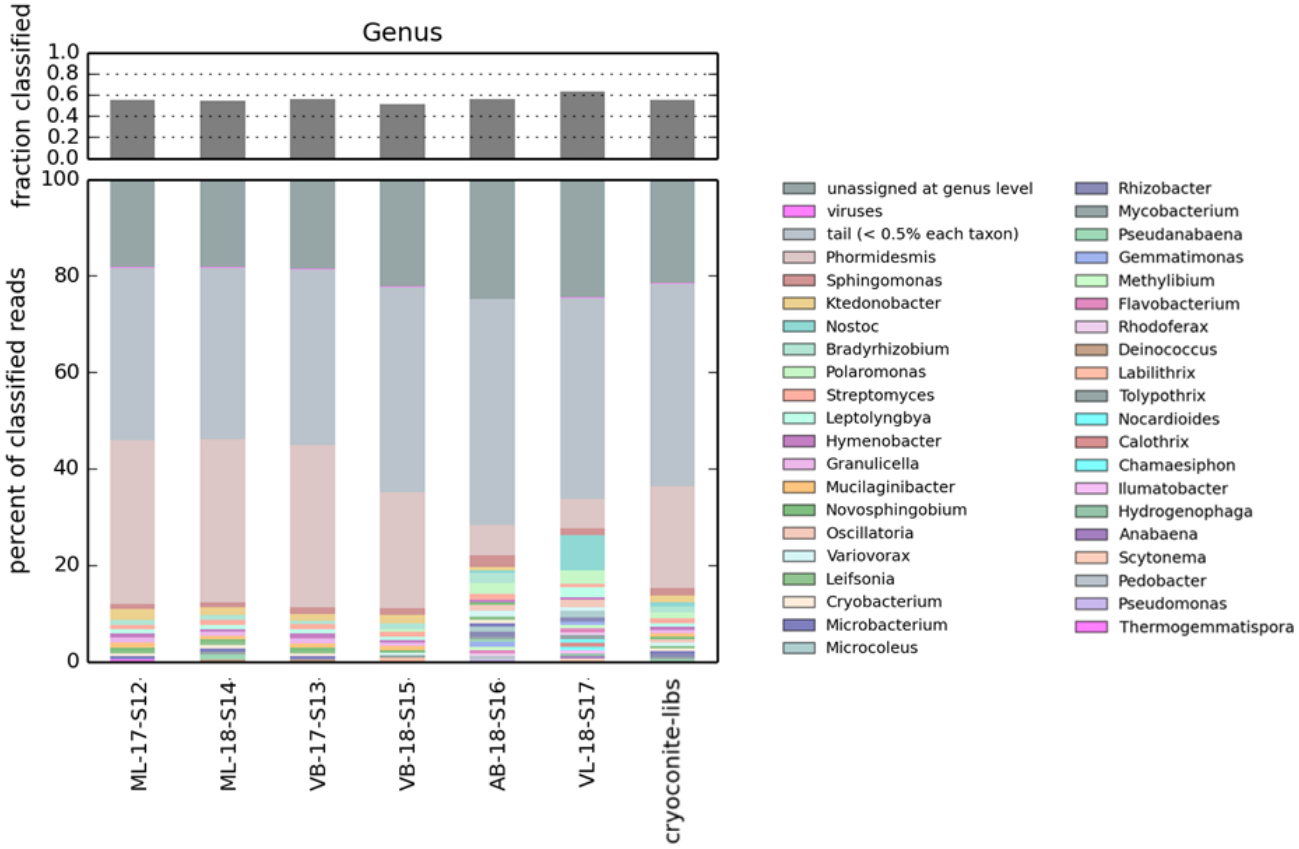

Figure 4-3 Reads-based taxonomic assignment of cryoconite libraries at the Genus level using Kaiju.

At the genus level, approximately 20% of the reads were unassigned, 40% of reads belonged to rare taxa, present at less than 0.5%, and the remaining 40% could be classified.

4.3.2.2 Soil

Approximately 60% of the reads in the soil libraries could be classified. The soil libraries were dominated by Bacterial phyla, of which the Proteobacteria, Actinobacteria and Bacteroidetes were the most abundant, followed by Acidobacteria, Cyanobacteria, Chloroflexi, Plantomycetes, Verrucomicrobia, Firmicutes, Gemmatimonadetes and Nitrospirae (Figure 4-4). Reads belonging to the fungal phyla Ascomycota made up a small proportion of the libraries.

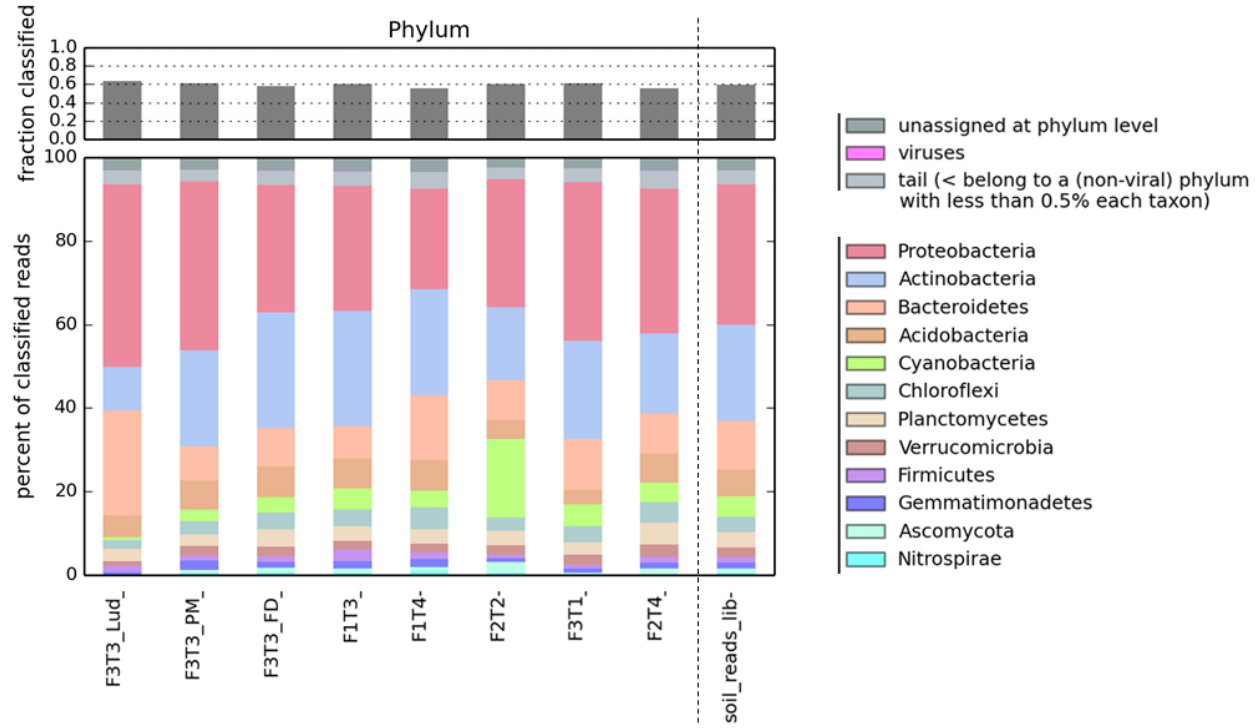

Figure 4-4 Reads-based taxonomic assignment of soil libraries at the Phylum level using Kaiju. Soil libraries are listed on the x-axis. A dashed lined separates the combined soil library from the individual libraries.

Although phylum-level diversity is similar across different soil samples, there is greater diversity at lower taxonomic ranks (Figure 4-5). There is a long tail of genera present at less than 0.5% relative abundance. The most abundant genera, which was also common to all sample sites were *Sphingomonas*, *Nocardioides*, *Streptomyces* and *Bradyrhizobium*. However, some genera are present at relatively high abundance at specific sites or when DNA was extracted using specific methods. Notably high abundance at the genus level include *Cecembia* (4.52 %), a genus that was not detected above 0.5% in either F3T3_PM or F3T3_FD, despite being from the same site. Other notable examples include *Nostoc*, present at 7.76% in F2T2, and at lower abundance in F1T3, F3T1, F2T4. The genus *Leptolyngba* was also found in all samples where *Nostoc* was identified.

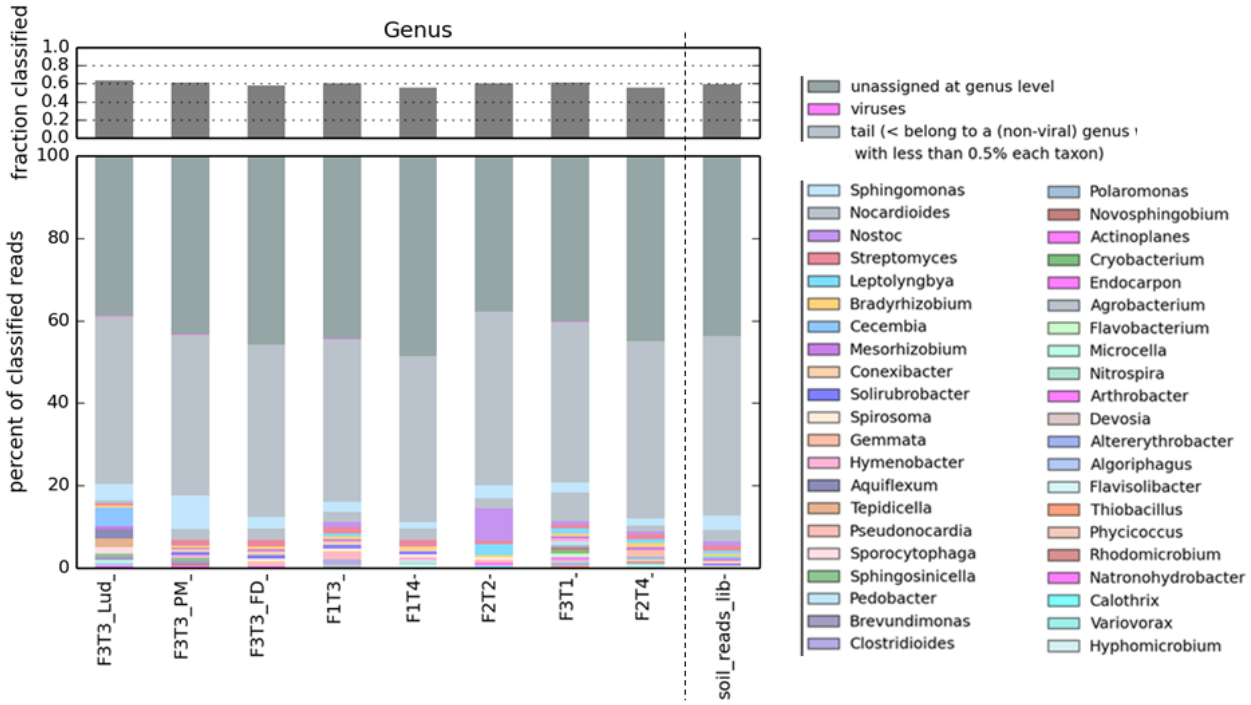

Figure 4-5 Reads-based taxonomic assignment of soil libraries at the Genus level using Kaiju. Soil libraries are listed on the x-axis. A dashed line separates the combined soil library.

4.3.2.3 Seawater

The SS1 library was slightly different to SS2 and SS3 in number of reads classified and in the composition of classified reads. In particular, the SS1 library had more classified reads overall, with a large proportion of sequences belonging to members of the Firmicutes and Actinobacteria, which was a relatively minor constituent of the SS2 and SS3 communities. The seawater libraries had the lowest percentage of classified reads of any environment type, with only 46.56%, 11.02% and 11.14% of reads classified in the SS1, SS2 and SS3 libraries, respectively.

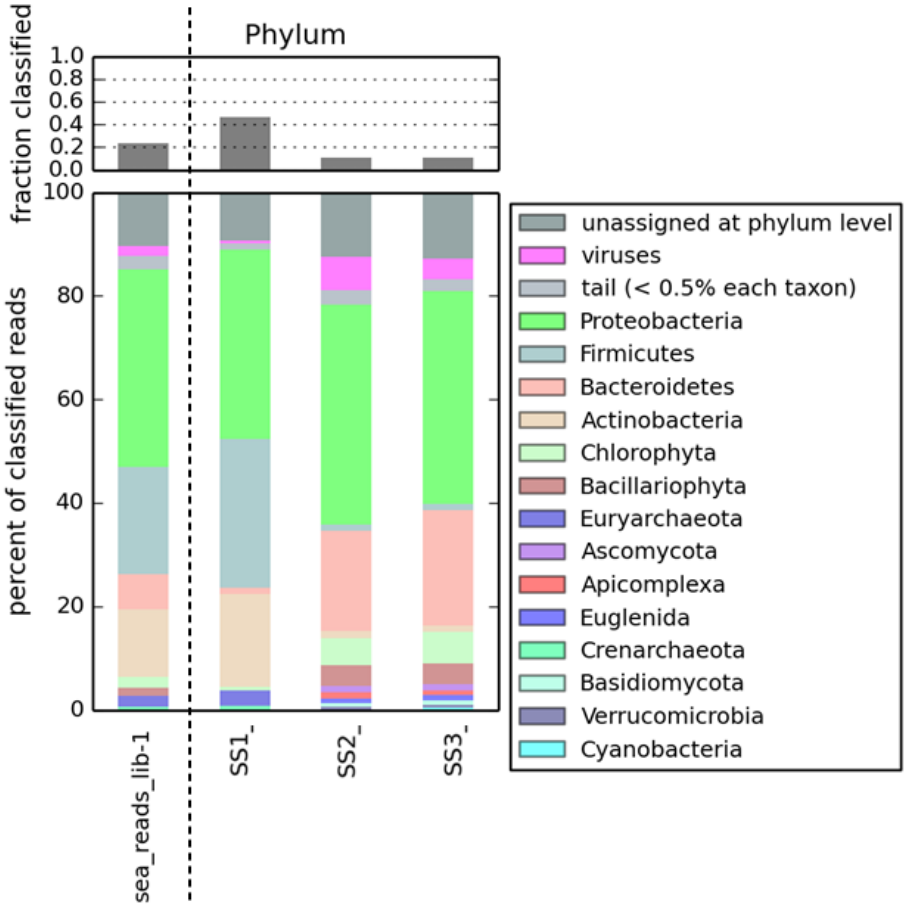

Figure 4-6 Reads-based taxonomic assignment of seawater libraries at the Phylum level using Kaiju.

Viruses were abundant in the SS2 (6.53%) and SS3 (3.96%) samples, and less abundant in SS1 (0.38%). The most abundant bacterial phyla in all samples were the Proteobacteria, (range 36.56% to 42.28%), with a high abundance of Bacteroidetes in SS2 (19.25%) and SS3 (22.36%) and a lower proportion in SS1 (1.13%). There was also notable number of Chlorophya (Green Algae), Bacillariophyta (Diatoms), Archaea (Euryarchaeota and Crenarchaeota), Fungi (Ascomycota, Basidiomycota), Apicomplexa and Euglenida.

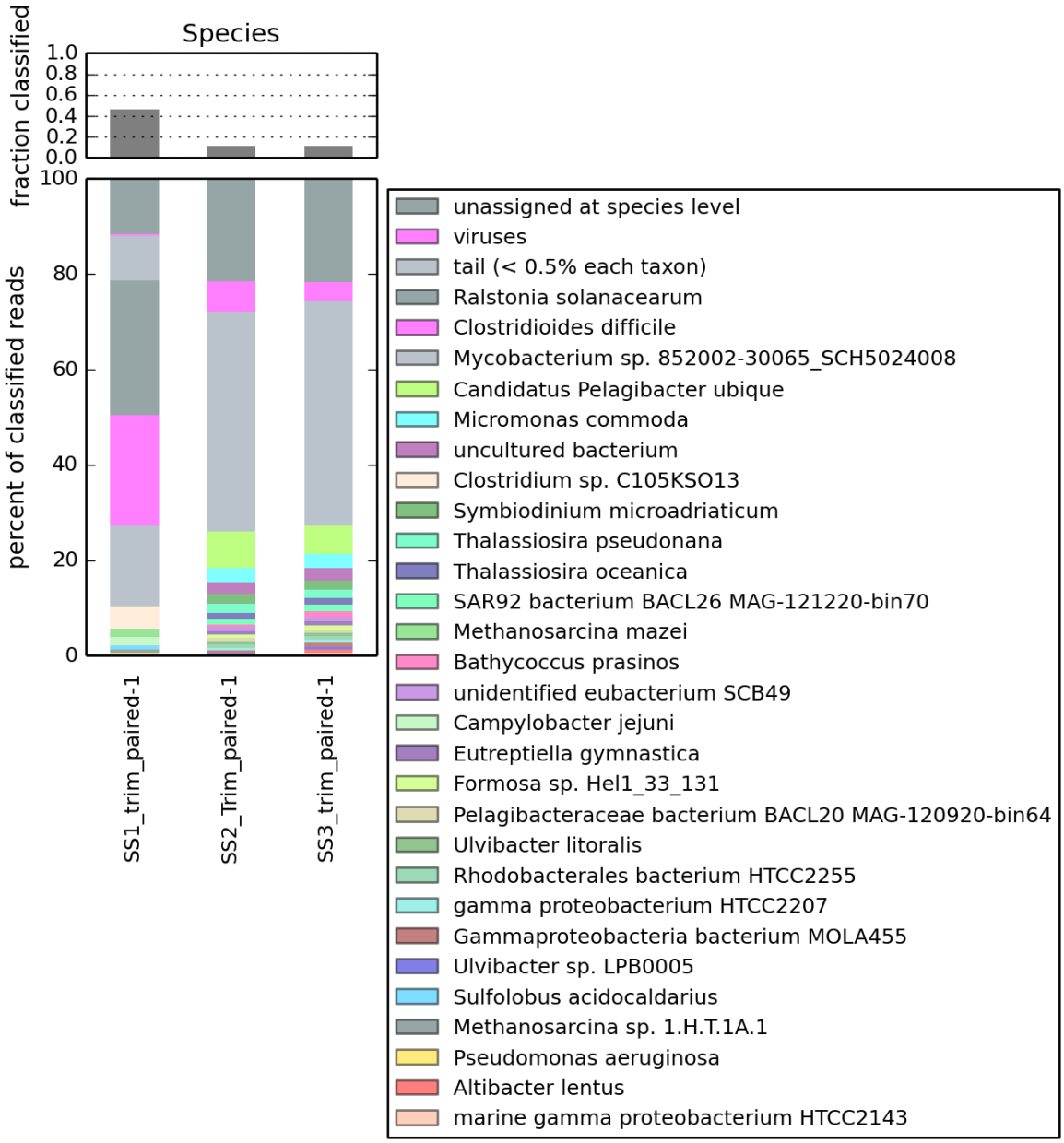

Figure 4-7 Reads-based taxonomic assignment of seawater libraries at the Species level using Kaiju.

At the species level, SS1 differs from SS2 and SS3. SS1 contained a high abundance of species commonly associated with sewerage. *Methanosarcina mazei* (1.88%), an anærobic archaeobacter is found in semi aquatic environments such as sewage receptacles and anoxygenic, moist soil. *Campylobacter jejuni* (1.60) is commonly found in animal faeces and is a leading cause of food-borne illness in humans.

4.3.3 Assembly statistics

The soil, cryoconite and seawater shotgun libraries were assembled by environment, and in a co-assembly of all environments. This was done to see whether co-assembly would increase library depth sufficiently to assemble additional/ longer contigs for bacterial species present in more than one of the Svalbard environments types. The co-assembly was similar in size to the sum of each of the soil, cryoconite and sea assemblies (Table 4-3). This suggests that co-assembly did not result in additional recruitment of reads into contigs or deeper coverage. This is likely because of little overlap in community members between soil, cryoconite and seawater (Chapter 3, Figure 3-17, Figure 3-19). As a result, a co-assembly of libraries from all Svalbard environments was used. The co-assembly provides extra information about the identity of genomes that are shared between environments, with minimal loss of information about genomes that are unique to one environment (or even one sample) in particular. The only assembly tool able to cope with the size of the library was MEGAHIT.

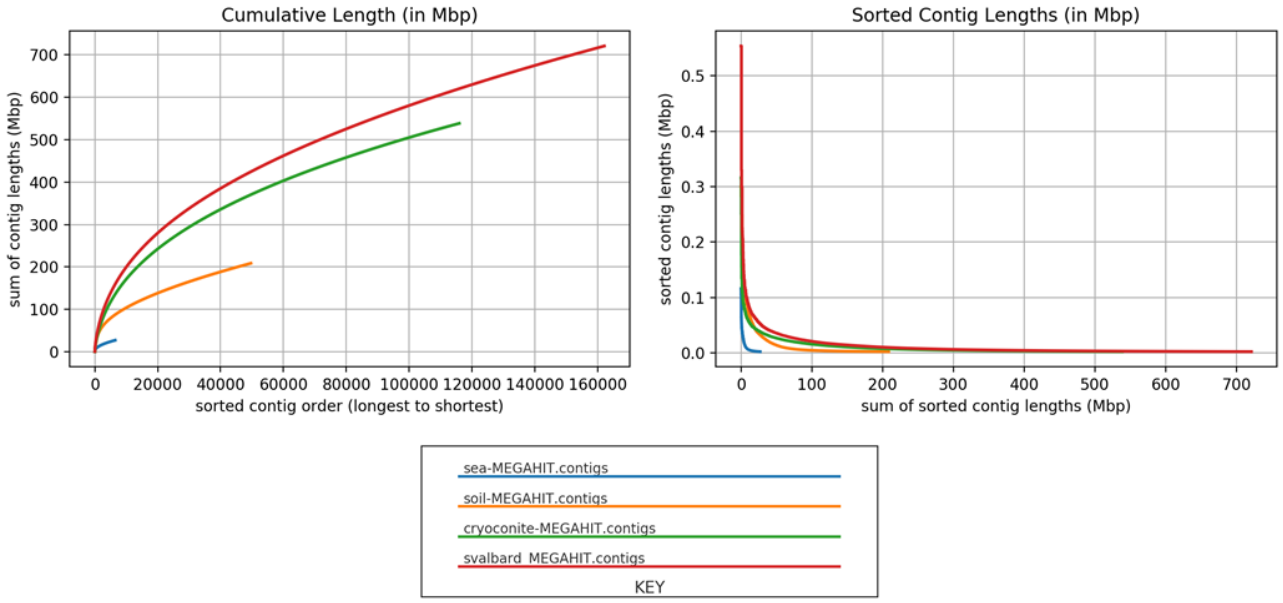

Figure 4-8 Comparison of cryoconite, soil and seawater co-assemblies and combined Svalbard co-assembly.

Table 4-3 Assembly Statistics for the Svalbard metagenomes

Assembly	Longest contig (bp)	Nx (Lx)		Length (bp)	Num Contigs	Sum Length (bp)	Contig Length Histogram (1bp <= len < 10Kbp)	Contig Length Histogram (10Kbp <= len < 100Kbp)	Contig Length Histogram (len >= 100Kbp)
cryoconite-MEGAHIT	315846	N50:	5126	>= 10^6	0	0	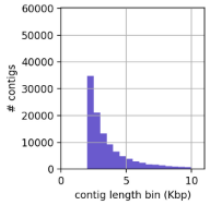	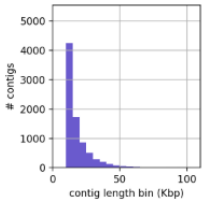	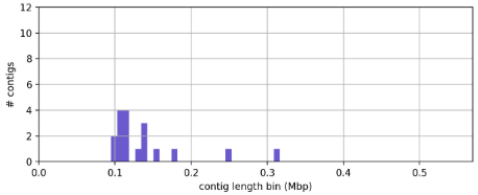
		L50:	(24906)	>= 10^5	18	2524410			
		N75:	2995	>= 10^4	8246	154707901			
		L75:	(60198)	>= 10^3	115949	538521980			
		N90:	2329	>= 500	115949	538521980			
		L90:	(90952)	>= 1	115949	538521980			
soil-MEGAHIT	300154	N50:	4111	>= 10^6	0	0	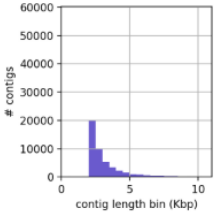	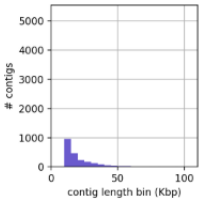	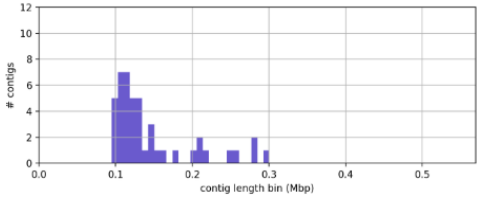
		L50:	(10133)	>= 10^5	45	6597658			
		N75:	2616	>= 10^4	2366	59047038			
		L75:	(26569)	>= 10^3	49641	208560096			
		N90:	2199	>= 500	49641	208560096			
		L90:	(39681)	>= 1	49641	208560096			
sea-MEGAHIT	115659	N50:	4236	>= 10^6	0	0	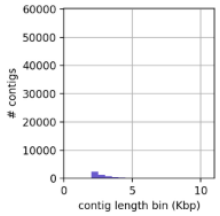	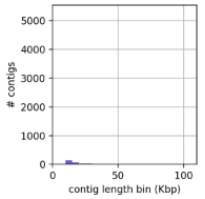	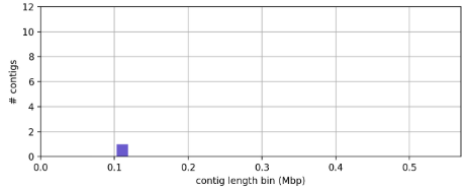
		L50:	(1450)	>= 10^5	2	221424			
		N75:	2686	>= 10^4	321	6766634			
		L75:	(3510)	>= 10^3	6451	26970110			
		N90:	2225	>= 500	6451	26970110			
		L90:	(5171)	>= 1	6451	26970110			
Svalbard MEGAHIT	554015	N50:	4739	>= 10^6	0	0	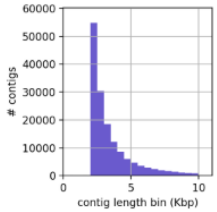	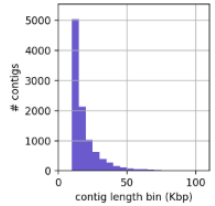	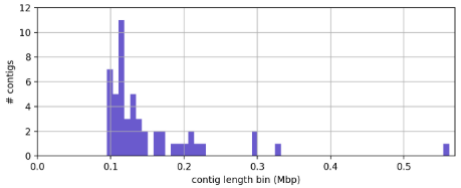
		L50:	(34565)	>= 10^5	51	7820617			
		N75:	2833	>= 10^4	10130	201062657			
		L75:	(85286)	>= 10^3	162105	720998358			
		N90:	2268	>= 500	162105	720998358			
		L90:	(128180)	>= 1	162105	720998358			

4.3.4 Metagenome Assembled Genomes

The contigs from the MEGAHIT assembly were clustered into 151 bins using CONCOCT (v 1.1.0) (Appendix Table D-5), 180 bins using MaxBin2 (version 2.2.7) (Appendix Table D-6), and 225 bins using metaBAT2 (v 2.12.1) (Appendix Table D-7). The bins in each collection were compared using DAS Tool (v 1.1.2) (Appendix Table D-8) and a refined collection of 95 bins with completion > 50% was created. The taxonomic classification of the bins from each binning method (collection) were checked using anvi-estimate-scg-taxonomy, using the contigs database, merged profile, and collection (Appendix Table D-4).

4.3.4.1 Manual Bin Refining

The bins were refined multiple times using anvi-refine and the method described in Chapter 8 (Section 8.2.5). A final collection consisting of 74 MAGs was kept for the remainder of the study. The final collection consists of 41 high quality draft genomes (completion > 90 % (prefix MAG) and 32 medium quality draft genomes (completion >70%, redundancy < 10% (prefix mag)). This collection of MAGS recruited 262,080,978 nucleotides, which represent only 36.35% of all nucleotides stored in the contigs and profile databases. The remaining contigs belonged to species present in too low abundance to properly be resolved into genomes by this sampling effort.

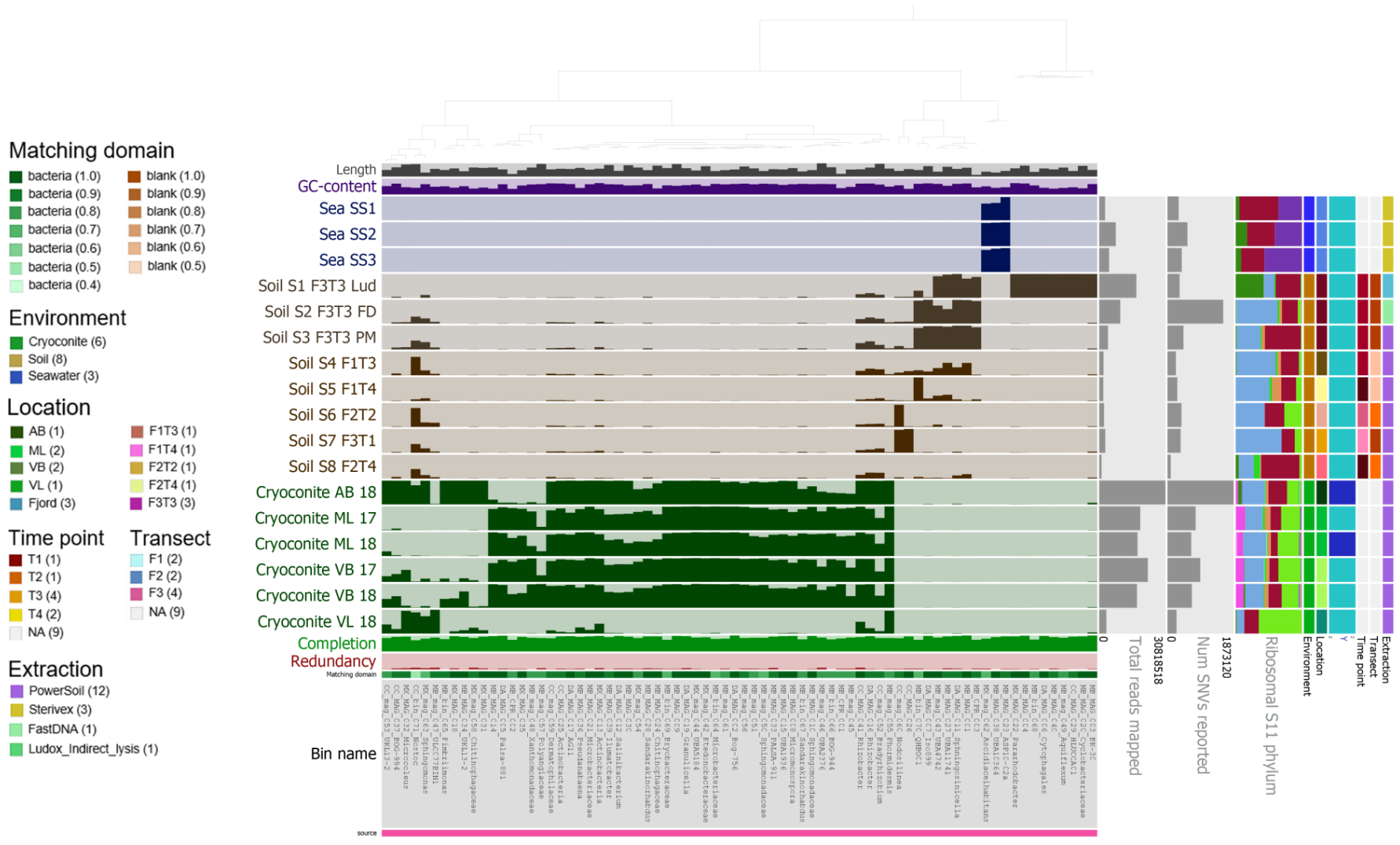

Figure 4-9 Figure showing the MAGS included in the dataset. Figure is generated using anvi-interactive from anvi'o. MAGS are ordered using mean-coverage and viewed using 'detection' which shows proportion of the MAG which has at least 1 X coverage.

Table 4-4 Table of high quality MAGS (completion >90%, redundancy < 10%)

Name	total length	num contigs	N50	GC content	percent completion	percent redundancy	SCG Taxonomy (GTDB)	n	Taxonomy kaiju	Kaiju %
Cryoconite										
DA_MAG_002_Bog-756	3194344	178	29706	65.93	100.00	1.41	Bog-756	21	Unknown_Iamiaceae	21.15
DA_MAG_005_Palsa-881	3232581	248	20887	64.11	98.59	4.23	Palsa-881 sp003136615	10	Caulobacter	27.72
MB_MAG_008_Micromonospora	3827765	339	16209	64.22	97.18	1.41	Micromonospora maris	1	Streptomyces	13.75
MB_MAG_010_Sphingomonadaceae	2931628	291	13543	65.14	97.18	2.82	Sphingomonadaceae	4	Sphingomonas	24.57
MB_MAG_009	5637460	593	12640	54.47	97.18	2.82	none	0	Candidatus Promineofilum	6.70
DA_MAG_012_Salinibacterium	2581198	166	23432	62.93	97.18	4.23	Salinibacterium sp001725325	21	Salinibacterium	34.25
MX_MAG_013_Actinobacteria	3574416	307	23221	71.23	97.18	7.04	Actinobacteria	4	Streptomyces	14.29
MB_MAG_015_UBA1936	3222436	215	27127	60.08	95.77	1.41	UBA1936 sp002336985	13	Sphingomonas	62.25
MB_MAG_014	4081280	530	9503	36.55	95.77	1.41	none	0	Haliscomenobacter	16.6
DA_MAG_017_AG11	3429033	213	24246	65.44	95.77	2.82	AG11 sp003223455	11	Gemmatirosa	63.98
DA_MAG_016_Rhizobacter	4051397	233	26619	68.71	95.77	2.82	Rhizobacter sp003152055	15	Rhizobacter	23.77
MX_MAG_018	3683642	435	12732	42.97	95.77	5.63	none	0	None	8.6
DA_MAG_019_Granulicella	3773816	296	17675	58.01	95.77	7.04	Granulicella tundricola	14	Granulicella	77.52
MB_MAG_021_Microbacteriaceae	3151193	231	19819	64.26	94.37	0.00	Microbacteriaceae	15	Salinibacterium	21.77
CC_MAG_025_Actinobacteria	3532430	250	17768	68.78	94.37	4.23	Actinobacteria	4	Streptomyces	18.89
MB_MAG_024_Chitinophagaceae	4943213	471	15645	37.88	94.37	4.23	Chitinophagaceae	5	Panacibacter	13.49
MB_MAG_028_Sandarakinorhabdus	2904960	437	7986	65.46	94.37	5.63	Sandarakinorhabdus sp002256005	4	Sphingomonas	29.75
MB_MAG_030	5120342	663	9491	56.41	92.96	4.23	none	0	Fimbriimonas	7.67
MX_MAG_031	3923198	439	13667	43.19	92.96	5.63	Unknown	1	None	10.96
MX_MAG_032_Microcoleus	5457007	948	6866	45.41	92.96	7.04	Microcoleus sp003003725	21	Oscillatoria	90.19
MB_MAG_033_PALSA-911	3340025	391	10992	65.58	92.96	8.45	PALSA-911 sp003133265	7	Acidibrevibacterium	14.47
MB_MAG_034_UKL13-2	2402288	476	5405	51.80	91.55	1.41	UKL13-2 sp001602455	7	Unknown_Betaproteobacteria	20.8
MX_MAG_035	2850025	287	13776	56.12	91.55	2.82	Unknown	0	Bdellovibrio	7.9
MB_MAG_036_Pseudanabaena	3926578	347	16026	41.06	91.55	4.23	Pseudanabaena	15	Pseudanabaena	81.84
CC_MAG_037_ BOG-994	4187073	330	18017	68.21	91.55	5.63	BOG-994 sp003136595	7	Variovorax	5.25
MB_MAG_039_Ilumatobacter	5220682	511	15028	64.26	90.14	1.41	Ilumatobacter coccineus	1	Unknown_Iamiaceae	17.05
CC_MAG_041_Rhizobacter	3284861	228	21863	68.04	90.14	9.86	Rhizobacter sp003152055	17	Rhizobacter	25.9

Table 4.5 continued…

Name	total length	num contigs	N50	GC content	percent completion	percent redundancy	SCG taxonomy (GTDB)	n	Taxonomy kaiju	Kaiju %
Seawater										
MB_MAG_023_ASP10-02a	2563445	129	32893	45.24	94.37	2.82	ASP10-02a sp002335115	20	Candidatus Thioglobus	6.75
MB_MAG_038_UBA10364	1841681	133	18813	41.70	90.14	0.00	UBA10364 sp002430755	21	Owenweeksia	21.43
Soil										
MB_MAG_001	3997738	152	39686	69.07	100.00	1.41	none	0	Luteitalea	5.8
MB_MAG_003_BK-30	3001625	147	29296	65.34	100.00	2.82	Burkholderiaceae_BK-30	21	Hydrogenophaga	45.35
MB_MAG_004	4947466	409	16841	68.99	98.59	1.41	none	0	Ferrovibrio	7.49
DA_MAG_006_Cytophagales	3673287	48	136173	42.04	97.18	0.00	Sporocytophaga myxococcoides	3	Cytophaga	33.53
DA_MAG_007_Iso899	4713114	185	33034	69.61	97.18	1.41	Iso899 sp000421445	11	Streptomyces	18.83
DA_MAG_011_Sphningosinicella	3477485	118	42505	66.66	97.18	4.23	Sphningosinicella sp003012735	12	Sphingosinicella	86.05
MB_MAG_020_ Cyclobacteriaceae	4845095	302	22910	38.78	94.37	0.00	Cyclobacteriaceae	4	Unknown_Flammeovirgaceae	18.15
MX_MAG_022_Pararhodobacter	3720906	603	7696	70.98	94.37	2.82	Pararhodobacter sp001314715	10	Rhodobaca	13.27
CC_MAG_026	3384069	404	11587	35.24	94.37	4.23	none	0	Haliscomenobacter	15.02
MB_MAG_027_UBA11741	4420110	372	16213	54.65	94.37	5.63	*UBA11741 sp002427845*	6	Chloracidobacterium	12.93
CC_MAG_029_HLUCCA01	2523900	60	69398	45.16	92.96	0.00	HLUCCA01	6	Candidatus Cyclonatronum	81.15
MB_MAG_040	3254196	446	8589	36.52	90.14	4.23	none	0	Flavobacterium	7.4

Table 4-5 Table of medium quality MAGS (completion >70%. Redundancy < 10%)

Name	total length	num contigs	N50	GC content	percent completion	percent redundancy	SCG Taxonomy (GTDB)	n	Taxonomy kaiju	Kaiju %
Cryoconite										
MX_mag_042_Ktedonobacteraceae	4685611	848	6700	53.2	88.73	1.41	Ktedonobacteraceae	4	Unknown_Ktedonobacteria	66.35
MB_mag_045	3183126	474	7727	47.61	87.32	4.23	none	0	Unknown_Ktedonobacteria	25.32
MB_mag_047_ULC077BIN1	3491281	719	5103	48.58	87.32	9.86	ULC077BIN1 sp003249025	18	*Leptolyngbya*	19.47
MX_mag_044_UBA5184	2744076	427	8453	62.42	87.32	2.82	Palsa-1515 sp003158195	4	Unknown_Bacteria	3.49
MB_mag_046_UBA2376	6278991	987	7373	66.04	87.32	9.86	UBA2376 sp002344285	2	*Haliangium*	27.86
MB_mag_048_Xanthomonadaceae	4060943	245	25552	62.82	85.92	0	Xanthomonadaceae	8	*Lysobacter*	15.77
MB_mag_051	3703043	665	6064	63.99	85.92	4.23	conflict	2	*Fimbriimonas*	5.86
MB_mag_050_Sphingomonadaceae	2515818	320	10297	67.47	85.92	2.82	Sphingomonadaceae	3	*Sphingomonas*	24.61
MX_mag_058_Chitinophagaceae	4091667	812	6024	37.06	84.51	9.86	Chitinophagaceae	6	*Panacibacter*	11.58
MB_mag_055_Phormidesmis	3621916	480	8841	49.44	84.51	2.82	*Phormidesmis priestleyi*	18	*Leptolyngbya*	55.49
CC_mag_053_UKL13-2	2993940	633	5373	52.59	84.51	1.41	UKL13-2 sp001602455	6	Unknown_Betaproteobacteria	19.75
MX_mag_054	4076001	831	5585	57.29	84.51	2.82	none	0	Unknown_Ktedonobacteria	19.86
CC_mag_052_Bradyrhizobium	5766360	626	13724	62.24	84.51	1.41	*Bradyrhizobium*	18	*Bradyrhizobium*	80.79
MB_mag_057_Polyangiaceae	5712704	946	6896	64.77	84.51	7.04	*Polyangiaceae Labilithrix*	4	*Labilithrix*	44.61
MB_mag_056	4563212	885	5536	67.99	84.51	4.23	none	0	*Streptomyces*	4.86
CC_mag_059_Dermatophilaceae	3256706	382	10773	69.57	83.1	1.41	*Dermatophilaceae*	10	*Intrasporangium*	18.85
MB_CPR_001	1237930	82	22880	39.7	81.69	4.23	none	0	None	11.36
MB_mag_061	2915558	669	4501	63.5	80.28	4.23	conflict	2	*Fimbriimonas*	4.63
MX_mag_063_Sphingomonas	1824331	443	4446	64.65	80.28	7.04	*Sphingomonas*	9	*Sphingomonas*	70.88
MB_bin_064_Microbacteriaceae	2485453	163	20769	66.28	78.87	1.41	*Microbacteriaceae*	9	*Lysinimonas*	44.63
MB_bin_065_Fimbriimonas	2967189	515	6437	51.23	77.46	0	*Fimbriimonas*	3	*Fimbriimonas*	64.47
MB_bin_066_BOG-944	4204385	780	5915	65.14	76.06	0	BOG-944 sp003134215	1	*Fimbriimonas*	5.51
MB_bin_067_Sandarakinorhabdus	2323251	375	7206	66.66	76.06	1.41	*Sandarakinorhabdus*	6	*Sphingomonas*	33.6
MB_CPR_002	1175402	195	7155	34.97	73.24	2.82	none	0	None	11.79
MB_bin_069_Bryobacteraceae	3840205	557	8316	57.14	73.24	2.82	*Bryobacteraceae*	2	*Candidatus Solibacter*	59.78
CC_bin_071_Nostoc	5614383	1271	4836	41.94	70.42	9.86	*Nostoc* sp002949735	11	*Nostoc*	91.82

Table 4.6 continued…

Name	total length	num contigs	N50	GC content	percent completion	percent redundancy	SCG Taxonomy (GTDB)	n	Taxonomy kaiju	Kaiju %
Seawater										
MX_mag_062_Ascidiaceihabitans	2223744	556	4225	50.99	80.28	4.23	*Ascidiaceihabitans* sp002478745	18	*Sulfitobacter*	32.37
Soil										
MB_mag_043_UBA4742	2225260	392	6786	66.48	87.32	1.41	UBA4742 sp002403895	1	*Unknown_Iamiaceae*	21.43
MB_mag_049_Aquiflexum	4067355	204	34607	41.04	85.92	1.41	*Aquiflexum balticum*	17	*Belliella*	66.53
CC_mag_060_Nodosilinea	2559317	740	3583	57.28	83.1	2.82	*Nodosilinea*	19	*Halomicronema*	21.89
MB_bin_068	2134956	206	13635	56.75	74.65	2.82	none	0	*Fimbriimonas*	46.19
MB_CPR_003	763139	102	9802	44.66	73.24	4.23	none	0	*Unknown_Candidatus_ Saccharibacteria*	45.1
MB_bin_070_QHBO01	2957152	263	15831	67.08	73.24	4.23	QHBO01 sp003243965	2	*Streptomyces*	6.39

4.3.5 Phylogenomic tree of Svalbard MAGs

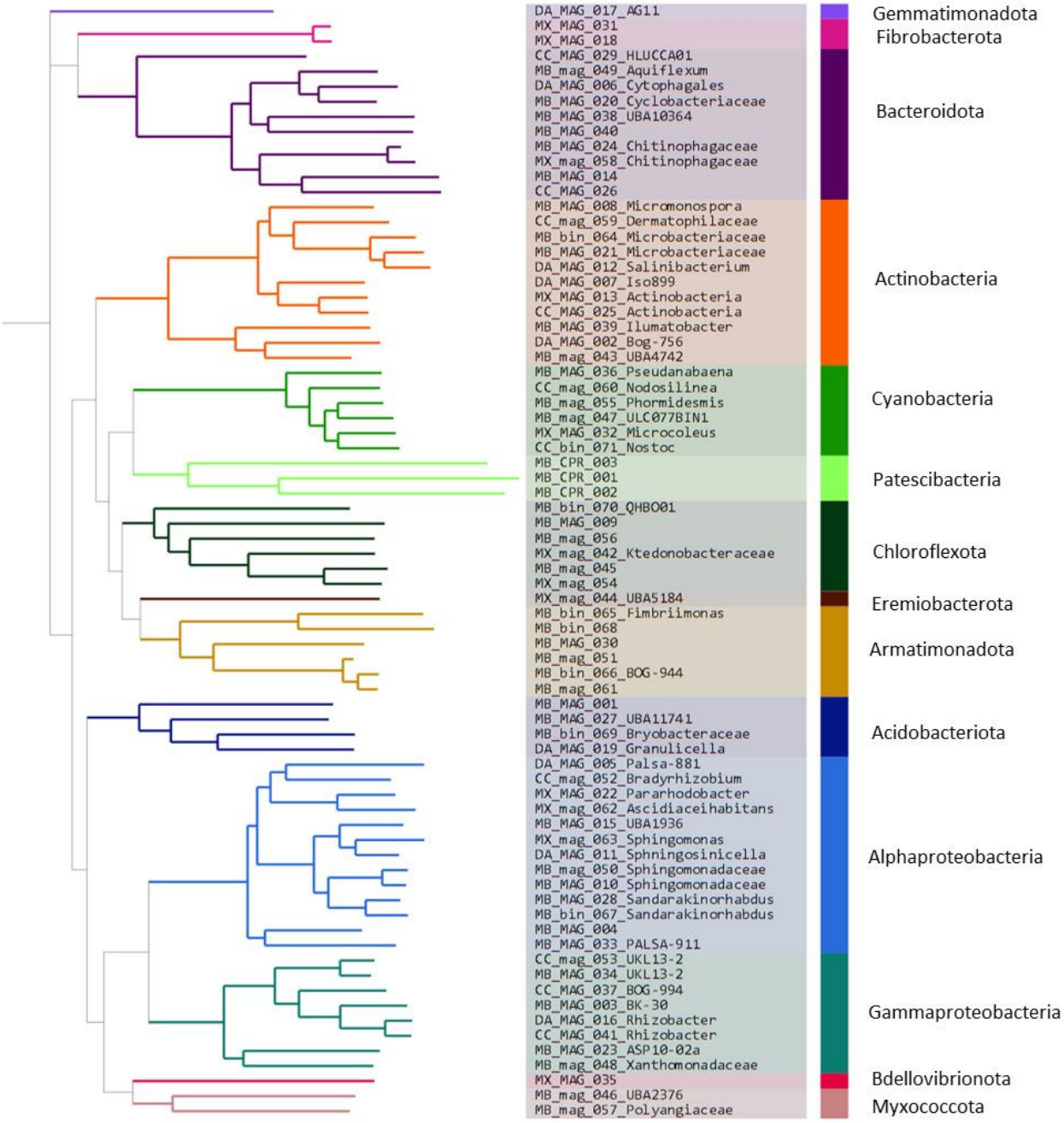

Figure 4-10 Phylogeny of MAGs created by Fast Tree of Muscle alignment of 71 single copy core genes.

4.3.5.1 GTDB-Tk Classification of MAGS

The MAGs were classified taxonomically using two different methods. A phylogenomic tree was constructed using a curated list of 71 genes (Lee, 2019) (Figure 4-10) and MAGs were classified using the GTDB-Tk (Table 4-7). Both methods gave similar results and clades within the phylogenomic tree (Figure 4-10) related to the 14 different phyla identified using GTDB-Tk (Table 4-7). In order of abundance, these were the Proteobacteria (α = 13, γ =8), Actinobacteriota (11), Bacteroidota (10) and the Cyanobacteria (6). The Chloroflexota (5) and Chloroflexota_A (1), Armatimonadota (6), Acidobacteriota (4) and Patescibacteria (3) also had several members. Finally, we resolved two MAGs each from the Myxococcota and Fibrobacterota, and a single MAG member from Bdellovibrionota, Eremiobacterota and Gemmatimonadota.

Two of the MAGs, MB_mag_055_Phormidesmis and MB_MAG_023_ASP10-02a were assigned to species-level using FastANI (Jain et al., 2018) within the GTDB-TK (Chaumeil et al., 2020) with ANI > 95% and an alignment fraction >65% (Table 4-6). MB_mag_055_Phormidesmis is very similar to the *Phormidesmis priestleyi* strain BC1401, isolated from cryoconite in a Greenland glacier. MB_MAG_023_ASP10-02a is very similar to an Oceanospirillaceae bacterium UBA2001 isolated from subsurface seawater marine metagenome from the North Sea (Parks et al., 2017). The remainder of the MAGS were assigned to novel species within their genus.

Table 4-6 Table of MAGS classified to species level using FastANI

User Genome	Classification	FastANI Reference	FastANI Reference	FastANI ANI	Alignment Fraction	Location	Reference
MB_mag_055_Phormidesmis	p__Cyanobacteria; c__Cyanobacteriia; o__Leptolyngbyales; f__Leptolyngbyaceae; g__Phormidesmis_A; s__Phormidesmis_A priestleyi_B	GCF_001650195.1	95	99.29	0.97	Cryoconite, Greenland	(Chrismas et al., 2016a)
MB_MAG_023_ASP10-02a	p__Proteobacteria; c__Gammaproteobacteria; o__Pseudomonadales; f__Nitrincolaceae; g__ASP10-02a; s__ASP10-02a sp002335115	GCA_002335115.1	95	95.44	0.86	Subsurface seawater, North Sea	(Parks et al., 2017)

Table 4-7 Classification of MAGS using GTDB-Tk

Phylum	Genus	MAG	Classification Method	Note	AA Percent	RED Value	Closest Placement Reference	Closest Placement Taxonomy	Closest Placement ANI	Closest Placement Alignment Fraction
Acidobacteriota	Granulicella	DA_MAG_019_Granulicella	P	C: TOP	89.15	0.961	GCF_000178975.2	*Granulicella tundricola*	78.41	0.23
	BOG-234	MB_bin_069_Bryobacteraceae	P	N: RED	70.56	0.891				
	UBA11741	MB_MAG_027_UBA11741	P	C: TOP	90.91	0.94				
		MB_MAG_001	P	N: RED	95.02	0.703				
Actinobacteriota		MB_mag_043_UBA4742	P	N: RED	76.59	0.598				
	Bog-756	DA_MAG_002_Bog-756	P	C: TOP	89.92	0.939				
		MB_MAG_039_Ilumatobacter	P	N: RED	87.76	0.82				
		MB_MAG_008_Micromonospora	P	C: TOP	96.69	0.604				
	GCA-2748155	CC_mag_059_Dermatophilaceae	P	N: RED	78.93	0.861				
	Salinibacterium	DA_MAG_012_Salinibacterium	P	C: TOP	94.03	0.967	GCF_900230175.1	*Salinibacterium xinjiangense*	77.83	0.26
	UBA10887	MB_MAG_021_Microbacteriaceae	P	N: RED	87.02	0.966	GCA_003454135.1	*UBA10887* sp003454135	79.23	0.43
	UBA1487	MB_bin_064_Microbacteriaceae	P	C: TOP	84.62	0.944	GCA_002325245.1	*UBA1487* sp002325245	78.91	0.36
		CC_MAG_025_Actinobacteria	P	N: RED	89.31	0.704				
		MX_MAG_013_Actinobacteria	P	N: RED	94.42	0.712				
	Iso899	DA_MAG_007_Iso899	P	N: RED	93.19	0.93				
Armatimonadota		MB_bin_066_BOG-944	P	N: RED	69.05	0.694				
		MB_mag_051	P	N: RED	69.8	0.693				
		MB_mag_061	P	N: RED	47.62	0.707				
		MB_MAG_030	P	N: RED	90.22	0.734				
		MB_bin_065_Fimbriimonas	P	N: RED	74.48	0.888				
		MB_bin_068	P	C: TOP	79.37	0.775				

Table 4-7 continued…

Phylum	Genus	MAG	Classification Method	Note	AA Perc ent	RED Value	Closest Placement Reference	Closest Placement Taxonomy	Closest Placement ANI	Closest Placement Alignment
Bacteroidota	Ferruginibacter	MB_MAG_024_Chitinophagaceae	P	C: TOP	95.36	0.902				
		MX_mag_058_Chitinophagaceae	P	C: TOP	78.41	0.901				
		MB_MAG_014	P	C: TOP	85.97	0.714				
	UBA3362	CC_MAG_026	P	N: RED	88.51	0.881				
		MB_MAG_020_Cyclobacteriaceae	P	N: RED	97.16	0.808				
	Cecembia	MB_mag_049_Aquiflexum	P	C: TOP	83.12	0.98	GCF_003014575.1	*Cecembia rubra*	82.37	0.69
		DA_MAG_006_Cytophagales	P	N: RED	98	0.845				
	UBA10364	MB_MAG_038_UBA10364	P	C: TOP	91.96	0.993	GCA_003487785.1	*UBA10364 sp003487785*	87.14	0.83
		MB_MAG_040	P	N: RED	83.23	0.848				
	UBA11400	CC_MAG_029_HLUCCA01	P	N: RED	91.45	0.879				
Bdellovibrionota	UBA1018	MX_MAG_035	P	N: RED	89.23	0.854				
Chloroflexota		MB_MAG_009	P	N: RED	91.19	0.797				
		MB_mag_045	P	N: RED	78.99	0.609				
		MX_mag_054	P	N: RED	72.24	0.608				
		MX_mag_042_Ktedonobacteraceae	P	C: TOP	85.36	0.869				
		MB_mag_056	P	N: RED	76.37	0.519				
Chloroflexota_A		MB_bin_070_QHBO01	P	N: RED	83.59	0.842	GCA_003243965.1	*QHBO01 sp003243965*	77.35	0.29
Cyanobacteria	Microcoleus	MX_MAG_032_Microcoleus	P	C: TOP	85.69	0.982	GCF_003003725.1	*Microcoleus sp003003725*	89.64	0.81
	Phormidesmis_A	MB_mag_055_Phormidesmis	ANI/ P	F: TOP+ ANI	80.42		GCF_001650195.1	*Phormidesmis_A priestleyi_B*	99.29	0.97
	ULC077BIN1	MB_mag_047_ULC077BIN1	P	N: RED	70.79	0.971	GCA_003249025.1	*ULC077BIN1 sp003249025*	83.83	0.8
	Nodosilinea	CC_mag_060_Nodosilinea	P	C: TOP	64.13	0.969				
	Pseudanabaena	MB_MAG_036_Pseudanabaena	P	C: TOP	91.17	0.978	GCA_003242085.1	*Pseudanabaena frigida*	80.5	0.68
	Nostoc	CC_bin_071_Nostoc	P	C: TOP	65.77	0.96				

Table 4-7 continued…

Phylum	Genus	MAG	Classification Method	Note	AA Percent	RED Value	Closest Placement Reference	Closest Placement Taxonomy	Closest Placement ANI	Closest Placement
Eremiobacterota	Palsa-1515	MX_mag_044_UBA5184	P	N: RED	80.12	0.893				
Fibrobacterota		MX_MAG_018	P	N: RED	87.7	0.787				
		MX_MAG_031	P	N: RED	92.6	0.783				
Gemmatimonadota	2013-60CM-65-52	DA_MAG_017_AG11	P	N: RED	84.44	0.929	GCA_002215645.1	2013-60CM-65-52 sp002215645	78.45	0.34
Myxococcota		MB_mag_046_UBA2376	P	N: RED	80.62	0.829	GCA_002344285.1	UBA2376 sp002344285	76.62	0.31
		MB_mag_057_Polyangiaceae	P	N: RED	70.63	0.831				
Patescibacteria	PJMF01	MB_CPR_002	P	C: TOP	55.38	0.806				
		MB_CPR_001	P	N: RED	64.76	0.895				
		MB_CPR_003	P	C: TOP	57.52	0.761				
Proteobacteria	BOG-908	MB_MAG_033_PALSA-911	P	N: RED	85.1	0.858				
	Palsa-881	DA_MAG_005_Palsa-881	P	C: TOP	93.61	0.961	GCA_003161535.1	Palsa-881 sp003161535	77.07	0.31
		MB_MAG_004	P	N: RED	93.63	0.749				
	Bradyrhizobium	CC_mag_052_Bradyrhizobium	P	C: TOP	81.43	0.987	GCA_001464035.1	*Bradyrhizobium* sp001464035	84.13	0.61
	Ascidiaceihabitans	MX_mag_062_Ascidiaceihabitans	P	C: TOP	72.22	0.998	GCA_002478745.1	*Ascidiaceihabitans* sp002478745	89.75	0.78
	Pararhodobacter	MX_MAG_022_Pararhodobacter	P	C: TOP	87.62	0.944				
		MB_bin_067_Sandarakinorhabdus	P	N: RED	58.47	0.86				
		MB_MAG_010_Sphingomonadaceae	P	N: RED	93.35	0.846				
		MB_MAG_028_Sandarakinorhabdus	P	N: RED	84.17	0.859				
		MB_mag_050_Sphingomonadaceae	P	C: TOP	78.97	0.812				
	Sphingomonas_A	MX_mag_063_Sphingomonas	P	C: TOP	55.46	0.944	GCF_000585415.1	*Sphingomonas_A jaspsi*	78.74	0.51
	Sphningosinicella	DA_MAG_011_Sphningosinicella	P	C: TOP	93.13	0.947	GCF_003012735.1	*Sphningosinicella* sp003012735	79.26	0.48

Table 4-6 continued…

Phylum	Genus	MAG	Classification Method	Note	AA Percent	RED Value	Closest Placement Reference	Closest Placement Taxonomy	Closest Placement ANI	Closest Placement Alignment Fraction
Proteobacteria	UBA1936	MB_MAG_015_UBA1936	P	C: TOP	96.37	0.956	GCA_002336985.1	UBA1936 sp002336985	77.31	0.24
		MB_MAG_003_BK-30	P	C: TOP	96.61	0.95				
	BOG-994	CC_MAG_037_BOG-994	P	N: RED	84.54	0.893				
	Rhizobacter	CC_MAG_041_Rhizobacter	P	C: TOP	89.25	0.974	GCA_003152055.1	*Rhizobacter* sp003152055	80.99	0.61
	Rhizobacter	DA_MAG_016_Rhizobacter	P	C: TOP	91.67	0.973	GCA_003152055.1	*Rhizobacter* sp003152055	82.36	0.61
	UKL13-2	CC_mag_053_UKL13-2	P	N: RED	80.63	0.898				
		MB_MAG_034_UKL13-2	P	N: RED	84.58	0.899				
	ASP10-02a	MB_MAG_023_ASP10-02a	ANI/ P	F: TOP+ANI:	92.24		GCA_002335115.1	ASP10-02a sp002335115	95.44	0.86
		MB_mag_048_Xanthomonadaceae	P	C: TOP	86.59	0.855				

P: Placement
C: TOP: taxonomic classification fully defined by topology
N: RED: taxonomic novelty determined using RED
F: T+ANI: topological placement and ANI have congruent species assignments

4.3.6 Spatial distribution of MAGs

Reads from each library (site) were mapped back to contigs by anvi'o to create a profile. High read coverage at a site reflects high abundance, whereas low coverage indicates the absence of the genome at the site. In this way it is possible to map relative abundance of the MAGs across different sites. By clustering the MAGs by site, groups of commonly co-occurring bacteria can be identified. The spatial distribution of the MAGs was plotted using MAG-centric (Figure 4-11; max-normalised ratio) and sample-centric (Figure 4-12; abundance) values. Both methods compare the coverage of each genome at each site but are normalised in different ways.

4.3.6.1 Max-normalized ratio to identify sites where MAG is most abundant

The max-normalised-ratio of coverage for the MAGs were clustered using the default hierarchical clustering withing the ComplexHeatmap package, and then divided into groups using k-means clustering into k=9 groups of MAGs and k=5 environments (set.seed=5). Groups of MAGs that are similar within sea, cryoconite and soil were identified. Notably, the MAGs in the VL cryoconite sample were very different to those in the cryoconite from ML, VB, and AB. The VL community was missing many of the members that make up the communities on VL, VB and VL, and instead, contained community members more commonly found in glacial forefield soil. The MAGs found in the seawater samples had absolutely no overlap with any of the other environments. Clustering in this way also revealed several MAGs that were present in a single sample or site. This was particularly true of MAGS present only in the F3T3_Ludox soil sample and the cryoconite from AB.

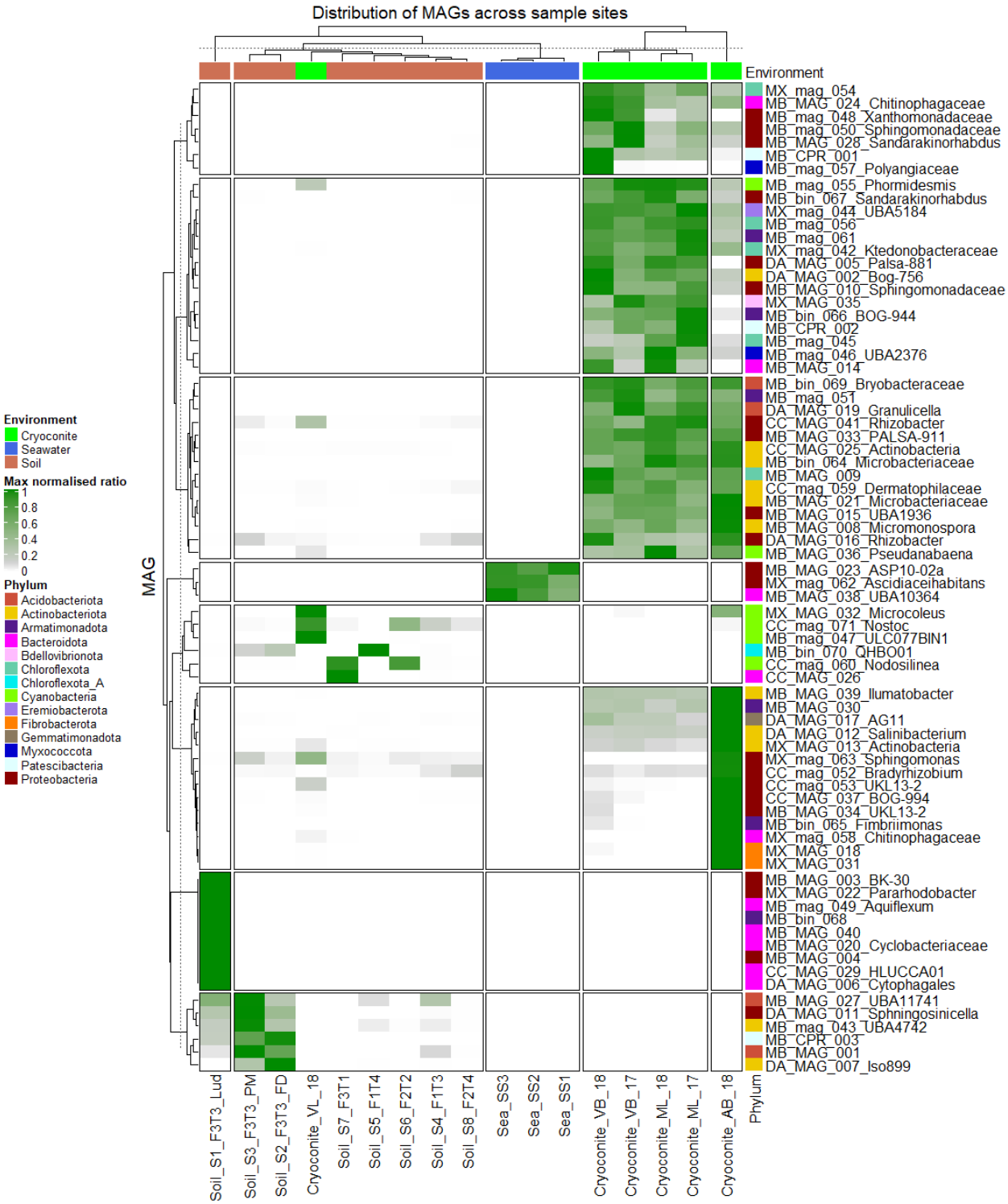

Figure 4-11 Heatmap showing distribution of MAGs across different environments and sites using a MAG-centric view. This view is useful to see in which environment each MAG is the most abundant. It compares each MAG to the same MAG in other environments.

4.3.6.2 The Abundance of MAGs across different sites.

Abundance values in anvi'o are calculated as the mean coverage of each MAG divided by that sample's overall mean coverage across all the MAGs. Abundance values therefore represent the ratio of a MAGs mean coverage to the mean coverage of all the MAGs in the sample. Therefore, MAGs with larger abundance values are more represented in that sample (i.e. recruited more reads) than those contigs with smaller abundance values. This is a useful view for highlighting abundant and rare taxa. Figure 4-12 shows the plotted abundance values of each of the MAGs across the different sites. This visualisation is particularly useful for highlighting the highly abundant (green to blue) MAGs compared to the rare MAGs (wheat and white).

Overall patterns are immediately evident. Firstly, the seawater has the fewest MAGs and these MAGs are not found in the other environments. Secondly, the cryoconite sample from VL is missing a large portion of the community that is present in AB, ML and VB samples. The ML and VB samples are very similar to each other and the VL and AB samples have several species in common that are not found on VB or ML. There are several MAGs, mainly belonging to the Actinobacteria and Proteobacteria that are highly abundant community members in cryoconite, and low abundance members of the soil community. There are also members of the soil community that were not detected in the cryoconite habitats.

There are several MAGs (dark blue) that are highly dominant community members at specific sites. MB_mag_055_Phormidesmis is the most abundant MAG in the cryoconite samples, especially from ML and VB, however it is also found in high abundance on AB and VL and is present at low abundance in soil samples. VL has three highly abundant cyanobacterial MAGs that are absent or extremely rare in the VB and ML samples. Two of these MAGs, CC_mag_071_Nostoc and MX_MAG_032_Microleus are also present in AB, however MB_mag_047_ULC077BIN1, is not found in any of the other cryoconite samples, but is found in all of the soil except F3T3_Lud.

The Cyanobacterial MAG, CC_mag_Nodoslinea_60, is not found in any of the cryoconite samples, but is highly abundant in the two early soil samples (F3T1 and F3T2) and is present, though less abundant, in later soils. The five MAGs belonging to the Chloroflexota are found exclusively in cryoconite, except for MX_mag_042_Ktedonobacteraceae, which is a low abundance member in all the soil samples.

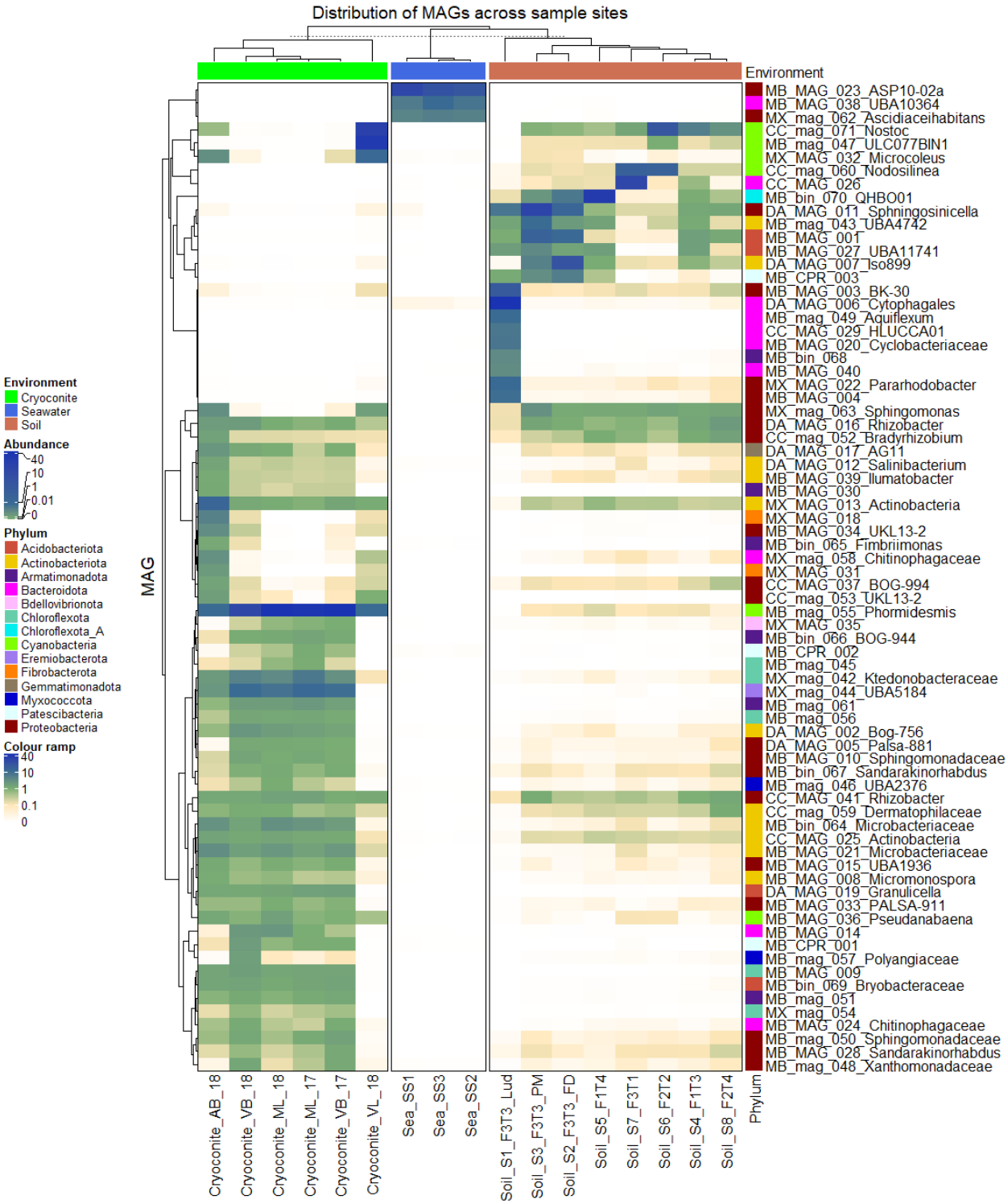

Figure 4-12 The distribution of Svalbard MAGS based on Abundance. Colour guide: Green: MAGs close to sample mean coverage; Blue: MAGs are highly abundant (10- 40x the sample mean); wheat: rare MAGs (0.1 of the sample mean); white: MAGs recruited zero reads in that sample. The phylum membership of MAGs is displayed using a colour legend and environments were forced to cluster together.

The Soil_S1_F3T3_Lud sample is different from all other soil samples, even though the library was extracted from the same soil site as (F3T3). This sample has several highly abundant Bacteroidota MAGs that are present only in this sample. This likely represent an extraction bias and further discussion of this sample will take place in the discussion.

4.3.7 Major biogeochemical cycles

The tool metabolisHMM was run to look for the presence of major genes involved in Carbon, Nitrogen, Sulfur, Oxygen and Hydrogen cycling (Figure 4-13, Figure 4-14).

4.3.7.1 Carbon cycling

Several MAGs had copies of form I RubisCO, including an Actinobacteria, CC_MAG_025_Actinobacteria, from the family Frankiaceae, two Alphaproteobacterial MAGs, MB_MAG_033_PALSA_911 and CC_mag_052_Bradyrhizobium belonging to the family Acetobacteraceae and Xanthobacteraceae respectively as well as a Gammaproteobacterial MAG CC_MAG_037_BOG_994, family Burkholderiaceae. The MAG MB_bin_070_QHBO01 from the phylum Chloroflexota_A and MX_mag_044_UBA5184 from the phylum Eremiobacterota also contained copies.

There were also Form I RubisCO genes in all the cyanobacterial MAGs, except for cc_mag_071_Nostoc_ and CC_mag_060_Nodoslinea. Of note, the cyanobacterial MAGs in this study had <90% completion, and therefore their absence may just reflect the incomplete bins. Interestingly, all MAGs harbouring RubisCO form I genes were most abundant in cryoconite, with the sole exception of MB_bin_070_QHBO01, which was more abundant in soil. Several methylotrophs were identified that had NDMA-dependent methanol dehydrogenase (nmda) and S-(hydroxymethyl)mycothiol dehydrogenase (smdh) genes in two and seven Actinobacterial MAGs, respectively. The smdh enzyme was found in seven of the ten Actinobacterial MAGs. Most of the Actinobacterial MAGs are more prevalent in cryoconite, but DA_MAG_007_Iso899 was more abundant in soil. There is evidence of carbon monoxide (CO) oxidation via carbon monoxide dehydrogenase (coxSML) genes in several Acidobacteria (3/4), Actinobacteria (5/11), Alphaproteobacteria (8/15) and Gammaproteobacteria (4/8) MAGs.

4.3.7.2 Nitrogen cycling

There was only one MAG capable of nitrogen fixation from the resolved genomes. The CC_bin_071_Nostoc had nifD and nifH genes (Figure 4-14), responsible for nitrogen fixation. Soil had a high number of genomes that has nosD and nosZ genes in involved in denitrification. An Alphaproteobacterial MAG, CC_mag_052_Brazyrhizobium, from the order Rhizobiales with a copy of the napA (nitrate reductase) gene was present in all soil and cryoconite samples. A second MAG, MB_MAG_020_Cyclobacteriaceae from the Bacteroidota had a copy of the napA gene but was present only in the F3T3_Ludox samples, which is believed to have been enriched (Section). The narG gene (respiratory nitrate reductase) was present in two Actinobacterial MAGs, CC_MAG_025_Actinobacteria and MB_MAG_008_Micromonospora and two Alphaproteobacterial MAGs, MB_MAG_004 and MX_MAG_022_Pararhodobacter (Figure 4-14). Both Actinobacterial MAGs were common in cryoconite samples, however the proteobacterial MAGs were from the F3T3_Ludox samples.

4.3.7.3 Sulfur cycling

The most common gene detected for sulfur cycling was sulfur dioxygenas (sdo). Sdo oxidizes the sulfane sulfur in GSSH to sulfite, and there were 39 MAGs that had at least one of these genes. The second most abundant gene was sulfate adenylyltransferase (sat), gene, which forms adenosine 5'-phosphosulfate (APS) from ATP and free sulfate, the first step in the formation of the activated sulfate donor 3'-phosphoadenylylsulfate (PAPS). Sat was found in the majority of Cyanobacterial (5/6) and Chloroflexota genomes (4/5) as well as in a few Acidobacteriota (2/5), Alphaproteobacteria (2/13) and Gammaproteobacteria (1/8).

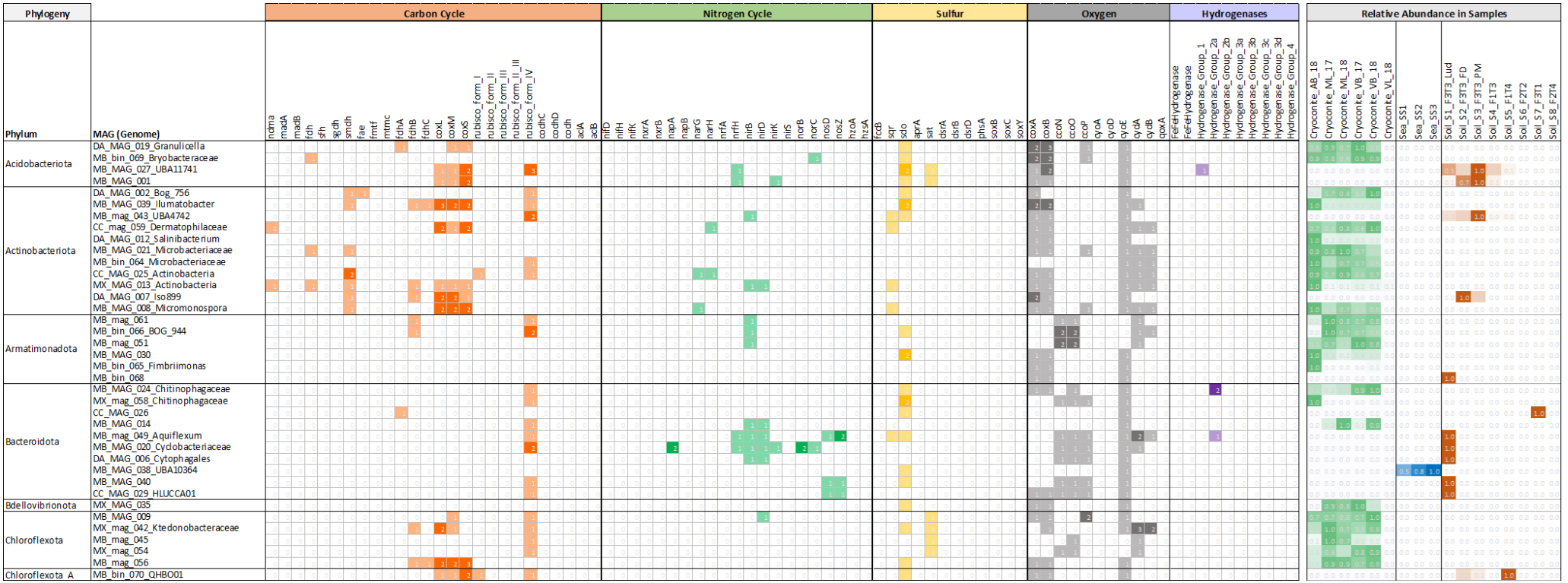

Figure 4-13 Figure 1 showing the detection of key genes in Svalbard MAGS involved in biogeochemical cycling.

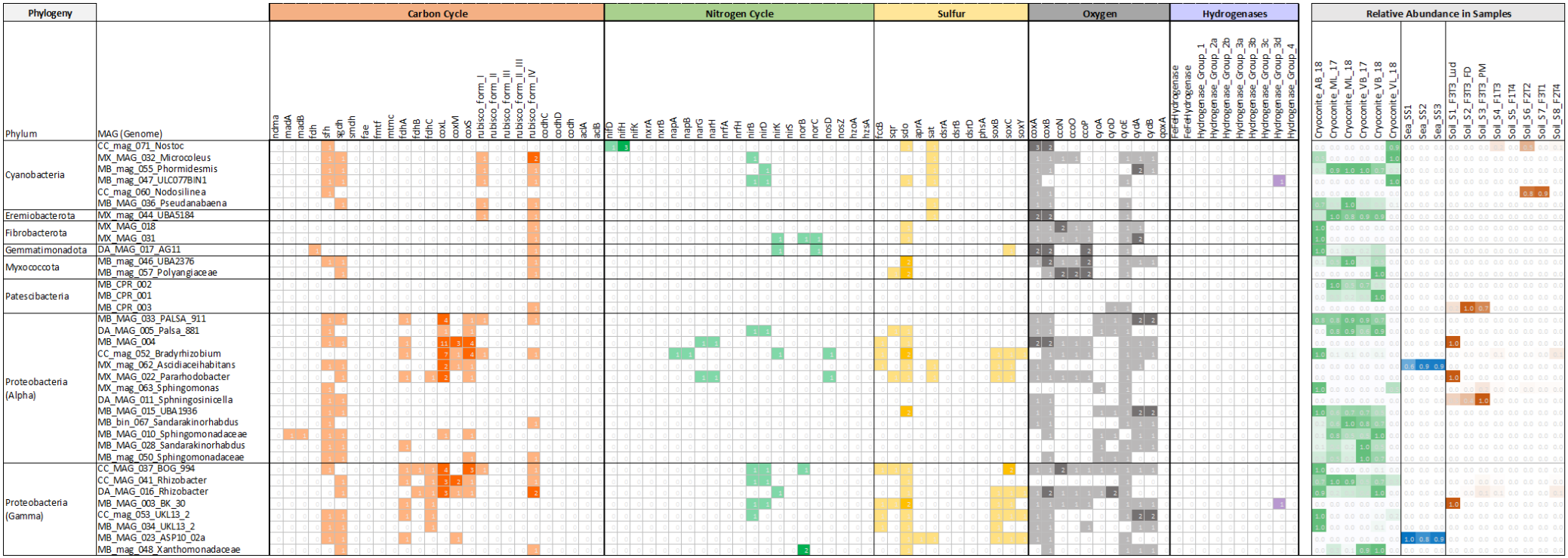

Figure 4-14 Figure 2 showing the detection of key genes in Svalbard MAGS involved in biogeochemical cycling.

4.3.8 Phormidesmis and Leptolyngba pangenome

A pangenome which included five MAGS: MB_mag_055_Phormidesmis, MB_mag_047_ULC077BIN1, MX_MAG_032_Microcoleus, MB_MAG_036_Pseudanabaena and CC_mag_060_Nodosilinea was created in order to confirm the correct taxonomic placement of the MAGs compared to well classified publicly available genomes (Appendix Figure D-3). Following this initial confirmation, a subsequent pangenome of more closely related species was created (Figure 4-15). The old NCBI taxonomy of the organisms has been rewritten by improved taxonomical classification by GTDB (Parks et al., 2018). This has resulted in the refinement and reclassification of the old Leptolyngba family into two new families, the Phormidesmiaceae and Leptolyngbyaceae, and the inclusion of several species previously classified as Synechococcaceae (Table 4-9). There have been rearrangements of genera within these families; Phormidesmis has been split into Phormidesmis and Phormidesmis_A, with Phormidesmis_A being classified within Leptolyngba rather than Phormidesmiaceae. Therefore, the old genus Phormidesmis has been split into different taxonomic orders. The genus Nodoslinea is now classified within Phormidesmiaceae. Based on the close relatedness of species within the Phormidesmiaceae and Leptolyngbyaceae families, and the presence of MAGs, within both families, a pangenome was created using MAGS (Table 4-8) and publicly available genomes (Table 4-9).

Table 4-8 Full GTDB classification of Cyanobacterial MAGs included in the Leptolyngba pangenome analysis

MAG name	Full GTDB-Tk Classification	Sequences for comparison in pangenome
MB_mag_055_Phormidesmis	p__Cyanobacteria; c__Cyanobacteriia; o__Leptolyngbyales; f__Leptolyngbyaceae; g__Phormidesmis_A; s__Phormidesmis_A priestleyi_B	GCF_001650195.1 GCF_001895925.1
MB_mag_047_ULC077BIN1	p__Cyanobacteria; c__Cyanobacteriia; o__Leptolyngbyales; f__Leptolyngbyaceae; g__ULC077BIN1	GCA_003249025.1
CC_mag_060_Nodosilinea	p__Cyanobacteria; c__Cyanobacteriia; o__Phormidesmiales; f__Phormidesmiaceae; g__Nodosilinea; s__	GCA_003249105.1

Table 4-9 Table of publicly available genomes included in the Leptolyngbya Pangenome

ID	NCBI Organism Name	NCBI Taxonomy	GTDB Taxonomy	MAG	Location	MAG or isolate	Ref
GCA_001314865.1	Phormidesmis priestleyi Ana	p__Cyanobacteria; c__; o__Synechococcales; f__Leptolyngbyaceae; g__Phormidesmis; s__Phormidesmis priestleyi	p__Cyanobacteria; c__Cyanobacteriia; o__Phormidesmiales; f__Phormidesmiaceae; g__Phormidesmis; s__Phormidesmis priestleyi_B		Hot Lake microbial mat, Washington	MAG: derived from metagenome Assembly method: IDBA_ud v. 1.1 Genome coverage: 490.0x Sequencing technology: Illumina	(Nelson et al., 2015)
GCA_002286735.1	Leptolyngbya sp. BC1307	p__Cyanobacteria; c__; o__Synechococcales; f__Leptolyngbyaceae; g__Leptolyngbya; s__	p__Cyanobacteria; c__Cyanobacteriia; o__Phormidesmiales; f__Phormidesmiaceae; g__Phormidesmis; s__Phormidesmis sp002286735		Surface ice layer of moat surrounding Lake Hoare, McMurdo Dry Valleys, Antarctica	Isolate: Strain: BC1307 Assembly method: SPAdes v. 3.5 Expected final version: yes Genome coverage: 181.0x Sequencing technology: Illumina HiSeq	(Chrismas et al., 2018)
GCA_003242035.1	Leptolyngbya foveolarum	p__Cyanobacteria; c__; o__Synechococcales; f__Leptolyngbyaceae; g__Leptolyngbya; s__Leptolyngbya foveolarum	p__Cyanobacteria; c__Cyanobacteriia; o__Phormidesmiales; f__Phormidesmiaceae; g__Phormidesmis; s__Phormidesmis foveolarum		Antarctica, Transantarctic Mountains	MAG non-axenic culture: ULC129 Assembly method: SPAdes v. 3.10.1 Expected final version: yes Genome coverage: 18.46x Sequencing technology: Illumina MiSeq	(Cornet et al., 2018)
GCA_003242115.1	Phormidesmis priestleyi	p__Cyanobacteria; c__; o__Synechococcales; f__Leptolyngbyaceae; g__Phormidesmis; s__Phormidesmis priestleyi	p__Cyanobacteria; c__Cyanobacteriia; o__Phormidesmiales; f__Phormidesmiaceae; g__Phormidesmis; s__Phormidesmis priestleyi_A		Antarctica, Larsemann Hills	MAG non-axenic-culture: ULC027bin1 Assembly method: SPAdes v. 3.10.1 Expected final version: yes Genome coverage: 6.26965x	(Cornet et al., 2018)
GCF_000155595.1	Synechococcus sp. PCC 7335	p__Cyanobacteria; c__; o__Synechococcales; f__Synechococcaceae; g__Synechococcus; s__	p__Cyanobacteria; c__Cyanobacteriia; o__Phormidesmiales; f__Phormidesmiaceae; g__Phormidesmis; s__Phormidesmis sp000155595		Shell (intertidal zone)	Craig Venter Institute (www.jcvi.org) sequenced, assembled, and auto-annotated the genomes	(Honda et al., 1999)
GCF_001650195.1	Phormidesmis priestleyi BC1401	p__Cyanobacteria; c__; o__Synechococcales; f__Leptolyngbyaceae; g__Phormidesmis; s__Phormidesmis priestleyi	p__Cyanobacteria; c__Cyanobacteriia; o__Leptolyngbyales; f__Leptolyngbyaceae; g__Phormidesmis_A; s__Phormidesmis_A priestleyi_B	MB_mag_055_ Phormidesmis (A)	Isolate from a cryoconite hole on the Greenland Ice Sheet	Isolate Strain: BC1401 Assembly method: SPAdes v. 3.5.0 Expected final version: no Genome coverage: 340.55x Sequencing technology: Illumina HiSeq	(Chrismas et al., 2016b)

ID	NCBI Organism Name	NCBI Taxonomy	GTDB Taxonomy	MAG	Location	MAG or isolate	Ref
GCF_001895925.1	Phormidesmis priestleyi ULC007	p__Cyanobacteria; c__; o__Synechococcales; f__Leptolyngbyaceae; g__Phormidesmis; s__Phormidesmis priestleyi	p__Cyanobacteria; c__Cyanobacteriia; o__Leptolyngbyales; f__Leptolyngbyaceae; g__Phormidesmis_A; s__Phormidesmis_A priestleyi_A	MB_mag_055_ Phormidesmis (B)	Antarctica, Larsemann Hills	MAG non-axenic-culture: ULC007bin1 Assembly method: SPAdes v. 3.10.1 Expected final version: yes Genome coverage: 26.62x Sequencing technology: Illumina MiSeq	(Cornet et al., 2018)
GCA_003249025.1	Leptolyngbya sp.	p__Cyanobacteria; c__; o__Synechococcales; f__Leptolyngbyaceae; g__Leptolyngbya; s__	p__Cyanobacteria; c__Cyanobacteriia; o__Leptolyngbyales; f__Leptolyngbyaceae; g__ULC077BIN1; s__ULC077BIN1 sp003249025	MB_mag_047_ ULC077BIN1 (A)	Canada microbial mat	derived from metagenome Assembly method: SPAdes v. 3.10.1 Expected final version: yes Genome coverage: 15.08x Sequencing technology: Illumina MiSeq	(Cornet et al., 2018)
GCA_003249105.1	Leptolyngbya sp.	p__Cyanobacteria; c__; o__Synechococcales; f__Leptolyngbyaceae; g__Leptolyngbya; s__	p__Cyanobacteria; c__Cyanobacteriia; o__Phormidesmiales; f__Phormidesmiaceae; g__Nodosilinea; s__Nodosilinea sp003249105	CC_mag_060_N odosilinea	Belgium, Renipont lake	MAG non-axenic culture: ULC186bin1 Assembly method: SPAdes v. 3.10.1 Expected final version: yes Genome coverage: 21.11x Sequencing technology: Illumina MiSeq	(Cornet et al., 2018)

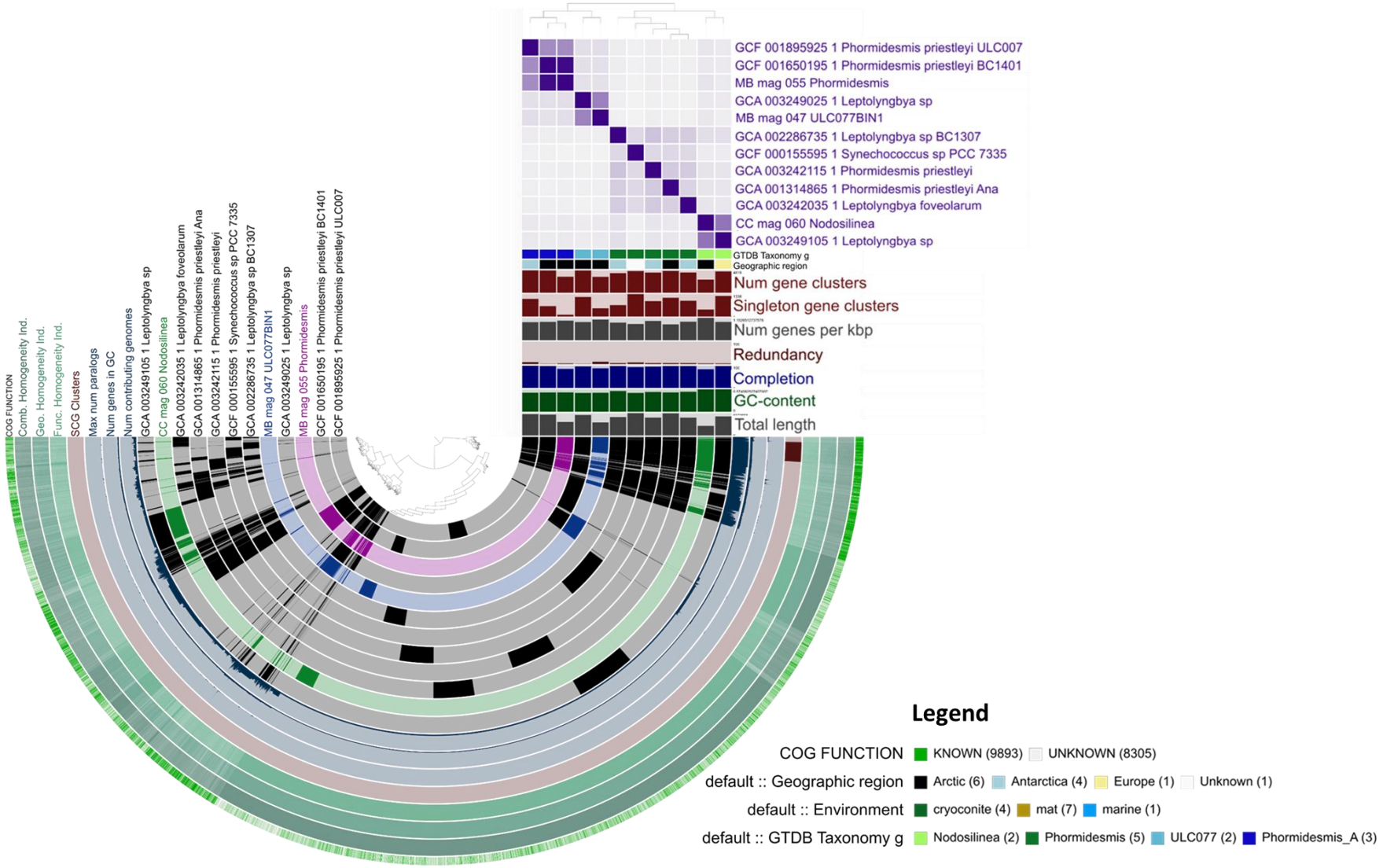

Figure 4-15 The Pangenome of *Phormidesmis* and *Leptolyngba* species and MAGs. Public genomes (black) are compared to MAGs (colour). Regions of overlap represent common gene clusters, and non-overlapping regions represent a unique accessory genome. An ANI results matrix (purple) reflects the relatedness of the MAGs and public genomes to each other.

4.3.8.1 Functional Enrichment analysis

Functional enrichment analysis based on geographic location, environment type and GTDB classification (Appendix Table D-14) was performed using the tool anvi-get-enriched-functions-per-pan-group. This tool creates a frequency table of functions in genomes and uses a Generalized Linear Model with the logit linkage function to compute an enrichment score and p-value for each function with False Detection Rate (FDR) correction to p-values to account for multiple tests is done using the package qvalue. The tool identifies groups within genomes, and then identifies functions that are enriched within those groups. In this way it is possible to identify functions that are characteristic of the genomes within a group, and absent from genomes from outside this group. There was no functional enrichment identified between groups of genomes based on Environment type, geographic location or GDTB classification. The non-significant results are likely due to a lack of statistical power, as the number of samples per group were not large enough to reach significance.

4.3.8.2 The functions of accessory genes in CC_mag_047 and cc_mag_055

After ordering the pangenome by gene cluster frequency and presence/ absence, the singleton gene clusters (accessory genome) of the MAGs included in this pangenome were identified (Figure 4-15). The identity and function of the singleton genes were analysed. MB_mag_047 had 472, CC_mag_060 had 407 and CC_mag_055 had 102 gene clusters that were unique and not shared with any other genome in the pangenome. Of these, 164 of the clusters were assigned to a COG functional category. The accessory genes were not known to be specific to cold-adaptation.

Table 4-10 COG Functional categories of accessory gene clusters in Leptolyngbya MAGs

COG Category	CC_mag_055	CC_mag_060	MB_mag_047
Information Storage and Processing			
[K] Transcription	0	19	5
[L] Replication, recombination, and repair	2	15	14
Cellular Processes and Signalling			
[D] Cell cycle control, cell division, chromosome partitioning	1	0	2
[V] Defence mechanisms	3	3	6
[T] Signal transduction mechanisms	0	15	19
[M] Cell wall/membrane/envelope biogenesis	1	17	9
[U] Intracellular trafficking, secretion, and vesicular transport	1	0	6
[O] Posttranslational modification, protein turnover, chaperones	0	10	9
Metabolism			
[C] Energy production and conversion	0	7	2
[G] Carbohydrate transport and metabolism	1	4	5
[E] Amino acid transport and metabolism	0	11	5
[F] Nucleotide transport and metabolism	0	3	1
[H] Coenzyme transport and metabolism	0	2	0
[I] Lipid transport and metabolism	0	1	0
[P] Inorganic ion transport and metabolism	0	4	6
[Q] Secondary metabolites biosynthesis, transport, and catabolism	0	6	5
Poorly Characterized			
[S] Function unknown	12	64	70
Mixed			
E, G	0	2	0
E, T	0	1	0
G, M	0	1	0
I, Q	0	3	0
N, T	0	1	0
Grand Total	21	189	164

4.4 Discussion

The chapter describes 74 metagenome-assembled-genomes (MAGs) recovered from sea, soil and cryoconite metagenomes from Ny-Ålesund, Svalbard. By their nature, reconstructed genomes represent the most abundant members of a community, because they are constructed from the longest contigs with the deepest coverage, proportional to their abundance in the original sample. They are therefore useful to understand the functional and metabolic potential of the most abundant members of a community. Using read mapping, the resolved genomes could be traced to exact environments types and geographical locations to provide additional ecological insights.

4.4.1 Effect of environment complexity on ability to resolve MAGs

Deep shotgun sequencing of these environments confirmed the presence of fungal, algal, and viral species in the sampled environments (Figure 4-4, Figure 4-6, and Figure 4-8). The higher the relative proportion of non-bacterial taxa, the greater the difficulty in resolving genomes. Seawater had a particularly high viral load. The relatively small assembly from seawater can be accounted for by the fact that many reads belonged to abundant, but non-bacterial sources, such as viruses, algae, and fungi. There were relatively fewer high quality MAGs reconstructed from soil, with fewer of their reads being aligned to the final assembly which reflects the enormous diversity of bacteria in the sample (Chapter 8, Table 8-7, Figure 8-7), which were not present in high enough abundance to assemble into contigs > 2000 bp or groups of contigs large enough to form bins. The high number of MAGs assembled from cryoconite libraries is due to a combination of (1) similarity across sites, relatively high bacterial population relative to eukaryotes, and a small core community of highly abundant species (Chapter 3). There was a good correlation between the taxonomy of the reconstructed MAGs and the taxonomic classification of reads. For example, the most abundant species from the reads-based taxonomic assignment in cryoconite were *Phormidesmis*, *Sphingomonas*, *Ktedonobacteria*, *Nostoc*, *Bradyrhizobium*, *Leptolyngba*, *Microbacteria*, *Pseudanabaena*, *Granulicella*, *Illumatobacter* and *Rhizobacte*r which were all present in the MAG collection. In soil, abundant reads-based taxa with MAG representatives include *Sphingomonas*, *Nostoc*, several Actinobacteria, *Leptolyngbya*, *Bradyrhizobium*, *Cecembia*, *Aquiflexum* and *Sphingosinicella*. Finally, the MAGs from seawater were from the most abundant phyla, the Proteobacteria and Bacteroidetes.

4.4.2 Phylogenomics of Svalbard MAGs

The vast majority of cultured isolates belong to just four phyla: Proteobacteria, Actinobacteria, Firmicutes and Bacteroidetes (Culligan et al., 2014), and this has resulted in their overrepresentation in genome databases. However, the use of metagenomics is greatly expanding the tree of life as we can construct genomes of as-yet uncultivatable organisms. The MAGs in this study belong to 14 different phyla. In order of abundance, these were the Proteobacteria (α = 13, γ =8), Actinobacteriota (11), Bacteroidota (10) and the Cyanobacteria (6). The Chloroflexota (5) and Chloroflexota_A (1), Armatimonadota (6), Acidobacteriota (4) and Patescibacteria (3) also had several members. Finally, two MAGs each from the Myxococcota and Fibrobacterota, and a single MAG member from Bdellovibrionota, Eremiobacterota and Gemmatimonadota were resolved. Only two of the MAGs belonged to known species, (according to FastANI, cutoff radius of 95). An additional 20 MAGs were closely related to know species (> 75% ANI) and the remainder of the MAGs represent novel species that do not yet have representatives in databases (Table 4-7).

GTDB-Tk was used to classify the MAGs taxonomically and revealed that many of the resolved genomes were closely related to isolates of cryospheric organisms from other sites and studies. MB_mag_055_Phormidesmis, the most abundant MAG in the cryoconite samples, was most similar to *Phormidesmis priestleyi* isolate (GCF_001650195.1) obtained from Greenland cryoconite (Chrismas et al., 2016b) and DA_MAG_019_Granulicella was closest to *Salinibacterium xinjiangense* (GCF_900230175.1), a novel psychrophilic, Gram-positive, yellow-pigmented, and aerobic bacterium, from the China No. 1 glacier (Zhang et al., 2008). There were also several MAGs that were closely related to species isolated from Arctic or Antarctic soils and permafrost. MB_bin_070_QHBO01 was closest to a MAG *QHBO01 sp003243965* (GCA_003243965.1) from desert soils of Antarctica (Ji et al., 2017), while DA_MAG_005_Palsa-881, CC_MAG_041_Rhizobacter and DA_MAG_016_Rhizobacter were closely related to isolates Palsa-881 sp003161535 (GCA_003161535.1) and Rhizobacter sp003152055 (GCA_003152055.1) from Arctic Swedish permafrost (Woodcroft et al., 2018). In addition, three of the cyanobacterial MAGs were from Canada; MB_MAG_036_Pseudanabaena and MB_mag_047_ULC077BIN1 both originate from microbial mats, and were closely related to *Pseudanabaena frigida* (GCA_003242085.1) and *ULC077BIN1 sp003249025* (GCA_003249025.1) respectively (Cornet et al., 2018), while MX_MAG_032_Microcoleus is similar to *Microcoleus sp003003725* from a freshwater lake. Two of the seawater-derived MAGs, MX_mag_062_Ascidiaceihabitans and MB_MAG_023_ASP10-02a were related to *Ascidiaceihabitans sp002478745* (GCA_002478745.1) and *ASP10-02a sp002335115* (GCA_002335115.1) which were both

reconstructed from a North Sea marine metagenome (Parks et al., 2017). There were, however, some surprises, such as the fact that MB_mag_049_Aquiflexuma is a close relative of *Cecembia rubra* (GCF_003014575.1), a thermophilic species from a hot spring sediment in Tengchong, Yunnan province, south-west China (Duan et al., 2015).

In addition to the bins included in this study, there were several bins possibly belonging to CPR group that were excluded because they did not meet the quality for inclusion (>70% complete). There were two bins that were identified as Candidatus Solibacter and one that was identified as unknown Candidatus Saccharibacteria. The completion percentage is based off a catalogue of 71 single copy genes present in most bacteria, but the CPR may very well be missing several of these genes and thus score below the threshold despite being complete. Because these MAGs could not be assessed for completeness, they were excluded, but may be investigated further in future work.

4.4.3 Spatial distribution of MAGs across different sites

Using binning methods that take coverage across different samples into account, it was possible to resolve highly related species with slightly different abundance and distribution across sample sites. For example, two Alphaproteobacterial MAGs MB_MAG_028_Sandarakinorhabdus and MB_bin_067_Sandarakinorhabdus, and four Gammaproteobacterial MAGs, DA_MAG_016_ Rhizobacter and CC_MAG_041_Rhizobacter and MB_MAG_034_UKL13-2 and CC_mag_053_ UKL13-2 could be distinguished based on differential coverage across different sites. Using a heat-map of coverage to describe spatial distribution also revealed that the MAGs show habitat preference. The Max-normalised ratio view (MAG-centric) showed a clear partitioning of cryoconite-only, and sea-specific MAGs (Figure 4-11). The heterogeneity of soil samples was also clear. The abundance view (sample-centric) showed that many of the MAGs are widely distributed, with a high abundance at a single site, or within a habitat type and extremely low coverage at other sites (Figure 4-12). Very low abundance at certain sites may be an artefact of read mapping, whereby reads align to contigs because short fragments of the genome are identical between related, but distinct species. Nonetheless, a pattern emerges that agrees with 16S rRNA gene amplicon studies of cryoconite, showing dominance by a cyanobacterial *Phormidesmis* MAG, and a less abundant tail community of Proteobacteria and Actinobacteria. Spatial mapping also revealed that ML and VB are more like each other than AB or VL. While cryoconite sites clearly resembled each other, the soil samples were far more heterogenous, particularly in cyanobacterial abundance. With a total of six different cyanobacteria in this dataset, which often proved the most abundant at their respective sites, MAGs from this phylum were examined in more detail.

4.4.4 Cyanobacteria

These Cyanobacterial MAGs are interesting because Cyanobacteria are known to play vital roles as ecosystem engineers in both cryoconite (Gokul et al., 2016; Hodson et al., 2010b; Langford et al., 2010) and early soil development (Pushkareva et al., 2015; Rossi and De Philippis, 2015). Two Leptolyngbya species could be resolved, MB_mag_055_Phormidesmis was dominant in AB, VB, and ML cryoconite, and a different MB_mag_047_ULC077BIN1 was dominant in VL cryoconite. A third closely related MAG (CC_mag_060_Nodosilinea) from the family Phormidesmiales, also used to be classified as Leptolyngbya before reclassification by GTDB to Phormidesmiaceae (Table 4.10). The MB_mag_055_Phormidesmis, is most similar to a Cyanobacterial strain isolated from Greenland cryoconite (Chrismas et al., 2016b), and was present as the main Cyanobacterial species and dominant community member in cryoconite on VB, ML and AB. It was also found at low levels in all forefield soil sites, suggesting that this glacial species might carried downstream in meltwaters and inoculate the soil. The MB_mag_047_ULC077BIN1 was the dominant Cyanobacterial species in VL cryoconite but was completely absent from cryoconite on other glaciers. It was however present at all forefield soil sites. VL is a markedly 'different' glacier in terms of its community make up (Figure 4-3, and Figure 4-11), and it is possible that 'cryoconite' on VL is caused by soil blown onto the glacier that nevertheless acts the same way as in terms of albedo and melting as true biological cryoconite granules would.

The CC_mag_060_Nodosilinea was found only in soil samples and was especially abundant in the soil collected from sites closer to the glacier snout (time point 1 (F3T1) and time point 2 (F2T2)). This raises the possibility that CC_mag_060_Nodosilinea is particularly important in the development and stabilisation of recently exposed glacial soils. A novel *Nodoslinea* species has recently been described in Svalbard (Davydov et al., 2020). Because there were three highly abundant and closely related MAGs in our dataset, a pangenome of MB_mag_047, CC_mag_060 and CC_mag_055 was constructed and of the MAGs and their closest relatives (Figure 4-15, Table 4-9).

The pangenome was used to show the MAGs relationship to each other and to relatives within the Leptolyngbya clade. Although these MAGs were closely related to known strains, they each had accessory genomes, which was examined to see whether the accessory genome had any genes responsible for specific habitat adaptation. However, the function of the accessory genes did not signify any particular cold adaptation (Table 4-10), which is similar to previous comparisons of cyanobacteria from different temperature zones (Chrismas et al., 2016b).

Cyanobacteria often live in community with other heterotrophic bacteria (Cornet et al., 2018). In this study two Alphaproteobacterial MAGs were identified in cryoconite that belong to the genus *Sandarakinorhabdus*, MB_MAG_028_Sandarakinorhabdus and MB_bin_067_ Sandarakinorhabdus. Members of the *Sandarakinorhabdus* genus have previously been found associated with cyanobacterial aggregates in freshwater lakes (Cai et al., 2018). Notably, two *Sandarakinorhabdus* MAGs were recently identified in glacial ice (Trivedi et al., 2020), which suggests that this genus might be common in glacial ice. *Sandarakinorhabdus* is a bacteriochlorophyll a-containing, obligately aerobic bacterium isolated from freshwater lakes (Gich and Overmann, 2006), however, a closely related strain (MC 3718T), which unfortunately has not been genome-sequenced, has also been isolated from a tundra soil near Ny-Ålesund (M. Kim et al., 2016).

4.4.5 Biogeochemical cycling in different environments

Biogeochemistry refers to the study of the processes by which organisms transform and recycle organic and inorganic substances in the environment, as well as evaluating the effects of these cycles (Madsen, 2011). In low nutrient glacial environments, microorganisms cycle nutrients to ensure the sustained availability of a variety of nutrients. Cryoconite communities therefore play a role in geochemical nutrient cycling of major nutrients such as carbon (C)(Anesio et al., 2009, 2010; Cameron et al., 2012b; Cook et al., 2016a; Hodson et al., 2010a; Langford et al., 2010), nitrogen (N)(Cameron et al., 2012b; Edwards et al., 2013a; Larose et al., 2013b) and phosphorous (P)(Cameron et al., 2012b; Cook et al., 2016b; Edwards et al., 2013a; Hodson et al., 2010a), as well as sulfur (S)(Edwards et al., 2013a; Simon et al., 2009b; Trivedi et al., 2020) and iron (Fe)(Edwards et al., 2013a). During the summer, in supraglacial regions where sunlight can penetrate the ice, photoautotrophy provides nutrients for many complex food webs (Boetius et al., 2015). However, during the winter polar night, and in the deeper subglacial habitats, chemoautotrophy is the main contributor to food webs (Boetius et al., 2015).

In addition, nutrients, and bacteria from cryoconite are regularly transported to downstream ecosystems during summer melt seasons (Anesio et al., 2009), therefore adding nutrients and seeding organisms in recently exposed, and therefore biologically and nutrient sparse soil (Bradley et al., 2014). The introduction of these nutrients to newly exposed glacial soils and the development of the microbial communities that can supplement and maintain nutrient cycling in soils is one of the most important factors driving soil development, and the eventual establishment of vegetation (Bradley et al., 2014). Recently, a study of the metabolic potential of MAGs from a subsurface

aquifer, revealed that very few microorganisms in a system can conduct multiple sequential redox reactions, suggesting that organisms rely on substantial metabolic trade-off of redox reaction products from one organism to another (Anantharaman et al., 2016). Interdependencies in nutrient cycling in microbial communities are continually revealed in studies of MAGs from environments such as a sulfur-rich glacial ecosystem (Trivedi et al., 2020), subsurface aquifer (Anantharaman et al., 2016), deep sea hydrothermal sediments (Dombrowski et al., 2017), Svalbard permafrost (Yaxin Xue et al., 2020), hypersaline soda lake brines (Vavourakis et al., 2016) and freshwater lakes (Linz et al., 2018).

4.4.5.1 Carbon cycling

The organisms of cryoconite holes are involved in both carbon fixation (e.g. photosynthesis) and carbon oxidation (e.g. respiration). The net ecosystem production (NEP) describes the balance between carbon fixation and carbon oxidation and is expressed by the following:

$NEP = PP - R$ (where PP is primary production and R is respiration)

When $NEP > 0$, photosynthesis (carbon fixation) exceeds respiration and cryoconite is acting as a carbon sink (removing atmospheric carbon). When $NEP < 0$, the cryoconite is a carbon source because carbon release via respiration exceeds the rate of carbon fixation (Cook et al., 2016b).

The external conditions which determine whether NEP is in positive or negative balance include: water state and characteristics, the availability of nitrogen and phosphorous (Stibal and Tranter, 2007), sediment size and arrangement (Cook et al., 2016a; Telling et al., 2012), solar angle and photosynthetically active radiation (PAR). The sediment angle, solar angle and PAR all affect the amount of solar energy which can be harnessed by microorganisms for carbon fixation via photosynthesis. For example, photoautotrophs may be responsible for net carbon fixation during the sunny summer months, and net carbon oxidation via respiration during the dark winter months. The availability of PAR explains why NEP is positive when sediment depth is less than 3mm favouring carbon fixation by autotrophic organisms, and carbon oxidation is favoured by heterotrophic organisms when sediment depth is greater than 3mm (Telling et al., 2012). This also explains why net autotrophy occurs in cryoconite holes with thin debris layers, while net heterotrophy occurs when sediment layers are deeper than 2-4 mm (Cook et al., 2010). Carbon cycling has been measured via a number of techniques including measuring the rates of photosynthesis and respiration, or via measuring the acquisition, storage or loss from cryoconite holes (Cameron et al., 2012b).

4.4.5.1.1 Carbon fixation

The contribution of cryoconite on the ML glacier surface on carbon cycling has previously been investigated using in situ incubations of cryoconite–water mixtures to estimate respiration (1.174 ± 0.182 μg C g^{-1} h^{-}) and bacterial carbon production (0.040 ± 0.019 μg C g^{-1} h^{-1}) (Hodson et al., 2007). These estimates were extrapolated, using uninhabited aerial vehicle (UAV) image acquisition to quantify the cryoconite over the entire glacier (0.42-1%). The results suggest that the carbon flux on this glacier could be up to 12–14 kg C km−2 a^{-1} in the summer, showing that cryoconite ecosystems can have a significant impact upon carbon cycling in glacial environments (Hodson et al., 2007). Using ^{14}C labelled bicarbonate to determine the rate of inorganic carbon uptake in cryoconite sediment in vitro, it was determined that cyanobacterial photosynthesis was the main process responsible for inorganic carbon fixation (75–93%), while heterotrophic uptake only accounted for a minor part (6–15%) (Stibal and Tranter, 2007). The rate of photosynthesis in meltwater on the ML glacier surface was lower than that of cryoconite, and within cryoconite holes, the rate of photosynthesis was much higher at the bottom of the holes (0.63–156.99 μg C l^{-1} h^{-1}) than in the overlying meltwater (60-8.33 μg C l^{-1} h^{-1}), which is not surprising considering the density of organisms associated with the granules in the bottom of the holes (Säwström et al., 2002).

The most important gene in carbon fixation, responsible for the first rate-limiting step of photosynthesis, is RubisCO (Ribulose-1,5-bisphosphate carboxylase/oxygenase), which has ribulose-1,5-bisphosphate and carbon dioxide (CO_2) as its substrates (Erb and Zarzycki, 2018). There are several forms of RubisCO. The form most common in autotrophic bacteria is RubisCO form I. Of these, there are several types, including the large subunit of form I red-like RubisCO (*cbbLR)*, the large subunit of form I green-like RubisCO (*cbbLG)* and the large subunit of RubisCO in eukaryotes (*rbcL)*. In a previous study, copies of the *cbbLR* gene from ML cryoconite most closely resembled gene sequences from an Actinobacteria family Mycobacterium and Alphaproteobacteria, order Rhizobiales (Cameron et al., 2012b). In this study, several MAGs had copies of form I RubisCO, including an Actinobacteria, CC_MAG_025_Actinobacteria, from the family Frankiaceae, two Alphaproteobacterial MAGs, MB_MAG_033_PALSA_911 and CC_mag_052_Bradyrhizobium belonging to the family Acetobacteraceae and Xanthobacteraceae respectively as well as a Gammaproteobacterial MAG CC_MAG_037_BOG_994, family Burkholderiaceae. The MAG MB_bin_070_QHBO01 from the phylum Chloroflexota_A and MX_mag_044_UBA5184 from the phylum Eremiobacterota also contained copies. There were also form I RubisCO genes in all the cyanobacterial MAGs, except for cc_mag_071_Nostoc_ and CC_mag_060_Nodoslinea. Previously amplicons of form I green-like RubisCO from

Leptolyngbya and Nostoc were identified in ML cryoconite (Cameron et al., 2012b). Of note, the cyanobacterial MAGs in this study had <90% completion, and therefore their absence may just reflect the incomplete bins. Interestingly, all MAGs harbouring RubisCO form I genes were most abundant in cryoconite, with the sole exception of MB_bin_070_QHBO01, which was more abundant in soil.

In addition to carbon fixation from CO_2, there are several pathways which take single-carbon sources as substrates for assimilatory carbon pathways. We identified several methylotrophs, methanol dehydrogenase (*nmda*) and S-(hydroxymethyl)mycothiol dehydrogenase (*smdh*) genes in two and seven Actinobacterial MAGs, respectively. The *nmda* enzyme takes methanol as its substrate and may play a role in extremely oligotrophic growth, or even or possibly enable chemoautotrophic growth (Ohhata et al., 2007). The *smdh* enzyme is specific to Actinobacteria, has formaldehyde (CH_2O) as one of its substrates and, was found in seven of the ten Actinobacterial MAGs (DA_MAG_002_Bog_756, MB_MAG_039_Ilumatobacter, MB_MAG_021_Micro bacteriaceae CC_MAG_025_Actinobacteria, MX_MAG_013_Actinobacteria, DA_MAG_007 _Iso899, and MB_MAG_008_Micromonospora). Most of the Actinobacterial MAGs are more prevalent in cryoconite, but DA_MAG_007_Iso899 was more abundant in soil. There is evidence of carbon monoxide (CO) oxidation via carbon monoxide dehydrogenase (coxSML) genes in several Acidobacteria (3/4), Actinobacteria (5/11), Alphaproteobacteria (8/15) and Gammaproteobacteria (4/8) MAGs. There is evidence that CO is a major energy source for aerobic heterotrophic bacteria in organic carbon deprived environments (Cordero et al., 2019).

4.4.5.2 Nitrogen cycling

Nitrogen can exist in multiple forms in the environment. It is present as N_2, the most abundant gas in our atmosphere (~78%). However, despite the abundance of N_2, the fixation of nitrogen gas is all but impossible for almost all organisms, save a few microorganisms. Nitrogen is mainly assimilated into organisms via reduced inorganic compounds such as ammonium and ammonia and oxidised inorganic forms, such nitrate, nitrite, nitric acid and nitrogen oxides (Larose et al., 2013b). It is also recycled between organisms in the form of organic nitrogen compounds such as urea, amines, and proteins. Prior to the invention of the Haber Process, the fixation and denitrification of nitrogen was in balance. However, as more nitrogen compounds have been produced via this process for agriculture and industry, the available nitrogen in the environment has been increasing, and there is evidence that this increase may be upsetting delicate ecosystems, including the Arctic (Larose et al., 2013b).

4.4.5.2.1 Nitrogen fixation

There was only one MAG capable of nitrogen fixation from the genomes we could resolve. The CC_bin_071_Nostoc had *nifD* and *nifH* genes (Figure 4-13 and Figure 4-14), responsible for nitrogen fixation. Nostoc is known to be capable of nitrogen fixation (Solheim et al., 1996). CC_bin_071_Nostoc was present in cryoconite on VL and AB and in all soil sites, with a particularly high abundance in VL cryoconite and F2T2 soil. Although previous studies have tried to identify genes associated with nitrogen fixation in cryoconite across four glacial sites on Svalbard, and one glacial site in Antarctica, no genes were amplified, despite evidence that taxa capable of fixation were present (Cameron et al., 2012b). A similar study on an Arctic snowpack metagenome found only a low number of reads associated to nitrogen fixation in their despite the presence of genera capable of nitrogen fixation (Larose et al., 2013b). Therefore, in this study, the gene responsible for nitrogen fixation in *Nostoc* species in cryoconite and soil was detected.

4.4.5.2.2 Nitrate reduction

The *napA* and *narG* genes are involved in denitrification and dissimilatory nitrate reduction. The *napA* and *narG* genes encode a periplasmic and membrane nitrate reductase respectively which reduce nitrate (NO_3^-) to nitrite (NO_2^-). Previously, *napA* and / or *narG* was amplified from all cryoconite communities from 8 different glaciers on Svalbard including ML (Cameron et al., 2012b). Clones with the *napA* gene from the Foxfanna glacier in Svalbard shared 76-84% sequence similarity with members of Alpha, Beta or Gammaproteobacteria classes (Cameron et al., 2012b). In this study, an Alphaproteobacterial MAG CC_mag_052_Brazyrhizobium from the order Rhizobiales with a copy of the *napA* gene was present in all soil and cryoconite samples. A second MAG, MB_MAG_020_Cyclobacteriaceae from the Bacteroidota had a copy of the *napA* gene but was present only in the F3T3_Ludox samples, which may not be representative of the microbial community due to extraction bias. The *narG* gene clones previously identified in Foxfanna cryoconite were most like uncultured and unclassified bacteria, as well as Rhodobacterales and Rhizobiales from the Alphaproteobacteria, and Burkholderiales from the Betaproteobacteria (Cameron et al., 2012b). In this study, the *narG* gene was present in two Actinobacterial MAGs, CC_MAG_025_Actinobacteria and MB_MAG_008_Micromonospora and two Alphaproteobacterial MAGs, MB_MAG_004 and MX_MAG_022_Pararhodobacter. Both Actinobacterial MAGs were common in cryoconite samples, however the proteobacterial MAGs were from the F3T3_Ludox samples.

4.4.5.3 Sulfur

The most common gene for sulfur cycling was sulfur dioxygenas (sdo). Sdo oxidizes the sulfane sulfur in GSSH to sulfite, and there were 39 MAGs that had at least one of these genes. The sulfate adenylyltransferase (sat), gene, was detected in the majority of Cyanobacterial (5/6) and Chloroflexota genomes (4/5) as well as in a few Acidobacteria (2/5), Alphabproeobacteria (2/13) and Gammaproteobacteria (1/8). Recently, a sulfur rich Canadian glacial system was investigated for sulfur genes (Trivedi et al., 2020). In addition, there was sulfur oxidation visa the Sulphur Oxidising (sox) pathways in several of the Alphaproteobacterial (3) and Gammaproteobacterial MAGs (6).

4.4.6 Advantages to this study

This study makes several important contributions. Firstly, and most importantly, this study describes a glacial ecosystem (cryoconite, forefield soil) that has previously only been described using 16S rRNA and biogeochemical gene amplicon studies. Based on GTDB-Tk classification, 72 of the MAGs represent new species that do not have representatives in known databases. The MAGs represent a dataset that can be annotated and interrogated to any effect using any of the available databases. Indeed, the mining of these genomes for bioactive secondary metabolites with useful industrial functions will be the focus of Chapter 5.

The ML glacier has been investigated for several decades, mostly using amplicon analysis, either 16S rRNA gene analysis or amplicon analysis of specific genes that form part of a biogeochemical pathway. Both approaches are beset by issues such as amplification bias, and although attempts are made to infer functional information from 16S rRNA phylotype, these inferences are guesses at best. The actual presence and annotation of function genes in microbial communities is vital to gain true insight into cooperation and ecosystem function. The investigation of biogeochemical cycling using amplicon sequencing relies on primers and therefore only captures highly similar sequences. HMMer analysis, like we performed in this study, is likely to capture a much more diverse set of sequences. Likewise, while amplicons can only capture single gene products, HMMer scanning of MAGs can capture different processes in the same pathway and tell us how many of those genes from different pathways occur in a single organism, and in different spatially co-occurring organisms. This analysis allows us to go from a ‘bag-of-genes’ to a ‘bag-of-genomes’ (Frioux et al., 2020).

4.4.7 Limitations of this study

MAGs still only describe the functional potential of the most abundant bacteria in a community, not necessarily the most active bacteria. Concurrent transcriptomics and metabolomics studies of these environments would give a far greater resolution of community metabolisms, regulation, and the contribution of various members. In addition, many reads and contigs from many of the less abundant bacteria failed to be binned and meet the criteria for MAG inclusion and are thus lost from the interpretation, providing an incomplete picture of the whole community.

4.4.7.1 Extraction bias and sample complexity

There were three samples sequenced from the same soil site (F3T3), using different methods which revealed that enormous bias is introduced by different extraction methods. DNA extracted using density gradient centrifugation to extract DNA from whole cells (F3T3_Lud) was missing several taxa that were abundant in samples extracted using alternate methods. This library also contained a greater relative number of reads aligning to contigs, and several bins that were absent in other samples. Five different Bacteroidota MAGs were constructed from the Ludox sample. However, the Bacteroidota are not overly abundant in soil from other sites or using other extraction methods.

4.4.7.2 Struggle to obtain 16S rRNA operons

Very few 16S rRNA operons were identified by HMM screening of the bins. This is a major drawback because it prevents the comparison of these MAGs to the vast literature which compares 16S rRNA genes at high resolution in this environment (Edwards et al., 2014). The problem has previously been described by other authors (Cornet et al., 2018; Hauptmann et al., 2017) who speculate that the frequent loss of rRNA genes is caused by the presence of multiple copies of the rRNA operon in many bacterial genomes, resulting in short rRNA-bearing contigs due to incomplete assembly of repeated regions. Because these contigs are dominated by the rRNA operon, they have higher sequencing coverage and divergent tetranucleotide frequencies (TNFs), two properties that are used by binning software to determine bin assignment (Cornet et al., 2018). Similarly, when comparing methods for determining microbial abundance in samples from the Greenland ice-sheet, EFM was the most accurate and reliable method for determining abundance, yet there was no correlation between qPCR and EFM abundance ratios, which could be due to a difference in the number of ribosomal RNA operon copies per cell (Stibal et al., 2015).

4.4.7.3 Inability to resolve highly similar strains

Co-assembly of several metagenomes containing very closely related populations often hinders confident assignments of shared contigs into individual bins (Shaiber and Eren, 2019). It is possible

that several of the MAGs in this collection reflect composite genomes. An example of a possible composite genome is CC-mag_Nostoc_071, which could reflect several related but distinct Nostoc species. The identification of composite and high-quality bins is discussed in Chapter 8.

4.4.8 Future work

Both the resolution of 16S rRNA genes in MAGs as well as the differentiation of closely related strains will be significantly aided by long-read sequencing. A hybrid assembly, which combines nanopore and Illumina data will create long scaffolds. Long sequences can bridge repetitive regions and regions of low coverage therefore solve issues of synteny and multi-gene operons. This approach has already been applied in wastewater studies, where several of the recovered genomes were complete circular genomes (Singleton et al., 2020).

4.5 Conclusion

In this study, via co-assembly of soil, cryoconite and seawater metagenomes, it was possible to reconstruct 74 high and medium quality MAGs from the most abundant community members. The mean coverage of these MAGs and their distribution across different samples, tells us about their abundance and distribution in various environmental sites. The MAGs belonged to species detected in high abundance by numerous 16S rRNA gene surveys, thus validating predictions by 16S rRNA amplicon studies. Notably, six cyanobacterial MAGs were resolved, which appear to have strong habitat preference and possibly play viral roles in cryoconite and early soil formation. In addition, the presence and absence of several enzymes involved in the major biogeochemical cycles were described. The MAGs assembled from this environment provide important ecological information about this highly threatened environment, which is highly valuable, however, they are also extremely useful for downstream bioprospecting applications. The genomic content and distribution of MAGS provides necessary information for strategic cocultivation and heterologous expression. In terms of cultivating ‘microbial dark matter’, the occurrence of several MAGs at a single site tells us which bacteria might be required for successful co-cultivation. Likewise, an analysis of KEGG pathways and modules will provide information on required nutrients and supplements and antimicrobial resistance. If a particular NP has been targeted for functional analysis and heterologous expression, the phylogenomic information will help in the selection of a closely related host, and access to the whole genomes will provide information on possible regulation, required substrates and chaperones. Finally, if a target is identified in one of the genomes, read mapping allows one to target future sampling efforts to the sites here it is in high abundance.

5 THE SECONDARY METABOLITES OF SOIL AND CRYOCONITE HAVE A RANGE OF BIOTECHNOLOGICAL APPLICATIONS

5.1 Introduction

Bioprospecting is the process by which organisms are investigated for natural products (NPs) that can be of societal benefit. Replication and rediscovery of the same compounds has become a major problem in bioprospecting, and one solution is to turn to environments that have extreme environmental conditions, and that have not yet been fully explored; as both of these factors increase the chance of a novel discovery (Knight et al., 2003). Although marine (Amoutzias et al., 2016; Giordano et al., 2015; Wietz et al., 2012) and soil (Feng et al., 2012, 2011) environments have been extensively investigated for antimicrobial compounds, the cryosphere remains under-explored.

Arctic microorganisms have adapted to extreme conditions such as cold temperatures, high summer UV radiation, and strong osmotic gradients- from extreme salinity to extremely dilute conditions (Maccario et al., 2015). Secondary metabolites form part of this adaptation arsenal, from pigments and antioxidants that protect against high UV radiation, to exopolysaccharides (EPS) that protect against desiccation and allow cells to form biofilms where they can sequester nutrients and create stable ecosystems, to a vast range of antimicrobial compounds that allow organisms to compete for limited nutrients (Piel, 2011). Replication in pharmaceutical bioprospecting is exacerbated because the detection of NPs has historically depended on cultivation of the producing strain and the expression and secretion of the NP of interest. However, this approach favours the rediscovery of compounds from highly investigated cultivatable strains and omits the biosynthetic potential of the 99% of uncultivatable bacteria and of cryptic biosynthetic gene clusters (BGCs)(Cimermancic et

al., 2014). Cryptic BGCs are gene clusters that synthesise unknown compounds, because they are expressed only under certain conditions (Butler et al., 2016). They may therefore be present in a cultivated strain, but the factors that regulate its expression remain unknown. An analysis of the genomes of 1154 archaeal and bacterial organisms predicted 33351 putative BGCs, many of which encode secondary metabolites that have never been detected and it is suspected that the current list of BGCs currently vastly underestimates the true number present. (Cimermancic et al., 2014). In addition, systematic surveys of thousands of sequenced microbial genomes showed that generally, silent clusters outnumber those that get expressed in laboratory cultures (Butler, 2004). Together, this suggests enormous untapped potential in the genomes of microbes (Butler, 2004). Sequence-based metagenomics is therefore a timely, much-needed tool to identify BGCs that otherwise elude detection because they allow us to access the biosynthetic potential of uncultivable bacteria and cryptic gene clusters.

The use of MAGs to search for BGCs is relatively new, but has previously been attempted from 26 metagenomic samples collected over various months in 2013, 2014 and 2015 from Lake Stechlin in north-eastern Germany (Cuadrat et al., 2018). Although MAGs have been constructed from several Arctic environments, including soil (Yaxin Xue et al., 2020), cryoconite (Hauptmann et al., 2017) and a Canadian glacier (Trivedi et al., 2020), this chapter is the first time that MAGs from an Arctic metagenome have been screened for biotechnologically relevant secondary metabolite BGCs.

In this chapter, the focus is on three main applications of secondary metabolites: EPS, antioxidants, and antimicrobial compounds, which are hypothesised to be abundant because of their role as adaption mechanisms to the environment. Exopolysaccharides (EPS) are synthesized by many bacteria, where they enable microorganisms to endure extremes of temperature, salinity and low nutrient availability (Poli et al., 2010). Depending on the nature of the EPS, these substances may find uses in the pharmaceutical to food-processing fields, or even be utilised in the remediation of polluted due to their detoxification capability (Poli et al., 2010). EPS synthesised by the Arctic bacterium, *Polaribacter sp.* SM1127, has high antioxidant activity and moisture-retaining properties make them excellent for use in cosmetic and food industries (Sun et al., 2015), while an EPS from *Pseudoalteromonas arctica* protects against freeze thaw injury and has utility as a cryoprotectant in the medical and food industries (Kim and Yim, 2007). The main Cyanobacterial strain in Svalbard cryoconite is *Phormidesmis Priestleyi*, which is similar to the Greenland *Phormidesmis Priestleyi* strain that is a prolific producer of EPS (Chrismas et al., 2016b).

Although carotenoids and terpenoid compounds from the Arctic are often investigated in relation to their role in glacier and ice-sheet darkening, and their contribution to glacier melt and sea level rise (Benning et al., 2014; Lutz et al., 2014), these compounds have numerous useful properties. Terpenoid and carotenoid clusters have known biotechnological applications as pigments, antioxidants, and UV compounds (Chrismas et al., 2016b, 2018; Mandelli et al., 2012). Select terpenoids and carotenoids also have potential antifungal, antitumor and antibacterial activity (Paduch et al., 2007; Sajjad et al., 2020). Finally, antimicrobial compounds can be synthesized by a vast array of BGCs ranging from saccharides to fatty acids to NRPS and polyketides. Growing antimicrobial resistance poses a serious threat to human health and novel antibiotics are urgently needed (Sabtu et al., 2015; Ventola, 2015). Some recently discovered antibiotics have been discovered from metagenomic approaches, illustrating the potential of this approach (Bauer et al., 2010; Feng et al., 2012; Kallifidas et al., 2012).

In this chapter the secondary metabolites of soil and cryoconite were examined to identify BGCs that may have useful application in pharmaceutical applications. Given the environmental conditions, terpenoid clusters such as carotenoids (pigments), EPS and antimicrobial compounds were a focus. Once BGCs of interest had been identified, the metabolome (LC-MS data) was searched to see whether the putative metabolites could be detected from amongst the raw metabolites.

5.1.1 Aims and objectives

1) Compare the types of BGC clusters detected in contigs of individual cryoconite, soil and seawater assemblies.
2) Run antiSMASH and BiG-SCAPE on the Svalbard MAGS (from Chapter 4) to identify BGCs with biotechnological potential.
3) Examine the BGCs of the Cyanobacterial MAGs in detail, as they are the most abundant species in the environment and play important roles as ecosystem engineers as well as contributing significantly to the metabolome because of their high proportion in the environment.
4) Try to identify possible antimicrobial compounds from the most talented Actinobacterial MAG in the dataset.
5) Compare the metabolomic profiles of soil and cryoconite using LC-MS to the predicted metabolites from MAGs to see if predicted and actual metabolic profiles are similar.

5.2 Methods

5.2.1 Samples

The shotgun libraries and the MAGs included in this chapter have been described previously (Chapter 4). The metabolite extractions were performed on cryoconite samples from several different cryoconite holes across four glaciers near Ny Ålesund, Svalbard in the summer of 2018. Raw metabolites from soil were extracted from 15 soil samples, comprising a three by five transect of the ML glacier forefield. A map of the locations of the cryoconite holes and the forefield transect are shown in Chapter 2, Figure 2-1, and the GPS coordinates of the cryoconite holes are in Appendix Table B-1. The samples included in the metabolite analysis are listed in Table 5-1.

Table 5-1 Table of sample sites for metabolite extractions and shotgun metagenome sequencing

Environment	Glacier	Metabolite analysis	Shotgun library	Library size (reads)
Cryoconite	Austre Brøggerbreen	AB1801, AB1802, AB1803, **AB1804**, AB1805, AB1805, AB1807, AB1808	**Cryoconite_AB_18**	64,909,032
	Midtre Lovénbreen	ML1801, **ML1802**, ML1803, ML1804, ML1805, ML1806	Cryoconite_ML_17, **Cryoconite_ML_18**	28,795,356, 28,471,672
	Vestre Brøggerbreen	VB1801, **VB1802**, VB1803, VB1804, VB1805, VB1806	Cryoconite_VB_17, **Cryoconite_VB_18**	34,504,862, 29,787,650
	Vestre Lovénbreen	**VL1801**, VL1802, VL1803, VL1804	**Cryoconite_VL_18**	14,939,536
Soil	Time0	F1T0, F2T0, F3T0	NA	NA
	Time1	F1T1, F2T1, **F3T1**	Soil_S7_**F3T1**	35,482,472
	Time2	F1T2, **F2T2**, F2T2	Soil_S6_**F2T2**	29,116,044
	Time3	**F1T3**, F2T3, **F3T3**	Soil_S1_**F3T3**_Lud, Soil_S2_**F3T3**_FD, Soil_S3_**F3T3**_PM, Soil_S4_**F1T3**	40,079,596, 113,754,008, 44,915,524, 37,684,166
	Time4	**F1T4**, **F2T4**, F3T4	Soil_S5_**F1T4,** Soil_S8_**F2T4**	38,762,496, 35,085,040

Bolded entries show the matching shotgun metagenomes and metabolite extractions. Only one cryoconite hole from each glacier was sequenced using shotgun sequencing, whereas metabolites were extracted from each cryoconite hole on each glacier. Likewise, metabolites were extracted from each glacier forefield soil site, but only selected sites were sequenced by shotgun sequencing. Two cryoconite shotgun libraries from 2017 were sequenced using shotgun sequencing, but there was not sufficient cryoconite left to do metabolite extractions.

5.2.2 Bioinformatics detection of BGCs

Reads from cryoconite, seawater and soil were assembled using MEGAHIT as described in Section 4.3.3 and Section 8.3.3. Analysis was run on single-environment co-assemblies (Table 5-2) and on the combined Svalbard libraries (Figure 4-8, Table 4-3) that had been binned into high quality MAGs in Chapter 4. The benefit of screening the MAGs is that the BGCs inherit the phylogenetic and spatial distribution information from the MAG, and clusters that co-occur together within the same genome can be identified. However, the MAGs represent only a small portion of the contigs database, and there may be many novel BGCs in the neglected contigs. Since one of the overall aims of the study was to link BGCs and metabolites from the same environment, it was decided to also screen the contigs databases of separate soil, cryoconite and seawater assemblies. Although these clusters will not have the information provided by the MAGs, such as coverage, distribution and phylogenetic origin, the databases are smaller, therefore easier to screen with antiSMASH; environment-specific and therefore easy to link to LC-MS data; and most importantly, all of the contigs can be screened., rather than just the contigs that could be binned into a high quality MAG.

5.2.2.1 antiSMASH to detect secondary metabolites

All contigs from the cryoconite, soil and seawater assemblies were run locally through antiSMASH (v.4) and submitted in batches to the antiSMASH server (v5) (https://antismash.secondarymetabolites.org). In addition, MAGs from the combined Svalbard assembly (Chapter 4) were submitted to the antiSMASH server (v.5).

5.2.2.2 Network analysis of secondary metabolites using Big-SCAPE

The genbank files from each cluster from each MAG were downloaded from the antiSMASH server and analysed using BiG-SCAPE (Biosynthetic Gene Similarity Clustering and Prospecting Engine) (Navarro-Muñoz et al., 2020). BiG-SCAPE is a software package that constructs sequence similarity networks of BGCs and groups them into gene cluster families (GCFs). BiG-SCAPE does this by rapidly calculating a distance matrix between gene clusters based on a comparison of their protein domain content, order, copy number, and sequence identity. BiG-SCAPE was run using the parameters --mix --cutoffs 0.7 and both included MiBIG database versions were compared (--mibig13, --mibig).

5.2.3 Metabolomics

Raw metabolites were extracted from soil and cryoconite. For cryoconite, each cryoconite hole from each of the four glaciers sampled (AB = 8; ML= 6; VB= 6; VL = 4) was treated as a replicate. Soil from the glacier forefield was collected from three time points in three transects, with each time point intended to from a replicate. Samples were stored at -20 °C until metabolite extraction.

5.2.3.1 Raw Metabolite extraction

Prior to metabolite extraction, soil and cryoconite samples were freeze dried. Thereafter, 100 mg ± 1 mg of dried soil and cryoconite were placed into 2 mL microcentrifuge tubes. Cells were lysed by repeated cycles of freeze-thaw in liquid nitrogen, then homogenised using a vortex at maximum speed. Samples were then put on ice and 1mL of chloroform: methanol: dH_2O (1**:** 2**.** 5**:** 1) was added. The samples were mixed again with a vortex prior to centrifuging at 3 °C at 5000 x *g* for 3 min. For 'whole' metabolite extractions (i.e. polar and non-polar phases together) the supernatants were decanted into clean labelled microcentrifuge tubes and dried, using a Buchi Rotavapor RE120 with Buchi $V5^{-1}$ vacuum and Buchi 461 water bath at 25 °C (Buchi Ltd., Postfach, Switzerland), alongside a Techne RB-5A refrigerated bath at 3 °C (Techne Inc., Burlington, NJ, US) and stored at -80 °C. An aliquot of 0.5 mL of 70% ethanol was added to the samples, mixed with a vortex and centrifuged at 3°C at 5000 x *g* for 3 min. Thereafter, 50 µL of supernatant was removed and added to 150 µL of ≈ 4°C 70% aqueous methanol (made up of HPLC grade methanol and ultrapure water) and mixed through vortexing for five seconds. Samples were stored at -20 °C until ready to use.

5.2.3.2 LC-MS (Liquid Chromatography –Mass Spectrometry)

Extracts were prepared for mass spectrometry by resuspending 50 µL of the solvent in 200 µL of 70% methanol:water (4°C) in a 2 mL borosilicate glass vial (HiChrom Limited) with Target MicroSert™ flat base inserts (National Scientific Company, Rockwood, TN, USA) and sealed with polytetrafluoroethylene (PTFE) seal aluminium crimp caps (Thermo Scientific™, Waltham, MA, USA). Vials were agitated for 5 seconds with a vortex and stored at -20°C until analysis by Flow Injection Electrospray Ionisation Mass Spectrometry (FI-ESI-MS) using a linear ion trap quadruple (LTQ) mass spectrometer (ThermoFinnigan, San Jose, CA) at the IBERS High Resolution Metabolomics Laboratory (Edward Llwyd Building, Penglais, Aberystwyth University).

5.2.3.3 Metabolomics analysis

Principle component analysis (PCA), multidimensional scaling (MDS) of unsupervised random forest proximities and supervised principle component linear discriminant analysis (PC-LDA) were used to assess the overall data structure and class relationships.

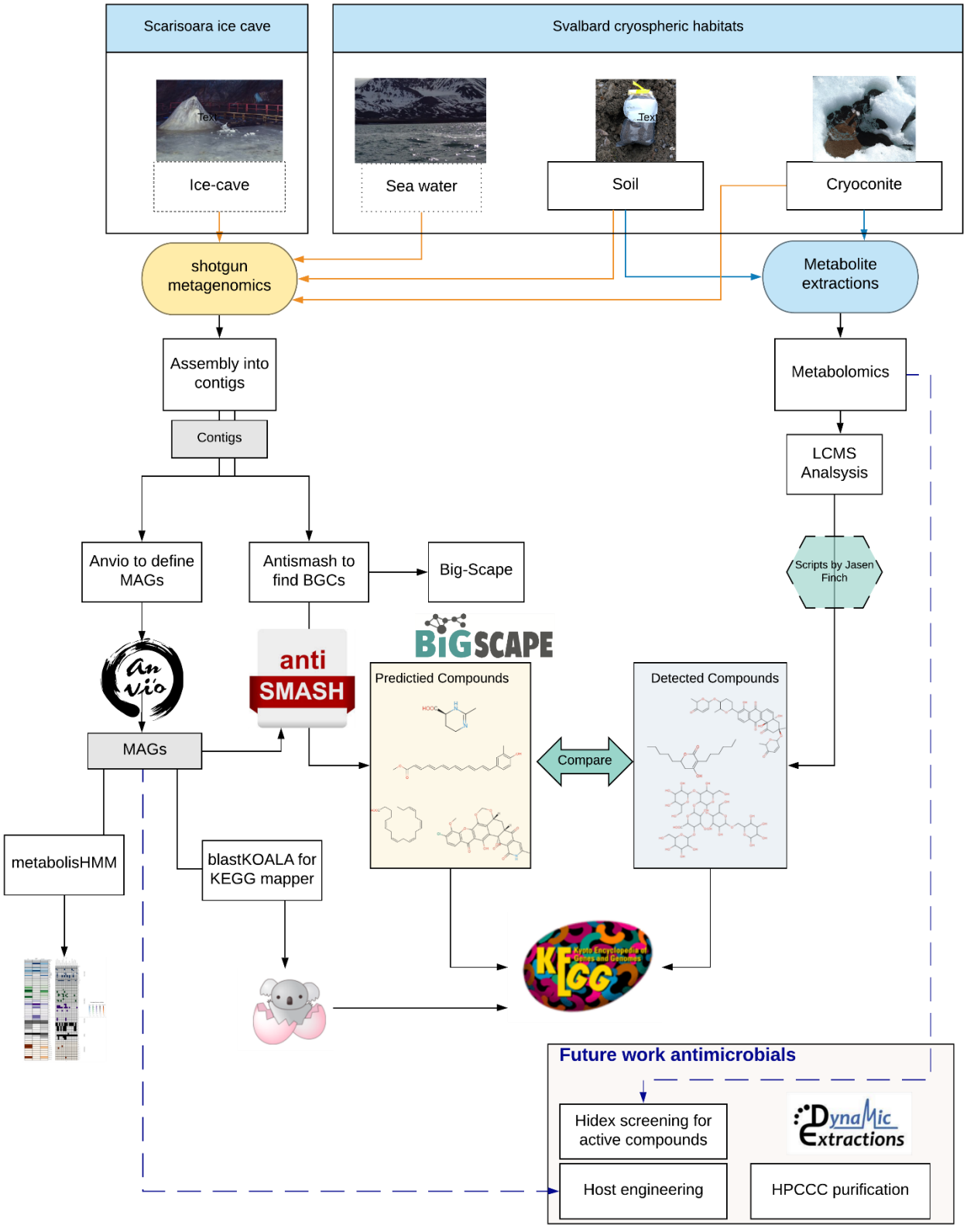

Figure 5-1 Ideal workflow for the exploring the metabolites of Svalbard soil and cryoconite using a mix of metabolomics and metagenomics.

5.3 Results

5.3.1 Assembly

The assembly statistics and contig distribution of the cryoconite, soil and seawater assemblies used in this chapter are shown in Table 5-2. The minimum contig size for inclusion in the assembly was 2000 bp. The cryoconite assembly was the largest (538 521 980 bp) from 115949 contigs, followed by the soil assembly (208 560 096 bp) from 49641 contigs, and finally the seawater assembly was considerably smaller than the others (26 970 110 bp) and 6451 contigs. Each of the individual environmental libraries was assembled separately, to compare contigs from the different environments. The MAGs included in this study from Chapter 4 are from a co-assembly of all the environments together.

Table 5-2 Table comparing Assembly statistics and contig size distribution of sea, soil and cryoconite assemblies.

Assembly	Longest contig (bp)	Nx (Lx)		Length (bp)	Number of contigs	Sum length (bp)	Contig Length Histogram (1bp <= len < 10Kbp)	Contig Length Histogram (10Kbp <= len < 100Kbp)	Contig Length Histogram (len >= 100Kbp)
sea-MEGAHIT.contigs	115659	N50:	4236	>= 10^6	0	0	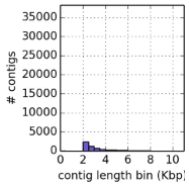	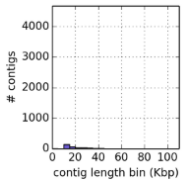	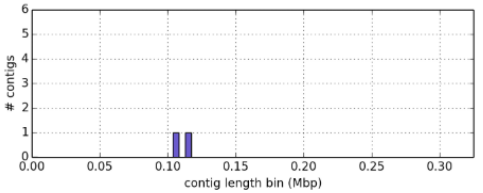
		L50:	(1450)	>= 10^5	2	221424			
		N75:	2686	>= 10^4	321	6766634			
		L75:	(3510)	>= 10^3	6451	26970110			
		N90:	2225	>= 500	6451	26970110			
		L90:	(5171)	>= 1	6451	26970110			
soil-MEGAHIT.contigs	300154	N50:	4111	>= 10^6	0	0	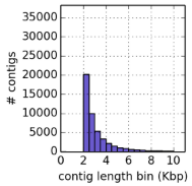	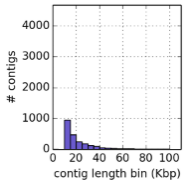	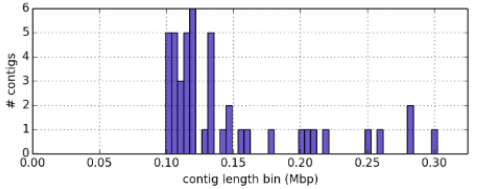
		L50:	(10133)	>= 10^5	45	6597658			
		N75:	2616	>= 10^4	2366	59047038			
		L75:	(26569)	>= 10^3	49641	208560096			
		N90:	2199	>= 500	49641	208560096			
		L90:	(39681)	>= 1	49641	208560096			
cryoconite-MEGAHIT.contigs	315846	N50:	5126	>= 10^6	0	0	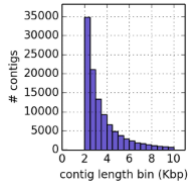	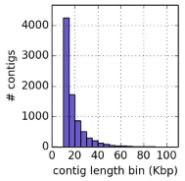	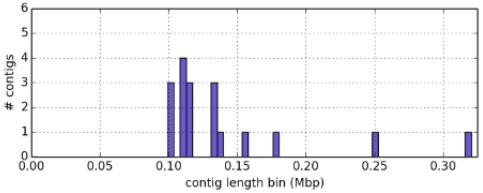
		L50:	(24906)	>= 10^5	18	2524410			
		N75:	2995	>= 10^4	8246	154707901			
		L75:	(60198)	>= 10^3	115949	538521980			
		N90:	2329	>= 500	115949	538521980			
		L90:	(90952)	>= 1	115949	538521980			

5.3.2 Screening MAGs for BGCs

The number and types of clusters detected in each MAG are tabulated in Figure 5-2 and Figure 5-3. There were 1742 BGCs detected in the 74 MAGs. Of these, 278 of the BGCs had similarity to known clusters in the MIBiG database (Appendix Table E-1). Of the 278 known compounds, 143 of them were unique. The compounds synthesized by the remaining 1464 clusters are unknown. Several large contigs had more than one cluster, or contained hybrid clusters, and therefore more than one cluster type was counted in a single region by the antiSMASH algorithm (Examples in Figure 5-11 and Figure 5-12). Notably, the primary cluster category detected by the antiSMASH algorithm is not always the same as the category of the closest BGC in the MIBiG database (Appendix Table E-1, Table E-2, Table E-3 and Table E-4).

The most abundant cluster type was the saccharides (1214), followed by fatty acids (212), and terpenes (122). There were a surprisingly high number of halogenated clusters (69), although these may simply be short clusters with halogenase tailoring enzymes that add halogen products to compound backbones synthesized by other BGCs.

In total there were 72 NRPS and 30 NRPS-like clusters across the MAGS. These BGC are quite abundant in the Chloroflexota (NRPS=22, NRPS-like=8) and in the Cyanobacteria (NRPS=7, NRPS-like=2), while a single Actinobacterial MAG (DA_MAG_007_Iso899) is extremely talented with 17 and 4 NRPS and NRPS-like clusters, respectively. The bacteriocins were also prevalent across many clades with 36 different clusters detected.

There are several BGC types that are more prevalent in certain clades than others. For example, there were only four lassopeptides detected, and three were in Actinobacterial MAGs. Across the Proteobacteria, six of the seven MAGs from the family Sphingomonadaceae have a T3PKS cluster, while 5/6 Burkholderiales had an arylpolyrene cluster.

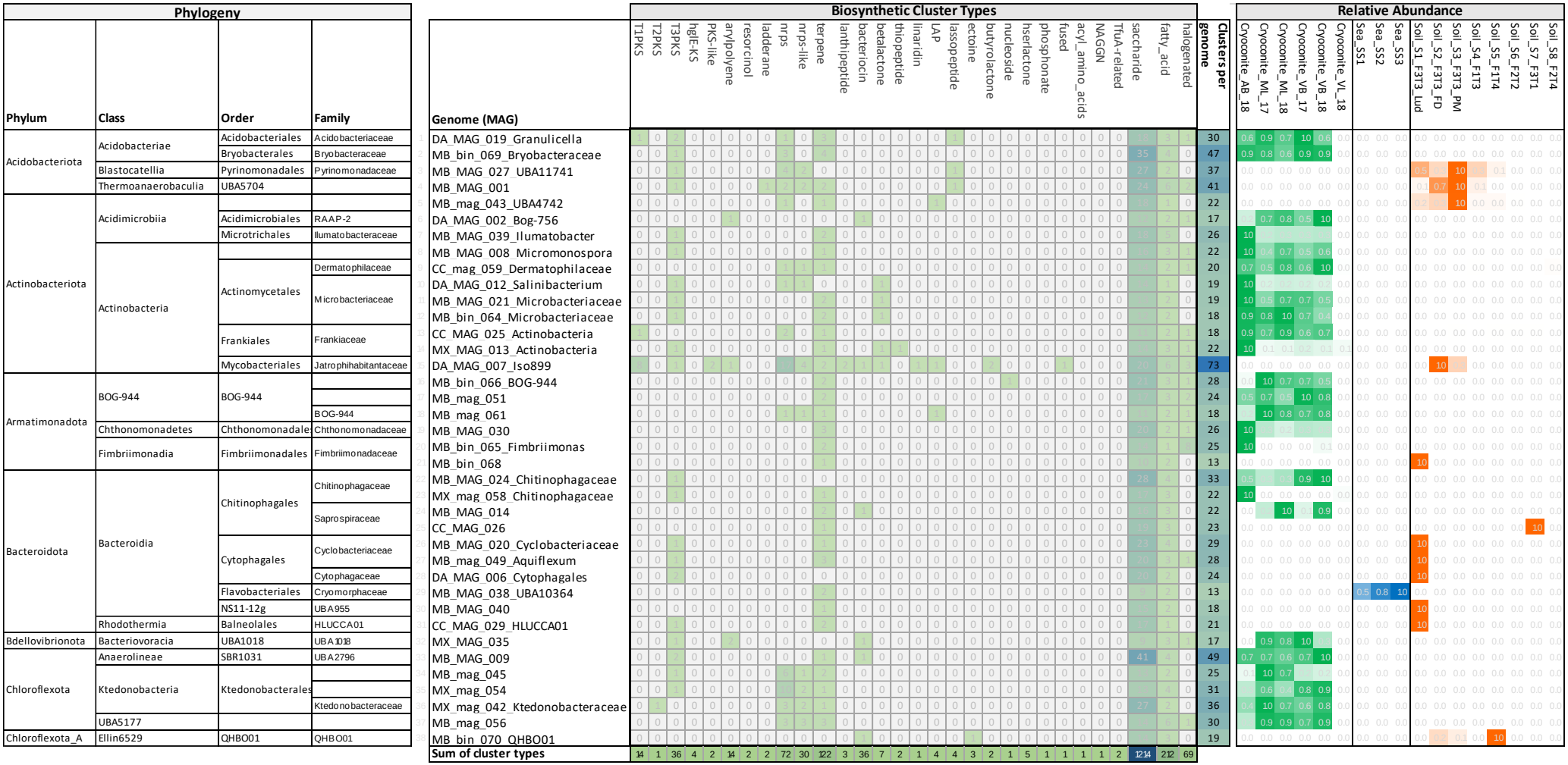

Figure 5-2 Secondary metabolite clusters in MAGs from the Acidobacteriota, Actinobacteriota, Armatimonadota, Bacteroidota, Bdellovibrionota, Chloroflexota, Chloroflexota_A phyla. Table showing the number and types of clusters detected by antiSMASH 5. The MAGs are arranged by taxonomic clade, and the relative abundance in each sample (expressed as max-normalised-abundance) is shown per MAG.

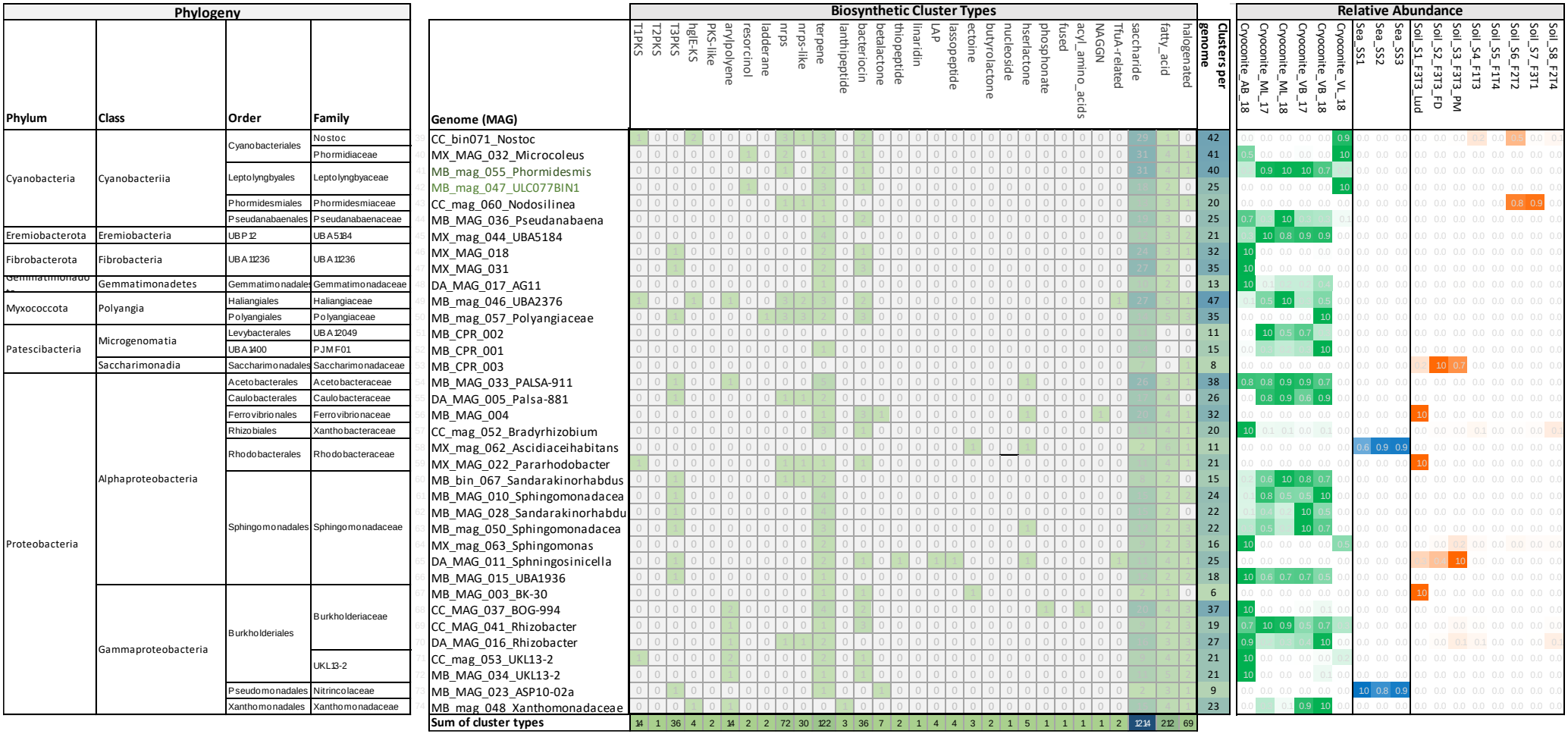

Figure 5-3 Secondary metabolite clusters in MAGs from the Cyanobacteria, Eremiobacterota, Fibrobacterota, Gemmatimonadota, Myxococcota, Patescibacteria and Proteobacteria phyla. Table showing the number and types of clusters detected by antiSMASH 5. The MAGs are arranged by taxonomic clade, and the relative abundance in each sample (expressed as max-normalised-abundance) is shown per MAG.

5.3.3 Network analysis of BGCs from MAGs

Although the vast majority of BGCs in the network analysis were singletons, there were several families of related BGCs that were similar to known compounds and these groups of related BGCs were examined because they tell us about metabolites that are enriched in these cryospheric samples.

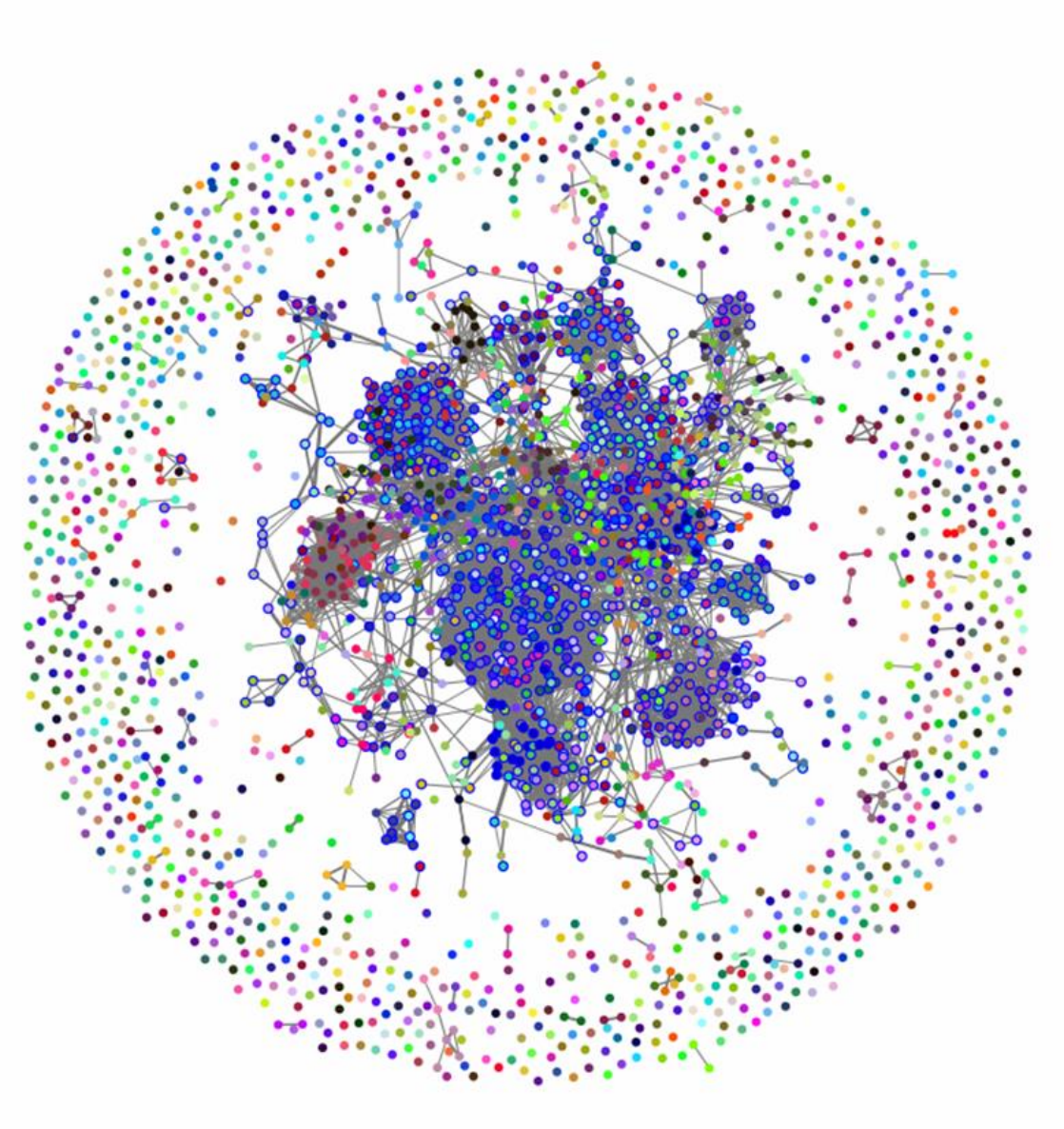

Figure 5-4 BiG-SCAPE network of 1742 BGCs from the Svalbard MAG collection and 1830 known biosynthetic gene clusters from the MiBIG database (v1.4). Total BGCs: 2649 (1096 singleton/s), links: 13454, families: 1433. Network generated using cutoff distance of 0.7. Clusters with a blue border represent BGCs with known compounds from the MiBIG database. Nodes without borders represent BGCs detected in the MAGs.

5.3.3.1 Terpenes and carotenoids

Terpenoid compounds were abundant in the MAGs, with 122 BGCs detected by antiSMASH in total. Of these, 40 had similarity to BGCS of known compounds in the MIBiG database, and the remaining 82 were novel. Network analysis with MIBiG compounds revealed nine different carotenoid cluster families that included a MIBiG cluster and at least four MAGs.

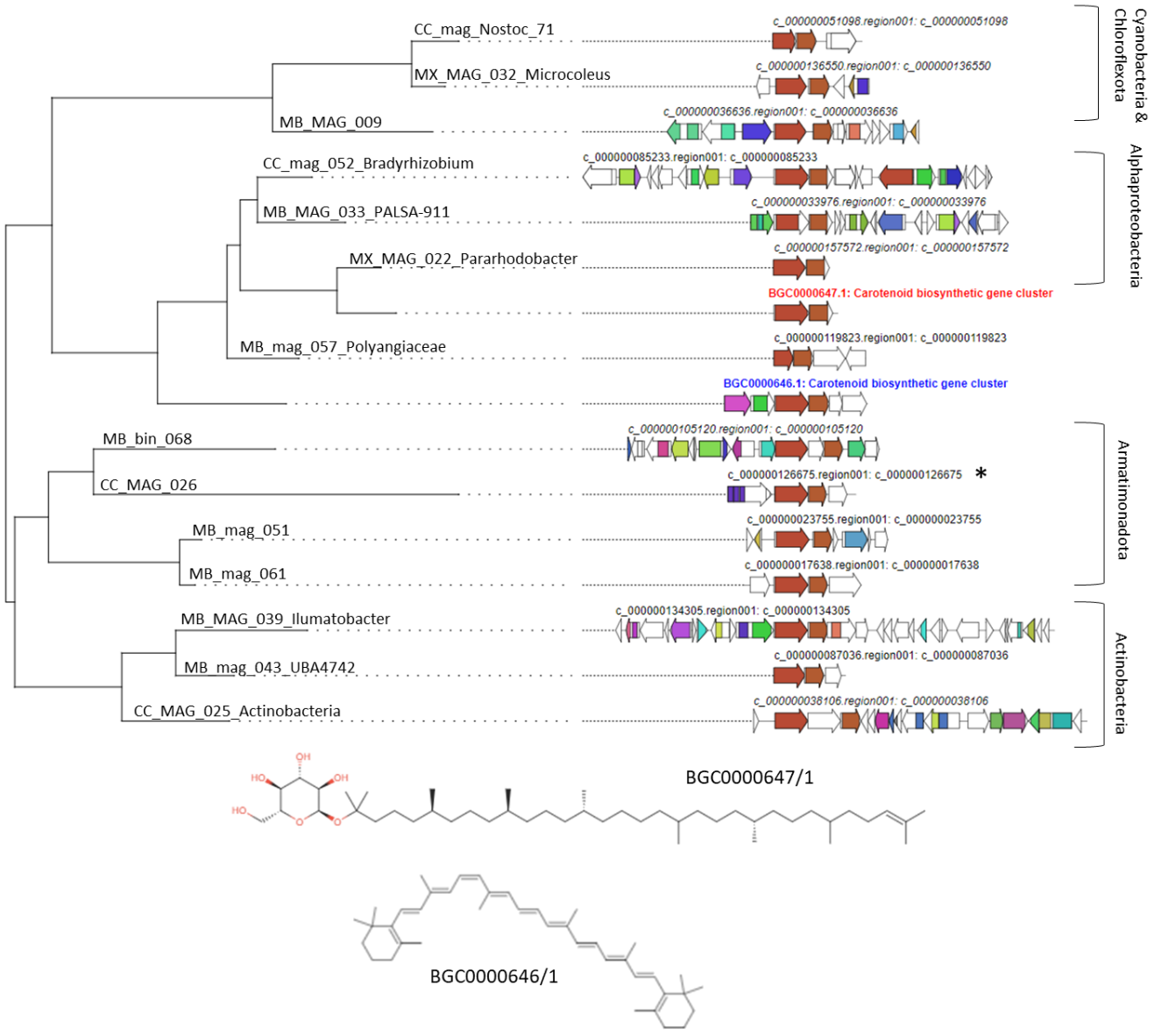

Figure 5-5 A Family of BGC s that synthesize carotenoid clusters similar to BGC0000646 and BGC0000647 are widely distributed across several phyla. Figure shows the contig id, MAG id and phyla membership of different tree branches. The molecules synthesized by the known BGCs are shown below. The * next to CC_MAG_026 because it does not belong to the same phylum (Armatimonadota) as the surrounding MAGs.

A large family of two known carotenoid clusters (BGC0000646 and BGC0000647) were detected, together with 14 BGCs from MAGs (Figure 5-5). These MAGs belonged to diverse phyla, such as the Cyanobacteria (CC_bin_071_Nostoc, MX_MAG_032_Microcoleus), Chloroflexota (MB_MAG_009), Armatimonadota (MB_bin_068, MB_mag_061, MB_mag_051), Actinobacteria (MB_MAG_039_Ilumatobacter, MB_mag_043_ UBA4742, CC_MAG_025_Actinobacteria), Alphaproteobacteria (CC_mag_052_Bradyrhizobium, MB_MAG_033_PALSA-911, MX_MAG_022_Pararhodobacter), and a single Myxococcota (MB_mag_057_Polyangiaceae).

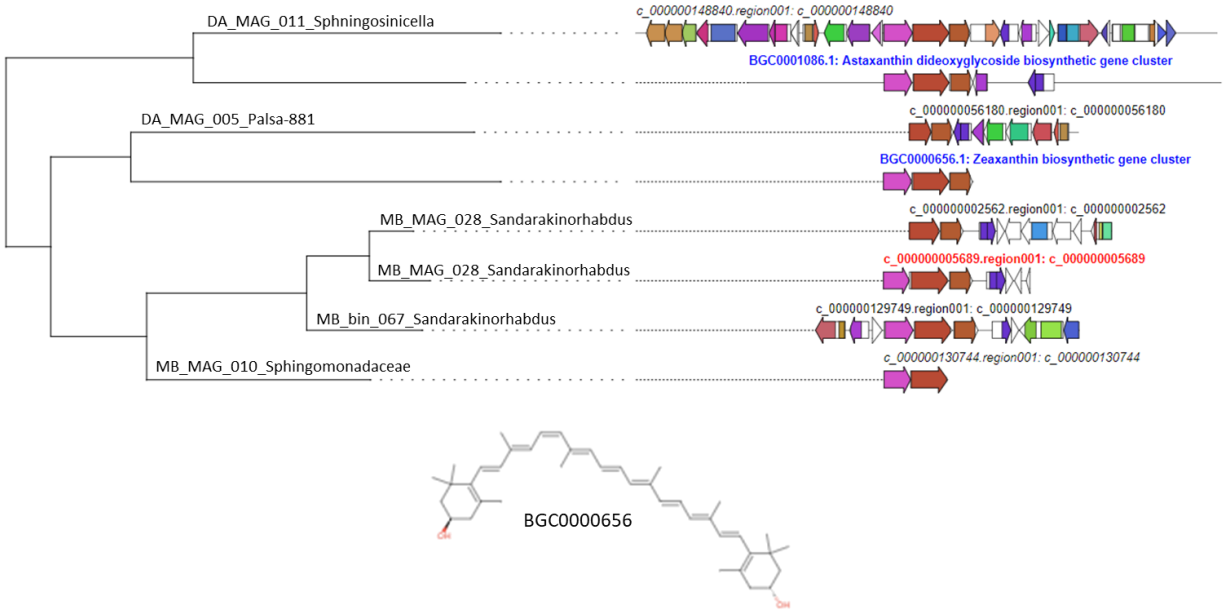

Figure 5-6 Family of BGCs that synthesize Astaxanthin dideoxyglycoside (BGC0001086) and Zeaxanthin (BGC0000656) gene clusters are all from the family Sphingomonadaceae. Figure shows the contig id and MAG id. The compound synthesized by the known BGCs are shown below.

A family of six BGCs that are similar to Astaxanthin dideoxyglycoside (BGC0001086) and Zeaxanthin (BGC0000656) were detected in five MAGs (DA_MAG_011_Sphningosinicella, DA_MAG_005_Palsa-881, MB_MAG_010_Sphingomonadaceae, MB_bin_067_Sandara-kinorhabdus and MB_MAG_028_Sandarakinorhabdus), which all belong to the family Sphingomonadaceae (Figure 5-6).

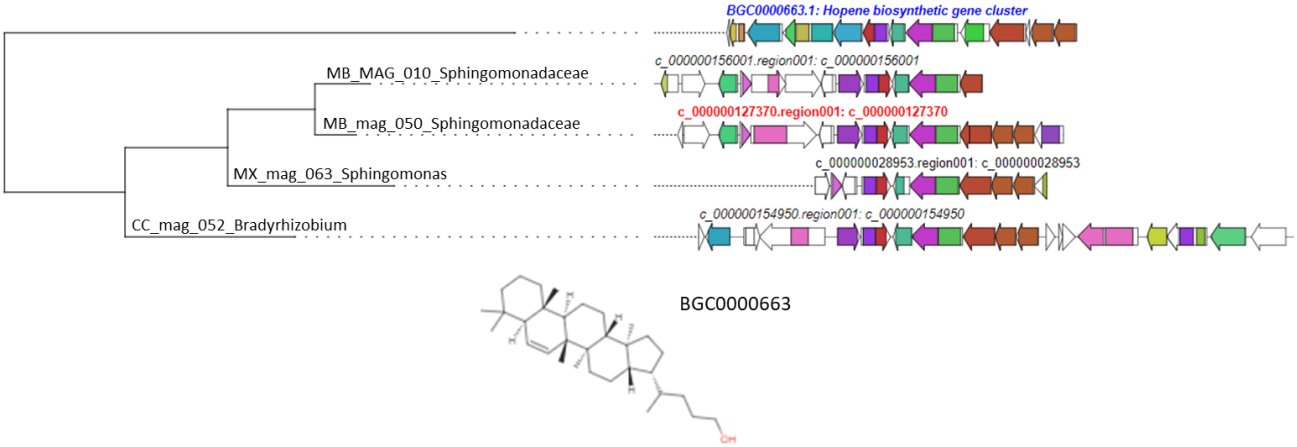

Figure 5-7 Family of BGCs similar to Hopene (BGC0000663) all from the Alphaproteobacteria. Figure shows the contig id and MAG id. The compound synthesized by the known BGCs are shown below the tree.

Several Alphaproteobacterial MAGs contained BGCs with partial similarity to the Hopene BGC (BGC0000663) (Figure 5-7).

5.3.3.2 Saccharides and EPS

The saccharide cluster class was the most abundant across all the MAGs, with 1214 clusters detected (Figure 5-2 and Figure 5-3). Most saccharides detected (1020) did not have hits to known compounds. Of those with hits to compounds in the MIBiG database, many of them were linked to the bacterial cell wall. For example, there were twelve MAGS with clusters similar to lipopolysaccharide (BGC0000774) and two similar to lipopolysaccharide (BGC0000773). There were also several clusters for the O-antigen portion of the gram-negative lipopolysaccharide layer. O-antigen BGCs in the dataset included two MAGs with clusters similar to BGC0000781, eleven MAGs similar to BGC0000782, three similar to BGC0000784, two like BGC0000788 and one similar to BGC0000791. Four Proteobacterial MAGs had similarity to the O&K-antigen (BGC0000780). Clusters in five MAGs were similar to the S-layer glycan BGC0000794 and two similar to S-layer glycan BGC0000795.

There were several clusters detected that are associated with bacterial capsules. The cell capsule is a polysaccharide layer that lies outside the cell envelope, also known as a glycocalyx or slime layer. Amongst the saccharides detected there were eight clusters similar to capsular polysaccharide (BGC0000730, BGC0000731, BGC0000732, BGC0000733). Four of these were in Cyanobacterial MAGs. In addition, duitan polysaccharide (BGC0000759) was found in three Alphaproteobacterial MAGs. Other EPS include one cluster similar to exopolysaccharide (BGC0000761), two clusters similar to galactoglucan (BGC0000801), two

K53 capsular polysaccharides (BGC0001947), three similar to phosphonoglycans (BGC0000806), four similar to polysaccharide B (BGC0001411), and two clusters from Alphaproteobacterial MAGs similar to sphingan polysaccharide (BGC0000797).

In addition to the EPS, there were several saccharide clusters with other functions. A BGC in the Acidobacterial MAG, MB_MAG_001, was similar to the aminoglycoside antibiotic hydroxystreptomycin (BGC0000690). There are several molecules that are synthesized by large BGCs that have modules similar to several type of clusters. An example is the glycopeptidolipid (BGC0000362), which is classed as an NRP, but has saccharide, fatty acid, and peptide moieties.

5.3.3.3 Nonribosomal peptide synthetases (NRPS)

Although there were 72 and 30 NRPS and NRPS-like clusters detected in the dataset, the vast majority of these were novel or singletons, and therefore cannot be explored via network analysis. However, BiG-SCAPE identified a family of BGCs that included the three BGCs from MiBIG, namely anabaenopeptin NZ857 and nostamide A (BGC0001479), aureusimine (BGC0000308), and AM-toxin (BGC0001261) and several BGCS in MAGs from the Cyanobacteria, Acidobacteria, Actinobacteria and Chloroflexota (Figure 5-8). MAGs with similarity to the BGC that synthesises the anabaenopeptin NZ857 and nostamide A (BGC0001479) compound from *Nostoc punctiforme* PCC 73102, include CC_mag_Nostoc_71. Several of the other clusters similar to the anabaenopeptin NZ857 (BGC0001479) BGC belong to Cyanobacteria (MX_MAG_032_Microcoleus) and Chloroflexota (MX_mag_054 and MB_mag_045). MB_MAG_027_UBA11741 was more similar to AM toxin (BGC0001261).

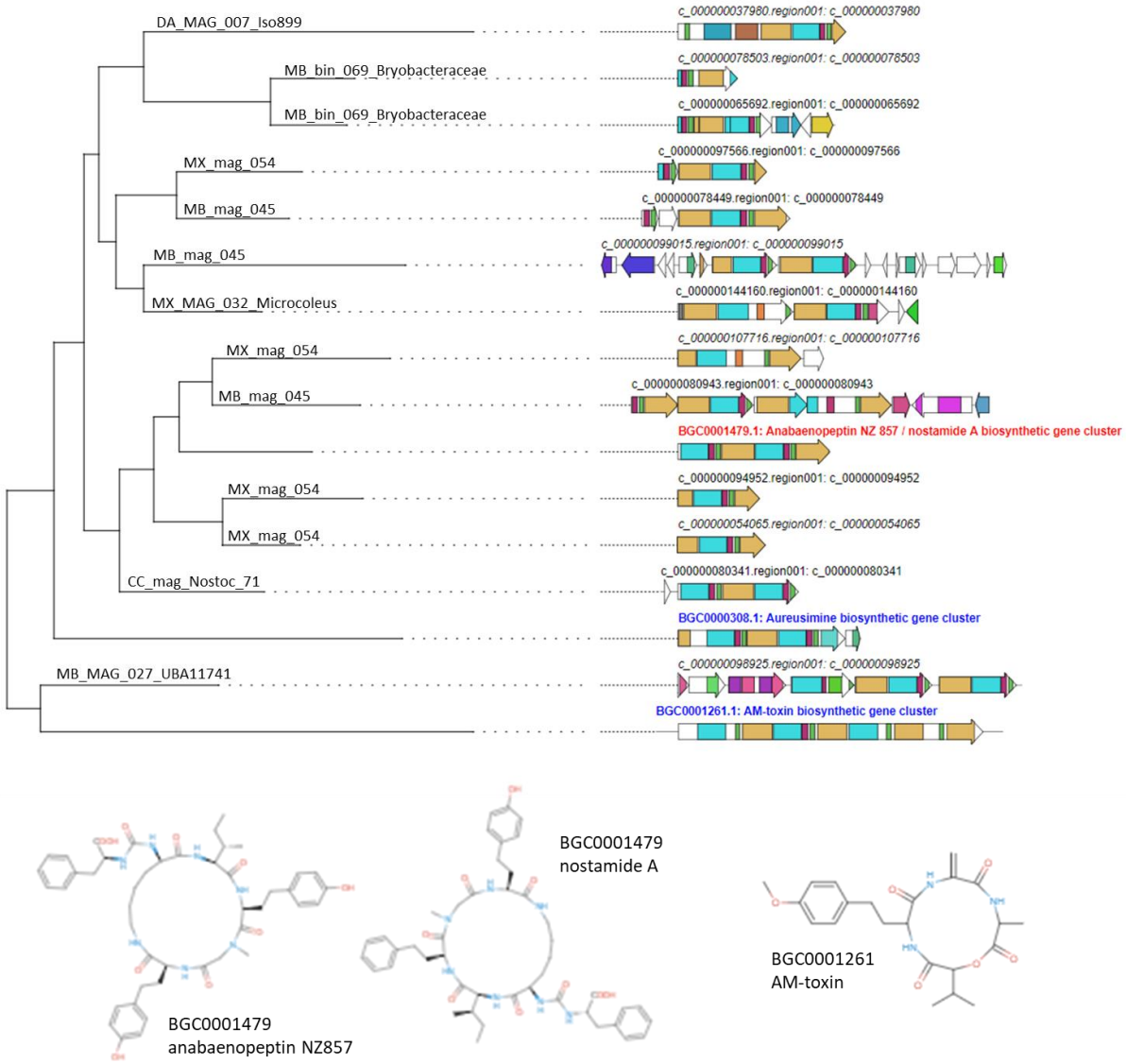

Figure 5-8 Several NRPs with similarity to anabaenopeptin NZ857 / nostamide A were identified in Chloroflexota and Cyanobacterial MAGs.

5.3.3.4 Polyketide Synthases Type III

Several Actinobacterial MAGs had T3PKS clusters for alkylresorcinol (BGC0000282), a phenolic compound that confers resistance against penicillin (Figure 5-9). The alkylresorcinol BGC is from *Streptomyces griseus* subsp. NBRC 13350. In addition, a related MAG from the Acidobacteria (MB_MAG_001) also clustered within this BGC family and was similar to the lagunapyrone A BGC (BGC0001647).

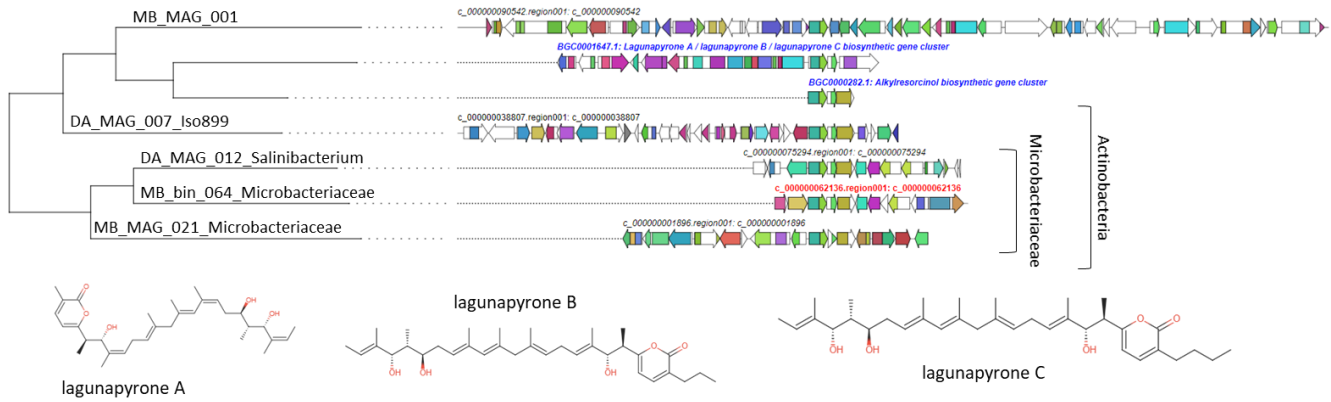

Figure 5-9 Several Actinobacterial MAGs contain a polyketide BGC for alkylresorcinol.

5.3.4 Cyanobacterial secondary metabolites

Because of their high abundance and importance as ecosystem engineers in cryoconite and soil habitats, some of the secondary metabolites of the Cyanobacterial MAGs were investigated in greater detail. The Cyanobacteria are photosynthetic and filamentous, known to excrete EPS which have a variety of functions (Chrismas et al., 2016b; Rossi and De Philippis, 2015). MX_MAG_032_Microcoleus had 31 saccharide clusters, including clusters similar to lipopolysaccharide (BGC0000774) and capsular polysaccharide (BGC0000730). MB_mag_047_ULC077BIN1 had 18 saccharide clusters, one of which was 13% similar to capsular polysaccharide (BGC0000731). MB_mag_055_Phormidesmis had 31 saccharide clusters, including a cluster with 13% similarity to capsular polysaccharide (BGC0000731). CC_mag_060_Nodosilinea had 13 saccharide clusters, including one with 13% similarity to S-layer glycan (BGC0000794). MB_MAG_036_Pseudanabaena had 18 saccharide clusters including a cluster with 13% similarity to S-layer glycan (BGC0000794). There were 29 saccharide clusters in CC_mag_071_Nostoc, including capsular polysaccharide (BGC0000731) and lipopolysaccharide (BGC0000774). CC_mag_071_Nostoc also had two clusters similar to hglE-KS (heterocyst glycolipid synthase-like PKS), including a cluster with 28% similarity to heterocyst glycolipids (BGC0000869).

Some of the diverse secondary metabolites of Cyanobacteria are shown in Figure 5-10. In MX_MAG_032_Microcoleus, there was a cluster with 14% similarity to the RiPP: Cyanobactin, anacyclamide A10 (BGC0000472), as well as a cluster with 16% similarity to barbamide (BGC0000962), a NRP + Polyketide: Modular type I cluster. MX_MAG_032_Microcoleus also had two NRPS, including a cluster with 16% similarity to gramicidin (BGC0000367) and several other compounds (Supplementary Table E-1).

MB_mag_055_Phormidesmis had a cluster that was only 3% similar to the known BGC for polyketide Sch-47554 / Sch-47555 (BGC0000268). ClusterBlast revealed that the most similar clusters belong related Cyanobacteria, *Lyngbya confervoides*. MB_MAG_036_Pseudanabaena had low similarity to murayaquinone (BGC0001675) and several other BGCs. CC_mag_071_Nostoc had a cluster with 25% similarity to the NRP + Polyketide, cryptophycin-327 (BGC0000975) as well as a NRPS cluster with no MiBIG hit. MX_MAG_032_Microcoleus, CC_mag_060_Nodosilinea and CC_mag_071_Nostoc all had clusters with 100% similarity to anabaenopeptin NZ857 / nostamide A (BGC0001479 (also shown in Figure 5-8). There were only two resorcinol clusters in the dataset, both of them in Cyanobacterial MAGs (MX_MAG_032_Microcoleus and MB_mag_047_ULC077BIN1).

Figure 5-10 KnownClusterBlast results of A NRPS from cc_MAG_Nostoc_71: The highly modular nature of NRPS gene clusters means that small reorganisations can result in a large number of different compounds.

5.3.5 Actinobacterial MAG DA_MAG_007_Iso899

The Actinobacterial MAG DA_MAG_007_Iso899 was the most prolific producer of secondary metabolites in the dataset (Figure 5-2, Appendix E-1). DA_MAG_007_Iso899 is high-quality with a length of 4,713,114 bp made up of 185 contigs. The N50 of the contigs is 33034, the GC content is 69.61% and the completion is 97.18% and redundancy was 1.41% (Chapter 4). The most similar genome in the GTDB (GCF_000421445.1) belongs to an isolate from North American forest soils and this MAG was also more abundant in the soil than cryoconite or seawater.

Table 5-3 BGCs from Actinobacterial MAG DA_MAG_007_Iso899

Cluster type (antiSMASH)	From	To	Most Similar Known Cluster	MIBiG Accession	MIBiG cluster type
T1PKS	12,798	58,653	calicheamicin	BGC0000033	PK
arylpolyene, fatty_acid	7,995	35,789	kedarcidin	BGC0000081	PK: Iterative type I + PK: Enediyne type I
T1PKS, halogenated	23,412	50,489	sporolide A / sporolide B	BGC0000150	NRP + PK: Enediyne type I
T1PKS, fatty_acid, saccharide, halogenated, NRPS, betalactone	1	84,052	sporolide A / sporolide B	BGC0000150	NRP + PK: Enediyne type I
saccharide	1	13,268	tiacumicin B	BGC0000165	PK: Modular type I
saccharide	1	46,555	arenimycin A	BGC0000198	PK: Type II + Saccharide: Hybrid/ tailoring
T3PKS	21,840	46,906	alkylresorcinol	BGC0000282	PK
saccharide	30,942	43,604	A-503083 A / A-503083 B / A-503083 E / A-503083 F	BGC0000288	NRP
NRPS	1	24,915	enduracidin	BGC0000341	NRP
saccharide	1	10,333	streptobactin	BGC0000368	NRP
terpene, halogenated	64,654	84,730	brasilicardin A	BGC0000632	Terpene + Saccharide
terpene, PKS-like, T1PKS	45,745	102,928	isorenieratene	BGC0000664	Terpene
saccharide	5,538	39,151	arginomycin	BGC0000883	Other
lanthipeptide, fatty_acid, NRPS	1	62,146	meridamycin	BGC0001011	NRP + PK
NRPS	1	30,199	WS9326	BGC0001297	NRP
NRPS, fatty_acid	1	28,845	lobosamide A / lobosamide B / lobosamide C	BGC0001303	PK
NRPS,fatty_acid, T1PKS	1	69,629	lobosamide A / lobosamide B / lobosamide C	BGC0001303/1	PK

Cluster type (antiSMASH)	From	To	Most Similar Known Cluster	MIBiG Accession	MIBiG cluster type
NRPS-like	1	26,151	malacidin A / malacidin B	BGC0001448/1	NRP:Ca+-dependent lipopeptide
saccharide,NRPS-like	24,435	56,187	amycolamycin A / amycolamycin B	BGC0001503/1	PK
NRPS	22,106	58,160	amycolamycin A / amycolamycin B	BGC0001503/1	PK
T1PKS	1	17,715	butyrolactol A	BGC0001537/1	PK
NRPS	10,871	65,454	ecumicin	BGC0001582/1	NRP
fused,T1PKS,fatty_acid,butyrolactone	10,290	60,923	ketomemicin B3 / ketomemicin B4	BGC0001633/1	Other
NRPS,LAP	1	31,351	paulomycin	BGC0001731/1	Other
NRPS	1	32,054	rimosamide	BGC0001760/1	NRP
saccharide	51,388	76,732	streptovaricin	BGC0001785/1	PK
NRPS,PKS-like	1	30,648	vazabitide A	BGC0001818/1	NRP
T1PKS,NRPS-like	1	11,407	(2S,6R)-diamino-(5R,7)-dihydroxy-heptanoic acid	BGC0001912/1	NRP

PK: Polyketide

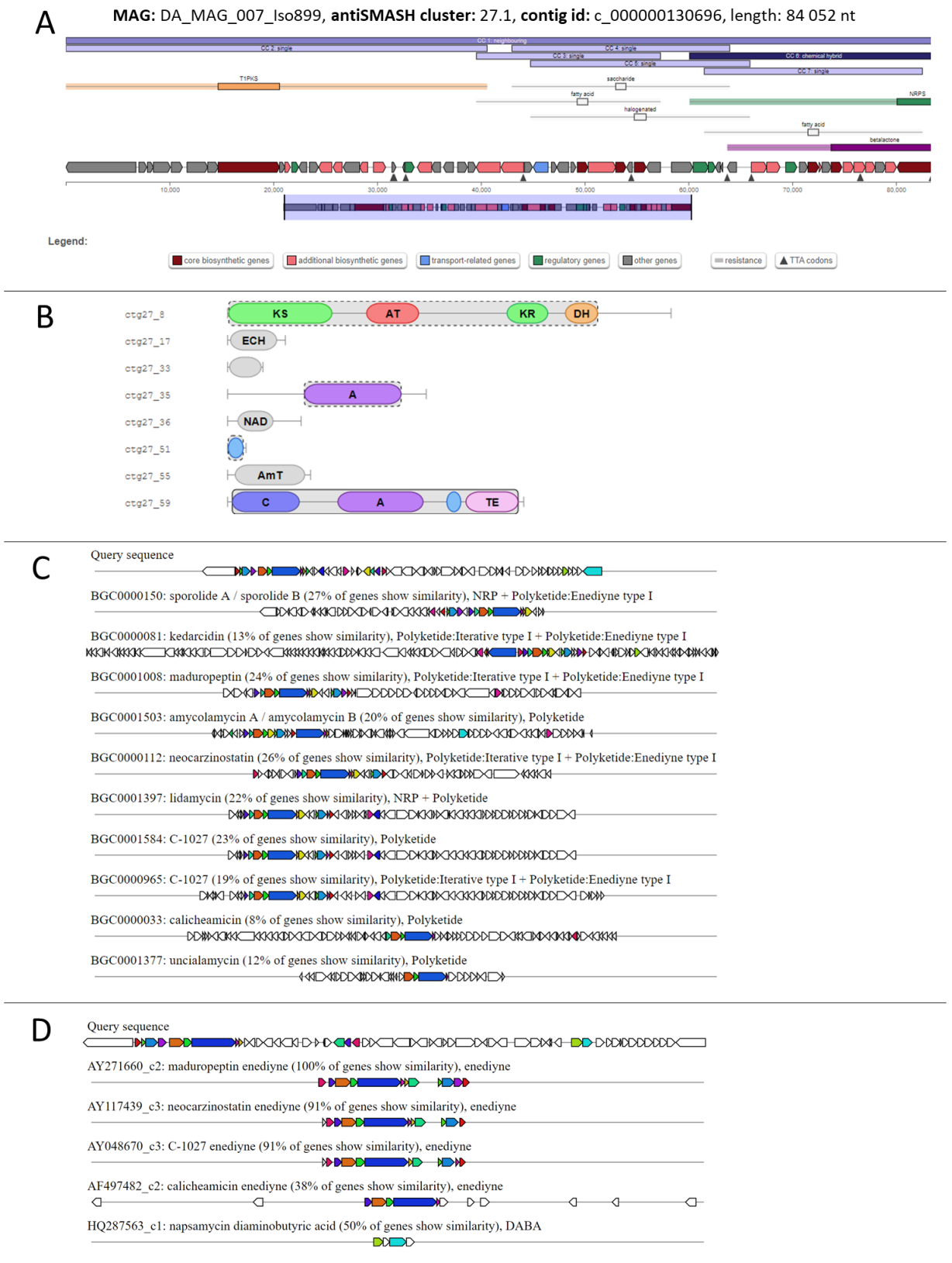

Figure 5-11 Cluster 27.1 has high similarity to several Polyketide: Enediyene type I BGCs. A Map of the location of the different clusters detected by antiSMASH on this contig. B shows the detailed NRPS/ PKS domain annotation. C shows known BGCs identified by KnownClusterBlast. D shows the accessions of similar clusters using SubClusterBlast.

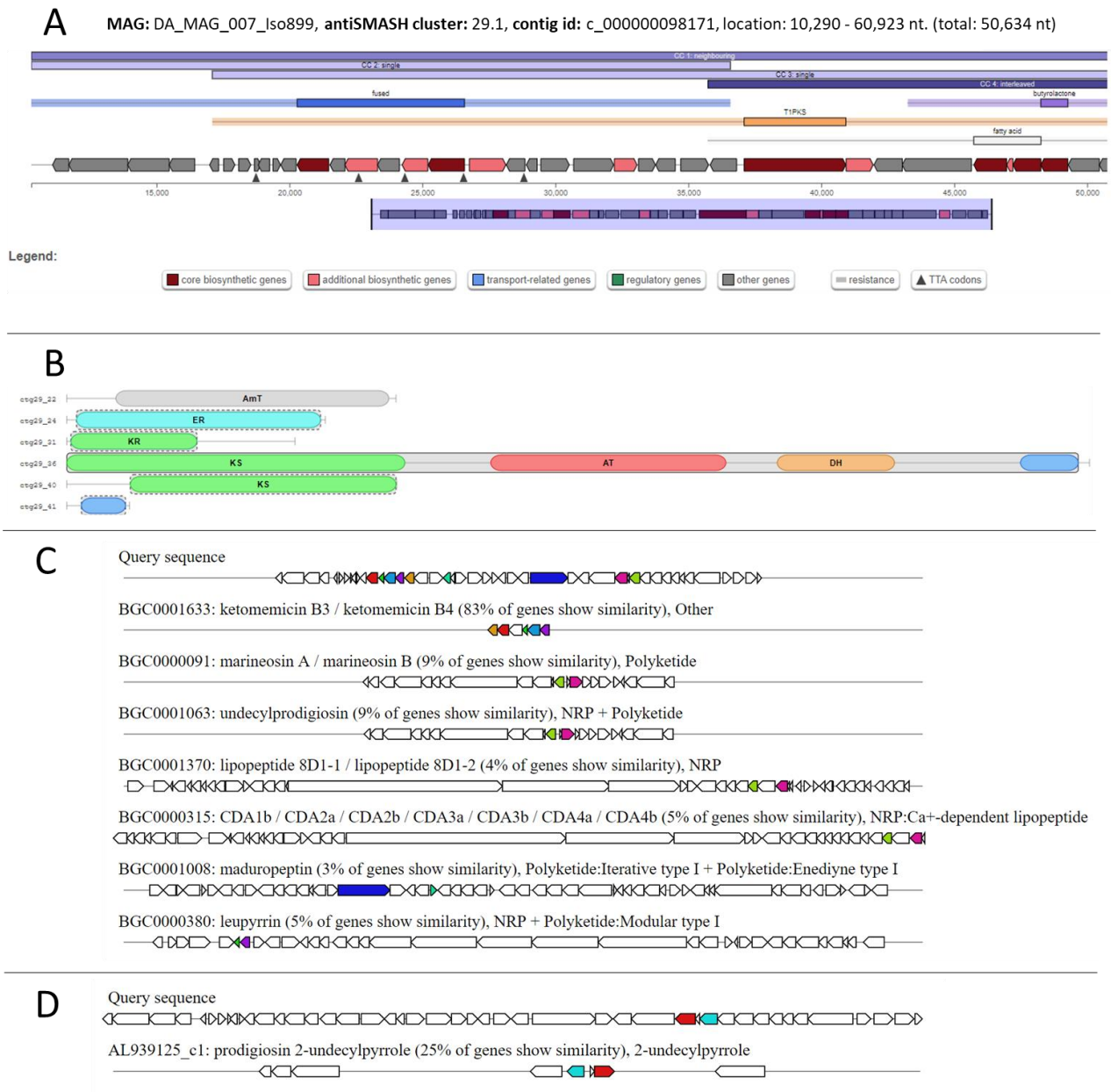

Figure 5-12 A Map of the location of the different clusters detected by antiSMASH on this contig. B shows the detailed NRPS/ PKS domain annotation**. C** shows known BGCs identified by KnownClusterBlast**. D** shows the accessions of similar clusters using SubClusterBlast.

5.3.6 Screening contigs by environment

Finally, to identify the metabolites from each of the environments that belonged to less abundant community members, the assemblies for each of the cryoconite, soil and seawater assemblies were submitted to antiSMASH. The saccharide and fatty acid clusters were not included in the analysis. There were 674 clusters detected from the cryoconite assembly (Appendix Table E-2), 325 clusters detected from the soil assembly (Appendix Table E-3) and 14 clusters detected from the seawater assembly (Appendix Table E-4).

Table 5-4 Types of secondary metabolites detected by antiSMASH

	Cryoconite (n=6)		Soil (n=8)		Seawater (n=3)	
Type	**count**	**Relative abundance (%)**	**count**	**Relative abundance (%)**	**count**	**Relative abundance (%)**
Terpene	273	40.50	84	25.85	6	42.86
NRPS	90	13.35	58	17.85	0	0.00
Bacteriocin	75	11.13	30	9.23	1	7.14
T3PKS	72	10.68	23	7.08	2	14.29
Nrps-like	49	7.27	41	12.62	0	0.00
Arylpolyene	36	5.34	15	4.62	1	7.14
T1PKS	13	1.93	17	5.23	2	14.29

Terpenes were the most abundant metabolite in all three environments. Despite small samples sizes, there was some difference in the types of secondary metabolites detected in soil, seawater and cryoconite. Of the 674 clusters detected in the cryoconite assembly, 172 of them were like 71 known BGCs from the MIBiG database (Appendix Table E-2). There were 177 BGCs with hits to clusters in MIBiG in the soil assembly (Appendix Table E-3), and three BGCs with hits to a single carotenoid MIBiG compound in the seawater assembly (Appendix Table E-4). The screening of the entire assemblies greatly increased the number of detected BGCs.

Table 5-5 Table of rare secondary metabolites detected in cryoconite, soil and seawater

	Cryoconite (n=6)		Soil (n=8)		Sea (n=3)	
Type	**count**	**Relative abundance (%)**	**count**	**Relative abundance (%)**	**count**	**Relative abundance (%)**
betalactone	7	1.04	3	0.92	1	7.14
ladderane	7	1.04	1	0.31	0	0.00
acyl_amino_acids	6	0.89	4	1.23	0	0.00
resorcinol	6	0.89	1	0.31	0	0.00
lassopeptide	5	0.74	7	2.15	0	0.00
hglE-KS	5	0.74	5	1.54	0	0.00
LAP	5	0.74	2	0.62	0	0.00
hserlactone	4	0.59	8	2.46	0	0.00
lanthipeptide	4	0.59	4	1.23	0	0.00
linaridin	4	0.59	1	0.31	0	0.00
phosphonate	2	0.30	4	1.23	0	0.00
cyanobactin	2	0.30	0	0.00	0	0.00
bottromycin	2	0.30	0	0.00	0	0.00
furan	2	0.30	0	0.00	0	0.00
PKS-like	1	0.15	1	0.31	0	0.00
T2PKS	1	0.15	0	0.00	0	0.00
thiopeptide	1	0.15	0	0.00	0	0.00
microviridin	1	0.15	0	0.00	0	0.00
proteusin	1	0.15	0	0.00	0	0.00
siderophore	0	0.00	4	1.23	0	0.00
ectoine	0	0.00	3	0.92	1	7.14
indole	0	0.00	3	0.92	0	0.00
other	0	0.00	3	0.92	0	0.00
butyrolactone	0	0.00	2	0.62	0	0.00
NAGGN	0	0.00	1	0.31	0	0.00

Sea – 7 types, soil – 25 types, cryoconite - 25

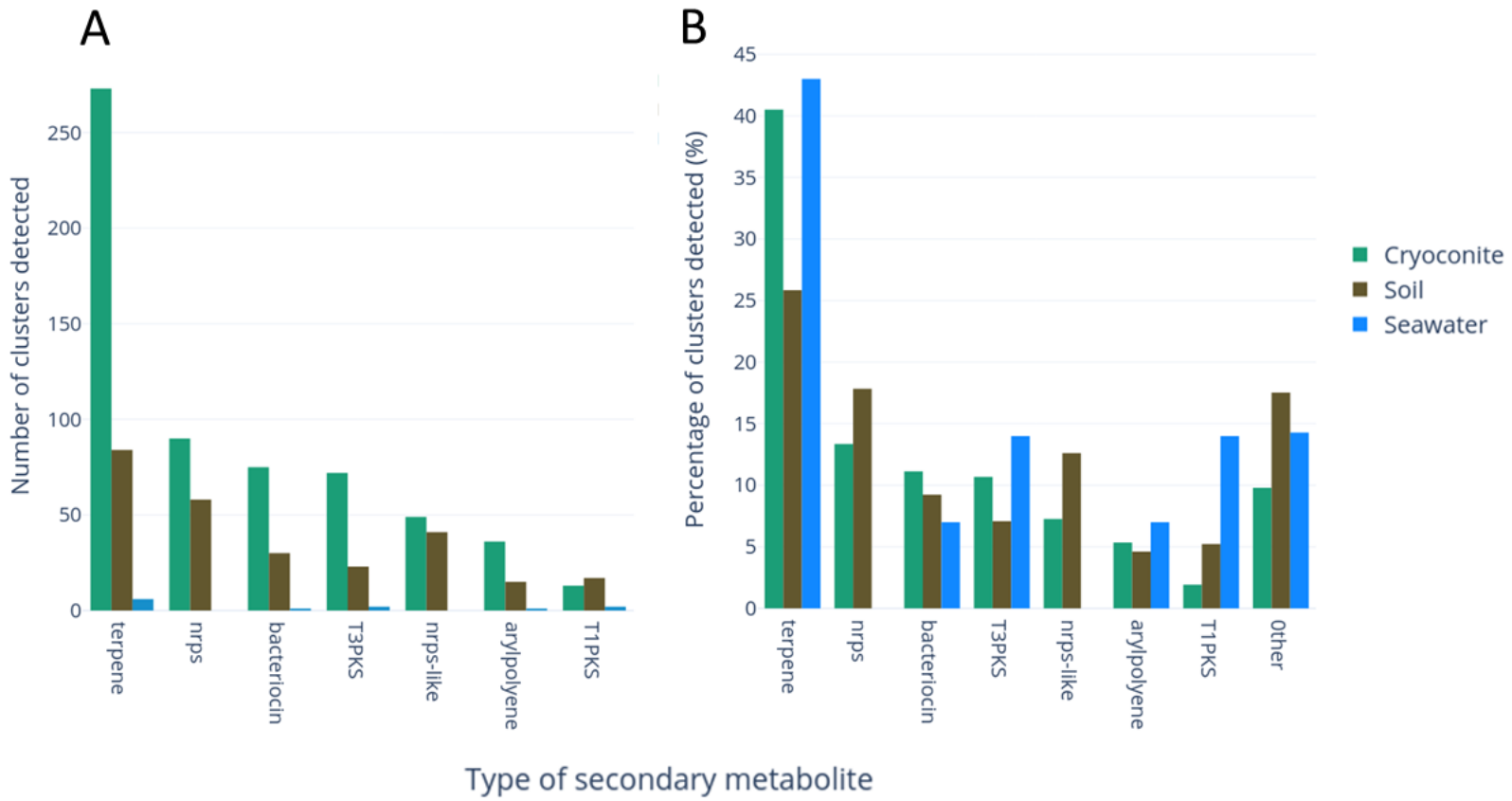

Figure 5-13 The number of biosynthetic gene clusters (BGCs) belonging to the most common types of secondary metabolite detected in cryoconite, soil and seawater. Figure shows only the most common secondary metabolite types (n> 10 in at least one environment). **A**) shows the absolute number of clusters detected in each environment. **B**) shows the relative proportion of the metabolites in each environment.

5.3.7 The metabolomes of cryoconite from different glaciers are similar

Principle component analysis (PCA), multidimensional scaling (MDS) of unsupervised random forest proximities and supervised principle component linear discriminant analysis (PC-LDA) were used to assess the overall data structure and class relationships between the metabolites of different samples. Cryoconite from different holes from four different glaciers (AB, ML, VB, and VL) were quite similar. However, there was some clustering observed between cryoconite holes from the same glacier, and in particular the cryoconite from VL tended to cluster together.

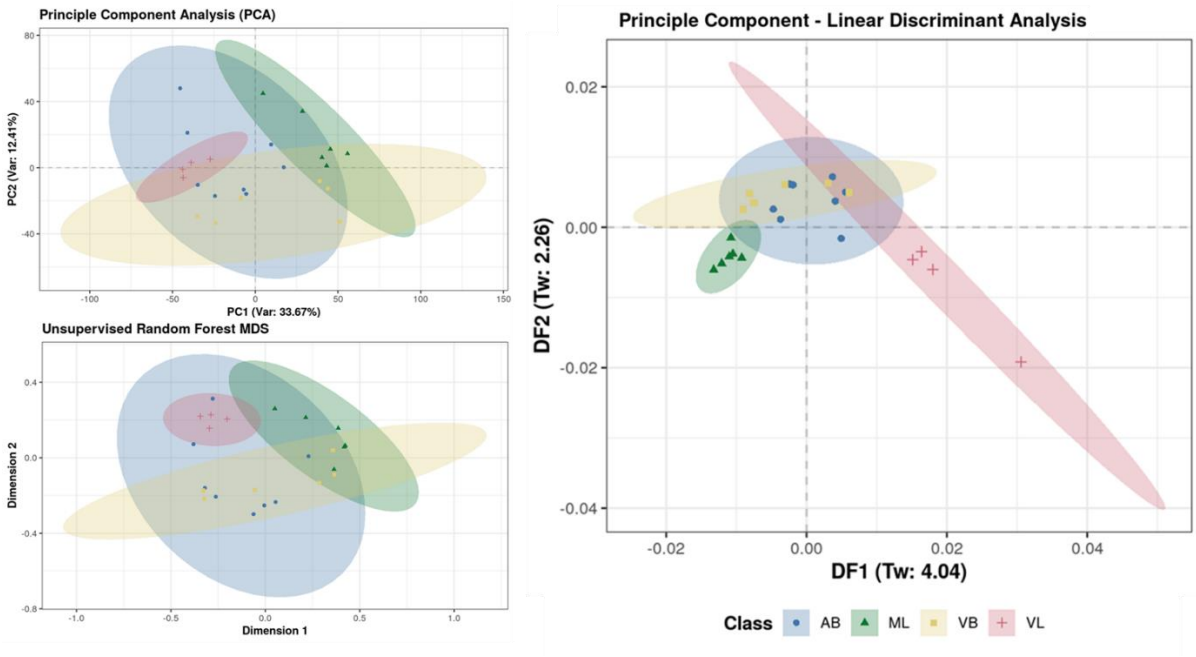

Figure 5-14 Principle Component Analysis (PCA), Principal Component- Linear Discriminant Analysis (PC-LDA) and Unsupervised Random Forest MDS of cryoconite of metabolites from four glaciers. Each point on the graph represents metabolites from a separate cryoconite hole.

The PCA and unsupervised random forest MDS plots show that there are no outliers present in that data set and that there is some grouping of sample classes such as VL. This is confirmed by explanatory discrimination in the PC-LDA plot where both DF1 and DF2 have Tw values > 2 (this is considered explanatory). Supervised random forest has not been performed due to the low numbers of replicates (<6) for the VL class. Unfortunately, the soil at each site, even though from the same time point, differed too much to be considered replicates (corroborated by taxonomic profiles (Chapter 3), and relative abundance of MAGs (Chapter 4).

ANOVA can be used to identify the metabolome features that are discriminatory between the four glaciers. ANOVA was preferable to random forest due to the low numbers of replicates and it identified 70 significant metabolome features, which are shown in a heat map of explanatory features for metabolite differences between four Svalbard glaciers. The list of metabolites is available in Appendix Table E-5. The metabolites were mapped to their KEGG categories, which is shown in Figure 5-15.

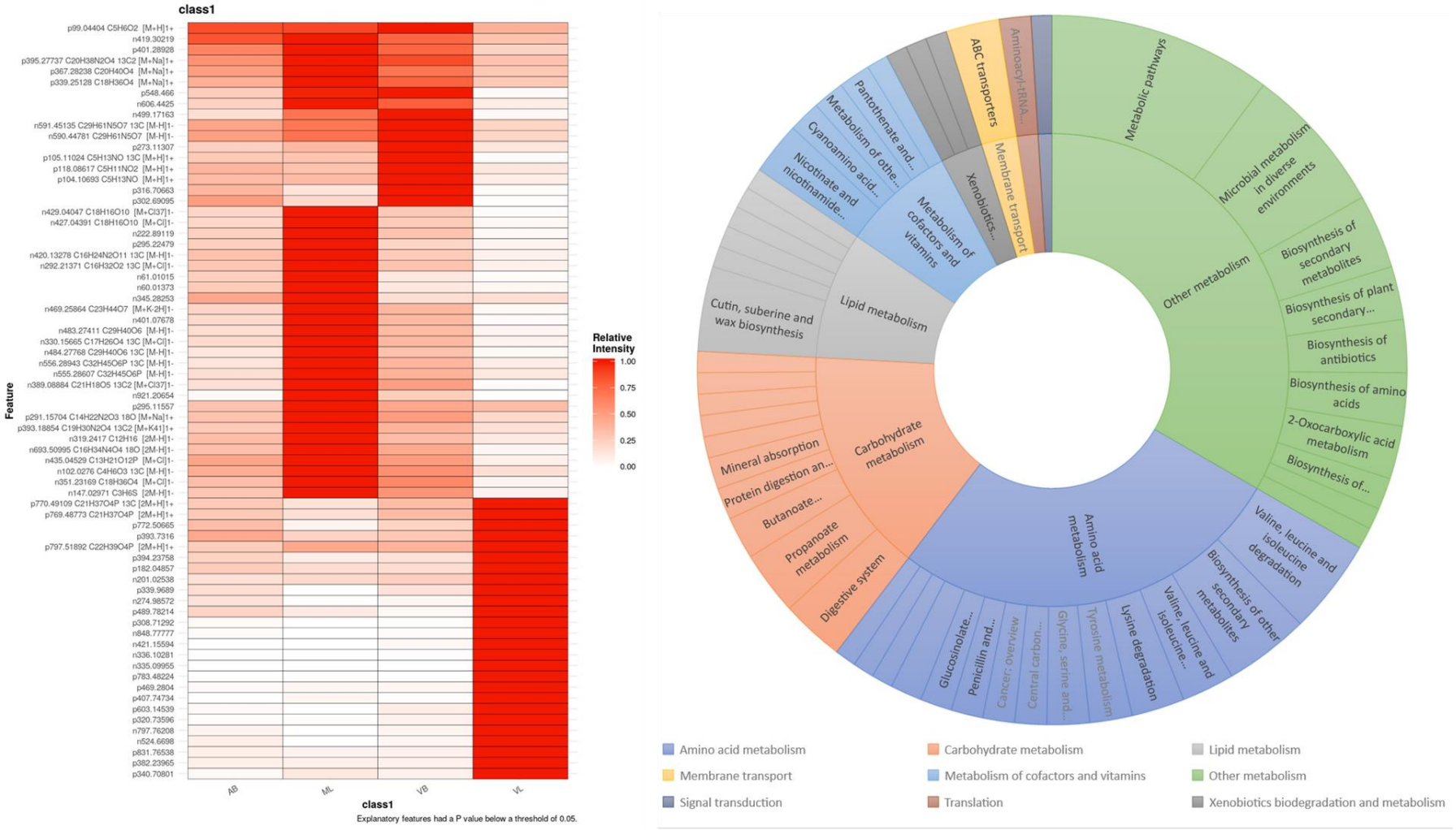

Figure 5-15 Heat map of explanatory features for metabolite differences between four Svalbard glaciers, and their KEGG categories .

5.4 Discussion

In Chapter 4, 74 MAGs were resolved from Svalbard cryoconite, soil and seawater metagenomes. These MAGs contain several novel species and therefore offer potentially novel metabolites from genomes that have never been sequenced or cultured before. Using antiSMASH, BGCs were annotated, and the resulting NP class was predicted based on similarity to reference BGCs and their known compounds in the MIBiG database. The separate cryoconite, soil and seawater assemblies include contigs that were not abundant enough to be included in MAGs but could still be linked to an environment origin. With this information, the LC-MS data was searched for evidence of the NP in the metabolome. Historically, BGC predictions do not always correlate well with detected metabolites via LC-MS and HPLC, because several metabolites are only synthesized under specific conditions (Chiang et al., 2011; van Bergeijk et al., 2020). The BGCs are better thought of as reflecting the potential rather than the actual biosynthetic activities of the organisms. However, once a high potential BGC has been predicted, genomic information makes it possible to strategically engineer the heterologous expression of those compounds. The focus of this chapter was therefore the identification of high potential BGCs in the genomes of highly abundant bacteria of cryoconite and soil.

5.4.1 Biosynthetic gene clusters are modular

Although the number of BGCs and their products are diverse, they consist of permutations in the sequence and modifications of a few key conserved core enzymes (Blin et al., 2017a). To identify BGCs, genome mining tools need to identify these conserved core biosynthetic genes, and then search upstream and downstream of the conserved region to identify other enzymes associated with the core sequence (Blin et al., 2017a). In addition to these core enzymes, there are a plethora of different tailoring enzymes that add extra structural diversity to the NPs (Banik et al., 2010; Owen et al., 2015). Therefore, very few BGCs fit neatly into a single class, and the classification of the BGC by the antiSMASH algorithm reflects just one way of classifying the BGC and resultant compound- which can differ from the MIBiG classification (Appendix Table E-1). In this study very few products with complete or even partial similarity to known compounds in the MIBiG database were found. In fact, 1464 (84%) BGCs had no similarity to known BGCs and compounds in the MIBiG database, suggesting that they synthesise novel compounds. Using network analysis with BiG-SCAPE, BGCs with similar domains were

identified and their similarity to each other viewed. In this way, even though exact compounds could not be identified, the class of the potential molecules could be inferred based on domain structure similarity, and families of BGCs and molecules that were enriched in this Arctic environment could be identified.

5.4.2 Secondary metabolites reflect adaptations to environmental stressors

The most abundant cluster type detected was the saccharides (1214 clusters), followed by fatty acids (212 clusters), and terpenes (122 clusters). These three cluster categories are known to play important roles in adaptation to cryospheric environments. The saccharides clusters detected by antiSMASH comprise several components of the cell wall as well as glycolipids and EPS which help to prevent against desiccation, allow the formation of biofilms and protect against UV stress (Poli et al., 2010). Fatty acids are known to maintain cellular membrane fluidity and permeability at low temperatures (D'Amico et al., 2006), and terpenes are often pigments and antioxidants capable of scavenging free radicals and protecting against the damaging effects of UV radiation (Paduch et al., 2007; Sajjad et al., 2020). However fatty acids and terpenoids have also been known to play antimicrobial roles (Karpiński and Adamczak, 2019; Yoon et al., 2018).

5.4.2.1 Terpenes and carotenoids

Terpenes are biosynthetically derived from isoprene units (C_5H_8) linked "head to tail" to form linear chains or arranged to form rings, where they have the formula $(C_5H_8)_n$ depending on the number of isoprene units (Paduch et al., 2007). Terpenes can be modified to include hydroxyl, carbonyl, ketone, or aldehyde groups, after which, they are referred to as terpenoids (Paduch et al., 2007). Terpenoids have been found to be useful in cancer prevention, have antimicrobial, antifungal, antiparasitic, antiviral, anti-allergenic, antispasmodic, antihyperglycemic, anti-inflammatory, and immunomodulatory properties and act as natural insecticides (Paduch et al., 2007). One of the major types of terpenoids is the carotenoids, most of which have 40 carbon atoms from 8 isoprene units. To date, there are over 1117 natural carotenoids from 683 source organisms (Yabuzaki, 2017). There were 122 terpene BGCs detected in the 74 screened MAGs, and 76 of these did not have hits to known compounds in the MiBIG database. Carotenoids perform diverse functions but are probably most useful as photosynthetic and photoprotective pigments, a function which is particularly important in Arctic habitats where UV radiation in snow and ice can damage bacterial DNA (Maccario et al., 2015). Some of the carotenoid BGCs, such as the family of clusters similar to BGC0000646 and BGC0000647, were widely

distributed across several phyla (Figure 5-5), whilst other terpenoid pigments were very clade specific. For example, all six BGCs that are like Astaxanthin dideoxyglycoside (BGC0001086) and Zeaxanthin (BGC0000656) were detected in five MAGs from the family Sphingomonadaceae (Figure 5-6). Zeaxanthin is a natural xanthophyll carotenoid is responsible for the synthesis of a yellow/ orange pigment and is used in the food, pharmaceutical and nutraceutical industries because of its strong antioxidant and anti-cancer properties (Y. Zhang et al., 2018). In this category we also include the arylpolyene cluster class, detected in 11 MAGs, which is structurally similar well-known carotenoids and play a similar antioxidative and photoprotective role (Schöner et al., 2016).

5.4.2.2 Exopolysaccharides (EPS)

Polysaccharides with diverse structures, functions and potential applications are synthesized by bacteria of all taxa and secreted into the external environment (Nwodo et al., 2012). They are also important components of the bacterial cell wall. There were several saccharides detected in this dataset that have links to know functions. The MAG (CC_mag_071_Nostoc) was previously shown to contain genes nifD and nifH for nitrogen fixation (Chapter 4, Figure 4-14) and antiSMASH also revealed the presence of heterocyst glycolipid BGC (BGC0000869) from a *Nostoc sp* in this same MAG. Without a combined nitrogen source, heterocysts (cells specialized in N_2 fixation) arise along the cyanobacterial filaments in a semi-regular pattern, with approximately one heterocyst to ten vegetative cells (Shvarev et al., 2019). Clusters similar to Phosphonoglycans (BGC0000806) were found in MB_bin_070_QHBO01, MB_MAG_008_Micromonospora and MX_mag_042_Ktedonobacteraceae, which was interesting as one of the speculative roles of phosphonoglycans is their action as phosphorus reservoirs in the environments of low phosphate concentration (Kafarski, 2019). This is interesting because phosphorus has previously been shown to be limiting in cryoconite (Stibal and Tranter, 2007).

Most saccharide clusters with similarity to known functions were related to various components of the bacterial cell wall. However, several clusters encoded polysaccharide clusters that form part of the glycocalyx. Unlike the lipopolysaccharides (including O-antigen portions), the saccharides of the glycocalyx are less likely to cause an immune response in humans. The function of these polysaccharides is to form a slime layer or hydration layer, and in this way protect against desiccation, sequester various nutrients, and form a resilient biofilm that enable microbial communities to adhere to each other (Poli et al., 2010).

5.4.2.3 Compatible solutes

The use of osmoprotectants, and acidic transmembrane proteins help resist precipitation in high salt environments (Saum et al., 2013). Simon et al showed that microorganisms in an alpine glacier contained genes encoding the synthesis of osmoprotectants such as glycine, betaine, choline, sarcosine and glutamate (Simon et al., 2009b). There are also a number of other organic compounds that can be concentrated in the cell without interfering with cellular functions (compatible solutes), such as free amino acids, sugars and polyols that may play a role in osmoprotection. The LC-MS data reflected an abundance of these compatible solutes, and betaine was one of the features detected by ANOVA as explanatory between the environments, because there was a higher concentration on VB, than the other glaciers (Figure 5-15, Appendix Table E-5). Very little research has been done to date on the possible role of these solutes on osmoprotection.

5.4.3 The NRPS metabolites of Cyanobacteria

The Cyanobacteria are the most abundant bacteria in cryoconite, and important organisms in stabilising recently deglaciated soil (Chrismas et al., 2016b; Langford et al., 2010; Pushkareva et al., 2015; Rossi and De Philippis, 2015). Cyanobacteria are also known to be excellent sources of peptides, trans-fatty acids, amino acids, vitamins, carotenes, chlorophyll, phycocyanin and minerals, and in fact the cyanobacteria *Arthrospira* (Spirulina) is widely used for several potential health-beneficial applications (Deng and Chow, 2010). However, they are known to produce several compounds toxic to humans and other organisms (Janssen, 2019; Kleinteich et al., 2013). Microcystins (MCs), the most well-known of these toxins, have been detected in many Arctic habitats including Baffin Island, Canada (Kleinteich et al., 2013), the north-west coast of Spitsbergen (Chrapusta et al., 2015), Greenland lakes (Trout-Haney et al., 2016) and Svalbard cyanobacterial mats (Kleinteich et al., 2018). Although MCs have dominated the attention of researchers due to their hepato- and neurotoxic potential in humans (Janssen, 2019), there are hundreds of other toxic bioactive peptides (TBPs) such as Anabaenopeptins (APs), cyanopeptolins (CPs), and microginins (MGs) (Janssen, 2019). These other TBPs have had far less attention, despite their vast range of bioactivity on cellular enzymes including proteases, chymotrypsin, thrombin (Janssen, 2019).

The high bioactivity of TBPs, means that they lend themselves to commercial or medicinal uses, such as antifungals, antimicrobials, or antivirals and interest in their potential as producers of antimicrobials, in particular, is growing (Swain et al., 2017). For example, Cyanobacteria

Phormidium Priestleyi strains ANT.L52.4 and ANT.L52.6 from an Antarctic lake have previously been shown to have potent antifungal and/or antibacterial activity (Biondi et al., 2008). Because of their excellent potential to produce a wide range of useful product, as well as several toxins, the secondary metabolites of Cyanobacteria were examined in greater detail.

In this study, there were three cyanobacterial MAGs (MX_MAG_032_Microcoleus, CC_mag_060_Nodosilinea and CC_mag_071_Nostoc) which all had BGCs with 100% similarity to the AP anabaenopeptin NZ857 / nostamide A (BGC0001479) (Figure 5-7). APs are cyclic hexapeptides consisting of five amino acid residues forming a ring and an exocyclic residue connected through an ureido bond (Entfellner et al., 2017). APs have potent bioactivity and can inhibit protein phosphatase 1 and 2A, serine proteases such as chymotrypsin and trypsin, and carboxypeptidase A and other metallocarboxypeptidases (Entfellner et al., 2017). There are numerous variants of APs reported to date, and the pharmacological effects and applications of these peptides is an emerging area of study (Spoof et al., 2015).

The vast array of structurally diverse oligopeptides produced by Caynobacteria suggests a high diversity of NRPS pathways and respective genes (Calteau et al., 2014; Welker and von Döhren, 2006). However, for each class of peptides, there are homologous synthetases and genes in all major branches of the cyanobacterial evolutionary tree, implying that NRPS genes are a very ancient part of the cyanobacterial genome (Welker and von Döhren, 2006). The diversity of peptide products can presumably be attributed to recombination and duplication events over evolutionary time. Evidence of this recombination and modularity is shown in (Figure 5-10), where a CC_mag_071_Nostoc NRPS BGC has similarity to ten different NRPS products. The persistence of NRPS genes in so many Cyanobacterial branches suggests that they are an essential part of Cyanobacterial physiology and survival (Welker and von Döhren, 2006). NRPS biosynthetic pathways can combine proteinogenic amino acids with non-proteinogenic amino acids, fatty acids, carbohydrates, and other building blocks into complex molecules.

MX_MAG_032_Microcoleus also had a cluster with 16% similarity to barbamide (BGC0000962), a NRP + Polyketide:Modular type I cluster that synthesises a chlorinated lipopeptide with potent molluscicidal activity (Chang et al., 2002). The MAG did also contain a halogenated cluster, which was perhaps a tailoring enzyme for the barbamide cluster. MX_MAG_032_Microcoleus also had two NRPS, including a cluster with 16% similarity to gramicidin (BGC0000367) and several other compounds. MX_MAG_032_Microcoleus, there

was a cluster with 14% similarity to the RiPP: Cyanobactin, anacyclamide A10 (BGC0000472). There were also several unknown halogenated clusters found in the Cyanobacterial MAGs, which is interesting because Chlorine is found in 22% of cyanobacterial metabolites (Guyot et al., 2004).

5.4.4 Talented Actinobacterial MAGs

Antimicrobial secondary metabolites are often synthesised by bacteria as a defence against competitive species and bacteria are therefore obvious sources of novel antibiotic compounds (Bérdy, 2005). There were several MAGs that were notable for the range and diversity of products that they synthesised. The Actinobacterial MAG DA_MAG_007_Iso899 from the family Jatrophihabitantaceae was particularly rich in complex metabolites. This MAG had several BGC clusters that were like known dieyne and PKS antibiotics sporolide A/ B (Figure 5-11). Some other hits to MIBiG compounds include ketomemicin B3/ B4 (BGC0001633), meridamycin (BGC0001011), amycolamycin A/ B (BGC0001503), ecumicin (BGC0001582), rimosamide (BGC0001760), lobosamide A/ B/ C (BGC0001303), paulomycin (BGC0001731), vazabitide A (BGC0001818). A full list is shown in Table 5-3.

5.4.5 Sequencing depth and metabolite detection

To some extent, the number of clusters is a consequence of sequencing effort rather than biosynthetic potential. The number of clusters detected depended on the size and number of contigs that were submitted to antiSMASH, which were in turn a consequence of library size, environment complexity and environment heterogeneity (Section 8.3.3). Likewise, the types of clusters detected is also affected by the average contig size. Some secondary metabolites are encoded by relatively small clusters, (such as some carotenoids) and are more easily detected than others (such as PKS and NRPs). The differences in the number of secondary metabolites detected is likely an artefact of the environmental complexity, and therefore the depth and coverage of the assembly for a given number of reads. Even though soil was the largest library and is known to contain a great variety of secondary metabolites, the cryoconite library provided better results because of a relatively less complex community structure, and therefore, a better assembly containing longer contigs.

As an additional caveat to this interpretation, it should be noted that because MAGs (which consist of collections of contigs) were analysed and not a single circular closed genome, large BGCs such as PKS and NRPS could have been split across contigs and the real number of

BGCs might be overestimated, or their similarity to known BGCs misattributed. There is evidence of this occurring in several of the MAGs, where more than one of the contigs had hits against the same compound in the MIBiG database (Table 5-3, Appendix Table E-1).

It is also worth noting that the completeness of the MAGs included in this study ranged from 70 – 100%. MAGs may therefore have clusters that are missing or incomplete. The DA_MAG_019_Granulicella MAG was closest to *Salinibacterium xinjiangense* (GCF_900230175.1), a novel psychrophilic, Gram-positive, yellow-pigmented, and aerobic bacterium, from the China No. 1 glacier (Zhang et al., 2008). However, we did not identify a pigment cluster from this strain.

5.4.6 Linking detected metabolites and predictions based on BGCs

Although the study intended to determine whether there was a link between detected metabolites (using LC-MS) and predicted metabolites from annotating BGCs, it was not possible to completely link both datasets. The initial analysis of LC-MS data did not analyse the compounds above 600 Da, and the carotenoids and APs are both larger than 600 Da in size. However, the LC-MS dataset can be reanalysed to specifically look for the compounds of interest in future research. The LC-MS data did reveal that the metabolites detected in cryoconite from VL was significantly different from the metabolites detected in the other three glaciers (Figure 5-14, Figure 5-15). From the study of the distribution of the MAGs across different sites (Chapter 4, Figure 4-11, and Figure 4-12) VL was shown to contain a significantly different microbial community. The fact that VL clustered differently using MAGs and metabolites provides a tantalising suggestion that different metabolites and microbial communities can be linked. In addition, by performing genome mining first, it as possible to search the LC-MS for specific metabolites of interest. This approach may help to focus the analysis of LC-MS datasets, and indeed, it revealed that future metabolite analyses of these samples should focus above the 600 Da range.

5.4.7 Future work

Currently, there are enormous databases of chemical compounds from secondary metabolism, many of which have no known synthesizing organism or mechanism. Likewise, there are hundreds of thousands of metagenome sequences. Although the algorithms to predict compounds from BGCs are complex, and based on assumptions that make them good estimates at beast, the ultimate goal is to link these datasets, and match the compounds with unknown

synthesis mechanism, to the BGCs with unknown compounds. There are already several initiatives working towards this aim, such as the Paired Omics Data Platform (https://pairedomicsdata.bioinformatics.nl/) which links Global Natural Products Social Molecular Networking (GNPS) data (Aron et al., 2020) with metagenomic and genomic MS data (Hooft et al., 2020). Because of homology, each BGC that can be successfully linked to a product, will act as a puzzle piece, and naturally make the picture clearer for similar BGCs and compounds.

Finally, the genome can be analysed for aspects that would enable the heterologous expression of the product, from codon usage, to required substrates to regulation and secretion. Although we did not have LC-MS data from seawater to compare against the MAGs, the seawater MAGs were included because the success rate of drug discovery from the marine world is roughly twofold to threefold better than the industry average (1 out of the 3140 known molecular entities) (Gerwick and Moore 2012; Giddings and Newman 2015).

5.5 Conclusion

This study attempted to link detected metabolites and predicted metabolites and identify BGCs that encode NPs of pharmaceutical value. Although exact metabolites and BGCs were not linked, there is evidence that metabolites from glaciers with different microbial communities could be distinguished from each other. Using antiSMASH and BiG-SCAPE, a range of secondary metabolites that could be used in biotechnology applications were identified. There were numerous EPS, which have applications as gums and thickening agents in the food, pharmaceuticals, and cosmetics industry and terpenoid clusters that synthesized a range of pigments and antioxidants, which also have roles as pigments, sunscreens, and nutraceuticals and even as preventatives and adjuvant therapies in cancers. There were numerous novel saccharides, NRPS, T1PKS, and T3PKS that have only partial similarity to compounds in the MIBIG database, but that could potentially be new sources of antimicrobial, insecticidal and antifungal treatments. The fight against antimicrobial resistance necessitates the discovery of novel antimicrobials, so these novel BGCs are intriguing for the possibility that they synthesize unique chemical compounds.

6 SCREENING OF ARCTIC SOIL AND CRYOCONITE METAGENOMES FOR COLD-ACTIVE POLYMERASES

6.1 Introduction

To cope with perennially low temperatures, cryospheric microorganims have evolved several interesting metabolic, physiological and structural adaptations to survive (reviewed in Chapter 1) (D'Amico et al., 2006; Maccario et al., 2015). One such adapation is cold-active enzymes, which help to maintain metabolism at extremely low temperatures. Biological enzymes are efficient and highly selective catalysts, and are generally more energy efficient, safer, and better for the environment (Santiago et al., 2016). Cold-active enzymes allow reactions to take place at lower temperatures, reducing the need for heating and preventing many undesirable chemical reactions that occur spontaneously at higher temperatures, resulting in a greater specificity of reaction and a higher yield (Santiago et al., 2016).

Several microorgnisms have the ability to grow and divide at tmperatures near or below freezing (Yuan Xue et al., 2020). This means that DNA replication via DNA polymerases need to function at exceptionally low temperatures. Enzymes from the family A DNA polymerases are of particular interest for bioprospecting because they are employed as tools in many molecular biology applications including polymerase chain reaction (PCR), probe labeling, DNA sequencing, and mutagenic PCR (Ishino and Ishino, 2014). While much research has focused on hot start enzymes, with high activation temperature to prevent non-specific primer binding and transcription during PCR preparation (Kellogg et al., 1994), there are several specific applications where cold active polymerases are desriable. For example, some of the DNA errors introduced by PCR are DNA damage caused by the high temperatures reached during thermocycling, and not introduced by polymerses (Potapov and Ong, 2017). Cold-active polymerases may therefore increase transcription accuracy. Similarly, template switching,

wherein a partially transcribed template anneals to a similar but not identical sequence in a subsequent PCR round and creates chimeric sequences, is less likely in a cold system where unintended DNA strand separation and the kinetics of individual molecules is reduced. An additional benefit is that low temperatures also inhibit nucleases (DNAse and RNAse) which degrade DNA. 'Cold biotechnlogy' has exploded in recent years, and the demand for cold active enzymes is growing (Mangiagalli et al., 2020). The engineering of psychrophlic strains that can express cold-active enzymes in therefore a focus of some research. A polymerase with high activity in cold temperatures that could be engineered into a heterolgous host could descrease the generation time for bacteria and their enzyme products and have masive impacts on enzyme yield. Finally, cold-active polymerases could have roles in DNA synthesis technology, such as DNA aptamer production.

Recently, the World Enzymes to 2017 Report forecast that enzyme demand would rise by 6.4 % to 6.9 billion p.a. in 2017 (http://www.rnrmarketresearch.com/world-enzymes-to-2017-market-report.html). However, to date, these enzymes have been sourced from the 1% of cultivatable bacteria and have neglected the 99% of uncultivatable bacteria. Sequence-based and functional metagenomics are approaches that enable the investigation of the other 99% of bacteria, and their genes. A previous screen for cold-active polymerases from a glacier ice metagenome successfully identified several polymerases from psychrophilic bacteria (Simon et al., 2009a). The study used cold-sensitive mutant of *E. coli*, unable to grow below 18°C, with a point mutation of the *polA* gene (designated *fcs*A29). The *fcs*A29 mutation phenotype is caused by a G(346) -> A transition, which causes Asp(116) (aspartic acid D) to be changed to a Asn (Asparagine N) (Nagano et al., 1999). These mutants therefore provide an excellent system in which to perform a cold-complementation assay for cold active polymerases, because only clones containing polymerase sequences that restore transcription in the *fcs*A29 mutants will be able to grow.

In this chapter, a functional screen for the presence of putative cold-active polymerases was performed. To do this, soil from the glacial forefield of Midtre Lovénbreen (ML) and pooled cryoconite DNA from Austre Brøggerbreen (AB), Midtre Lovénbreen (ML), Vestre Brøggerbreen (VB) and Vestre Lovénbreen (VL) glaciers in Svalbard was used to create a clone library of environmental DNA. The environmental DNA was cloned into pJET1.2/blunt plasmids and transformed into *E. coli* DH10B competent cells to make a clone library. The library was amplified, and the extracted plasmids were expressed in cold-sensitive *E. coli*

strains HCS1 and cs2-29 and grown at 15°C to screen for clones that restored polymerase activity.

6.1.1 Aims and objectives

1) Create a clone library of cryoconite and soil eDNA in chemically competent DH10B *E.coli.*
2) Screen for cold-active polymerases in cold-sensitive mutant *E. coli* strains cs2-29 and HCS1.

6.2 Materials and Methods

6.2.1 Samples and environmental DNA extraction

Soil and cryoconite sampling and DNA extractions were performed as described in previous chapters. Various DNA extraction methods (Lucigen MasterPure DNA and RNA extraction kit) were tested to obtain a high concentration of high molecular weight DNA (> 40 kb) for cloning.

Table 6-1 Tables of environments and DNA extraction methods

Environment	Extraction method	Details	Number of samples
Cryoconite	FastDNA	2.2.4	All
	PowerSoil	2.2.3	
Soil	FastDNA	2.2.4	All
	PowerSoil	2.2.3	All
	Ludox	2.2.6	F3T3
	PowerMax	2.2.7	F3T3

6.2.2 Bacterial strains

The One Shot™ MAX Efficiency™ DH10B chemically competent cells (Invitrogen, Life technologies) were used to create clone libraries of soil and cryoconite DNA for long-term storage, and for plasmid amplification prior to transformation and screening of clones in mutant strains. Two *E.coli* strains, cs2-29 and HCS1 harbouring a point mutation (designated *fcsA29)* of the *polA* gene were kindly provided by Dr Masaaki Wachi at the Department of Bioengineering, Tokyo Institute of Technology, Japan (Nagano et al., 1999). The *fcsA29* mutation phenotype is thought to be caused by a G(346) -> A transition, which causes Asp(116) (aspartic acid D) to be changed to a Asn (Asparagine N). The cs2-29 and HCS1 strains were used to screen for cold-active polymerases. The strains and their genomic background are listed in Table 6-2.

Table 6-2 Table of bacterial strains used in this thesis

	Mutations	Antibiotic resistance	Supplements
DH10B	F- mcrA Δ(mrr-hsdRMS-mcrBC) ϕ80lacZΔM15 ΔlacX74 recA1 endA1 araD139 Δ (ara, leu) 7697 galU galK λ- rpsL nupG /pMON14272 / pMON7124		N/A
HCS1	(thi-1, leu-6, proC32, hisF860, thyA54, cycC43, lacZ36, ara-14, mtl-1, xyl-5, str-109, spc-15, fcsA29).	Streptomycin	Thymine
Cs2-29	(F-, thr, leuB, trp, his, thy, ara, lac, gal, xyl, mtl, str, tonA, fcsA29).	Streptomycin	Thymine

6.2.2.1 Media

The cs2-29 strain was grown on L-agar (1% Bactopeptone, 0.5% yeast extract, 0.5% NaCl, 0.1% glucose, pH 7.2 with 20 mg/L thymine and solidified with 1.5% agar). For sub-culturing, cells were grown at 37 °C. For complementation tests, cells were grown at 15 °C. The cs2-29, HCS1 and DH10B cells were also grown on LB media with appropriate supplementation.

Table 6-3 Table of Media Supplements

Supplements	Purpose
None	Growing untransformed cells,
Thymine	Cs2-29 and HCS1 require thymine for growth
Carbenicillin	Antibiotic to select for transformants
Streptomycin	cs2-s29 and HCS1 have natural streptomycin resistance

6.2.3 PCR of *polA* gene

To confirm that the mutant strains contained the *fcsA*29 point mutation, the suspected regions of the *polA* gene of both strains were amplified by PCR and sequenced using Sanger Sequencing (Section 2.6.3). The primers used to amplify the *polA* gene were designed using primerBLAST and are show in Figure 6-1 and Table 6-4. PCR was performed in 50µL reaction volumes using 5µl 10X Titanium Taq DNA Buffer, 1µL 50X Titanium Taq DNA polymerase, 1µL 50X DNTP mix (10mM) and 1uM concentration of forward and reverse primers. The PCR was performed on the Biometra T1 Thermocycler (Biometra GmbH, Göttingen, Germany), with the following cycle conditions, 5 minutes at 95°C followed by 30 cycles of 95°C for 30 seconds, 60°C for 1 minute and 68°C for 2 minutes.

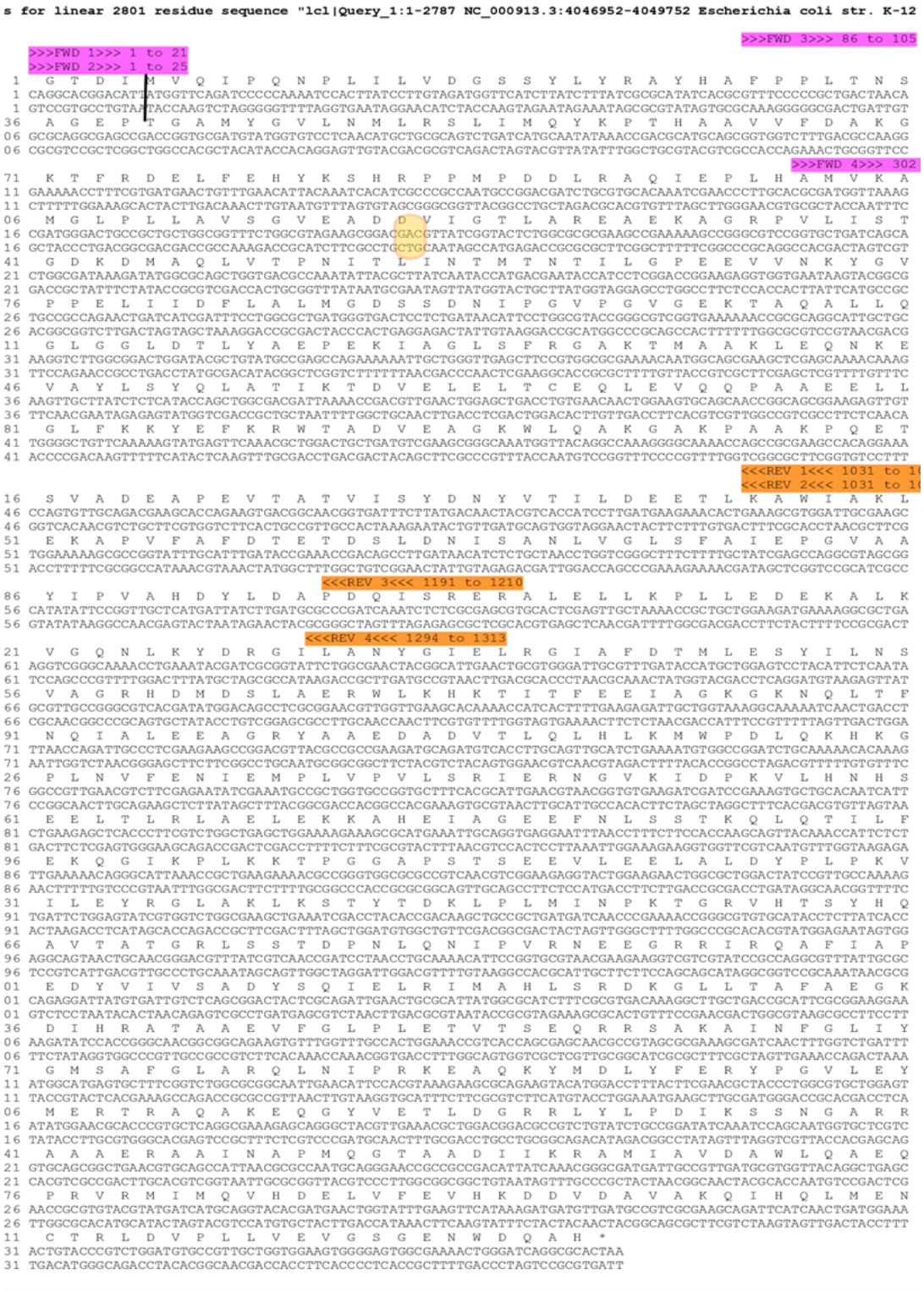

Figure 6-1. Position of primer binding sites for the *E.coli polA* gene. The location of the mutation and the codon that is affected is indicated in yellow. A G(346) -> A transition causes Asp(116) (aspartic acid D) to be changed to a Asn (Asparagine N). The different primer pairs that were tested are indicated on the figure. FWD primers are in pink and REV primers are in orange.

Table 6-4 Table of primers used to amplify the *polA* gene.

Pair	Sequence (5'->3')	Template strand	Length	Start	Stop	Tm	GC%	Self comp.	Self 3' comp.	Product size (bp)
1F	Forward CAGGCACGGACATTATGGTTC	Plus	21	1	21	59.33	52.38	5.0	3.0	
1R	Reverse AGCTTCGCAATCCACGCTTTC	Minus	21	1051	1031	62.13	52.38	4.0	1.0	1051
3F	Forward GTTTCCCCCGCTGACTAACA	Plus	20	72	91	59.96	55.00	3.0	0.0	
3R	Reverse TCGCGAGAGATTTGATCGGG	Minus	20	1196	1177	59.97	55.00	6.0	2.0	1125
8F	Forward CGCGATGGTTAAAGCGATGG	Plus	20	288	307	60.04	55.00	4.0	3.0	
8R	Reverse AATGCCGTAGTTCGCCAGAA	Minus	20	1299	1280	60.04	50.00	5.0	3.0	1012

6.2.4 Cloning and transformation

6.2.4.1 Size selection and gel extraction

The *polA* gene is ~3kb in length and the maximum insert size of the pJET2.1/blunt plasmid is 10kb, therefore DNA fragments between 4kb and 10kb were required. DNA was therefore size selected by running the metagenomic DNA on a 0.8% agarose gel and cutting bands between 5kb and 10kb in size. The gel was run without stain, with dilutions of the DNA library, the concentrated DNA pools, and two DNA ladders (Cleaver Scientific Broad Range Ladder, and the NEB 1kb Ladder (New England Biosystems). The lanes containing DNA ladder and library dilutions were cut from the gel and post-stained in SybrSafe DNA stain. The gel was then reassembled and visualised on a Dark Reader. The libraries dilutions showed the size spread of the library, and the Ladder was used as a guide to cut the sample lanes. Gel slices of approximately 300mg were then purified using the PureLink^{TM} Quick Gel Extraction and PCR Purification Combo Kit (Invitrogen, Life technologies) according the manufacturer's instructions. Where libraries had been pre-concentrated on a speedivac, the DNA was eluted in 50 ul of 10mM Tris-HCl, pH 8.5. Where the DNA had not been pre-concentrated, the DNA was eluted in DNAse-free water and concentrated on a speedivac to get the required concentration for the ligation reaction. Figure 6-2 demonstrates the size-selection procedure.

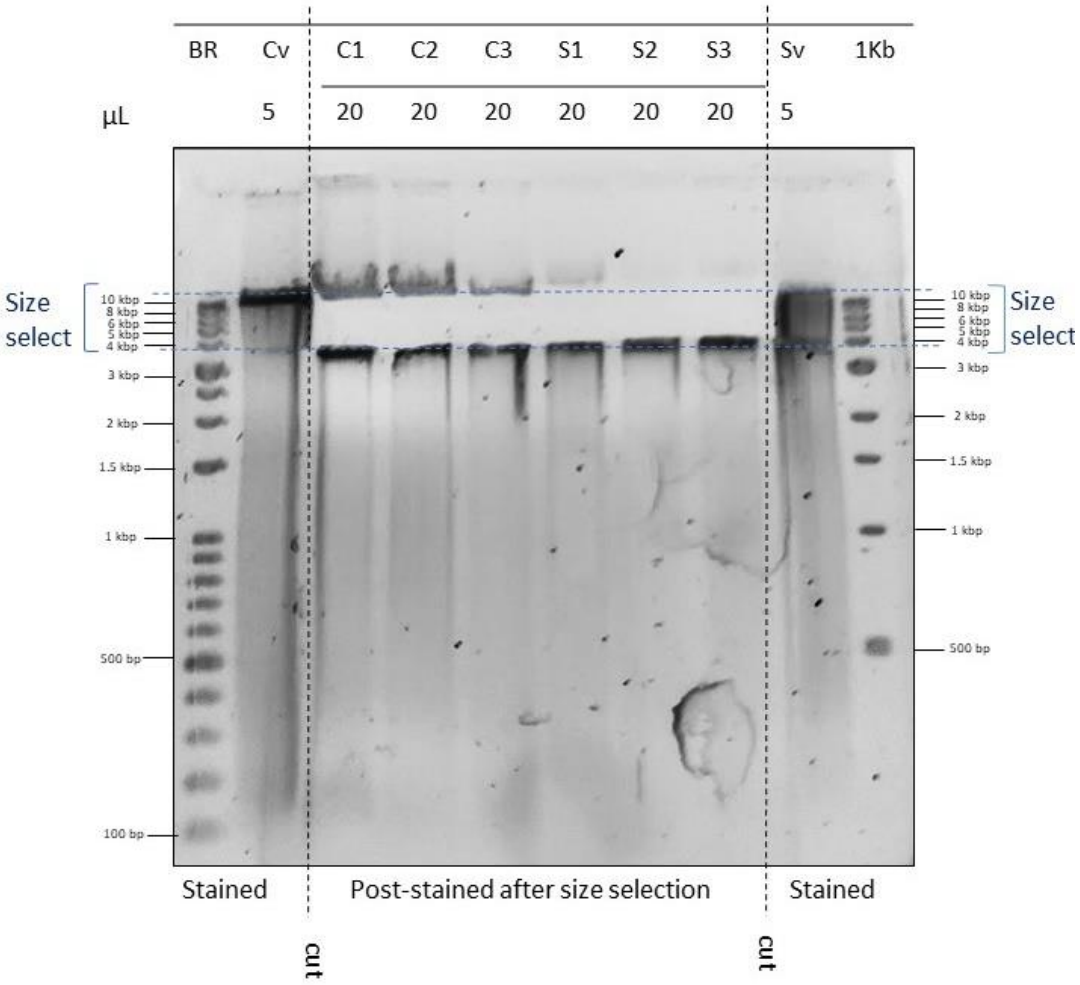

Figure 6-2 DNA size selection via agarose gel electrophoresis. An example of gel used to size select DNA fragments for clone library construction. **BR** is Cleaver Scientific Broad Range DNA Ladder, **1Kb** is the NEB 1kb DNA Ladder. 5ul of cryoconite and soil respectively was added to the second and second last columns for visualization of the pool fragment sizes.

6.2.4.1.1 Size selection

Pooled cryoconite and soil DNA libraries were run on a 1.3% agarose gel in clean gel tanks with new TBE buffer and no DNA staining products. After running the gels at 150V for 2 hours, the first two and last two lanes were carefully removed with a scalpel and placed in a tray with TBE and 20 µL SybrSafe. The gel slices were gently agitated in the stain for 15-30 minutes. The gel was reassembled and viewed on a Dark Reader blue transilluminator. The DNA staining of the first two and rows contained a DNA ladder and a diluted amount of the DNA pool, which allowed visualisation of the sizes of gels and the distribution of DNA sizes in the pool. The bands corresponding to the region between 4 and 10kbp from each sample lane was sliced out using a scalpel (Figure 6-2).

6.2.4.1.2 Gel Extraction

The Invitrogen™ PureLink™ Quick Gel Extraction and PCR Purification Combo Kit (Catalog no. K2200-01) was used to extract size-selected DNA from agarose gel slices. Before Starting, ethanol was added to the Wash Buffer (W1) according to the label on the bottle and heat block was equilibrated to 50°C. A clean, sharp razor blade was used to excise an area of gel weighing approximately 200-350 mg containing the DNA fragment of interest. Gel Solubilization Buffer (L3) in a ratio of 3.1, was added to the tube containing the excised gel to solubilise the agarose. The tube was incubated at 50°C for 15 minutes with gentle inversion every 3 minutes. After the gel slice had dissolved, the tubes were incubated for an additional 5 minutes. Approximately 750 µL of the dissolved gel piece was then pipetted onto a column inside a Wash Tube. The column was centrifuged at >12,000 × g for 1 minute and the flow-through discarded. This step was repeated until all the solubilised gel had been processed. Next, 500 µL of Wash Buffer (W1) containing ethanol was added, and the column was centrifuged at >12,000 × g for 1 minute. The flow-through was discarded and the column placed into the Wash Tube. The column was centrifuged at maximum speed for 2–3 minutes and the flow-through discarded. To elute the DNA, the column was placed into a Recovery Tube and 50 µL of Elution Buffer (E1) was added. Finally, the tube was incubated at room temperature for 1 minute, then centrifuged at >12,000 × g for 1 minute. The purified DNA was then stored at 4°C when needed for immediate use or at −20°C for long-term storage.

6.2.4.2 Plasmids and vectors

After considerable attempts to obtain high molecular weight (40kb +) DNA at high concentrations for fosmid library construction (See Section 2.2.6), it was decided to try construct a plasmid library instead, as there was ample DNA in the 8-20 kb range. The pJET1.2/Blunt vector was chosen for its ability to take relatively large insert sizes of 10 kbp, its resistance (bla(Ap^R)) to a the common antibiotic ampicillin (and carbenicillin) and the eco47IR gene which is lethal unless disrupted by an insert, therefore allowing positive selection of transformants. An additional benefit of the vector is that it can accept blunt-end DNA fragments and inserts, which is vital for a metagenomic library in which DNA is randomly sheared and has 5’ and 3’ overhangs of random size and sequence. The use of restriction digestion to insert sites for ligation would likely reduce insert size and introduce bias; therefore, we sought to avoid it.

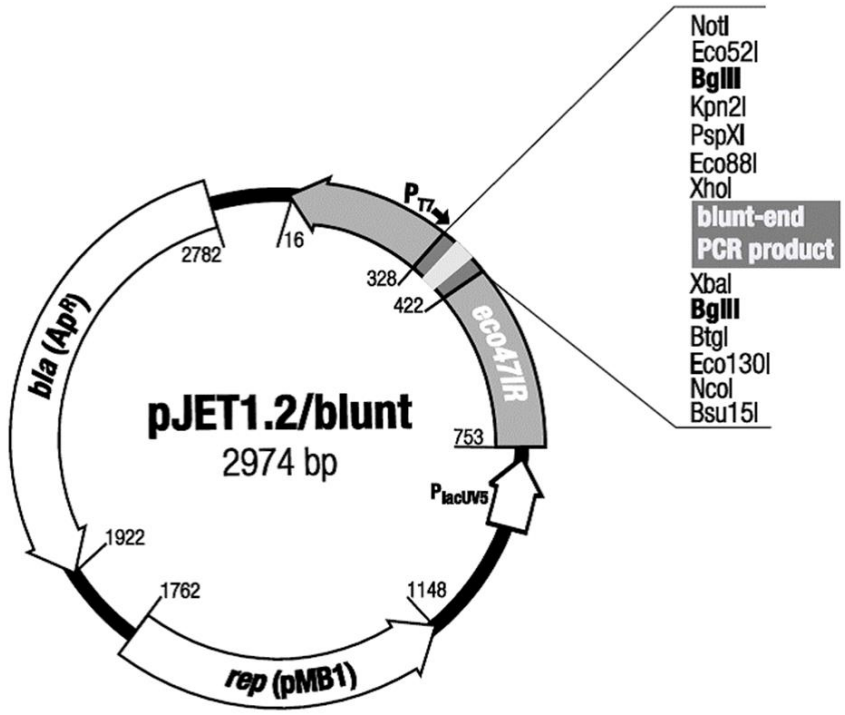

Figure 6-3 Vector map of the pJET1.2/blunt plasmid. The vector contains the (bla(ApR)) sequence which confers resistance to ampicillin (and carbenicillin) and the eco47IR gene which is lethal unless disrupted by an insert.

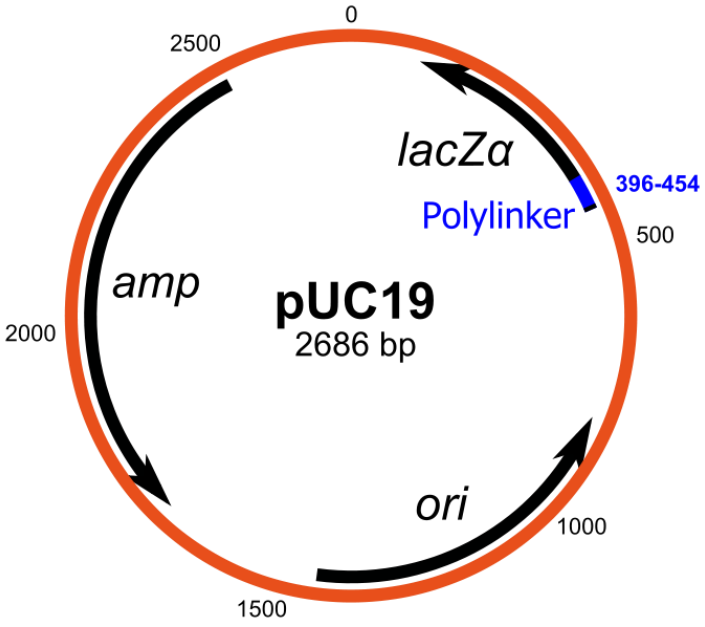

Figure 6-4 A Map of the pUC19 plasmid used as a transformation control in all cloning experiments. The pUC19 plasmid has high transformation efficiency, is resistant to carbenicillin antibiotics and is a similar size to empty pJET1.2/blunt. It was therefore used as transformation efficiency control.

6.2.4.2.1 Ligation of DNA into pJET1.2/blunt

Cloning was performed using the CloneJET PCR Cloning Kit (Thermo Scientific). The vector was selected for its ability to accept inserts from 6kb to 10kb in size. After size selection and gel extraction and clean-up the environmental DNA needed to be prepared for ligation into the pJET1.2/Blunt vector by a blunting reaction to end-repair 3' and 5' ends. The DNA Blunting Enzyme is a proprietary thermostable DNA polymerase with proofreading activity from Thermo Scientific that removes 3'- overhangs and fills in 5'-overhangs. Nucleotides for the blunting reaction are included in the reaction buffer. The blunting reaction was set up on ice as follows:

Table 6-5 Components and volumes for DNA Blunting reaction

Component	Volume
2X Reaction Buffer	10 µL
Environmental DNA fragments	1 µL (0.15 pmol ends)
Water, nuclease-free	6 µL
DNA Blunting Enzyme	1 µL
Total volume	**18 µL**

The reaction mixtures were then vortexed briefly and centrifuged for 3–5 seconds before incubation at 70°C for 5 min. After incubation, the reaction mixtures were placed on ice and the ligation reaction was set up as follows.

Table 6-6 Components and volumes for ligation Reaction

Component	Volume
Blunting reaction (from previous step)	18 µL
pJET1.2/blunt Cloning Vector (50 ng/µL)	1 µL (0.05 pmol ends)
T4 DNA Ligase	1 µL
Total volume	**20 µL**

The ligation mixture was then vortexed briefly and centrifuged for 3–5 seconds to collect drops. The ligation mixture was then incubated the at room temperature (22°C) for 30 minutes (as recommended for DNA fragment inserts >3kb). The ligation mixture was kept at –20 °C when transformation was postponed, otherwise the ligation mixture was kept on ice and used the same day for transformations. A 976bp PCR product was also cloned into the vector as a ligation control. The PUC19 plasmid was transformed into the cells as a transformation control. The protocol recommends an insert/vector ratio of 3:1, however, ligation can be completed over a wide range of ratios from 0.5: 1 to 15:1.

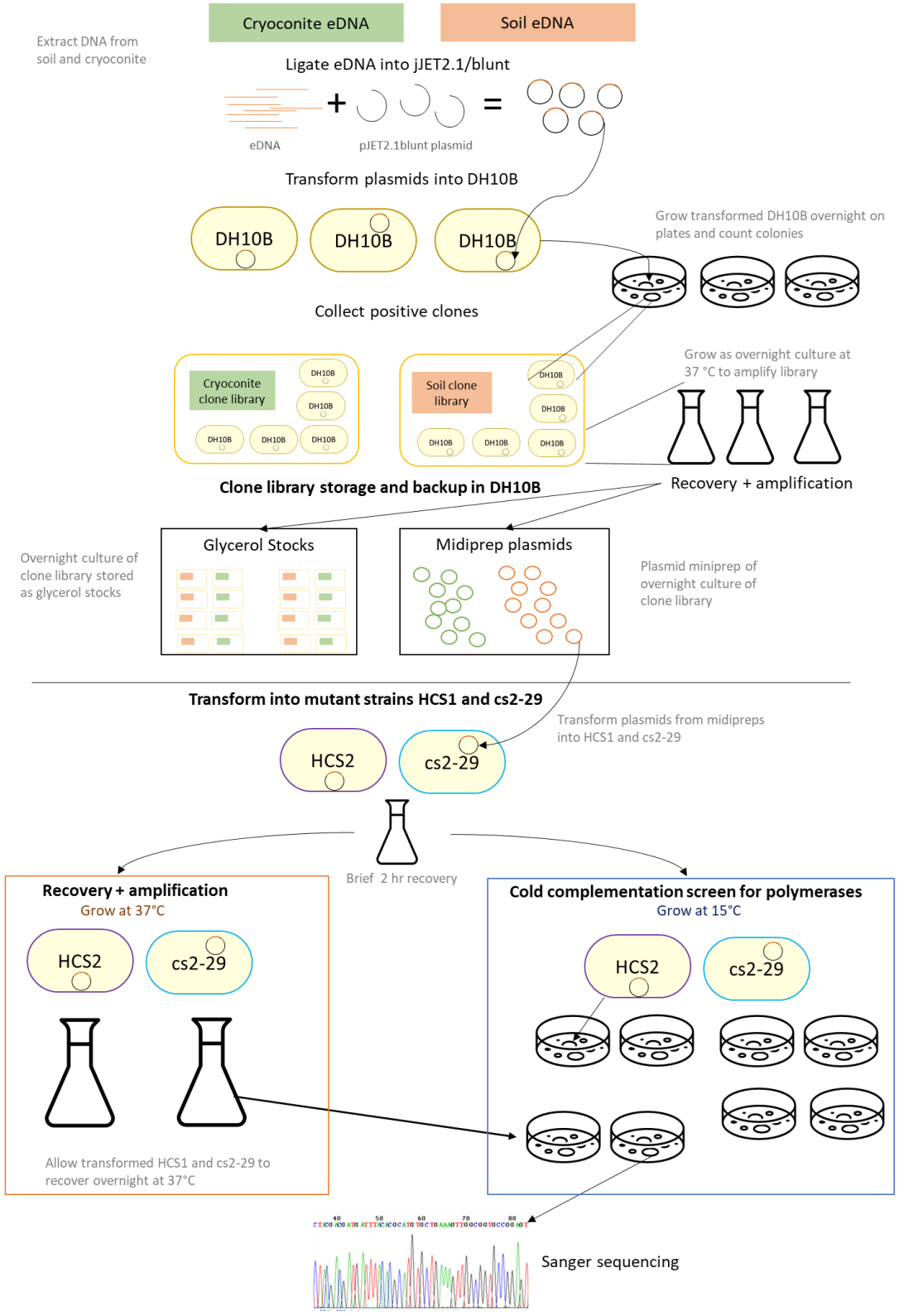

Figure 6-5 Cloning strategy to identify cold-active polymerases. The pJET2.1/blunt plasmids were first transformed into chemically competent *E. coli* DH10B. Clones were washed off, amplified in an O/N culture, midiprepped and then transformed into the mutant *E.coli* HCS1 and cs2-29 strains. The *E.coli* HCS1 and cs2-29 were grown at 15°C to identify clones with potential polymerases.

6.2.4.3 Transformation

Various transformation methods were tested. Electroporation straight into HCS1 and cs2-29 was attempted (Appendix F-1), but due to low transformation efficiency, the strategy was changed to transformation into highly chemically competent One Shot® DH10B *E. coli* cells (Invitrogen) to establish the clone library. This library could be amplified, midiprep and the plasmids transformed into cs2-29 and HCS1.

6.2.4.3.1 Transformation into chemically competent E. coli DH10B

The pJET2.1/blunt ligation reaction was placed on ice while the 50 µl vials of One Shot® cells for each ligation/transformation were thawed on ice. Once thawed, 1 to 5 µl of each ligation reaction was pipetted directly into the competent cells and mixed by gentle tapping. The vials containing cells and ligation mixture were incubated on ice for 30 minutes, while a water bath was warmed to exactly 42 °C. The vials were transferred to 42°C water bath for exactly 30 seconds then placed immediately on ice. Thereafter, 250 µl of pre-warmed SOC medium was added to each vial. The vials were placed in a microcentrifuge rack on its side, secured with tape and incubated for exactly 1 hour at 225 rpm in a 37°C shaking incubator. After recovery, between 20 µl to 200 µl from each transformation vial was spread on separate, labelled LB agar plates. The plates were inverted and incubate at 37°C overnight. The number of colonies that came from each transformation vial (for each plasmid library, including a PCR ligation control and a PUC19 transformation control) were counted the following day.

6.2.4.3.2 Calcium Chloride transformation

For $CaCl_2$ transformation, overnight cultures of HCS1 and cs2-29 *E. coli* were grown at 37°C in LB broth + Thy. Approximately 2 hours before the transformation, 1.0 mL of the overnight culture was used to inoculate 125 mL aliquots of fresh LB broth + Thy in several 500 mL Erlenmeyer flasks. This culture was grown at 37°C with shaking at 150 rpm, and after 90 minutes, 1 mL aliquots were removed, and the OD was measured using a spectrophotometer. Once the OD_{600} reached 0.4, the flasks were immediately placed on ice for 10 minutes to halt growth. The cells were kept below 4°C for the remainder of the procedure. Approximately 30 mL of the broth was transferred into 50 mL pre-cooled Falcon tubes, and cells were pelleted by centrifugation at 5000rpm for 5 minutes. The supernatant was poured off and the cells were resuspended in 15 mL of ice-cold 0.1M $CaCl_2$. The Falcon tubes were left on ice for at least 20 minutes with very gentle swirling to wash the pellet. The cells were then centrifuged at 5000 rpm for 5 minutes a second time and the supernatant poured off. One mL of ice cold 0.1M

$CaCl_2$ was added to the pellet, and gently swirled to resuspend. On ice, 100 µL aliquots of the cells were added to 8 strip thin-walled 200 µL PCR tubes. The pJET2.1/blunt plasmids (with soil and cryoconite eDNA) from the DH10B midiprep (100ng) were then added to the tubes, which were tapped to mix, and then placed in ice, in a 4°C cold room for 1 hour. A water bath was prewarmed to exactly 42°C. The HCS1 and cs2-29 *E.coli* with plasmids were then placed in the 42°C water bath for exactly 40 seconds and then returned briefly to ice. The contents of each tube were added to 2 mL of LB + Thy broth in a 15 mL Falcon tube and incubated with shaking at 37°C for 90 minutes to 2 hours. Thereafter, 0.1 mL aliquots of the broth were spread onto LB + thy plates to which carbenicillin had been added and moved to 15 °C for the cold complementation assay. To try and increase the chances of a positive clone, some of the recovery broth (for each strain, and each library) was transferred into an Erlenmeyer flask with fresh LB + thy broth with carbenicillin and grown overnight with shaking at 37°C. The O/N cultures were then plated the next morning and moved to the 15 °C incubator.

6.2.4.4 Plasmid DNA midiprep

Plasmid minipreps were performed using the Invitrogen™ PureLink™ HiPure Plasmid Midiprep Kit (Catalog no. K210004). Before starting, RNase A was added to Resuspension Buffer (R3) according to the instructions on the label and Lysis Buffer (L7) was warmed to 37°C to redissolve particulate matter. Transformed *E. coli* was grown in LB medium with carbenicillin and required supplements (20 µM/ ml Thy for HCS1 and cs2-29). Between 15–25 mL of the overnight culture was used in the extraction. During column purification steps, the provided Column Holders were used to place columns in the mouth of an Erlenmeyer flask (or 50mL Falcon Tube). To equilibrate the column, 10 mL Equilibration Buffer (EQ1) was added to the HiPure Midi Column and the solution allowed to drain by gravity flow. Simultaneously cells were harvested by centrifugation at 4,000 × g for 10 min. The medium was discarded, and the cells resuspended in 4 mL Resuspension Buffer (R3) with RNase A. The cell pellet was resuspended by pipetting until homogeneous. To lyse the cells, 4 mL Lysis Buffer (L7) was added and mixed by gentle inverting of the capped tube until the mixture was homogeneous. The tubes were then incubated at room temperature for 5 minutes. To precipitate cell debris and proteins, 4 mL Precipitation Buffer (N3) was added and mix immediately by inverting the tube. The lysate was centrifuged at >12,000 × g for 10 minutes at room temperature. The supernatant was then loaded onto the equilibrated column and allowed drain by gravity flow. A wash step in which 10 mL Wash Buffer (W8) was added to the column, allowed to drain by gravity flow, and the flow-through discarded, was

repeated twice. To elute the DNA, a sterile 15-mL centrifuge tube was placed under the column and 5 mL Elution Buffer added (E4) to the column and allowed to drain by gravity flow. The elution tube containing the purified DNA was precipitated by adding 3.5 mL isopropanol to the eluate, mixing well, and centrifuging the tube at >12,000 × g for 30 minutes at 4°C. The supernatant was carefully removed, and the DNA pellet was washed in 3 mL 70% ethanol. The tube was centrifuged at >12,000 × g for 5 minutes at 4°C and the supernatant discarded. Finally, after air-drying the pellet for 10 minutes, the purified plasmid DNA pellet was resuspended in 100–200 µL TE Buffer (TE). The plasmid size and quantity of the DNA was checked on an agarose gel and Qubit, respectively. DNA which was to be used within 24 hours for transformations of mutant strains were stored at 4 °C. Plasmid DNA intended for long-term storage was placed at −20°C.

6.2.4.5 Restriction digestion using Xho1

Restriction digestion using the restriction endonuclease Xho1 (Promega) was performed to linearize the pJET.2/blunt plasmid. The linearized fragment was required to determine insert length. Restriction digestion also interrupted the insertion site, flanked by the FWD and REV primers. Restriction digestion prior to PCR was necessary to ensure the sequencing of the DNA insert, and not the entire vector length. Restriction Digestion was carried out in reaction volume of 20 µL, with 2 ul of Buffer D (10x), 2 µl of 3000 U Xho1 and 2 µL of plasmid DNA (200 – 800 ng). The reaction was incubated at 37°C for 1 hour. The restriction products were run on an agarose gel, together with uncut plasmid to determine plasmid size, or used to perform PCR of the plasmid insert.

6.2.4.6 Colony PCR

Colony PCR was performed to amplify the PJET1.2/blunt insert, confirm the *polA* mutation and amplify the 16S rRNA gene for taxonomic identification. A single colony was selected using a pipette tip, and tip was added to 20 µL PCR water. A PCR reaction was set up in a total reaction volume of 40 µL as follows, 20 µL PCR Mastermix, 0.8 µL FWD primer, 0.8 µL REV primer, 1 µL dilute bacteria, 17.4 µL PCR-grade water. A selection of clones from the DH10B library were selected to determine average insert size. The PCR reaction was performed using OneTaq® 2X Master Mix with Standard Buffer (New England Biosystems) in a reaction volume of 30 ul.

6.2.5 Glycerol stocks

Glycerol stocks were made of strains and clone libraries for long-term storage at -80 °C. To make stocks of mutant strains, colonies were streaked on LB+Thymine agar and grown overnight. Five colonies of each strain were picked and added to 10 mL LB broth supplemented with Thymine, then grown overnight at 37°C in a shaking incubator. The stocks were made by adding 500 µL of the overnight culture to 500 µL of 50% glycerol in a 2 mL microcentrifuge tube, resulting in a glycerol concentration of 25%.

6.2.5.1 Clone library stocks

Glycerol stocks of *E.coli* DH10B, cs2-29 and HCS1 clone libraries were made by washing colonies of transformants from agar plates using a small amount of LB and diluting the mixture in fresh LB, supplemented with carbenicillin (and thymine for cs2-29 and HCS1). The stocks were made by adding 500 µL of the diluted library to 500 µL of 50% glycerol in a 2 mL microcentrifuge tube, resulting in a glycerol concentration of 25%.

Table 6-7 Table of glycerol stocks of different strains with different supplements

Strain	Description	Supplements
cs2-29	Strain stock	Thymine
HCS1	Strain stock	Thymine
DH10B Max Efficiency	Clone library	Carbenicillin
cs2-29	Clone library	Thymine + Carbenicillin
HCS1	Clone library	Thymine + Carbenicillin

6.2.5.2 DNA extraction from glycerol stocks

Glycerol stocks were revived in overnight culture and then streaked onto LB agar and L-agar plates supplemented with thymine. For DNA extraction, single colonies were picked from LB plates and DNA was extracted using the ZymoBIOMICS^{TM} DNA Mini Kit (Zymo Research, Irvine, CA).

6.2.6 Bioinformatics

Low quality bases were trimmed from the Sanger sequences using Chromas. Sequences were aligned using ClustalW on Mega. The Sanger sequences of the pJET 2.1/ blunt vector inserts were submitted to BLAST and aligned using blastx (translated nucleotide sequence against the non-redundant protein database).

6.3 Results

6.3.1 Sanger sequencing to confirm mutation

Sequencing of the *polA* PCR products confirmed the presence of the G>A transition in the cs2-29 and HCS1 mutant strains at position 346 that confer the cold-sensitivity phenotype.

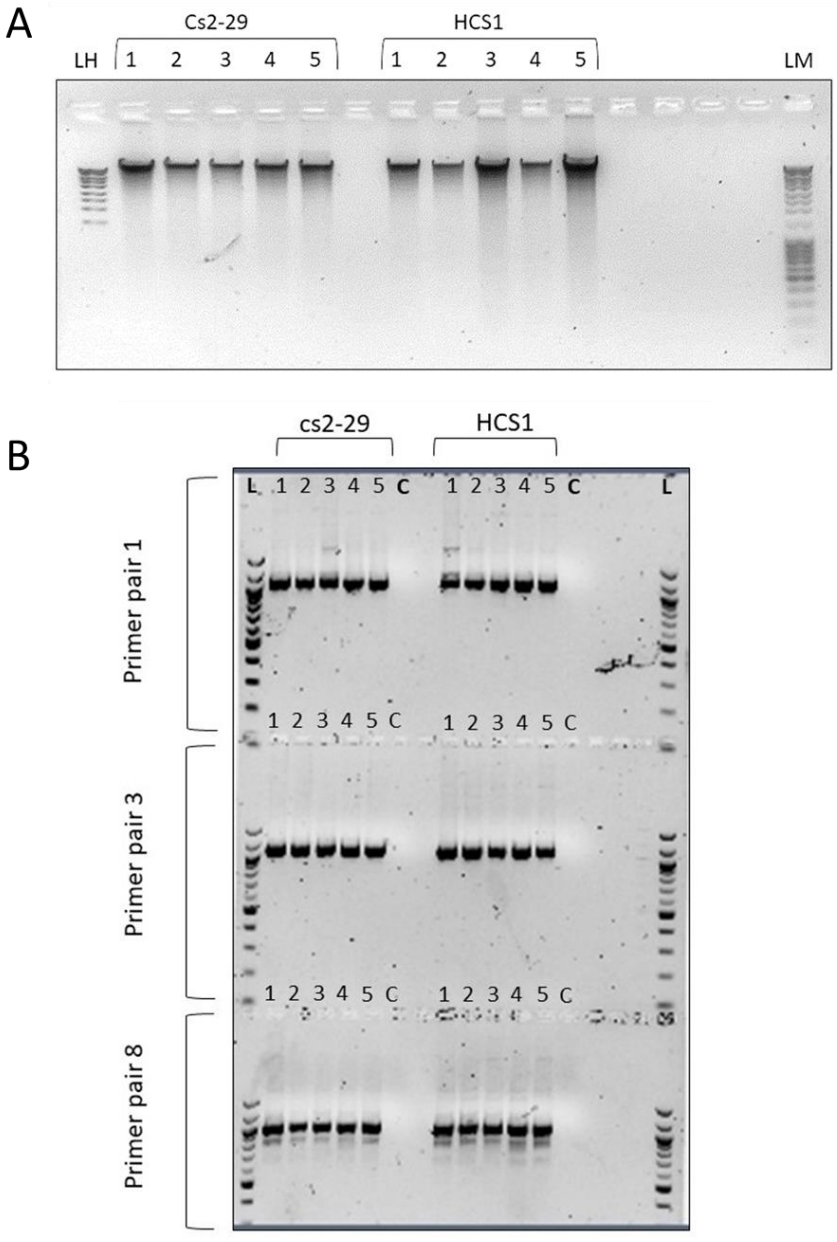

Figure 6-6. A: Agarose gel of *E. coli* cs2-29 and HCSI genomic DNA. Lane numbers refer to the glycerol stock number. LH: Thermo Scientific™ MassRuler DNA Ladder Mix. LM: Thermo Scientific™ MassRuler DNA Ladder High Range. **B: Agarose gel of *polA* PCR products.** The *polA* gene was amplified using three different primer pairs [1, 3, 8] that contained the mutation site. **L:** The DNA ladder is the NEB 100 bp ladder. **C:** is a PCR negative control.

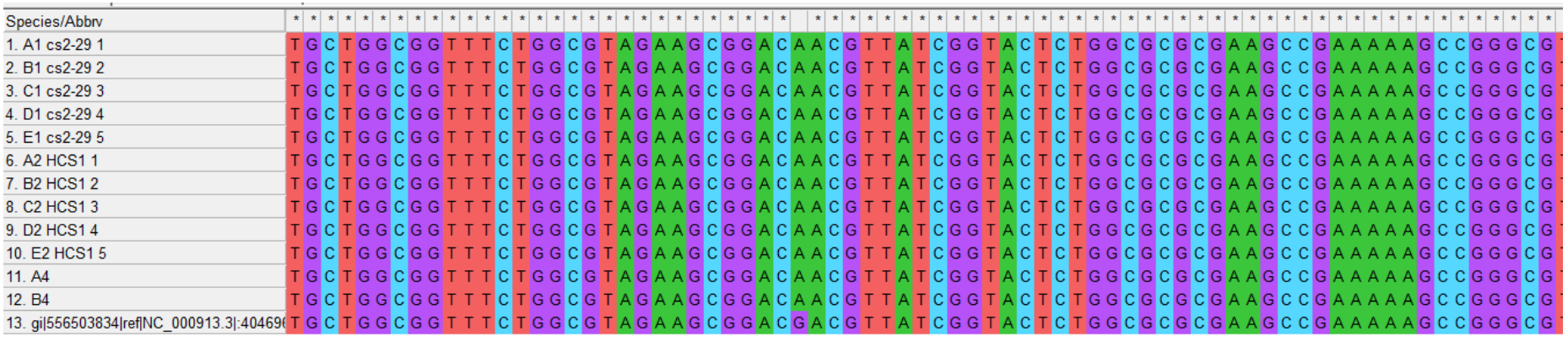

Figure 6-7. Alignment of *polA* amplicons and polA gene showing the position of the mutation conferring cold sensitivity. There is a G>A transition in the sc2-29 and HCS1 mutant strains at position 346.

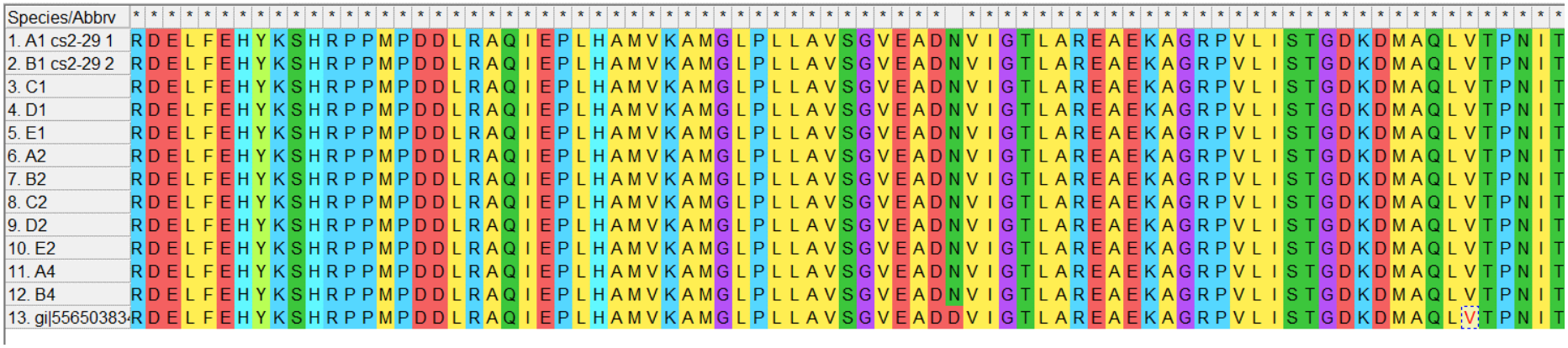

Figure 6-8. Alignment of translated polA gene showing the position of the amino acid change causing cold sensitivity. The G>A transition in the cs2-29 and HCS1 mutant strains at position results in an amino acid change from D (Aspartic acid) to be changed to a N (Asparagine) at position 116.

6.3.2 Transformation of DH10B with soil and cryoconite eDNA

The ligations and transformations were repeated twice. The first transformation resulted in a library of approximately ~3400 cryoconite clones and ~1800 soil clones. The second transformation resulted in an improved library size of 5760 cryoconite clones and ~2700 soil clones. Between both transformation batches, a clone library of 9160 cryoconite clones and 4500 soil clones was created.

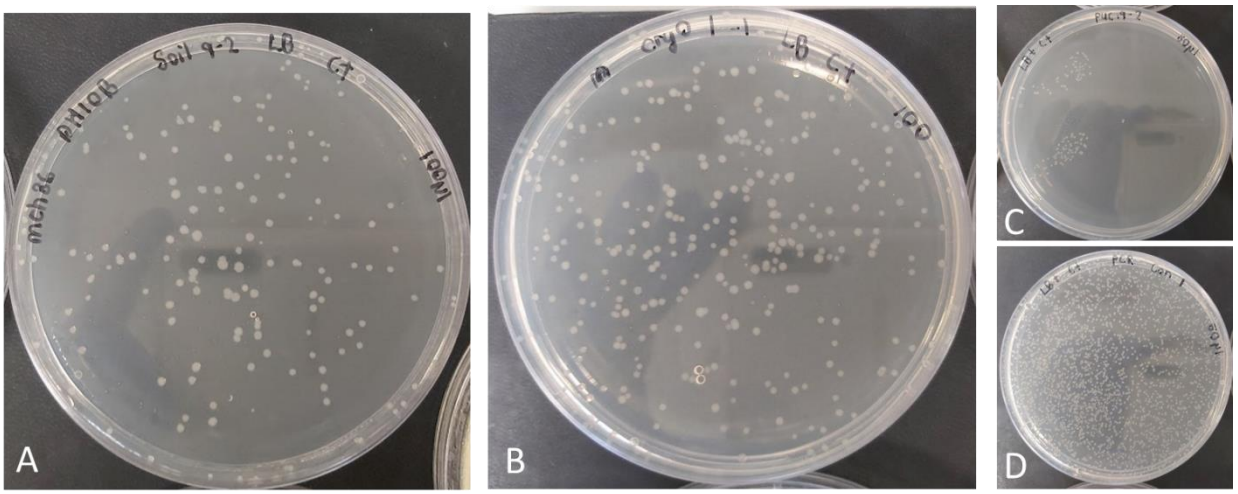

Figure 6-9 Examples of clones obtained by transformation into DH10B. A shows clones derived from soil DNA. **B** shows clones obtained from cryoconite DNA. **C** is a PUC19 control to check transformation efficiency and **D** is a PCR product control to check ligation efficiency. Plates are LB, supplemented with carbenicillin.

Several clones were randomly selected from each plate for colony PCR of the pJET2.1/blunt plasmid insert. The gel (Figure6-10), showing insert sizes, and the BLAST results from Sanger sequencing of the PCR products are shown in Table 6-8. The size of the inserts was within the intended range. Clones 1A, 1B and 1D were approximately 5 kb or greater. Although 1A, 1E and 1H were the largest inserts, the Sanger sequences appeared to be heterozygous or contained mixed sequences. The ~5 kB sequence from cryoconite clone 1B is related to a hypothetical protein from *Phormidesmis priestleyi* ULC0007.

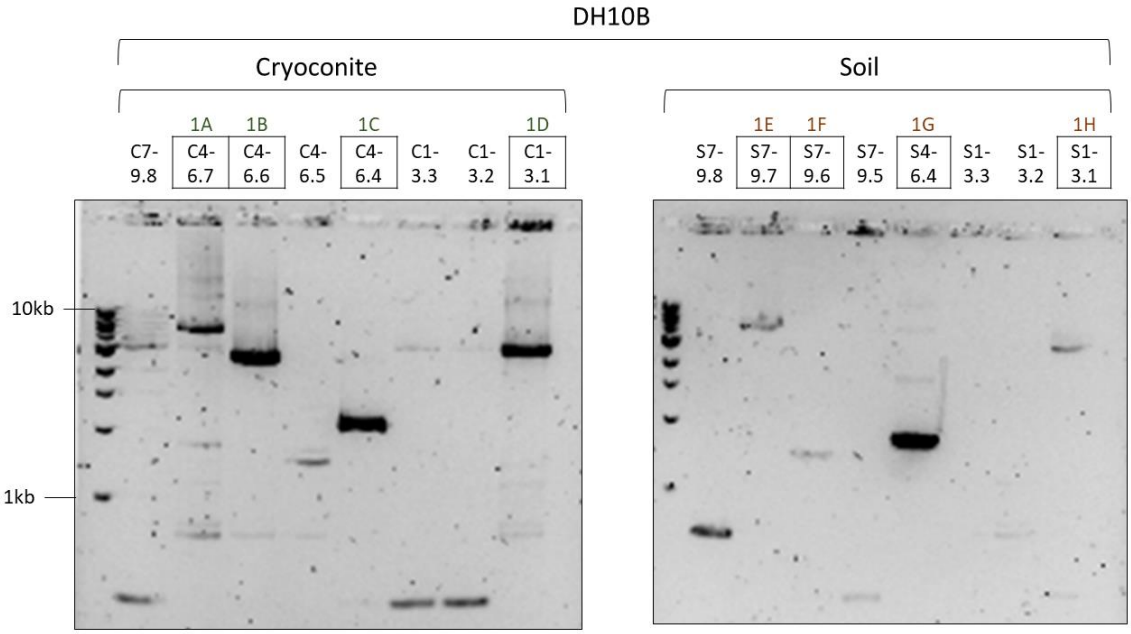

Figure 6-10 Agarose gel of PCR of pJET1.2/blunt inserts from randomly selected DH10B cryoconite and soil clones.

Table 6-8 Table of blastx hits of randomly selected soil and cryoconite clones in DH10B cells.

	Description	Max Score	Total Score	Query Cover	E value	Per. Ident	Accession
Random selection of inserts from DH10B clones							
1B	hypothetical protein C7B65_04385 [Phormidesmis priestleyi ULC007]	99.4	99.4	43%	$1e^{-20}$	73.03%	PSB21180.1
1C	ketol-acid reductoisomerase [Isosphaera pallida]	316	316	77%	$3e^{-105}$	89.70%	WP_013563169.1
1D	alpha-D-glucose phosphate-specific phosphoglucomutase [Afipia sp. GAS231]	391	391	99%	$6e^{-132}$	97.18%	WP_092511167.1
1F	TPA: acetate--CoA ligase [Ktedonobacter sp.]	191	191	65%	$3e^{-57}$	67.88%	HBE27042.1
1G	30S ribosomal protein S5 [Bdellovibrionales bacterium]	136	136	38%	$8e^{-37}$	76.19%	MSP19036.1

6.3.3 Size of cryoconite and soil eDNA inserts

As mentioned previously, we were aiming for an insert length of 3kB to 10kB. To check the size of the clone library, the plasmids were pooled. Colonies from all the plates from a single ligation mixture were pooled, and then all the ligation mixtures from the same environment were pooled. The entire transformation was repeated twice (batch 1 and batch 2). In the end there were two libraries, a cryoconite and soil library. We ran these on a gel to check the size of the plasmids (Figure 6-11). We expected a smear, which can be interpreted as the size distribution of the plasmids from each library. An empty pJET2.1/blunt plasmid is 2974 bp in size, but self-ligated vectors without an insert should be lethal and so we did not expect many 3kB plasmids. Unfortunately, because plasmids are circular, they do not run in the same manner as linear DNA and therefore the ladder is not a good indicator of library size. To linearize the library, the plasmids were incubated with Xho1 restriction enzyme. The library is unfortunately skewed towards shorter sequences, which is due to greater ligation efficiency for shorter DNA sequences. However, there are some inserts above the desired length of 6kB.

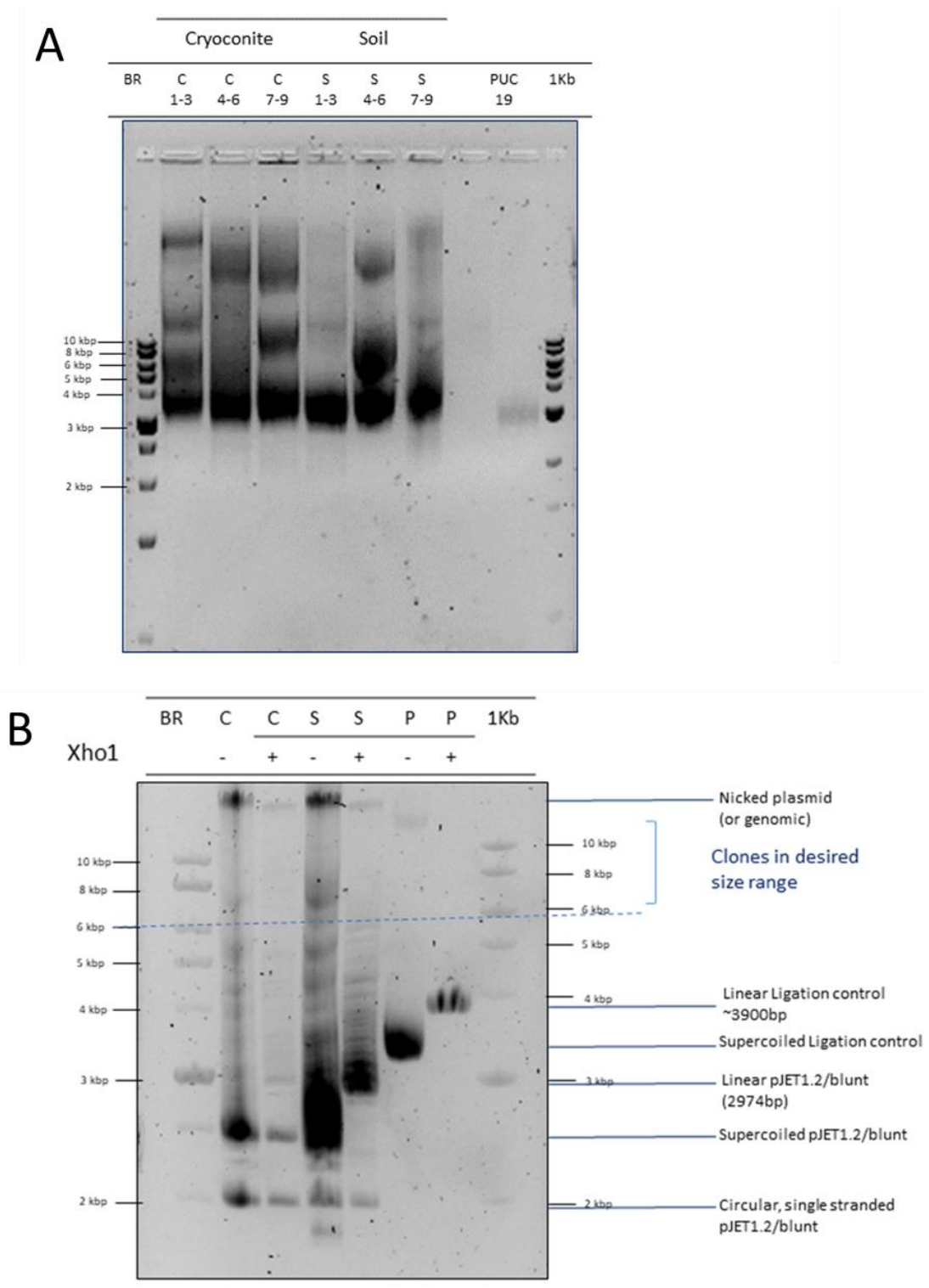

Figure 6-11 A: Example of an agarose gel of undigested plasmids extracted from Batch 2 cryoconite and soil clone libraries. S: soil, C: cryoconite, (n-n) refer to the mixed ligation batches. **B: Restriction digestion of Batch 1 plasmids to check linear size.** C Cryoconite library. S: soil library. P: PCR ligation control. BR: Cleaver Scientific Broad Range Ladder. +/– reflects whether the library was (+) or was not (-) incubated with Xho1 restriction enzyme.

6.3.4 Cold complementation

Several clones were found to be growing at 15° after 10 days of incubation.

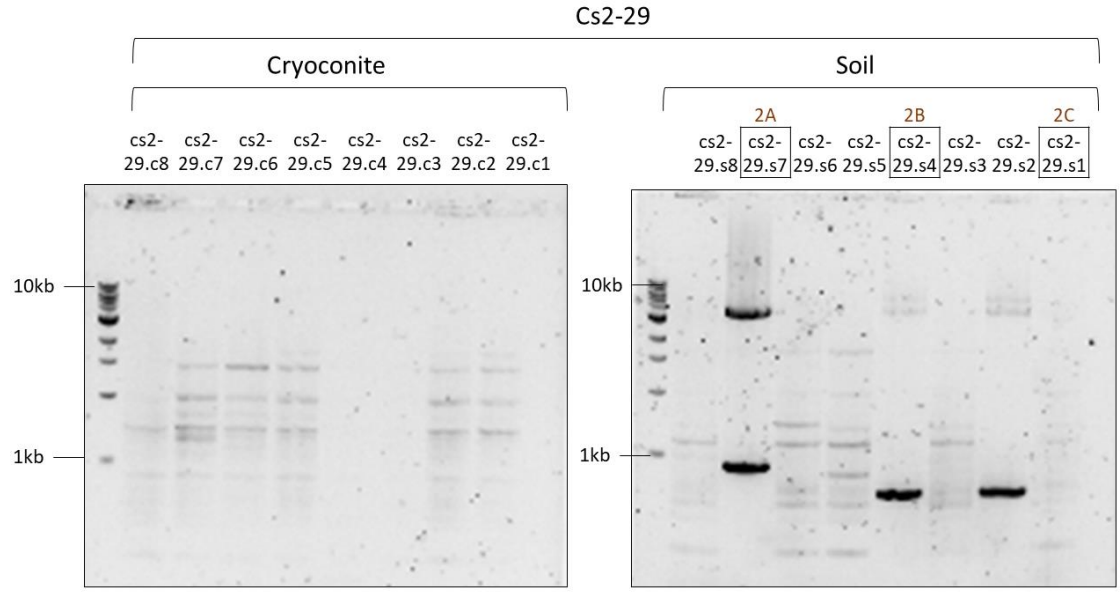

Figure 6-12 Agarose gel of PCR of pJET1.2/blunt inserts from randomly selected cs2-29 cryoconite and soil clones.

	Description	Max Score	Total Score	Query Cover	E value	Per. Ident	Accession
Random selection of inserts from cs2-29 clones							
2A	TIGR03545 family protein [Planctomycetes bacterium Pla175]	46.6	46.6	52%	0.001	47.73%	WP_145289226.1
2B	DUF4981 domain-containing protein [Escherichia coli]	137	137	70%	9e-40	98.46%	WP_123055588.1

Sanger sequencing of the inserts of clones able to grow at 15°C revealed several of the clones had DNA binding activity, even when the sequences were not necessarily hits to polymerase genes (Clone 2D, 2F, 3A and 3C). Furthermore, there were clones with hits to proteins of unknown function, such as a Plantomycetes sequence (WP_145289226.1) which codes for rare but broadly distributed uncharacterized proteinfamily (TIGR03545),and another similar to a domain of unknown function (DUF4981) in E.coli (WP_123055588).

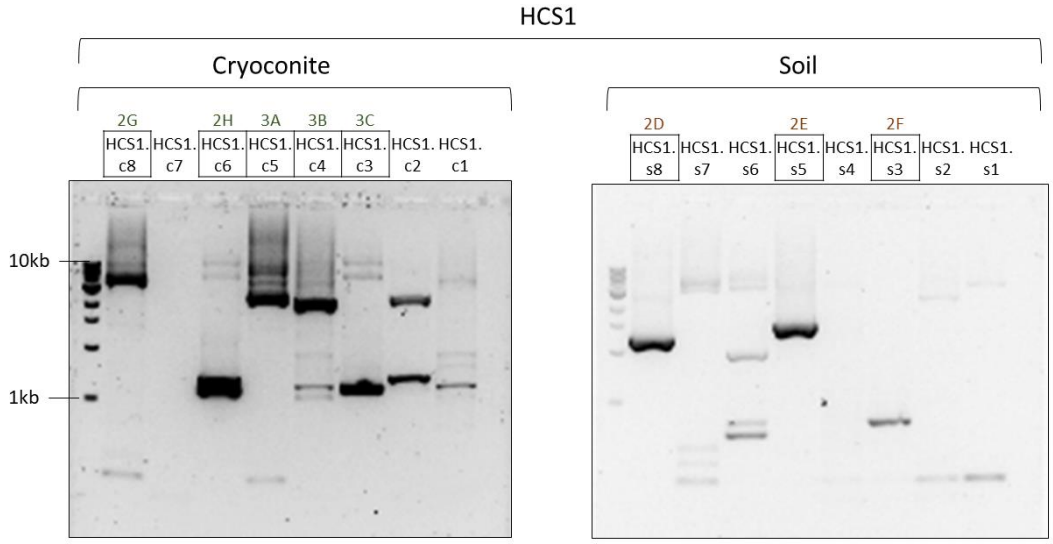

Figure 6-13 Agarose gel of PCR of pJET1.2/blunt inserts from randomly selected HCS1 cryoconite and soil clones.

	Description	Max Score	Total Score	Query Cover	E value	Per. Ident	Accession
Random selection of inserts from HCS1 clones							
2D	groupII intron-encoded protein [Listeria monocytogenes SHL001]	104	184	98%	2e-37	52.68%	KHK05566.1
2F	transcription elongation factor GreAB [Betaproteobacteria bacterium RIFCSPLOWO2_02_FULL_67_19]	74.7	74.7	59%	6e-15	63.08%	OGA25544.1
2G	antimicrobial protein [uncultured bacterium]	134	134	37%	8e-34	88.89%	AQW80360.1
3A	TetR family transcriptional regulator [Actinobacteria bacterium]	110	110	67%	1e-27	65.91%	MSZ50992.1
3C	IS630 family transposase [Pseudanabaena sp.]	155	155	39%	1e-42	93.59%	PZU98931.1

Clone 3C, from the cryoconite library, was similar to an IS630 family transposase (PZU98931.1) from a *Pseudanabaena sp*. One of the clones that grew in the cold also contained an insert similar to an antimicrobial protein (AQW80360) from an uncultured bacterium.

6.4 Discussion

Functional screening of metagenomic libraries remains a vital arm of the bioprospecting enterprise. The use of purely bioinformatic approaches to identify enzymes relies on homology to known proteins, and therefore misses truly novel sequences that do not already exist in databases. In this chapter we cloned soil and cryoconite eDNA into *E. coli* DH10B cells to create a clone library and then extracted the plasmids and transformed them into cold-sensitive mutant *E. coli* strains HCS1 and cs2-29. Clones from the DH10B backup library and HCS1 and cs2-29 clones that grew in the cold were selected and sequenced using Sanger sequencing.

6.4.1 Difficulties encountered

There were several issues encountered in this cloning experiment. The initial experiment was meant to use the PCCFOS1 cloning vector system, which makes use of fosmids that can take inserts of 40 kB in size. This was the system previously used with success to identify polymerases from glacier ice (Simon et al., 2009a). It is also the system of choice in several other screens of metagenomic libraries (Fu et al., 2013; Jeon et al., 2009; Vester et al., 2014). Large inserts are ideal in cloning experiments because they capture several genes at once, which reduces the number of clones that are needed to cover a genome. However, the use of fosmids, requires both long inserts of around 40 kb and enormous quantities of DNA ranging in the 10s to 100s of μg. Several months and many DNA extraction kits and methods were tested to get the DNA length and quantities needed to be packaged into the lambda phage. Several of these methods are listed in Section 2.2. Unfortunately, to get long DNA fragments, direct lysis methods like DNA beating are inappropriate and so the focus is to separate the cells from the environment matrix in which they are embedded and then to perform gentle lysis. Although we attempted many of these methods, from soil agitation in a blender followed by filtering through miracloth and filter paper, to a Ludox Density gradient, we were unable to isolate the quantities of DNA described in the literature (Bakken and Lindahl, 1995; Robe et al., 2003). In addition, most of the methods for long DNA require indirect lysis, which severely reduced the taxonomic diversity and the abundance. The diversity loss is likely due to a combination of factors, such as bacteria forming biofilms and adhering to soil particles with different affinity, size exclusion where larger bacteria or bacterial aggregates don’t get past filters or settle out of the density gradient, and different sensitivity to lysis (Section 4.4.7.1).

Although several metagenome studies have used soil in the past, glacial forefield may have been more tricky than loamy soils because of the high clay content. It is incredibly difficult to separate the microorganisms from the clay in the first place. DNA also adsorbs to any clay carry over in subsequent lysis steps, resulting in further DNA loss.

Instead, we decided to use a plasmid system. We had intended to use the TOPO XL (Invitrogen) which can take inserts of up to 13kb and is ideal for long inserts. However, there was a worldwide shortage of these plasmids and so the pJET1.2/Blunt system which can take inserts of up to 10kB was chosen instead. Plasmids are ideally used with cleaned PCR products of a specific length. In this sample we had sheared metagenomic DNA which ranged in size. To obtain the ideal length for the plasmids, we performed a gel size selection, followed by clean-up. This resulted in some loss of DNA, and the purification, which could only be done in 50uL volumes needed to be reduced via speedivac to the concentrations required for the ligation reaction. The ligation reaction itself is most efficient for short inserts and efficient at specific vector: DNA ratios. Unfortunately, based on our midiprep gels and restriction digestions, it seems that many of the plasmids contained incredibly short inserts, which makes sense as these have a higher probability of proper ligation and plasmid closure. A 976 bp PCR product was included with the cloning kit to act as ligation control. The plasmids with the PCR control repeatedly had much higher transformation efficiencies that the environmental DNA. This perhaps reflects the fact that ligation of smaller DNA fragments is far more efficient than ligation of long inserts.

Cloning of environmental DNA into a plasmid vector and transformation of that vector into a heterologous host was performed multiple times. Initially, electroporation was attempted to transform plasmids directly into the cold-sensitive mutant HCS1 and cs2-29 *E. coli* strains (Appendix Section F-1). However, various difficulties with the electroporation, lead to changes in strategy to Calcium Chloride chemical transformation. The benefit of the Calcium Chloride method is that it is relatively inexpensive and can be repeated many times at very low cost. The initial decision to clone directly into the mutant strains was made to screen the greatest biodiversity possible, with the understanding that cloning into another competent host strain first might reduce the diversity in the library that gets cloned into the mutant strain in the complementation screen. However, the competency of the mutant strains was unknown, and it was decided instead to clone into a commercial competent strain, like *E. coli* DH10B to maximise the efficiency of DNA take up. The successfully transformed DH10B cells would be amplified and their plasmids extracted to allow massive rescreening of the library. The use of

Calcium Chloride transformation method and amplified plasmids from a competent cell library, made unlimited attempts to clone the plasmids into the mutant strains possible.

Cloning into the chemically competent *E. coli* cells resulted in a much bigger library than electroporation directly into HCS1 and cs2-29. Using this method, we were able to create a clone library of approximately 9160 cryoconite clones and 4500 soil clones

6.4.2 The clones reflect the most abundant taxa in cryoconite and soil

The clones we sequenced were from the most abundant taxa in these environments. There was good correlation between the taxonomy of the clone sequences and what we know to be the most abundant species in these environments. For example, *Phormidesmis priestleyi* (1B), *Ktedonobacte*r sp (1F), *Bdellovibrionales* (1G), *Pseudanabaena* sp (3C), Actinobacteria bacterium.

6.4.3 The clones from the cold-complementation assay tended to have DNA-binding activity

Sanger sequencing of the clones reflected that many of the clones that grew in the cold had inserts with genes that had DNA binding activity. Unfortunately, we were limited to Sanger sequencing of the PCR inserts from the clones, with only several hundred high quality bases from which to base our BLAST search. Several of the clones had large inserts, and therefore it is possible that there was a polymerase gene downstream of the short section we sequenced. The HCSI cryoconite clone (2G) was > 6kB in size. For example, clone 3C from cryoconite had a sequence similar to a transposase from *Pesudoanabaena*. This raises the possibility of mutation correction by the *Pseudanabaena* transposase. In any community of bacteria, with a given mutation rate, and sufficient generations, it is possible for point mutations to revert to their original WT. This may be what happened in the case of the empty inserts we sequenced. There were also several instances where we cloned the empty vector or where the Sanger PCR products were clearly mixtures, containing inserts from more than one clone. This was partly a consequence of time pressure, and generations of sub-culturing could have separated the mixed clones, although it might have taken PCRs of several colonies to capture both, (or all) of the clones that were in the mixture.

Although we did not have any clear clones with a polymerase, this is not improbable given other studies of this nature. The previous study that used the *fcsA* mutation to screen for polymerases identified 1 fosmid clone, and 8l plasmid clones, although several were

duplications (Simon et al., 2009a). They calculated a success rate of approximately 1 polymerase clone per 1000 plasmids screened. This is a success rate many times higher than most metagenomic screens (Ferrer et al., 2016). In this study, we had approximately 9160 cryoconite clones and 4500 soil clones. However, the study by Simon et al, used plasmids with insert sizes of 14 kB (Simon et al., 2009a). The insert sizes in our library were 10kB maximum, and occasionally much smaller, which drives down the actual coverage in our clone library as well as the number that might contain full and functional polymerase sequences.

6.4.4 Future work

The cryoconite and soil clone libraries created in this chapter have been stored as glycerol stocks and as plasmids. They remain a resource for future investigation. The intention was to catalogue the entire library by performing a PCR of the pJET2.1/blunt vector insert site, followed by sequencing of the library on a Nanopore minION. Long-read sequencing by Nanopore could easily capture the entire insert, with no need for assembly, and allow the determination of the exact number of clones, together with the taxonomic and functional classification. The screening of clone libraries can be an exceptionally laborious exercise, generally requiring hundreds of plates, meticulously poured, marked, and catalogued and then grown for long periods of time for a relatively low hit rate (Ferrer et al., 2016). A bioinformatic catalogue of a clone library lends itself to many applications. In this study we employed a relatively easy complementation assay for polymerases. However, based on a bioinformatic screen of the library, specific assays could be designed to target specific clones that we know to be present and complete.

If a clone with a full enzyme sequences is present, the clone can then be analysed for signatures of cold adaptation. The types of structural adaptations that signify cold-adaption include decreased core hydrophobicity and increased surface hydrophilicity, alterations in the types, and proportions of amino acids present, such as less Isoleucine, more histidine and methionine, a high (Glu + Asp) / (Lys + Arg) ratio, and a low Low Arg/ Lys ratio (Siddiqui and Cavicchioli, 2006). In addition, there is more Gly, less pro in loops, and more proline in a-helices, resulting in more loops and/ or loops of longer length. Because there are fewer total charged residues, there tend to be fewer hydrogen bonds, disulphide bridges and salt bridges. There are also fewer metal-binding sites and/ or lower affinity for metal-binding, less aromatic interactions and weaker intersubunit/ interdomain contacts (Siddiqui and Cavicchioli, 2006).

Unfortunately, only part of the inserts from the clones could be sequenced using Sanger sequencing (~1000 bp). An obvious extension of this work would be to sequence the full-length inserts using long read technology such as Nanopore, or alternatively, Illumina shotgun sequencing of the clone library and assembly of the contigs.

6.5 Conclusion

In this chapter, clone libraries of cryoconite and soil environmental DNA were created in DH10B *E. coli* for storage, propagation, and future screens, as well as in cold-sensitive mutant *E. coli strains* cs2-29 and HCS1. Several clones capable of growth at 15°C, suggesting they were able to rescue transcription in the mutant strains. The sequenced clones were similar to proteins that had DNA binding ability and should be investigated in further.

7 A METAGENOMIC ANALYSIS OF THE FUNCTIONAL POTENTIAL OF THE SCĂRIȘOARA ICE CAVE

7.1 Introduction

The Scărișoara Ice Cave is one of the oldest and largest perennial underground ice-blocks in the world, being older than 3000 years and greater than 100 000 m^3 in volume (Perşoiu and Pazdur, 2011). The cave is located in the Bihor Mountains of North West Romania (46°29’23”N, 22°48’35”E) at an altitude of 1165m. The Scărișoara ice block differs from surface glaciers and glacier caves because it is not formed by snow accumulation. Rather, it grows via the annual freezing of a layer of water that trickles into the cave during summer months, forming a shallow lake on top of the existing ice block (Holmlund et al., 2005). This layer, which can be up to 20 cm deep, freezes every winter, trapping at its bottom a layer of sediment deposited during the summer. The ice block therefore consists of sequential layers of ice of variable thickness, separated by organic-rich sediment layers. This makes it a fascinating record of past climactic conditions, as each year remains frozen, like layers of sedimentary rock. Secondly, the environment is oligotrophic and dark, and many of the deeper layers are also anaerobic, meaning that bacteria that thrive here will be adapted to extreme conditions.

Although there may be annual injections of nutrients into the cave via the water and sediment that trickles into the cave each summer, there is likely to be significant recycling of nutrients. Without photoautotrophy to continuously add organic carbon into the environment, there will need to be alternative pathways for carbon fixation. To investigate this environment, bacterial MAGs were constructed from shotgun metagenomes collected from seven sites within the cave. The abundance of the MAGs at various sites was inferred via read mapping, and the MAGs were investigated for their biogeochemical cycling potential, which was used in turn to infer the types of nutrient cycling occurring at each site.

In addition, the MAGs were also screened for secondary metabolite BGCs. Growing antimicrobial resistance poses a serious threat to human health and novel antibiotics are urgently needed (Sabtu et al., 2015; Ventola, 2015). Antimicrobial secondary metabolites are often synthesised by bacteria as weapons against competitive species (Bérdy, 2005; van Bergeijk et al., 2020). Low nutrient environments are especially harsh and competitive environments in which cell death is often required to recycle nutrients for continued growth (Bérdy, 2005; van Bergeijk et al., 2020). It has been suggested that a resistome is innate in some cave environments (Bhullar et al., 2012), and since resistance develops in response to the presence of antimicrobials, this raises the possibility that the microorganisms of cave microbiomes may synthesise a novel and distinct arsenal of antimicrobial compounds (Ghosh et al., 2017). Because caves are such isolated habitats, in which organisms predominantly enter the cave, and do not tend to leave, it possible that that there are distinct and endemic bacterial communities, with a novel, unknown BGCs. Although several caves have been explored for potential antimicrobials, from the subterranean Kotumsar cave, India (Rajput et al., 2012), to a volcanic cave in western Canada (Rule and Cheeptham, 2013) to Magura Cave, Bulgaria (Tomova et al., 2013), these studies relied on cultured bacteria, and none have investigated a solid ice block like the one present in the Scărișoara Ice Cave.

7.1.1 Aims and objectives

The aims of this chapter were as follows:

1. Construct high quality metagenome-assembled genomes (MAGs) from seven samples collected from different sites within the Scărișoara Ice Cave.
2. Classify the MAGs using phylogenomic methods and identify novel species from these environments.
3. Use read mapping and coverage information to identify:
   3.1. distribution of these species across different sample sites.
   3.2. co-occurrence of different species at specific locations.
4. Identify the presence of genes involved in biogeochemical cycling of major nutrients at specific sites:
5. Use antiSMASH to identify the main categories of secondary metabolites synthesized by Ice Cave Bacteria

7.2 Materials and methods

7.2.1 Site description

Seven metagenomes from the perennial ice block of Scărișoara Ice Cave in Romania were included in this study (Iţcuş et al., 2016). Ice samples of three different ages were collected from the cave in 2012. At the time of collection, samples with the prefix 1 were collected in 2012, samples designated 400 were from 385 calendar years before the collection date and samples with the prefix 900 were 943 calendar years before 2012. The most recent samples were collected from a sun-exposed site in the immediate vicinity of the entrance (**IS**), a second sample was collected from an indirect light exposed area in the centre of the cave (**1L**). A description of sample locations and characteristics are in Table 7-1. A table describing the age, location and characteristics of samples collected in the Scărișoara Ice Cave.

Table 7-1. A table describing the age, location and characteristics of samples collected in the Scărișoara Ice Cave.

Sample Name	Age	location	description	Organic or inorganic
1S (2)	Present	Great Hall, immediate vicinity of entrance	Sunlight exposed	
1L (13)	Present	Great Hall, centre of cave	Light-exposed	
400-O (6)	-385	Little Reservation, horizontal drilling of ice-wall surface		Organic
900-O (15)	-943	Little Reservation, horizontal drilling of ice-wall surface		Organic
900-I (7)	-943	Little Reservation horizontal drilling of ice-wall surface		Inorganic, clear ice
1500 (18)	~1200 (?)			
2000 (14)	~1500 (?)			

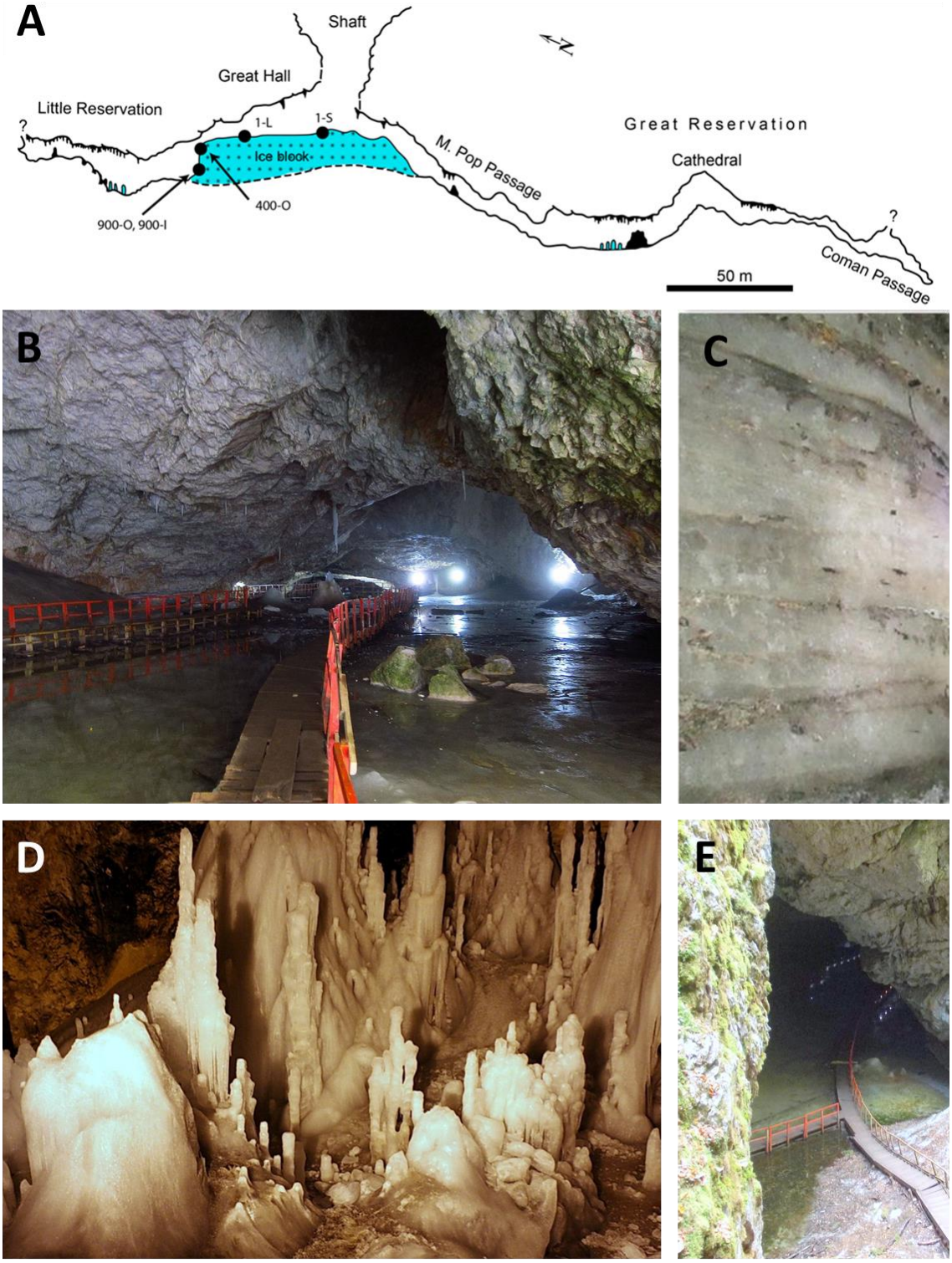

A) Shared with permission to use in thesis. **B)** CC BY-SA 4.0 (By Mpdus at https://commons.wikimedia.org/wiki/File:Kirchensaal_Sommer_2017.jpg), **C)** Shared with permission to use in thesis, **D)** CC BY-SA 3.0 (By Beradrian at https://commons.wikimedia.org/w/index.php?curid=3126173), **E)** CC BY-SA 4.0 (By Țetcu Mircea Rareș at https://commons.wikimedia.org/wiki/File:RO_AB_Pestera_Scarisoara_(2).jpg

Figure 7-1 A) Schematic diagram of the Scărișoara Ice Cave showing the locations of sample collection. B) The Great Hall. C) Layers of sediment and water deposited in annual layers. D) The Church contains stalagmites and is accessed from the Great Hall (not shown on map). E) Entrance to the Cave (Shaft).

7.2.2 Sequencing and bioinformatics

The metagenomes were sequenced on an Illumina HiSeq and are available from the nanuq platform at McGill University and Génome Québec Innovation Centre (https://genomequebec.mcgill.ca/nanuqAdministration). The sequences were uploaded to KBase and adapters were removed and low quality bases trimmed using Trimmomatic (Bolger et al., 2014) with a minimum Phred score threshold of 30. The seven ice cave libraries were assembled together on the KBase server, using three different assembly tools: metaSPAdes (Nurk et al., 2017), MEGAHIT (D. Li et al., 2015) and IDBA-UD (Peng et al., 2012).

7.2.2.1 Taxonomy

Taxonomy was determined from the trimmed reads for each library individually and for the combined library using the kaiju (Menzel et al., 2016) module hosted on the KBase server (Arkin et al., 2018).

7.2.3 Metagenome assembled genomes (MAGs)

Genomes were assembled from metagenomes using Anvi'o (Section 8.2.4). Analysis was started in Anvi'o v5 "margaret" (https://github.com/merenlab/anvio/releases/tag/v5), which was then updated to Anvi'o v6.1 "esther" (https://github.com/merenlab/anvio/releases/v6). The existing profile.db and contigs.db were migrated to the latest versions using anvi-migrate. Functions were added to the contigs database using anvi-run-hmms and anvi-run-ncbi-cogs -c contigs.db -T 8. The contigs were also functionally annotated using KEGG annotations and Eggnog mapper (Chapter 8).

7.2.3.1 Binning and refinement of MAGs

The contigs database of 179753 contigs was too large to run anvi-interactive with hierarchical clustering and run manual binning. Therefore, the contigs were binned using anvi-cluster-contigs as part of the anvi'o workflow using CONCOCT, MaxBin2 and MetaBAT2 (Section 8.3.6). The DAS Tool was then run on all three collections, using diamond as a search engine. The taxonomic classification of the bins, and bin refinement was performed as previously described in Chapter 4 and detailed in Chapter 8. The dataset was trimmed to contain high quality MAGs. The genomes had to be larger than 1.8 MB, have greater 70% completion and less than 10% redundancy (Bowers et al., 2017). The list of medium to low quality bins not included for further analysis is shown in Appendix Table G-7.

7.2.3.2 Check genome quality with CheckM and GTDB-Tk

The completeness, redundancy and taxonomic classification of the MAGs was performed using CheckM (Parks et al., 2015) and the GTDB-Tk module on KBase (Chaumeil et al., 2020) as previously described (Section 4.2.6). The phylogenomic relationship of the MAGs was calculated using the HMM hits from a curated collection of single copy core genes for the GToTree workflow (Lee, 2019) as previously described (Section 4.2.6).

7.2.3.3 Spatial distribution of the MAGs across sample sites

A heatmap of max-normalised ratio (number of reads recruited to a contig divided by the maximum number of reads recruited to that contig in any sample) was created using the R package ComplexHeatmap to visualise the spatial distribution of the MAGs (http://www.bioconductor.org/packages/devel/bioc/html/ComplexHeatmap.html) (Gu et al., 2016).

7.2.3.4 Biogeochemical cycles

The fasta files from the MAGs were analysed for major metabolic pathways using MetabolisHMM (https://github.com/elizabethmcd/metabolisHMM).

7.2.3.5 Screening for antimicrobial secondary metabolites

The MAGs were submitted to antiSMASH v 5 to screen for secondary metabolite BGCs (Blin et al., 2019b).

7.3 Results

Table 7-2 Ice-cave library shotgun library statistics

				Read Length		Duplicate reads		Quality		
Environment	**Sample**	**Reads**	**No Bases**	**mean**	**std dev**	**Number**	**%**	**mean**	**std dev**	**GC%**
Ice-cave dataset										
Present, sun	**1S_2**	69,575,748	8,530,226,859	122.60	10.58	29,675	0.04	35.48	3.95	53.19
Present, light	**1L_13**	72,190,896	8,860,007,146	122.73	10.26	36,821	0.05	35.48	3.94	56.84
-385, organic	**400_O_6**	76,039,348	9,324,467,510	122.63	10.53	161,544	0.21	35.47	3.97	54.29
-943. Organic	**900_O_15**	73,462,594	9,019,960,422	122.78	10.20	353,401	0.48	35.51	3.90	54.57
-943, inorganic	**900_I_7**	75,113,102	9,213,747,381	122.67	10.46	145,477	0.19	35.43	4.03	59.89
~1200	**1500_18**	75,510,556	9,278,999,040	122.88	9.77	1,286,620	1.70	35.67	3.59	42.33
~1500	**2000_14**	63,569,516	7,815,266,055	122.94	9.78	84,276	0.13	35.48	3.93	61.72

7.3.1 Sequencing results

The library size (number of reads), average read length, quality (average Phred score) and GC content of the seven shotgun metagenome libraries included in the study are described in Table 7-2.

7.3.2 Taxonomy

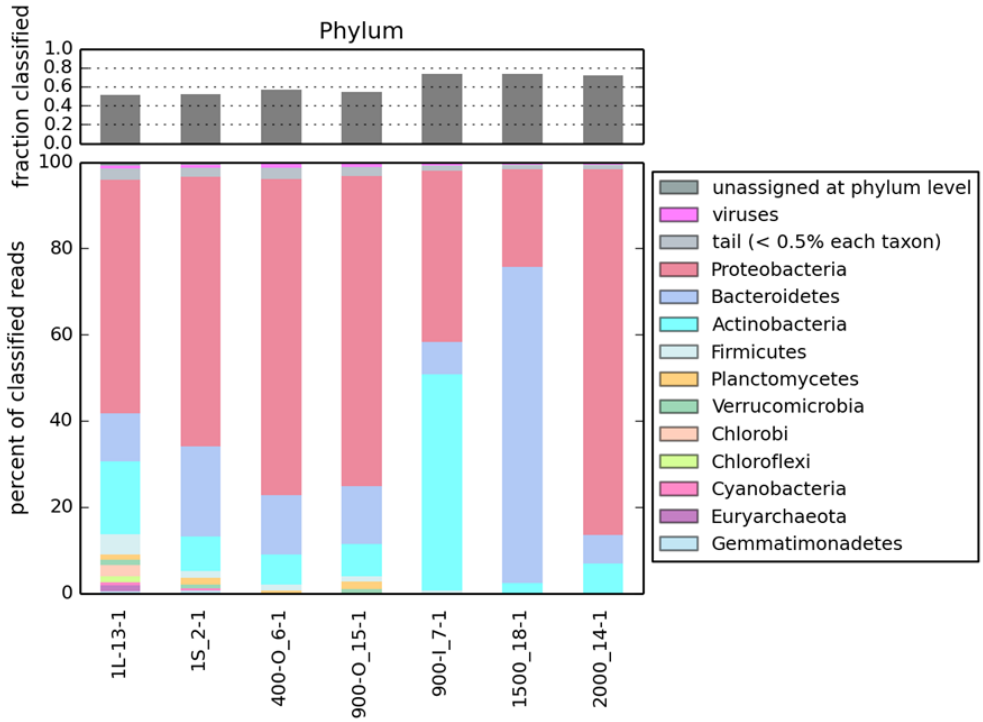

Figure 7-2 Phylum-level taxonomic profile of individual samples from various locations in the Scărișoara Ice Cave.

Samples 1L and 1S from the cave Great Hall as well as 400-O and 900-O which were older in age, but from organic layers, were similar in profile with approximately 50% of reads classified to Phylum level. The Proteobacteria dominated these samples, with Bacteroidetes and Actinobacteria comprising the second and third most abundant phyla. The present-day samples contained a greater diversity of Phyla, with small proportions of Firmicutes, Plantomycetes, Verrucobacteria, Chlorobi, Chloroflexi and Cyanobacteria also present. The older samples 1500 and 2000 and the inorganic sample 900-I had more reads (~70%) classified to Phylum level. Sample 900-I from an inorganic layer had fewer Proteobacteria and the largest proportion of Actinobacteria. Sample 1500 was unique with most reads classified as Bacteroidetes, while Sample 2000 was dominated by Proteobacteria.

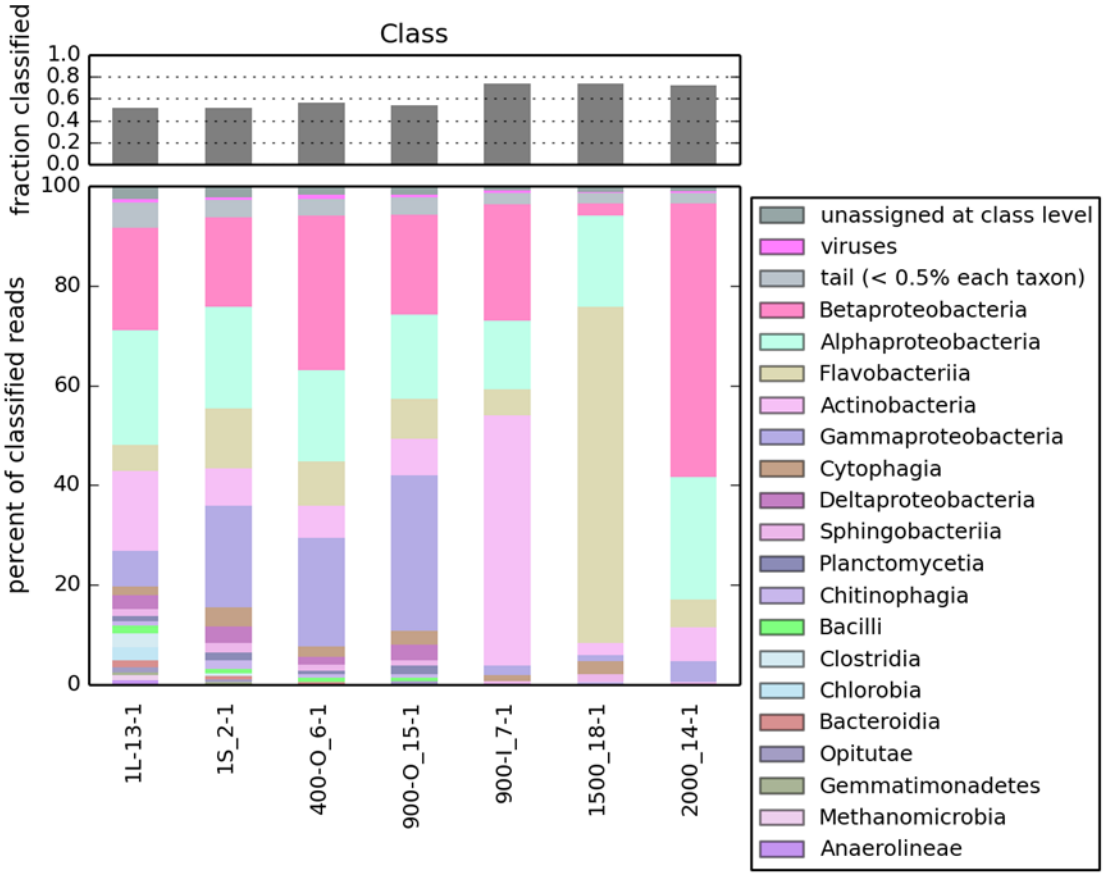

Figure 7-3 Class-level taxonomic profile of individual samples from various locations in the Scărișoara Ice Cave.

Samples 1L and 1S from the cave Great Hall as well as 400-O and 900-O which were older in age, but from organic layers, were similar in profile with approximately 50% of reads classified to Class level. The Beta-, Alpha- and Gammaproteobacterial classes were in high abundance, with a smaller number of Deltaproteobacteria present. Flavobacteriia from the Bacteroidetes phylum and Actinobacteria comprised the second and third most abundant non-proteobacterial classes. The present-day samples contained a greater diversity of Classes. The older samples 1500 and 2000 and the inorganic sample 900-I had more reads (~70%) classified to Class level. Sample 900-I from an inorganic layer had the largest proportion of Actinobacteria. Sample 1500 was unique with most reads classified as Flavobacteriia from the Bacteroidetes, while Sample 2000 was dominated by Beta-, Alpha- and Gammaproteobacteria in that order, with some Actinobacteria and Flavobacteriia also present.

Table 7-3 Table comparing Ice Cave assemblies

Assembly	Longest contig (bp)	Nx (Lx)		Length (bp)	Number of contigs	Sum Length (bp)	Contig Length Histogram (1bp <= len < 10Kbp)	Contig Length Histogram (10Kbp <= len < 100Kbp)	Contig Length Histogram (len >= 100Kbp)
MEGAHIT	1388828	N50:	8767	>= 10^6	2	2540240	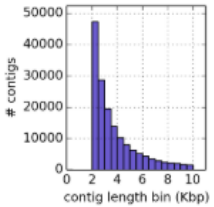	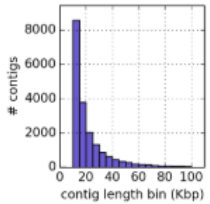	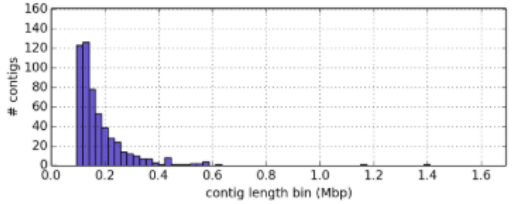
		L50:	(24021)	>= 10^5	547	99933809			
		N75:	3819	>= 10^4	19855	522690257			
		L75:	(74910)	>= 10^3	179753	1123284953			
		N90:	2539	>= 500	179753	1123284953			
		L90:	(129650)	>= 1	179753	1123284953			
IDBA-UD	1388786	N50:	11935	>= 10^6	1	1388786	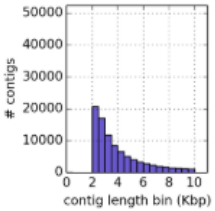	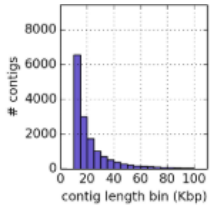	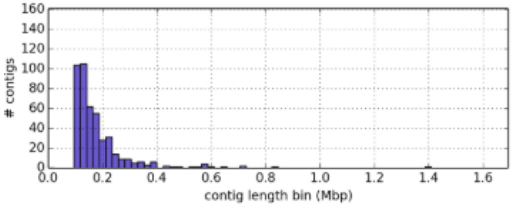
		L50:	(12589)	>= 10^5	453	81591909			
		N75:	4631	>= 10^4	15812	430080664			
		L75:	(40483)	>= 10^3	106360	789866587			
		N90:	2828	>= 500	106360	789866587			
		L90:	(73683)	>= 1	106360	789866587			
metaSPAdes	1644450	N50:	9447	>= 10^6	4	4899394	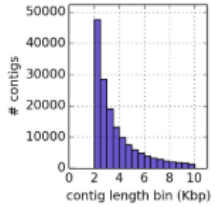	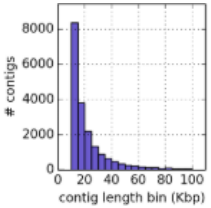	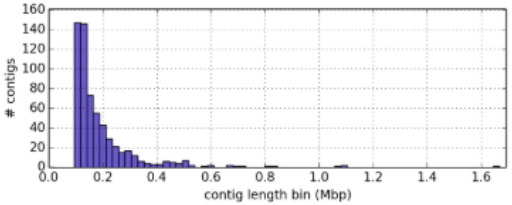
		L50:	(21521)	>= 10^5	611	116757355			
		N75:	3862	>= 10^4	19998	549270645			
		L75:	(70816)	>= 10^3	175966	1128145066			
		N90:	2538	>= 500	175966	1128145066			
		L90:	(125621)	>= 1	175966	1128145066			

7.3.3 Assembly

The combined ice-cave library was assembled using MEGAHIT v1.1.1 and metaSPAdes 1.1.3 and IDBA-UD v1.1.3 on the KBase server. The assembly contig distributions were compared using Compare Assembled Contig Distributions - v1.1.2. The assemblies were remarkably similar in size and contig distribution (Table 7-3). MEGAHIT was the assembly used for MAG construction.

7.3.4 Metagenome assembled genomes

The contigs from the MEGAHIT assembly were clustered into 270 bins using CONCOCT (v 1.1.0) (Appendix Table G-2), 253 bins using MaxBin2 (version 2.2.7) (Appendix Table G-3), and 401 bins using metaBAT2 (v 2.12.1) (Appendix Table G-4). The bins in each collection were compared using DAS Tool (v 1.1.2) (Appendix Table G-5) and a refined collection of 145 bins with completion > 50% was created. The taxonomic classification of the bins from each binning method (collection) were checked using anvi-estimate-scg-taxonomy, using the contigs database, merged profile, and collection (Appendix Table G-8).

The DAS Tool collection consisted of 145 bins, accounting for 502,443,977 nucleotides, which represent 44.73% of all nucleotides stored in the contigs and profile databases. This collection was refined using anvi-refine, resulting in the collection ice-mags, which describes 146 bins accounting for 472,098,455 nucleotides, representing 42.03% of all nucleotides stored in the contigs and profile database. The fastas from each of the MAGs in the ice-mags collection were downloaded and submitted to CheckM on KBase. Based on the KBase completion and redundancy estimates, the collection was reduced to 121 bins (ice_mags_final) which had completion above 70% (Appendix Table G-6). Bins excluded from the dataset at this point can be found in Appendix Table G-7. This final dataset comprises 430,185,758 nucleotides, which represent 38.30% of all nucleotides stored in the contigs database.

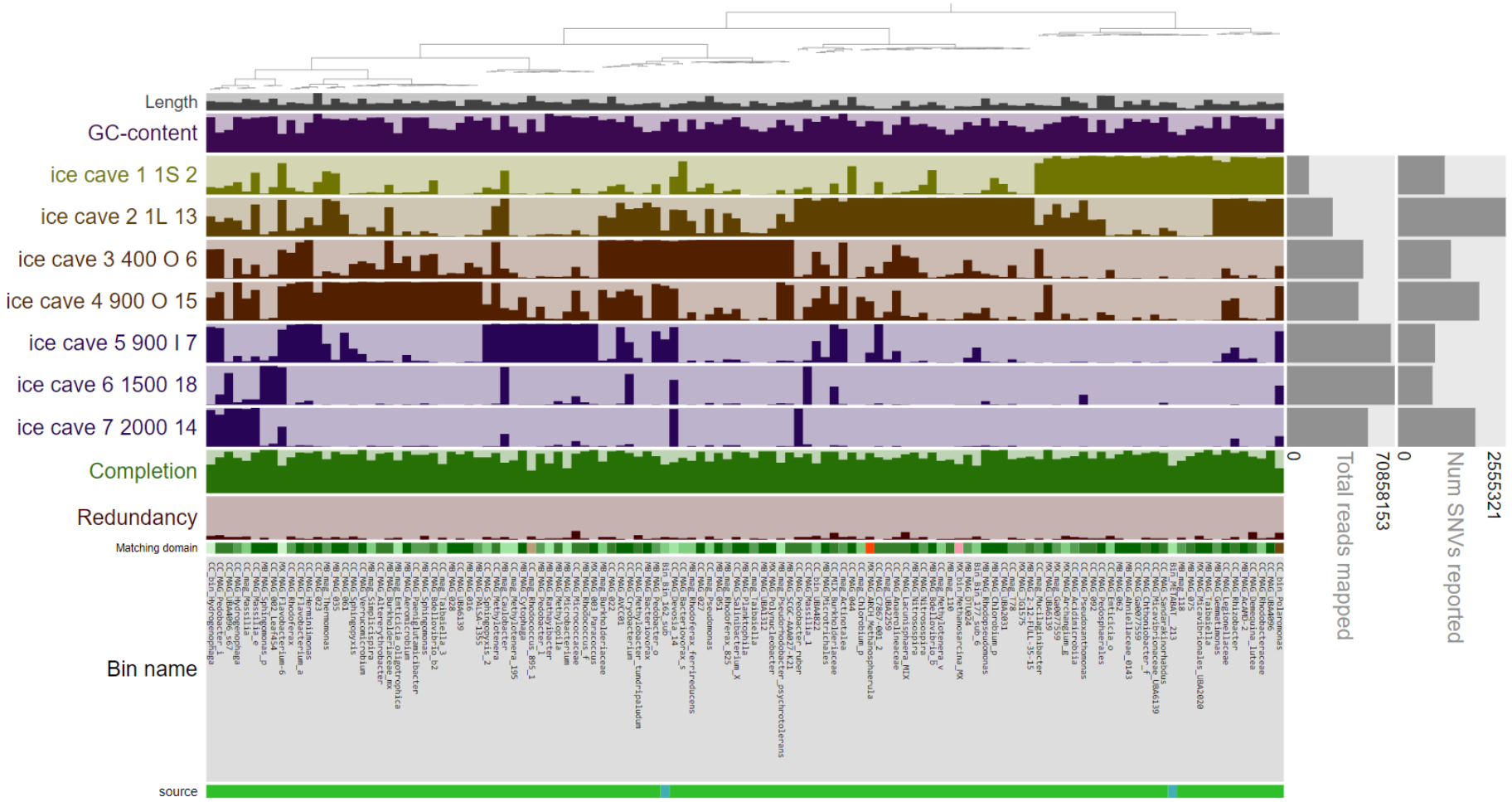

Figure 7-4 Phylogram of the 121 MAGs in the Ice cave dataset. The Items order: Abundance (D: Euclidean; L: Ward) | Current view: detection. Bars represent proportion of contigs that have at least 1x coverage.

7.3.4.1 Metagenome-assembled-genomes (MAGS)

Table 7-4 Table of MAG characteristics

Bin	Taxon (Kaiju estimate)	Total length	Num contigs	N50	GC content	Completion (%)	Redundancy (%)	CM Completeness	CM Contamination
MB_MAG_Bdellovibrio_b	Bdellovibrio	3881963	52	127279	47.93	94.37	0.00	100	0
MB_MAG_Rhodococcus_f	Rhodococcus	5177775	92	80063	64.68	97.18	2.82	99.75	2.44
CC_MAG_Sandarakinorhabdus	Sphingosinicella	3891944	56	112443	65.45	92.96	2.82	99.62	1.3
CC_MAG_002_Leaf454	Aureimonas	5585765	58	277120	66.90	100.00	0.00	99.6	0.6
MB_MAG_Taibaiella	Chitinophaga	5052740	113	61840	45.10	100.00	1.41	99.51	1.51
MB_MAG_Rhodopseudomonas	Rhodopseudomonas	5682077	87	123697	63.64	100.00	1.41	99.47	1.17
MB_MAG_Chlorobium_p	Pelodictyon	2609204	10	377055	48.74	98.59	0.00	99.45	0.55
CC_MAG_Micrococcaceae	Pseudarthrobacter	5121799	64	179917	64.80	91.55	19.72	99.42	4.43
CC_MAG_Verrucomicrobium	Akkermansia	5589208	289	28819	59.98	100.00	2.82	99.32	5.24
MB_MAG_Sphingomonas_p	Sphingomonas	3632561	39	143436	65.84	100.00	4.23	99.3	1.1
MB_MAG_Cytophaga	Cytophaga	3841174	36	188784	36.41	98.59	0.00	99.11	0
MB_MAG_UBA1312	Chitinophaga	3328700	60	76584	38.65	97.18	1.41	99.01	0.66
MX_MAG_003_Paracoccus	Paracoccus	3525589	26	250083	67.22	100.00	0.00	98.94	0.71
CC_MAG_UBA2031	Unknown	3414998	164	41523	58.31	100.00	0.00	98.77	2.25
CC_MAG_Herminiimonas	Herminiimonas	3077735	8	327690	55.54	92.96	1.41	98.72	0.1
MX_MAG_Polynucleobacter	beta proteobacterium CB	2151838	39	114400	46.02	97.18	0.00	98.47	0.83
MB_MAG_Aeromicrobium	Aeromicrobium	3406021	26	270508	64.77	97.18	0.00	98.45	0.69
MB_MAG_Pedobacter_l	Pedobacter	4329052	103	69015	38.70	91.55	1.41	98.43	0.97
CC_mag_Pseudomonas	Paucimonas	6734602	413	28806	56.50	73.24	7.04	98.41	2.28
CC_MAG_Legionellaceae	Legionella	2853258	160	26752	43.83	100.00	1.41	98.25	0.97
CC_MAG_027	Unknown	3987049	91	69217	43.05	95.77	0.00	98.1	0.03
MB_mag_Emticicia_oligotrophica	Emticicia	5202269	96	87793	35.53	76.06	4.23	97.69	1.49
MB_MAG_SCGC-AAA027-K21	Achromobacter	3521530	42	174330	50.49	94.37	0.00	97.66	0.85
CC_MAG_Pedobacter_ruber	Pedobacter	3987695	205	31064	38.90	83.10	5.63	97.56	1.59
CC_MAG_Flavobacterium_a	Flavobacterium	3392991	35	202201	35.67	94.37	2.82	97.15	0.62
MB_MAG_Methylopila	Unknown	3850659	205	28627	67.62	95.77	2.82	97.04	2.57
MB_MAG_Pedobacter_o	Pedobacter	3560853	175	30001	39.91	85.92	2.82	97.02	2.39
MB_MAG_PALSA-1355	Pirellula	5002409	193	36281	58.72	83.10	0.00	96.88	0.57
MB_MAG_Burkholderiaceae_mx	Rhodoferax	3404216	45	113992	55.37	94.37	2.82	96.86	0.26
MB_mag_Pseudorhodobacter_psychrotolerans	Gemmobacter	3830488	55	124416	60.36	70.42	2.82	96.64	0.4
CC_MAG_022	Unknown	6571728	523	20806	61.91	97.18	5.63	96.6	7.17
CC_mag_Methylotenera_195	Methylotenera	2976345	176	23350	47.67	76.06	1.41	96.52	3.02
CC_MAG_Bdellovibrio_b2	Bdellovibrio	4772976	203	36723	44.87	92.96	0.00	96.3	3.78
CC_MAG_Rhizobacter	Rhizobacter	4321097	570	10096	67.77	92.96	5.63	96	4.15
CC_MAG_Pedosphaerales	Unknown	6928595	188	57823	60.38	95.77	2.82	95.95	1.35
CC_MAG_Altererythrobacter	Altererythrobacter	3456033	223	26472	64.85	91.55	0.00	95.88	7.37
CC_MAG_Cryobacterium	Salinibacterium	2583124	202	18291	67.50	92.96	0.00	95.2	1.17
CC_MAG_Massilia_1	Massilia	4880312	192	42305	62.46	91.55	5.63	95.03	3.12
CC_MAG_Rhodobacteraceae	Gemmobacter	4033570	361	15969	63.12	80.28	2.82	94.99	1.57
MB_MAG_AcAMD-2	Unknown	2362746	108	37212	65.48	97.18	0.00	94.81	1.08
MB_MAG_016	Unknown	5008661	53	149673	66.82	97.18	0.00	94.62	0
MB_MAG_Ahniellaceae_0143	Ahniella	4333603	268	24388	62.74	98.59	0.00	94.49	1.63

Bin	Taxon (Kaiju estimate)	Total length	Num contigs	N50	GC content	Completion (%)	Redundancy (%)	CM Completeness	CM Contamination
CC_MAG_Salinibacterium_X	Salinibacterium	3312337	328	16214	65.60	95.77	5.63	94.43	6.78
MB_MAG_028	Bacteroidetes bacterium UKL13-3	4449372	182	38646	41.63	95.77	0.00	94.29	0.74
CC_MAG_Sphingopyxis	Sphingopyxis	3092699	278	16862	63.24	90.14	7.04	94.15	4.79
MB_mag_Caulobacter	Caulobacter	3592269	170	34828	68.06	70.42	5.63	93.6	2.39
CC_MIX_Burkholderiaceae	Noviherbaspirillum	4927372	289	25856	62.28	95.77	15.49	93.52	4.3
CC_MAG_Emticicia_o	Emticicia	6873062	340	32339	36.14	80.28	8.45	93.38	3.45
CC_MAG_Pseudoxanthomonas	Lysobacter	3621813	422	12254	63.72	95.77	4.23	92.85	7.43
MB_MAG_Microtrichales	Ilumatobacter	2607163	319	9872	67.06	95.77	2.82	92.64	3.59
MB_MAG_035	Unknown	5555582	380	21768	61.83	95.77	5.63	92.18	2.08
CC_MAG_044	Planctomyces	6289724	452	20527	58.72	94.37	7.04	92.13	3.65
CC_MAG_Massilia_e	Massilia	4954318	557	11658	64.35	94.37	0.00	91.81	3.13
CC_mag_Massilia	Massilia	5479085	228	43741	62.36	74.65	7.04	91.79	6.26
MB_mag_Rhodoferax_825	Rhodoferax	3195297	129	35496	60.99	78.87	0.00	91.73	1.62
MB_mag_Thermomonas	Thermomonas	2699415	59	83838	62.66	78.87	2.82	91.68	1.54
MB_MAG_051	Bdellovibrio	3850901	22	295428	52.34	92.96	1.41	91.59	1.79
MX_MAG_ARCH_Methanosphaerula	Methanosphaerula	1920527	254	10438	58.13	93.42	6.58	91.48	1.63
MB_MAG_Rathayibacter	Rathayibacter	3744026	74	86938	71.70	69.01	2.82	91.39	3.89
MB_MAG_Sphingomonas	Sphingomonas	3543038	303	16646	65.13	88.73	8.45	90.82	5.46
CC_MAG_AVCC01	Noviherbaspirillum	3225531	322	13377	56.16	98.59	1.41	90.81	2.88
CC_MAG_Methylotenera	Methylotenera	2450063	237	14460	41.66	92.96	2.82	90.6	3.59
MB_MAG_062	Candidatus Protochlamydia	1527864	10	366162	44.28	90.14	2.82	90.37	0.68
CC_MAG_Pedobacter_i	Pedobacter	3901671	687	6933	37.16	83.10	9.86	90.33	7.44
CC_mag_Methylotenera_v	Methylotenera	2344679	236	13140	42.47	74.65	1.41	89.96	1.5
MB_MAG_Planktophila	Candidatus Planktophila	1810513	48	59808	47.65	94.37	0.00	89.84	0
CC_MAG_UBA4096	Bacteriovorax	3035644	116	48894	42.99	98.59	4.23	89.43	1.79
MX_MAG_UBA6139	Micavibrio	2258108	89	36391	52.93	100.00	0.00	89.24	1.34
CC_MAG_Ga0077559	Sphingopyxis	2647559	420	7832	56.87	88.73	0.00	89.05	3.53
CC_MAG_Paeniglutamicibacter	Glutamicibacter	4376895	434	12630	64.66	88.73	0.00	88.21	4.74
MB_MAG_Bacteriovorax	Bacteriovorax	3410402	204	25869	37.74	97.18	1.41	87.55	4.02
CC_MAG_Rhodoferax	Rhodoferax	3830090	723	6566	60.01	83.10	7.04	87.2	7.12
MB_MAG_2-12-FULL-35-15	Unknown	3406027	380	11687	38.37	84.51	0.00	87.04	1.27
CC_MAG_Sphingopyxis_2	Sphingopyxis	4111480	497	11188	64.34	83.10	5.63	86.41	6.25
CC_MAG_UBA4096_s67	Bacteriovorax	3950664	368	15117	41.55	95.77	5.63	86.38	4.37
CC_mag_Chlorobium_p	Pelodictyon	2224110	379	7577	48.05	77.46	1.41	86.22	2.75
MB_MAG_Nitrosospira	Nitrosospira	1776121	198	10752	51.25	94.37	2.82	86.16	2.11
CC_MAG_023	Unknown	8138496	1227	7984	72.05	97.18	5.63	85.81	3.57
CC_MAG_Micavibrionaceae_UBA6139	Micavibrio	2247450	270	11967	54.90	95.77	2.82	85.51	1.01
CC_MAG_Demequina_lutea	Unknown	2659767	451	7170	65.88	84.51	16.90	85.4	7.64
CC_MAG_Nitrosospira	Nitrosospira	2568230	490	5946	52.75	80.28	5.63	85.27	8.94
CC_MAG_Bacteriovorax_s	Bacteriovorax	3316357	488	8566	38.83	81.69	2.82	84.93	4.07
MB_mag_Simplicispira	Simplicispira	3144367	224	19976	64.38	76.06	0.00	83.87	0.77
CC_MAG_Acidimicrobiia	Ilumatobacter	4300832	713	8014	67.52	85.92	5.63	83.02	8.55
CC_MAG_061	Unknown	3695421	762	5575	59.87	90.14	2.82	82.26	4.3
CC_MAG_C7867-001_2	Candidatus Campbellbacteria bacterium GW2011_OD1_34_28	786490	24	77072	57.49	83.10	0.00	82.18	0

Bin	Taxon (Kaiju estimate)	Total length	Num contigs	N50	GC content	Completion (%)	Redundancy (%)	CM Completeness	CM Contamination
MB_MAG_DTU024	Unknown	1792322	223	10828	56.49	88.73	2.82	81.99	2.65
CC_MAG_Anaerolineaceae	Brevefilum	2160356	458	5311	51.00	81.69	5.63	81.82	7.56
CC_MAG_Devosia_14	Devosia	2966599	631	5324	62.07	71.83	4.23	81.37	4.41
CC_mag_T78	Brevefilum	2379041	440	6296	49.94	78.87	4.23	81.15	5
CC_MAG_Lacunisphaera_MIX	Lacunisphaera	4502698	1132	4180	66.31	90.14	16.90	80.93	8.19
CC_MAG_UBA6139	Micavibrio	2043176	357	6721	55.04	90.14	2.82	80.36	1.88
MB_mag_Burkholderiaceae	Rhodoferax	3355550	252	19993	59.58	73.24	5.63	80.16	5.49
MB_mag_Rhodoferax_ferrireducens	Rhodoferax	4385890	201	33231	60.95	74.65	4.23	79.74	9.02
MX_mag_Ga0077559	Sphingorhabdus	2002653	365	6284	55.95	78.87	1.41	79.26	3.85
MB_MAG_Microbacterium	Microbacterium	3130372	416	8640	68.02	57.75	4.23	78.84	9.51
CC_mag_UBA2259	Unknown	786234	18	100936	33.12	77.46	1.41	78.13	0
CC_mag_Taibaiella_3	Unknown	4191268	1044	4291	43.67	67.61	4.23	78	9.52
CC_MAG_Methylobacter_tundripaludum	Methylovulum	2969009	672	4942	47.45	84.51	9.86	77.87	1.07
MX_MAG_Micavibrionales_UBA2020	Micavibrio	2325853	389	6954	49.09	94.37	8.45	77.62	3.57
CC_MAG_092	Candidatus Campbellbacteria bacterium GW2011_OD1_34_28	1016293	9	154946	37.69	80.28	2.82	76.22	0
CC_mag_Taibaiella	Unknown	4393797	803	6472	42.34	81.69	2.82	76.07	2.71
MX_MAG_Flavobacterium-6	Flavobacterium	2625055	60	61210	34.33	63.38	0.00	75.98	5.27
MB_MAG_Gemmatimonas	Gemmatimonas	3002341	602	5554	65.72	88.73	0.00	75.82	1.1
CC_MAG_Chthoniobacter_f	Unknown	4874552	1070	4992	61.41	92.96	4.23	75.72	1.01
MB_mag_110	Candidatus Beckwithbacteria bacterium GW2011_GWC1_49_16	869644	87	12429	33.14	77.46	1.41	75.24	1.72
MB_mag_118	candidate division SR1 bacterium RAAC1_SR1_1	1240642	80	20658	32.17	74.65	4.23	75.13	1.72
CC_mag_Rhodococcus_895_1	Rhodococcus	6901278	838	11143	61.39	52.11	7.04	74.83	3.45
MX_bin_Methanosarcina_MX	Methanosarcina	1948321	472	4753	42.03	67.11	2.63	74.46	2.48
CC_MAG_Hydrogenophaga	Hydrogenophaga	3735540	933	4183	65.77	81.69	5.63	73.61	9.31
CC_mag_Actinotalea	Cellulomonas	2327837	712	3242	71.79	77.46	5.63	73.25	2.29
MX_MAG_JG1575	Unknown	2150409	382	6672	47.76	81.69	1.41	73.01	1.86
CC_bin_Hydrogenophaga	Hydrogenophaga	4330368	902	5593	65.50	66.20	8.45	72.94	8.63
Bin_Bin_162_sub	Caldisericum	1422177	247	6994	57.25	66.20	5.63	72.81	6.57
Bin_METABAT__213	Unknown	3717713	676	5933	38.35	63.38	0.00	72.31	2.49
Bin_Bin_177_sub_6	Brevefilum	2027050	503	4236	49.78	63.38	7.04	71.99	8.64
MX_MAG_Archangium_g	Unknown	6300226	1491	4631	66.26	81.69	8.45	71.36	1.14
CC_bin_UBA4822	Caldisericum	1680086	313	5874	56.60	69.01	8.45	71.17	4.63
CC_bin_Polaromonas	Polaromonas	3506572	961	3654	62.60	57.75	15.49	70.69	9.25
CC_mag_Mucilaginibacter	Mucilaginibacter	2532027	713	3672	42.44	78.87	2.82	70.19	1.1
MB_MAG_075	Candidatus Campbellbacteria bacterium GW2011_OD1_34_28	883026	10	122784	43.04	85.92	0.00	70.04	1.12

7.3.5 Phylogenomics

Using GTDB-Tk, the MAGs were classified taxonomically into 13 different bacterial phyla and one archaeal phylum (Figure 7-5 and Table 7-6). The two archaeal MAGs belonged to the Halobacterota. The phylum with the largest MAG membership was the Proteobacteria, with 50 MAGs in total, 30 of which belonged to the Gammaproteobacteria, and 20 belonging to the Alphaproteobacteria. The second largest phylum was the Bacteroidota (20), followed by the Actinobacteria (15) and the Bdellovibrionota (7). The Verrucomicrobiae and Patesibacteria had six MAGs each, the Plantomycetota had four, the Chloroflexota had three and the Myxococcota, Caldisericota, Firmicutes_A each had two MAGs. There was a single MAG in each of the Gemmatimonadota and Verrucomicrobiota_A. The majority of the MAGs represent new species, however 10 of the MAGs were identified to species level using FastANI (Table 7-5).

Table 7-5 Table of MAGS classified to species level using FastANI

User Genome	FastANI Reference	FastANI Reference Radius	FastANI Taxonomy	FastANI ANI	FastANI Alignment Fraction
MB_MAG_Sphingomonas_p	GCF_000739895.2	95	*Sphingomonas paucimobilis*	99.89	0.96
MB_mag_Caulobacter	GCF_002737765.1	95	*Caulobacter sp002737765*	97.46	0.9
MX_MAG_003_Paracoccus	GCF_000787695.1	95	*Paracoccus sp000787695*	97.02	0.83
MX_MAG_Polynucleobacter	GCF_002206635.1	95	*Polynucleobacter aenigmaticus*	98.22	0.82
CC_bin_Polaromonas	GCF_000709345.1	95	*Polaromonas glacialis*	95.02	0.8
MB_MAG_Rathayibacter	GCF_003044275.1	95	*Rathayibacter caricis*	98.3	0.92
MB_MAG_Rhodococcus_f	GCF_001894785.1	95	*Rhodococcus fascians*	97.69	0.92
CC_MAG_Pedobacter_ruber	GCF_900103545.1	95	*Pedobacter_A ruber*	97.11	0.9
MX_MAG_Flavobacterium-6	GCA_003312425.1	95	*Flavobacterium psychrolimnae*	95.01	0.87
MX_bin_Methanosarcina_MX	GCA_001714685.2	95	*Methanosarcina sp001714685*	96.8	0.89

A phylogenomic tree of Ice-Caves MAGS (Figure 7-5) was created by using Fast Tree on a Muscle alignment of 71 single copy core genes. The clades on the phylogenomic tree agree with the taxonomic assignment of the MAGs by GTDB-Tk.

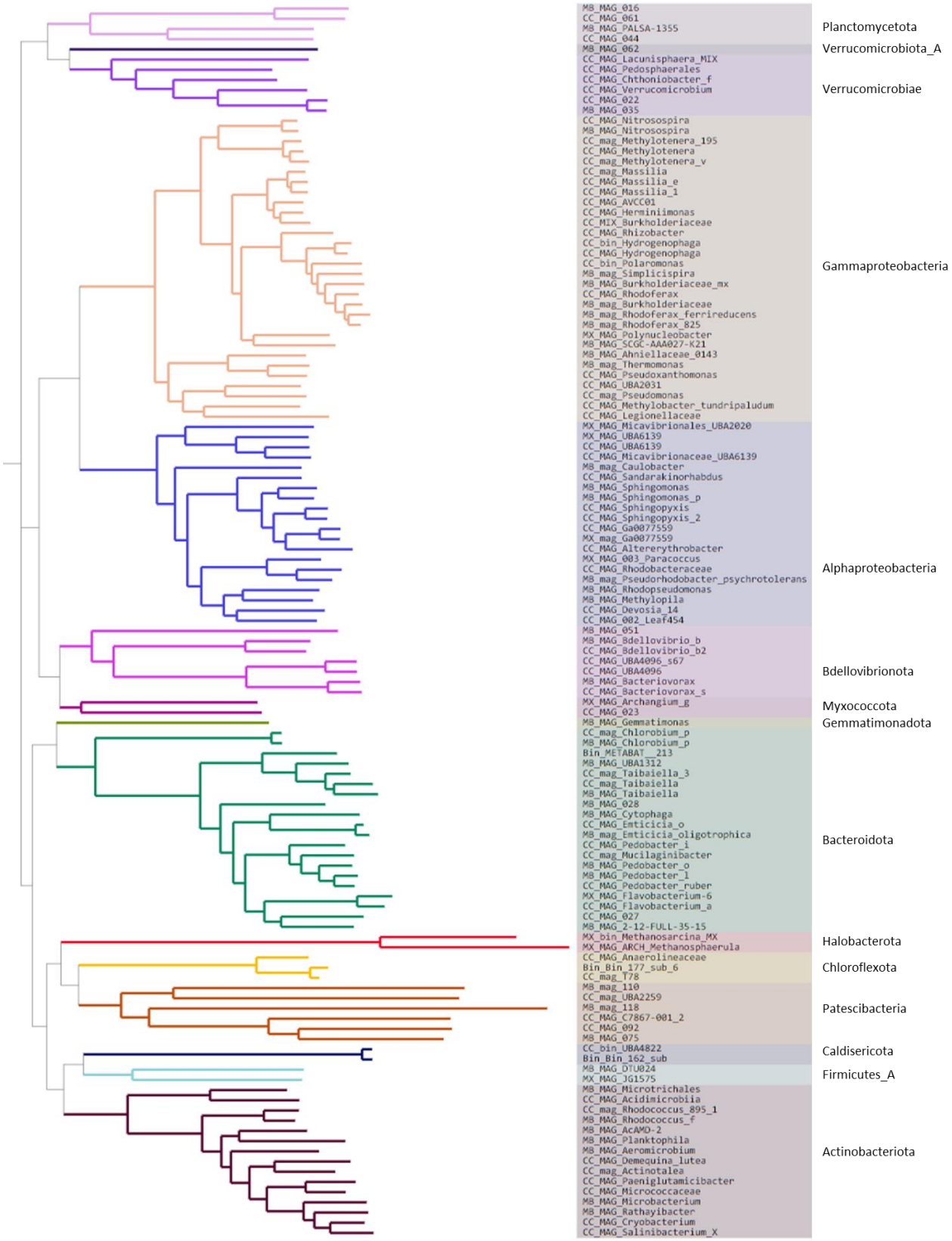

Figure 7-5 Phylogenomic tree of Ice-Caves MAGS. Fast Tree of Muscle alignment of 71 single copy core genes.

Table 7-6 GTDB-Yk classification of Ice Cave MAGS

phylum	Class	Genus	MAG	Closest Placement Reference	Closest Placement Taxonomy	Closest Placement ANI	Close. Place. AF	Class. Method	Note	AA Percent	RED Value
			Archaea								
Halobacterota	Methanomicrobia	Methanosphaerula	MX_MAG_ARCH_Methanosphaerula	GCF_000021965.1	*Methanosphaerula palustris*	86.34	0.87	P	N: RED	91.02	0.96
	Methanosarcinia	Methanosarcina	MX_bin_Methanosarcina_MX	GCA_001714685.2	*Methanosarcina* sp001714685	96.8	0.89	ANI/P	F: T+ANI	68.77	
			Bacteria								
Actinobacteriota	Acidimicrobiia	UBA11034	CC_MAG_Acidimicrobiia					P	N: RED	77.82	0.88
		f_UBA8139	MB_MAG_Microtrichales					P	N: RED	81.41	0.77
	Actinobacteria	Actinotalea	CC_mag_Actinotalea	GCA_000767215.1	*Actinotalea fermentans*	80.22	0.46	P	C: TOP	66.9	0.92
		Demequina	CC_MAG_Demequina_lutea	GCF_000975075.1	*Demequina lutea_B*	82.62	0.53	P	C: TOP	80.69	0.99
		Cryobacterium_A	CC_MAG_Cryobacterium	GCF_003065485.1	*Cryobacterium_A* sp003065485	79.83	0.47	P	C: TOP	87.3	0.97
		Microbacterium	MB_MAG_Microbacterium	GCF_002024885.1	*Microbacterium foliorum_A*	91.58	0.87	P	C: TOP	64.05	1.00
		Rathayibacter	MB_MAG_Rathayibacter	GCF_003044275.1	*Rathayibacter caricis*	98.3	0.92	ANI/P	F: T+ANI	72.8	
		Salinibacterium	CC_MAG_Salinibacterium_X	GCF_900230175.1	*Salinibacterium xinjiangense*	78.87	0.34	P	C: TOP	88.93	0.97
		Paeniglutamicibacter	CC_MAG_Paeniglutamicibacter	GCF_900010755.1	*Paeniglutamicibacter antarcticus*	83.91	0.61	P	C: TOP	76.59	0.98
		Pseudarthrobacter_A	CC_MAG_Micrococcaceae					P	C: TOP	95.06	0.99
		Rhodococcus	CC_mag_Rhodococcus_895_1	GCF_002245895.1	*Rhodococcus* sp002245895	94.44	0.78	P	C: TOP	65.52	1.00
		Rhodococcus	MB_MAG_Rhodococcus_f	GCF_001894785.1	*Rhodococcus fascians*	97.69	0.92	ANI/P	F: T+ANI	97.46	
		Planktophila	MB_MAG_Planktophila					P	C: TOP	94.66	0.94
		f_UBA12327	MB_MAG_AcAMD-2					P	N: RED	92.3	0.79
		Aeromicrobium	MB_MAG_Aeromicrobium					P	C: TOP	96.87	0.93
Bacteroidota	Bacteroidia	o_AKYH767	CC_MAG_027					P	N: RED	96.39	0.67
		2-12-FULL-35-15	MB_MAG_2-12-FULL-35-15					P	C: TOP	81.51	0.93
		Ferruginibacter	Bin_METABAT__213					P	C: TOP	61.09	0.92
		Taibaiella_B	CC_mag_Taibaiella					P	C: TOP	71.35	0.92
		Taibaiella_B	MB_MAG_Taibaiella					P	C: TOP	97.38	0.92
		Taibaiella_B	CC_mag_Taibaiella_3					P	C: TOP	63.97	0.92
		UBA1312	MB_MAG_UBA1312	GCA_002482815.1	*UBA1312* sp002482815	78.54	0.25	P	C: TOP	97.56	0.97
		Cytophaga	MB_MAG_Cytophaga	GCF_000379725.1	*Cytophaga aurantiaca*	79.99	0.44	P	C: TOP	97.7	0.98
		Emticicia	CC_MAG_Emticicia_o	GCA_000263195.1	*Emticicia oligotrophica*	78.36	0.37	P	C: TOP	80.65	0.96
		Emticicia	MB_mag_Emticicia_oligotrophica	GCA_000263195.1	*Emticicia oligotrophica*	77.69	0.33	P	C: TOP	83.1	0.96

Phylum	Class	Genus	MAG	Closest Placement Reference	Closest Placement Taxonomy	Closest Placement ANI	Close. Place. AF	Class. Method	Note	AA Percent	RED Value
Bacteroidota	Bacteroidia	Flavobacterium	CC_MAG_Flavobacterium_a					P	C: TOP	95.69	0.95
		Flavobacterium	MX_MAG_Flavobacterium-6	GCA_003312425.1	*Flavobacterium psychrolimnae*	95.01	0.87	ANI/P	F: T+ANI	64.78	
		f_UBA8524	MB_MAG_028					P	N: RED	96.73	0.83
		f_Sphingobacteriaceae	CC_mag_Mucilaginibacter					P	N: RED	71.07	0.80
		Pedobacter	CC_MAG_Pedobacter_i	GCF_900113525.1	*Pedobacter insulae*	79.41	0.43	P	C: TOP	77.14	0.98
		Pedobacter_A	MB_MAG_Pedobacter_l	GCF_900168015.1	*Pedobacter_A luteus*	78.18	0.22	P	C: TOP	96.17	0.95
		Pedobacter_A	MB_MAG_Pedobacter_o					P	C: TOP	90.99	0.91
		Pedobacter_A	CC_MAG_Pedobacter_ruber	GCF_900103545.1	*Pedobacter_A ruber*	97.11	0.9	ANI/P	F: T+ANI	90	
	Chlorobia	Chlorobium	CC_mag_Chlorobium_p	GCF_000020645.1	*Chlorobium phaeoclathratiforme*	81.26	0.59	P	C: TOP	75.75	0.96
		Chlorobium	MB_MAG_Chlorobium_p	GCF_000020645.1	*Chlorobium phaeoclathratiforme*	82.99	0.65	P	C: TOP	98.12	0.97
Bdellovibrionota	Bacteriovoracia	Bacteriovorax	MB_MAG_Bacteriovorax					P	C: TOP	87.7	0.95
		Bacteriovorax	CC_MAG_Bacteriovorax_s	GCA_002428265.1	*Bacteriovorax* sp002428265	79.08	0.42	P	C: TOP	76.41	0.98
		UBA4096	CC_MAG_UBA4096					P	C: TOP	93.47	0.93
		UBA4096	CC_MAG_UBA4096_s67					P	C: TOP	86.53	0.95
	Bdellovibrionia	f_Bdellovibrionaceae	MB_MAG_Bdellovibrio_b					P	N: RED	97.8	0.86
		Bdellovibrio	CC_MAG_Bdellovibrio_b2					P	C: TOP	91.77	0.92
	UBA2394	f_UBA2428	MB_MAG_051					P	N: RED	89.84	0.79
Caldisericota	Caldisericia	UBA4822	Bin_Bin_162_sub					P	C: TOP	65.22	0.98
		UBA4822	CC_bin_UBA4822					P	C: TOP	65.73	0.97
Chloroflexota	Anaerolineae	T78	Bin_Bin_177_sub_6					P	C: TOP	66.61	0.91
		T78	CC_MAG_Anaerolineaceae					P	C: TOP	77.92	0.91
		T78	CC_mag_T78					P	C: TOP	81.65	0.91
Firmicutes_A	Clostridia	UBA1038	MB_MAG_DTU024					P	N: RED	84.48	0.91
		JG1575	MX_MAG_JG1575					P	N: RED	78.15	0.91
Gemmatimonadota	Gemmatimonadetes	Gemmatimonas	MB_MAG_Gemmatimonas	GCA_002737115.1	*Gemmatimonas* sp002737115	84.56	0.49	P	C: TOP	70.97	0.99
Myxococcota	Myxococcia	Archangium_A	MX_MAG_Archangium_g	GCA_003243425.1	*Archangium_A gephyra*	79.92	0.53	P	N: RED	70.36	0.94
	UBA796	o_UBA796	CC_MAG_023					P	N: RED	93.45	0.64
Patescibacteria	Dojkabacteria	UBA2259	CC_mag_UBA2259	GCA_002419125.1	UBA2259 sp002419125	83.8	0.77	P	C: TOP	71.17	0.99
	Gracilibacteria	f_X112	MB_mag_118					P	C: TOP	58.15	0.79
	Microgenomatia	UBA1435	MB_mag_110					P	N: RED	58.04	0.87
		f_UBA11359	CC_MAG_092					P	C: TOP	67.32	0.80
	Paceibacteria	C7867-001	CC_MAG_C7867-001_2	GCA_001189075.1	C7867-001 sp001189075	78.84	0.4	P	C: TOP	68.17	0.96
		f_UBA9973	MB_MAG_075					P	C: TOP	70.02	0.79

Phylum	Class	Genus	MAG	Closest Placement Reference	Closest Placement Taxonomy	Closest Placement ANI	Close. Pl.ace AF	Classification Method	Note	AA Percent	RED Value
Planctomycetota	Planctomycetes	o_Pirellulales	MB_MAG_PALSA-1355					P	N: RED	85.14	0.69
		Planctomyces_A	CC_MAG_044					P	N: RED	86.09	0.88
	UBA11346	f_UBA11346	CC_MAG_061					P	N: RED	78.33	0.84
		BOG-1363	MB_MAG_016	GCA_003136555.1	*BOG-1363* sp003136555	77.11	0.18	P	N: RED	89.48	0.86
Proteobacteria	Alphaproteobacteria	Caulobacter	MB_mag_Caulobacter	GCF_002737765.1	*Caulobacter* sp002737765	97.46	0.9	ANI/P	F: T+ANI	81.65	
		f_Micavibrionaceae	MX_MAG_UBA6139					P	C: TOP	87.68	0.88
		UBA6139	CC_MAG_Micavibrionaceae_UBA6139					P	N: RED	87.24	0.94
		UBA6139	CC_MAG_UBA6139	GCA_002423285.1	UBA6139 sp002423285	78.22	0.46	P	N: RED	76.61	0.97
		UBA2020	MX_MAG_Micavibrionales_UBA2020					P	C: TOP	82.9	0.90
		Devosia	CC_MAG_Devosia_14	GCF_000971275.1	*Devosia psychrophila*	84.91	0.75	P	C: TOP	61.01	0.99
		Methylopila	MB_MAG_Methylopila	GCF_000384475.1	*Methylopila* sp000384475	82.5	0.68	P	C: TOP	85.24	0.97
		Leaf454	CC_MAG_002_Leaf454					P	N: RED	97.24	0.95
		Rhodopseudomonas	MB_MAG_Rhodopseudomonas	GCF_000014825.1	*Rhodopseudomonas palustris_B*	91.74	0.74	P	C: TOP	96.94	0.99
		Paracoccus	MX_MAG_003_Paracoccus	GCF_000787695.1	*Paracoccus* sp000787695	97.02	0.83	ANI/P	F: T+ANI	97.86	
		Pseudorhodobacter_A	CC_MAG_Rhodobacteraceae					P	N: RED	84.42	0.97
		Pseudorhodobacter_A	MB_mag_Pseudorhodobacter_psychrotolerans	GCF_001294535.1	*Pseudorhodobacter_A psychrotolerans*	89.46	0.85	P	C: TOP	86.19	1.00
		Altererythrobacter_B	CC_MAG_Altererythrobacter					P	C: TOP	88.61	0.98
		Ga0077559	CC_MAG_Ga0077559	GCA_001464315.1	Ga0077559 sp001464315	79.1	0.43	P	C: TOP	84.37	0.99
		Ga0077559	MX_mag_Ga0077559	GCA_002299895.1	Ga0077559 sp002299895	80.69	0.65	P	C: TOP	75.58	0.99
		Sandarakinorhabdus	CC_MAG_Sandarakinorhabdus	GCA_003241875.1	*Sandarakinorhabdus* sp003241875	82.13	0.58	P	C: TOP	94.25	0.97
		Sphingomonas	MB_MAG_Sphingomonas	GCF_001591025.1	Sphingomonas soli	83.51	0.65	P	C: TOP	79.33	0.98
		Sphingomonas	MB_MAG_Sphingomonas_p	GCF_000739895.2	Sphingomonas paucimobilis	99.89	0.96	ANI/P	F: T+ANI	95.48	
		Sphingopyxis	CC_MAG_Sphingopyxis					P	N: RED	83.29	0.94
		Sphingopyxis	CC_MAG_Sphingopyxis_2					P	C: TOP	72.36	0.99
Proteobacteria	Gammaproteobacteria	AVCC01	CC_MAG_AVCC01	GCF_000622895.1	AVCC01 sp000622895	85.02	0.63	P	N: RED	91.63	0.97
		Herminiimonas	CC_MAG_Herminiimonas					P	C: TOP	92.4	0.98
		Herminiimonas	CC_MIX_Burkholderiaceae					P	C: TOP	83.95	0.94
		Hydrogenophaga	CC_bin_Hydrogenophaga	GCF_001571225.1	Hydrogenophaga palleronii	83.11	0.57	P	C: TOP	55.73	0.99
		Hydrogenophaga	CC_MAG_Hydrogenophaga					P	C: TOP	68.85	0.99
		Massilia	CC_MAG_Massilia_1					P	N: RED	87.84	0.96
		Massilia_B	CC_mag_Massilia	GCF_900129765.1	Massilia_B sp900129765	81.72	0.53	P	C: TOP	70.99	0.98
		Massilia_B	CC_MAG_Massilia_e	GCF_002760655.1	Massilia_B eurypsychrophila	88.13	0.79	P	C: TOP	88.53	0.99
		Polaromonas	MB_MAG_Burkholderiaceae_mx					P	N: RED	90.48	0.95
		Polaromonas	CC_bin_Polaromonas	GCF_000709345.1	Polaromonas glacialis	95.02	0.8	ANI/P	F: T+ANI	64.01	
		Polynucleobacter	MX_MAG_Polynucleobacter	GCF_002206635.1	Polynucleobacter aenigmaticus	98.22	0.82	ANI/P	F: T+ANI	98.77	

Phylum	Class	Genus	MAG	Closest Placement Reference	Closest Placement Taxonomy	Close. Place. ANI	Close. Place. AF:	Class Method	Note	AA Percent	RED Value
Proteobacteria	Gammaproteobacteria	Rhizobacter	CC_MAG_Rhizobacter	GCF_001425865.1	Rhizobacter sp001425865	86.28	0.77	P	C: TOP	87.16	0.98
		Rhodoferax	CC_MAG_Rhodoferax	GCA_001770935.1	Rhodoferax sp001770935	81.19	0.54	P	C: TOP	75.38	0.98
		Rhodoferax	MB_mag_Burkholderiaceae	GCA_002413825.1	Rhodoferax sp002413825	80.24	0.49	P	C: TOP	66.23	0.98
		Rhodoferax	MB_mag_Rhodoferax_825	GCA_002422455.1	Rhodoferax sp002422455	83.07	0.65	P	C: TOP	83.53	0.98
		Rhodoferax	MB_mag_Rhodoferax_ferrireducens	GCF_000013605.1	Rhodoferax ferrireducens	83.52	0.6	P	C: TOP	70.81	0.98
		SCGC-AAA027-K21	MB_MAG_SCGC-AAA027-K21					P	C: TOP	87.58	0.96
		Simplicispira_A	MB_mag_Simplicispira	GCF_003008595.1	Simplicispira_A suum	87.14	0.84	P	C: TOP	67.18	0.99
		Methylotenera	CC_MAG_Methylotenera	GCA_002429455.1	Methylotenera sp002429455	79.2	0.39	P	C: TOP	86.25	0.97
		Methylotenera	CC_mag_Methylotenera_195	GCA_002429455.1	Methylotenera sp002429455	78.1	0.31	P	C: TOP	87.66	0.97
		Methylotenera	CC_mag_Methylotenera_v	GCF_000093025.1	Methylotenera versatilis	78.99	0.48	P	C: TOP	85.52	0.98
		Nitrosospira	CC_MAG_Nitrosospira					P	C: TOP	78.27	0.96
		Nitrosospira	MB_MAG_Nitrosospira	GCF_900102495.1	Nitrosospira sp900102495	79.39	0.65	P	C: TOP	89.46	0.92
		Legionella_A	CC_MAG_Legionellaceae					P	C: TOP	97.12	0.90
		Methylobacter_A	CC_MAG_Methylobacter_tundripaludum	GCF_000190755.2	Methylobacter_A tundripaludum	84.34	0.72	P	C: TOP	75.73	0.98
		f_Moraxellaceae	CC_MAG_UBA2031					P	N: RED	98.63	0.88
		Pseudomonas_E	CC_mag_Pseudomonas					P	C: TOP	88.23	0.98
		0-14-3-00-62-12	MB_MAG_Ahniellaceae_0143	GCA_002785585.1	0-14-3-00-62-12 sp002785585	77.37	0.29	P	N: RED	92.32	0.92
		Pseudoxanthomonas_A	CC_MAG_Pseudoxanthomonas	GCF_900104085.1	Pseudoxanthomonas_A sp900104085	83.77	0.72	P	C: TOP	90.18	0.99
		Thermomonas	MB_mag_Thermomonas					P	N: RED	79.19	0.95
Verrucomicrobiota	Verrucomicrobiae	Chthoniobacter	CC_MAG_Chthoniobacter_f					P	N: RED	67.5	0.86
		Lacunisphaera	CC_MAG_Lacunisphaera_MIX					P	C: TOP	65.83	0.94
		f_Palsa-1400	CC_MAG_Pedosphaerales					P	N: RED	90.75	0.80
		o_Verrucomicrobiales	CC_MAG_022					P	N: RED	91.01	0.72
		o_Verrucomicrobiales	MB_MAG_035					P	N: RED	85.28	0.72
		Verrucomicrobium	CC_MAG_Verrucomicrobium					P	N: RED	91.17	0.89
Verrucomicrobiota_A	Chlamydiia	o_Parachlamydiales	MB_MAG_062					P	C: TOP	83.95	0.60

P: Placement

C: TOP: taxonomic classification fully defined by topology

N: RED: taxonomic novelty determined using RED

F: T+ANI: topological placement and ANI have congruent species assignments

Column Headings: Close. Place. ANI: Closest Placement ANI; **Close. Place.AF:** Closest Placement Alignment Fraction; **Class. Method,** Classification Method

7.3.6 Spatial distribution of MAGs throughout the Ice-Cave

The spatial distribution of the MAGs is plotted using a MAG-centric (Appendix Figure G-2) and sample-centric views as described in Section 4.2.9. One of the striking observations of this Ice-Cave metagenome is that many of the community members are predominantly present at a single site. The cave locations with the fewest number of MAGs and the least coverage were the two oldest sites, Ice_cave_7_2000_14 (ice deposited approximately 1500 years ago) and Ice_cave_6_1500_18 (ice deposited approximately 1200 years ago). The oldest site (Ice_cave_7_2000_14) was dominated by CC_MAG_Hydrogenophaga and CC_MAG_Massilia_e, while Ice_cave_6_1500_18 was dominated by MX_MAG_Flavobacterium-6 and CC_MAG_002_Leaf454. Although a MAG may be site-specific, there are several genera that have MAG representatives at different sites.

Site IL_13 has several phyla that are unique to that site. Both Archaeal MAGs occur at site 1L_13, as do the three Patescibacteria MAGs. Two Chlorobium MAGs are also found solely at this site. Site 900_I is particularly rich in Actinobacteria compared to other sites.

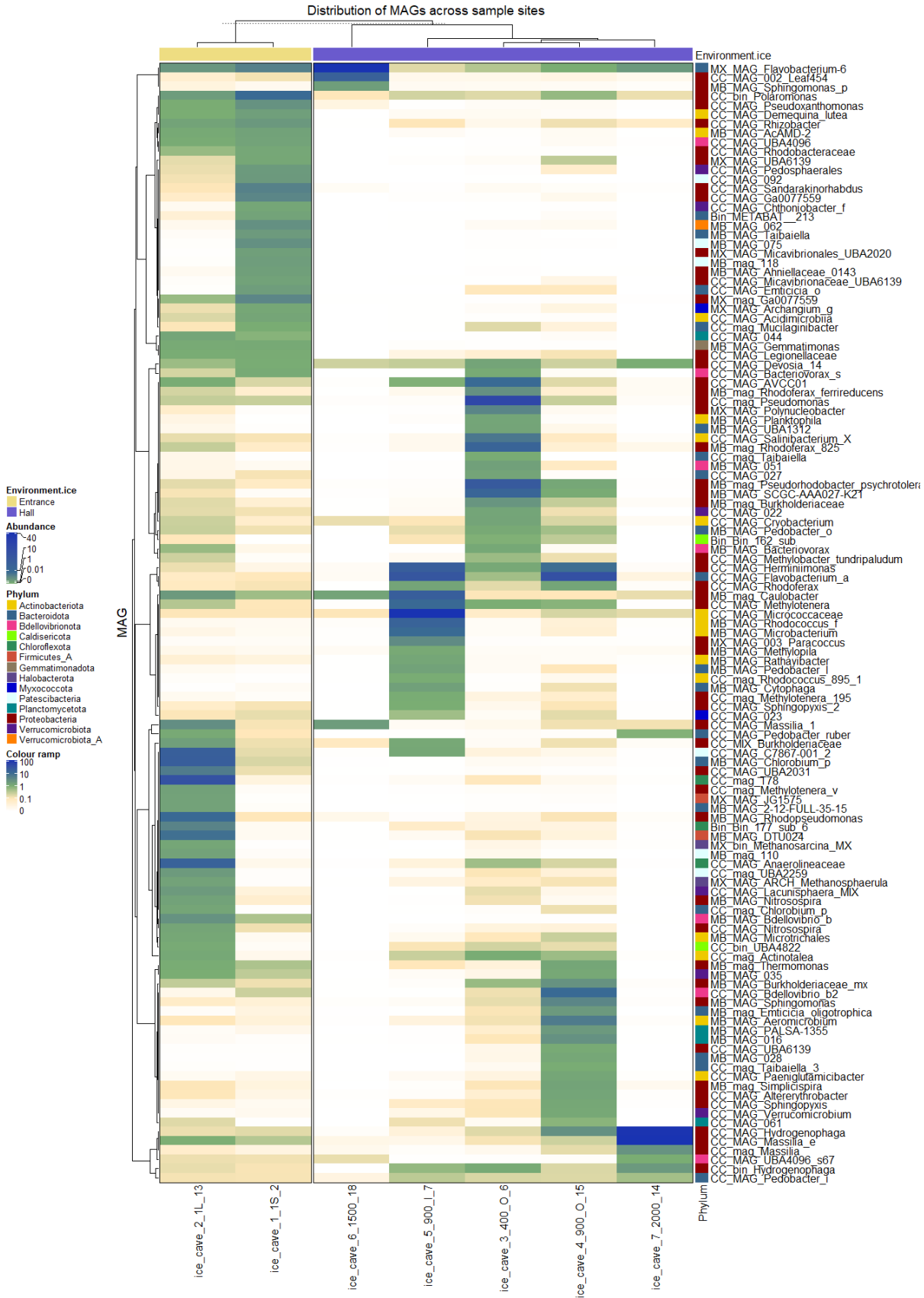

Figure 7-6 Abundance and spatial distribution of community members in the Scărișoara Ice Cave.

7.3.7 Biogeochemical cycles

The Scărișoara ice-cave is an oligotrophic environment. It is freezing, receives very little light for photosynthesis and so much of its metabolism is chemolithotrophic.

7.3.7.1 Carbon cycling

Out of 122 MAGs, there were only eight that had RubisCO Form 1 genes involved in carbon fixation, and all of these were Proteobacterial MAGs. The two MAGs belonging to the Phylum Bacteroidetes, order Chlorobiales, were found in Ice_Cave_2_1L_13 had the genes acetate citrate lyase genes *aclA* and *aclB*, which enables carbon fixation in anaerobic conditions.

7.3.7.2 Nitrogen cycling

There were only four MAGs capable of nitrogen fixation via one or more of nifH/D/K. Three of these MAGs (MB_MAG_Rhodopseudomonas, MB_MAG_Chlorobium_p and MX_MAG_ARCH_Methanosphaerula) were found predominantly at site IL. The Gammaproteobacterial MB_mag_Rhodoferax_ferrireducens from site 400-O also had the genes for nifD/H. The napA/B and narG/H genes are involved in denitrification and dissimilatory nitrate reduction. The napA/B and narG/H genes encode genes that reduce nitrate (NO3-) to nitrite (NO2-). Both napA/B were present in a Planctomycetales MAG (CC_MAG_044), a single Alphaproteobacterial MAG (MB_MAG_Rhodopseudomonas) and three Gammaproteobacterial MAGs (CC_MAG_Massilia_1, CC_MAG_Rhodoferax and MB_mag_Burkholderiaceae). The narG/H genes were far more abundant, and found in four Actinobacterial MAGs, four Alphaproteobacterial MAGs and 18 Gammaproteobacterial MAGs. MAGs CC_MAG_Massilia_1 and CC_MAG_Rhodoferax had all four genes for napA/B and narG/H. NirB/D genes were detected in eight Actinobacterial MAGs, five Bacteroidota MAGs (including all three Cytophagales MAGs), three Plantomycetes, eight Alphaproteobacteria and 21 Gammaproteobacterial MAGs. The NorB/C genes encode a respiratory nitric oxide reductase that reduces NO to N_2O.

7.3.7.3 Sulfur

The sdo gene was the most common gene across all the phyla. Sulfur oxidation via the Sulfur Oxidising (soxBCY) pathways was highly prevalent in the Gammaproteobacteria, and specifically, within the order Burkholderiales, where 13/23 had at least one sox gene, and 10 had all three of soxBCY. There were two Rhizobiales MAGs in the Alphaproteobacteria with at least one sox gene and a single sox gene in MB_MAG_Gemmatimonas.

7.3.7.4 Oxygen cycling

The coxAB genes were present in 13 Actinobacterial MAGs, none of the Bacteroidetes and all but one of the Proteobacteria. The genes for the CcoNOP complex was ubiquitous across Bacteroidetota (15/16), the Alphaproteobacteria (11/20), Gammaproteobacteria (27/31) Bdellovibrionota (7/7), Planctomycetota (2/4), Verrucomicrobiota (5/6) the Gemmatimonadota (1/1), Myxococcota (2/2), but completely absent from the Actinobacteria, Caldisericota, Chloroflexota, Firmicutes_A, Patescibacteria and Verrucomicrobiota_A. Whilst the Actinobacteria tend to have all three of cyoE, cydA and cydB, most of the Bacteroidetes only have cyoE, except for MX_mag_Flavobacterium_6 and the two Chlorobium MAGs which only have cydA and cydB.

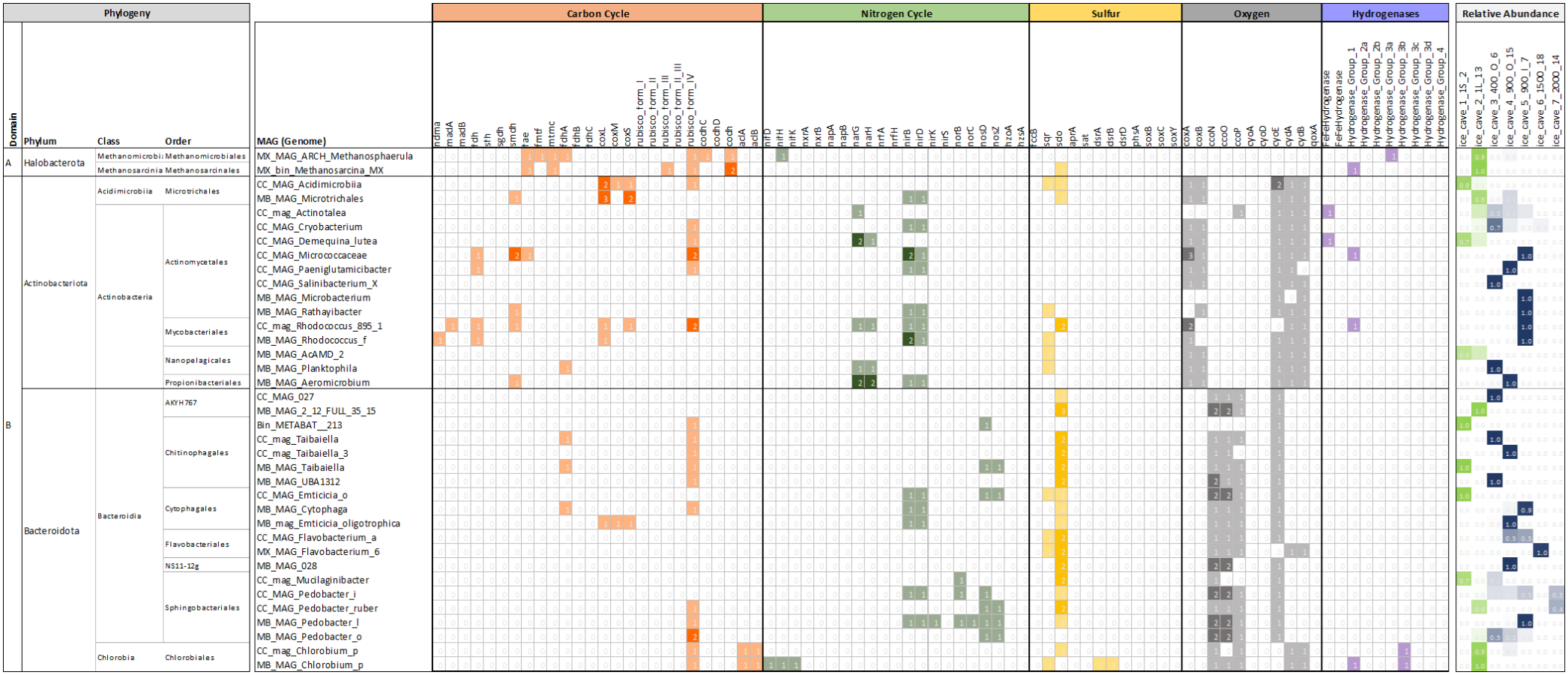

Figure 7-7 Table of genes involved in major biogeochemical cycles in MAGs belonging to Archaeal, Actinobacteriota and Bacteroidota phyla. The table shows Phylogeny of each of the mags, presence, absence, and count data for selected genes in the Carbon, Nitrogen, Sulfur, Oxygen and Hydrogen cycling pathway. The relative abundance of the MAGs in each environment is shown in a panel to the right.

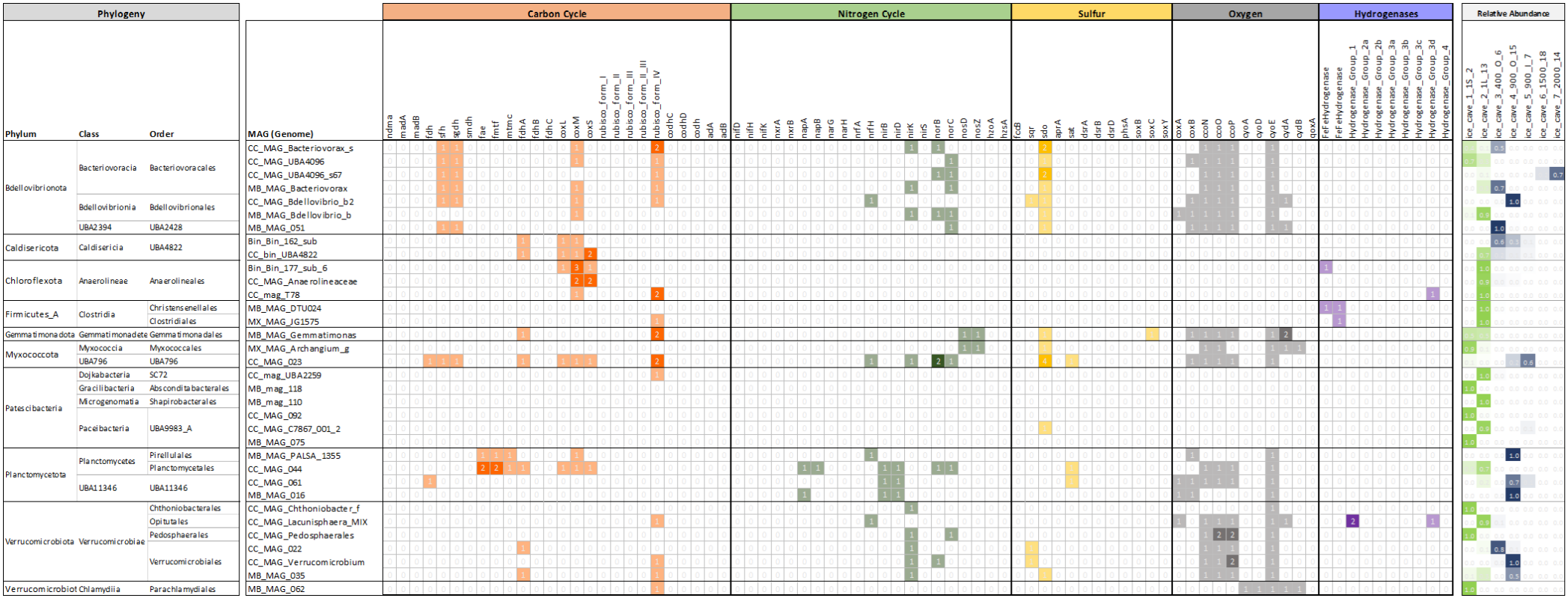

Figure 7-8 Table of genes involved in major biogeochemical cycles in MAGs belonging to Bdellovibrionota, Caldisericota, Chloroflexota, Firmicutes_A, Gemmatimonadota, Myxococcota, Patescibacteria, Planctomycetota, Verrucomicrobiota, Verrucomicrobiota_Aphyla. The table shows Phylogeny of each of the mags, presence, absence, and count data for selected genes in the Carbon, Nitrogen, Sulfur, Oxygen and Hydrogen cycling pathway. The relative abundance of the MAGs in each environment is shown in a panel to the right.

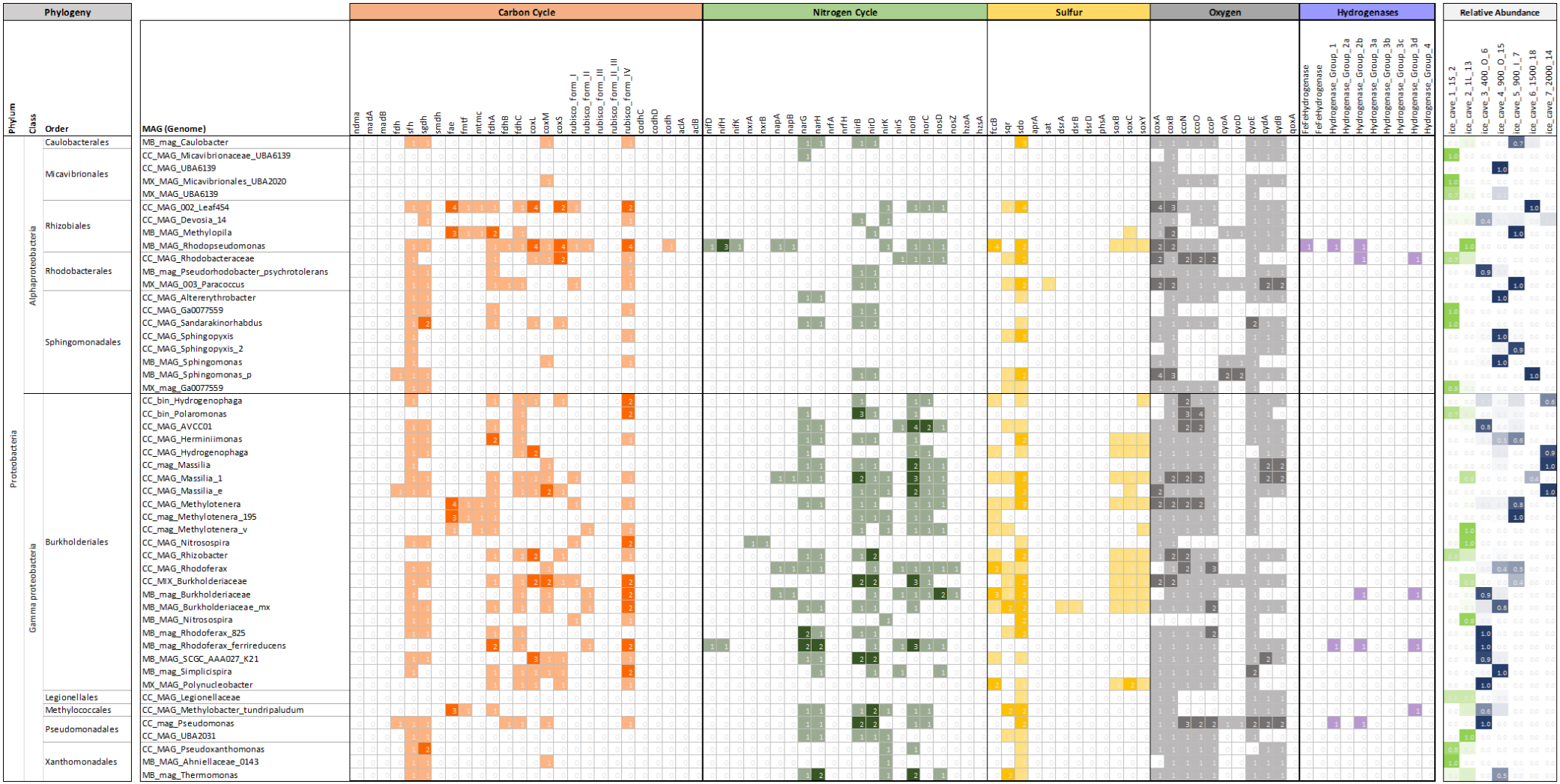

Figure 7-9 Table of genes involved in major biogeochemical cycles in Proteobacterial MAGs. The table shows Phylogeny of each of the mags, presence, absence, and count data for selected genes in the Carbon, Nitrogen, Sulfur, Oxygen and Hydrogen cycling pathway. The relative abundance of the MAGs in each environment is shown in a panel to the right.

7.3.8 Antimicrobial secondary metabolites

The 122 MAGs were submitted to antiSMASH to mine for novel BGCs (Figure 7-10, Figure 7-11, and Figure 7-12). There were 2694 clusters detected in total. Of the cluster types detected, the most common was saccharide clusters (1597), followed by fatty acids (344) and halogenated clusters (131). Together, there were more NRPS and NRPS-like clusters (NRPS=122, NRPS-like=41, combined=163) than there were terpenes (124). The NRPS and NRPS-like compounds are somewhat distributed throughout several phyla, but they are especially concentrated in the Actinobacteria. Together, 47/122 of the NRPS clusters and 14 of the 41 NRPS-like clusters occur in just eight Actinobacterial MAGs. Interestingly, all eight of these MAGs occur in the older and darker ice from sites 400-O (2), 900-O (1) and 900-I (5). Of note, there was a single Actinobacterial MAG (CC_mag_Rhodococcus_895_1) that had 28 NRPS clusters. This represents 23% of the NRPS clusters in the whole dataset. Of these, only four are similar to known compounds with described BGCs in the MiBIG database, and the remainder represent novel NRPS clusters.

The known clusters include one with 45% similarity to heterobactin A and heterobactin S2 (BGC0000371) from *Rhodococcus erythropolis PR4*, two different clusters with 5 and 7 % similarity to atratumycin (BGC0001975) from *Streptomyces atratus*, and a fourth cluster with similarity to SF2575 (BGC0000269) from *Streptomyces sp. SF2575*. There were eight siderophores detected, two of which had 100% similarity to known BGCs in the MIBiG database.

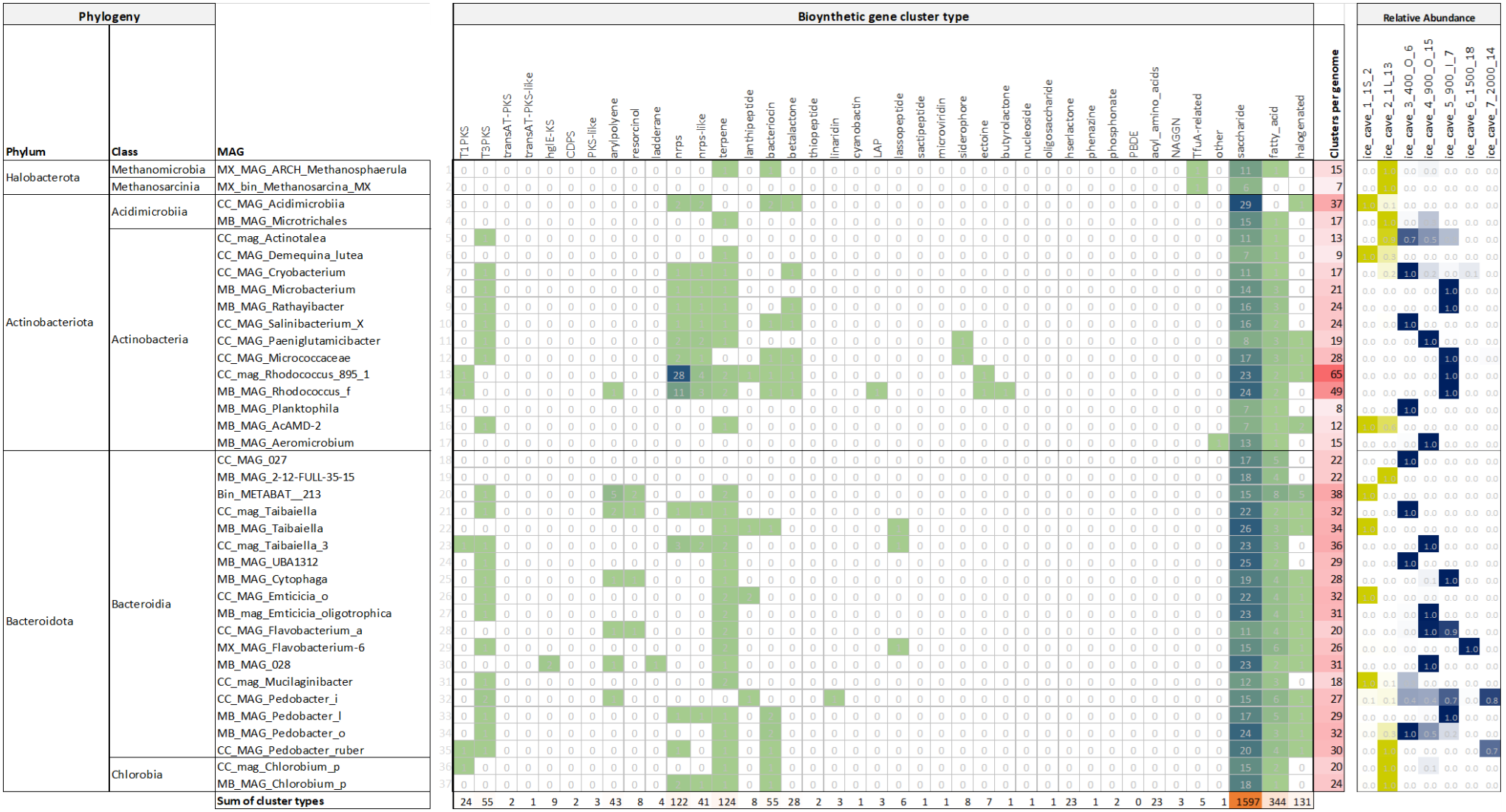

Figure 7-10 Secondary metabolites detected by antiSMASH in the Halobacterota, Actinobacteria and Bacteroidota MAGS.

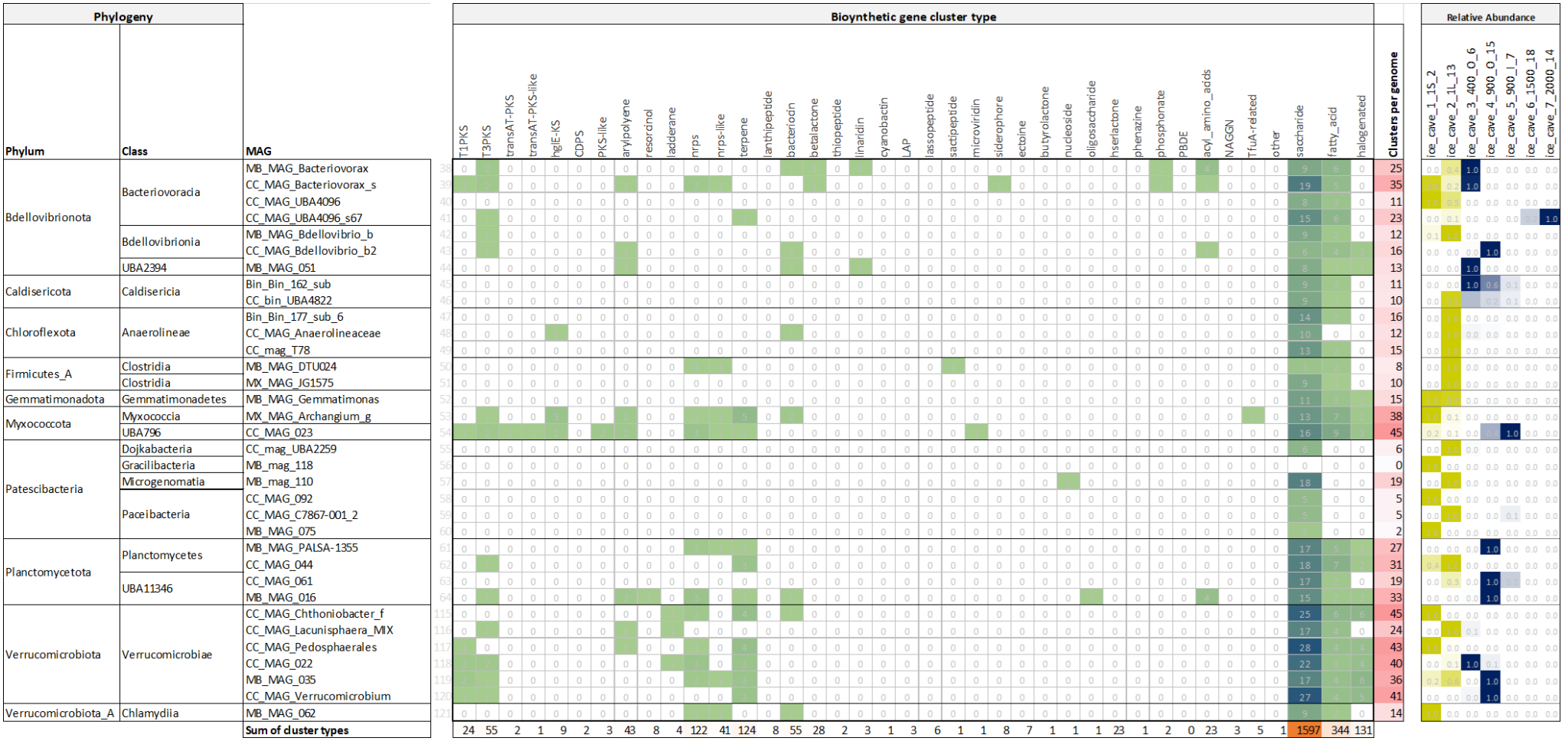

Figure 7-11 Secondary metabolites detected by antiSMASH in the Bdellovibrionota, Caldisericota, Chloroflexota, Firmicutes, Gemmatimonadota, Myxococcota, Patescibacteria, Planctomycetota and Verrucomicrobiota MAGS.

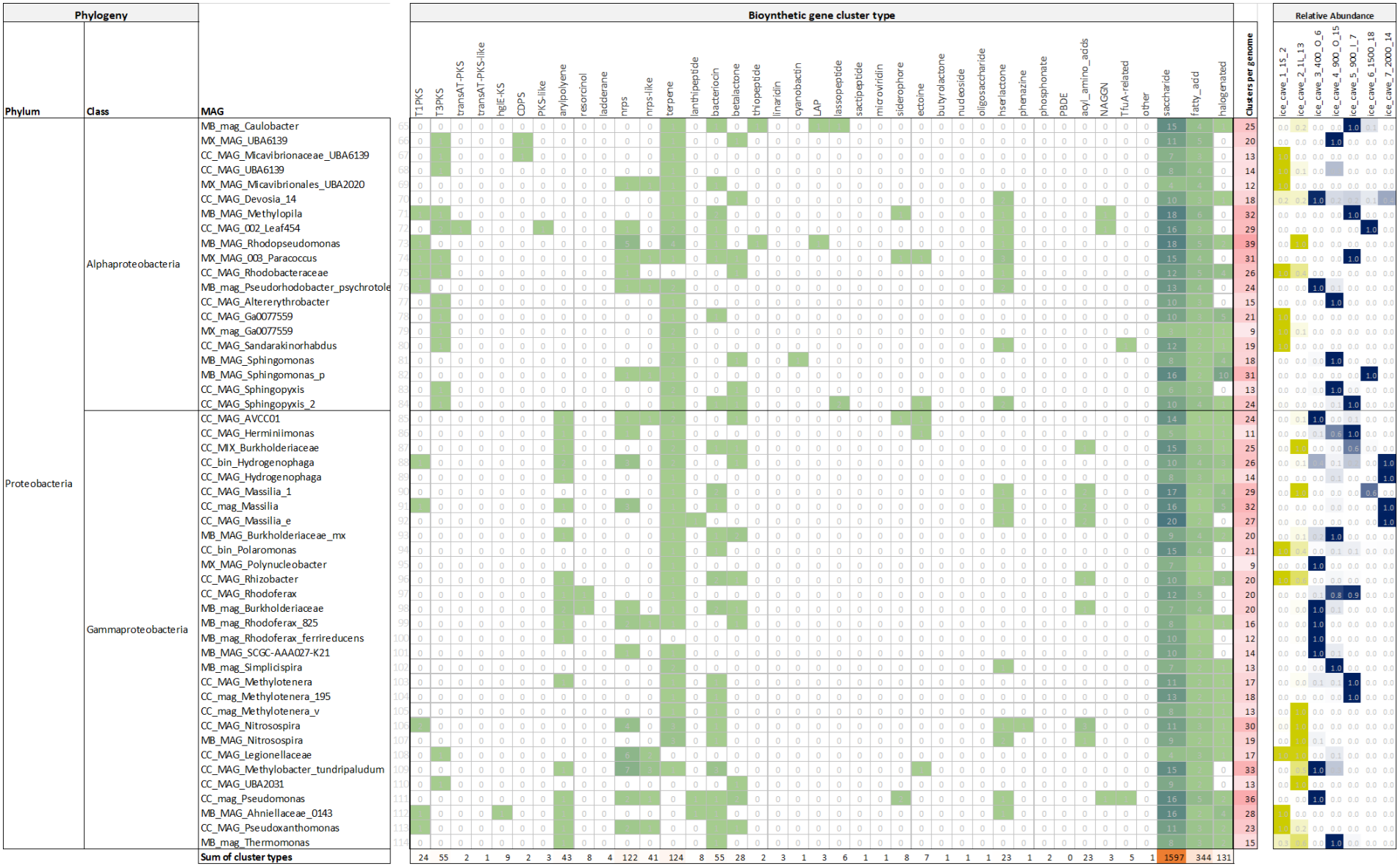
Phylogeny
Phylum
Class
MAG
Bioynthetic gene cluster type
T1PKS
T3PKS
transAT-PKS
transAT-PKS-like
hglE-KS
CDPS
PKS-like
arylpolyene
resorcinol
ladderane
nrps
nrps-like
terpene
lanthipeptide
bacteriocin
betalactone
thiopeptide
linaridin
cyanobactin
LAP
lassopeptide
sactipeptide
microviridin
siderophore
ectoine
butyrolactone
nucleoside
oligosaccharide
hserlactone
phenazine
phosphonate
PBDE
acyl_amino_acids
NAGGN
TfuA-related
other
saccharide
fatty_acid
halogenated
Clusters per genome
Relative Abundance
ice_cave_1_15_2
ice_cave_2_1L_13
ice_cave_3_400_O_6
ice_cave_4_900_O_15
ice_cave_5_900_I_7
ice_cave_6_1500_18
ice_cave_7_2000_14
Proteobacteria
Alphaproteobacteria
Gammaproteobacteria
MB_mag_Caulobacter
MX_MAG_UBA6139
CC_MAG_Micavibrionaceae_UBA6139
CC_MAG_UBA6139
MX_MAG_Micavibrionales_UBA2020
CC_MAG_Devosia_14
MB_MAG_Methylopila
CC_MAG_002_Leaf454
MB_MAG_Rhodopseudomonas
MX_MAG_003_Paracoccus
CC_MAG_Rhodobacteraceae
MB_mag_Pseudorhodobacter_psychrotole
CC_MAG_Altererythrobacter
CC_MAG_Ga0077559
MX_mag_Ga0077559
CC_MAG_Sandarakinorhabdus
MB_MAG_Sphingomonas
MB_MAG_Sphingomonas_p
CC_MAG_Sphingopyxis
CC_MAG_Sphingopyxis_2
CC_MAG_AVCC01
CC_MAG_Herminiimonas
CC_MIX_Burkholderiaceae
CC_bin_Hydrogenophaga
CC_MAG_Hydrogenophaga
CC_MAG_Massilia_1
CC_mag_Massilia
CC_MAG_Massilia_e
MB_MAG_Burkholderiaceae_mx
CC_bin_Polaromonas
MX_MAG_Polynucleobacter
CC_MAG_Rhizobacter
CC_MAG_Rhodoferax
MB_mag_Burkholderiaceae
MB_mag_Rhodoferax_825
MB_mag_Rhodoferax_ferrireducens
MB_MAG_SCGC-AAA027-K21
MB_mag_Simplicispira
CC_MAG_Methylotenera
CC_mag_Methylotenera_195
CC_mag_Methylotenera_v
CC_MAG_Nitrosospira
MB_MAG_Nitrosospira
CC_MAG_Legionellaceae
CC_MAG_Methylobacter_tundripaludum
CC_MAG_UBA2031
CC_mag_Pseudomonas
MB_MAG_Ahniellaceae_0143
CC_MAG_Pseudoxanthomonas
MB_mag_Thermomonas
Sum of cluster types
24 55 2 1 9 2 3 43 8 4 122 41 124 8 55 28 2 3 1 3 6 1 1 8 7 1 1 1 23 1 2 0 23 3 5 1 1597 344 131

Figure 7-12 Secondary metabolites detected by antiSMASH in the Proteobacterial MAGS.

7.4 Discussion

The Scărișoara Ice Cave has several unique features that make it a fascinating environment for study. Firstly, it is a perennially cold environment, where the bulk of ice remains frozen year-round, and only a top liquid layer is added annually, making it a fascinating record of past climactic conditions (Perşoiu and Pazdur, 2011). Secondly, the ice cave is an extremely unique and rare environment because of its steady, year-round cold temperatures, variable light conditions, and oligotrophic conditions. Nonetheless, several studies have shown that bacteria (Hillebrand-Voiculescu et al., 2015; Itcus et al., 2018; Iţcuş et al., 2016; Paun et al., 2019) and fungi (Brad et al., 2018; Mondini et al., 2018) can thrive in these systems. The previous investigations relied on culturing and amplicon sequencing studies, which have two disadvantages- they can only capture the diversity of cultivable organisms, and secondly, they only provide information about phylotype, and do not tell us anything about functional adaptations to this environment. In this study, 121 high-quality MAGs were assembled from metagenomic DNA collected from seven sites. The spatial distribution of the MAGs (Figure 7-6), their phylogenetic relatedness to each other (Figure 7-5) and to reference species (Table 7-6), their biogeochemical cycling ability (Figure 7-7, Figure 7-8 and Figure 7-9) and their repertoire of secondary metabolites (Figure 7-10, Figure 7-11 and Figure 7-12) were all investigated.

7.4.1 Phylogeny and novel species

There were 121 MAGS resolved from the Ice Cave, and they belonged to 14 different phyla. The phylogenetic classification of these MAGs corroborates recent 16S rRNA amplicon studies of this same cave environment (Paun et al., 2019). The most abundant phylum by far was the Proteobacteria, which was in agreement with previous 16S rRNA studies of this environment (Iţcuş et al., 2016). We also managed to resolve two Archaea from the dataset.

Several MAGs from the Ice Cave were species-level matches to known bacteria and archaea according to FastANI (Table 7-5). When we looked at the habitats of these close relatives, we found that they were isolated predominantly in oligotrophic and cold environments. The Archaea, MX_bin_Methanosarcina_MX, is a close relative of *Methanosarcina* sp001714685 (GCA_001714685.2), which was assembled from a permafrost metagenome from near Miers Lake, McMurdo Dry Valleys, Antarctica. MX_MAG_Flavobacterium-6 is like the type strain *Flavobacterium psychrolimnae* (GCA_003312425.1) collected from an Antarctic lake. CC_bin_Polaromonas is similar to *Polaromonas glacialis* (GCF_000709345.1) which was

collected from glacial foreland till in Norway. MX_MAG_003_Paracoccus is a close relation of *Paracoccus* sp000787695 (GCF_000787695.1) collected from a marine sediment near Ny-Ålesund, Svalbard. There was no geographic information associated with the assembly for *Pedobacter_A ruber* (GCF_900103545.1) which was the closest relative of CC_MAG_Pedobacter_ruber, however, the species *Pedobacter_A ruber* was first described as a psychrophilic soil bacteria (Margesin and Zhang, 2013). MB_mag_Caulobacter is similar to Caulobacter sp002737765 (GCF_002737765.1), an isolate from littorial waters of Lake Michigan that had been stored at 4 degrees C for one year. MX_MAG_Polynucleobacter, relative of *Polynucleobacter aenigmaticus* (GCF_002206635.1) from a freshwater lake, Lake Krottensee, from the Salzkammergut Area, Austria.

The exceptions to the overwhelming majority of psychrophilic microorganisms was MB_MAG_Rhodococcus_f, was similar to *Rhodococcus fascians* (GCF_001894785.1) and MB_MAG_Rathayibacter, similar to *Rathayibacter caricis* (GCF_003044275.1) and MB_MAG_Sphingomonas_p related to *Sphingomonas paucimobilis* (GCF_000739895.2), which was isolated from a hospital respirator.

There were many more MAGs that fell short of the 95 radius set by FastANI, but that could be identified to species level using GTDB-tk. For example, there were three MAGs belonging to the *Massilia*, which are known to be psychrophilic.

This ice block has previously been investigated using 16S rRNA sequencing, and the assembled MAGs bear striking and reassuring similarity to the communities detected using 16S rRNA amplicon studies. Previously, methanogenic species belonging to *Methanosphaerula* and *Methanosarcina* were detected in 2,000- and 5,000-year-old samples (Paun et al., 2019), however, in this study we found these MAGs predominantly in ice from site 1L-13 ice from the present day (Figure 7-6).

7.4.2 Spatial distribution of the MAGs

There was significant variation in the ages and environmental properties of the different sites that were sampled. Some areas of the cave, near the entrance, receive direct light (1S), others receive indirect light (1L) and still others are in complete darkness. In addition, some layers have higher organic and inorganic content (due to the settling of sediment within each annual layer) than others, which appear as clear ice. Apart from site 1S and 1L, sampled layers were quite old and have remained frozen for hundreds (400-O: 385 years) to thousands of years (1800: ~1500 years ago). The bacteria within, have therefore been trapped (dead or alive), for

significant periods of time, and they provide a fascinating insight into the conditions outside of the cave, during the summer when the water first trickled in and then froze. In a previous study of these same sites, cell density and number of cultivatable organisms was negatively correlated to the age of the ice (Iţcuş et al., 2016), which is corroborated in this study as because the cave locations with the fewest number of MAGs and the least coverage were the two oldest sites.

A striking observation was the strong spatial preference of specific MAGs for a single site (Figure 7-6). This could be explained by the fact that the Ice Cave remains frozen, and that community members become trapped within a single layer with each freezing. Nonetheless, this obvious spatial organisation of the microbial communities suggests that it is a priceless resource for looking the changing climate conditions over recent millennia.

The spatial distribution of the MAGs also highlights the incredible power of read mapping to distinguish between closely related strains when the assembly is good. There were three different Bacteroidete MAGs from the genus *Taibaiella_B*, however, they could be distinguished because they occurred in completely different samples. MB_MAG_Taibaiella occurred at location 1S_2, CC_mag_Taibaiella was found in location 400_O_6 and CC_mag_Taibaiella_3 occurred at location 900_O_15. There is a Flavobacterium (MX_MAG_Flavobacterium-6) that occurs exclusively at site 1500_18 and a Flavobacterium (CC_MAG_Flavobacterium_a) that can be found at sites 400_O_6, 900_O_15 and 900_I_7. It is evident that the locations of each of the three Massilia MAGs differ. CC_MAG_Massilia_1 is found in location 1500_18, while CC_mag_Massilia (GCF_900129765.1) and CC_MAG_Massilia_e (GCF_002760655.1) are found mainly in location 2000_14, and to different extents in nearby locations. The same can be said of Methylotenera MAGs.

The fact that similar MAGs crop up again and again at different sites suggests that the ice cave community is not particularly diverse. The passage of times between freezing events allows us to assemble and distinguish different strains of the same species and genera, but the genera and species making up the core community in the different layers is relatively constant.

7.4.3 Biogeochemical cycling

Analysis of several biogeochemical cycling genes revealed that the Ice Cave is a highly reducing environment (Figure 7-7, Figure 7-8, and Figure 7-9).

7.4.3.1 Carbon cycling

The Calvin–Benson–Bassham (CBB) cycle assimilates CO_2 for the primary production of organic matter and the key enzyme of this cycle is ribulose-bisphosphate carboxylase/oxygenase (RubisCO). Of the three carboxylating forms of RubisCO (I, II and III), form I is the main enzyme responsible for photoautotrophy in bacteria (Tabita et al., 2008). Given the low levels of light in the cave, we did not expect to find much evidence photoautotrophy. Indeed, there were only eight MAGs in total with Form *1 RubisCO* genes, three Alphaproteobacterial MAGs, and five Gammaproteobacterial MAGs, all of which belong to the family Burkholderia. Of these, five came from sites IS and IL which received light. We also found a *form III RubisCO* gene in MX_bin_Methanosarcina_MX. Until recently, *form III* RubisCO was thought to exist exclusively in archaea where it aided in the utilization of ribonucleotides and ribonucleosides via the pentose-bisphosphate pathway (Frolov et al., 2019). However, *Form III RubisCO* has just recently been implicated in autotrophic CO_2 fixation (Frolov et al., 2019).

The two MAGs belonging to the Phylum Chlorobia, order Chlorobiales, found predominantly at site 1L_13, had acetate citrate lyase genes *aclA* and *aclB*, which enable carbon fixation in anaerobic conditions (Kanao et al., 2001). Chlorobium, which have previously been detected in the Scărișoara Ice Cave (Itcus et al., 2018; Paun et al., 2019), generally grow photoautotrophically in strict anaerobic environments and are known to contain acetate citrate lyase genes (Kanao et al., 2001). These genes encode a key enzyme (ATP-citrate lyase) in the reductive tricarboxylic acid (RTCA) cycle because it determines the direction of this cycle (Kanao et al., 2001). The (RTCA) cycle fixes four molecules of CO_2 to generate one molecule of oxaloacetate in one cycle. Even though these bacteria are exposed to light, they are too deeply embedded in the ice to photosynthesize aerobically.

7.4.3.2 Nitrogen cycling

There were only four MAGs capable of nitrogen fixation via one or more of *nifH/D/K* (Fani et al., 2000). Three of these MAGs were found predominantly at site IL, which receives some sunlight and represents a ‘present day’ community. The *napA/B* and *narG/H* genes are involved in denitrification and dissimilatory nitrate reduction and encode genes that reduce nitrate (NO_3^-) to nitrite (NO_2^-) (Sparacino-Watkins et al., 2014). Both *napA/B* were present in a Planctomycetales MAG, a single Alphaproteobacterial MAG and three Gammaproteobacterial MAGs. The *narG/H* genes were far more abundant, and found in four Actinobacterial MAGs, four Alphaproteobacterial MAGs and 18 Gammaproteobacterial MAGs. MAGs

CC_MAG_Massilia_1 and CC_MAG_Rhodoferax had all four genes for napA/B and narG/H. Nitrite reductase (NirBD) functions during aerobic growth where is reduces nitrite (NO_3^-) to ammonium (NH_4^+) (Harborne et al., 1992). *NirB/D* genes were detected in eight Actinobacterial MAGs, five Bacteroidota MAGs (including all three Cytophagales MAGs), three Plantomycetes, eight Alphaproteobacteria and 21 Gammaproteobacterial MAGs. The *norB/C* genes encode a respiratory nitric oxide reductase that reduces NO to N_2O (Hendriks et al., 2000). *NorB/C* genes were present in several Bdellovibrionota and Alphaproteobacterial MAGs and in 20 Gammaproteobacterial MAGs. Several of the MAGs with *norB/C* genes also had *nosD/Z* genes, which reduce N_2O further to N_2 (McGuirl et al., 1998).

7.4.3.3 Sulfur cycling

The sdo (sulfuf dioxygenase) gene was the most common gene across all the phyla. Sulfur dioxygenases (SDOs) were originally found in the cell extracts of chemolithotrophic bacteria as glutathione (GSH)-dependent sulfur dioxygenases (Liu et al., 2014). GSH spontaneously reacts with elemental sulfur to generate glutathione persulfide (GSSH), and SDOs oxidize GSSH to sulfite and GSH (Liu et al., 2014). Sulfur oxidation via the Sulfur Oxidising (soxBCY) pathways (Bagchi and Ghosh, 2005; Bagchi and Roy, 2005) was highly prevalent in the Gammaproteobacteria, and specifically, within the order Burkholderiales, where 13/23 had at least one *sox* gene, and 10 had all three of *soxBCY*. There were two Rhizobiales MAGs in the Alphaproteobacteria with at least one *sox* gene and a single *sox* gene in the Gemmatimonadota MAG (MB_MAG_Gemmatimonas).

7.4.3.4 Oxygen cycling

There are also some striking clade-specific differences in biogeochemical cycling pathways for oxygen cycling. The *coxAB* genes encode for a cytochrome c oxidase that couples the oxidation of reduced cytochrome c with the reduction of molecular oxygen to water (Schmetterer et al., 1994). These genes are present in 13 Actinobacterial MAGs, none of the Bacteroidetes and all but one of the Proteobacteria. CcoNOP is a cbb3 cytochrome c oxidase that exhibits oxygen reductase activity (Swem and Bauer, 2002). The genes for this complex was ubiquitous across Bacteroidetota (15/16), the Alphaproteobacteria (11/20), Gammaproteobacteria (27/31) Bdellovibrionota (7/7), Planctomycetota (2/4), Verrucomicrobiota (5/6) the Gemmatimonadota (1/1), Myxococcota (2/2), but completely absent from the Actinobacteria, Caldisericota, Chloroflexota, Firmicutes_A, Patescibacteria and Verrucomicrobiota_A. Whilst the Actinobacteria tend to have all three of *cyoE*, *cydA* and *cydB*, most of the Bacteroidetes only

have *cyoE*, except for MX_mag_Flavobacterium_6 and the two Chlorobium MAGs which only have *cydA* and *cydB*. The *cyoE* gene encodes a cytochrome o oxidase complex and *cydAB* encodes a cytochrome d oxidase complex, which act as terminal oxidases that catalyse the oxidation of ubiquinol-8 and the reduction of oxygen to water (Cotter et al., 1990).

7.4.4 Secondary metabolites

Several caves have been explored in the past for novel antimicrobial compounds (Ghosh et al., 2017). Examples include the subterranean Kotumsar cave, India (Rajput et al., 2012), to a volcanic cave in western Canada (Rule and Cheeptham, 2013) to Magura Cave, Bulgaria (Tomova et al., 2013). However, all of these studies have relied on cultivated strains, which can exceptionally difficult to grow because of complicated cultivation conditions and exceptionally slow growth (Ghosh et al., 2017).

We submitted the 121 MAGs to antiSMASH, and there was a total of 2694 clusters detected. Of the cluster types detected, the most common was saccharide clusters (1597), followed by fatty acids (344) and halogenated clusters (131). Together, there were more NRPS and NRPS-like clusters (NRPS=122, NRPS-like=41, combined=163) than there were terpenes (124). Since terpenes are often carotenoids and other photoprotective antioxidants, the low-light cave environment is not unexpected.

The NRPS and NRPS-like compounds are somewhat distributed throughout several phyla, but they are especially concentrated in the Actinobacteria. Together, 47/122 of the NRPS clusters and 14 of the 41 NRPS-like clusters occur in just 8 Actinobacterial MAGs. Of note, there was a single Actinobacterial MAG (CC_mag_Rhodococcus_895_1) that had 28 NRPS clusters. This represents 23% of the NRPS clusters in the whole dataset. Of these, only four are similar to known compounds with described BGCs in the MiBIG database, and the remainder represent novel NRPS clusters. These clusters and compounds are worth exploring for novel bioactivities.

7.5 Conclusion

Ice Caves are unusual habitats characterized by extreme conditions for life, and to our knowledge, this is the first study to study shotgun metagenomes from an ice cave. There were 121 high quality MAGs assembled from this environment, including genomes from 111 novel species. There were strong spatial patterns amongst the community members and mapping reads back to contigs enabled the resolution of distinct, yet closely related species. There were

several biogeochemical pathways suggesting that anaerobic photoautotrophy is possible near the entrance to the cave, but chemolithotrophy is common at other sites. Cave microbiomes have been hypothesized to be rich resources for antimicrobial products and this study identified thousands of clusters for secondary metabolites in the MAGs of this biome.

8 BIOINFORMATICS WORKFLOW FOR BIOPROSPECTING FROM METAGENOMES

8.1 Introduction

Bioprospecting is the search for NPs that provide health, societal or environmental benefits. Increasingly, with a reduction in the cost of DNA sequencing, it is possible to investigate the bioprospecting potential of an environment as a precursor to obtaining physiological proof of function. Recently, there has been a major paradigm shift in microbial ecology to the construction of genomes from metagenomic datasets (Parks et al., 2018; Pasolli et al., 2019), which is partly fueled by the increased sequencing depth, and to some extent by new long-read sequencing methods, like Nanopore (Moss et al., 2020; Overholt et al., 2019; Singleton et al., 2020). This genome-centric view has several advantages in bioprospecting, such as the resolution of genomes belonging to novel species that have no cultivable relatives and additional information about regulatory factors, nutrient requirements and metabolism and antibiotic resistance that all help inform strategic heterologous expression and cultivation efforts. However, it also comes with disadvantages, the major of these being that only the most abundant members of a community can be resolved using this method, which means that a large portion of a dataset is not explored. However, the benefits of a genome-centric bioprospecting are great, particularly because of the insights it provides when it comes to community cooperation and the way it opens possibilities for strategic cultivation efforts. In addition, the contigs of rarer community members that cannot be binned into MAGs are still a catalogue of diversity that can be mined in the same way as MAGs. The contigs can be submitted to numerous databases, specialized to identify genes and gene clusters for specific NP products and gene functions.

In this thesis, MAGs were constructed from two very different environments, a Svalbard glacial system comprising cryoconite, soil and seawater metagenomes (Chapter 4) and the Scărișoara Ice-cave in Romania (Chapter 7). The bioinformatic approach involved the assembly, annotation, binning, and comparison of genomes from these metagenomic datasets.

This chapter is a review some of some of the benchmarking, method optimization, and decision-making employed in the construction of the MAGs. The application of these methods on two different datasets also provided some insights into the effect of sequencing depth and community complexity on MAG reconstruction.

8.1.1 Aims and Objectives

The aims of this chapter were as follows:

1. Based on knowledge of environmental stressors, create a list of genes and gene products that have useful applications.
2. Describe a workflow that goes from raw reads to contigs and metagenome-assembled genomes using readily available open-access tools.
3. Curate a catalogue of tools that can be used and substituted in this workflow
4. Test and compare tools on different cryospheric datasets to compare:
   4.1. The effect of the data: i.e. the effect of sampling depth and environment complexity.
   4.2. The use of different tools: i.e. the use of different assembly tools and binning methods.
5. Highlight the advantages and disadvantages of using reads, contigs and MAGs in bioprospecting.

8.2 Methods

8.2.1 Environmental sample types

In accordance with the project objectives, a range of different environmental sample types was analysed. There were two datasets analysed in detail for their bioprospecting potential. A Svalbard dataset consisting of 17 paired-end (PE) libraries from soil (8), cryoconite (6) and seawater (3) (see Chapter 4). An ice cave dataset consisting of seven libraries from the perennial ice block of Scărișoara Ice Cave in Romania (see Chapter 7). The libraries for the different datasets differ in sequencing depth, community heterogeneity and complexity.

8.2.2 Quality control

All libraries form both metagenome datasets were uploaded to KBase (http://kbase.us/)(Arkin et al., 2018). The quality of the raw libraries was assessed using FastQC (J. Brown et al., 2017). Adapters were removed and low-quality bases were trimmed using Trimmomatic (Bolger et al., 2014) with a minimum Phred score threshold of 30. The quality of the read libraries was then reassessed using FastQC.

8.2.3 Assembly

Assembly is the process by which individual reads are split into predefined segments (k-mers), which are overlapped into a network, and paths are traversed iteratively to create longer contigs (van der Walt et al., 2017). Assembly is a very computationally expensive step, and all downstream analyses depend on the quality of the contigs. There are a range of different assembly tool available, many of which can be tailored with different parameters such as k-mer length (Vollmers et al., 2017). Metagenome libraries, consisting of the DNA from a single site, can either be assembled individually, or co-assembled together, wherein all the libraries are combined in the assembly step, and reads are mapped to the contigs to determine the contribution of different libraries to the contigs in the final assembly. In this thesis, the performance of three different assembly tools: MEGAHIT (D. Li et al., 2015), metaSPAdes (Nurk et al., 2017) and IDBA-UD (Peng et al., 2012) were tested, as was the effect of co-assembly vis single-sample assembly. MetaQUAST was used to compared the assemblies (Gurevich et al., 2013).

8.2.4 Metagenome-assembled genomes (MAGs) using anvi'o

With large shotgun metagenomic libraries, it is possible to assemble putative genomes or metagenome-assembled genomes (MAGs). To do this, we used the tool anvi'o (versions 5, 6.1 and 6.2) (Eren et al., 2015) following the Anvi'o User Tutorial for Metagenomic Workflow (http://merenlab.org/2016/06/22/anvio-tutorial-v2/). An anvi'o contigs databases is created using anvi-gen-contigs-database, with an assembly fasta file as input. The contigs database is an essential component of the anvi'o metagenomic workflow because it stores information on positions of open reading frames (ORFs), identified using Prodigal (Hyatt et al., 2010), and k-mer frequencies for each contig.

8.2.4.1 Functional Annotation of contigs

The contigs database can be annotated from within the anvi'o workflow using scripts that access external databases.

8.2.4.1.1 Single copy gene HMMs

To estimate the number of bacterial genomes in the metagenome, anvi'o runs HMMER (Eddy, 2008; Mistry et al., 2013) against a series of single-copy gene (SCG) databases. In anvi'o-6.1, these include specially curated HMM profiles of SCGs for Archaea (76 genes), Protista (83 genes) and Bacteria (71 genes)(Lee, 2019). There is also a script to detect candidate phyla radiation (CPR) that relies on the SCG HMM dataset from (Campbell et al., 2013). Therefore, the Campbell HMMs, together with the three profiles with anvio-6.1 were included in the HMMER scan.

8.2.4.1.2 NCBI COGs

The genes in the contigs database can be annotated with functions from the NCBI's Clusters of Orthologus Groups (COGs) using anvi-setup-ncbi-cogs to download the database (http://www.ncbi.nlm.nih.gov/COG/) and anvi-run-ncbi-cogs to annotate the contigs database. Each COG consists of individual orthologous proteins or orthologous sets of paralogs from several (minimum of three) lineages (Galperin et al., 2015; Tatusov et al., 1997). Orthologs generally have the same function, which means functional information from one member can be transferred to an entire COG, allowing functional predictions of poorly characterized genomes (Galperin et al., 2015; Tatusov et al., 1997).

8.2.4.1.3 KEGG annotations

The Kyoto Encyclopedia of Genes and Genomes (KEGG) (https://www.genome.jp/kegg/) database integrates functional information, biological pathways, and sequence similarity in order to infer high level functions of organisms or ecosystems (Kanehisa and Goto, 2000). GhostKOALA (https://www.kegg.jp/ghostkoala/) is a web-server-based tool that provides automatic annotation of KEGG Identifiers to metagenomes (Kanehisa et al., 2016). In order to import KEGG annotations into the anvi'o contigs database(s), a workflow (http://merenlab.org/2018/01/17/importing-ghostkoala-annotations/) and its associated tools (https://github.com/edgraham/GhostKoalaParser.git) were used as described. Gene calls were exported from the contigs database and submitted in batches of an appropriate size.

8.2.4.1.4 Eggnog mapper

Annotations were computed using eggnog-mapper (Huerta-Cepas et al., 2017) based on eggNOG 4.5 orthology data (Huerta-Cepas et al., 2016) using the eggNOG mapper v.1 web-server (http://eggnogdb.embl.de/#/app/emapper). Gene calls from the contig database were exported, and the file split into multiple files of 80 000 sequences (Svalbard) or 100 000 sequences (Ice-cave), and then submitted to the webserver.

8.2.4.2 Taxonomic Assignment

8.2.4.2.1 Assign Taxonomy from kaiju- refseq

Taxonomic information was added to the genes and contigs using Kaiju (Menzel et al., 2016). Kaiju was installed locally on the CLIMB VM using instructions available on the Kaiju Github (https://github.com/bioinformatics-centre/kaiju). The Kaiju database was made using the 'refseq' database, which contains 63 million sequences from completely assembled and annotated reference genomes of Archaea, Bacteria, and viruses from the NCBI RefSeq database (O'Leary et al., 2016). The sequences for the gene-calls in the contigs database were exported using anvi-get-sequences-for-gene-calls, and Kaiju was run on these gene-calls. The script addTaxonNames adds taxon information so that is can be parsed back into the contig database, and finally taxonomy for the gene calls was added by running anvi-import-taxonomy-for-genes.

8.2.4.2.2 Single-Copy Core Genes (SCGs)

The taxonomy of the MAGs was estimated using the anvi'o scg-taxonomy workflow described here: http://merenlab.org/scg-taxonomy. The workflow uses the taxonomy determined by the Genome Taxonomy Database (GTDB) (Parks et al., 2018) and makes use

of DIAMOND (Buchfink et al., 2015), a fast alternative to the NCBI's BLAST. The command anvi-setup-scg-databases downloads the SCGs and the GTDB taxonomy of the genomes and builds a search database for a subset of 22 SCGs. The script anvi-run-scg-taxonomy searches the contigs.db for the 22 SCGs, compares them against the corresponding genes in the GTDB databases and selects the best hit, which it stores in a table in the contigs database. The anvi-run-scg-taxonomy script can be run on a contigs database to estimate how many genomes are in the assembly, or on a contigs database + profile database to determine the coverage or relative proportion of the different genomes in different samples, or it can be run on a contigs.db, profile.db and a collection to get the taxonomy of each of the bins in a collection. There were 1,377 SCG Ribosomal genes with taxonomic affiliations in the Svalbard contigs database. (Appendix: Figure D-2 shows the number of hits per Ribosomal gene and Appendix Table D-3 shows the probable identity of the genomes, based on the most abundant SCG, Ribosomal_S11, (n=112). There were 3,025 SCG genes with taxonomic affiliations in the Ice Cave contig database (Appendix Figure G-1). Appendix Table G-1 shows the probable identity of the genomes in the data set as well as their coverage and distribution across samples, based on the most abundant SCG, Ribosomal_S2 (n=202).

8.2.4.3 Mapping and creating a sample profile

Mapping of individual trimmed read libraries to co-assemblies was performed within the anvi'o environment using Bowtie2 (Langmead and Salzberg, 2012)(version 2.3.4.3). Samtools (Li et al., 2009) was used to convert the .sam file to raw .bam files, and an anvi'o script 'anvi-init-bam to get indexed .bam files for each of the samples. Next, anvi-profile creates a single profile that reports properties for each contig in a single sample based on mapping results. Profiling includes calculating the mean coverage, standard deviation of coverage, and the average coverage for the inner quartiles (Q1 and Q3) as well as coverage and single nucleotide variation at each nucleotide position for a given contig. Once samples have been individually profiled, all samples sharing a contigs database can be merged using anvi-merge.

8.2.5 Binning and refinement of MAGs

8.2.5.1 Binning

CONCOCT (v.1.1.0) was the built-in binning program in anvi'o until V. 6.1 because it uses Gaussian mixture models to cluster contigs into genomes based on sequence composition and coverage across multiple samples (Alneberg et al., 2014). The cross-sample comparison was especially suited to binning contigs from co-assemblies. However, additional binning tools

such as metaBAT2 (v2.12.1) (Kang et al., 2015) and MaxBin2 (v2.2.7) (Wu et al., 2016) were installed and then run from within anvi'o using the script anvi-cluster-contigs. The tool DAS Tool (v1.1.1) (Sieber et al., 2018), which optimises bins based on bins generated by other tools was then run, using the metaBAT2, MaxBin2 and CONCOCT collections as input for the refinement. The DAS Tool bins were then manually refined, and DAS Tool run again, to determine whether refining resulted in better or worse bins. The iteration and refining of DAS Tool bins were repeated twice: each time, the DAS Tool results were run on all the original bins, and the newly refined bins. Where DAS Tool reverted previously refined bins to unrefined bins, those refinements were checked. If the previous refinement could be clearly justified, the bin was refined again. Where the decision was unclear, the original bin was kept, regardless of high redundancy values.

8.2.5.2 Comparing binning results and refining bins

After binning, the collections were exported, merged and them re-imported as an additional layer. The steps were followed as described in http://merenlab.org/tutorials/infant-gut/ Chapter II: Automatic Binning: Comparing multiple binning approaches, with some modifications. The results of each collection, including those that had been through refinement steps were exported as tab-limited (.tsv) files. These files contained information on split-name and bin membership. In anvi'o, large contigs are divided into 'splits' of approximately 20 kB for processing, but all information about the original contig is kept, and splits have the same contig_id, with a unique suffix which comprises the split id. To import the bin membership information, the .tsv files were edited to remove split details from the contig id using (sed) (https://www.gnu.org/software/sed/manual/), and then were sorted and deduplicated using uniq (sort | uniq). The collections were then merged using anvi-script-merge-collections to create a .tsv file where each line represents a contig id, and each column has the bin id for each binning result. The .tsv was imported to the profile database as an 'item' using anvi-import-misc-data, which allowed visualisation of bin membership of each contig. Therefore, any collection could be loaded in anvi-interactive or in anvi-refine and the binning results of each tool compared. Where there was disagreement between bins, contig membership could be compared, and a 'consensus' bin visualised (Figure 8-1). The contigs of chimeric bins are more likely to be grouped different using different binning methods.

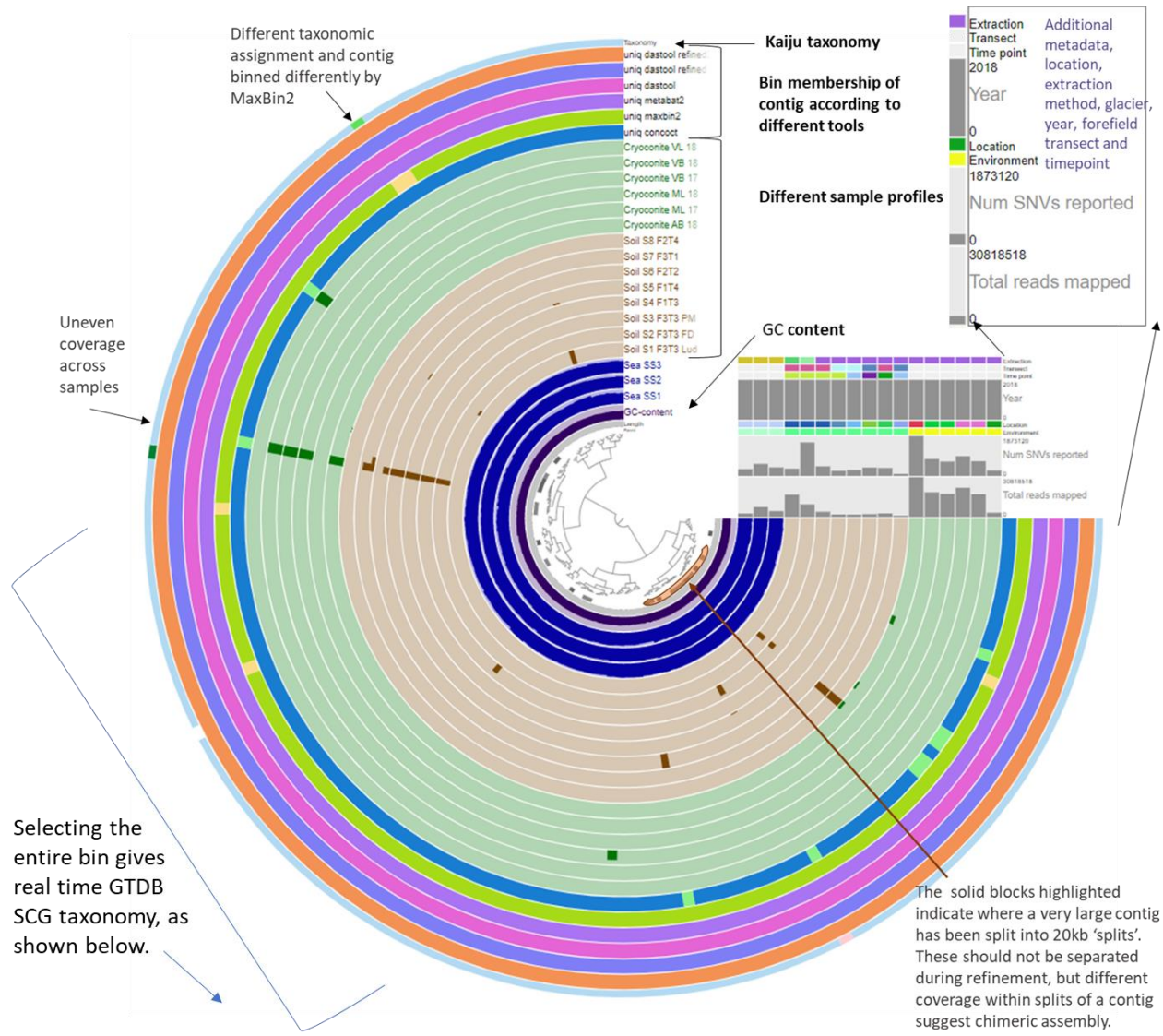

Bin name	Total SCGs	Supporting SCGs	Domain	Phylum	Class	Order	Family	Genus	Species
MB_MAG_023_ASP10-02a_1	20	15	Bacteria	Proteobacteria	Gammaproteobacteria	Pseudomonadales	Nitrincolaceae	ASP10-02a	*ASP10-02a sp002335115*

SCG Name	Gene Caller's Id	Percent Identity	<3?	Domain	Phylum	Class	Order	Family	Genus	Species
Ribosomal_L20	17334	100.0	true	Bacteria	Proteobacteria	Gammaproteobacteria	Pseudomonadales	Nitrincolaceae	ASP10-02a	*ASP10-02a sp002335115*
Ribosomal_S9	17402	100.0	true	Bacteria	Proteobacteria	Gammaproteobacteria	Pseudomonadales	Nitrincolaceae	ASP10-02a	*ASP10-02a sp002335115*
Ribosomal_L13	17403	100.0	true	Bacteria	Proteobacteria	Gammaproteobacteria	Pseudomonadales	Nitrincolaceae	ASP10-02a	*ASP10-02a sp002335115*
Ribosomal_S20p	347183	98.8	true	Bacteria	Proteobacteria	Gammaproteobacteria	Pseudomonadales	Nitrincolaceae	ASP10-02a	*ASP10-02a sp002335115*
Ribosomal_L21p	347189	99.0	true	Bacteria	Proteobacteria	Gammaproteobacteria	Pseudomonadales	Nitrincolaceae	ASP10-02a	*ASP10-02a sp002335115*
Ribosomal_S2	347251	99.6	false	Bacteria	Proteobacteria	Gammaproteobacteria	Pseudomonadales	Nitrincolaceae	ASP10-02a	*ASP10-02a sp002312935*
Ribosomal_L9_C	358492	93.2	false	Bacteria	Proteobacteria	Gammaproteobacteria	Pseudomonadales	Nitrincolaceae	ASP10-02a	*ASP10-02a sp002312935*
Ribosomal_S6	358495	98.9	true	Bacteria	Proteobacteria	Gammaproteobacteria	Pseudomonadales	Nitrincolaceae	ASP10-02a	*ASP10-02a sp002335115*

Figure 8-1 Figure showing an example of a 'good' bin during refinement. Anvi'o shows contig coverage across samples, GC content, splits, total reads mapped and single nucleotide variants (SNVs). Bin membership of each contig using different binning tools is export as an additional data layer. Kaiju contig classification, and various other metadata and statistics such as extraction method, year and glacier are also displayed. By selecting the bin, a real-time estimate of taxonomy based on SCG hits to GTDB can be viewed.

8.2.5.3 Visualisation and refinement of MAGs

The MAGS were refined, visualised, and compared using the anvi'o anvi-interactive and anvi-refine tools. In the view, Kaiju taxonomy is shown in colour of the contigs, the SCG taxonomy (including the number of GTDB SCGs and their identity) is shown from the bin information, and the binning tool membership is added as a layer (Figure 8-1). After refinement, the collection of complete bins could be exported using anvi-summarise. This summary contains information about contig coverage, GC content, number of contigs, N50, total size, MAG completion and redundancy based SCG genes from HMM profiles. The fasta files for each MAG were also separately uploaded to KBase and the completion and redundancy (heterogeneity or contamination) of the MAGs was assessed using CheckM (Parks et al., 2015), and the taxonomic classification was checked using GTDB-Tk (Chaumeil et al., 2020).

8.2.6 Screening MAGs and contigs

Finally, the MAGs can be screened for sequences responsible for the synthesis of desired NPs. In this chapter, the results of screening these datasets for secondary metabolites using (antiSMASH) and carbohydrate-active enzymes (dbCAN2) is described.

8.2.6.1 dbCAN2 to detect carbohydrate active enzymes

The contigs from the MEGAHIT assemblies of the Ice Cave and Svalbard datasets were submitted in batches to the dbCAN2 webserver (http://bcb.unl.edu/dbCAN2/index.php) (Zhang et al., 2018), which queries the Carbohydrate-Active EnZymes database (CAZy) (Cantarel et al., 2009; Lombard et al., 2014) (http://www.cazy.org/) using DIAMOND (Buchfink et al., 2015), HMMER (Mistry et al., 2013) and HotPep (Busk et al., 2017).

8.2.6.2 Biosynthetic gene cluster detection

AntiSMASH has algorithms able to detect a vast range of different BGCs, and many different molecule families. AntiSMASH is developed by several collaborating institutions, that makes use of a variety of tools such as NCBI BLAST+, HMMer 3, Muscle 3, Glimmer 3, FastTree, TreeGraph 2, Indigo-depict, PySVG and JQuery SVG. It can be run using a web application (https://antismash.secondarymetabolites.org) or as a standalone tool. The antiSMASH v5 results from the Svalbard MAGs (Chapter5) and Ice-Cave MAGs (Chapter7, Figure 7-10 to 7-12.) have been shown in previous chapters. In addition, all of the contigs from three different Ice-Cave assemblies, and the contigs from Svalbard cryoconite, soil and seawater were also screened using antiSMASH.

8.2.7 Workflow steps

A schematic diagram of the bioinformatics workflow is shown in Figure 8-2. A general outline

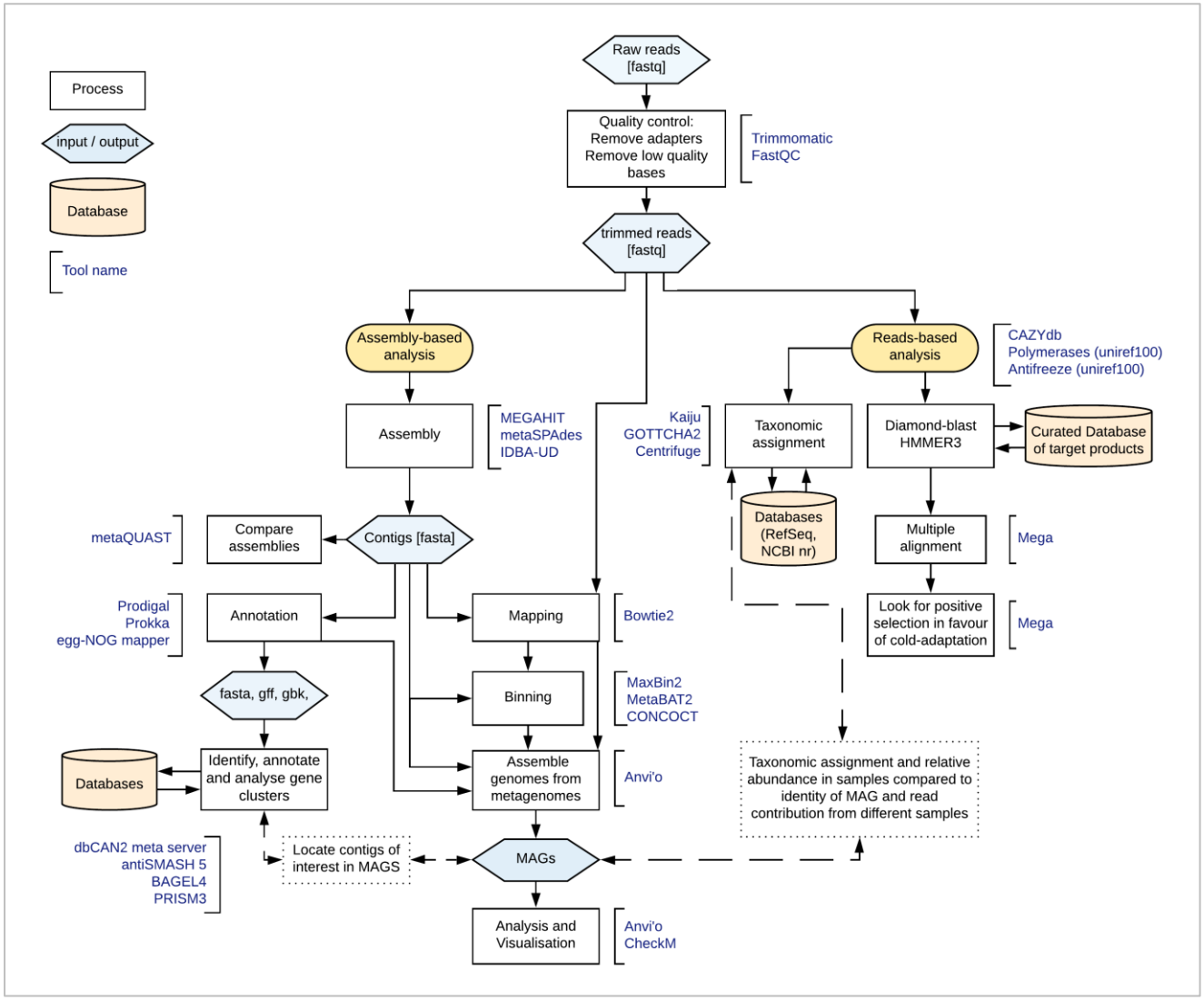

Figure 8-2: Schematic diagram of the bioinformatics workflow for Bioprospecting. Analyses can be performed on the trimmed reads or on assembled contigs. The reads and contigs can also be mapped back to MAGs.

Summary of terms in figure: Quality control: trimming adapters and primers, removing bases with a low Phred score. **Assembly**: assembling millions of short reads into longer contigs. **Mapping**: aligning reads back to the contigs to calculate contig coverage and assembly quality. **Annotation**: processing the data to look for open reading frames (ORFs) and coding sequences. **Alignment**: comparing the amino acids in these samples to reference strains and each other. **Binning**: grouping contigs into taxonomic groups based on similar coverage, GC content and tetranucleotide repeats to resolve genomes.

8.3 Results

8.3.1 Identification of bioprospecting targets

One of the aims of this project was to interrogate cryospheric metagenomes for industrially useful natural products such as enzymes and antimicrobial metabolites using open and freely available bioinformatics tools. To focus the project, potentially common and useful product-types were identified based on likely microbial adaptations to known cryospheric environmental stresses.

Table 8-1 Bioprospecting targets for cryospheric environments

Product	Adaptation	Application	Steps	List of product-specific tools
Cold-active enzymes	Amino acid changes that increase enzyme flexibility	Food industry, detergents, molecular biology tools	QC, alignment, assembly, annotation, BGC mining, binning	DIAMOND-blastx, HMMER3, UniRef, Pfam, CAZy, dbCAN2
Polyunsaturated fatty acids	PUFAs increase membrane permeability at low temperatures	Dietary supplements for humans, livestock, and fish	QC, assembly, annotation, BGC mining, binning	antiSMASH
Ice nucleation proteins	Seed small crystals instead of large damaging crystals	Food industry, synthetic snow	QC, alignment	DIAMOND-blastx, HMMER3, MEGA, UniRef, Pfam
Antifreeze proteins and solutes	Disrupt orderely arrangement of water molecules from forming ice-crystal structure	Cryoprotectants, food industry	QC, alignment	
Antioxidants and UV pigments	Protect microrganisms from seasonally high UV irradiation in snow	Biomedical, pharmaceutical, food technology and cosmetics	QC, assembly, annotation, BGC mining, binning	antiSMASH
Exopolysaccharide	Trap liquid water, preventing freezing	Biomedical, pharmaceutical, food technology and cosmetics	QC, assembly, annotation, BGC mining, binning	antiSMASH, dbCAN2 webserver
Antimicrobial compounds	Chemical defenses and weapons against competeing bacteria in low-resource environments	Pharmaceutical industry-antibiotics, antifungals, anti-tumour medications and pesticides	QC, assembly, annotation, BGC mining, binning	antiSMASH, PRISM, BAGEL

The adaptation strategy, application of the natural product, workflow steps involved, and specific tools and databases are listed.

8.3.2 Datasets

The shotgun metagenome libraries from the Svalbard dataset and Scărișoara Ice Cave dataset are shown in in Table 8-2 and Table 8-3 respectively.

Table 8-2 Characteristics of the Svalbard Soil, Seawater and Cryoconite datasets that contributed to the design and implementation of the bioinformatics workflow

				Read Length		Duplicate reads		Quality		
Environment	**Sample**	**Reads**	**No Bases**	**mean**	**std dev**	**Number**	**%**	**mean**	**std dev**	**GC%**
Svalbard dataset										
Soil	F3T3_Lud	40,079,596	5,866,959,800	146.38	17.23	595,443	1.49	34.05	4.75	57.43
Soil	F3T3_PM	44,915,524	6,576,965,385	146.43	17.22	43,387	0.10	34.05	4.76	62.47
Soil	F3T3_FD	113,754,008	16,645,206,349	146.33	17.43	594,826	0.52	34.04	4.77	61.04
Soil	F1T3-3	37,684,166	5,477,450,552	145.35	18.97	121,309	0.32	33.89	5.01	61.17
Soil	F1T4-2	38,762,496	5,660,342,037	146.03	17.92	881,337	2.27	34.00	4.85	57.65
Soil	F2T2-1	29,116,044	4,232,776,792	145.38	19.00	310,829	1.07	33.88	5.02	56.75
Soil	F3T1-3	35,482,472	5,166,716,509	145.61	18.70	336,628	0.95	33.92	4.97	58.63
Soil	F2T4-2	35,085,040	5,124,389,299	146.06	17.92	74,333	0.21	34.00	4.83	58.69
Sea	SS1	51,330,724	7,191,372,496	140.10	25.89	1,100,183	2.14	34.20	4.54	50.69
Sea	SS2	55,019,496	7,445,759,578	135.33	32.31	1,412,286	2.57	33.89	5.02	49.25
Sea	SS3	35,985,822	4,971,626,677	138.16	29.48	775,768	2.16	33.96	4.92	49.01
Cryoconite	ML-17	28,795,356	4,194,553,943	145.67	18.57	441,991	1.53	33.89	5.02	55.16
Cryoconite	VB-17	34,504,862	5,049,762,759	146.35	17.40	601,414	1.74	34.05	4.77	54.68
Cryoconite	ML-18	28,471,672	4,149,307,242	145.73	18.46	471,631	1.66	33.94	4.93	54.46
Cryoconite	VB-18	29,787,650	4,347,438,702	145.95	18.08	384,887	1.29	33.94	4.93	55.41
Cryoconite	AB-18	64,909,032	9,494,783,816	146.28	17.54	131,932	0.20	34.02	4.81	56.75
Cryoconite	VL-18	14,939,536	2,184,519,311	146.22	17.69	78,246	0.52	34.04	4.78	54.47

Library statistics are reported after quality trimming using Trimmomatic.

Table 8-3 Characteristics of the Scărișoara Ice-Cave dataset that contributed to the design and implementation of the bioinformatics workflow

				Read Length		Duplicate reads		Quality		
Environment	**Sample**	**Reads**	**No Bases**	**mean**	**std dev**	**Number**	**%**	**mean**	**std dev**	**GC%**
Ice-cave dataset										
Present, sun	1S_2	69,575,748	8,530,226,859	122.60	10.58	29,675	0.04	35.48	3.95	53.19
Present, light	1L_13	72,190,896	8,860,007,146	122.73	10.26	36,821	0.05	35.48	3.94	56.84
-385, organic	400_O_6	76,039,348	9,324,467,510	122.63	10.53	161,544	0.21	35.47	3.97	54.29
-943. Organic	900_O_15	73,462,594	9,019,960,422	122.78	10.20	353,401	0.48	35.51	3.90	54.57
-943, inorganic	900_I_7	75,113,102	9,213,747,381	122.67	10.46	145,477	0.19	35.43	4.03	59.89
~1200	1500_18	75,510,556	9,278,999,040	122.88	9.77	1,286,620	1.70	35.67	3.59	42.33
~1500	2000_14	63,569,516	7,815,266,055	122.94	9.78	84,276	0.13	35.48	3.93	61.72

8.3.3 Assembly comparisons

8.3.3.1 Assembly tool: MEGAHIT vs metaSPAdes vs IDBA-UD

MEGAHIT, metaSPAdes and IDBA-UD were used to assemble the Svalbard cryoconite libraries (n=6, PE reads= 201 408 108 reads) and the Scărișoara Ice cave libraries (n=7, PE reads= 505 461 760) to compare the performance of the tools (Table 8-4, Table 7-3). The cryoconite co-assembly was tested rather than the combined Svalbard assembly because IDBA-UD and metaSPAdes were unable to assemble the large combined Svalbard metagenome (n= 17, PE reads = 718 623 496), or the smaller, but high complexity metagenomes from soil (n=8, PE reads =374 879 346) and seawater (n=3, PE reads =142 336 042). Assembly with metaSPAdes and IDBA-UD failed despite the large size of these libraries and the large allocation of memory and cores provided by KBase. Since the allocation by KBase is likely larger than most institutions can provide themselves, this is essentially a cap on what can be accomplished.

As shown in Figure 8-3, the metaSPAdes and MEGAHIT assemblies provided similar results, while IDBA-UD differed in both assembly size and contig distribution. Modification of the default MEGAHIT assembly parameters to parameters optimal for large complex assemblies did not result in a significant difference. Changing the minimum contig length to include in the assembly resulted in a considerable inflation of the total assembly size, but negligible difference in the distribution of contigs. This suggests potential loss of information about less abundant species occurs when setting a higher contig length cut-off.

However, the most important downstream analyses based on these assemblies includes MAG assembly via anvi'o and the identification of BGCs with potential antimicrobial activity using antiSMASH, both of which have minimum contig length cut-offs. Anvi'o does not include contigs smaller than 2000 bp, and antiSMASH cannot detect large gene clusters from small contigs. Therefore, the assemblies with a lower contig length cut-off are larger overall, there is no impacts on the resulting MAGs due to the requirements of anvi'o. The fact that MEGAHIT provided similar (or superior assemblies) and was faster and more efficient and successful than the other assembly tools made it the assembler of choice for both datasets.

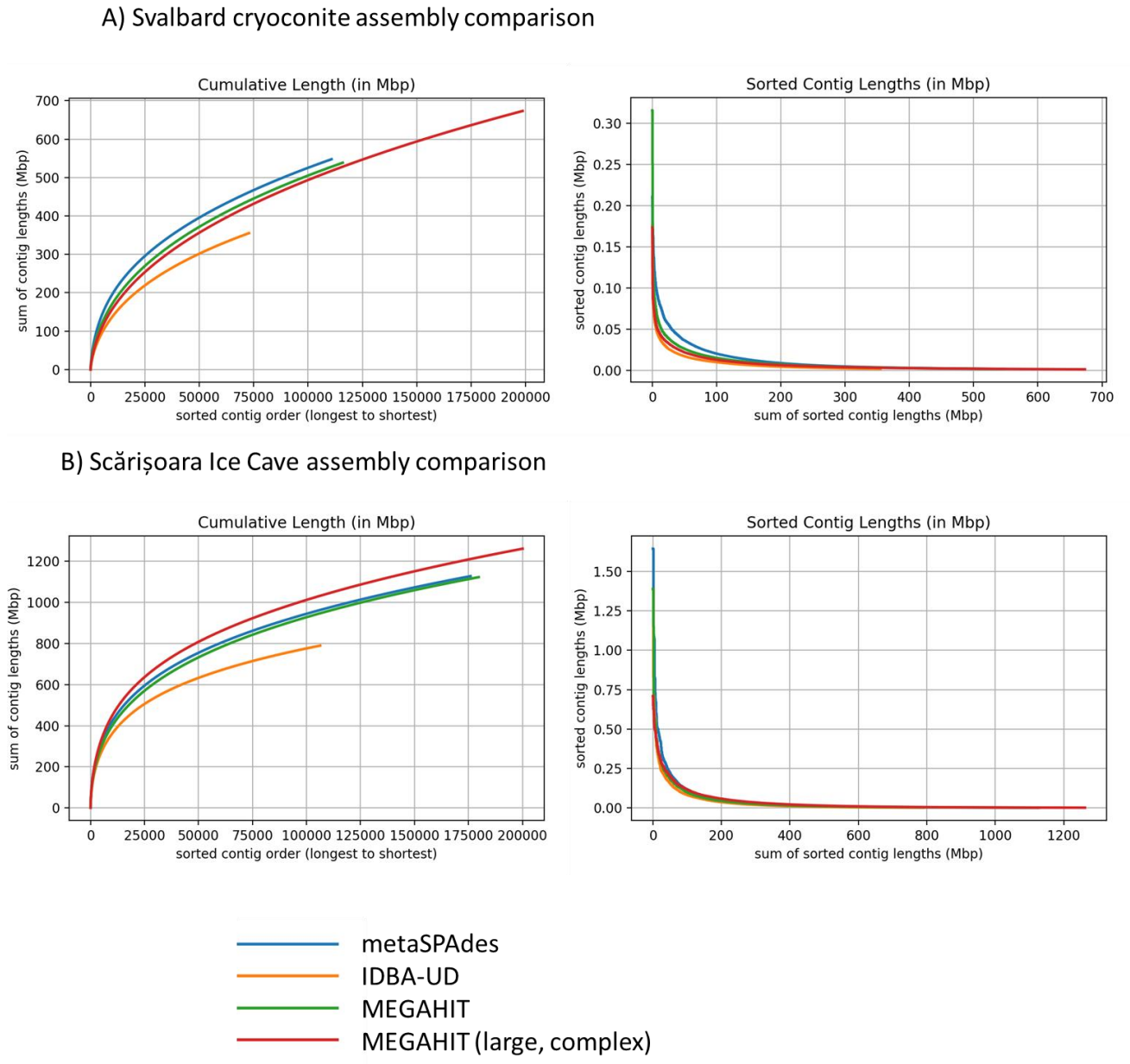

Figure 8-3 Comparison of Svalbard cryoconite and Scărișoara Ice Cave contigs from metaSPAdes, IDBA-UD and MEGAHIT assemblies.

Table 8-4: Comparison of cryoconite metagenome assembly statistics using QUAST

Assembly	Longest Contig (bp)	Nx (Lx)		Length (bp)	Num Contigs	Sum Length (bp)	Contig Length Histogram (1bp - 10Kbp)	Contig Length Histogram (10Kbp - 100Kbp)	Contig Length Histogram (len >= 100Kbp)
cryoconite_ SPAdes.contigs	210693	N50:	5678	>= 10^6	0	0	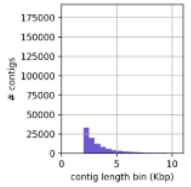	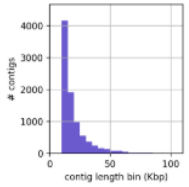	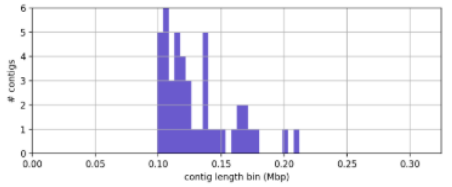
		L50:	(20919)	>= 10^5	45	5887565			
		N75:	3090	>= 10^4	8969	186135969			
		L75:	(54780)	>= 10^3	110819	547654561			
		N90:	2351	>= 500	110819	547654561			
		L90:	(85495)	>= 1	110819	547654561			
cryoconite_ IDBA.contigs	176515	N50:	5506	>= 10^6	0	0	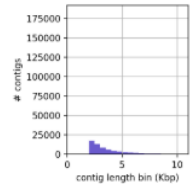	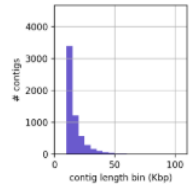	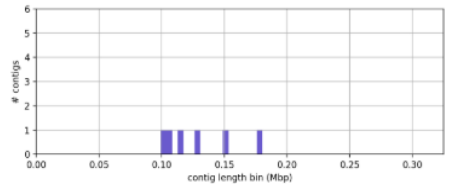
		L50:	(16320)	>= 10^5	6	780937			
		N75:	3206	>= 10^4	5957	102757056			
		L75:	(37936)	>= 10^3	72852	355141001			
		N90:	2451	>= 500	72852	355141001			
		L90:	(57051)	>= 1	72852	355141001			
cryoconite-MEGAHIT .contigs	315846	N50:	5126	>= 10^6	0	0	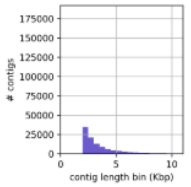	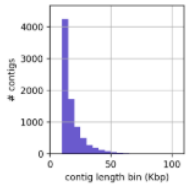	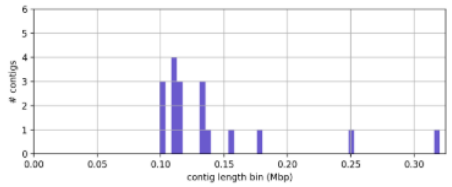
		L50:	(24906)	>= 10^5	18	2524410			
		N75:	2995	>= 10^4	8246	154707901			
		L75:	(60198)	>= 10^3	115949	538521980			
		N90:	2329	>= 500	115949	538521980			
		L90:	(90952)	>= 1	115949	538521980			
large_complex_ MEGAHIT_1500. assembly	173759	N50:	3651	>= 10^6	0	0	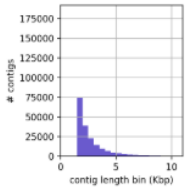	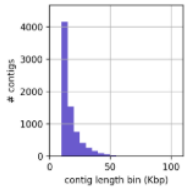	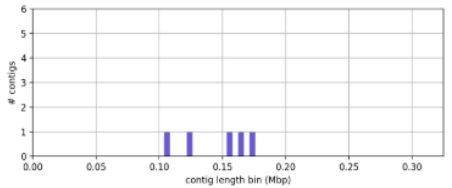
		L50:	(44415)	>= 10^5	5	719522			
		N75:	2212	>= 10^4	7588	135209030			
		L75:	(105081)	>= 10^3	198637	673213276			
		N90:	1736	>= 500	198637	673213276			
		L90:	(156849)	>= 1	198637	673213276			
cryo_MEGAHIT_ 1000.assembly	173758	N50:	2616	>= 10^6	0	0	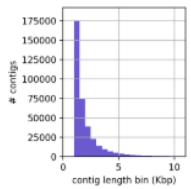	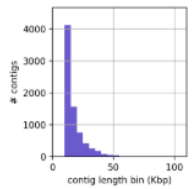	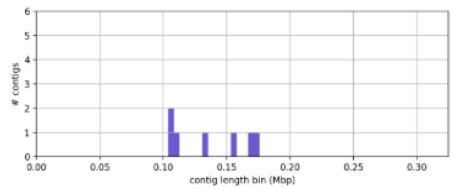
		L50:	(78785)	>= 10^5	7	950683			
		N75:	1533	>= 10^4	7586	135122332			
		L75:	(191785)	>= 10^3	372891	883628882			
		N90:	1174	>= 500	372891	883628882			
		L90:	(291143)	>= 1	372891	883628882			

8.3.3.2 Single or co-assembly

The next comparison was to compare the effect of single assembly and co-assembly on contig distribution and assembly size. Libraries from the Scărișoara Ice Cave were assembled individually and in a co-assembly. As expected, the greater the number of samples combined, the greater the resultant assembly. However, co-assembly works best when samples are similar. Similar samples tend to result in assemblies that are larger than the sum of their parts, because reads from different libraries can combine to build longer contigs, whereas co-assemblies of samples with different microbial communities are generally similar to the sum of the single assemblies. The Ice-Cave co-assembly is quite close to the sum of the individual assemblies (Appendix Table H-5), and the Svalbard co-assembly of all the samples was similar to the sum of the cryoconite, seawater and soil assemblies (Appendix Table H6 and Appendix Figure H-1). Co-assembly was selected for these datasets because there is enormous insight that can be gained from differential mapping, which is best performed on a co-assembly.

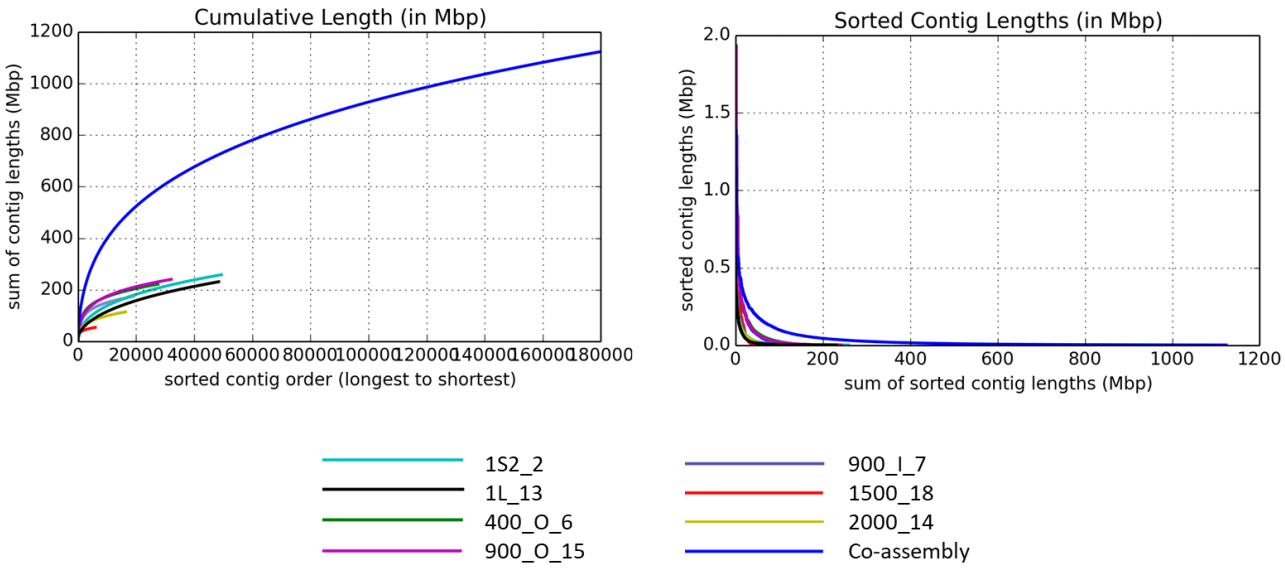

Figure 8-4 Testing single assembly vs co-assembly on the Scărișoara Ice Cave libraries. Scărișoara Ice cave assemblies were assembled individually in a single assembly, and in a co-assembly.

8.3.3.3 Environment complexity

The final test was to compare the effect of environment complexity and heterogeneity on assembly size. To do this, the libraries for each environment type were co-assembled to create seawater (n=3), soil (n=8) and cryoconite (n=6) co-assemblies. From previous analysis of these environments (Chapter 3), the environments differ substantially in heterogeneity and in community composition. For example, soil was found to be extremely heterogenous, with very few shared ASVs between sites, and there were many species, all of which made minor contributions to relative abundance. In comparison, there were many ASVs shared between cryoconite sites on different glaciers, and there were several species that dominated the community with extremely high relative abundance. Finally, the seawater samples were extremely similar and shared many species with each other.

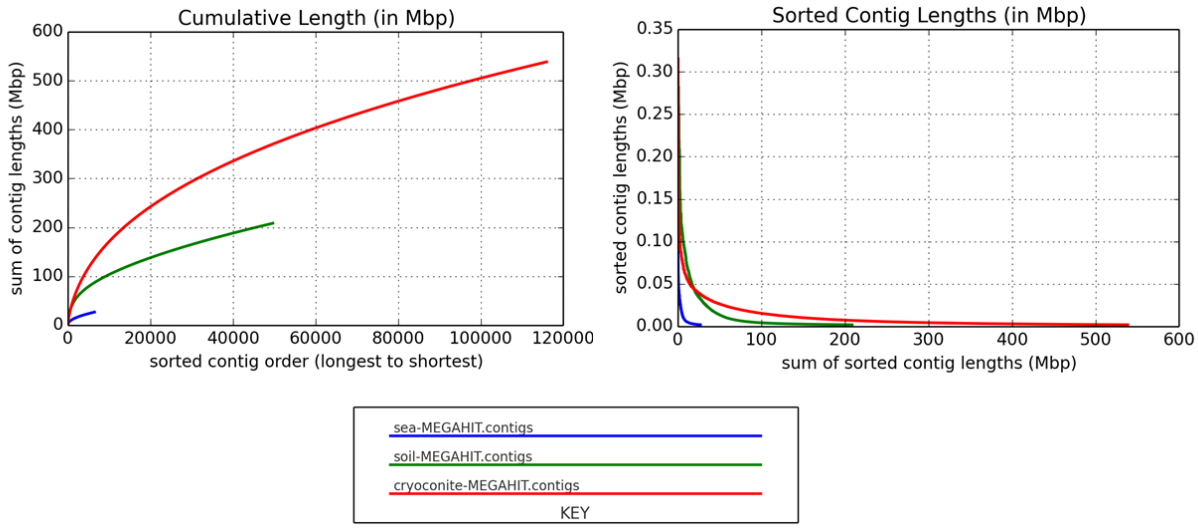

Figure 8-5 Comparison of assembly of different environments. All three assemblies were performed using MEGAHIT with the default parameters.

The seawater assembly is 26 970 110 bp from 142,336,042 reads, the cryoconite assembly is 538 521 980 bp from 201,408,108 reads and the soil assembly is 208 560 096 bp from 374,879,346 reads (Table 8-5). The cryoconite library is significantly larger than both the soil and seawater libraries (Figure 8.5), despite being created from fewer reads than the soil assembly. This comparison reveals the dramatic effect of community heterogeneity and complexity on the size of the assembly, and subsequently, the number and quality of the MAGs that can be constructed.

Table 8-5 Table comparing Assembly statistics and contig distribution of sea, soil and cryoconite assemblies.

Assembly	Longest contig (bp)	Nx (Lx)		Length (bp)	Number of contigs	Sum length (bp)	Contig Length Histogram (1bp <= len < 10Kbp)	Contig Length Histogram (10Kbp <= len < 100Kbp)	Contig Length Histogram (len >= 100Kbp)
sea-MEGAHIT.contigs	115659	N50:	4236	>= 10^6	0	0	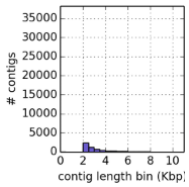	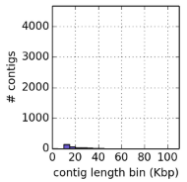	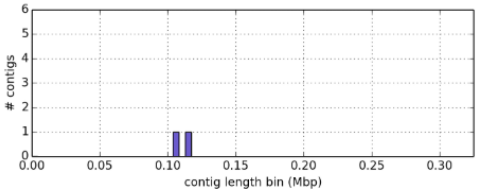
		L50:	(1450)	>= 10^5	2	221424			
		N75:	2686	>= 10^4	321	6766634			
		L75:	(3510)	>= 10^3	6451	26970110			
		N90:	2225	>= 500	6451	26970110			
		L90:	(5171)	>= 1	6451	26970110			
soil-MEGAHIT.contigs	300154	N50:	4111	>= 10^6	0	0	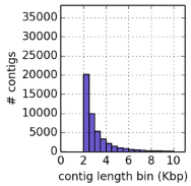	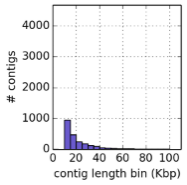	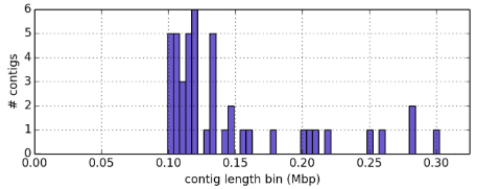
		L50:	(10133)	>= 10^5	45	6597658			
		N75:	2616	>= 10^4	2366	59047038			
		L75:	(26569)	>= 10^3	49641	208560096			
		N90:	2199	>= 500	49641	208560096			
		L90:	(39681)	>= 1	49641	208560096			
cryoconite-MEGAHIT.contigs	315846	N50:	5126	>= 10^6	0	0	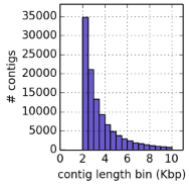	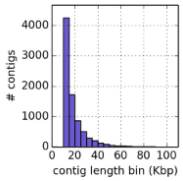	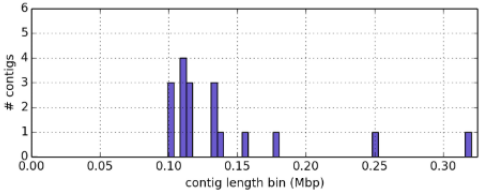
		L50:	(24906)	>= 10^5	18	2524410			
		N75:	2995	>= 10^4	8246	154707901			
		L75:	(60198)	>= 10^3	115949	538521980			
		N90:	2329	>= 500	115949	538521980			
		L90:	(90952)	>= 1	115949	538521980			

8.3.3.4 Comparison of functional annotation of contigs from different assemblies

In addition to understanding how the different assembly tools affected contig length, and assembly size, the assembly tools were compared to see whether there were differences in the downstream functional analyses from these assemblies. Table 8.6 shows a comparison of three assemblers, MEGAHIT (Appendix Table H-2), metaSPAdes (Appendix Table H-3) and IDBA-UD (Appendix Table H-4) on secondary metabolite detection from the Scărișoara Ice Cave using antiSMASH 4.

Table 8-6 Table comparing BGCs detected from contigs form the MEGAHIT, metaSPAdes and IDBA-UD assemblies.

	MEGAHIT	metaSPAdes	IDBA-UD
terpene	269	270	181
nrps	195	174	118
T3PKS	131	130	92
bacteriocin	125	133	88
arylpolyene	118	111	89
nrps-like	109	108	69
betalactone	61	62	42
lassopeptide	54	56	39
hserlactone	53	61	44
acyl_amino_acids	45	45	30
siderophore	31	27	22
T1PKS	30	33	13
resorcinol	21	22	14
hglE-KS	14	11	10
lanthipeptide	11	12	7
ectoine	9	7	7
CDPS	7	7	5
phosphonate	7	5	5
indole	5	3	3
linaridin	4	3	3
butyrolactone	4	5	2
other	4	4	3
ladderane	3	5	3
LAP	3	5	3
NAGGN	3	3	3
PKS-like	1	1	0
PUFA	1	1	0
thiopeptide	1	3	1
cyanobactin	1	1	1
sactipeptide	1	1	1
microviridin	1	2	0
nucleoside	1	1	1
phenazine	1	1	0
T2PKS	0	1	0

The similarity between metaSPAdes and MEGAHIT assemblies (Figure 8-2) are reflected in the antiSMASH results, which are very similar between contigs databases. The greatest number of BGCs were detected using the MEGAHIT assembly (1374) followed by metaSPAdes (1368) and then IDBA-UD (934). The most abundant BGCs were the terpenes, with MEGAHIT and metaSPAdes and IDBA-UD detecting clusters on 269, 270 and 181 contigs respectively. The NRPS were the second most abundant biosynthetic gene cluster type with MEGAHIT, metaSPAdes and IDBA-UD detecting clusters on 195, 174 and 118 contigs, respectively. The similarity between contig annotations suggest that the tools are equivalent.

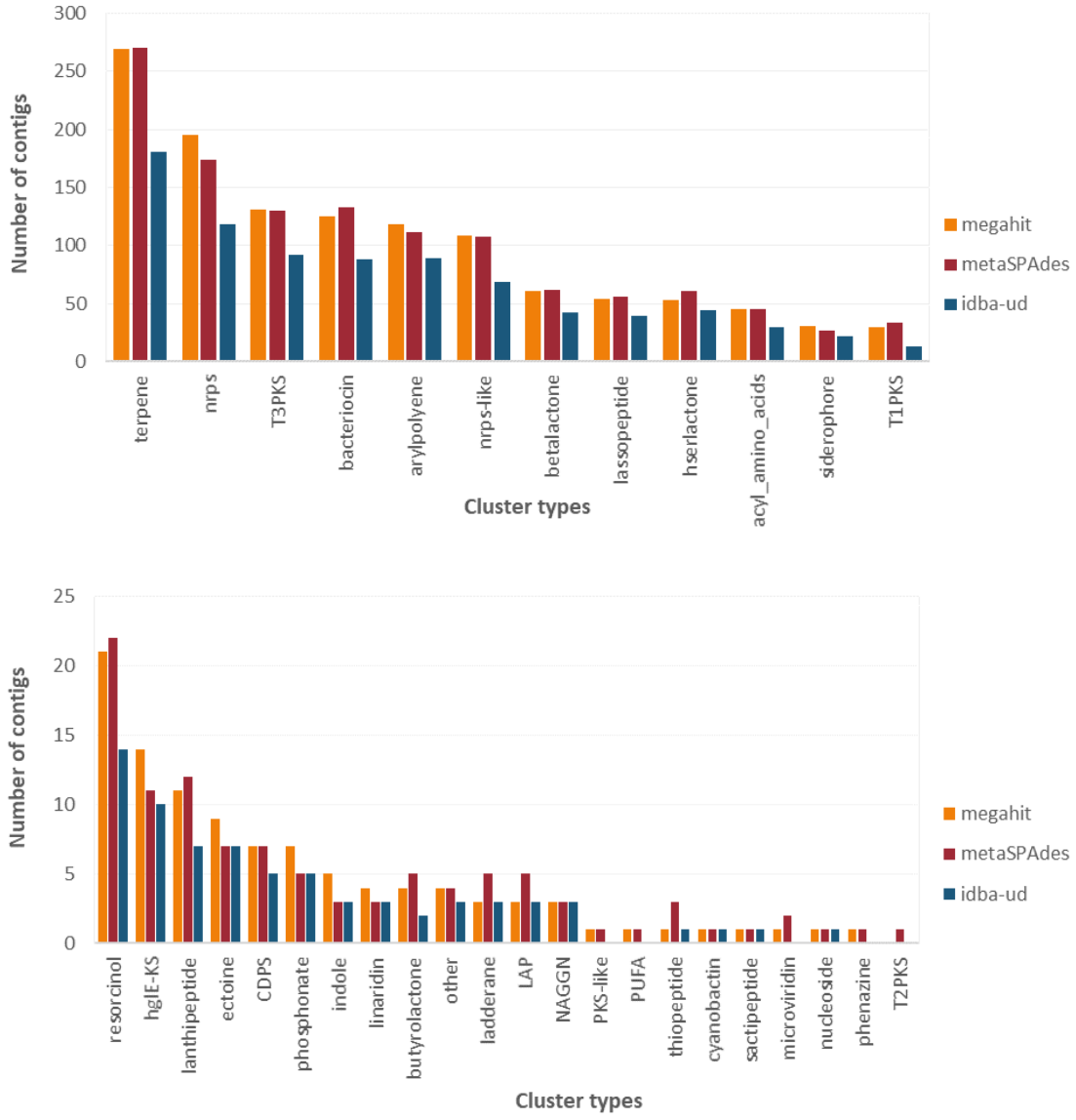

Figure 8-6: Comparison of the choice of assembler on the number and type of secondary metabolite clusters detected by antismash5.

8.3.4 Read Mapping

Read mapping is important because it enables the calculation of coverage across the contigs, (and MAGs) across the different samples. However, it can also be used as a crude indication of sequencing depth. Reads were mapped back to the assembly using Bowtie2. Mapping tells us a lot about the complexity of the environments that were sampled, and the extent to which sampling depth was sufficient to reconstruct the microbial community. The percentage mapped correlates strongly with the size of the assembly for each sample. This in turn depends on the complexity and evenness of the environment. Cryoconite recruited the most reads by far, largely due to skewness in the community structure, with a few key taxa contributing disproportionately to the overall abundance (Chapter 3). Likewise, many reads from the Ludox extraction of Soil sample F3T3 contributed to the assembly, likely because the Ludox extraction method resulted in a lower diversity of organisms (Section 4.4.7.1).

Table 8-7 Alignment rate of reads mapped back to assembly

Sample	Trimmed Paired reads	Overall alignment rate (%)
Svalbard samples		
AB-18	32 454 516	47.48
ML-17	14 397 678	66.29
ML-18	14 235 836	62.62
VB-17	17 252 431	65.56
VB-18	14 893 825	58.97
VL-18	7 469 768	22.32
SS1	25 665 362	5.32
SS2	27 509 748	14.02
SS3	17 992 911	12.79
F3T3_Lud	20 039 798	43.10
F3T3_FD	56 877 004	8.61
F3T3_PM	22 457 762	9.07
F1T3_S4	18 842 083	5.29
F1T4_S5	19 381 248	4.88
F2T2_S6	14 558 022	7.75
F3T1_S7	17 741 236	7.94
F2T4_S8	17 542 420	3.00
Scărișoara Ice Cave		
1S_2	69 575 748	21.59
1L_13	72 190 896	9.96
400_O_6	76 039 348	32.94
900_O_15	73 462 594	31.98
900_I_7	75 113 102	45.46
1500_18	75 510 556	46.92
2000_14	63 569 516	41.86

The soil libraries had the lowest proportion of reads mapped back to contigs, ranging from 3% to 9.07% (Table 8-7, Figure 8-7). The F3T3_Lud library was an exception with a much higher alignment rate (43.10%), which is reflective of a significant enrichment, caused by diversity loss in this specific DNA extraction method. The low alignment rate of the soil libraries reflects the high diversity and heterogeneity of this environment, (also shown in Chapter 3). The cryoconite libraries had the best alignment rate. Cryoconite is dominated by a core of highly prevalent and abundant bacteria, and a long tail of rare taxa. The high alignment fraction likely represents the high coverage of contigs (and MAGs) belonging to this abundant core community.

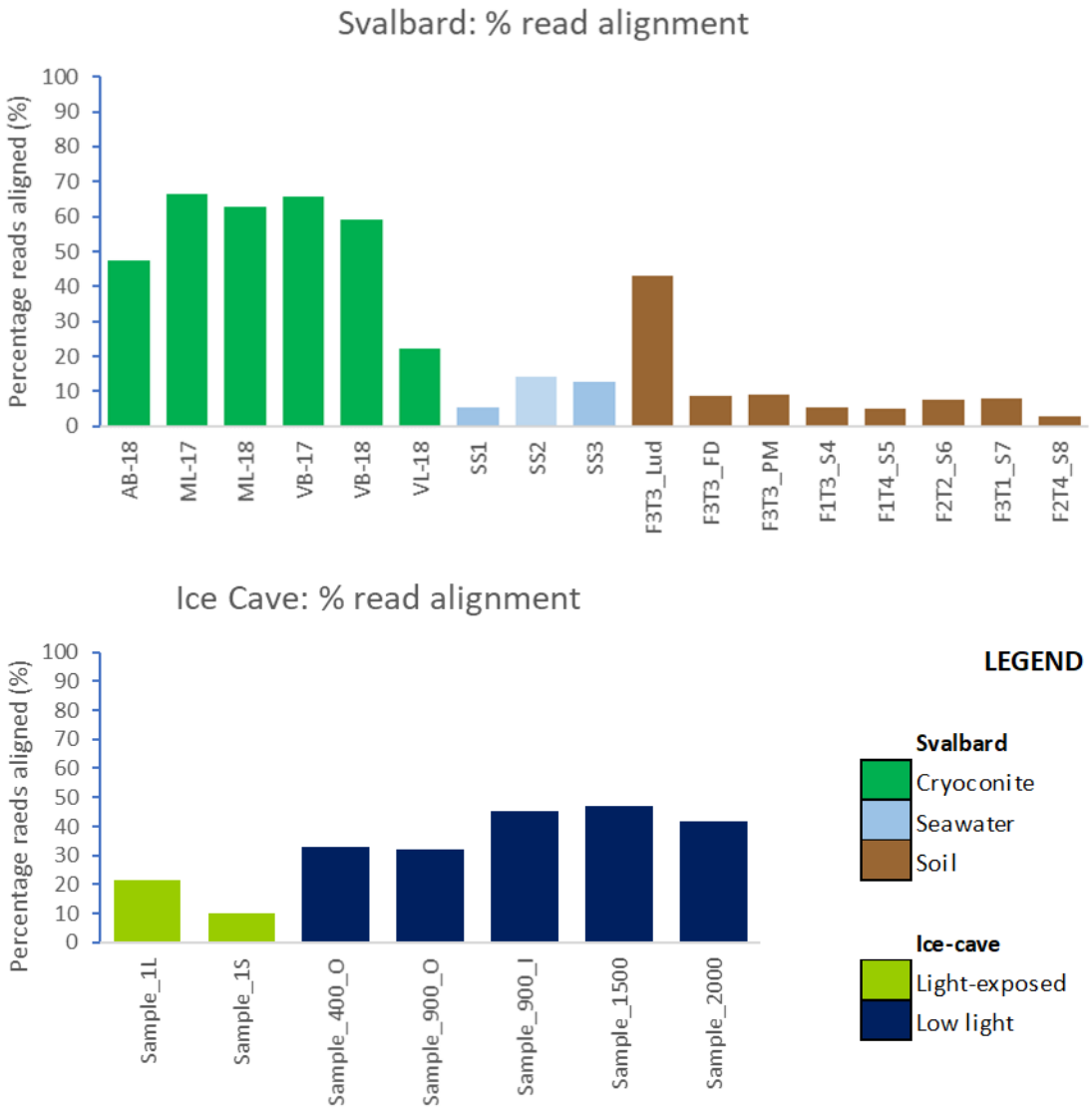

Figure 8-7: The percentage of reads aligned to the contigs reflects the complexity of the communities in each environment type and at each site.

8.3.5 The performance of different binning tools

Both datasets were binned using four different binding methods: CONCOCT (Alneberg et al., 2014), MetaBAT2(Kang et al., 2015), MaxBin2 (Wu et al., 2016) and DAS Tool (Sieber et al., 2018). DAS Tool is designed to score, select, and optimise bins produced using other binning methods. A summary of the number of bins and the average completion and redundancy estimates obtained using each binning methods is shown in Table 8-8, and Figure 8-8.

Table 8-8 Binning tool comparison for the Svalbard and Ice-Cave datasets

Ice Cave				
Tool	**CONCOCT**	**MaxBin2**	**MetaBAT2**	**DAS Tool**
Number of bins	270	253	401	145
No of Nucleotides	1,123,284,953	758,127,487	790,621,951	502,443,977
% Nucleotides	100	67.49	70.38	44.73
Number of contigs	179753	132573	84984	53815
% contigs included	100	73.75	47.28	29.94
Ave completion	57.45	46.06	32.59	85.12
SD completion	36.78	32.21	35.91	11.48
Ave redundancy	28.84	15.62	2.28	5.71
SD redundancy	61.17	19.79	6.95	6.62
Ave size (length) (bp)	4160315	2996551	1971626	3465131
SD length (bp)	3867430	2137964	1758817	1620512
Svalbard				
Tool	**CONCOCT**	**MaxBin2**	**MetaBAT2**	**DAS Tool**
Number of bins	151	180	226	95
No of Nucleotides	720,998,358	664,863,606	471,439,592	322,990,650
% Nucleotides	100%	92.21	65.39	44.80
Number of contigs	162,105	150,327	73,975	45,400
% contigs included	100%	92.73	45.63	28.01
Ave completion	50.17%	55.05	39.48	83.11
SD completion	36.99%	32.24	36.94	14.09
Ave redundancy	52.78%	20.48	3.25	6.42
SD redundancy	131.14%	21.93	6.28	7.04
Ave size (length) (bp)	4 774 824	3 693 687	2 086 016	3 399 902
SD length (bp)	7 825 034	1 893 821	1 648 078	1 369 520

CONCOCT always binned 100% of the contigs. However, although it retained the largest portion of the data, it has the highest level of redundancy and largest bin sizes. This is likely a choice by the anvi'o team, who set the default parameters to err on the size of having bins that were too large, and could therefore be split in manual refining, rather than bins that had accidentally been split, which are much harder to detect and combine at a later stage. In both datasets, MaxBin2 retained the second greatest number of contigs. In the Svalbard dataset, contigs were split into slightly more bins than CONCOCT, whereas the Ice Cave dataset had fewer bins.

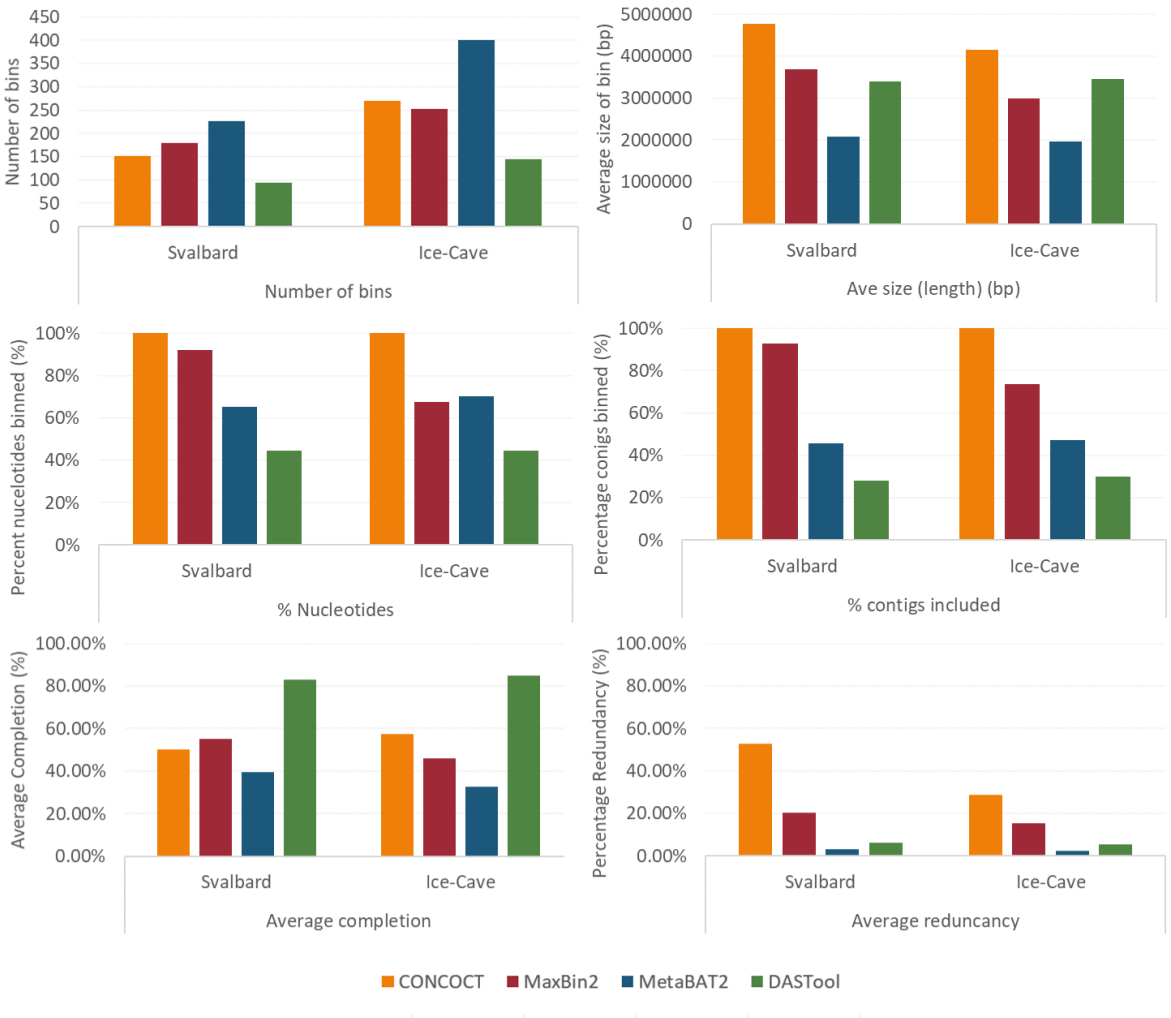

Figure 8-8: Comparison of different CONCOCT, MaxBin2, MetaBAT2 and DAS Tool binning methods on the Svalbard and Ice Cave datasets.

The average completion of those bins was higher in the Svalbard dataset, and lower in the Ice Cave dataset, and the redundancy was greatly reduced, compared to CONCOCT, but still higher than metaBAT2 and DAS Tool. MetaBAT2 had the largest number of bins in both datasets. In comparison to CONCOCT, the algorithm seems to have favoured splitting the bins, which is why this method had both the largest number of bins, but also the lowest redundancy in both datasets. This aggressive splitting did influence completion, where it had the lowest percentage completions of all the methods. Finally, DAS Tool, which optimises bins created using the other tools, had the highest completion, the second lowest redundancy, with a good average bin size commensurate with expected bacterial genome sizes. However, this quality came at the expense of data, and this tool resulted in the least number of bins, and the lowest percentage contigs and nucleotides. The individual bins from the Svalbard and Ice-Cave datasets are plotted in Figure 8-9 and Figure 8-10 respectively.

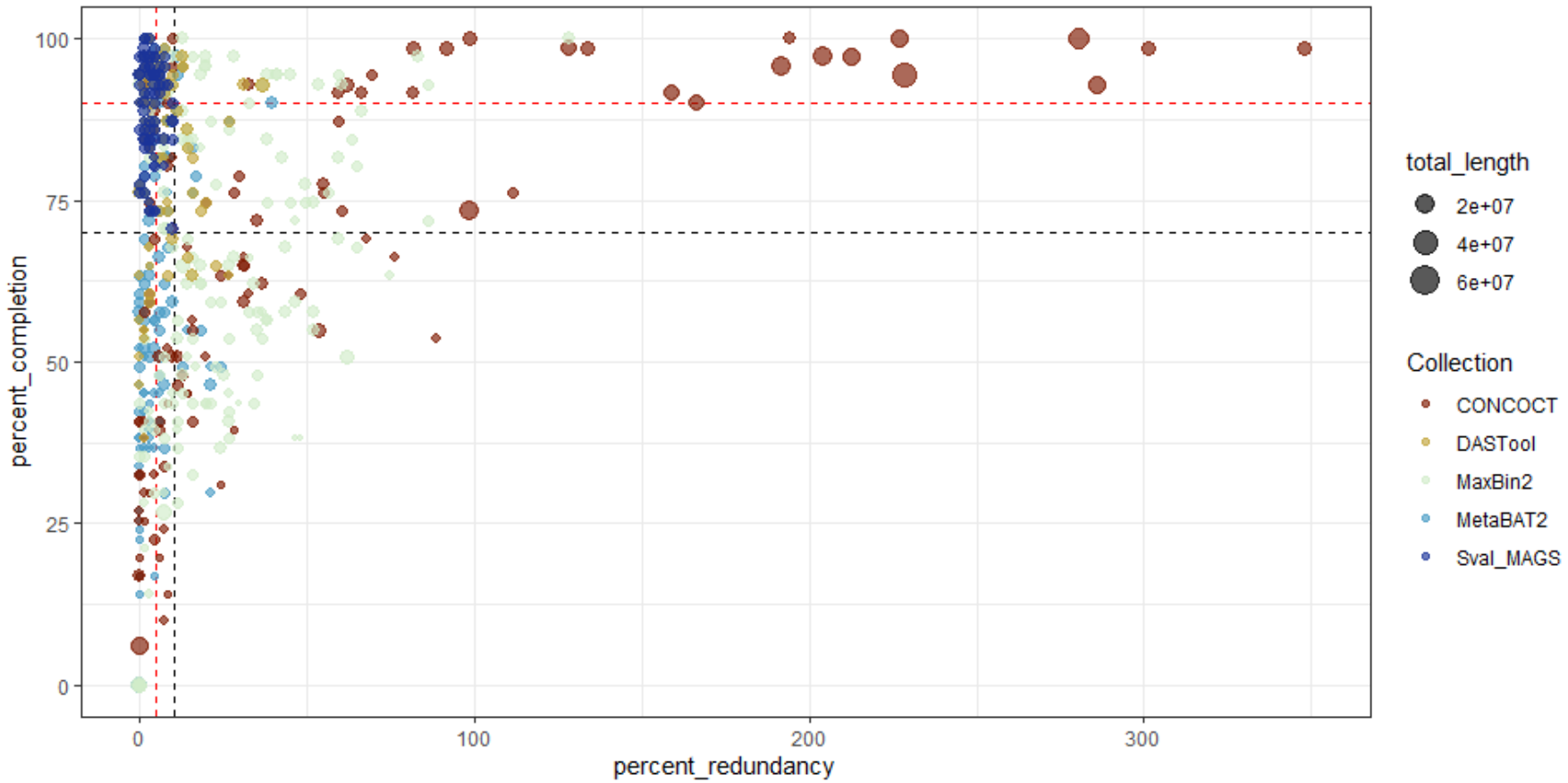

Figure 8-9 Comparison of binning tools for refining MAGs from the Svalbard dataset. Scatterplot showing percent redundancy (x-axis) and percent completion (y-axis) for the bins resolved using CONCOCT, MaxBin2, MetaBAT2 and DAS Tool, as well as the final MAG collection. The binning tool is shown represented by colour, and the size of the bin is represented by point size. A horizontal line at 5% and 90% on the x- and y-axis respectively represent the criteria for high quality MAGs. The grey dashed line at 10% and 70% on the x- and y-axis respectively represent the criteria for inclusion in this study. Four outlier bins from CONCOCT with redundancy > 350% are not shown.

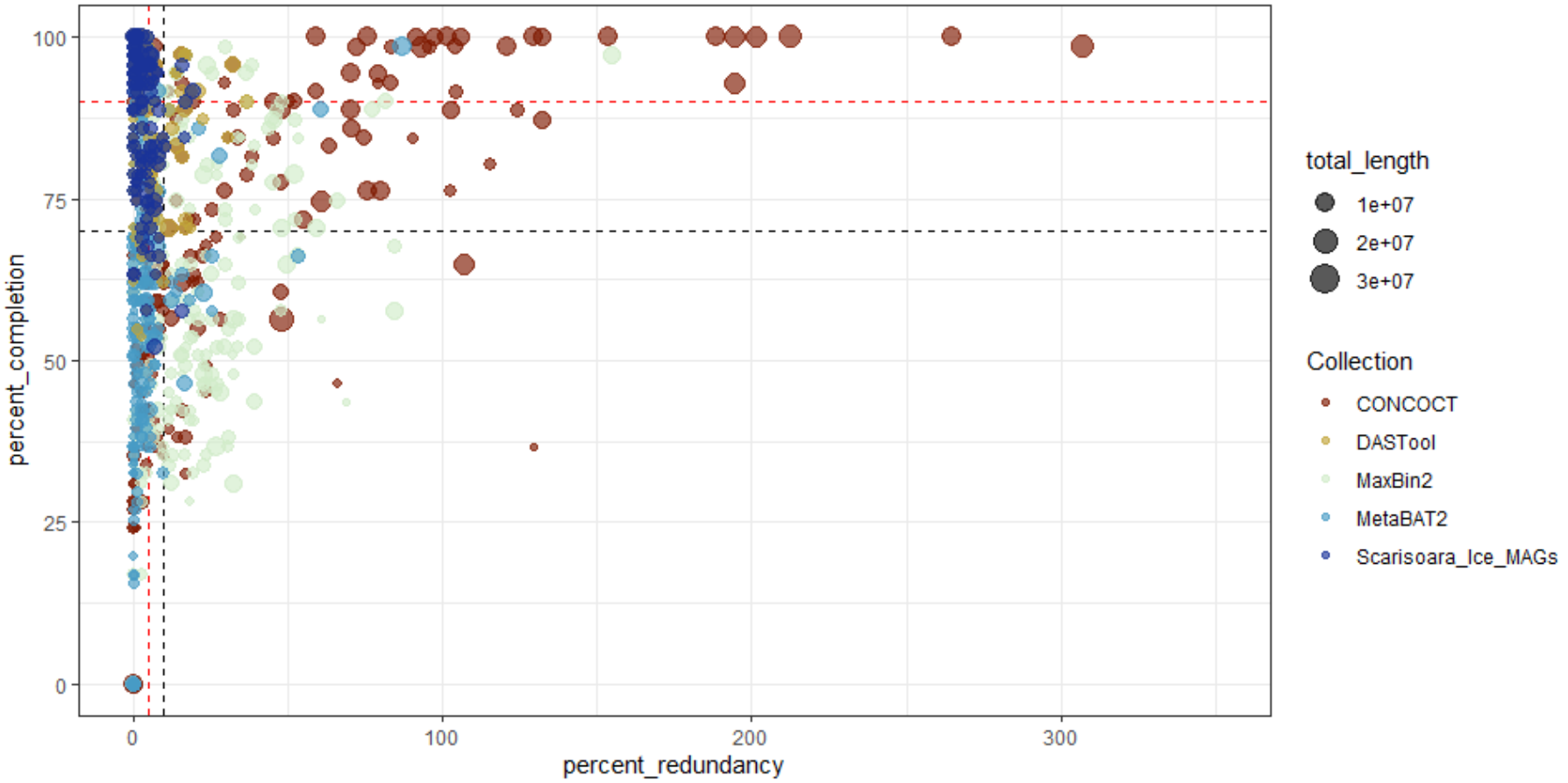

Figure 8-10 Comparison of binning tools for refining MAGs from the Ice-Cave dataset. Scatterplot showing percent redundancy (x-axis) and percent completion (y-axis) for the bins resolved using CONCOCT, MaxBin2, MetaBAT2 and DAS Tool, as well as the final MAG collection. The binning tool is shown represented by colour, and the size of the bin is represented by point size. A horizontal line at 5% and 90% on the x- and y-axis respectively represent the criteria for high quality MAGs. The grey dashed line at 10% and 70% on the x- and y-axis respectively represent the criteria for inclusion in this study. Two outlier bins from CONCOCT with redundancy > 350% are not shown.

8.3.6 Manual refinement in anvi'o

There are several studies, especially when they involve enormous datasets and thousands of MAGs, that do not go beyond the automatic binning of contigs by binning tools (Parks et al., 2015; Shaiber and Eren, 2019). However, automatic binning tools can often get contig membership wrong, and here, anvi'o provides an excellent tool for the manual refinement of bins (Eren et al., 2015). Every bin in the two datasets was manually refined. Occasionally this was done in an iterative process, where refined bins were rerun through DAS Tool, together with unrefined bins to see whether the newly defined bins scored better or worse than the automatic bins. A comparison between all the different binning methods, which also includes the final bins is shown in Figures 8-9 and Figure 8-10 for the Svalbard and Ice Cave datasets, respectively. The effect of the final manual refinement on the DAS Tool bins quality is shown in Figure 8-14 and Figure 8-15. Manual refinement was greatly assisted by the method described (Section 8.2.5) where the bin membership of each contig was imported as a data layer and could be viewed in anvi-refine. This view enabled several easy refinements that could be performed unambiguously and confidently.

8.3.6.1 High-quality and poor-quality bins

In a complete and uncontaminated bin, one expects coverage to be even across a single sample, and the relative proportion of reads across samples to be relatively constant. There should be at least one sample that contains every single contig. Figure 8-11 is a good example of a bin that contains mis-binned contigs. In Figure 8-11 no samples contain all the contigs. Contigs from several organisms, from different environments and sites, have erroneously been binned together. The mis-binning may have occurred because these are related species, with similar GC content and TNF ratios that resulted in the binning algorithm clustering them together. If this is a large bin with high redundancy, this bin may still be salvaged by and be maintained in the dataset as at least one, and possibly more refined bins.

An example of a high-quality bin is shown in Figure 8-12. The coverage is even across a single sample site and relative coverage cross the sample sites is also even. The different binning methods all concur on bin membership. In a poor-quality (incomplete, mixed, or chimeric) bin (Figure 8-13), contigs might have different distribution within and across samples. As a result, binning methods might disagree about bin membership of different contigs. These aspects of bin quality do not often come out in summary statistics. However, the visualisation of contigs, and their bin membership quickly highlights ambiguous contigs and bins.

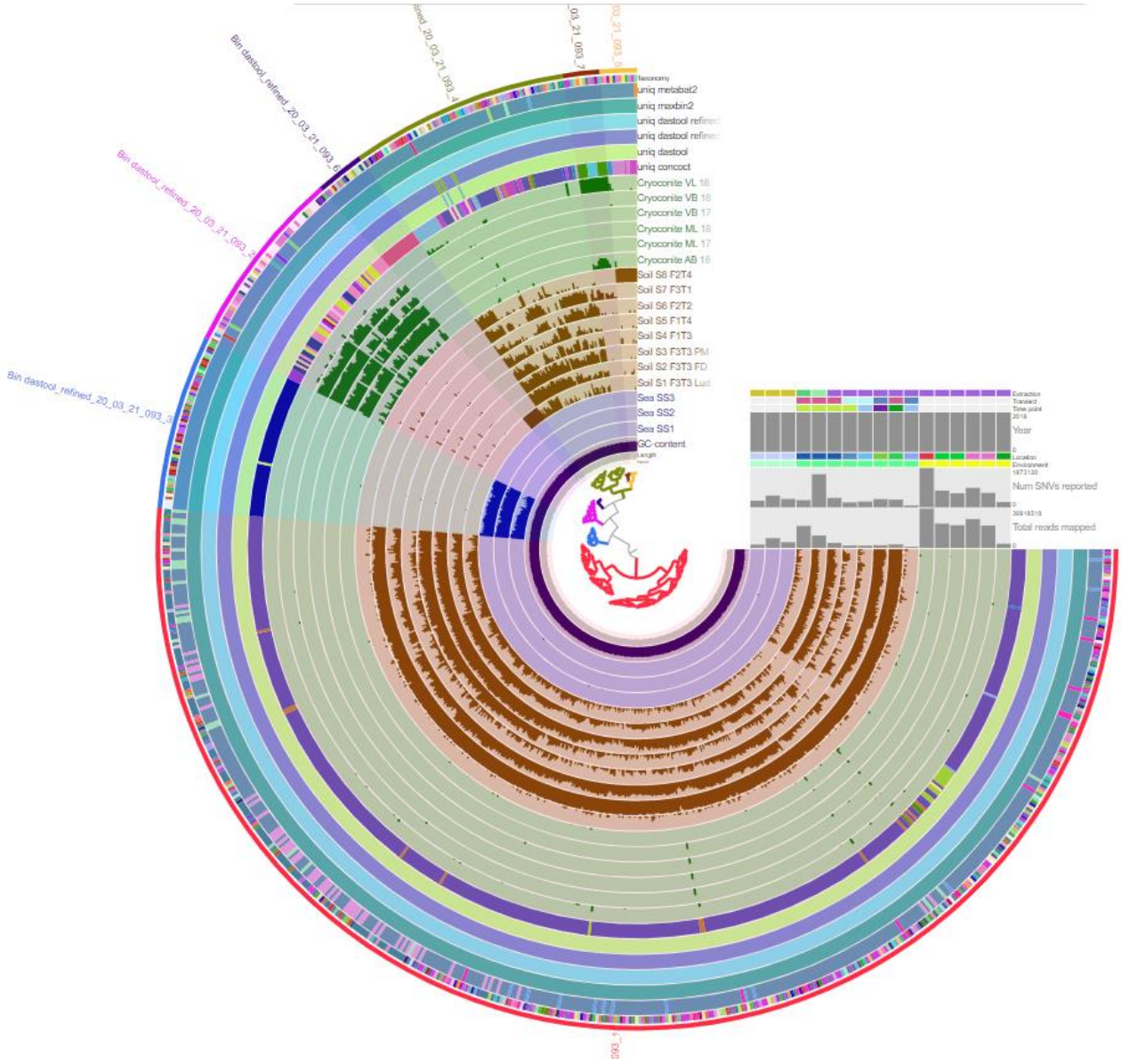

Figure 8-11 Example A: Bin that is not complete across a single sample, and has varying levels of coverage in different samples

This is a refined DAS Tool bin based off a MaxBin2 bin. The bin is easy to refine based on coverage across different samples. Contigs belonging to seawater species, at least two different cryoconite species and several soil species are easy to discern. This bin is likely not salvageable, as each ‘refined’ bin from this collection will likely contain too few contigs and be too incomplete to meet miMAG standards. However, refinement is iterative, and the split bins can be viewed and assessed in subsequent rounds.

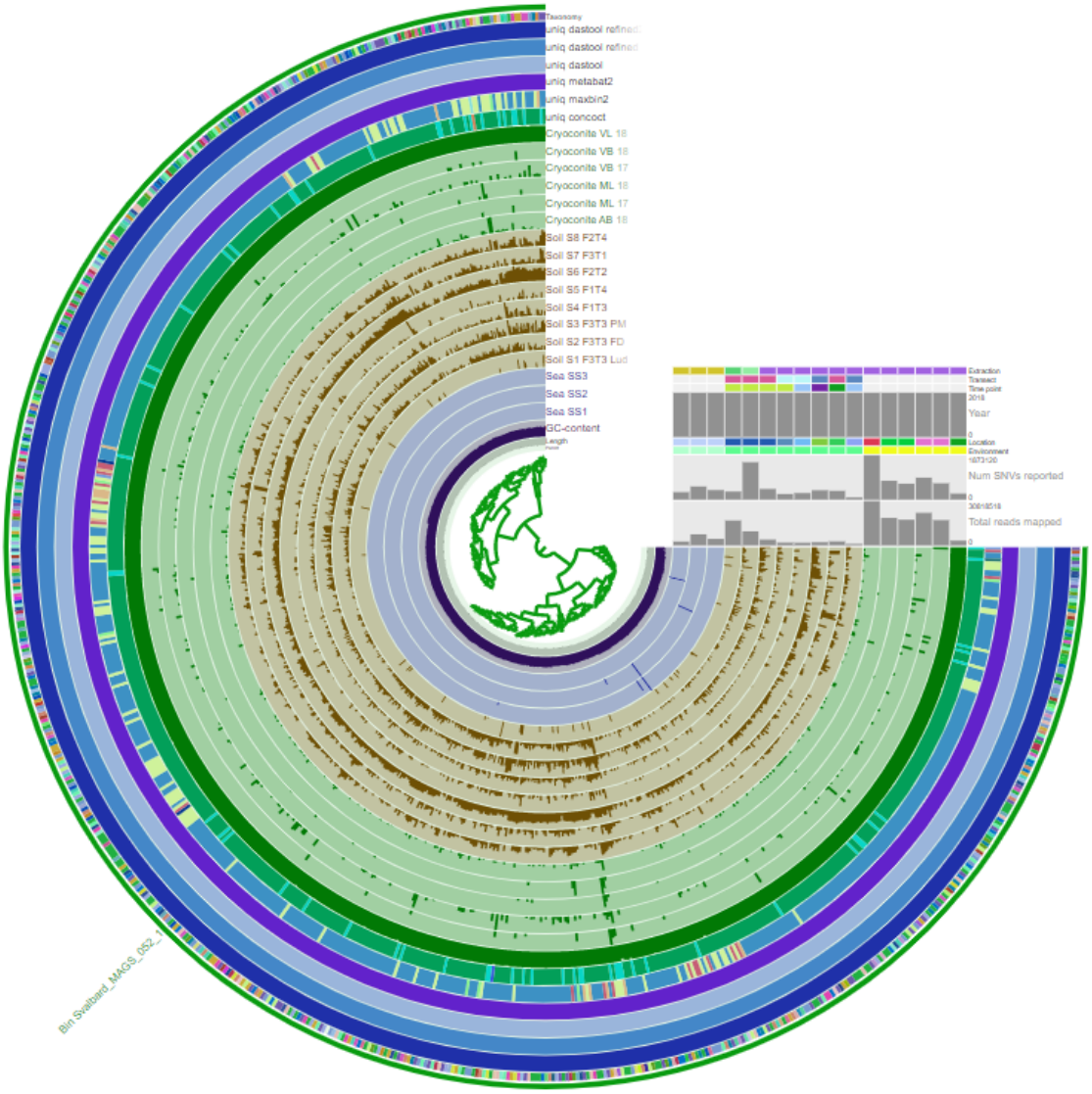

Figure 8-12: Example B: Bin has high consensus between binning methods and consistent coverage cross a single site.

This bin has high consensus between all the binning tools and even coverage across all of the contigs. DAS Tool selected this bin from a metaBAT2 bin.

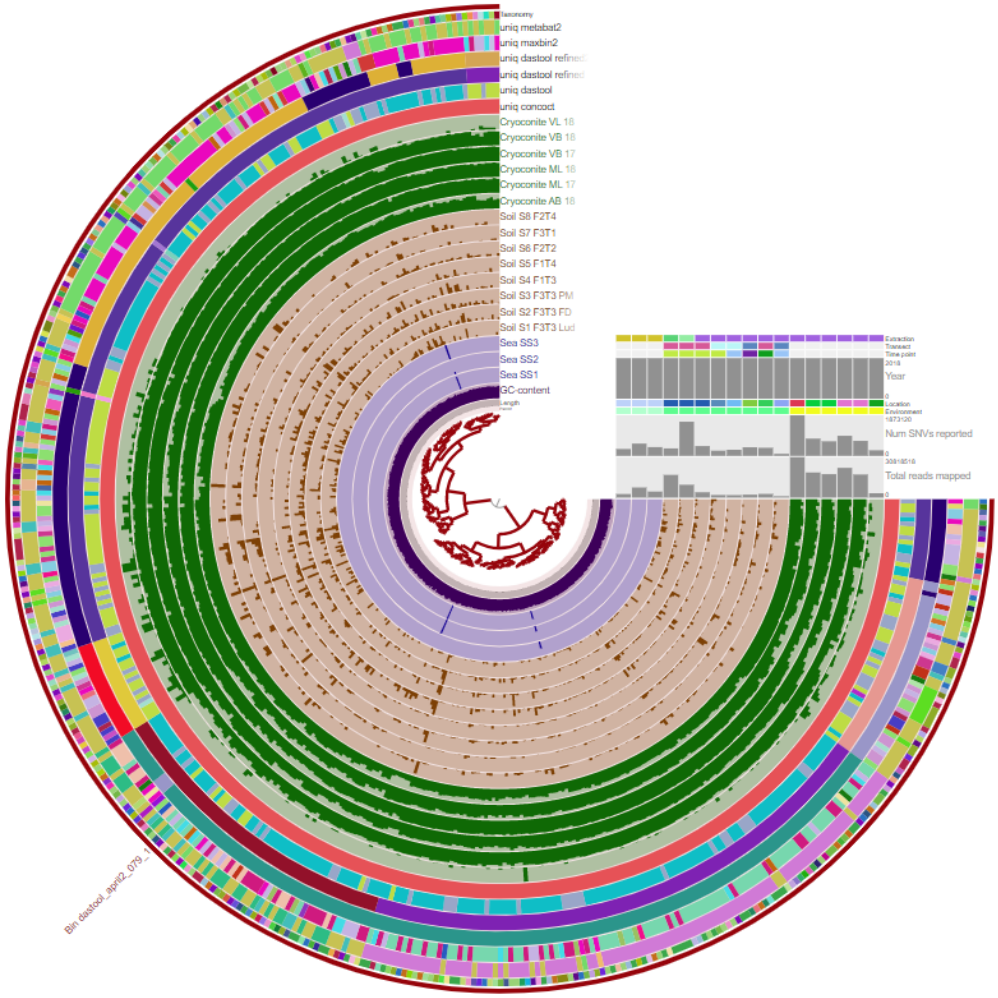

Figure 8-13: Example C: Bin with low consensus between binning methods, and variable coverage across contigs and across samples.

This bin is from the CONCOCT collection. There is very little consensus between this bin and the other binning tools. CONCOCT has accurately binned contigs with high coverage in cryoconite and low coverage in soil and seawater. However, there is variability in the depth of coverage in the different contigs, and he GC content is also variable. The Kaiju taxonomy is mixed.

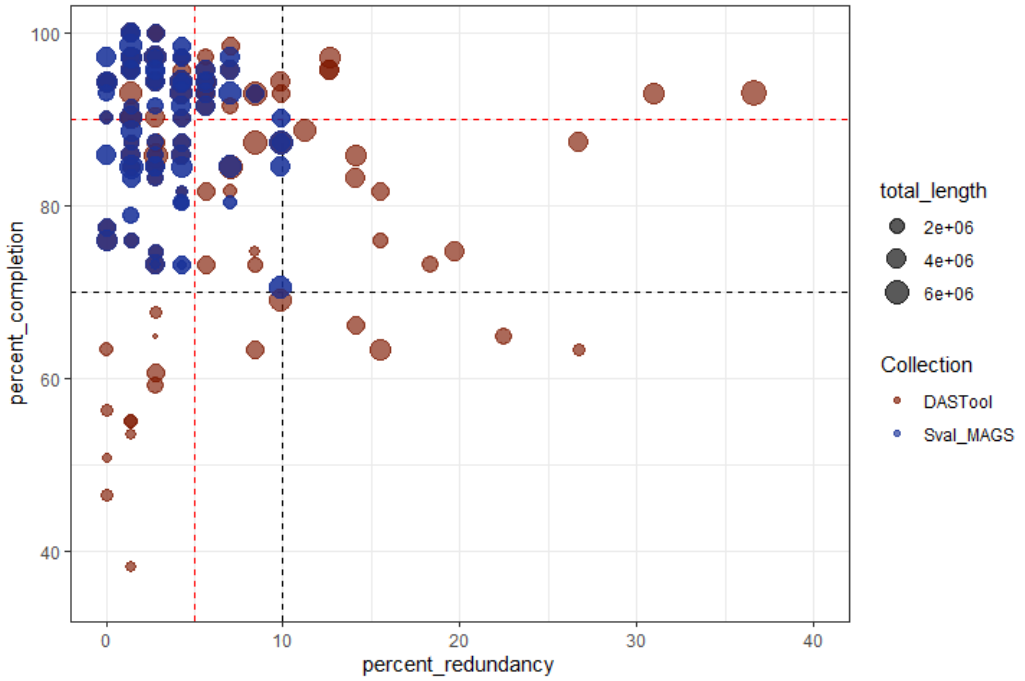

Figure 8-14 Scatterplot showing the effect of the manual refinement step on bin quality (completion and redundancy). A red horizontal line at 5% and 90% on the x- and y-axis respectively represent the criteria for high quality MAGs. The grey dashed line at 10% and 70% on the x- and y-axis respectively represent the criteria for inclusion in this study.

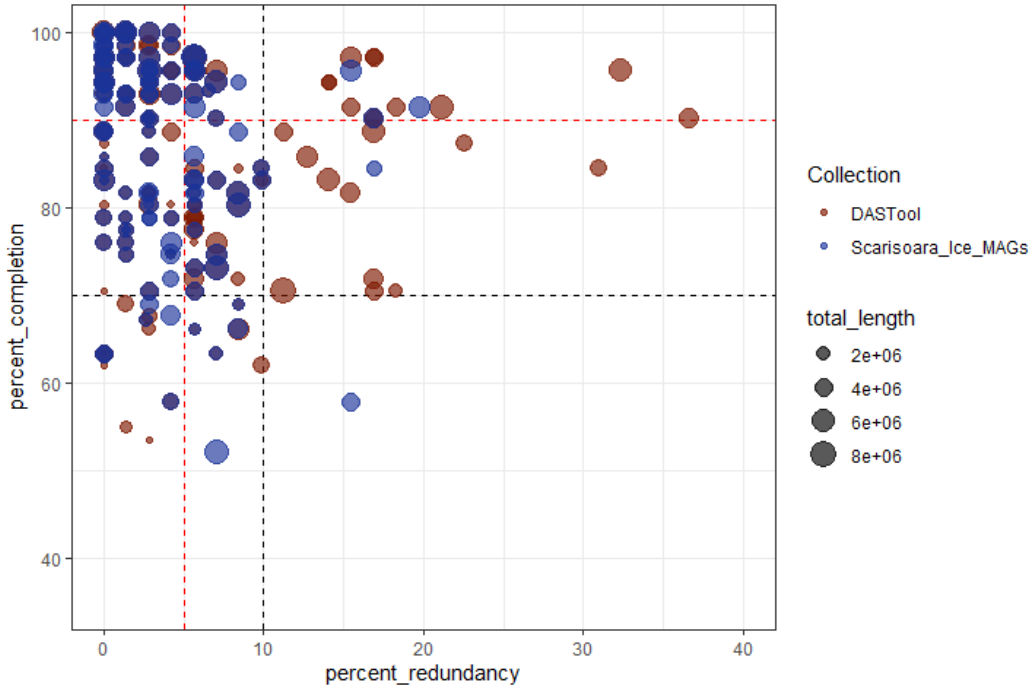

Figure 8-15 Scatterplot showing the effect of the manual refinement step on bin quality (completion and redundancy). A red horizontal line at 5% and 90% on the x- and y-axis respectively represent the criteria for high quality MAGs. The grey dashed line at 10% and 70% on the x- and y-axis respectively represent the criteria for inclusion in this study.

8.3.7 Genome completeness and quality

The completeness and quality of MAGs can be assessed using several tools. Within the anvi'o workflow, it is possible to estimate completeness and redundancy of the contigs in a bin by using HMM hits against a curated collection of 70 single copy bacterial genes (Lee, 2019). This estimate is available during the refinement process and makes it possible to refine bins, and discard those that fall short of the quality criteria set out by Genomic Standards Consortium (GSC), in the Minimum information about a metagenome-assembled genome (MIMAG) standard, one of the most important of which being that completion should be at least 80% and redundancy or 'contamination' less than 10% (Bowers et al., 2017). Although a fantastic method for refinement and estimates, applying the quality cutoff criteria for the bins at this stage may ultimately lead to over-fragmentation of bins, or discarding bins that may be complete. CheckM is another tool that estimates completeness, but it does so by using SCGs that belong to different lineages of bacteria (Parks et al., 2015). CheckM is arguably a better tool, since it considers the fact that some clades will contain more than one copy of certain genes and may be missing others.

The difference between the completion and redundancy estimates of the Ice Cave MAGs using the 71 Bacterial SCGs and CheckM is shown in Table7-4.

8.3.8 Databases and tools for the annotation of reads, contigs and MAGs

8.3.8.1 BGC detection

There are a number of bioinformatics tools that can be used in NP research (reviewed in (Chavali and Rhee, 2018; Loureiro et al., 2018; Tracanna et al., 2017; Weber and Kim, 2016). The various tools and databases can be specialised by class of molecule, by organism or domain, or by its ability to predict NP product structure and link to external databases. One of the most commonly used and comprehensive of these tools is antiSMASH (antibiotics and Secondary Metabolite Analysis SHell) (Blin et al., 2019b; Weber et al., 2015). AntiSMASH has algorithms able to detect a vast range of different BGCs, and many different molecule families. These different molecules families have diverse functions such as antimicrobial compounds, exopolysaccharides, UV pigments, antioxidants, fatty acids.The antiSMASH results from the Svalbard MAGs (Section 5.3.2), individual cryoconite, soil and seawater assemblies (Section 5.3.6) and Ice-Cave MAGs (Section 7.3.8), and entire MEGAHIT, IDBA-UD and metSPAdes assemblies (Section 8.3.3.4) have previously been shown.

8.3.8.2 Enzyme bioprospecting

The contigs from the megahit assemblies of the Ice Cave and Svalbard datasets were submitted in batches to the dbCAN2 webserver (http://bcb.unl.edu/dbCAN2/index.php) (Zhang et al., 2018), which queries the Carbohydrate-Active EnZymes database (CAZy) (Cantarel et al.,2009; Lombard et al., 2014) (http://www.cazy.org/) using DIAMOND, HMMER and HotPep (Figure 8-16).

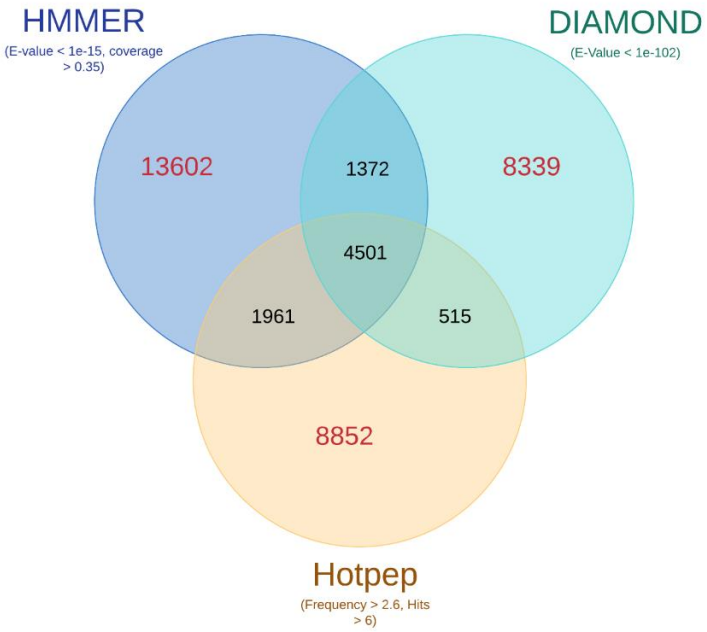

Figure 8-16 Example of a summary of carbohydrate-active enzymes hits in contigs from the cryoconite MEGAHIT assembly, using each of the tools: HMMER, DIAMOND and HotPep. A total of 8349 of the detected enzymes were detected by more than one tool, while 4501 of the enzymes were detected using all three tools.

Screening the contigs databases of the different environments is useful to distinguish the range of different enzyme families present, and the number of variants within each family. In bioprospecting, an extremely useful enzyme may be found in a rare taxon and cloned into a model organism. Therefore, the present of the enzyme is more important than the abundance of the enzyme in the community, as these genes, once identified, can be amplified using specific primers. Therefore, dbCAN2 screening of contigs rather than MAGs can be used to make abundance agnostic screening, and the contigs of interest can be identified independent of taxonomic affiliation and abundance.

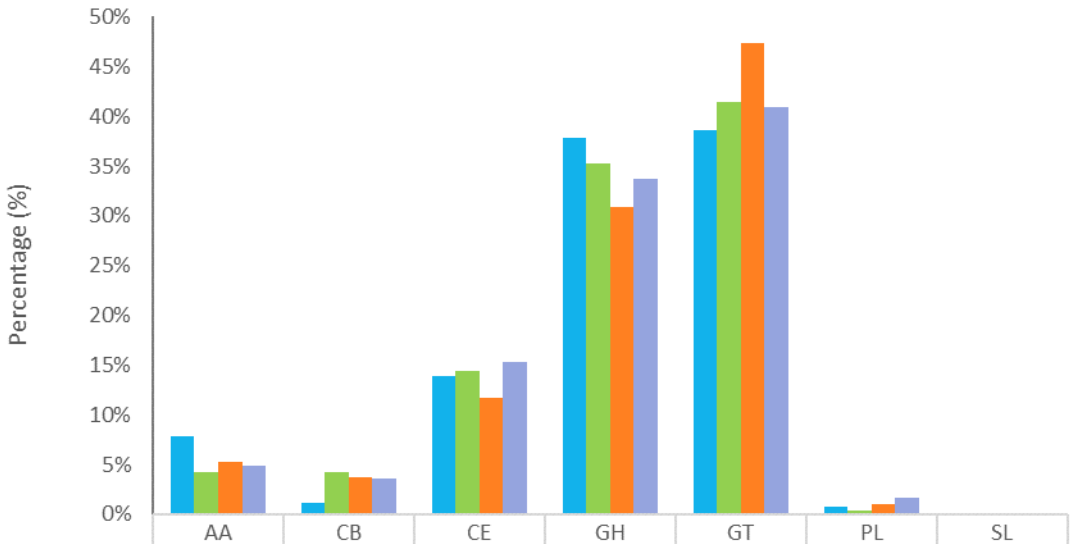

	AA	CB	CE	GH	GT	PL	SL
Seawater	8%	1%	14%	38%	39%	1%	0%
Cryoconite	4%	4%	14%	35%	41%	0%	0%
Soil	5%	4%	12%	31%	47%	1%	0%
Ice-cave	5%	4%	15%	34%	41%	2%	0%

Figure 8-17 Relative abundance of carbohydrate active families in seawater, cryoconite, soil and Ice-Cave contigs.

In total, there were 267 enzymes in the seawater, 13604 in cryoconite, 5053 in soil and 24313 enzymes detected in the Ice Cave. The largest proportion of enzymes belonged to the Glycosyl Transferases (GTs) class, ranging from 39% in seawater to 47% in soil, which are responsible for the formation of glycosidic bonds. Enzymes like these would be important during EPS synthesis. The second most abundant class was the Glycoside Hydrolases (GHs) which are responsible for the hydrolysis and/or rearrangement of glycosidic bonds. These enzymes had the highest relative abundance (RA) in seawater (47%), and the lowest RA in soil (31%). Carbohydrate Esterases (CEs) which perform hydrolysis of carbohydrate esters were the next most abundant family, followed by the Auxiliary Activities (AAs) family of redox enzymes that act in conjunction with CAZymes. Several enzymes with carbohydrate-binding modules (CBM), were also detected. The lowest abundance enzymes were the Polysaccharide Lyases (PLs) which perform non-hydrolytic cleavage of glycosidic bonds.

A Sunburst plot in Figure 8-18 shows some of the most abundant families within these classes. These environments seem enriched with enzymes from the GT4, GT2_Glycos_transf_2, GT2 families from the GT class, GH23 and GH3 from the GH class, CE10, CE1 and CE4 from the CE class, and AA3 from the AA class.

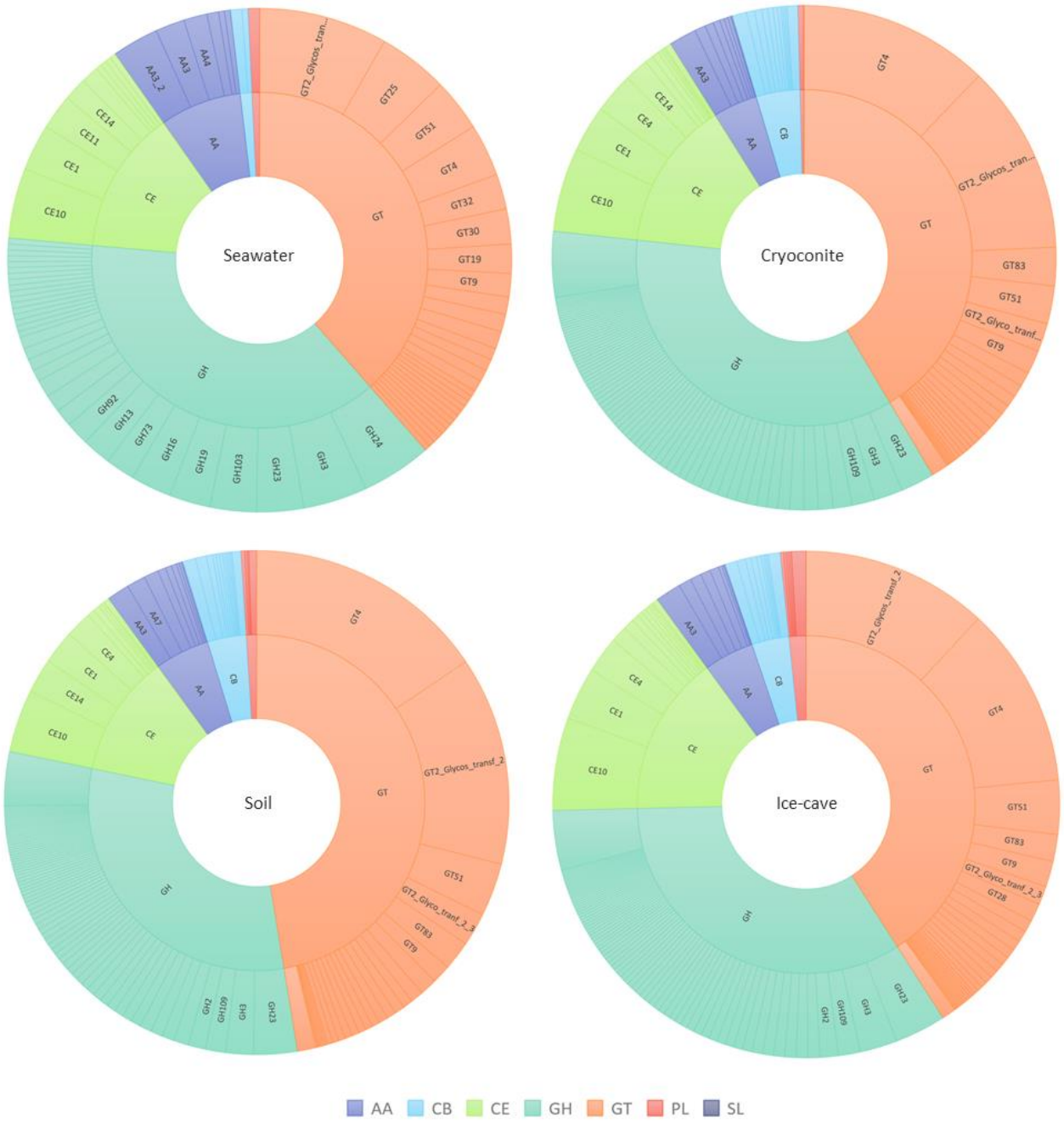

Figure 8-18 Sunburst plots of the major carbohydrate active enzyme classes and the most abundant enzyme families within each class.

Table 8-9 Table of tool and databases

Database	Full name	NP	Applications	Website	Databases accessed	Reference
antiSMASH	antibiotics and Secondary Metabolite Analysis SHell	Polyketides, NRPS, bacteriocins, RiPPs, terpenes, saccharides, fatty acids (and many more)	Antimicrobial compounds, EPS, UV screens, pigments, antioxidants, fatty acids.	https://antismash.secondarymetabolites.org/	MIBiG	(Blin et al., 2017, 2019b, 2019a)
PRISM	PRediction Informatics for Secondary Metabolomes	NRPS, Polyketides	Antimicrobial compounds.	http://grid.adapsyn.com/prism/#!/prism		(Skinnider et al., 2017, 2015)
BAGEL4	BAGEL	Bacteriocins, RiPPs	Antimicrobial compounds.	http://bagel4.molgenrug.nl/index.php		(van Heel et al., 2018)
dbCAN2	(database for) automated Carbohydrate-active enzyme ANnotation	Carbohydrate active enzymes	Food, paper, alcohol synthesis, EPS.	http://bcb.unl.edu/dbCAN2/index.php	CAZy	(H. Zhang et al., 2018)
LED	Lipase Engineering Database	Lipases and esterases	Detergent, food, bioremediation.	http://www.led.uni-stuttgart.de	LED	(Fischer and Pleiss, 2003)
LccED	Laccase Engineering Database	Laccases	Plastic degradation.	https://lcced.biocatnet.de/)	LccED	(Sirim et al., 2011)
Redoxibase	Peroxibase, now Redoxibase	Peroxidases, oxido-reductase	Antioxidants.	http://peroxibase.toulouse.inra.fr/	Redoxibase	(Passardi et al., 2007)

8.4 Discussion

The number and range of tools available to analyse genetic data has rapidly expanded in recent years. In this chapter, the bioinformatics workflow that resulted in two MAG collections is described. In the process of optimizing the workflow, several tools were tested and compared. In addition, a catalogue of additional tools and databases that can be used to investigate these datasets for additional products was compiled. In this thesis, the focus was on the assembly of MAGs as the unit of investigation for bioinformatic bioprospecting. MAGs are useful because phylogenomic information about the microorganism that harbors the gene for the NP of interest can be vital in strategic expression and cultivation efforts.

8.4.1 The effect of environment on assembly size

There were several insights from the comparison of the Scărișoara Ice cave and Svalbard assemblies. The Svalbard library (718 623 496 reads) was larger than the Ice Cave library (reads= 505 461 760), however the Svalbard assembly (contigs= 162 105, bp = 720 998 358) was smaller than the Ice Cave assembly (contigs= 179 753, bp= 1 123 284 953) (Table 8 5), and this was also reflected in the number of high quality MAGs that were resolved from each assembly (Svalbard=74, Ice Cave = 121). This comparison, together insights from the comparison of sea, soil and cryoconite libraries (Figure 8-5), highlights the enormous effect microbial diversity and complexity has on the assembly and resultant MAGs. The greater the number of bacterial species in a sample, the fewer reads will overlap to form contigs, and this can be extremely detrimental to downstream analysis. Considering that longer contigs are needed to obtain good functional annotation of genes, with complete genes and ORFs, this suggest that it is far better to sequence deeply (few libraries with maximum number of reads) than widely (many samples with fewer reads). The balance between depth and breadth of sequencing can be weighed up by considering the heterogeneity of the selected environments. The use of co-assembly vs single assembly also needs to be considered. A recent study showed co-assembly recovered a larger genome fraction than a combination of single assemblies (Hofmeyr et al., 2020). However, single assembly was better at identifying variation between closely related strains, but the combined single assembly dataset suffered from duplications. The effect of co-assembly on these datasets appeared to be positive on balance. Microbially diverse environments are tempting for bioprospecting because greater diversity suggests a greater probability of genetic novelty. However, in this study of different environments, it is

clear that extremely diverse and heterogenous environments may result in less complete and robust data for meaningful analysis.

A further consideration when sampling environments include, considering the contribution of non-bacterial DNA in the environmental DNA. Seawater is known to contain many diverse bacteria and the marine metagenomes have been explored in several studies. However, Kaiju revealed many reads had non-bacterial origin, and this substantially reduced the number of reads that could contribute to the assembly. Although the ability to resolve eukaryotic MAGs from fungal and algal species will soon be possible (Saary et al., 2020), the size of eukaryotic genomes, as well as the increased number of repeat regions makes this a formidable challenge. The number of recovered genomes could be considerably increased via greater sequencing depth.

8.4.2 The advantages and disadvantages of reads, contigs and metagenome-assembled genomes

While using the described bioinformatics pipeline, there is information loss at several stages. For the Svalbard dataset, the initial library was 1.038 x 10^{11} bases in size. However, read-mapping back to contigs revealed that only 3% – 9.07% of soil library reads, 22.32% - 66.62% of cryoconite library reads, and 5.32% - 14.02% of seawater library reads aligned to contigs. This represents an enormous loss of information, with up to 97% of the reads in the soil library not being included in the assembly and downstream analysis. Read mapping also confirms the observation from testing assembly tools, that higher diversity libraries suffer from lack of incorporation into contigs. During binning and MAG refinement, the information loss continues, as only 28.01% of the Svalbard contigs and 29.97 % of the Ice-Cave contigs were included in MAGs (Table 8-8). The use of contigs as a dataset is useful because it detects diversity in the rarer taxa in environmental samples.

8.4.3 Optimisation and benchmarking are necessary

In this chapter, several tools were compared, from assemblers (Section 8.3.3.1), to binning tools (Section 8.3.5). Whilst some of these comparisons were reassuring, and gave similar results, there were sometimes significant differences that are severe enough to potentially interfere with result interpretation. The use of a consensus approach to select tools and results assumes that if results converge, despite using different methods to get there, then the probability of the result being accurate is higher. MetaSPAdes and MEGAHIT gave similar results in assembly size (Figure 8-3), and in BGC annotation using antiSMASH (Figure 8-6),

although MEGAHIT got the results more efficiently, which was the justification for using MEGAHIT. This kind of consensus approach to method selection and optimisation is also being built into several other tools. For example, dbCAN2 uses several methods to screen contigs for carbohydrate-active enzymes and suggests that the dataset be trimmed to include only hits where there is agreement between at least two different tools (Figure 8-16).

The presence or absence of results convergence can be used in several ways. In the comparison of binning tools there was an alarming lack of overlap between the bins created by metaBAT2, MaxBin2 and CONCOCT. Parameter tweaking may have resulted in slightly different, and more similar bins, but nonetheless, the bins were different in size and redundancy (Table 8-8, Figure 8-9, Figure 8-10). DAS Tool did not particularly favour one tool over the other, with the final bins coming from all three of the tools. While it is almost impossible to get 'accurate' bins, the degree to which results agree or disagree can be used to assign a confidence value. Where all three tools converge on a similar bin, there is greater confidence in the quality of the MAG. Where there is a large discrepancy in contig membership between the different binning tools, it serves as a warning that the data is of poorer quality (Figure 8-13). This method of consensus seeking can be applied when refining MAGs too. There is growing evidence that many MAGs in databases are of poor quality, consisting of chimeric bins and even chimeric contigs (Shaiber and Eren, 2019). The manual refinement of bins is therefore an important step, however, is made difficult and impractical when there are hundreds to thousands of contigs in a single bin, and hundreds of bins in a dataset. The visualisation of binning results as a data layer, used in this thesis, is a way to quickly identify suspect contigs.

During bin-refinement, it is always easier to create large bins, that may contain contaminant contigs, and the refine the bins, than to accidentally split bins that belong together. Manual refinement therefore involves a whittling away of contaminant sequences. Figure 8-1 and Figure 8-11 show how bin refinement can easily be accomplished using differential coverage across samples, GC content and TNFs. Additional clues can be provided by the taxonomic classification of MAGs, which can be done in two ways. Kaiju can be used to classify each gene call and contig taxonomically and viewed on a contig-by contig basis. The HMM scan of 71 bacterial genes is used to estimate the completion and redundancy information for each bin in real time, and the results from the SCG scan of 22 genes from GTDB can be used to view a taxonomic prediction in real time. The SCG taxonomy from GTDB can once again be used to find consensus, where all 22 genes are present have the same closest relative, that is an excellent indicator of a complete and uncontaminated bin. Occasionally, GTDB SCGs may belong to

several different species from within the same genus, which could indicate contamination, and chimera or hybrid of closely related species, or a novel species that is related to both, having diverged from a shared common ancestor. However, the presence of GTDB SCGs from different orders, classes or phyla are a clear sign that the bin is contaminated or chimeric and requires further refinement. This approach was very good at identifying bins that were likely to be chimeric. Chimeras are more likely when there are lots of closely related species or strains present in a sample. These are may appear as a bin with lots of contigs with uneven coverage or distribution amongst samples.

Anvi'o is growing and increasing functionality constantly, with several updates annually. Within the next updates, automatic KEGG functionality is to be included, as well as screening for tRNAs, which will allow easier fulfilment of the criteria by the miMAG standards (Bowers et al., 2017).

8.4.4 Long-read technologies will improve MAG quality

The use of long-read sequencing is poised to revolutionise microbial ecology. Currently, bins are often composed of multiple closely relates species, and these consortia are often very difficult to separate bioinformatically using the current short-read technology and assembly methods. However, new long-read technologies such as Nanopore are poised to reinvigorate genome assembly from metagenomes (Moss et al., 2020; Overholt et al., 2019). The benefit of long reads is immense, as long reads can act as scaffolds, helping to bridge caps between contigs and close genomes. Closely related species can also be resolved because deletions/ insertions and rearrangements can highlight differences in strains. It will vastly improve binning, as long reads that span multiple genes, possible rearrangements and deletion will address issues of synteny, and help to resolve closely related species within a population (Moss et al., 2020; Overholt et al., 2019).

8.4.5 Contigs and MAGs are a catalogue of diversity that can be explored

The MAGs and contigs databases are catalogues of diversity that are amenable to a large range of downstream analysis. In this thesis, the MAGs and contigs were screened for BGCs using the tool antiSMASH, which also links to several databases and dbCAN2 which links to the CAZy database. However, multifastas from assemblies can be screened using several databases using a variety of tools.

The antiSMASH results are discussed throughout the chapters of this thesis. The dbCAN2 scan identified abundant carbohydrate active enzymes from the contigs of seawater (267), cryoconite (13604), soil (5053) and the Ice Cave (24313) (Appendix Table H1). These environments seem enriched with enzymes from the GT4, GT2_Glycos_transf_2, GT2 from the GT class, GH23 and GH3 from the GH class, CE10, CE1 and CE4 from the CE class, and AA3 from the AA class.

Some additional tools, which have been used at various stages (but not included in this thesis) are listed in Table 8-9 and represent avenues for future work. For example, BAGEL4 (van Heel et al., 2018) focuses on identifying bacteriocins or ribosomally synthesized and post translationally modified peptides (RiPPs), which are not commonly covered by other tools. PRISM (PRediction Informatics for Secondary Metabolomes) is a computational resource that implements novel algorithms to identify BCGs and predict genetically encoded nonribosomal peptides and type I and II polyketides (Skinnider et al., 2015). It also uses and bio- and cheminformatics to detect replication of known natural products, which is a huge advantage since rediscovery' of existing molecules has plagued pharmaceutical research.

The Lipase Engineering Database (LED) (http://www.led.uni-stuttgart.de) is a database that attempts to integrate sequence, structure, and function information of a range of enzymes with similar catalytic machinery (Fischer and Pleiss, 2003). Within this family, the cutinases are of interest as enzymes potentially capable of PET and PUR plastic degradation (Fischer and Pleiss, 2003; Wei and Zimmermann, 2017). Likewise, the non-heme peroxidases, detected using RedoxiBASE (Passardi et al., 2007; Savelli et al., 2019) may also contain plastic-degrading enzymes. The Laccase Engineering Database (LccED) (https://lcced.biocatnet.de/) is a database that contains information about the sequence, structure and function of laccases and their homologues from the multicopper oxidase (MCO) superfamily (Sirim et al., 2011). MCOs catalyse the one-electron reduction of substrates concurrent with the four-electron reduction of molecular oxygen to water. Fungal laccases play a role in lignin degradation, pigment production and plant pathogenesis, while bacterial laccases play a role in melanin production, spore coat resistance, morphogenesis, and copper detoxification (Sirim et al., 2011). In addition to potential plastic-degrading capabilities, laccases are also excellent candidates for other biotechnological applications, in the textile, pulp and paper, food and organic synthesis industries as well as in bioremediation (Sirim et al., 2011).

8.4.5.1 Custom databases for specific NP discovery

Finally, it is possible to create custom databases of sequences of specific interest. This was done for example by downloading sequences and HMM profiles for anti-freeze proteins and polymerases from Uniprot (data not shown). DIAMOND and HMMER3 can then be used to query the custom databases and identify products. To ensure good quality data, the use of both HMMER and DIAMOND can be used, and only hits to both datasets used in analysis (similar to dbCAN2 recommendations).

8.4.6 MAGs enable strategic bioprospecting

Once the gene or BGC responsible for the synthesis of a NP of interest has been identified, additional information provided by the entire MAG genome can be used to aid strategic sampling, cultivation, and heterologous expression efforts.

8.4.6.1 Optimisation of sampling strategy and environmental sites

By their nature, reconstructed genomes represent the most abundant members of a community, because they are constructed from the longest contigs with the deepest coverage, proportional to their abundance in the original sample. Because anvi'o maps the reads from individual libraries, it is possible to see which libraries (i.e. sampling sites, environment types, or environmental conditions) contribute most to the contig of interest, and therefore, which environments/ sample sites/ conditions should be favoured in future sampling activities.

8.4.6.2 Host engineering and expression optimisation

Understanding the genomic context overcomes some of the difficulties of BGC expression, which relies on compatible promoters, ribosome binding sites, substrate metabolites and secretion machinery for natural products to be correctly expressed (Zhang et al., 2010). Therefore, locating a BGC inside of a genomic context helps greatly with the genetic engineering of suitable hosts and the identification of optimal conditions for expression of the desired natural product.

Traditional cloning methods rely on a random shearing of DNA and insertion of putative BGCs into cosmids, fosmids and BACs. This approach relies on chance, and fragments are rarely long enough to capture a BGC in its entirety. However, by conducting a bioinformatic screen and identifying a BGC of interest, it is possible to target a specific BGC using newer recombinant DNA technologies. Examples of recombinant DNA technologies that have been successfully employed to specifically and precisely target and capture BGCs of interest include high

efficiency linear-linear homologous recombination (LLHR)(Yin et al., 2015), Transformation-associated recombination (TAR) cloning (Kouprina and Larionov, 2016), serine integrase-mediated site-specific recombination (SSR)(Du et al., 2015; Olorunniji et al., 2016) and Cas9-associated targeting of chromosome segments (CATCH) (Jiang et al., 2015). Meanwhile, advances in synthetic biology, referred to as bottom-up assembly methods, involve assembling the desired BGCs from several smaller fragments (Li et al., 2017). Examples include methylation-assisted tailorable ends rational (MASTER) ligation based on the type IIs endonuclease *Msp*JI (Chen et al., 2013) site-specific recombination-based tandem assembly (SSTRA) (Zhang et al., 2011), Modified Gibson assembly (L. Li et al., 2015) and DNA assembler (Shao et al., 2011).

8.5 Conclusion

Two datasets were used in this bioinformatic workflow and tool comparison, a Svalbard metagenome consisting of cryoconite (6), soil (8) and seawater (3) libraries and an Ice-Cave dataset (7). The complexity and heterogeneity of the environments played a role in the size quality of the assembly, which affected all downstream analyses. Nonetheless, using careful manual refinement, a collection of high-quality MAGs was constructed. These MAGs and contigs represent catalogues of biodiversity that can be explored for several categories of products. The insights from MAGS enable strategic sampling, heterologous expression, and co-cultivation efforts.

Table 8-10 Table of tools used in the workflow.

Tool name	Link	Reference
Trimmomatic	http://www.usadellab.org/cms/?page=trimmomatic	(Bolger et al., 2014)
FastQC	https://www.bioinformatics.babraham.ac.uk/projects/fastqc/	(J. Brown et al., 2017)
Kaiju	http://kaiju.binf.ku.dk/	(Menzel et al., 2016)
Centrifuge	https://ccb.jhu.edu/software/centrifuge/	(D. Kim et al., 2016)
GOTTCHA	https://lanl-bioinformatics.github.io/GOTTCHA/	(Freitas et al., 2015)
eggnog-mapper	http://eggnog-mapper.embl.de/	(Huerta-Cepas et al., 2017)
DIAMOND	https://ab.inf.uni-tuebingen.de/software/diamond/	(Buchfink et al., 2015)
HMMER	http://hmmer.org/	(Mistry et al., 2013)
MEGA	https://www.megasoftware.net/	(Kumar et al., 2018)
MEGAHIT	https://github.com/voutcn/megahit	(D. Li et al., 2015)
metaSPAdes	http://cab.spbu.ru/software/spades/	(Nurk et al., 2017)
IDBA-UD	https://i.cs.hku.hk/~alse/hkubrg/projects/idba_ud/	(Peng et al., 2012)
metaQUAST	http://cab.spbu.ru/software/metaquast/	(Mikheenko et al., 2016)
Prokka	http://www.bioinformatics.net.au/software.prokka.shtml	(Seemann, 2014)
antiSMASH 4	https://antismash.secondarymetabolites.org/ *Previous version*	(Blin et al., 2017)
antiSMASH 5	https://antismash.secondarymetabolites.org/	(Blin et al., 2019b)
BAGEL4	http://bagel.molgenrug.nl/index.php/bagel3	(van Heel et al., 2018)
PRISM	http://grid.adapsyn.com/prism/#!/prism	(Skinnider et al., 2017)
dbCAN2	http://bcb.unl.edu/dbCAN2/	(H. Zhang et al., 2018)
Bowtie2	http://bowtie-bio.sourceforge.net/index.shtml	(Langmead et al., 2009)
CONCOCT	https://github.com/BinPro/CONCOCT	(Alneberg et al., 2014)
MaxBin2	https://sourceforge.net/projects/maxbin2/	(Wu et al., 2016)
metaBAT2	https://bitbucket.org/berkeleylab/metabat	(Kang et al., 2015)
Anvi'o	http://merenlab.org/software/anvio/	(Eren et al., 2015)
GTDB-tk	https://github.com/Ecogenomics/GTDBTk	(Chaumeil et al., 2020)
CheckM	https://ecogenomics.github.io/CheckM/	(Parks et al., 2015)
GhostKoala	https://www.kegg.jp/ghostkoala/	(Kanehisa et al., 2016)

The link to the software and publication reference are provided for the main tools used. Many of these tools make use of additional tools and software as well as several databases.

Table 8-11 List of databases used in the workflow

Database name	Link	Reference
UniRef100	https://www.uniprot.org/uniref/	(Suzek et al., 2015)
Pfam	http://pfam.xfam.org/	(El-Gebali et al., 2019)
CAZy	http://www.cazy.org/	(Cantarel et al., 2009)
RefSeq	https://www.ncbi.nlm.nih.gov/refseq/	(O'Leary et al., 2016)
NCBI COG	https://www.ncbi.nlm.nih.gov/COG/	(Galperin et al., 2015)
GTDB	https://gtdb.ecogenomic.org/	(Parks et al., 2018)
NCBI BLAST nr	ftp://ftp.ncbi.nlm.nih.gov/blast/db/FASTA/nr.gz	(Benson et al., 2013)
KEGG	https://www.genome.jp/kegg/	(Kanehisa and Goto, 2000)
antiSMASH-db2	https://antismash-db.secondarymetabolites.org/	(Blin et al., 2019a)
MIBiG	https://mibig.secondarymetabolites.org/	(Medema et al., 2015)

Table of most important databases used in the bioinformatics analysis. The link to the software and publication reference are provided for the main tools used. Many databases that are referenced and used by the tools described in Table 8.12 are not mentioned specifically.

Table 8-12: Table of high performance and cloud computing facilities

Tool name	Link	Reference
Kbase	http://kbase.us/	(Arkin et al., 2018)
CLIMB	https://www.climb.ac.uk/	(Connor et al., 2016)
IBERS HPC	https://bioinformatics.ibers.aber.ac.uk/wiki/index.php/Main_Page	

9 DISCUSSION

This thesis sought to explore the biotechnological potential of the cryosphere. The scope for applications from cryospheric microorganisms is enormous and ranges from novel antimicrobials to cold-active enzymes to ecosystem services such as soil remediation and plastic degradation (Chapter 1). In this thesis, Svalbard soil, cryoconite and seawater were investigated for putative antimicrobials, antioxidants, and EPS (Chapter 5) and cold-active polymerases (Chapter 6) using mixed sequence-based bioinformatics and functional screening methods. In addition, shotgun metagenomic data from Svalbard soil, cryoconite and seawater (Chapter 4), and the Scărișoara ice Cave (Chapter7) were assembled to create contigs databases and MAGs that can be interrogated for enzymes, secondary metabolites and biodegradation pathways using bioinformatic tools described in Chapter 8. Crucially, a 16S rRNA amplicon-based survey of a Svalbard glacial ecosystem showed that the window for undertaking these bioprospecting activities from these highly specialized cryospheric bacteria is rapidly closing because of global climate change (Chapter 3).

9.1 Bioprospecting and global climate change

Bioprospecting in the Arctic has the potential to be beneficial for humans and for the environment. Not only are there multiple products that could benefit human health and industry, from novel antimicrobials, EPS and antioxidants in the pharmaceutical industry to enzymes and antifreeze proteins in the food, detergent and molecular biology industries, but several of these solutions can have positive feedback on the environment (Chapter 1). Cold-active enzymes can lower energy costs (and carbon footprint) in large scale chemical reactions (Table 1-5) or degrade persistent organic pollutants (Table 1-11) and plastics (Table 1-12). Furthermore, the recognition of this environment as having economic value helps to justify its protection and maintenance.

The importance of these bioprospecting ventures is becoming increasingly urgent because habitats in the Arctic are rapidly changing as glaciers and sea ice retreat due to global climate change (Barry, 2017; Fountain, 2012). The potential loss of these extreme environments, and the unique biodiversity therein, necessitates urgent efforts to understand and uncover the

potential of these cryospheric microorganisms before the opportunity is lost (Stibal et al., 2020). Worryingly, the temperatures in the Arctic, (particularly Winter temperatures (Graham et al., 2017)) are increasing faster than the models predict (Graversen et al., 2008), and sea ice retreat is also about two decades ahead of predicted rates (Barry, 2017).

To identify how resilient Arctic bacteria are to climate change, several habitats within a glacier ecosystem, including cryoconite, snow, slush, glacial meltwater, proglacial water, forefield soil and seawater were investigated to identify a core microbiome for each habitat type and determine the extent to which bacteria can exist in different environments (Chapter 3). This helped identify whether Arctic microbial communities consist predominantly of specialists, able to live only within a narrow ecological niche, or whether they were more cosmopolitan, able to live across a broad range of environmental parameters. The 16S rRNA gene amplicon analysis revealed that many of the bacteria inhabiting the High Arctic have strict habitat preferences (Chapter 3). The survey used ASVs rather than OTUs because it allows the resolution of exact variants. An UpsetR plot of shared ASVs between environments (Figure 3-17), and a co-occurrence network (Figure 3-19) revealed that there are very few ASVs able to occupy several environments. The narrow spatial range suggests significant specialisation, and therefore a high risk of extinction, should global climate change continue to alter the environment. Moreover, filtering of the dataset to include only ASVs occurring in more than two samples resulted in a significant reduction of diversity in the dataset (Figure 3-16), which suggests that the community is extremely heterogenous, and/or that there is a large and diverse rare microbiome. The following chapters in this thesis sought to catalogue some of that unique diversity.

9.2 Genome-centred metagenomics enables strategic bioprospecting

The main contribution of this thesis was the creation of two MAG collections, which form the foundation for further bioinformatic bioprospecting (Chapter 4,5,7,8). MAGs are reconstructed genomes from the assembly and then binning of metagenomic DNA. Ideally, a single MAG represents an exact strain or species from the sampled environment, however MAGs can represent several closely related species that have assembled together because of their high level of sequence overlap. MAGs can therefore be thought of as in a similar way to OTUs, as representing a cluster of highly similar strains or species. MAGs represent a biological catalogue, with information on phylogenetic relatedness to reference species (Table 4-7, Table 7-6), and metabolic and functional potential (Figure 4-13 to Figure 4-14, Figure 5-2 to Figure

5-3, Figure 7-7 to Figure 7-12). In addition, the use of differential coverage contributes additional insights, such a map of spatial distribution and abundance across sites (Figure 4-12, Figure 7-6) and information about co-occurring bacteria and possible symbionts. This information can then be used in strategic bioprospecting activity, including, but not limited to the selection of specific habitat types and sites for further work, strategic co-cultivation efforts and host engineering for heterologous expression of NPs of interest.

In this thesis, 74 high quality MAGs were assembled from cryoconite, soil and seawater from a glacial ecosystem (Chapter 4) and 121 high quality MAGs were assembled from the Scărișoara Ice Cave in Romania (Chapter 7). In addition, a bioinformatic workflow was tested and described, where both the MAG construction process, as well as insights from the comparison of the two different datasets were compared (Chapter 8).

9.2.1 MAGs vs phylotypes from previous 16S rRNA gene analysis

One of the first observations is that the reconstructed MAGs belonged to the most abundant species identified using both 16S rRNA analysis, and culturing studies of these environments (Chapter 3, and (Edwards et al., 2013c; Gokul et al., 2016; Hillebrand-Voiculescu et al., 2015; Itcus et al., 2018; Paun et al., 2019). The MAG with the highest coverage (a proxy for relative abundance) in Svalbard cryoconite was classified as *Phormidesmis priestleyi*, exactly as expected based on the 16S rRNA analysis (Chapter 3) and previous studies of Svalbard cryoconite (Gokul et al., 2016; Segawa et al., 2017; Takeuchi et al., 2019). However, several of the other MAGs belong to members of the cryoconite core community such as Microbacteriaceae, including *Salinibacterium* (3), *Pseudanabaena* (1), Ktedonobacteria (1), *Granulicella* (1) and *Rhizobacter* (2) (Figure 3-6, Figure 4-3, Table 4-4, Appendix Table C-12). Abundant genera in soil were also present, such as *Nostoc* (1), *Rhizobacter* (2), *Phormidium (Microcoleus)* (1) and *Sphingomonas* (1) (Figure 3-12, Figure 4-5, Table 4-4, Appendix Table C-17). According to the 16S rRNA amplicon analysis, the most abundant family in the seawater was Nitrincolaceae (39.62%) (Figure 3-14), and a species-level MAG belonging to the uncultured genus ASP10-02a of within the family Nitrincolaceae was constructed (Table 4-6).

The same correspondence was observed in the Scărișoara Ice Cave MAGs. Two Archaeal MAGs were classified as *Methanosarcina* and *Methanosphaerula* (Table 7-6), which were the exact two Archaeal species detected using 16S rRNA amplicon analysis of this same cave glacier (Paun et al., 2019). Other abundant community members detected using 16S rRNA

analayis that matched with constructed MAGs, include *Cryobacterium* (1), *Pedobacter* (4), *Aeromicrobium* (1), *Clostridium sensu stricto* (2), *Pseudomonas* (1), and *Massilia* (3). While these genus and species-level matches are impressive, there is also overlap in representatives at the family and order level. Perfect matches are difficult and probably inaccurate, as sequences in the 16S rRNA and reference genome databases represent only a fraction of the true diversity in these environments. Nonetheless, taxonomic classification of MAGs to full reference genomes in the GTDB tended to have been collected in Arctic, Antarctic or other cryospheric environments (Appendix Table D-11).

Unfortunately, during the bioinformatic processing steps that take place during MAG construction, there is attrition of reads and contigs at each step, which results in the loss of information about rare taxa, because these fail to be incorporated into the analysis (Chapter 8). Of the hundreds of millions of reads that are assembled, the portion that are not incorporated into contigs are gene fragments of species at too low abundance to overlap into contigs. Likewise, there are contigs that either fail to meet the length criteria, or that are not incorporated into bins, which also contributes to a loss of diversity in the data. This loss is unfortunate because the rare taxa could represent endemic, specialised species with the biological novelty that is highly desirable in bioprospecting.

The reduction in diversity can be seen from the decrease in the number of taxa identified using reads-based taxonomic classification with tools like Kaiju (Figure 4-2 to Figure 4-7; Figure 7-1, Figure 7-2), versus the taxonomic identity of the MAGs (Table 4-5 to Table 4-8, Figure 4-4; Table 7-4 to Table 7.6, Figure 7-5). However, the MAGs do successfully represent the most abundant bacterial species detected in these environments. Therefore, there is excellent correspondence between 16S rRNA amplicon studies (Chapter 3), reads-based taxonomic classification of shotgun data, and MAGs. The rare taxa are unfortunate casualties of the MAG approach, but the rare microbiome is often neglected in 16S rRNA amplicon studies too, due to OTU clustering and rarefaction (Bay et al., 2020; McMurdie and Holmes, 2014).

The construction of MAGs has additional advantages over 16S rRNA amplicon studies, including the fact that several species, including members of the CPR, which can be 16S rRNA primer blind, can be reconstructed (Brown et al., 2015). In fact, several of the MAGs from these environments represented members of the CPR. From the Scărișoara Ice Cave, there were six MAGs belonging to the CPR phylum Patescibacteria, and they belonged to four classes, the Paceibacteria (3), Dojkabacteria (1), Gracilibacteria (1) and Microgenomatia (1) (Table 7-6, Appendix Table G-8). In the Svalbard dataset, there were three CPR MAGs, which belonged

to the Microgenomatia (2) and Saccharimonadia (1) classes (Table 4-8, Appendix Table D-4). The construction of MAGs is the first, and to date, the only way, that researchers can identify and describe these CPR species and evaluate their abundance and function in these environments. This represents an important contribution to glacier and cave biology because CPR species have been shown to be abundant in oligotrophic environments and may play an important role in microbial community dynamics (Herrmann et al., 2019).

9.2.2 Environment choice for bioprospecting

Metagenomes were constructed from soil samples because of the high biodiversity in this environment (Chapter 3). Soil is considered the most biodiverse environment on Earth (Roesch et al., 2007), and is likely to contain diversity and novelty in enzymes, proteins, and NPs. In addition, the various environmental influences (like pH, salinity, underlying geology, and minerals present) are likely to be diverse, and the interaction of these factors are likely to lead to changes in species composition over even small areas (Bach et al., 2018; Malard et al., 2019; Malard and Pearce, 2018). This high biodiversity was confirmed by the fact that soil had the highest species-richness, despite small library sizes (Figure 3-12, Appendix Figure C-22), and the heterogeneity is reflected by the difficulty in identifying core ASVs present in all 15 glacier forefield sites (Figure 3-13, Appendix Table C-17). Compared to soil, cryoconite is far less heterogenous, with a core community of highly abundant and prevalent ASVs that were present on both VB and ML glaciers (Figure 3-6, Figure 4-11, Appendix Table C-12). In addition, while the species composition in soil is relatively even, with many species contributing a minor proportion to the community composition, cryoconite is dominated by a single species, with several members of the core community that contribute moderately to community composition, and a long tail of rare species.

To construct MAGs, hundreds of millions of pair-end reads are first assembled into contigs, then binned, annotated, and screened for useful functions (Chapter 8). However, due to current limitations in sequencing, such as the expense, number and lengths of reads that can be feasibly sequenced, and limitations in computational resources (memory and cores), and bioinformatics approaches (efficient algorithms), the high diversity and heterogeneity of environments were found to have a detrimental effect on the resulting dataset (Chapter 8). The greater the number of bacterial species in a sample, the fewer reads overlap to form contigs, and this can be extremely detrimental to downstream analysis. Considering that longer contigs are needed to obtain good functional annotation of genes, with complete genes and ORFs, this suggest that it

is far better to sequence deeply (few libraries with maximum number of reads) than widely (many samples with fewer reads). The balance between depth and breadth of sequencing can be weighed up by considering the heterogeneity of the selected environments. The cryoconite and Ice-Cave libraries reflect this relationship, and these environments provided the largest number of high-quality MAGs.

Differences between the Svalbard glacier system and the Scărișoara Ice Cave environment extend beyond just the complexity of the environment, but also illustrate how environmental factors influence the identity and composition of bacteria in different habitats. While both cryoconite and the Ice Cave metagenomes are frozen freshwater environments, they contain completely different communities, which is likely due to differences in geology, light regimes, temperature stability as well as the manner, quantity, regularity and types of nutrients that are imported and exported from the ice systems. For example, photoautotrophic cyanobacteria were both diverse (6 MAGs) and abundant in the Svalbard samples where glaciers experience sunlight for more than six months of the year, whereas there were no Cyanobacteria detected in the Ice Cave, which experiences perennial dark. This highlights a second vital aspect of environment selection, which is to seek out environments with environmental pressures that are likely to favour the synthesis of specific NPs as an adaptation mechanism.

9.3 Environmental pressures select for specific genes and products

Microorganisms synthesise a suite of diverse secondary metabolites, which may or may not be directly related to their survival (Bérdy, 2005; Calteau et al., 2014; Cimermancic et al., 2014). These secondary metabolites have been of considerable interest in the food, cosmetic and pharmaceutical industry, where these metabolites find functions as antioxidants, UV screens, gums, emollients, nutraceuticals, pigments and antimicrobial compounds (Poli et al., 2010; Sajjad et al., 2020; Tracanna et al., 2017).

AntiSMASH was used to interrogate the BGCs in the dataset and the most abundant cluster types reflected adaptation to cryospheric environments but may also have useful biotechnological applications. There were 2694 BGCs from the 121 MAGs in the Scărișoara ice Cave dataset (Figures 7-10- 7-12), and 1742 BGCs from the 74 MAGs in the Svalbard dataset (Figures 5-2, 5-3). The most abundant BGC types detected in the Svalbard MAGs (Chapter 5) were saccharides (1214), followed by fatty acids (212), and terpenes (122) (Figure 5-2 and Figure 5-3). However, the most abundant clusters detected in the Scărișoara Ice Cave (Chapter 7) were saccharides (1597), fatty acids (344) and halogenated clusters (131), with

only 124 terpenes. Terpenes therefore represent 4.6% of BGCs in the Ice Cave, but 7.0% of BGCs in the Svalbard dataset. As many of the terpenes within these MAGs were carotenoid pigments, which are known to be protective against high UV light, a lower portion of BGCs in this environment may reflect the low light environment within the Scărișoara Ice Cave, compared to the Svalbard glacial environment, which will experience high and constant UV radiation during the summer.

The saccharides clusters detected by antiSMASH comprise several components of the cellular wall as well as EPS which help to prevent against desiccation, allow the formation of biofilms and protect against UV stress (Poli et al., 2010). These polysaccharides have diverse functions as emollients, antioxidants and gums which makes them useful in food technology and pharmaceutical industries (Poli et al., 2010). In addition, some EPS act as biosurfactants, where they influence the biodegradation of hydrocarbons, and can be used in bioremediation and detoxification of petrochemical oil-polluted areas (Gutierrez et al., 2013).

Fatty acids are known to maintain cellular membrane fluidity and permeability at low temperatures (D'Amico et al., 2006), and terpenes are often pigments and antioxidants capable of scavenging free radicals and protecting against the damaging effects of UV radiation (Paduch et al., 2007; Sajjad et al., 2020). However fatty acids and terpenoids have also been known to play antimicrobial roles (Karpiński and Adamczak, 2019; Yoon et al., 2018).

The potential of some of these compounds to act as antimicrobials is especially attractive, because increasing antimicrobial resistance to a broad range of antibiotics is a significant threat to human and animal welfare (Ventola, 2015). To overcome resistance mechanisms, new classes of antibiotics are urgently needed. Rediscovery and replication of BGCs and their products is a major problem in bioprospecting, where the same bioactive ingredients are rediscovered repeatedly in cultured bacteria (Coates et al., 2011; Demain and Sanchez, 2009). Of the 278 BGCs with hits to MIBiG compounds, only 21 of those had > 85% similarity to the reference BGC. The remaining 257 clusters with hits to MIBiG compounds ranged from just 1% to 85% similarity, suggesting incredible NP diversity. The low similarity to known BGCs and compounds in cryospheric bacteria suggests that this is an excellent environment for novel metabolites, and potential antimicrobials.

9.3.1 Same genes, but with a twist

Sometimes, it is not the gene product that is specific to cold environments, but rather cryospheric bacteria will have the same genes, with alterations in codon preference or

regulation that result in differences in protein structure, kinetics, stability or quantity. This was shown in Chapter 4, where a pangenome of Cyanobacterial genomes consisting of Svalbard MAGs and their closest temperate relatives revealed that there were no specific genes in the accessory genome for cold adaptation (Table 4-10). Rather, cryospheric bacteria have a similar suite of genes, but may have differences in codon preference, that result in differential regulation or amino acid changes with consequences on protein structure and function in cold temperatures. Higher activity at lower temperatures is thought to be achieved via amino acid changes that confer greater conformation flexibility, which has the effect of making the enzyme-active site able to bind the substrate at a slightly greater range of orientations, as well as allowing a "tighter fit" (Casanueva et al., 2010).

When dealing with small datasets it is difficult to interpret whether changes in amino acids in proteins have occurred as an adaptive response to the cold, or whether the changes are purely the result of evolution and genetic drift. However, the use of very large datasets, such as genomic, and especially metagenomic data, to compare psychrophilic, mesophilic and thermophilic organisms from cold, moderate and hot environments respectively, tends to highlight common trends in cold-adapted organism that are more likely to be due to adaptations to the extreme environment, as opposed to the random background noise of evolution (Casanueva et al., 2010; Siddiqui and Cavicchioli, 2006). Previously, the protein sequences of psychrophilic bacteria were found to have a reduced number of salt-bridge-forming residues, such as arginine, glutamic acid, and aspartic acid, as well as reduced proline contents, and a reduction in stabilising hydrophobic clusters (Grzymski et al., 2006). This dataset lends itself to that type of investigation in future work.

Because of these changes in amino acid preference, there is a high probability that an enzyme from a cryospheric bacteria will have a lower temperature optimum than an enzyme from a thermophile. With this is mind, the contigs database was submitted to dbCAN2 to screen for carbohydrate active enzymes (Figure 8-18). Most studies of carbohydrate- active metabolism have investigated soils (Jiménez et al., 2015) and ruminant mammals (Stewart et al., 2019), where the amount of carbohydrate metabolism and breakdown by bacteria is expected to be high. However, gut microbiomes, and soils with high plant content are likely to be warmer. The environments investigated in this thesis were extremely low nutrient, and so carbohydrate metabolism could differ markedly from studies conducted on microbiomes that have carbohydrate surplus. In total, there were 267 carbohydrate active enzymes in the seawater contigs, 13604 in cryoconite, 5053 in soil and 24313 enzymes in soil (Figure 8-18). The most

abundant family of enzymes were the Glycosyl Transferases (GTs), which are responsible for the formation of glycosidic bonds, and important enzymes during EPS synthesis. The second most abundant class was the Glycoside Hydrolases (GHs) which are responsible for the hydrolysis and/or rearrangement of glycosidic bonds. Although the trends in enzyme relative abundance were similar across all environments, the ratio of relative abundance between enzyme families differed. For example, the ratio of GT:GH was 39%:38% in seawater and 47%:31% in soil.

9.4 The choice of appropriate methods and multiple lines of evidence

The use of 16S rRNA gene based taxonomic surveys may provide insight into taxonomic diversity, however they will never capture the full metabolic novelty and functional potential of a community. To do this one needs genotypes not phylotypes. MAGs are a vast improvement for understanding the functional potential of a microbial community. However, they too, are limited in their ability to capture the activity of microbes. To truly capitalise on the biotechnological potential of microbes, the functional predictions based on sequenced-based genomics, will always need to be ground truthed using functional and physiological data. The use of transcriptomics and metabolomics will be required to identify the actual activity of the bacteria, and the novel genes and gene products will need to be purified, expressed, and characterised to truly gain insights into which bacteria are present, what they are doing, and how they are doing it.

9.4.1 Functional studies are vital to ground-truth bioinformatics predictions

Bioinformatics is truly entering a golden era, however, reliance on reference databases and algorithms is not sufficient to make inroads into the truly novel and unknown because new discoveries are always tethered by what limited knowledge we have. Currently, the number of hypothetical proteins and proteins of unknown function form the majority of many organisms' genomes (Vanni et al., 2020). In addition, many of the functions that have been ascribed to genomes are based on predictions themselves, using homology to known genes (El-Gebali et al., 2019; Galperin et al., 2015; Huerta-Cepas et al., 2017; Mistry et al., 2013).

The utility of bioinformatics to ascribe functions to hypothetical proteins is severely limited and would represent guesses at best. The role of traditional wet lab techniques, such as culturing, cloning and expression experiments is therefore a vital aspect of both bioprospecting and understanding microbial physiology and ecology. Therefore, in this thesis, a functional

metagenomics screen was used to identify novel polymerases (Chapter 6). A clone library of soil and cryoconite eDNA was created in *E. coli* DH10B for storage, propagation and for future functional screening, and in two mutant strains, *E. coli* cs2-29 and HCS1, to screen for cold-active polymerases. The cs2-29 and HCSI strains harbour a mutation in the *PolA* gene that is lethal below 20°C. Several clones grew at 18°C, suggesting that the clone inserts contained sequences capable of rescuing DNA transcription at low temperatures. Sanger sequencing of the inserts of clones able to grow at 18°C revealed several of the clones had DNA binding activity, even when the sequences were not necessarily hits to polymerase genes. Furthermore, there were clones with hits to proteins of unknown function, such as a Plantomycetes sequence (WP_145289226.1) which codes for rare but broadly distributed uncharacterized protein family (TIGR03545), and another similar to a domain of unknown function (DUF4981) in *E. coli* (WP_123055588). One of the clones that grew in the cold also contained an insert similar to an antimicrobial protein (AQW80360) from an uncultured bacterium.

In addition to the clones that grew in the cold, random sequencing of clones from the *E. coli* DH10B library reflected inserts belong to highly abundant taxa in these environments, such as *Phormidesmis Priestleyi*, a Ktedonobacter species and Bdellovibrionales. The clone libraries created in this library therefore represent a second resource and 'catalogue' of functional biodiversity from this thesis. Future work is planned to sequence the full inserts of the clones that grew in the cold in the mutant cs2-29 and HCSI. In addition, the clone library in *E. coli* in DH10B can be screened for various enzymes such as lipases, esterases, glucuronidases using traditional assays.

9.4.2 Non-representative samples

One would like to assume that when DNA is extracted directly from an environmental sample, it represents the entire community of microbes that are present, in their correct proportions. However, there are several reasons why this may not be the case. One of the challenges in sampling from the environment is the heterogeneity of the species in the sample which extends both to the abundance of different species, and to their resistance to lysis. As a result, there are multiple steps at which the true structure of the community can be obscured by preferentially lysing, amplifying or otherwise advantaging some taxa of organisms over others. The method of lysis can result in unintentional biases (Culligan et al., 2014; Vester et al., 2015). For example, Gram-positive and Gram-negative cells respond differently to different lysis methods; gentle lysis is often preferable in order to protect the integrity of the DNA, however

it may lead to under-representation of hard-to-lyse gram-positive cells (Culligan et al., 2014). In this thesis, three of the shotgun metagenome samples from the same glacier forefield site (F3T3) were sequenced after using different DNA extraction methods to compare methods (Chapter 4).

DNA from all samples in this thesis was extracted using direct lysis methods, except for F3T3_Ludox. F3T3_Ludox DNA was extracted using a custom method that made use of a Ludox density gradient centrifugation step (Section 2.2.6) to separate bacteria from soil. Bacteria were then lysed using lysozyme to obtain high molecular weight DNA for cloning. The DNA obtained using this method was sequenced using shotgun sequencing in Chapter 4, to determine whether the Ludox microbial DNA was comparable to the microbial DNA extracted from the same site using PowerSoil and FastDNA methods. Perhaps unsurprisingly, the Ludox community was significantly altered, with a large reduction in the diversity of community members.

This observation has several implications for further research. Firstly, it highlights the importance of using the same DNA extraction techniques when aiming to make comparisons about community composition. Secondly, indirect lysis approaches are growing in popularity because of the need for high molecular weight DNA in both cloning experiments, and recently, in ultra-long read nanopore sequencing (Amarasinghe et al., 2020). However, these results serve as a warning that these gentler lysis methods may be introducing biases into experiments, which should be acknowledged, and measured by comparison to direct lysis methods if possible. Finally, the F3T3_Ludox also confirms the observation from Section 9.2.2, that lower diversity samples result in superior number and quality of MAGs. The F3T3_Ludox samples contributed 9 MAGs to the Svalbard metagenome dataset.

9.5 Microbial communities are cooperative

Prior to the metagenomics era, bioprospecting was often performed at a strain or isolate level. However, zooming out to the ecosystem level and examining how communities cooperate is a promising strategy. The use of microbial communities has been used in bioremediation and plastic degradation (Bell et al., 2013; Wei and Zimmermann, 2017; Yergeau et al., 2009). Several studies of environmental MAGs, many of them without cultured representatives, have revealed extreme cooperation between different members within a community (Anantharaman et al., 2016). In fact, most bacteria are symbiotic, working in symphony with other microorganism to obtain metabolites and energy. The recent discovery of candidate phyla

radiation (CPR) shows that certain bacteria are wholly dependent on other species for survival (Brown et al., 2015). The resolution and then annotation of communities of MAGs from environments can tell us what individual members need in terms of requirements, but also who they co-occur with. Ecology-level bioprospecting is therefore a promising avenue to describe community-level solutions, as well as to finally make inroads into the 'unculturable' microbial dark matter by suggesting non-axenic culturing strategies.

9.5.1 Co-cultivation to investigate 'uncultivatable' species

Cryoconite emerged as an interesting environment, that may present an ideal system for co-cultivation efforts. Compared to the highly heterogeneous soil environment, the cryoconite community was relatively stable across glaciers and years (Chapter 4, Spatial distribution). Cryoconite in Svalbard is dominated by a single cyanobacterial species, *Phormidesmis priestleyi*, although the literature suggests that the dominant cyanobacterial species can vary in different regions (Segawa et al., 2017). A fascinating observation is the core community or 'keystone taxa' that seem to cooccur with the Cyanobacteria, as well as several members of the CPR. Previous studies show that Cyanobacteria grow more easily in non-axenic culture with other bacteria (Cornet et al., 2018). In Chapter 3, a strong network of highly prevalent bacteria was present across many cryoconite samples, and in the MAG reconstruction, the ML, VB, and AB glacier also shared many similar heterotrophic bacteria. Both Chapter 3, and the MAG spatial distribution also showed that these species do not necessarily colonise downstream soil environments. Cryoconite therefore presents an excellent system in which to attempt co-cultivation of previously uncultivated species from cryoconite, as this ecosystem seems to form as a symbiotic collaboration between several different species.

9.6 Applications of the results of this thesis

The unique adaptations of bacteria to environmental pressures not only improves our understanding of general biology and the resilience of life under taxing conditions; but may also provide us with biotechnological tools that can improve human life in a number of ways (Cavicchioli et al., 2002).

9.6.1 Strategic cultivation

One of the main reasons for the turn to metagenomics is the realisation that the majority of microorganism cannot yet be cultured. It is estimated that 99% of bacterial species have not yet been cultured, and there are entire phyla, classes and orders that have no known cultured

isolates. There are many reasons for this difficulty in culturing bacteria, from a lack of knowledge of their nutrient, temperature, pH and salinity requirements to obligate dependence on other species for metabolic substrates, to the regulation of their growth by secondary metabolites of nearby bacteria. From studies of environmental MAGs, many of them without cultured representatives, there is growing evidence of extreme cooperation between different members within a community (Anantharaman et al., 2016). MAGs can be used to inform strategic cultivation of uncultured species by looking at the genome for information on nutrient sources and co-occurrence of different species.

9.6.2 Host engineering

Understanding the genomic context overcomes some of the difficulties of BGC expression, which relies on compatible promoters, ribosome binding sites, substrate metabolites and secretion machinery for NPs to be correctly expressed. Therefore, locating a BGC inside of a MAG, assists greatly with the genetic engineering of suitable hosts and the identification of optimal conditions for expression of the desired NP.

By conducting a bioinformatic screen and identifying a BGC of interest, it is possible to target a specific BGC using recombinant DNA technologies. Examples of recombinant DNA technologies that have been successfully employed to specifically and precisely target and capture BGCs of interest include high efficiency linear-linear homologous recombination (LLHR)(Yin et al., 2015), Transformation-associated recombination (TAR) cloning (Kouprina and Larionov, 2016), serine integrase-mediated site-specific recombination (SSR)(Du et al., 2015; Olorunniji et al., 2016) and Cas9-associated targeting of chromosome segments (CATCH) (Jiang et al., 2015). Meanwhile, advances in synthetic biology, referred to as bottom-up assembly methods, involve assembling the desired BGCs from several smaller fragments (Li et al., 2017). Examples include methylation-assisted tailorable ends rational (MASTER) ligation based on the type IIs endonuclease MspJI (Chen et al., 2013) site-specific recombination-based tandem assembly (SSTRA) (Zhang et al., 2011), Modified Gibson assembly (L. Li et al., 2015) and DNA assembler (Shao et al., 2011).

9.7 Genetic novelty in the cryosphere

Recent surveys of extreme environments reveal that the genetic diversity and novelty of extreme environments has not even begun to be catalogued by scientists (Duarte et al., 2020). In this thesis, the enormous depth of phylogenetic and functional diversity in the cryosphere

was revealed. Firstly, in the 16S rRNA amplicon study of ASVs in a glacial ecosystem, rare ASVs made up a significant proportion of the samples (Figure 3-16). Secondly, shotgun analyses of the microbial communities of Svalbard cryoconite, soil and seawater (Chapter 4) and the Scărișoara Ice Cave in Romania (Chapter 7) resulted in only two MAGs from the Svalbard dataset (Table 4-7), and ten MAGs from the Scărișoara Ice Cave (Table 7-4) dataset that could be classified to species level. The remaining MAGs represented novel species within their genus, or novel genera within their family. Thirdly, when the Svalbard MAGs were screened for BGCS, there were 1742 BGCs detected, and only 278 of the clusters had hits to clusters that synthesize known compounds within the MIBiG database (Chapter 5). Of the 278 BGCs with hits to MIBiG compounds, only 21 of those had > 85% similarity to MIBiG compounds. The remaining 257 clusters with hits to MIBiG compounds ranged from just 1% to 85% similarity, suggesting incredible NP diversity.

9.8 Conclusion

Bioprospecting in the cryosphere has the potential to provide NPs that benefit human health and the environment. Although the cryosphere is often considered an extreme environment, it is an incredibly diverse biome, and most bacteria that inhabit this environment are exquisitely adapted to their specific ecological niche. These adaptations translate into a range of enzymes and secondary metabolites that have a wide range of applications in the pharmaceutical, cosmetics, food, and bioremediation industries. A bioinformatics workflow designed to assemble MAGs from shotgun data was used to explore the genetic potential of cryoconite, soil and seawater habitats in Svalbard, and an Ice Cave glacier from Romania. Both settings were found to have a high level of genetic novelty, with 72 MAGs from the Svalbard data and 111 MAGs from the Scărișoara Ice Cave representing new species. Furthermore, bioinformatics screens of the MAGs and contigs revealed a wealth of novel BGCs for EPS, carotenoids, and NRPS secondary metabolites which are useful as emollients, gums, antioxidants, pigments, and antimicrobial compounds. A clone library of cryoconite and soil eDNA was also created and can be used in future research to conduct functional screens for novel enzymes. This thesis therefore represents a contribution to the understanding of cryospheric bacteria, their adaptations to their environments, and their utility as sources of useful products.

10 REFERENCES

Abedi, E., Sahari, M.A., 2014. Long-chain polyunsaturated fatty acid sources and evaluation of their nutritional and functional properties. Food Sci. Nutr. 2, 443–463. https://doi.org/10.1002/fsn3.121

Aislabie, J., Foght, J., Saul, D., 2000. Aromatic hydrocarbon-degrading bacteria from soil near Scott Base, Antarctica. Polar Biol. 23, 183–188. https://doi.org/10.1007/s003000050025

Aislabie, J., Saul, D.J., Foght, J.M., 2006. Bioremediation of hydrocarbon-contaminated polar soils. Extremophiles 10, 171–179. https://doi.org/10.1007/s00792-005-0498-4

Albino, A., Marco, S., Di Maro, A., Chambery, A., Masullo, M., De Vendittis, E., 2012. Characterization of a cold-adapted glutathione synthetase from the psychrophile *Pseudoalteromonas haloplanktis*. Mol. Biosyst. 8, 2405. https://doi.org/10.1039/c2mb25116g

Alikkunju, A.P., Sainjan, N., Silvester, R., Joseph, A., Rahiman, M., Antony, A.C., Kumaran, R.C., Hatha, M., 2016. Screening and Characterization of Cold-Active β-Galactosidase Producing Psychrotrophic *Enterobacter ludwigii* from the Sediments of Arctic Fjord. Appl. Biochem. Biotechnol. 180, 477–490. https://doi.org/10.1007/s12010-016-2111-y

Alikunju, A.P., Joy, S., Salam, J.A., Silvester, R., Antony, A.C., Rahiman, K.M.M., Krishnan, K.P., Hatha, A.A.M., 2018. Functional Characterization of a New Cold-Adapted β-Galactosidase from an Arctic Fjord Sediment Bacteria *Enterobacter ludwigii* MCC 3423. Catal. Lett. 148, 3223–3235. https://doi.org/10.1007/s10562-018-2504-3

Allen, E.E., Bartlett, D.H., 2002. Structure and regulation of the omega-3 polyunsaturated fatty acid synthase genes from the deep-sea bacterium *Photobacterium profundum* strain SS9The GenBank accession numbers for the sequences reported in this paper are AF409100 and AF467805. Microbiology, 148, 1903–1913. https://doi.org/10.1099/00221287-148-6-1903

Allison, S.D., Martiny, J.B.H., 2008. Resistance, resilience, and redundancy in microbial communities. Proc. Natl. Acad. Sci. 105, 11512–11519. https://doi.org/10.1073/pnas.0801925105

Alneberg, J., Bjarnason, B.S., de Bruijn, I., Schirmer, M., Quick, J., Ijaz, U.Z., Lahti, L., Loman, N.J., Andersson, A.F., Quince, C., 2014. Binning metagenomic contigs by coverage and composition. Nat. Methods 11, 1144–1146. https://doi.org/10.1038/nmeth.3103

Al-Zereini, W., Schuhmann, I., Laatsch, H., Helmke, E., Anke, H., 2007. New Aromatic Nitro Compounds from *Salegentibacter* sp. T436, an Arctic Sea Ice Bacterium: Taxonomy, Fermentation, Isolation and Biological Activities. J. Antibiot. (Tokyo) 60, 301–308. https://doi.org/10.1038/ja.2007.38

Amarasinghe, S.L., Su, S., Dong, X., Zappia, L., Ritchie, M.E., Gouil, Q., 2020. Opportunities and challenges in long-read sequencing data analysis. Genome Biol. 21, 30. https://doi.org/10.1186/s13059-020-1935-5

Amato, P., Hennebelle, R., Magand, O., Sancelme, M., Delort, A.-M., Barbante, C., Boutron, C., Ferrari, C., 2007. Bacterial characterization of the snow cover at Spitzberg,

Svalbard: Bacterial characterization of an Arctic snow cover. FEMS Microbiol. Ecol. 59, 255–264. https://doi.org/10.1111/j.1574-6941.2006.00198.x

Amoutzias, G.D., Chaliotis, A., Mossialos, D., 2016. Discovery Strategies of Bioactive Compounds Synthesized by Nonribosomal Peptide Synthetases and Type-I Polyketide Synthases Derived from Marine Microbiomes. Mar. Drugs 14, 80. https://doi.org/10.3390/md14040080

Anantharaman, K., Brown, C.T., Hug, L.A., Sharon, I., Castelle, C.J., Probst, A.J., Thomas, B.C., Singh, A., Wilkins, M.J., Karaoz, U., Brodie, E.L., Williams, K.H., Hubbard, S.S., Banfield, J.F., 2016. Thousands of microbial genomes shed light on interconnected biogeochemical processes in an aquifer system. Nat. Commun. 7, 13219. https://doi.org/10.1038/ncomms13219

Anesio, A.M., Hodson, A.J., Fritz, A., Psenner, R., Sattler, B., 2009. High microbial activity on glaciers: importance to the global carbon cycle. Glob. Change Biol. 15, 955–960. https://doi.org/10.1111/j.1365-2486.2008.01758.x

Anesio, A.M., Laybourn-Parry, J., 2012. Glaciers and ice sheets as a biome. Trends Ecol. Evol. 27, 219–225. https://doi.org/10.1016/j.tree.2011.09.012

Anesio, A.M., Lutz, S., Chrismas, N.A.M., Benning, L.G., 2017. The microbiome of glaciers and ice sheets. Npj Biofilms Microbiomes 3, 1–11. https://doi.org/10.1038/s41522-017-0019-0

Anesio, A.M., Sattler, B., Foreman, C., Telling, J., Hodson, A., Tranter, M., Psenner, R., 2010. Carbon fluxes through bacterial communities on glacier surfaces. Ann. Glaciol. 51, 32–40. https://doi.org/10.3189/172756411795932092

Angelaccio, S., Florio, R., Consalvi, V., Festa, G., Pascarella, S., 2012. Serine Hydroxymethyltransferase from the Cold Adapted Microorganism *Psychromonas ingrahamii*: A Low Temperature Active Enzyme with Broad Substrate Specificity. Int. J. Mol. Sci. 13, 1314–1326. https://doi.org/10.3390/ijms13021314

Arkin, A.P., Cottingham, R.W., Henry, C.S., Harris, N.L., Stevens, R.L., Maslov, S., Dehal, P., Ware, D., Perez, F., Canon, S., Sneddon, M.W., Henderson, M.L., Riehl, W.J., Murphy-Olson, D., Chan, S.Y., Kamimura, R.T., Kumari, S., Drake, M.M., Brettin, T.S., Glass, E.M., Chivian, D., Gunter, D., Weston, D.J., Allen, B.H., Baumohl, J., Best, A.A., Bowen, B., Brenner, S.E., Bun, C.C., Chandonia, J.-M., Chia, J.-M., Colasanti, R., Conrad, N., Davis, J.J., Davison, B.H., DeJongh, M., Devoid, S., Dietrich, E., Dubchak, I., Edirisinghe, J.N., Fang, G., Faria, J.P., Frybarger, P.M., Gerlach, W., Gerstein, M., Greiner, A., Gurtowski, J., Haun, H.L., He, F., Jain, R., Joachimiak, M.P., Keegan, K.P., Kondo, S., Kumar, V., Land, M.L., Meyer, F., Mills, M., Novichkov, P.S., Oh, T., Olsen, G.J., Olson, R., Parrello, B., Pasternak, S., Pearson, E., Poon, S.S., Price, G.A., Ramakrishnan, S., Ranjan, P., Ronald, P.C., Schatz, M.C., Seaver, S.M.D., Shukla, M., Sutormin, R.A., Syed, M.H., Thomason, J., Tintle, N.L., Wang, D., Xia, F., Yoo, H., Yoo, S., Yu, D., 2018. KBase: The United States Department of Energy Systems Biology Knowledgebase. Nat. Biotechnol. 36, 566–569. https://doi.org/10.1038/nbt.4163

Aron, A.T., Gentry, E.C., McPhail, K.L., Nothias, L.-F., Nothias-Esposito, M., Bouslimani, A., Petras, D., Gauglitz, J.M., Sikora, N., Vargas, F., van der Hooft, J.J.J., Ernst, M., Kang, K.B., Aceves, C.M., Caraballo-Rodríguez, A.M., Koester, I., Weldon, K.C., Bertrand, S., Roullier, C., Sun, K., Tehan, R.M., P, C.A.B., Christian, M.H., Gutiérrez, M., Ulloa, A.M., Tejeda Mora, J.A., Mojica-Flores, R., Lakey-Beitia, J., Vásquez-Chaves, V., Zhang, Y., Calderón, A.I., Tayler, N., Keyzers, R.A., Tugizimana, F., Ndlovu, N., Aksenov, A.A., Jarmusch, A.K., Schmid, R., Truman, A.W., Bandeira, N., Wang, M., Dorrestein, P.C., 2020. Reproducible molecular

networking of untargeted mass spectrometry data using GNPS. Nat. Protoc. 15, 1954–1991. https://doi.org/10.1038/s41596-020-0317-5

Arrigo, K.R., 2014. Sea Ice Ecosystems. Annu. Rev. Mar. Sci. 6, 439–467. https://doi.org/10.1146/annurev-marine-010213-135103

Asthana, R.K., Deepali, Tripathi, M.K., Srivastava, A., Singh, A.P., Singh, S.P., Nath, G., Srivastava, R., Srivastava, B.S., 2009. Isolation and identification of a new antibacterial entity from the Antarctic cyanobacterium *Nostoc* CCC 537. J. Appl. Phycol. 21, 81. https://doi.org/10.1007/s10811-008-9328-2

Bach, E.M., Williams, R.J., Hargreaves, S.K., Yang, F., Hofmockel, K.S., 2018. Greatest soil microbial diversity found in micro-habitats. Soil Biol. Biochem. 118, 217–226. https://doi.org/10.1016/j.soilbio.2017.12.018

Bagchi, A., Ghosh, T.C., 2005. A structural study towards the understanding of the interactions of SoxY, SoxZ, and SoxB, leading to the oxidation of sulfur anions via the novel global sulfur oxidizing (sox) operon. Biochem. Biophys. Res. Commun. 335, 609–615. https://doi.org/10.1016/j.bbrc.2005.07.115

Bagchi, A., Roy, P., 2005. Structural insight into SoxC and SoxD interaction and their role in electron transport process in the novel global sulfur cycle in *Paracoccus pantotrophus*. Biochem. Biophys. Res. Commun. 331, 1107–1113. https://doi.org/10.1016/j.bbrc.2005.04.028

Bakken, L.R., Lindahl, V., 1995. Recovery of Bacterial Cells from Soil, in: Trevors, J.T., van Elsas, J.D. (Eds.), Nucleic Acids in the Environment, Springer Lab Manuals. Springer Berlin Heidelberg, Berlin, Heidelberg, pp. 9–27. https://doi.org/10.1007/978-3-642-79050-8_2

Banik, J.J., Craig, J.W., Calle, P.Y., Brady, S.F., 2010. Tailoring Enzyme-Rich Environmental DNA Clones: A Source of Enzymes for Generating Libraries of Unnatural Natural Products. J. Am. Chem. Soc. 132, 15661–15670. https://doi.org/10.1021/ja105825a

Bar Dolev, M., Braslavsky, I., Davies, P.L., 2016. Ice-Binding Proteins and Their Function. Annu. Rev. Biochem. 85, 515–542. https://doi.org/10.1146/annurev-biochem-060815-014546

Baraniecki, C.A., Aislabie, J., Foght, J.M., 2002. Characterization of *Sphingomonas* sp. Ant 17, an Aromatic Hydrocarbon-Degrading Bacterium Isolated from Antarctic Soil. Microb. Ecol. 43, 44–54. https://doi.org/10.1007/s00248-001-1019-3

Barletta, R.E., Priscu, J.C., Mader, H.M., Jones, W.L., Roe, C.H., 2012. Chemical analysis of ice vein microenvironments: II. Analysis of glacial samples from Greenland and Antarctica. J. Glaciol. 58, 1109–1118. https://doi.org/10.3189/2012JoG12J112

Barry, R.G., 2017. The Arctic Cryosphere in the Twenty-First Century. Geogr. Rev. 107, 69–88. https://doi.org/10.1111/gere.12227

Bastian, M., Heymann, S., Jacomy, M., 2009. Gephi: An Open Source Software for Exploring and Manipulating Networks, in: International AAAI Conference on Web and Social Medi. Presented at the International AAAI Conference on Web and Social Media.

Bauer, J.D., King, R.W., Brady, S.F., 2010. Utahmycins A and B, Azaquinones Produced by an Environmental DNA Clone. J. Nat. Prod. 73, 976–979. https://doi.org/10.1021/np900786s

Bay, S.K., McGeoch, M.A., Gillor, O., Wieler, N., Palmer, D.J., Baker, D.J., Chown, S.L., Greening, C., 2020. Soil Bacterial Communities Exhibit Strong Biogeographic Patterns at Fine Taxonomic Resolution. mSystems 5. https://doi.org/10.1128/mSystems.00540-20

Bazinet, R.P., Layé, S., 2014. Polyunsaturated fatty acids and their metabolites in brain function and disease. Nat. Rev. Neurosci. 15, 771–785. https://doi.org/10.1038/nrn3820

Bej, A.K., Saul, D., Aislabie, J., 2000. Cold-tolerant alkane-degrading *Rhodococcus* species from Antarctica. Polar Biol. 23, 100–105. https://doi.org/10.1007/s003000050014

Bell, T.H., Yergeau, E., Maynard, C., Juck, D., Whyte, L.G., Greer, C.W., 2013. Predictable bacterial composition and hydrocarbon degradation in Arctic soils following diesel and nutrient disturbance. ISME J. 7, 1200–1210. https://doi.org/10.1038/ismej.2013.1

Benning, L.G., Anesio, A.M., Lutz, S., Tranter, M., 2014. Biological impact on Greenland's albedo. Nat. Geosci. 7, 691–691. https://doi.org/10.1038/ngeo2260

Benson, D.A., Cavanaugh, M., Clark, K., Karsch-Mizrachi, I., Lipman, D.J., Ostell, J., Sayers, E.W., 2013. GenBank. Nucleic Acids Res. 41, D36-42. https://doi.org/10.1093/nar/gks1195

Bérdy, J., 2005. Bioactive Microbial Metabolites. J. Antibiot. (Tokyo) 58, 1–26. https://doi.org/10.1038/ja.2005.1

Bergmann, M., Mützel, S., Primpke, S., Tekman, M.B., Trachsel, J., Gerdts, G., 2019. White and wonderful? Microplastics prevail in snow from the Alps to the Arctic. Sci. Adv. 5, eaax1157. https://doi.org/10.1126/sciadv.aax1157

Bhullar, K., Waglechner, N., Pawlowski, A., Koteva, K., Banks, E.D., Johnston, M.D., Barton, H.A., Wright, G.D., 2012. Antibiotic Resistance Is Prevalent in an Isolated Cave Microbiome. PLOS ONE 7, e34953. https://doi.org/10.1371/journal.pone.0034953

Blin, K., Pascal Andreu, V., de los Santos, E.L.C., Del Carratore, F., Lee, S.Y., Medema, M.H., Weber, T., 2019a. The antiSMASH database version 2: a comprehensive resource on secondary metabolite biosynthetic gene clusters. Nucleic Acids Res. 47, D625–D630. https://doi.org/10.1093/nar/gky1060

Blin, K., Shaw, S., Steinke, K., Villebro, R., Ziemert, N., Lee, S.Y., Medema, M.H., Weber, T., 2019b. antiSMASH 5.0: updates to the secondary metabolite genome mining pipeline. Nucleic Acids Res. 47, W81–W87. https://doi.org/10.1093/nar/gkz310

Blin, K., Wolf, T., Chevrette, M.G., Lu, X., Schwalen, C.J., Kautsar, S.A., Suarez Duran, H.G., de Los Santos, E.L.C., Kim, H.U., Nave, M., Dickschat, J.S., Mitchell, D.A., Shelest, E., Breitling, R., Takano, E., Lee, S.Y., Weber, T., Medema, M.H., 2017. antiSMASH 4.0-improvements in chemistry prediction and gene cluster boundary identification. Nucleic Acids Res. https://doi.org/10.1093/nar/gkx319

Boetius, A., Anesio, A.M., Deming, J.W., Mikucki, J.A., Rapp, J.Z., 2015. Microbial ecology of the cryosphere: sea ice and glacial habitats. Nat. Rev. Microbiol. 13, 677–690. https://doi.org/10.1038/nrmicro3522

Bolger, A.M., Lohse, M., Usadel, B., 2014. Trimmomatic: a flexible trimmer for Illumina sequence data. Bioinformatics 30, 2114–2120. https://doi.org/10.1093/bioinformatics/btu170

Bowers, R.M., Kyrpides, N.C., Stepanauskas, R., Harmon-Smith, M., Doud, D., Reddy, T.B.K., Schulz, F., Jarett, J., Rivers, A.R., Eloe-Fadrosh, E.A., Tringe, S.G., Ivanova, N.N., Copeland, A., Clum, A., Becraft, E.D., Malmstrom, R.R., Birren, B., Podar, M., Bork, P., Weinstock, G.M., Garrity, G.M., Dodsworth, J.A., Yooseph, S., Sutton, G., Glöckner, F.O., Gilbert, J.A., Nelson, W.C., Hallam, S.J., Jungbluth, S.P., Ettema, T.J.G., Tighe, S., Konstantinidis, K.T., Liu, W.-T., Baker, B.J., Rattei, T., Eisen, J.A., Hedlund, B., McMahon, K.D., Fierer, N., Knight, R., Finn, R., Cochrane, G., Karsch-Mizrachi, I., Tyson, G.W., Rinke, C., Lapidus, A., Meyer, F., Yilmaz, P., Parks, D.H., Eren, A.M., Schriml, L., Banfield, J.F., Hugenholtz, P., Woyke, T., 2017. Minimum information about a single amplified genome (MISAG) and a metagenome-assembled

genome (MIMAG) of bacteria and archaea. Nat. Biotechnol. 35, 725–731. https://doi.org/10.1038/nbt.3893

Bowman, J.P., Gosink, J.J., McCammon, S.A., Lewis, T.E., Nichols, D.S., Nichols, P.D., Skerratt, J.H., Staley, J.T., McMeekin, T.A., 1998. *Colwellia deming*iae sp. nov., *Colwellia hornerae* sp. nov., *Colwellia rossensis* sp. nov. and *Colwellia psychrotropica* sp. nov.: psychrophilic Antarctic species with the ability to synthesize docosahexaenoic acid (22: 63). Int. J. Syst. Bacteriol. 48, 1171–1180. https://doi.org/10.1099/00207713-48-4-1171

Bowman, J.P., McCammon, S.A., Nichols, D.S., Skerratt, J.H., Rea, S.M., Nichols, P.D., McMeekin, T.A., 1997. *Shewanella gelidimarina* sp. nov. and *Shewanella frigidimarina* sp. nov., Novel Antarctic Species with the Ability To Produce Eicosapentaenoic Acid (20:5 3) and Grow Anaerobically by Dissimilatory Fe(III) Reduction. Int. J. Syst. Bacteriol. 47, 1040–1047. https://doi.org/10.1099/00207713-47-4-1040

Box, J.E., Fettweis, X., Stroeve, J.C., Tedesco, M., Hall, D.K., Steffen, K., 2012. Greenland ice sheet albedo feedback: thermodynamics and atmospheric drivers. The Cryosphere 6, 821–839. https://doi.org/10.5194/tc-6-821-2012

Brad, T., Itcus, C., Pascu, M.-D., Perșoiu, A., Hillebrand-Voiculescu, A., Iancu, L., Purcarea, C., 2018. Fungi in perennial ice from Scărișoara Ice Cave (Romania). Sci. Rep. 8, 10096. https://doi.org/10.1038/s41598-018-28401-1

Bradley, J.A., Singarayer, J.S., Anesio, A.M., 2014. Microbial community dynamics in the forefield of glaciers. Proc. R. Soc. B Biol. Sci. 281, 20140882. https://doi.org/10.1098/rspb.2014.0882

Brown, B.L., Watson, M., Minot, S.S., Rivera, M.C., Franklin, R.B., 2017. MinION™ nanopore sequencing of environmental metagenomes: a synthetic approach. GigaScience 6. https://doi.org/10.1093/gigascience/gix007

Brown, C.T., Hug, L.A., Thomas, B.C., Sharon, I., Castelle, C.J., Singh, A., Wilkins, M.J., Wrighton, K.C., Williams, K.H., Banfield, J.F., 2015. Unusual biology across a group comprising more than 15% of domain Bacteria. Nature 523, 208–211. https://doi.org/10.1038/nature14486

Brown, J., Pirrung, M., McCue, L.A., 2017. FQC Dashboard: integrates FastQC results into a web-based, interactive, and extensible FASTQ quality control tool. Bioinformatics 33, 3137–3139. https://doi.org/10.1093/bioinformatics/btx373

Bruntner, C., Binder, T., Pathom-aree, W., Goodfellow, M., Bull, A.T., Potterat, O., Puder, C., Hörer, S., Schmid, A., Bolek, W., Wagner, K., Mihm, G., Fiedler, H.-P., 2005. Frigocyclinone, a Novel Angucyclinone Antibiotic Produced by a *Streptomyces griseus* Strain from Antarctica†. J. Antibiot. (Tokyo) 58, 346–349. https://doi.org/10.1038/ja.2005.43

Buchfink, B., Xie, C., Huson, D.H., 2015. Fast and sensitive protein alignment using DIAMOND. Nat. Methods 12, 59–60. https://doi.org/10.1038/nmeth.3176

Buck, M., Hamilton, C., 2011. The Nagoya Protocol on Access to Genetic Resources and the Fair and Equitable Sharing of Benefits Arising from their Utilization to the Convention on Biological Diversity. Rev. Eur. Community Int. Environ. Law 20, 47–61. https://doi.org/10.1111/j.1467-9388.2011.00703.x

Busi, S.B., Pramateftaki, P., Brandani, J., Fodelianakis, S., Peter, H., Halder, R., Wilmes, P., Battin, T., 2020. Optimised biomolecular extraction for metagenomic analysis of microbial biofilms from high-mountain streams. bioRxiv 2020.04.30.069724. https://doi.org/10.1101/2020.04.30.069724

Busk, P.K., Pilgaard, B., Lezyk, M.J., Meyer, A.S., Lange, L., 2017. Homology to peptide pattern for annotation of carbohydrate-active enzymes and prediction of function. BMC Bioinformatics 18, 214. https://doi.org/10.1186/s12859-017-1625-9

Butler, M.S., 2004. The Role of Natural Product Chemistry in Drug Discovery †. J. Nat. Prod. 67, 2141–2153. https://doi.org/10.1021/np040106y

Butler, M.S., Blaskovich, M.A., Owen, J.G., Cooper, M.A., 2016. Old dogs and new tricks in antimicrobial discovery. Curr. Opin. Microbiol. 33, 25–34. https://doi.org/10.1016/j.mib.2016.05.011

Cai, H., Cui, H., Zeng, Y., An, M., Jiang, H., 2018. *Sandarakinorhabdus cyanobacteriorum* sp. nov., a novel bacterium isolated from cyanobacterial aggregates in a eutrophic lake. Int. J. Syst. Evol. Microbiol. 68, 730–735. https://doi.org/10.1099/ijsem.0.002571

Callahan, B.J., McMurdie, P.J., Holmes, S.P., 2017. Exact sequence variants should replace operational taxonomic units in marker-gene data analysis. ISME J. 11, 2639–2643. https://doi.org/10.1038/ismej.2017.119

Callahan, B.J., McMurdie, P.J., Rosen, M.J., Han, A.W., Johnson, A.J.A., Holmes, S.P., 2016. DADA2: High-resolution sample inference from Illumina amplicon data. Nat. Methods 13, 581–583. https://doi.org/10.1038/nmeth.3869

Calteau, A., Fewer, D.P., Latifi, A., Coursin, T., Laurent, T., Jokela, J., Kerfeld, C.A., Sivonen, K., Piel, J., Gugger, M., 2014. Phylum-wide comparative genomics unravel the diversity of secondary metabolism in Cyanobacteria. BMC Genomics 15, 977. https://doi.org/10.1186/1471-2164-15-977

Cameron, K.A., Hodson, A.J., Osborn, A.M., 2012a. Structure and diversity of bacterial, eukaryotic and archaeal communities in glacial cryoconite holes from the Arctic and the Antarctic. FEMS Microbiol. Ecol. 82, 254–267. https://doi.org/10.1111/j.1574-6941.2011.01277.x

Cameron, K.A., Hodson, A.J., Osborn, A.M., 2012b. Carbon and nitrogen biogeochemical cycling potentials of supraglacial cryoconite communities. Polar Biol. 35, 1375–1393. https://doi.org/10.1007/s00300-012-1178-3

Cameron, K.A., Müller, O., Stibal, M., Edwards, A., Jacobsen, C.S., 2020a. Glacial microbiota are hydrologically connected and temporally variable. Environ. Microbiol. n/a. https://doi.org/10.1111/1462-2920.15059

Campbell, J.H., O'Donoghue, P., Campbell, A.G., Schwientek, P., Sczyrba, A., Woyke, T., Söll, D., Podar, M., 2013. UGA is an additional glycine codon in uncultured SR1 bacteria from the human microbiota. Proc. Natl. Acad. Sci. 110, 5540–5545. https://doi.org/10.1073/pnas.1303090110

Cantarel, B.L., Coutinho, P.M., Rancurel, C., Bernard, T., Lombard, V., Henrissat, B., 2009. The Carbohydrate-Active EnZymes database (CAZy): an expert resource for Glycogenomics. Nucleic Acids Res. 37, D233–D238. https://doi.org/10.1093/nar/gkn663

Casanueva, A., Tuffin, M., Cary, C., Cowan, D.A., 2010. Molecular adaptations to psychrophily: the impact of 'omic' technologies. Trends Microbiol. 18, 374–381. https://doi.org/10.1016/j.tim.2010.05.002

Cavicchioli, R., Ripple, W.J., Timmis, K.N., Azam, F., Bakken, L.R., Baylis, M., Behrenfeld, M.J., Boetius, A., Boyd, P.W., Classen, A.T., Crowther, T.W., Danovaro, R., Foreman, C.M., Huisman, J., Hutchins, D.A., Jansson, J.K., Karl, D.M., Koskella, B., Mark Welch, D.B., Martiny, J.B.H., Moran, M.A., Orphan, V.J., Reay, D.S., Remais, J.V., Rich, V.I., Singh, B.K., Stein, L.Y., Stewart, F.J., Sullivan, M.B., van Oppen, M.J.H., Weaver, S.C., Webb, E.A., Webster, N.S., 2019. Scientists' warning to

humanity: microorganisms and climate change. Nat. Rev. Microbiol. 17, 569–586. https://doi.org/10.1038/s41579-019-0222-5

Cavicchioli, R., Siddiqui, K.S., Andrews, D., Sowers, K.R., 2002. Low-temperature extremophiles and their applications. Curr. Opin. Biotechnol. 13, 253–261. https://doi.org/10.1016/S0958-1669(02)00317-8

Chang, Z., Flatt, P., Gerwick, W.H., Nguyen, V.-A., Willis, C.L., Sherman, D.H., 2002. The barbamide biosynthetic gene cluster: a novel marine cyanobacterial system of mixed polyketide synthase (PKS)-non-ribosomal peptide synthetase (NRPS) origin involving an unusual trichloroleucyl starter unit. Gene 296, 235–247. https://doi.org/10.1016/S0378-1119(02)00860-0

Chattopadhyay, M.K., 2006. Mechanism of bacterial adaptation to low temperature. J. Biosci. 31, 157–165.

Chaumeil, P.-A., Mussig, A.J., Hugenholtz, P., Parks, D.H., 2020. GTDB-Tk: a toolkit to classify genomes with the Genome Taxonomy Database. Bioinformatics 36, 1925–1927. https://doi.org/10.1093/bioinformatics/btz848

Chavali, A.K., Rhee, S.Y., 2018. Bioinformatics tools for the identification of gene clusters that biosynthesize specialized metabolites. Brief. Bioinform. 19, 1022–1034. https://doi.org/10.1093/bib/bbx020

Chen, W.-H., Qin, Z.-J., Wang, J., Zhao, G.-P., 2013. The MASTER (methylation-assisted tailorable ends rational) ligation method for seamless DNA assembly. Nucleic Acids Res. 41, e93. https://doi.org/10.1093/nar/gkt122

Chiang, Y.-M., Chang, S.-L., Oakley, B.R., Wang, C.C., 2011. Recent advances in awakening silent biosynthetic gene clusters and linking orphan clusters to natural products in microorganisms. Curr. Opin. Chem. Biol., Omics 15, 137–143. https://doi.org/10.1016/j.cbpa.2010.10.011

Chrapusta, E., Węgrzyn, M., Zabaglo, K., Kaminski, A., Adamski, M., Wietrzyk, P., Bialczyk, J., 2015. Microcystins and anatoxin-a in Arctic biocrust cyanobacterial communities. Toxicon 101, 35–40. https://doi.org/10.1016/j.toxicon.2015.04.016

Chrismas, N.A.M., Barker, G., Anesio, A.M., Sánchez-Baracaldo, P., 2016a. Genomic mechanisms for cold tolerance and production of exopolysaccharides in the Arctic cyanobacterium *Phormidesmis priestleyi* BC1401. BMC Genomics 17, 533. https://doi.org/10.1186/s12864-016-2846-4

Chrismas, N.A.M., Williamson, C.J., Yallop, M.L., Anesio, A.M., Sánchez-Baracaldo, P., 2018. Photoecology of the Antarctic cyanobacterium *Leptolyngbya* sp. BC1307 brought to light through community analysis, comparative genomics and in vitro photophysiology. Mol. Ecol. 27, 5279–5293. https://doi.org/10.1111/mec.14953

Cimermancic, P., Medema, M.H., Claesen, J., Kurita, K., Wieland Brown, L.C., Mavrommatis, K., Pati, A., Godfrey, P.A., Koehrsen, M., Clardy, J., Birren, B.W., Takano, E., Sali, A., Linington, R.G., Fischbach, M.A., 2014. Insights into Secondary Metabolism from a Global Analysis of Prokaryotic Biosynthetic Gene Clusters. Cell 158, 412–421. https://doi.org/10.1016/j.cell.2014.06.034

Coates, A.R., Halls, G., Hu, Y., 2011. Novel classes of antibiotics or more of the same? Br. J. Pharmacol. 163, 184–194. https://doi.org/10.1111/j.1476-5381.2011.01250.x

Connor, T.R., Loman, N.J., Thompson, S., Smith, A., Southgate, J., Poplawski, R., Bull, M.J., Richardson, E., Ismail, M., Thompson, S.E.-, Kitchen, C., Guest, M., Bakke, M., Sheppard, S.K., Pallen, M.J., 2016. CLIMB (the Cloud Infrastructure for Microbial Bioinformatics): an online resource for the medical microbiology community. Microb. Genomics 2. https://doi.org/10.1099/mgen.0.000086

Conte, A., Papale, M., Amalfitano, S., Mikkonen, A., Rizzo, C., De Domenico, E., Michaud, L., Lo Giudice, A., 2018. Bacterial community structure along the subtidal sandy

sediment belt of a high Arctic fjord (Kongsfjorden, Svalbard Islands). Sci. Total Environ. 619–620, 203–211. https://doi.org/10.1016/j.scitotenv.2017.11.077

Conway, J.R., Lex, A., Gehlenborg, N., 2017. UpSetR: an R package for the visualization of intersecting sets and their properties. Bioinformatics 33, 2938–2940. https://doi.org/10.1093/bioinformatics/btx364

Cook, J.M., Edwards, A., Bulling, M., Mur, L.A.J., Cook, S., Gokul, J.K., Cameron, K.A., Sweet, M., Irvine-Fynn, T.D.L., 2016a. Metabolome-mediated biocryomorphic evolution promotes carbon fixation in Greenlandic cryoconite holes. Environ. Microbiol. https://doi.org/10.1111/1462-2920.13349

Cook, J.M., Edwards, A., Takeuchi, N., Irvine-Fynn, T., 2016b. Cryoconite The dark biological secret of the cryosphere. Prog. Phys. Geogr. 40, 66–111. https://doi.org/10.1177/0309133315616574

Cook, J.M., Hodson, A., Telling, J., Anesio, A., Irvine-Fynn, T., Bellas, C., 2010. The mass–area relationship within cryoconite holes and its implications for primary production. Ann. Glaciol. 51, 106–110. https://doi.org/10.3189/172756411795932038

Cordero, P.R.F., Bayly, K., Man Leung, P., Huang, C., Islam, Z.F., Schittenhelm, R.B., King, G.M., Greening, C., 2019. Atmospheric carbon monoxide oxidation is a widespread mechanism supporting microbial survival. ISME J. 13, 2868–2881. https://doi.org/10.1038/s41396-019-0479-8

Cormack, W.P.M., Fraile, E.R., 1997. Characterization of a hydrocarbon degrading psychrotrophic Antarctic bacterium. Antarct. Sci. 9. https://doi.org/10.1017/S0954102097000199

Cornet, L., Bertrand, A.R., Hanikenne, M., Javaux, E.J., Wilmotte, A., Baurain, D., 2018. Metagenomic assembly of new (sub)polar Cyanobacteria and their associated microbiome from non-axenic cultures. Microb. Genomics 4. https://doi.org/10.1099/mgen.0.000212

Cotter, P.A., Chepuri, V., Gennis, R.B., Gunsalus, R.P., 1990. Cytochrome o (cyoABCDE) and d (cydAB) oxidase gene expression in *Escherichia coli* is regulated by oxygen, pH, and the fnr gene product. J. Bacteriol. 172, 6333–6338. https://doi.org/10.1128/jb.172.11.6333-6338.1990

Craig, J.W., Chang, F.-Y., Kim, J.H., Obiajulu, S.C., Brady, S.F., 2010. Expanding Small-Molecule Functional Metagenomics through Parallel Screening of Broad-Host-Range Cosmid Environmental DNA Libraries in Diverse Proteobacteria. Appl. Environ. Microbiol. 76, 1633–1641. https://doi.org/10.1128/AEM.02169-09

Cuadrat, R., Ionescu, D., Dávila, A., Grossart, H.-P., 2018. Recovering Genomics Clusters of Secondary Metabolites from Lakes using Genome-Resolved Metagenomics. Front. Microbiol. 9. https://doi.org/10.3389/fmicb.2018.00251

Culligan, E.P., Sleator, R.D., Marchesi, J.R., Hill, C., 2014. Metagenomics and novel gene discovery. Virulence 5, 399–412. https://doi.org/10.4161/viru.27208

Cusano, A.M., Parrilli, E., Marino, G., Tutino, M.L., 2006. A novel genetic system for recombinant protein secretion in the Antarctic *Pseudoalteromonas haloplanktis* TAC125. Microb. Cell Factories 5, 40. https://doi.org/10.1186/1475-2859-5-40

Cuthbertson, L., Amores-Arrocha, H., Malard, L.A., Els, N., Sattler, B., Pearce, D.A., 2017. Characterisation of Arctic Bacterial Communities in the Air above Svalbard. Biology 6. https://doi.org/10.3390/biology6020029

Dai, X.-Z., Kawamoto, J., Sato, S.B., Esaki, N., Kurihara, T., 2012. Eicosapentaenoic acid facilitates the folding of an outer membrane protein of the psychrotrophic bacterium, *Shewanella livingstonensis* Ac10. Biochem. Biophys. Res. Commun. 425, 363–367. https://doi.org/10.1016/j.bbrc.2012.07.097

D'Amico, S., Collins, T., Marx, J.-C., Feller, G., Gerday, C., 2006. Psychrophilic microorganisms: challenges for life. EMBO Rep. 7, 385–389. https://doi.org/10.1038/sj.embor.7400662

Dani, K.G.S., Mader, H.M., Wolff, E.W., Wadham, J.L., 2012. Modelling the liquid-water vein system within polar ice sheets as a potential microbial habitat. Earth Planet. Sci. Lett. 333–334, 238–249. https://doi.org/10.1016/j.epsl.2012.04.009

Danso, D., Chow, J., Streit, W.R., 2019. Plastics: Environmental and Biotechnological Perspectives on Microbial Degradation. Appl. Environ. Microbiol. 85. https://doi.org/10.1128/AEM.01095-19

Davis, N.M., Proctor, D., Holmes, S.P., Relman, D.A., Callahan, B.J., 2018. Simple statistical identification and removal of contaminant sequences in marker-gene and metagenomics data. https://doi.org/10.1101/221499

Davydov, D., Shalygin, S., Vilnet, A., 2020. New cyanobacterium *Nodosilinea svalbardensis* sp. nov. (*Prochlorotrichaceae, Synechococcales*) isolated from alluvium in Mimer river valley of the Svalbard archipelago. Phytotaxa 442, 61–79. https://doi.org/10.11646/phytotaxa.442.2.2

de Goffau, M.C., Lager, S., Salter, S.J., Wagner, J., Kronbichler, A., Charnock-Jones, D.S., Peacock, S.J., Smith, G.C.S., Parkhill, J., 2018. Recognizing the reagent microbiome. Nat. Microbiol. 3, 851–853. https://doi.org/10.1038/s41564-018-0202-y

De Santi, C., Leiros, H.-K.S., Di Scala, A., de Pascale, D., Altermark, B., Willassen, N.-P., 2016. Biochemical characterization and structural analysis of a new cold-active and salt-tolerant esterase from the marine bacterium *Thalassospira* sp. Extremophiles 20, 323–336. https://doi.org/10.1007/s00792-016-0824-z

De Santi, C., Tedesco, P., Ambrosino, L., Altermark, B., Willassen, N.-P., de Pascale, D., 2014. A new alkaliphilic cold-active esterase from the psychrophilic marine bacterium *Rhodococcus* sp.: functional and structural studies and biotechnological potential. Appl. Biochem. Biotechnol. 172, 3054–3068. https://doi.org/10.1007/s12010-013-0713-1

Debroas, D., Mone, A., Ter Halle, A., 2017. Plastics in the North Atlantic garbage patch: A boat-microbe for hitchhikers and plastic degraders. Sci. Total Environ. 599–600, 1222–1232. https://doi.org/10.1016/j.scitotenv.2017.05.059

Demain, A.L., Sanchez, S., 2009. Microbial drug discovery: 80 years of progress. J. Antibiot. (Tokyo) 62, 5–16. https://doi.org/10.1038/ja.2008.16

Deng, R., Chow, T.-J., 2010. Hypolipidemic, Antioxidant and Anti-inflammatory Activities of Microalgae *Spirulina*. Cardiovasc. Ther. 28, e33–e45. https://doi.org/10.1111/j.1755-5922.2010.00200.x

Dineen, S.M., Aranda, R., Anders, D.L., Robertson, J.M., 2010. An evaluation of commercial DNA extraction kits for the isolation of bacterial spore DNA from soil. J. Appl. Microbiol. 109, 1886–1896. https://doi.org/10.1111/j.1365-2672.2010.04816.x

Ding, H., Nunes, P., Muso, I., 2006. Is Bioprospecting Contract an Efficient Market based Policy Instrument for Biodiversity Conservation?, in: BIOECON 2006 Annual Conference.

Dombrowski, N., Seitz, K.W., Teske, A.P., Baker, B.J., 2017. Genomic insights into potential interdependencies in microbial hydrocarbon and nutrient cycling in hydrothermal sediments. Microbiome 5. https://doi.org/10.1186/s40168-017-0322-2

Donia, M.S., Cimermancic, P., Schulze, C.J., Wieland Brown, L.C., Martin, J., Mitreva, M., Clardy, J., Linington, R.G., Fischbach, M.A., 2014. A Systematic Analysis of Biosynthetic Gene Clusters in the Human Microbiome Reveals a Common Family of Antibiotics. Cell 158, 1402–1414. https://doi.org/10.1016/j.cell.2014.08.032

Du, D., Wang, L., Tian, Y., Liu, H., Tan, H., Niu, G., 2015. Genome engineering and direct cloning of antibiotic gene clusters via phage ϕBT1 integrase-mediated site-specific recombination in *Streptomyces*. Sci. Rep. 5. https://doi.org/10.1038/srep08740

Duarte, C.M., Ngugi, D.K., Alam, I., Pearman, J., Kamau, A., Eguiluz, V.M., Gojobori, T., Acinas, S.G., Gasol, J.M., Bajic, V., Irigoien, X., 2020. Sequencing Effort Dictates Gene Discovery in Marine Microbial Metagenomes. Environ. Microbiol. https://doi.org/10.1111/1462-2920.15182

Dubnick, A., Kazemi, S., Sharp, M., Wadham, J., Hawkings, J., Beaton, A., Lanoil, B., 2017. Hydrological controls on glacially exported microbial assemblages. J. Geophys. Res. Biogeosciences 122, 1049–1061. https://doi.org/10.1002/2016JG003685

Eckford, R., Cook, F.D., Saul, D., Aislabie, J., Foght, J., 2002. Free-living heterotrophic nitrogen-fixing bacteria isolated from fuel-contaminated Antarctic soils. Appl. Environ. Microbiol. 68, 5181–5185.

Eddy, S.R., 2008. A Probabilistic Model of Local Sequence Alignment That Simplifies Statistical Significance Estimation. PLOS Comput. Biol. 4, e1000069. https://doi.org/10.1371/journal.pcbi.1000069

Edgar, R.C., 2004. MUSCLE: multiple sequence alignment with high accuracy and high throughput. Nucleic Acids Res. 32, 1792–1797. https://doi.org/10.1093/nar/gkh340

Edwards, A., Anesio, A.M., Rassner, S.M., Sattler, B., Hubbard, B., Perkins, W.T., Young, M., Griffith, G.W., 2011. Possible interactions between bacterial diversity, microbial activity and supraglacial hydrology of cryoconite holes in Svalbard. ISME J. 5, 150–160. https://doi.org/10.1038/ismej.2010.100

Edwards, A., Cameron, K.A., Cook, J.M., Debbonaire, A.R., Furness, E., Hay, M.C., Rassner, S.M.E., 2020. Microbial genomics amidst the Arctic crisis. Microb. Genomics 6. https://doi.org/10.1099/mgen.0.000375

Edwards, A., Debbonaire, A.R., Sattler, B., Mur, L.A., Hodson, A.J., 2016. Extreme metagenomics using nanopore DNA sequencing: a field report from Svalbard, 78 N. bioRxiv 073965. https://doi.org/10.1101/073965

Edwards, A., Mur, L.A.J., Girdwood, S.E., Anesio, A.M., Stibal, M., Rassner, S.M.E., Hell, K., Pachebat, J.A., Post, B., Bussell, J.S., Cameron, S.J.S., Griffith, G.W., Hodson, A.J., Sattler, B., 2014. Coupled cryoconite ecosystem structure–function relationships are revealed by comparing bacterial communities in alpine and Arctic glaciers. FEMS Microbiol. Ecol. 89, 222–237. https://doi.org/10.1111/1574-6941.12283

Edwards, A., Pachebat, J.A., Swain, M., Hegarty, M., Hodson, A.J., Irvine-Fynn, T.D.L., Rassner, S.M.E., Sattler, B., 2013a. A metagenomic snapshot of taxonomic and functional diversity in an alpine glacier cryoconite ecosystem. Environ. Res. Lett. 8, 035003. https://doi.org/10.1088/1748-9326/8/3/035003

Edwards, A., Rassner, S.M.E., Anesio, A.M., Worgan, H.J., Irvine-Fynn, T.D.L., Wyn Williams, H., Sattler, B., Wyn Griffith, G., 2013b. Contrasts between the cryoconite and ice-marginal bacterial communities of Svalbard glaciers. Polar Res. 32. https://doi.org/10.3402/polar.v32i0.19468

El-Gebali, S., Mistry, J., Bateman, A., Eddy, S.R., Luciani, A., Potter, S.C., Qureshi, M., Richardson, L.J., Salazar, G.A., Smart, A., Sonnhammer, E.L.L., Hirsh, L., Paladin, L., Piovesan, D., Tosatto, S.C.E., Finn, R.D., 2019. The Pfam protein families database in 2019. Nucleic Acids Res. 47, D427–D432. https://doi.org/10.1093/nar/gky995

Elleuche, S., Qoura, F.M., Lorenz, U., Rehn, T., Brück, T., Antranikian, G., 2015. Cloning, expression and characterization of the recombinant cold-active type-I pullulanase from *Shewanella arctica*. J. Mol. Catal. B Enzym. 116, 70–77. https://doi.org/10.1016/j.molcatb.2015.03.001

Enright, A.J., Van Dongen, S., Ouzounis, C.A., 2002. An efficient algorithm for large-scale detection of protein families. Nucleic Acids Res. 30, 1575–1584. https://doi.org/10.1093/nar/30.7.1575

Entfellner, E., Frei, M., Christiansen, G., Deng, L., Blom, J., Kurmayer, R., 2017. Evolution of Anabaenopeptin Peptide Structural Variability in the Cyanobacterium *Planktothrix*. Front. Microbiol. 8. https://doi.org/10.3389/fmicb.2017.00219

Erb, T.J., Zarzycki, J., 2018. A short history of RubisCO: the rise and fall (?) of Nature's predominant CO2 fixing enzyme. Curr. Opin. Biotechnol., Food biotechnology • Plant biotechnology 49, 100–107. https://doi.org/10.1016/j.copbio.2017.07.017

Eren, A.M., Esen, Ö.C., Quince, C., Vineis, J.H., Morrison, H.G., Sogin, M.L., Delmont, T.O., 2015. Anvi'o: an advanced analysis and visualization platform for 'omics data. PeerJ 3, e1319. https://doi.org/10.7717/peerj.1319

Eriksson, M., Dalhammar, G., Mohn, W.W., 2002. Bacterial growth and biofilm production on pyrene. FEMS Microbiol. Ecol. 40, 21–27. https://doi.org/10.1111/j.1574-6941.2002.tb00932.x

Fani, R., Gallo, R., Liò, P., 2000. Molecular Evolution of Nitrogen Fixation: The Evolutionary History of the nifD, nifK, nifE, and nifN Genes. J. Mol. Evol. 51, 1–11. https://doi.org/10.1007/s002390010061

Feng, Z., Chakraborty, D., Dewell, S.B., Reddy, B.V.B., Brady, S.F., 2012. Environmental DNA-Encoded Antibiotics Fasamycins A and B Inhibit FabF in Type II Fatty Acid Biosynthesis. J. Am. Chem. Soc. 134, 2981–2987. https://doi.org/10.1021/ja207662w

Feng, Z., Kallifidas, D., Brady, S.F., 2011. Functional analysis of environmental DNA-derived type II polyketide synthases reveals structurally diverse secondary metabolites. Proc. Natl. Acad. Sci. U. S. A. 108, 12629–12634. https://doi.org/10.1073/pnas.1103921108

Ferrer, M., Martínez-Martínez, M., Bargiela, R., Streit, W.R., Golyshina, O.V., Golyshin, P.N., 2016. Estimating the success of enzyme bioprospecting through metagenomics: current status and future trends: Enzyme bioprospecting by metagenomics. Microb. Biotechnol. 9, 22–34. https://doi.org/10.1111/1751-7915.12309

Fischer, M., Pleiss, J., 2003. The Lipase Engineering Database: a navigation and analysis tool for protein families. Nucleic Acids Res. 31, 319–321. https://doi.org/10.1093/nar/gkg015

Fountain, A.G., 2012. The Disappearing Cryosphere: Impacts and Ecosystem Responses to Rapid Cryosphere Loss. BioScience 62, 405–415. https://doi.org/10.1525/bio.2012.62.4.11

Freitas, T.A.K., Li, P.-E., Scholz, M.B., Chain, P.S.G., 2015. Accurate read-based metagenome characterization using a hierarchical suite of unique signatures. Nucleic Acids Res. 43, e69. https://doi.org/10.1093/nar/gkv180

Frioux, C., Singh, D., Korcsmaros, T., Hildebrand, F., 2020. From bag-of-genes to bag-of-genomes: metabolic modelling of communities in the era of metagenome-assembled genomes. Comput. Struct. Biotechnol. J. https://doi.org/10.1016/j.csbj.2020.06.028

Frolov, E.N., Kublanov, I.V., Toshchakov, S.V., Lunev, E.A., Pimenov, N.V., Bonch-Osmolovskaya, E.A., Lebedinsky, A.V., Chernyh, N.A., 2019. Form III RubisCO-mediated transaldolase variant of the Calvin cycle in a chemolithoautotrophic bacterium. Proc. Natl. Acad. Sci. 116, 18638–18646. https://doi.org/10.1073/pnas.1904225116

Fu, J., Leiros, H.-K.S., de Pascale, D., Johnson, K.A., Blencke, H.-M., Landfald, B., 2013. Functional and structural studies of a novel cold-adapted esterase from an Arctic intertidal metagenomic library. Appl. Microbiol. Biotechnol. 97, 3965–3978. https://doi.org/10.1007/s00253-012-4276-9

Fuentes-Tristan, S., Parra-Saldivar, R., Iqbal, H.M.N., Carrillo-Nieves, D., 2019. Bioinspired biomolecules: Mycosporine-like amino acids and scytonemin from *Lyngbya* sp. with UV-protection potentialities. J. Photochem. Photobiol. B 201, 111684. https://doi.org/10.1016/j.jphotobiol.2019.111684

Gabor, E.M., Alkema, W.B.L., Janssen, D.B., 2004. Quantifying the accessibility of the metagenome by random expression cloning techniques. Environ. Microbiol. 6, 879–886. https://doi.org/10.1111/j.1462-2920.2004.00640.x

Galperin, M.Y., Makarova, K.S., Wolf, Y.I., Koonin, E.V., 2015. Expanded microbial genome coverage and improved protein family annotation in the COG database. Nucleic Acids Res. 43, D261-269. https://doi.org/10.1093/nar/gku1223

Ghosh, S., Kuisiene, N., Cheeptham, N., 2017. The cave microbiome as a source for drug discovery: Reality or pipe dream? Biochem. Pharmacol., Antibiotics - Meeting the Challenges of 21st Century Health Care: Part II 134, 18–34. https://doi.org/10.1016/j.bcp.2016.11.018

Gich, F., Overmann, J., 2006. *Sandarakinorhabdus limnophila* gen. nov., sp. nov., a novel bacteriochlorophyll a-containing, obligately aerobic bacterium isolated from freshwater lakes. Int. J. Syst. Evol. Microbiol. 56, 847–854. https://doi.org/10.1099/ijs.0.63970-0

Gilbert, J.A., Hill, P.J., Dodd, C.E.R., Laybourn-Parry, J., 2004. Demonstration of antifreeze protein activity in Antarctic lake bacteria. Microbiology, 150, 171–180. https://doi.org/10.1099/mic.0.26610-0

Giordano, D., Coppola, D., Russo, R., Denaro, R., Giuliano, L., Lauro, F.M., di Prisco, G., Verde, C., 2015. Marine Microbial Secondary Metabolites: Pathways, Evolution and Physiological Roles. Adv. Microb. Physiol. 66, 357–428. https://doi.org/10.1016/bs.ampbs.2015.04.001

Gokul, J.K., Hodson, A.J., Saetnan, E.R., Irvine-Fynn, T.D.L., Westall, P.J., Detheridge, A.P., Takeuchi, N., Bussell, J., Mur, L.A.J., Edwards, A., 2016. Taxon interactions control the distributions of cryoconite bacteria colonizing a High Arctic ice cap. Mol. Ecol. 25, 3752–3767. https://doi.org/10.1111/mec.13715

Gomez-Escribano, J.P., Bibb, M.J., 2014. Heterologous expression of natural product biosynthetic gene clusters in *Streptomyces coelicolor*: from genome mining to manipulation of biosynthetic pathways. J. Ind. Microbiol. Biotechnol. 41, 425–431. https://doi.org/10.1007/s10295-013-1348-5

Gowers, G.-O.F., Vince, O., Charles, J.-H., Klarenberg, I., Ellis, T., Edwards, A., 2019. Entirely Off-Grid and Solar-Powered DNA Sequencing of Microbial Communities during an Ice Cap Traverse Expedition. Genes 10, 902. https://doi.org/10.3390/genes10110902

Graham, R.M., Cohen, L., Petty, A.A., Boisvert, L.N., Rinke, A., Hudson, S.R., Nicolaus, M., Granskog, M.A., 2017. Increasing frequency and duration of Arctic winter warming events. Geophys. Res. Lett. 44, 6974–6983. https://doi.org/10.1002/2017GL073395

Grannas, A.M., Bogdal, C., Hageman, K.J., Halsall, C., Harner, T., Hung, H., Kallenborn, R., Klán, P., Klánová, J., Macdonald, R.W., Meyer, T., Wania, F., 2013. The role of the global cryosphere in the fate of organic contaminants. Atmospheric Chem. Phys. 13, 3271–3305. https://doi.org/10.5194/acp-13-3271-2013

Graversen, R.G., Mauritsen, T., Tjernström, M., Källén, E., Svensson, G., 2008. Vertical structure of recent Arctic warming. Nature 451, 53–56. https://doi.org/10.1038/nature06502

Grzymski, J.J., Carter, B.J., DeLong, E.F., Feldman, R.A., Ghadiri, A., Murray, A.E., 2006. Comparative Genomics of DNA Fragments from Six Antarctic Marine Planktonic

Bacteria. Appl. Environ. Microbiol. 72, 1532–1541. https://doi.org/10.1128/AEM.72.2.1532-1541.2006

Gu, Z., Eils, R., Schlesner, M., 2016. Complex heatmaps reveal patterns and correlations in multidimensional genomic data. Bioinformatics 32, 2847–2849. https://doi.org/10.1093/bioinformatics/btw313

Gurevich, A., Saveliev, V., Vyahhi, N., Tesler, G., 2013. QUAST: quality assessment tool for genome assemblies. Bioinforma. Oxf. Engl. 29, 1072–1075. https://doi.org/10.1093/bioinformatics/btt086

Gutierrez, T., Berry, D., Yang, T., Mishamandani, S., McKay, L., Teske, A., Aitken, M.D., 2013. Role of Bacterial Exopolysaccharides (EPS) in the Fate of the Oil Released during the Deepwater Horizon Oil Spill. PLOS ONE 8, e67717. https://doi.org/10.1371/journal.pone.0067717

Hamilton, T.L., Peters, J.W., Skidmore, M.L., Boyd, E.S., 2013. Molecular evidence for an active endogenous microbiome beneath glacial ice. ISME J. 7, 1402–1412. https://doi.org/10.1038/ismej.2013.31

Harborne, N.R., Griffiths, L., Busby, S.J., Cole, J.A., 1992. Transcriptional control, translation and function of the products of the five open reading frames of the *Escherichia coli* nir operon. Mol. Microbiol. 6, 2805–2813. https://doi.org/10.1111/j.1365-2958.1992.tb01460.x

Hauksson, J.B., Andrésson, Ó.S., Ásgeirsson, B., 2000. Heat-labile bacterial alkaline phosphatase from a marine *Vibrio* sp. Enzyme Microb. Technol. 27, 66–73. https://doi.org/10.1016/S0141-0229(00)00152-6

Hauptmann, A.L., Sicheritz-Pontén, T., Cameron, K.A., Bælum, J., Plichta, D.R., Marlene Dalgaard, Stibal, M., 2017. Contamination of the Arctic reflected in microbial metagenomes from the Greenland ice sheet. Environ. Res. Lett. 12, 074019. https://doi.org/10.1088/1748-9326/aa7445

Head, I.M., Saunders, J.R., Pickup, R.W., 1998. Microbial Evolution, Diversity, and Ecology: A Decade of Ribosomal RNA Analysis of Uncultivated Microorganisms. Microb. Ecol. 35, 1–21. https://doi.org/10.1007/s002489900056

Hell, K., Edwards, A., Zarsky, J., Podmirseg, S.M., Girdwood, S., Pachebat, J.A., Insam, H., Sattler, B., 2013. The dynamic bacterial communities of a melting High Arctic glacier snowpack. ISME J. 7, 1814–1826. https://doi.org/10.1038/ismej.2013.51

Hendriks, J., Oubrie, A., Castresana, J., Urbani, A., Gemeinhardt, S., Saraste, M., 2000. Nitric oxide reductases in bacteria. Biochim. Biophys. Acta BBA - Bioenerg. 1459, 266–273. https://doi.org/10.1016/S0005-2728(00)00161-4

Herrmann, M., Wegner, C.-E., Taubert, M., Geesink, P., Lehmann, K., Yan, L., Lehmann, R., Totsche, K.U., Küsel, K., 2019. Predominance of Cand. Patescibacteria in Groundwater Is Caused by Their Preferential Mobilization From Soils and Flourishing Under Oligotrophic Conditions. Front. Microbiol. 10. https://doi.org/10.3389/fmicb.2019.01407

Hess, M., Sczyrba, A., Egan, R., Kim, T.-W., Chokhawala, H., Schroth, G., Luo, S., Clark, D.S., Chen, F., Zhang, T., Mackie, R.I., Pennacchio, L.A., Tringe, S.G., Visel, A., Woyke, T., Wang, Z., Rubin, E.M., 2011. Metagenomic Discovery of Biomass-Degrading Genes and Genomes from Cow Rumen. Science 331, 463–467. https://doi.org/10.1126/science.1200387

Hillebrand-Voiculescu, A., Itcus, C., Ardelean, I., Pascu, D., Persoiu, A., Rusu, A., Brad, T., Popa, E., Onac, B.P., Purcarea, C., 2015. Searching for cold-adapted microorganisms in the underground glacier of Scarisoara Ice Cave, Romania. Acta Carsologica 43. https://doi.org/10.3986/ac.v43i2-3.604

Hodson, A., Anesio, A.M., Ng, F., Watson, R., Quirk, J., Irvine-Fynn, T., Dye, A., Clark, C., McCloy, P., Kohler, J., Sattler, B., 2007. A glacier respires: Quantifying the distribution and respiration CO $_2$ flux of cryoconite across an entire Arctic supraglacial ecosystem: respiration rates upon an Arctic glacier. J. Geophys. Res. Biogeosciences 112, n/a-n/a. https://doi.org/10.1029/2007JG000452

Hodson, A., Anesio, A.M., Tranter, M., Fountain, A., Osborn, M., Priscu, J., Laybourn-Parry, J., Sattler, B., 2008. Glacial Ecosystems. Ecol. Monogr. 78, 41–67. https://doi.org/10.1890/07-0187.1

Hodson, A., Cameron, K., Bøggild, C., Irvine-Fynn, T., Langford, H., Pearce, D., Banwart, S., 2010a. The structure, biological activity and biogeochemistry of cryoconite aggregates upon an Arctic valley glacier: Longyearbreen, Svalbard. J. Glaciol. 56, 349–362. https://doi.org/10.3189/002214310791968403

Hodson, A., Roberts, T.J., Engvall, A.-C., Holmén, K., Mumford, P., 2010b. Glacier ecosystem response to episodic nitrogen enrichment in Svalbard, European High Arctic. Biogeochemistry 98, 171–184. https://doi.org/10.1007/s10533-009-9384-y

Hofmeyr, S., Egan, R., Georganas, E., Copeland, A.C., Riley, R., Clum, A., Eloe-Fadrosh, E., Roux, S., Goltsman, E., Buluç, A., Rokhsar, D., Oliker, L., Yelick, K., 2020. Terabase-scale metagenome coassembly with MetaHipMer. Sci. Rep. 10, 10689. https://doi.org/10.1038/s41598-020-67416-5

Holmlund, P., Onac, B.P., Hansson, M., Holmgren, K., Mörth, M., Nyman, M., Persoiu, A., 2005. Assessing the Palaeoclimate Potential of Cave Glaciers: The Example of the Scărişoara Ice Cave (romania). Geogr. Ann. Ser. Phys. Geogr. 87, 193–201. https://doi.org/10.1111/j.0435-3676.2005.00252.x

Honda, D., Yokota, A., Sugiyama, J., 1999. Detection of Seven Major Evolutionary Lineages in Cyanobacteria Based on the 16S rRNA Gene Sequence Analysis with New Sequences of Five Marine *Synechococcus* Strains. J. Mol. Evol. 48, 723–739. https://doi.org/10.1007/PL00006517

Hooft, J.J.J. van der, Mohimani, H., Bauermeister, A., C. Dorrestein, P., R. Duncan, K., H. Medema, M., 2020. Linking genomics and metabolomics to chart specialized metabolic diversity. Chem. Soc. Rev. 49, 3297–3314. https://doi.org/10.1039/D0CS00162G

Hu, A., Ju, F., Hou, L., Li, J., Yang, X., Wang, H., Mulla, S.I., Sun, Q., Bürgmann, H., Yu, C.-P., 2017. Strong impact of anthropogenic contamination on the co-occurrence patterns of a riverine microbial community. Environ. Microbiol. 19, 4993–5009. https://doi.org/10.1111/1462-2920.13942

Huerta-Cepas, J., Forslund, K., Coelho, L.P., Szklarczyk, D., Jensen, L.J., von Mering, C., Bork, P., 2017. Fast Genome-Wide Functional Annotation through Orthology Assignment by eggNOG-Mapper. Mol. Biol. Evol. 34, 2115–2122. https://doi.org/10.1093/molbev/msx148

Huerta-Cepas, J., Szklarczyk, D., Forslund, K., Cook, H., Heller, D., Walter, M.C., Rattei, T., Mende, D.R., Sunagawa, S., Kuhn, M., Jensen, L.J., von Mering, C., Bork, P., 2016. eggNOG 4.5: a hierarchical orthology framework with improved functional annotations for eukaryotic, prokaryotic and viral sequences. Nucleic Acids Res. 44, D286–D293. https://doi.org/10.1093/nar/gkv1248

Hyatt, D., Chen, G.-L., LoCascio, P.F., Land, M.L., Larimer, F.W., Hauser, L.J., 2010. Prodigal: prokaryotic gene recognition and translation initiation site identification. BMC Bioinformatics 11, 119. https://doi.org/10.1186/1471-2105-11-119

Irvine-Fynn, T.D.L., Edwards, A., 2014. A frozen asset: The potential of flow cytometry in constraining the glacial biome: Communication to the Editor. Cytometry A 85, 3–7. https://doi.org/10.1002/cyto.a.22411

Ishino, S., Ishino, Y., 2014. DNA polymerases as useful reagents for biotechnology – the history of developmental research in the field. Front. Microbiol. 5. https://doi.org/10.3389/fmicb.2014.00465

Iţcuş, C., Pascu, M.-D., Brad, T., Perşoiu, A., Purcarea, C., 2016. Diversity of cultured bacteria from the perennial ice block of Scarisoara Ice Cave, Romania. Int. J. Speleol. 45. http://dx.doi.org/10.5038/1827-806X.45.1.1948

Itcus, C., Pascu, M.D., Lavin, P., Perşoiu, A., Iancu, L., Purcarea, C., 2018. Bacterial and archaeal community structures in perennial cave ice. Sci. Rep. 8. https://doi.org/10.1038/s41598-018-34106-2

Iulia, L., Bianca, I.M., Octavian, P., 2013. The evidence of contaminant bacterial DNA in several commercial Taq polymerases. Romanian Biotechnol. Lett. 18, 6.

Jacomy, M., Venturini, T., Heymann, S., Bastian, M., 2014. ForceAtlas2, a Continuous Graph Layout Algorithm for Handy Network Visualization Designed for the Gephi Software. PLOS ONE 9, e98679. https://doi.org/10.1371/journal.pone.0098679

Jain, A., Krishnan, K.P., 2017. Differences in free-living and particle-associated bacterial communities and their spatial variation in Kongsfjorden, Arctic. J. Basic Microbiol. 57, 827–838. https://doi.org/10.1002/jobm.201700216

Jain, C., Rodriguez-R, L.M., Phillippy, A.M., Konstantinidis, K.T., Aluru, S., 2018. High throughput ANI analysis of 90K prokaryotic genomes reveals clear species boundaries. Nat. Commun. 9, 5114. https://doi.org/10.1038/s41467-018-07641-9

Jambeck, J.R., Geyer, R., Wilcox, C., Siegler, T.R., Perryman, M., Andrady, A., Narayan, R., Law, K.L., 2015. Marine pollution. Plastic waste inputs from land into the ocean. Science 347, 768–771. https://doi.org/10.1126/science.1260352

Janssen, E.M.-L., 2019. Cyanobacterial peptides beyond microcystins – A review on co-occurrence, toxicity, and challenges for risk assessment. Water Res. 151, 488–499. https://doi.org/10.1016/j.watres.2018.12.048

Jeon, H.J., Kim, M.N., 2015. Functional analysis of alkane hydroxylase system derived from *Pseudomonas aeruginosa* E7 for low molecular weight polyethylene biodegradation. Int. Biodeterior. Biodegrad. 103, 141–146. https://doi.org/10.1016/j.ibiod.2015.04.024

Jeon, J.H., Kim, J.-T., Kang, S.G., Lee, J.-H., Kim, S.-J., 2009. Characterization and its Potential Application of Two Esterases Derived from the Arctic Sediment Metagenome. Mar. Biotechnol. 11, 307–316. https://doi.org/10.1007/s10126-008-9145-2

Ji, M., Greening, C., Vanwonterghem, I., Carere, C.R., Bay, S.K., Steen, J.A., Montgomery, K., Lines, T., Beardall, J., van Dorst, J., Snape, I., Stott, M.B., Hugenholtz, P., Ferrari, B.C., 2017. Atmospheric trace gases support primary production in Antarctic desert surface soil. Nature 552, 400–403. https://doi.org/10.1038/nature25014

Jiang, W., Zhao, X., Gabrieli, T., Lou, C., Ebenstein, Y., Zhu, T.F., 2015. Cas9-Assisted Targeting of CHromosome segments CATCH enables one-step targeted cloning of large gene clusters. Nat. Commun. 6, 8101. https://doi.org/10.1038/ncomms9101

Jiménez, D.J., Chaves-Moreno, D., van Elsas, J.D., 2015. Unveiling the metabolic potential of two soil-derived microbial consortia selected on wheat straw. Sci. Rep. 5, 13845. https://doi.org/10.1038/srep13845

Jøstensen, J.-P., Landfald, B., 1997. High prevalence of polyunsaturated-fatty-acid producing bacteria in arctic invertebrates. FEMS Microbiol. Lett. 151, 95–101. https://doi.org/10.1111/j.1574-6968.1997.tb10400.x

Ju, F., Xia, Y., Guo, F., Wang, Z., Zhang, T., 2014. Taxonomic relatedness shapes bacterial assembly in activated sludge of globally distributed wastewater treatment plants. Environ. Microbiol. 16, 2421–2432. https://doi.org/10.1111/1462-2920.12355

Ju, F., Zhang, T., 2015. Bacterial assembly and temporal dynamics in activated sludge of a full-scale municipal wastewater treatment plant. ISME J. 9, 683–695. https://doi.org/10.1038/ismej.2014.162

Kaczmarek, Ł., Jakubowska, N., Celewicz-Gołdyn, S., Zawierucha, K., 2016. The microorganisms of cryoconite holes (algae, Archaea, bacteria, cyanobacteria, fungi, and Protista): a review. Polar Rec. 52, 176–203. https://doi.org/10.1017/S0032247415000637

Kafarski, P., 2019. Phosphonates: Their Natural Occurrence and Physiological Role. Contemp. Top. Phosphorus Biol. Mater. https://doi.org/10.5772/intechopen.87155

Kallifidas, D., Kang, H.-S., Brady, S.F., 2012. Tetarimycin A, an MRSA-Active Antibiotic Identified through Induced Expression of Environmental DNA Gene Clusters. J. Am. Chem. Soc. 134, 19552–19555. https://doi.org/10.1021/ja3093828

Kanao, T., Fukui, T., Atomi, H., Imanaka, T., 2001. ATP-citrate lyase from the green sulfur bacterium *Chlorobium limicola* is a heteromeric enzyme composed of two distinct gene products. Eur. J. Biochem. 268, 1670–1678. https://doi.org/10.1046/j.1432-1327.2001.02034.x

Kanehisa, M., Goto, S., 2000. KEGG: Kyoto Encyclopedia of Genes and Genomes. Nucleic Acids Res. 28, 27–30. https://doi.org/10.1093/nar/28.1.27

Kanehisa, M., Sato, Y., Morishima, K., 2016. BlastKOALA and GhostKOALA: KEGG Tools for Functional Characterization of Genome and Metagenome Sequences. J. Mol. Biol., Computation Resources for Molecular Biology 428, 726–731. https://doi.org/10.1016/j.jmb.2015.11.006

Kang, D.D., Froula, J., Egan, R., Wang, Z., 2015. MetaBAT, an efficient tool for accurately reconstructing single genomes from complex microbial communities. PeerJ 3, e1165. https://doi.org/10.7717/peerj.1165

Karpiński, T.M., Adamczak, A., 2019. Fucoxanthin—An Antibacterial Carotenoid. Antioxidants 8. https://doi.org/10.3390/antiox8080239

Kaštovská, K., Elster, J., Stibal, M., Šantrůčková, H., 2005. Microbial Assemblages in Soil Microbial Succession After Glacial Retreat in Svalbard (High Arctic). Microb. Ecol. 50, 396. https://doi.org/10.1007/s00248-005-0246-4

Kaštovská, K., Stibal, M., Šabacká, M., Černá, B., Šantrůčková, H., Elster, J., 2007. Microbial community structure and ecology of subglacial sediments in two polythermal Svalbard glaciers characterized by epifluorescence microscopy and PLFA. Polar Biol. 30, 277–287. https://doi.org/10.1007/s00300-006-0181-y

Katz, L., Baltz, R.H., 2016. Natural product discovery: past, present, and future. J. Ind. Microbiol. Biotechnol. 43, 155–176. https://doi.org/10.1007/s10295-015-1723-5

Kellogg, D.E., Rybalkin, I., Chen, S., Mukhamedova, N., Vlasik, T., Siebert, P.D., Chenchik, A., 1994. TaqStart Antibody: "hot start" PCR facilitated by a neutralizing monoclonal antibody directed against Taq DNA polymerase. BioTechniques 16, 1134–1137.

Kim, D., Song, L., Breitwieser, F.P., Salzberg, S.L., 2016. Centrifuge: rapid and sensitive classification of metagenomic sequences. Genome Res. https://doi.org/10.1101/gr.210641.116

Kim, E.H., Jeong, H.-J., Lee, Y.K., Moon, E.Y., Cho, J.-C., Lee, H.K., Hong, S.G., 2011. *Actimicrobium antarcticum* gen. nov., sp. nov., of the family Oxalobacteraceae, isolated from Antarctic coastal seawater. Curr. Microbiol. 63, 213–217. https://doi.org/10.1007/s00284-011-9962-9

Kim, M., Kang, O., Zhang, Y., Ren, L., Chang, X., Jiang, F., Fang, C., Zheng, C., Peng, F., 2016. *Sphingoaurantiacus polygranulatus* gen. nov., sp. nov., isolated from high-Arctic tundra soil, and emended descriptions of the genera *Sandarakinorhabdus*, *Polymorphobacter* and *Rhizorhabdus* and the species *Sandarakinorhabdus*

limnophila, *Rhizorhabdus argentea* and *Sphingomonas wittichii*. Int. J. Syst. Evol. Microbiol. 66, 91–100. https://doi.org/10.1099/ijsem.0.000677

Kim, M.-K., Park, H., Oh, T.-J., 2014. Antibacterial and antioxidant capacity of polar microorganisms isolated from Arctic lichen *Ochrolechia* sp. Pol. J. Microbiol. 63, 317–322.

Kim, S.-J., Yim, J.-H., 2007. Cryoprotective Properties of Exopolysaccharide (P-21653) Produced by the Antarctic Bacterium, *Pseudoalteromonas arctica* KOPRI 21653. J. Microbiol. 45, 510–514.

Kleinteich, J., Puddick, J., Wood, S.A., Hildebrand, F., Laughinghouse IV, H.D., Pearce, D.A., Dietrich, D.R., Wilmotte, A., 2018. Toxic Cyanobacteria in Svalbard: Chemical Diversity of Microcystins Detected Using a Liquid Chromatography Mass Spectrometry Precursor Ion Screening Method. Toxins 10, 147. https://doi.org/10.3390/toxins10040147

Kleinteich, J., Wood, S.A., Puddick, J., Schleheck, D., Küpper, F.C., Dietrich, D., 2013. Potent toxins in Arctic environments – Presence of saxitoxins and an unusual microcystin variant in Arctic freshwater ecosystems. Chem. Biol. Interact. 206, 423–431. https://doi.org/10.1016/j.cbi.2013.04.011

Klindworth, A., Pruesse, E., Schweer, T., Peplies, J., Quast, C., Horn, M., Glöckner, F.O., 2013. Evaluation of general 16S ribosomal RNA gene PCR primers for classical and next-generation sequencing-based diversity studies. Nucleic Acids Res. 41, e1–e1. https://doi.org/10.1093/nar/gks808

Knight, C.A., Hallett, J., DeVries, A.L., 1988. Solute effects on ice recrystallization: An assessment technique. Cryobiology 25, 55–60. https://doi.org/10.1016/0011-2240(88)90020-X

Knight, V., Sanglier, J.-J., DiTullio, D., Braccili, S., Bonner, P., Waters, J., Hughes, D., Zhang, L., 2003. Diversifying microbial natural products for drug discovery. Appl. Microbiol. Biotechnol. 62, 446–458. https://doi.org/10.1007/s00253-003-1381-9

Kohler, T.J., Vinšová, P., Falteisek, L., Žárský, J.D., Yde, J.C., Hatton, J.E., Hawkings, J.R., Lamarche-Gagnon, G., Hood, E., Cameron, K.A., Stibal, M., 2020. Patterns in Microbial Assemblages Exported From the Meltwater of Arctic and Sub-Arctic Glaciers. Front. Microbiol. 11. https://doi.org/10.3389/fmicb.2020.00669

Komatsu, M., Komatsu, K., Koiwai, H., Yamada, Y., Kozone, I., Izumikawa, M., Hashimoto, J., Takagi, M., Omura, S., Shin-ya, K., Cane, D.E., Ikeda, H., 2013. Engineered *Streptomyces avermitilis* Host for Heterologous Expression of Biosynthetic Gene Cluster for Secondary Metabolites. ACS Synth. Biol. 2, 384–396. https://doi.org/10.1021/sb3001003

Kouprina, N., Larionov, V., 2016. Transformation-associated recombination (TAR) cloning for genomics studies and synthetic biology. Chromosoma 125, 621–632. https://doi.org/10.1007/s00412-016-0588-3

Kumar, S., Stecher, G., Li, M., Knyaz, C., Tamura, K., 2018. MEGA X: Molecular Evolutionary Genetics Analysis across Computing Platforms. Mol. Biol. Evol. 35, 1547–1549. https://doi.org/10.1093/molbev/msy096

Langford, H., Hodson, A., Banwart, S., Bøggild, C., 2010. The microstructure and biogeochemistry of Arctic cryoconite granules. Ann. Glaciol. 51, 87–94. https://doi.org/10.3189/172756411795932083

Langmead, B., Salzberg, S.L., 2012. Fast gapped-read alignment with Bowtie 2. Nat. Methods 9, 357–359. https://doi.org/10.1038/nmeth.1923

Langmead, B., Trapnell, C., Pop, M., Salzberg, S.L., 2009. Ultrafast and memory-efficient alignment of short DNA sequences to the human genome. Genome Biol. 10, R25. https://doi.org/10.1186/gb-2009-10-3-r25

Larose, C., Dommergue, A., Vogel, T., 2013a. The Dynamic Arctic Snow Pack: An Unexplored Environment for Microbial Diversity and Activity. Biology 2, 317–330. https://doi.org/10.3390/biology2010317

Larose, C., Dommergue, A., Vogel, T.M., 2013b. Microbial nitrogen cycling in Arctic snowpacks. Environ. Res. Lett. 8, 035004. https://doi.org/10.1088/1748-9326/8/3/035004

Leary, D., 2008. Bioprospecting in the Arctic. United Nations University Institute of Advanced Studies.

Lee, J.K., Park, K.S., Park, S., Park, H., Song, Y.H., Kang, S.-H., Kim, H.J., 2010. An extracellular ice-binding glycoprotein from an Arctic psychrophilic yeast. Cryobiology 60, 222–228. https://doi.org/10.1016/j.cryobiol.2010.01.002

Lee, Learn-Han, Cheah, Y.-K., Mohd Sidik, S., Ab Mutalib, N.-S., Tang, Y.-L., Lin, H.-P., Hong, K., 2012. Molecular characterization of Antarctic actinobacteria and screening for antimicrobial metabolite production. World J. Microbiol. Biotechnol. 28, 2125–2137. https://doi.org/10.1007/s11274-012-1018-1

Lee, L.-H., Cheah, Y.-K., Nurul Syakima, A.M., Shiran, M.S., Tang, Y.-L., Lin, H.-P., Hong, K., 2012. Analysis of Antarctic proteobacteria by PCR fingerprinting and screening for antimicrobial secondary metabolites. Genet. Mol. Res. GMR 11, 1627–1641. https://doi.org/10.4238/2012.June.15.12

Lee, M.D., 2019. GToTree: a user-friendly workflow for phylogenomics. Bioinformatics 35, 4162–4164. https://doi.org/10.1093/bioinformatics/btz188

Lee, S.-H., Jang, I., Chae, N., Choi, T., Kang, H., 2013. Organic Layer Serves as a Hotspot of Microbial Activity and Abundance in Arctic Tundra Soils. Microb. Ecol. 65, 405–414. https://doi.org/10.1007/s00248-012-0125-8

Lex, A., Gehlenborg, N., Strobelt, H., Vuillemot, R., Pfister, H., 2014. UpSet: Visualization of Intersecting Sets. IEEE Trans. Vis. Comput. Graph. 20, 1983–1992. https://doi.org/10.1109/TVCG.2014.2346248

Li, D., Liu, C.-M., Luo, R., Sadakane, K., Lam, T.-W., 2015. MEGAHIT: an ultra-fast single-node solution for large and complex metagenomics assembly via succinct de Bruijn graph. Bioinformatics 31, 1674–1676. https://doi.org/10.1093/bioinformatics/btv033

Li, H., Handsaker, B., Wysoker, A., Fennell, T., Ruan, J., Homer, N., Marth, G., Abecasis, G., Durbin, R., 1000 Genome Project Data Processing Subgroup, 2009. The Sequence Alignment/Map format and SAMtools. Bioinforma. Oxf. Engl. 25, 2078–2079. https://doi.org/10.1093/bioinformatics/btp352

Li, L., Jiang, W., Lu, Y., 2017. New strategies and approaches for engineering biosynthetic gene clusters of microbial natural products. Biotechnol. Adv. 35, 936–949. https://doi.org/10.1016/j.biotechadv.2017.03.007

Li, L., Zhao, Y., Ruan, L., Yang, S., Ge, M., Jiang, W., Lu, Y., 2015. A stepwise increase in pristinamycin II biosynthesis by *Streptomyces pristinaespiralis* through combinatorial metabolic engineering. Metab. Eng. 29, 12–25. https://doi.org/10.1016/j.ymben.2015.02.001

Li, W., Xue, Y., Li, J., Yuan, J., Wang, X., Fang, W., Fang, Z., Xiao, Y., 2016. A cold-adapted and glucose-stimulated type II α-glucosidase from a deep-sea bacterium *Pseudoalteromonas* sp. K8. Biotechnol. Lett. 38, 345–349. https://doi.org/10.1007/s10529-015-1987-x

Linz, A.M., He, S., Stevens, S.L.R., Anantharaman, K., Rohwer, R.R., Malmstrom, R.R., Bertilsson, S., McMahon, K.D., 2018. Freshwater carbon and nutrient cycles revealed through reconstructed population genomes. PeerJ 6, e6075. https://doi.org/10.7717/peerj.6075

Liu, S.-B., Chen, X.-L., He, H.-L., Zhang, X.-Y., Xie, B.-B., Yu, Y., Chen, B., Zhou, B.-C., Zhang, Y.-Z., 2013. Structure and Ecological Roles of a Novel Exopolysaccharide from the Arctic Sea Ice Bacterium *Pseudoalteromonas* sp. Strain SM20310. Appl. Environ. Microbiol. 79, 224–230. https://doi.org/10.1128/AEM.01801-12

Lo Giudice, A., Fani, R., 2016. Antimicrobial Potential of Cold-Adapted Bacteria and Fungi from Polar Regions, in: Rampelotto, P.H. (Ed.), Biotechnology of Extremophiles: Advances and Challenges, Grand Challenges in Biology and Biotechnology. Springer International Publishing, Cham, pp. 83–115. https://doi.org/10.1007/978-3-319-13521-2_3

Lombard, V., Golaconda Ramulu, H., Drula, E., Coutinho, P.M., Henrissat, B., 2014. The carbohydrate-active enzymes database (CAZy) in 2013. Nucleic Acids Res. 42, D490-495. https://doi.org/10.1093/nar/gkt1178

Lorv, J.S.H., Rose, D.R., Glick, B.R., 2014. Bacterial Ice Crystal Controlling Proteins. Scientifica 2014, 1–20. https://doi.org/10.1155/2014/976895

Loureiro, C., Medema, M.H., van der Oost, J., Sipkema, D., 2018. Exploration and exploitation of the environment for novel specialized metabolites. Curr. Opin. Biotechnol., Energy biotechnology • Environmental biotechnology 50, 206–213. https://doi.org/10.1016/j.copbio.2018.01.017

Lutz, S., Anesio, A.M., Edwards, A., Benning, L.G., 2016. Linking microbial diversity and functionality of Arctic glacial surface habitats. Environ. Microbiol. https://doi.org/10.1111/1462-2920.13494

Lutz, S., Anesio, A.M., Jorge Villar, S.E., Benning, L.G., 2014. Variations of algal communities cause darkening of a Greenland glacier. FEMS Microbiol. Ecol. 89, 402–414. https://doi.org/10.1111/1574-6941.12351

Lyutskanova, D., Ivanova, V., Stoilova-Disheva, M., Kolarova, M., Aleksieva, K., Raykovska, V., Peltekova, V., 2009. Isolation, Characterization and Screening for Antimicrobial Activities of Psychrotolerant Streptomycetes Isolated from Polar Permafrost Soil. Biotechnol. Biotechnol. Equip. 23, 305–309. https://doi.org/10.1080/13102818.2009.10818425

Maccario, L., Sanguino, L., Vogel, T.M., Larose, C., 2015. Snow and ice ecosystems: not so extreme. Res. Microbiol. 166, 782–795. https://doi.org/10.1016/j.resmic.2015.09.002

Macherla, V.R., Liu, J., Bellows, C., Teisan, S., Nicholson, B., Lam, K.S., Potts, B.C.M., 2005. Glaciapyrroles A, B, and C, Pyrrolosesquiterpenes from a *Streptomyces* sp. Isolated from an Alaskan Marine Sediment. J. Nat. Prod. 68, 780–783. https://doi.org/10.1021/np049597c

Madsen, E.L., 2011. Microorganisms and their roles in fundamental biogeochemical cycles. Curr. Opin. Biotechnol. 22, 456–464. https://doi.org/10.1016/j.copbio.2011.01.008

Malard, L.A., Anwar, M.Z., Jacobsen, C.S., Pearce, D.A., 2019. Biogeographical patterns in soil bacterial communities across the Arctic region. FEMS Microbiol. Ecol. 95. https://doi.org/10.1093/femsec/fiz128

Malard, L.A., Pearce, D.A., 2018. Microbial diversity and biogeography in Arctic soils. Environ. Microbiol. Rep. 10, 611–625. https://doi.org/10.1111/1758-2229.12680

Mandelli, F., Miranda, V.S., Rodrigues, E., Mercadante, A.Z., 2012. Identification of carotenoids with high antioxidant capacity produced by extremophile microorganisms. World J. Microbiol. Biotechnol. 28, 1781–1790. https://doi.org/10.1007/s11274-011-0993-y

Mangiagalli, M., Brocca, S., Orlando, M., Lotti, M., 2020. The “cold revolution”. Present and future applications of cold-active enzymes and ice-binding proteins. New Biotechnol. 55, 5–11. https://doi.org/10.1016/j.nbt.2019.09.003

Margesin, R., Collins, T., 2019. Microbial ecology of the cryosphere (glacial and permafrost habitats): current knowledge. Appl. Microbiol. Biotechnol. 103, 2537–2549. https://doi.org/10.1007/s00253-019-09631-3

Margesin, R., Miteva, V., 2011. Diversity and ecology of psychrophilic microorganisms. Res. Microbiol. 162, 346–361. https://doi.org/10.1016/j.resmic.2010.12.004

Margesin, R., Zhang, D.-C., 2013. *Pedobacter ruber* sp. nov., a psychrophilic bacterium isolated from soil. Int. J. Syst. Evol. Microbiol. 63, 339–344. https://doi.org/10.1099/ijs.0.039107-0

Martin, M., 2011. Cutadapt removes adapter sequences from high-throughput sequencing reads. EMBnet.journal 17, 10–12. https://doi.org/10.14806/ej.17.1.200

McAlpine, J.B., Bachmann, B.O., Piraee, M., Tremblay, S., Alarco, A.-M., Zazopoulos, E., Farnet, C.M., 2005. Microbial Genomics as a Guide to Drug Discovery and Structural Elucidation: ECO-02301, a Novel Antifungal Agent, as an Example †. J. Nat. Prod. 68, 493–496. https://doi.org/10.1021/np0401664

McClerren, A.L., Cooper, L.E., Quan, C., Thomas, P.M., Kelleher, N.L., van der Donk, W.A., 2006. Discovery and in vitro biosynthesis of haloduracin, a two-component lantibiotic. Proc. Natl. Acad. Sci. 103, 17243–17248. https://doi.org/10.1073/pnas.0606088103

McDaniel, E.A., Anantharaman, K., McMahon, K.D., 2019. metabolisHMM: Phylogenomic analysis for exploration of microbial phylogenies and metabolic pathways. bioRxiv 2019.12.20.884627. https://doi.org/10.1101/2019.12.20.884627

McGuirl, M.A., K. Nelson, L., Bollinger, J.A., Chan, Y.-K., Dooley, D.M., 1998. The nos (nitrous oxide reductase) gene cluster from the soil bacterium *Achromobacter cycloclastes*: Cloning, sequence analysis, and expression. J. Inorg. Biochem. 70, 155–169. https://doi.org/10.1016/S0162-0134(98)10001-6

McMahon, M.D., Guan, C., Handelsman, J., Thomas, M.G., 2012. Metagenomic Analysis of *Streptomyces lividans* Reveals Host-Dependent Functional Expression. Appl. Environ. Microbiol. 78, 3622–3629. https://doi.org/10.1128/AEM.00044-12

McMurdie, P.J., Holmes, S., 2014. Waste Not, Want Not: Why Rarefying Microbiome Data Is Inadmissible. PLOS Comput. Biol. 10, e1003531. https://doi.org/10.1371/journal.pcbi.1003531

McMurdie, P.J., Holmes, S., 2013. phyloseq: An R Package for Reproducible Interactive Analysis and Graphics of Microbiome Census Data. PLOS ONE 8, e61217. https://doi.org/10.1371/journal.pone.0061217

Medema, M.H., Kottmann, R., Yilmaz, P., Cummings, M., Biggins, J.B., Blin, K., de Bruijn, I., Chooi, Y.H., Claesen, J., Coates, R.C., Cruz-Morales, P., Duddela, S., Düsterhus, S., Edwards, D.J., Fewer, D.P., Garg, N., Geiger, C., Gomez-Escribano, J.P., Greule, A., Hadjithomas, M., Haines, A.S., Helfrich, E.J.N., Hillwig, M.L., Ishida, K., Jones, A.C., Jones, C.S., Jungmann, K., Kegler, C., Kim, H.U., Kötter, P., Krug, D., Masschelein, J., Melnik, A.V., Mantovani, S.M., Monroe, E.A., Moore, M., Moss, N., Nützmann, H.-W., Pan, G., Pati, A., Petras, D., Reen, F.J., Rosconi, F., Rui, Z., Tian, Z., Tobias, N.J., Tsunematsu, Y., Wiemann, P., Wyckoff, E., Yan, X., Yim, G., Yu, F., Xie, Y., Aigle, B., Apel, A.K., Balibar, C.J., Balskus, E.P., Barona-Gómez, F., Bechthold, A., Bode, H.B., Borriss, R., Brady, S.F., Brakhage, A.A., Caffrey, P., Cheng, Y.-Q., Clardy, J., Cox, R.J., De Mot, R., Donadio, S., Donia, M.S., van der Donk, W.A., Dorrestein, P.C., Doyle, S., Driessen, A.J.M., Ehling-Schulz, M., Entian, K.-D., Fischbach, M.A., Gerwick, L., Gerwick, W.H., Gross, H., Gust, B., Hertweck, C., Höfte, M., Jensen, S.E., Ju, J., Katz, L., Kaysser, L., Klassen, J.L., Keller, N.P., Kormanec, J., Kuipers, O.P., Kuzuyama, T., Kyrpides, N.C., Kwon, H.-J., Lautru, S., Lavigne, R., Lee, C.Y., Linquan, B., Liu, X., Liu, W., Luzhetskyy, A., Mahmud, T.,

Mast, Y., Méndez, C., Metsä-Ketelä, M., Micklefield, J., Mitchell, D.A., Moore, B.S., Moreira, L.M., Müller, R., Neilan, B.A., Nett, M., Nielsen, J., O'Gara, F., Oikawa, H., Osbourn, A., Osburne, M.S., Ostash, B., Payne, S.M., Pernodet, J.-L., Petricek, M., Piel, J., Ploux, O., Raaijmakers, J.M., Salas, J.A., Schmitt, E.K., Scott, B., Seipke, R.F., Shen, B., Sherman, D.H., Sivonen, K., Smanski, M.J., Sosio, M., Stegmann, E., Süssmuth, R.D., Tahlan, K., Thomas, C.M., Tang, Y., Truman, A.W., Viaud, M., Walton, J.D., Walsh, C.T., Weber, T., van Wezel, G.P., Wilkinson, B., Willey, J.M., Wohlleben, W., Wright, G.D., Ziemert, N., Zhang, C., Zotchev, S.B., Breitling, R., Takano, E., Glöckner, F.O., 2015. Minimum Information about a Biosynthetic Gene cluster. Nat. Chem. Biol. 11, 625–631. https://doi.org/10.1038/nchembio.1890

Menzel, P., Ng, K.L., Krogh, A., 2016. Fast and sensitive taxonomic classification for metagenomics with Kaiju. Nat. Commun. 7, 11257. https://doi.org/10.1038/ncomms11257

Mikheenko, A., Saveliev, V., Gurevich, A., 2016. MetaQUAST: evaluation of metagenome assemblies. Bioinforma. Oxf. Engl. 32, 1088–1090. https://doi.org/10.1093/bioinformatics/btv697

Mistry, J., Finn, R.D., Eddy, S.R., Bateman, A., Punta, M., 2013. Challenges in homology search: HMMER3 and convergent evolution of coiled-coil regions. Nucleic Acids Res. 41, e121–e121. https://doi.org/10.1093/nar/gkt263

Miteva, V., 2008. Bacteria in Snow and Glacier Ice, in: Margesin, R., Schinner, F., Marx, J.-C., Gerday, C. (Eds.), Psychrophiles: From Biodiversity to Biotechnology. Springer Berlin Heidelberg, Berlin, Heidelberg, pp. 31–50.

Mojib, N., Philpott, R., Huang, J.P., Niederweis, M., Bej, A.K., 2010. Antimycobacterial activity in vitro of pigments isolated from Antarctic bacteria. Antonie Van Leeuwenhoek 98, 531–540. https://doi.org/10.1007/s10482-010-9470-0

Mondini, A., Donhauser, J., Itcus, C., Marin, C., Perșoiu, A., Lavin, P., Frey, B., Purcarea, C., 2018. High-throughput sequencing of fungal communities across the perennial ice block of Scărișoara Ice Cave. Ann. Glaciol. 59, 134–146. https://doi.org/10.1017/aog.2019.6

Moss, E.L., Maghini, D.G., Bhatt, A.S., 2020. Complete, closed bacterial genomes from microbiomes using nanopore sequencing. Nat. Biotechnol. 38, 701–707. https://doi.org/10.1038/s41587-020-0422-6

Mu, D.-S., Ouyang, Y., Chen, G.-J., Du, Z.-J., 2020. Strategies for culturing active/dormant marine microbes. Mar. Life Sci. Technol. https://doi.org/10.1007/s42995-020-00053-z

Mueller, D.R., Vincent, W.F., Bonilla, S., Laurion, I., 2005. Extremotrophs, extremophiles and broadband pigmentation strategies in a high arctic ice shelf ecosystem. FEMS Microbiol. Ecol. 53, 73–87. https://doi.org/10.1016/j.femsec.2004.11.001

Muñoz, P.A., Márquez, S.L., González-Nilo, F.D., Márquez-Miranda, V., Blamey, J.M., 2017. Structure and application of antifreeze proteins from Antarctic bacteria. Microb. Cell Factories 16. https://doi.org/10.1186/s12934-017-0737-2

Muryoi, N., Sato, M., Kaneko, S., Kawahara, H., Obata, H., Yaish, M.W.F., Griffith, M., Glick, B.R., 2004. Cloning and expression of afpA, a gene encoding an antifreeze protein from the arctic plant growth-promoting rhizobacterium *Pseudomonas putida* GR12-2. J. Bacteriol. 186, 5661–5671. https://doi.org/10.1128/JB.186.17.5661-5671.2004

Nagano, K., Wachi, M., Takada, A., Takaku, F., Hirasawa, T., Nagai, K., 1999. *fcsA29* Mutation is an Allele of *polA* Gene of *Escherichia coli*. Biosci. Biotechnol. Biochem. 63, 427–429. https://doi.org/10.1271/bbb.63.427

Navarro-Muñoz, J.C., Selem-Mojica, N., Mullowney, M.W., Kautsar, S.A., Tryon, J.H., Parkinson, E.I., De Los Santos, E.L.C., Yeong, M., Cruz-Morales, P., Abubucker, S.,

Roeters, A., Lokhorst, W., Fernandez-Guerra, A., Cappelini, L.T.D., Goering, A.W., Thomson, R.J., Metcalf, W.W., Kelleher, N.L., Barona-Gomez, F., Medema, M.H., 2020. A computational framework to explore large-scale biosynthetic diversity. Nat. Chem. Biol. 16, 60–68. https://doi.org/10.1038/s41589-019-0400-9

Nelson, W.C., Maezato, Y., Wu, Y.-W., Romine, M.F., Lindemann, S.R., 2015. Identification and Resolution of Microdiversity through Metagenomic Sequencing of Parallel Consortia. Appl. Environ. Microbiol. 82, 255–267. https://doi.org/10.1128/AEM.02274-15

Nichols, D.S., 2003. Prokaryotes and the input of polyunsaturated fatty acids to the marine food web. FEMS Microbiol. Lett. 219, 1–7. https://doi.org/10.1016/S0378-1097(02)01200-4

Nichols, D.S., McMeekin, T.A., 2002. Biomarker techniques to screen for bacteria that produce polyunsaturated fatty acids. J. Microbiol. Methods 48, 161–170. https://doi.org/10.1016/S0167-7012(01)00320-7

Novototskaya-Vlasova, K., Petrovskaya, L., Yakimov, S., Gilichinsky, D., 2012. Cloning, purification, and characterization of a cold-adapted esterase produced by *Psychrobacter cryohalolentis* K5 ^{T} from Siberian cryopeg. FEMS Microbiol. Ecol. 82, 367–375. https://doi.org/10.1111/j.1574-6941.2012.01385.x

Novototskaya-Vlasova, K.A., Petrovskaya, L.E., Rivkina, E.M., Dolgikh, D.A., Kirpichnikov, M.P., 2013. Characterization of a cold-active lipase from *Psychrobacter cryohalolentis* K5T and its deletion mutants. Biochem. Mosc. 78, 385–394. https://doi.org/10.1134/S000629791304007X

Nurk, S., Meleshko, D., Korobeynikov, A., Pevzner, P.A., 2017. metaSPAdes: a new versatile metagenomic assembler. Genome Res. 27, 824–834. https://doi.org/10.1101/gr.213959.116

Nwodo, U.U., Green, E., Okoh, A.I., 2012. Bacterial Exopolysaccharides: Functionality and Prospects. Int. J. Mol. Sci. 13, 14002–14015. https://doi.org/10.3390/ijms131114002

O'Brien, A., Sharp, R., Russell, N.J., Roller, S., 2004. Antarctic bacteria inhibit growth of food-borne microorganisms at low temperatures. FEMS Microbiol. Ecol. 48, 157–167. https://doi.org/10.1016/j.femsec.2004.01.001

Ochsenreither, K., Glück, C., Stressler, T., Fischer, L., Syldatk, C., 2016. Production Strategies and Applications of Microbial Single Cell Oils. Front. Microbiol. 7. https://doi.org/10.3389/fmicb.2016.01539

Ohhata, N., Yoshida, N., Egami, H., Katsuragi, T., Tani, Y., Takagi, H., 2007. An extremely oligotrophic bacterium, *Rhodococcus erythropolis* N9T-4, isolated from crude oil. J. Bacteriol. 189, 6824–6831. https://doi.org/10.1128/JB.00872-07

O'Leary, N.A., Wright, M.W., Brister, J.R., Ciufo, S., Haddad, D., McVeigh, R., Rajput, B., Robbertse, B., Smith-White, B., Ako-Adjei, D., Astashyn, A., Badretdin, A., Bao, Y., Blinkova, O., Brover, V., Chetvernin, V., Choi, J., Cox, E., Ermolaeva, O., Farrell, C.M., Goldfarb, T., Gupta, T., Haft, D., Hatcher, E., Hlavina, W., Joardar, V.S., Kodali, V.K., Li, W., Maglott, D., Masterson, P., McGarvey, K.M., Murphy, M.R., O'Neill, K., Pujar, S., Rangwala, S.H., Rausch, D., Riddick, L.D., Schoch, C., Shkeda, A., Storz, S.S., Sun, H., Thibaud-Nissen, F., Tolstoy, I., Tully, R.E., Vatsan, A.R., Wallin, C., Webb, D., Wu, W., Landrum, M.J., Kimchi, A., Tatusova, T., DiCuccio, M., Kitts, P., Murphy, T.D., Pruitt, K.D., 2016. Reference sequence (RefSeq) database at NCBI: current status, taxonomic expansion, and functional annotation. Nucleic Acids Res. 44, D733-745. https://doi.org/10.1093/nar/gkv1189

Olorunniji, F.J., Rosser, S.J., Stark, W.M., 2016. Site-specific recombinases: molecular machines for the Genetic Revolution. Biochem. J. 473, 673–684. https://doi.org/10.1042/BJ20151112

Oman, T.J., Lupoli, T.J., Wang, T.-S.A., Kahne, D., Walker, S., van der Donk, W.A., 2011. Haloduracin α binds the peptidoglycan precursor lipid II with 2:1 stoichiometry. J. Am. Chem. Soc. 133, 17544–17547. https://doi.org/10.1021/ja206281k

Overholt, W.A., Hölzer, M., Geesink, P., Diezel, C., Marz, M., Küsel, K., 2019. Inclusion of Oxford Nanopore long reads improves all microbial and phage metagenome-assembled genomes from a complex aquifer system. bioRxiv 2019.12.18.880807. https://doi.org/10.1101/2019.12.18.880807

Owen, J.G., Charlop-Powers, Z., Smith, A.G., Ternei, M.A., Calle, P.Y., Reddy, B.V.B., Montiel, D., Brady, S.F., 2015. Multiplexed metagenome mining using short DNA sequence tags facilitates targeted discovery of epoxyketone proteasome inhibitors. Proc. Natl. Acad. Sci. U. S. A. 112, 4221–4226. https://doi.org/10.1073/pnas.1501124112

Paduch, R., Kandefer-Szerszeń, M., Trytek, M., Fiedurek, J., 2007. Terpenes: substances useful in human healthcare. Arch. Immunol. Ther. Exp. (Warsz.) 55, 315. https://doi.org/10.1007/s00005-007-0039-1

Panicker, G., Aislabie, J., Saul, D., Bej, A., 2002. Cold tolerance of *Pseudomonas* sp. 30-3 isolated from oil-contaminated soil, Antarctica. Polar Biol. 25, 5–11. https://doi.org/10.1007/s003000100304

Papale, M., Giannarelli, S., Francesconi, S., Di Marco, G., Mikkonen, A., Conte, A., Rizzo, C., De Domenico, E., Michaud, L., Giudice, A.L., 2017. Enrichment, isolation and biodegradation potential of psychrotolerant polychlorinated-biphenyl degrading bacteria from the Kongsfjorden (Svalbard Islands, High Arctic Norway). Mar. Pollut. Bull. 114, 849–859. https://doi.org/10.1016/j.marpolbul.2016.11.011

Park, D., Swayambhu, G., Pfeifer, B.A., 2020. Heterologous biosynthesis as a platform for producing new generation natural products. Curr. Opin. Biotechnol. 66, 123–130. https://doi.org/10.1016/j.copbio.2020.06.014

Parks, D.H., Chuvochina, M., Waite, D.W., Rinke, C., Skarshewski, A., Chaumeil, P.-A., Hugenholtz, P., 2018. A standardized bacterial taxonomy based on genome phylogeny substantially revises the tree of life. Nat. Biotechnol. 36, 996–1004. https://doi.org/10.1038/nbt.4229

Parks, D.H., Imelfort, M., Skennerton, C.T., Hugenholtz, P., Tyson, G.W., 2015. CheckM: assessing the quality of microbial genomes recovered from isolates, single cells, and metagenomes. Genome Res. 25, 1043–1055. https://doi.org/10.1101/gr.186072.114

Parks, D.H., Rinke, C., Chuvochina, M., Chaumeil, P.-A., Woodcroft, B.J., Evans, P.N., Hugenholtz, P., Tyson, G.W., 2017. Recovery of nearly 8,000 metagenome-assembled genomes substantially expands the tree of life. Nat. Microbiol. 2, 1533–1542. https://doi.org/10.1038/s41564-017-0012-7

Parrilli, E., De Vizio, D., Cirulli, C., Tutino, M.L., 2008. Development of an improved *Pseudoalteromonas haloplanktis* TAC125 strain for recombinant protein secretion at low temperature. Microb. Cell Factories 7, 2. https://doi.org/10.1186/1475-2859-7-2

Pasolli, E., Asnicar, F., Manara, S., Zolfo, M., Karcher, N., Armanini, F., Beghini, F., Manghi, P., Tett, A., Ghensi, P., Collado, M.C., Rice, B.L., DuLong, C., Morgan, X.C., Golden, C.D., Quince, C., Huttenhower, C., Segata, N., 2019. Extensive Unexplored Human Microbiome Diversity Revealed by Over 150,000 Genomes from Metagenomes Spanning Age, Geography, and Lifestyle. Cell 176, 649-662.e20. https://doi.org/10.1016/j.cell.2019.01.001

Passardi, F., Theiler, G., Zamocky, M., Cosio, C., Rouhier, N., Teixera, F., Margis-Pinheiro, M., Ioannidis, V., Penel, C., Falquet, L., Dunand, C., 2007. PeroxiBase: the peroxidase database. Phytochemistry 68, 1605–1611. https://doi.org/10.1016/j.phytochem.2007.04.005

Pathak, J., Pandey, A., Maurya, P.K., Rajneesh, R., Sinha, R.P., Singh, S.P., 2020. Cyanobacterial Secondary Metabolite Scytonemin: A Potential Photoprotective and Pharmaceutical Compound. Proc. Natl. Acad. Sci. India Sect. B Biol. Sci. 90, 467–481. https://doi.org/10.1007/s40011-019-01134-5

Paun, V.I., Icaza, G., Lavin, P., Marin, C., Tudorache, A., Perşoiu, A., Dorador, C., Purcarea, C., 2019. Total and Potentially Active Bacterial Communities Entrapped in a Late Glacial through Holocene Ice Core from Scarisoara Ice Cave, Romania. Front. Microbiol. 10. https://doi.org/10.3389/fmicb.2019.01193

Peng, Y., Leung, H.C.M., Yiu, S.M., Chin, F.Y.L., 2012. IDBA-UD: a de novo assembler for single-cell and metagenomic sequencing data with highly uneven depth. Bioinforma. Oxf. Engl. 28, 1420–1428. https://doi.org/10.1093/bioinformatics/bts174

Pereira, J.O., de Souza, A.Q.L., de Souza, A.D.L., de Castro França, S., de Oliveira, L.A., 2017. Overview on Biodiversity, Chemistry, and Biotechnological Potential of Microorganisms from the Brazilian Amazon, in: de Azevedo, J.L., Quecine, M.C. (Eds.), Diversity and Benefits of Microorganisms from the Tropics. Springer International Publishing, Cham, pp. 71–103. https://doi.org/10.1007/978-3-319-55804-2_5

Pereira, S., Zille, A., Micheletti, E., Moradas-Ferreira, P., De Philippis, R., Tamagnini, P., 2009. Complexity of cyanobacterial exopolysaccharides: composition, structures, inducing factors and putative genes involved in their biosynthesis and assembly. FEMS Microbiol. Rev. 33, 917–941. https://doi.org/10.1111/j.1574-6976.2009.00183.x

Perşoiu, A., Pazdur, A., 2011. Ice genesis and its long-term mass balance and dynamics in Scărişoara Ice Cave, Romania. The Cryosphere 5, 45–53. https://doi.org/10.5194/tc-5-45-2011

Petrovskaya, L.E., Novototskaya-Vlasova, K.A., Kryukova, E.A., Rivkina, E.M., Dolgikh, D.A., Kirpichnikov, M.P., 2015. Cell surface display of cold-active esterase EstPc with the use of a new autotransporter from *Psychrobacter cryohalolentis* K5(T). Extrem. Life Extreme Cond. 19, 161–170. https://doi.org/10.1007/s00792-014-0695-0

Pham, V.H.T., Kim, J., 2012. Cultivation of unculturable soil bacteria. Trends Biotechnol. 30, 475–484. https://doi.org/10.1016/j.tibtech.2012.05.007

Piel, J., 2011. Approaches to capturing and designing biologically active small molecules produced by uncultured microbes. Annu. Rev. Microbiol. 65, 431–453. https://doi.org/10.1146/annurev-micro-090110-102805

Poli, A., Anzelmo, G., Nicolaus, B., 2010. Bacterial Exopolysaccharides from Extreme Marine Habitats: Production, Characterization and Biological Activities. Mar. Drugs 8, 1779–1802. https://doi.org/10.3390/md8061779

Potapov, V., Ong, J.L., 2017. Examining Sources of Error in PCR by Single-Molecule Sequencing. PLOS ONE 12, e0169774. https://doi.org/10.1371/journal.pone.0169774

Price, M.N., Dehal, P.S., Arkin, A.P., 2010. FastTree 2 – Approximately Maximum-Likelihood Trees for Large Alignments. PLOS ONE 5, e9490. https://doi.org/10.1371/journal.pone.0009490

Pritchard, L., Glover, R.H., Humphris, S., Elphinstone, J.G., Toth, I.K., 2015. Genomics and taxonomy in diagnostics for food security: soft-rotting enterobacterial plant pathogens. Anal. Methods 8, 12–24. https://doi.org/10.1039/C5AY02550H

Pruthi, V., Cameotra, S.S., 1997. Production and properties of a biosurfactant synthesized by *Arthrobacter protophormiae* — an antarctic strain. World J. Microbiol. Biotechnol. 13, 137–139. https://doi.org/10.1007/BF02770822

Pushkareva, E., Pessi, I.S., Wilmotte, A., Elster, J., 2015. Cyanobacterial community composition in Arctic soil crusts at different stages of development. FEMS Microbiol. Ecol. 91. https://doi.org/10.1093/femsec/fiv143

Qoura, F., Kassab, E., Reiße, S., Antranikian, G., Brueck, T., 2015. Characterization of a new, recombinant thermo-active subtilisin-like serine protease derived from *Shewanella arctica*. J. Mol. Catal. B Enzym. Complete, 16–23. https://doi.org/10.1016/j.molcatb.2015.02.015

Quast, C., Pruesse, E., Yilmaz, P., Gerken, J., Schweer, T., Yarza, P., Peplies, J., Glöckner, F.O., 2013. The SILVA ribosomal RNA gene database project: improved data processing and web-based tools. Nucleic Acids Res. 41, D590–D596. https://doi.org/10.1093/nar/gks1219

Quesada, A., Vincent, W.F., Lean, D.R.S., 1999. Community and pigment structure of Arctic cyanobacterial assemblages: the occurrence and distribution of UV-absorbing compounds. FEMS Microbiol. Ecol. 28, 315–323. https://doi.org/10.1111/j.1574-6941.1999.tb00586.x

Räisänen, O., 2008. English: Topographic map of Svalbard. Suomi: Huippuvuorten topografinen kartta. Norsk bokmål: Topografisk kart over Svalbard.Polski: Mapa topograficzna Svalbardu.Русский: Топографическая_карта Шпицбергена.Українська: Топографічна_карта Свальбарда.

Rajput, Y., Biswas, J., Rai, V., 2012. Potentiality test in antimicrobial activity and antibiotic sensitivity of subterranean *Streptomyces* strains isolated from Kotumsar cave of India. Int. J. Biol. Chem. 6, 53–60.

Rashid, M., Stingl, U., 2015. Contemporary molecular tools in microbial ecology and their application to advancing biotechnology. Biotechnol. Adv. 33, 1755–1773. https://doi.org/10.1016/j.biotechadv.2015.09.005

Ratledge, C., 2004. Fatty acid biosynthesis in microorganisms being used for Single Cell Oil production. Biochimie, Recent advances in lipid metabolism and related disorders 86, 807–815. https://doi.org/10.1016/j.biochi.2004.09.017

Rime, T., Hartmann, M., Brunner, I., Widmer, F., Zeyer, J., Frey, B., 2015. Vertical distribution of the soil microbiota along a successional gradient in a glacier forefield. Mol. Ecol. 24, 1091–1108. https://doi.org/10.1111/mec.13051

Rime, T., Hartmann, M., Frey, B., 2016. Potential sources of microbial colonizers in an initial soil ecosystem after retreat of an alpine glacier. ISME J. 10, 1625–1641. https://doi.org/10.1038/ismej.2015.238

Robe, P., Nalin, R., Capellano, C., Vogel, T.M., Simonet, P., 2003. Extraction of DNA from soil. Eur. J. Soil Biol. 39, 183–190. https://doi.org/10.1016/S1164-5563(03)00033-5

Roesch, L.F.W., Fulthorpe, R.R., Riva, A., Casella, G., Hadwin, A.K.M., Kent, A.D., Daroub, S.H., Camargo, F.A.O., Farmerie, W.G., Triplett, E.W., 2007. Pyrosequencing enumerates and contrasts soil microbial diversity. ISME J. 1, 283–290. https://doi.org/10.1038/ismej.2007.53

Rossi, F., De Philippis, R., 2015. Role of cyanobacterial exopolysaccharides in phototrophic biofilms and in complex microbial mats. Life Basel Switz. 5, 1218–1238. https://doi.org/10.3390/life5021218

Rule, D., Cheeptham, N., 2013. The effects of UV light on the antimicrobial activities of cave actinomycetes. Int. J. Speleol. 42. http://dx.doi.org/10.5038/1827-806X.42.2.7

Saary, P., Mitchell, A.L., Finn, R.D., 2020. Estimating the quality of eukaryotic genomes recovered from metagenomic analysis. bioRxiv 2019.12.19.882753. https://doi.org/10.1101/2019.12.19.882753

Sabtu, N., Enoch, D.A., Brown, N.M., 2015. Antibiotic resistance: what, why, where, when and how? Br. Med. Bull. 116, 105–113. https://doi.org/10.1093/bmb/ldv041

Sajjad, W., Din, G., Rafiq, M., Iqbal, A., Khan, S., Zada, S., Ali, B., Kang, S., 2020. Pigment production by cold-adapted bacteria and fungi: colorful tale of cryosphere with wide range applications. Extremophiles 24, 447–473. https://doi.org/10.1007/s00792-020-01180-2

Salter, S.J., Cox, M.J., Turek, E.M., Calus, S.T., Cookson, W.O., Moffatt, M.F., Turner, P., Parkhill, J., Loman, N.J., Walker, A.W., 2014. Reagent and laboratory contamination can critically impact sequence-based microbiome analyses. BMC Biol. 12, 87. https://doi.org/10.1186/s12915-014-0087-z

Santiago, M., Ramírez-Sarmiento, C.A., Zamora, R.A., Parra, L.P., 2016. Discovery, Molecular Mechanisms, and Industrial Applications of Cold-Active Enzymes. Front. Microbiol. 7. https://doi.org/10.3389/fmicb.2016.01408

Santo, M., Weitsman, R., Sivan, A., 2013. The role of the copper-binding enzyme – laccase – in the biodegradation of polyethylene by the actinomycete *Rhodococcus ruber*. Int. Biodeterior. Biodegrad. 84, 204–210. https://doi.org/10.1016/j.ibiod.2012.03.001

Sato, S., Kurihara, T., Kawamoto, J., Hosokawa, M., Sato, S.B., Esaki, N., 2008. Cold adaptation of eicosapentaenoic acid-less mutant of *Shewanella livingstonensis* Ac10 involving uptake and remodeling of synthetic phospholipids containing various polyunsaturated fatty acids. Extremophiles 12, 753–761. https://doi.org/10.1007/s00792-008-0182-6

Saul, D.J., Aislabie, J.M., Brown, C.E., Harris, L., Foght, J.M., 2005. Hydrocarbon contamination changes the bacterial diversity of soil from around Scott Base, Antarctica. FEMS Microbiol. Ecol. 53, 141–155. https://doi.org/10.1016/j.femsec.2004.11.007

Saum, S.H., Pfeiffer, F., Palm, P., Rampp, M., Schuster, S.C., Müller, V., Oesterhelt, D., 2013. Chloride and organic osmolytes: a hybrid strategy to cope with elevated salinities by the moderately halophilic, chloride-dependent bacterium *Halobacillus halophilus*: Genome of *H. halophilus*. Environ. Microbiol. 15, 1619–1633. https://doi.org/10.1111/j.1462-2920.2012.02770.x

Savelli, B., Li, Q., Webber, M., Jemmat, A.M., Robitaille, A., Zamocky, M., Mathé, C., Dunand, C., 2019. RedoxiBase: A database for ROS homeostasis regulated proteins. Redox Biol. 26, 101247. https://doi.org/10.1016/j.redox.2019.101247

Säwström, C., Mumford, P., Marshall, W., Hodson, A., Laybourn-Parry, J., 2002. The microbial communities and primary productivity of cryoconite holes in an Arctic glacier (Svalbard 79°N). Polar Biol. 25, 591–596. https://doi.org/10.1007/s00300-002-0388-5

Schmetterer, G., Alge, D., Gregor, W., 1994. Deletion of cytochrome c oxidase genes from the cyanobacterium *Synechocystis* sp. PCC6803: Evidence for alternative respiratory pathways. Photosynth. Res. 42, 43–50. https://doi.org/10.1007/BF00019057

Schmidt, M., Stougaard, P., 2010. Identification, cloning and expression of a cold-active β-galactosidase from a novel Arctic bacterium, *Alkalilactibacillus ikkense*. Environ. Technol. 31, 1107–1114. https://doi.org/10.1080/09593331003677872

Schöner, T.A., Gassel, S., Osawa, A., Tobias, N.J., Okuno, Y., Sakakibara, Y., Shindo, K., Sandmann, G., Bode, H.B., 2016. Aryl Polyenes, a Highly Abundant Class of Bacterial Natural Products, are Functionally Related to Antioxidative Carotenoids. Chembiochem Eur. J. Chem. Biol. 17, 247–253. https://doi.org/10.1002/cbic.201500474

Schostag, M., Stibal, M., Jacobsen, C.S., Bælum, J., Taş, N., Elberling, B., Jansson, J.K., Semenchuk, P., Priemé, A., 2015. Distinct summer and winter bacterial communities in the active layer of Svalbard permafrost revealed by DNA- and RNA-based analyses. Front. Microbiol. 6. https://doi.org/10.3389/fmicb.2015.00399

Schulz, S., Brankatschk, R., Dümig, A., Kögel-Knabner, I., Schloter, M., Zeyer, J., 2013. The role of microorganisms at different stages of ecosystem development for soil formation. Biogeosciences 10, 3983–3996. https://doi.org/10.3929/ethz-b-000070776

Seemann, T., 2014. Prokka: rapid prokaryotic genome annotation. Bioinforma. Oxf. Engl. 30, 2068–2069. https://doi.org/10.1093/bioinformatics/btu153

Segawa, T., Yonezawa, T., Edwards, A., Akiyoshi, A., Tanaka, S., Uetake, J., Irvine-Fynn, T., Fukui, K., Li, Z., Takeuchi, N., 2017. Biogeography of cryoconite forming cyanobacteria on polar and Asian glaciers. J. Biogeogr. 44, 2849–2861. https://doi.org/10.1111/jbi.13089

Seipke, R.F., 2015. Strain-Level Diversity of Secondary Metabolism in *Streptomyces albus*. PLOS ONE 10, e0116457. https://doi.org/10.1371/journal.pone.0116457

Seok, Y.J., Song, E.-J., Cha, I.-T., Lee, H., Roh, S.W., Jung, J.Y., Lee, Y.K., Nam, Y.-D., Seo, M.-J., 2016. Microbial Community of the Arctic Soil from the Glacier Foreland of Midtre Lovénbreen in Svalbard by Metagenome Analysis. Microbiol. Biotechnol. Lett. 44, 171–179. https://doi.org/10.4014/mbl.1601.01003

Setlow, R.B., Swenson, P.A., Carrier, W.L., 1963. Thymine Dimers and Inhibition of DNA Synthesis by Ultraviolet Irradiation of Cells. Science 142, 1464–1466. https://doi.org/10.1126/science.142.3598.1464

Shaiber, A., Eren, A.M., 2019. Composite Metagenome-Assembled Genomes Reduce the Quality of Public Genome Repositories. mBio 10. https://doi.org/10.1128/mBio.00725-19

Shao, Z., Luo, Y., Zhao, H., 2011. Rapid Characterization and Engineering of Natural Product Biosynthetic Pathways via DNA Assembler. Mol. Biosyst. 7, 1056–1059. https://doi.org/10.1039/c0mb00338g

Shi, Y., Wang, Q., Hou, Y., Hong, Y., Han, X., Yi, J., Qu, J., Lu, Y., 2014. Molecular cloning, expression and enzymatic characterization of glutathione S-transferase from Antarctic sea-ice bacteria *Pseudoalteromonas* sp. ANT506. Microbiol. Res. 169, 179–184. https://doi.org/10.1016/j.micres.2013.06.012

Shvarev, D., Nishi, C.N., Maldener, I., 2019. Glycolipid composition of the heterocyst envelope of *Anabaena* sp. PCC 7120 is crucial for diazotrophic growth and relies on the UDP-galactose 4-epimerase HgdA. Microbiology Open 8. https://doi.org/10.1002/mbo3.811

Siddiqui, K.S., Cavicchioli, R., 2006. Cold-Adapted Enzymes. Annu. Rev. Biochem. 75, 403–433. https://doi.org/10.1146/annurev.biochem.75.103004.142723

Sieber, C.M.K., Probst, A.J., Sharrar, A., Thomas, B.C., Hess, M., Tringe, S.G., Banfield, J.F., 2018. Recovery of genomes from metagenomes via a dereplication, aggregation and scoring strategy. Nat. Microbiol. 3, 836–843. https://doi.org/10.1038/s41564-018-0171-1

Simon, C., Herath, J., Rockstroh, S., Daniel, R., 2009a. Rapid Identification of Genes Encoding DNA Polymerases by Function-Based Screening of Metagenomic Libraries Derived from Glacial Ice. Appl. Environ. Microbiol. 75, 2964–2968. https://doi.org/10.1128/AEM.02644-08

Simon, C., Wiezer, A., Strittmatter, A.W., Daniel, R., 2009b. Phylogenetic Diversity and Metabolic Potential Revealed in a Glacier Ice Metagenome. Appl. Environ. Microbiol. 75, 7519–7526. https://doi.org/10.1128/AEM.00946-09

Singh, B., Mal, G., Gautam, S.K., Mukesh, M., 2019. Metagenomics for Utilizing Herbivore Gut Potential, in: Singh, B., Mal, G., Gautam, S.K., Mukesh, M. (Eds.), Advances in Animal Biotechnology. Springer International Publishing, Cham, pp. 3–15. https://doi.org/10.1007/978-3-030-21309-1_1

Singh, P., Hanada, Y., Singh, S.M., Tsuda, S., 2014a. Antifreeze protein activity in Arctic cryoconite bacteria. FEMS Microbiol. Lett. 351, 14–22. https://doi.org/10.1111/1574-6968.12345

Singh, P., Singh, S.M., Dhakephalkar, P., 2014b. Diversity, cold active enzymes and adaptation strategies of bacteria inhabiting glacier cryoconite holes of High Arctic. Extremophiles 18, 229–242. https://doi.org/10.1007/s00792-013-0609-6

Singleton, C.M., Petriglieri, F., Kristensen, J.M., Kirkegaard, R.H., Michaelsen, T.Y., Andersen, M.H., Kondrotaite, Z., Karst, S.M., Dueholm, M.S., Nielsen, P.H., Albertsen, M., 2020. Connecting structure to function with the recovery of over 1000 high-quality activated sludge metagenome-assembled genomes encoding full-length rRNA genes using long-read sequencing. bioRxiv 2020.05.12.088096. https://doi.org/10.1101/2020.05.12.088096

Sirim, D., Wagner, F., Wang, L., Schmid, R.D., Pleiss, J., 2011. The Laccase Engineering Database: a classification and analysis system for laccases and related multicopper oxidases. Database J. Biol. Databases Curation 2011. https://doi.org/10.1093/database/bar006

Skinnider, M.A., Dejong, C.A., Rees, P.N., Johnston, C.W., Li, H., Webster, A.L.H., Wyatt, M.A., Magarvey, N.A., 2015. Genomes to natural products PRediction Informatics for Secondary Metabolomes (PRISM). Nucleic Acids Res. 43, 9645–9662. https://doi.org/10.1093/nar/gkv1012

Skinnider, M.A., Merwin, N.J., Johnston, C.W., Magarvey, N.A., 2017. PRISM 3: expanded prediction of natural product chemical structures from microbial genomes. Nucleic Acids Res. 45, W49–W54. https://doi.org/10.1093/nar/gkx320

Solheim, B., Endal, A., Vigstad, H., 1996. Nitrogen fixation in Arctic vegetation and soils from Svalbard, Norway. Polar Biol. 16, 35–40. https://doi.org/10.1007/BF01876827

Sparacino-Watkins, C., Stolz, J.F., Basu, P., 2014. Nitrate and periplasmic nitrate reductases. Chem. Soc. Rev. 43, 676–706. https://doi.org/10.1039/c3cs60249d

Spoof, L., Błaszczyk, A., Meriluoto, J., Cegłowska, M., Mazur-Marzec, H., 2015. Structures and Activity of New Anabaenopeptins Produced by Baltic Sea Cyanobacteria. Mar. Drugs 14. https://doi.org/10.3390/md14010008

Staley, J.T., Konopka, A., 1985. Measurement of in Situ Activities of Nonphotosynthetic Microorganisms in Aquatic and Terrestrial Habitats. Annu. Rev. Microbiol. 39, 321–346. https://doi.org/10.1146/annurev.mi.39.100185.001541

Steinrücken, P., Erga, S.R., Mjøs, S.A., Kleivdal, H., Prestegard, S.K., 2017. Bioprospecting North Atlantic microalgae with fast growth and high polyunsaturated fatty acid (PUFA) content for microalgae-based technologies. Algal Res. 26, 392–401. https://doi.org/10.1016/j.algal.2017.07.030

Stewart, E.J., 2012. Growing Unculturable Bacteria. J. Bacteriol. 194, 4151–4160. https://doi.org/10.1128/JB.00345-12

Stewart, R.D., Auffret, M.D., Warr, A., Walker, A.W., Roehe, R., Watson, M., 2019. Compendium of 4,941 rumen metagenome-assembled genomes for rumen microbiome biology and enzyme discovery. Nat. Biotechnol. 37, 953–961. https://doi.org/10.1038/s41587-019-0202-3

Stibal, M., Bradley, J.A., Edwards, A., Hotaling, S., Zawierucha, K., Rosvold, J., Lutz, S., Cameron, K.A., Mikucki, J.A., Kohler, T.J., Šabacká, M., Anesio, A.M., 2020. Glacial ecosystems are essential to understanding biodiversity responses to glacier retreat. Nat. Ecol. Evol. https://doi.org/10.1038/s41559-020-1163-0

Stibal, M., Šabacká, M., Kaštovská, K., 2006. Microbial Communities on Glacier Surfaces in Svalbard: Impact of Physical and Chemical Properties on Abundance and Structure of

Cyanobacteria and Algae. Microb. Ecol. 52, 644–654. https://doi.org/10.1007/s00248-006-9083-3

Stibal, M., Tranter, M., 2007. Laboratory investigation of inorganic carbon uptake by cryoconite debris from Werenskioldbreen, Svalbard. J. Geophys. Res. Biogeosciences 112, G04S33. https://doi.org/10.1029/2007JG000429

Stibal, M., Tranter, M., Benning, L.G., Řehák, J., 2008. Microbial primary production on an Arctic glacier is insignificant in comparison with allochthonous organic carbon input. Environ. Microbiol. 10, 2172–2178. https://doi.org/10.1111/j.1462-2920.2008.01620.x

Stibal, M., Wadham, J.L., Lis, G.P., Telling, J., Pancost, R.D., Dubnick, A., Sharp, M.J., Lawson, E.C., Butler, C.E.H., Hasan, F., Tranter, M., Anesio, A.M., 2012. Methanogenic potential of Arctic and Antarctic subglacial environments with contrasting organic carbon sources. Glob. Change Biol. 18, 3332–3345. https://doi.org/10.1111/j.1365-2486.2012.02763.x

Stokke, R., Reeves, E.P., Dahle, H., Fedøy, A.-E., Viflot, T., Lie Onstad, S., Vulcano, F., Pedersen, R.B., Eijsink, V.G.H., Steen, I.H., 2020. Tailoring Hydrothermal Vent Biodiversity Toward Improved Biodiscovery Using a Novel in situ Enrichment Strategy. Front. Microbiol. 11. https://doi.org/10.3389/fmicb.2020.00249

Sun, M.-L., Zhao, F., Shi, M., Zhang, X.-Y., Zhou, B.-C., Zhang, Y.-Z., Chen, X.-L., 2015. Characterization and Biotechnological Potential Analysis of a New Exopolysaccharide from the Arctic Marine Bacterium *Polaribacter* sp. SM1127. Sci. Rep. 5, 18435. https://doi.org/10.1038/srep18435

Sun, M.-L., Zhao, F., Zhang, X.-K., Zhang, X.-Y., Zhang, Y.-Z., Song, X.-Y., Chen, X.-L., 2020. Improvement of the production of an Arctic bacterial exopolysaccharide with protective effect on human skin cells against UV-induced oxidative stress. Appl. Microbiol. Biotechnol. 104, 4863–4875. https://doi.org/10.1007/s00253-020-10524-z

Suzek, B.E., Wang, Y., Huang, H., McGarvey, P.B., Wu, C.H., 2015. UniRef clusters: a comprehensive and scalable alternative for improving sequence similarity searches. Bioinformatics 31, 926–932. https://doi.org/10.1093/bioinformatics/btu739

Swain, S.S., Paidesetty, S.K., Padhy, R.N., 2017. Antibacterial, antifungal and antimycobacterial compounds from cyanobacteria. Biomed. Pharmacother. 90, 760–776. https://doi.org/10.1016/j.biopha.2017.04.030

Swem, D.L., Bauer, C.E., 2002. Coordination of Ubiquinol Oxidase and Cytochrome cbb3 Oxidase Expression by Multiple Regulators in *Rhodobacter capsulatus*. J. Bacteriol. 184, 2815–2820. https://doi.org/10.1128/JB.184.10.2815-2820.2002

Tabita, F.R., Satagopan, S., Hanson, T.E., Kreel, N.E., Scott, S.S., 2008. Distinct form I, II, III, and IV Rubisco proteins from the three kingdoms of life provide clues about Rubisco evolution and structure/function relationships. J. Exp. Bot. 59, 1515–1524. https://doi.org/10.1093/jxb/erm361

Takeuchi, N., 2002. Optical characteristics of cryoconite (surface dust) on glaciers: the relationship between light absorbency and the property of organic matter contained in the cryoconite. Ann. Glaciol. 34, 409–414. https://doi.org/10.3189/172756402781817743

Takeuchi, N., Tanaka, S., Konno, Y., Irvine-Fynn, T.D.L., Rassner, S.M.E., Edwards, A., 2019. Variations in Phototroph Communities on the Ablating Bare-Ice Surface of Glaciers on Brøggerhalvøya, Svalbard. Front. Earth Sci. 7. https://doi.org/10.3389/feart.2019.00004

Tatusov, R.L., Koonin, E.V., Lipman, D.J., 1997. A genomic perspective on protein families. Science 278, 631–637. https://doi.org/10.1126/science.278.5338.631

Tedesco, P., Maida, I., Palma Esposito, F., Tortorella, E., Subko, K., Ezeofor, C.C., Zhang, Y., Tabudravu, J., Jaspars, M., Fani, R., de Pascale, D., 2016. Antimicrobial Activity of Monoramnholipids Produced by Bacterial Strains Isolated from the Ross Sea (Antarctica). Mar. Drugs 14, 83. https://doi.org/10.3390/md14050083

Telling, J., Anesio, A.M., Tranter, M., Stibal, M., Hawkings, J., Irvine-Fynn, T., Hodson, A., Butler, C., Yallop, M., Wadham, J., 2012. Controls on the autochthonous production and respiration of organic matter in cryoconite holes on high Arctic glaciers: Carbon Production on Arctic Glaciers. J. Geophys. Res. Biogeosciences 117, n/a-n/a. https://doi.org/10.1029/2011JG001828

Terashima, M., Umezawa, K., Mori, S., Kojima, H., Fukui, M., 2017. Microbial Community Analysis of Colored Snow from an Alpine Snowfield in Northern Japan Reveals the Prevalence of Betaproteobacteria with Snow Algae. Front. Microbiol. 8. https://doi.org/10.3389/fmicb.2017.01481

Thomas, F.A., Sinha, R.K., Krishnan, K.P., 2020. Bacterial community structure of a glacio-marine system in the Arctic (Ny-Ålesund, Svalbard). Sci. Total Environ. 718, 135264. https://doi.org/10.1016/j.scitotenv.2019.135264

Thomas, T., Gilbert, J., Meyer, F., 2012. Metagenomics - a guide from sampling to data analysis. Microb. Inform. Exp. 2, 3. https://doi.org/10.1186/2042-5783-2-3

Thomassin-Lacroix, E.J., Yu, Z., Eriksson, M., Reimer, K.J., Mohn, W.W., 2001. DNA-based and culture-based characterization of a hydrocarbon-degrading consortium enriched from Arctic soil. Can. J. Microbiol. 47, 1107–1115.

Tomova, I., Lazarkevich, I., Tomova, A., Kambourova, M., Vasileva-Tonkova, E., 2013. Diversity and biosynthetic potential of culturable aerobic heterotrophic bacteria isolated from Magura Cave, Bulgaria. Int. J. Speleol. 42, 65–76. https://doi.org/10.5038/1827-806X.42.1.8

Tracanna, V., de Jong, A., Medema, M.H., Kuipers, O.P., 2017. Mining prokaryotes for antimicrobial compounds: from diversity to function. FEMS Microbiol. Rev. 41, 417–429. https://doi.org/10.1093/femsre/fux014

Trevors, J. T., van Elsas, J. D., 1995. Introduction to Nucleic Acids in the Environment: Methods and Applications, in: Trevors, Jack T., van Elsas, J. Dick (Eds.), Nucleic Acids in the Environment, Springer Lab Manuals. Springer Berlin Heidelberg, Berlin, Heidelberg, pp. 1–7. https://doi.org/10.1007/978-3-642-79050-8_1

Trivedi, C.B., Stamps, B.W., Lau, G.E., Grasby, S.E., Templeton, A.S., Spear, J.R., 2020. Microbial Metabolic Redundancy Is a Key Mechanism in a Sulfur-Rich Glacial Ecosystem. mSystems 5. https://doi.org/10.1128/mSystems.00504-20

Trout-Haney, J.V., Wood, Z.T., Cottingham, K.L., 2016. Presence of the Cyanotoxin Microcystin in Arctic Lakes of Southwestern Greenland. Toxins 8, 256. https://doi.org/10.3390/toxins8090256

Tveit, A., Schwacke, R., Svenning, M.M., Urich, T., 2013. Organic carbon transformations in high-Arctic peat soils: key functions and microorganisms. ISME J. 7, 299–311. https://doi.org/10.1038/ismej.2012.99

Uchiyama, T., Miyazaki, K., 2010. Product-Induced Gene Expression, a Product-Responsive Reporter Assay Used to Screen Metagenomic Libraries for Enzyme-Encoding Genes. Appl. Environ. Microbiol. 76, 7029–7035. https://doi.org/10.1128/AEM.00464-10

Uchiyama, T., Watanabe, K., 2008. Substrate-induced gene expression (SIGEX) screening of metagenome libraries. Nat. Protoc. 3, 1202–1212. https://doi.org/10.1038/nprot.2008.96

Urbanek, A.K., Rymowicz, W., Strzelecki, M.C., Kociuba, W., Franczak, Ł., Mirończuk, A.M., 2017. Isolation and characterization of Arctic microorganisms decomposing bioplastics. AMB Express 7, 148. https://doi.org/10.1186/s13568-017-0448-4

van Bergeijk, D.A., Terlouw, B.R., Medema, M.H., van Wezel, G.P., 2020. Ecology and genomics of Actinobacteria: new concepts for natural product discovery. Nat. Rev. Microbiol. https://doi.org/10.1038/s41579-020-0379-y

van der Walt, A.J., van Goethem, M.W., Ramond, J.-B., Makhalanyane, T.P., Reva, O., Cowan, D.A., 2017. Assembling metagenomes, one community at a time. BMC Genomics 18, 521. https://doi.org/10.1186/s12864-017-3918-9

van Heel, A.J., de Jong, A., Song, C., Viel, J.H., Kok, J., Kuipers, O.P., 2018. BAGEL4: a user-friendly web server to thoroughly mine RiPPs and bacteriocins. Nucleic Acids Res. 46, W278–W281. https://doi.org/10.1093/nar/gky383

Vanni, C., Schechter, M.S., Acinas, S.G., Barberán, A., Buttigieg, P.L., Casamayor, E.O., Delmont, T.O., Duarte, C.M., Eren, A.M., Finn, R.D., Kottmann, R., Mitchell, A., Sanchez, P., Siren, K., Steinegger, M., Glöckner, F.O., Fernandez-Guerra, A., 2020. Light into the darkness: Unifying the known and unknown coding sequence space in microbiome analyses. bioRxiv 2020.06.30.180448. https://doi.org/10.1101/2020.06.30.180448

Vavourakis, C.D., Ghai, R., Rodriguez-Valera, F., Sorokin, D.Y., Tringe, S.G., Hugenholtz, P., Muyzer, G., 2016. Metagenomic Insights into the Uncultured Diversity and Physiology of Microbes in Four Hypersaline Soda Lake Brines. Front. Microbiol. 7. https://doi.org/10.3389/fmicb.2016.00211

Ventola, C.L., 2015. The Antibiotic Resistance Crisis. Pharm. Ther. 40, 277–283.

Vester, J., Glaring, M., Stougaard, P., 2014. Discovery of novel enzymes with industrial potential from a cold and alkaline environment by a combination of functional metagenomics and culturing. Microb. Cell Factories 13, 72. https://doi.org/10.1186/1475-2859-13-72

Vester, J.K., Glaring, M.A., Stougaard, P., 2015. Improved cultivation and metagenomics as new tools for bioprospecting in cold environments. Extremophiles 19, 17–29. https://doi.org/10.1007/s00792-014-0704-3

Vollmers, J., Wiegand, S., Kaster, A.-K., 2017. Comparing and Evaluating Metagenome Assembly Tools from a Microbiologist's Perspective - Not Only Size Matters! Plos One 12, e0169662. https://doi.org/10.1371/journal.pone.0169662

Wang, Q., Hou, Y., Shi, Y., Han, X., Chen, Q., Hu, Z., Liu, Y., Li, Y., 2014. Cloning, Expression, Purification, and Characterization of Glutaredoxin from Antarctic Sea-Ice Bacterium *Pseudoalteromonas* sp. AN178. BioMed Res. Int. 2014, 1–6. https://doi.org/10.1155/2014/246871

Weber, T., Blin, K., Duddela, S., Krug, D., Kim, H.U., Bruccoleri, R., Lee, S.Y., Fischbach, M.A., Müller, R., Wohlleben, W., Breitling, R., Takano, E., Medema, M.H., 2015. antiSMASH 3.0—a comprehensive resource for the genome mining of biosynthetic gene clusters. Nucleic Acids Res. 43, W237–W243. https://doi.org/10.1093/nar/gkv437

Weber, T., Kim, H.U., 2016. The secondary metabolite bioinformatics portal: Computational tools to facilitate synthetic biology of secondary metabolite production. Synth. Syst. Biotechnol., Special Issue on "Bioinformatic tools and approaches for Synthetic Biology of natural products" 1, 69–79. https://doi.org/10.1016/j.synbio.2015.12.002

Wei, R., Zimmermann, W., 2017. Microbial enzymes for the recycling of recalcitrant petroleum-based plastics: how far are we? Microb. Biotechnol. n/a-n/a. https://doi.org/10.1111/1751-7915.12710

Welker, M., von Döhren, H., 2006. Cyanobacterial peptides - nature's own combinatorial biosynthesis. FEMS Microbiol. Rev. 30, 530–563. https://doi.org/10.1111/j.1574-6976.2006.00022.x

Wicka, M., Wanarska, M., Krajewska, E., Pawlak-Szukalska, A., Kur, J., Cieśliński, H., 2016. Cloning, expression, and biochemical characterization of a cold-active GDSL-esterase of a *Pseudomonas* sp. S9 isolated from Spitsbergen island soil. Acta Biochim. Pol. 63, 117–125. https://doi.org/10.18388/abp.2015_1074

Wietz, M., Månsson, M., Bowman, J.S., Blom, N., Ng, Y., Gram, L., 2012. Wide Distribution of Closely Related, Antibiotic-Producing *Arthrobacter* Strains throughout the Arctic Ocean. Appl. Environ. Microbiol. 78, 2039–2042. https://doi.org/10.1128/AEM.07096-11

Wong, C.M.V.L., Tam, H., Alias, S., González, M., González-Rocha, G., Domínguez-Yévenes, M., 2011. *Pseudomonas* and *Pedobacter* isolates from King George Island inhibited the growth of foodborne pathogens. https://doi.org/10.2478/V10183-011-0003-Y

Woodcroft, B.J., Singleton, C.M., Boyd, J.A., Evans, P.N., Emerson, J.B., Zayed, A.A.F., Hoelzle, R.D., Lamberton, T.O., McCalley, C.K., Hodgkins, S.B., Wilson, R.M., Purvine, S.O., Nicora, C.D., Li, C., Frolking, S., Chanton, J.P., Crill, P.M., Saleska, S.R., Rich, V.I., Tyson, G.W., 2018. Genome-centric view of carbon processing in thawing permafrost. Nature 560, 49–54. https://doi.org/10.1038/s41586-018-0338-1

Wu, Y.-W., Simmons, B.A., Singer, S.W., 2016. MaxBin 2.0: an automated binning algorithm to recover genomes from multiple metagenomic datasets. Bioinforma. Oxf. Engl. 32, 605–607. https://doi.org/10.1093/bioinformatics/btv638

Xue, Yuan, Braslavsky, I., Quake, S.R., 2020. Kinetics and Fidelity of Psychrophilic DNA Polymerases. bioRxiv 2020.08.04.236919. https://doi.org/10.1101/2020.08.04.236919

Xue, Yaxin, Jonassen, I., Øvreås, L., Taş, N., 2020. Metagenome-assembled genome distribution and key functionality highlight importance of aerobic metabolism in Svalbard permafrost. FEMS Microbiol. Ecol. 96. https://doi.org/10.1093/femsec/fiaa057

Yabuzaki, J., 2017. Carotenoids Database: structures, chemical fingerprints and distribution among organisms. Database J. Biol. Databases Curation 2017. https://doi.org/10.1093/database/bax004

Yamanaka, K., Reynolds, K.A., Kersten, R.D., Ryan, K.S., Gonzalez, D.J., Nizet, V., Dorrestein, P.C., Moore, B.S., 2014. Direct cloning and refactoring of a silent lipopeptide biosynthetic gene cluster yields the antibiotic taromycin A. Proc. Natl. Acad. Sci. 111, 1957–1962. https://doi.org/10.1073/pnas.1319584111

Yarza, P., Yilmaz, P., Pruesse, E., Glöckner, F.O., Ludwig, W., Schleifer, K.-H., Whitman, W.B., Euzéby, J., Amann, R., Rosselló-Móra, R., 2014. Uniting the classification of cultured and uncultured bacteria and archaea using 16S rRNA gene sequences. Nat. Rev. Microbiol. 12, 635–645. https://doi.org/10.1038/nrmicro3330

Yergeau, E., Arbour, M., Brousseau, R., Juck, D., Lawrence, J.R., Masson, L., Whyte, L.G., Greer, C.W., 2009. Microarray and Real-Time PCR Analyses of the Responses of High-Arctic Soil Bacteria to Hydrocarbon Pollution and Bioremediation Treatments. Appl. Environ. Microbiol. 75, 6258–6267. https://doi.org/10.1128/AEM.01029-09

Yin, J., Hoffmann, M., Bian, X., Tu, Q., Yan, F., Xia, L., Ding, X., Stewart, A.F., Müller, R., Fu, J., Zhang, Y., 2015. Direct cloning and heterologous expression of the salinomycin biosynthetic gene cluster from *Streptomyces albus* DSM41398 in Streptomyces coelicolor A3(2). Sci. Rep. 5, 15081. https://doi.org/10.1038/srep15081

Yoon, B.K., Jackman, J.A., Valle-González, E.R., Cho, N.-J., 2018. Antibacterial Free Fatty Acids and Monoglycerides: Biological Activities, Experimental Testing, and Therapeutic Applications. Int. J. Mol. Sci. 19, 1114. https://doi.org/10.3390/ijms19041114

Yoon, M., Jeon, H., Kim, M., 2012. Biodegradation of polyethylene by a soil bacterium and alkB cloned recombinant cell. J. Bioremediation Biodegrad. 3.

Yoshitake, S., Uchida, M., Iimura, Y., Ohtsuka, T., Nakatsubo, T., 2018. Soil microbial succession along a chronosequence on a High Arctic glacier foreland, Ny-Ålesund, Svalbard: 10 years' change. Polar Sci. 16, 59–67. https://doi.org/10.1016/j.polar.2018.03.003

Yu, Z., Stewart, G.R., Mohn, W.W., 2000. Apparent Contradiction: Psychrotolerant Bacteria from Hydrocarbon-Contaminated Arctic Tundra Soils That Degrade Diterpenoids Synthesized by Trees. Appl. Environ. Microbiol. 66, 5148–5154. https://doi.org/10.1128/AEM.66.12.5148-5154.2000

Yuan, M., Yu, Y., Li, H.-R., Dong, N., Zhang, X.-H., 2014. Phylogenetic diversity and biological activity of actinobacteria isolated from the Chukchi Shelf marine sediments in the Arctic Ocean. Mar. Drugs 12, 1281–1297. https://doi.org/10.3390/md12031281

Zarsky, J.D., Stibal, M., Hodson, A., Sattler, B., Schostag, M., Hansen, L.H., Jacobsen, C.S., Psenner, R., 2013. Large cryoconite aggregates on a Svalbard glacier support a diverse microbial community including ammonia-oxidizing archaea. Environ. Res. Lett. 8, 035044. https://doi.org/10.1088/1748-9326/8/3/035044

Zeng, Y.-X., Yu, Y., Li, H.-R., Luo, W., 2017. Prokaryotic Community Composition in Arctic Kongsfjorden and Sub-Arctic Northern Bering Sea Sediments as Revealed by 454 Pyrosequencing. Front. Microbiol. 8. https://doi.org/10.3389/fmicb.2017.02498

Zhang, D.-C., Liu, H.-C., Xin, Y.-H., Yu, Y., Zhou, P.-J., Zhou, Y.-G., 2008. *Salinibacterium xinjiangense* sp. nov., a psychrophilic bacterium isolated from the China No. 1 glacier. Int. J. Syst. Evol. Microbiol. 58, 2739–2742. https://doi.org/10.1099/ijs.0.65802-0

Zhang, H., Boghigian, B.A., Armando, J., Pfeifer, B.A., 2010. Methods and options for the heterologous production of complex natural products. Nat. Prod. Rep. 28, 125–151. https://doi.org/10.1039/C0NP00037J

Zhang, H., Yohe, T., Huang, L., Entwistle, S., Wu, P., Yang, Z., Busk, P.K., Xu, Y., Yin, Y., 2018. dbCAN2: a meta server for automated carbohydrate-active enzyme annotation. Nucleic Acids Res. 46, W95–W101. https://doi.org/10.1093/nar/gky418

Zhang, H.L., Hua, H.M., Pei, Y.H., Yao, X.S., 2004. Three New Cytotoxic Cyclic Acylpeptides from Marine *Bacillus* sp. Chem. Pharm. Bull. (Tokyo) 52, 1029–1030. https://doi.org/10.1248/cpb.52.1029

Zhang, L., Demain, A.L., 2005. Natural products: drug discovery and therapeutic medicine. Humana Press, Totowa, N.J.

Zhang, L., Zhao, G., Ding, X., 2011. Tandem assembly of the epothilone biosynthetic gene cluster by in vitro site-specific recombination. Sci. Rep. 1. https://doi.org/10.1038/srep00141

Zhang, S., Hou, S., Qin, X., Du, W., Liang, F., Li, Z., 2015. Preliminary Study on Effects of Glacial Retreat on the Dominant Glacial Snow Bacteria in Laohugou Glacier No. 12. Geomicrobiol. J. 32, 113–118. https://doi.org/10.1080/01490451.2014.929761

Zhang, Y., Liu, Z., Sun, J., Xue, C., Mao, X., 2018. Biotechnological production of zeaxanthin by microorganisms. Trends Food Sci. Technol. 71, 225–234. https://doi.org/10.1016/j.tifs.2017.11.006